Relicensing Study 3.1.2

Northfield Mountain / Turners Falls Operations Impact on Existing Erosion and Potential Bank Instability Study Report

Volume I – Executive Summary and Summary Report

Northfield Mountain Pumped Storage Project (No. 2485) and Turners Falls Hydroelectric Project (No. 1889)

Prepared for:

FirstLight Power Resources

Prepared by:

Simons & associates

Cardno Shaping the Future

Gomez and Sullivan Engineers

Kit Choi, PhD, PE

OCTOBER 2016

PREFACE

As part of the Federal Energy Regulatory Commission (FERC or the Commission) relicensing process for the Northfield Mountain Pumped Storage Project (FERC No. 2485) and Turners Falls Hydroelectric Project (FERC No. 1889) FirstLight Hydro Generating Company (FirstLight) conducted Relicensing Study No. 3.1.2 *Northfield Mountain / Turners Falls Operations Impacts on Existing Erosion and Potential Bank Instability* (Study No. 3.1.2). The goal of this study was to evaluate and identify the causes of erosion in the Turners Falls Impoundment (Connecticut River) and to determine to what extent they are related to Northfield Mountain and Turners Falls Project operations. The study was conducted over the period 2013-2016 and included various field data collection, analysis, and modeling efforts. In accordance with the FERC approved Revised Study Plan (RSP), this report provides a detailed discussion of all tasks identified in the RSP as well as the findings of each task.

Due to the extensive nature of the study, the robust datasets which were collected and analyzed, and the complex nature of this resource issue, the final report has been divided into three volumes to enable an easier review. These volumes include:

- Volume I – Executive Summary and Summary Report;
- Volume II – Main Report; and
- Volume III – Appendices

EXECUTIVE SUMMARY

The primary goal of Relicensing Study No. 3.1.2 *Northfield Mountain / Turners Falls Operations Impacts on Existing Erosion and Potential Bank Instability* (Study No. 3.1.2) was to evaluate and identify the causes of erosion in the Turners Falls Impoundment (TFI) and to determine to what extent they are related to Northfield Mountain Pumped Storage Hydroelectric Project (FERC No. 2485) and Turners Falls Hydroelectric Project (FERC No. 1889) operations. In order to achieve the goals and objectives of the study, the study methodology was divided into seven tasks which included data gathering and literature review; developing a geomorphic understanding of the Connecticut River; identifying the potential causes of erosion present in the TFI; conducting field studies and data collection efforts; data analyses; evaluation of the causes of erosion; and, finally, developing a final report and deliverables.

In order to identify and evaluate the causes of erosion, a list of potential causes was first identified during development of the study methodology. This list was based on past experience conducting geomorphic assessments of the Connecticut River, and other alluvial rivers, as well as from preliminary investigation of existing documentation. The list of potential causes was then divided into two categories: (1) potential primary causes of erosion, and (2) potential secondary causes of erosion. The list of potential causes provided the foundation for this study and included the following:

Potential Primary Causes of Erosion

- Hydraulic shear stress due to flowing water
- Water level fluctuations associated with hydropower operations
- Boat waves
- Land management practices and anthropogenic influences
- Ice

Potential Secondary Causes of Erosion

- Animals
- Wind Waves
- Seepage and piping
- Freeze-thaw

Potential primary causes of erosion were those which were thought to be most prevalent throughout the TFI where erosion occurs. These causes were studied at a number of detailed study sites which were located throughout the geographic extent of the TFI. In addition to encompassing the geographic extent of the TFI, the detailed study sites spanned the various hydraulic reaches of the TFI and exhibited the full range of riverbank features and characteristics as observed during the 2013 Full River Reconnaissance (FRR) survey (Relicensing Study No. 3.1.1). The results from the various field investigations which occurred at each site were then incorporated into the Bank Stability and Toe Erosion Model (BSTEM) and/or were used for independent, supplemental analyses. Dominant and contributing primary causes of erosion were then identified at each detailed study site. In order to be considered a dominant cause of erosion the specific cause had to be responsible for greater than 50% of the erosion at that site. Conversely, to be considered a contributing cause the specific cause had to be responsible for greater than 5% (but less than 50%) of the erosion at that site.

Once the dominant and contributing causes of erosion were identified at each detailed study site, the results were extrapolated throughout the TFI such that every riverbank segment identified during the 2013 FRR was assigned dominant and contributing primary causes of erosion. The extrapolation process was a multi-step process that took into consideration the riverbank features and characteristics of each riverbank segment as well as the hydraulic characteristics present. At the completion of the extrapolation process

summary statistics were developed for the dominant and contributing primary causes of erosion throughout the TFI.

During study plan development it was anticipated that the potential secondary causes of erosion could be present at specific locations in the TFI, however, it was likely that they would have minimal to no influence on erosion processes (other than in any specific location where they may exist). Accordingly, these causes of erosion were analyzed sufficiently to determine their relative contribution to erosion but not to the level of detail and specificity as the potential primary causes of erosion mentioned above. Any potential secondary causes of erosion that were found to be a contributing cause(s) at a specific site were taken into consideration during the extrapolation process.

Results

The results of the study found that naturally occurring high flows were the dominant primary cause of erosion, followed by boat waves, and Vernon operations. Northfield Mountain or Turners Falls Project operations were not found to be a dominant primary cause of erosion at any riverbank segment in the TFI. The dominant primary causes of erosion followed a clear spatial pattern with Vernon Project operations being the dominant cause from Vernon Dam to downstream of detailed study site 11L, natural high flows from downstream of detailed study site 11L to upstream of Barton Cove, and boat waves from upstream of Barton Cove to Turners Falls Dam. The basis of the conclusions of the study are set out in the paragraphs that follow.

Review of the hydraulic model results, and more specifically the Energy Grade Line slope[1], revealed four distinct hydraulic reaches within the TFI. The four hydraulic reaches included the Upper (Reach 4), Middle (Reach 3), Northfield Mountain (Reach 2), and Lower (Reach 1) reaches. The Upper reach extends from Vernon Dam to just upstream of the NH/MA border, the Middle reach from upstream of the NH/MA border to just downstream of Kidds Island, the Northfield Mountain reach from just downstream of Kidds Island to just downstream of the Northfield Mountain tailrace, and the Lower reach from just downstream of the Northfield Mountain tailrace to the Turners Falls Dam.

The results of the hydraulic and BSTEM models indicated that hydropower operations can only potentially impact erosion processes within the hydraulic reach where the project is located due to the varying hydraulic characteristics of the TFI. In other words, the models showed that Northfield Mountain operations can only potentially impact erosion processes at riverbank segments within the Northfield Mountain reach. Vernon operations can only potentially impact erosion processes within the Upper reach, and likewise Turners Falls operations can only affect the Lower reach. Although Project operations can impact flows and water levels beyond their given hydraulic reach, the impacts at flows which cause erosion (as determined by BSTEM) are minor enough that they do not alter the EGL slope, and therefore the velocity or shear stress, outside of their reach.

The models assessed the erosive impact of flows within thresholds established by the hydraulic characteristic of each reach. Through further analysis of the various modeling results two flow thresholds were established in the upper reach of the TFI (hydraulic reach 4): (1) <17,130 cubic feet per second (cfs), and (2) >17,130 cfs. This threshold value was identified as it corresponds with the hydraulic capacity of the Vernon Hydroelectric Project and is consistent with the hydraulic characteristics of this more riverine reach

[1] The Energy Grade Line is the elevation of the energy head of the water in the river and is the hydraulic grade line plus the velocity head between each model transect. Generally, a greater slope of the energy grade line indicates a higher water velocity and a higher potential for hydraulic erosion. The Energy Grade Line is an important component in the hydraulic-erosion sub-model of BSTEM as it forms the basis for calculating boundary shear stress for nodes along the wetted perimeter along with the hydraulic radius of the segmented flow and the unit weight of water.

of the TFI. In the remaining three hydraulic reaches (i.e., from just upstream of the NH/MA border to Turners Falls Dam), three flow thresholds were established, including: (1) <17,130 cfs; (2) 17,130 to 37,000 cfs; and (3) >37,000 cfs. 37,000 cfs was chosen as the high flow threshold as it represents the combined hydraulic capacity of Vernon and Northfield Mountain, is at a flow above which the French King Gorge becomes the hydraulic control for the mid and upper TFI, and represents periods when Northfield Mountain does not regularly operate. Flow thresholds represent flows as measured at a given site at a given time and can be the combination of a number of factors including hydroelectric operations, tributary inflow, or natural flows. Given that flow can vary across different locations at the same time, these flow thresholds are not based exclusively on Vernon inflow or naturally routed flow (i.e. Vernon inflow plus inflow from the Ashuelot and Millers Rivers) but are instead representative of all hydrologic influences.

For the purpose of this study, flows equal to or less than 17,130 cfs were considered low flows. This threshold was established based on the hydraulic capacity of the Vernon Hydroelectric Project which is 17,130 cfs. At flows equal to or less than this value flows and water levels throughout the TFI are controlled by hydroelectric operations (i.e., Vernon, Northfield Mountain, and/or Turners Falls operations). During these low flow periods Vernon operations can impact flow and water levels downstream to the Turners Falls Dam while water level management at the Turners Falls Dam and Northfield Mountain Project operation can impact flows and water levels upstream to Vernon. Water levels during these low flow periods are almost exclusively on the lower riverbank regardless of water level fluctuations from hydroelectric operations.

At flows between 17,130 and 37,000 cfs (i.e., moderate flows) a number of hydraulic influences are observed throughout the TFI, specifically in hydraulic reaches 3 (middle), 2 (Northfield Mountain), and 1 (lower)[2]. While Vernon and Turners Falls operations are no longer the controlling hydraulic factor they can still have a contributing impact on flows and water levels depending on the location in the TFI. Northfield Mountain operations cans also impact flows and water levels throughout the TFI during the full range of moderate flows. Additionally, water level management at the Turners Falls Dam can still impact water levels throughout the TFI up to flows of 30,000 cfs; however, as moderate flows increase, the upstream impact of water level management at the Turners Falls Dam diminishes until having no impact at all. At flows of 30,000 cfs or greater the French King Gorge becomes the hydraulic control for the middle and upper portions of the TFI. That is, Turners Falls Dam water level management has a very limited impact on flows or water levels above the French King Gorge at flows greater than 30,000 cfs. Water levels during moderate flow periods may be on either the lower or upper riverbank depending on the flow and the location in the TFI.

In hydraulic reaches 3 (middle), 2 (Northfield Mountain), and 1 (lower) flows equal to or greater than 37,000 cfs represent natural high flows.[3] At flows of this magnitude neither the Vernon or Turners Falls Project impacts flows or water levels as they are operated in run-of-river mode (i.e., inflow is equal to outflow). Additionally, the French King Gorge acts as the hydraulic control for the upper and middle portion of the TFI. While Northfield Mountain has the ability to operate at flows of this magnitude, analysis of Project operations data over the evaluation period (2000-2014) found that the Project only operated 0.025% (4 units) to 2.6% (1 unit) of the time when flows exceeded 37,000 cfs. This equates to approximately 0.1 to 9 days per year, respectively. During these high flow periods, the water level rests almost exclusively on the upper bank.

[2] While downstream hydraulic influences can have an impact on flows and water levels in hydraulic reach 4 (upper) during these moderate flow periods, the impact is not as pronounced as in the middle and downstream reaches. As such, for the purposes of this study, the upper reach has only two defined flow thresholds – those below 17,130 cfs and those above 17,130 cfs.

[3] As previously noted, the natural high flow threshold in hydraulic reach 4 (upper) is 17,130 cfs.

In order to quantify the primary causes of erosion at each detailed study site a number of analyses were conducted utilizing BSTEM. The results of these analyses were then compared against the results of various supplemental analyses (e.g., hydraulics, sediment transport, etc.) as a means of verification. Each primary cause of erosion was determined as follows:

- **Moderate or High Flows** *(hydraulic shear stress due to flowing water)*: a flow analysis was conducted which resulted in the identification of the erosion flow threshold at which 50% and 95% of all erosion occurs at a given site. Based on the results of this analysis, and the flow thresholds previously discussed, a determination was then made as to the sites where natural moderate or high flows were found to be a dominant or contributing cause of erosion;

- **Boats** *(boat waves)*: BSTEM was enhanced with a built-in boat wave module for this study. Two BSTEM runs were executed utilizing this module, one with boat waves "turned on" and the other with boat waves "turned off." The difference in observed erosion between the two model runs determined the sites where boat waves were a cause of erosion;

- **Vernon Operations** *(hydraulic shear stress due to flowing water, water level fluctuations associated with hydropower operations)*: the results of the flow analysis were used to identify areas within the Upper reach where erosion was observed at flows below 17,130 cfs;

- **Northfield Mountain Operations** *(hydraulic shear stress due to flowing water, water level fluctuations associated with hydropower operations)***:** two BSTEM runs were executed, one representing the Baseline Condition (i.e., what actually happened during the modeling period) and one representing Northfield Mountain as idle. The difference in observed erosion between the two model runs determined the sites where Northfield Mountain operations were a cause of erosion; and

- **Turners Falls Operations** *(hydraulic shear stress due to flowing water, water level fluctuations associated with hydropower operations)***:** as previously discussed, due to the hydraulic characteristics of the TFI, Turners Falls Project operations could only be a potential cause of erosion in hydraulic reach 1 (lower). Detailed study sites in the lower reach only existed in the vicinity of Barton Cove and were not located in the more riverine portion of the reach (spanning just upstream of Barton Cove to upstream of the French King Gorge). As such, a modified extrapolation approach was used to determine the causes of erosion in the Lower reach upstream of Barton Cove. The modified extrapolation approach utilized a combination of BSTEM results, geomorphic assessment, and hydraulic model analysis.

The two remaining potential primary causes of erosion (land-use and land management practices and ice) were evaluated independently of BSTEM. In regard to land-use and land management practices, while riverbank vegetative conditions were analyzed as contributing factors in BSTEM, the potential for land-use and land management practices adjacent to the riverbanks to contribute to erosion were evaluated through geospatial analysis using GIS software. Ice was evaluated primarily through a combination of TFI monitoring during the winter of 2015/2016 (as well as limited monitoring during the winter of 2014/2015) and analysis of historic information from throughout the Connecticut River (including upstream impoundments) and other river systems.

As shown below, the results of the study found that naturally occurring high flows were the dominant primary cause of erosion, followed by boat waves, and Vernon operations. Northfield Mountain or Turners Falls Project operations were not found to be a dominant primary cause of erosion at any riverbank segment in the TFI. The dominant primary causes of erosion followed a clear spatial pattern with Vernon Project operations being the dominant cause from Vernon Dam to downstream of detailed study site 11L, natural high flows from downstream of detailed study site 11L to upstream of Barton Cove, and boat waves from upstream of Barton Cove to Turners Falls Dam.

Dominant Primary Causes of Erosion	% of Total Riverbank Length	Total length
Natural High Flows	78%	175,900 ft. (33 mi.)
Boat waves	13%	30,800 ft. (6 mi.)
Vernon Operations	9%	20,200 ft. (4 mi)
Northfield Mountain Operations	0%	0 ft.
Turners Falls Operations	0%	0 ft.
Ice	I	I

I = Indeterminate

As observed in the table, the impact of ice on erosion processes could not be quantified as it was not a cause of erosion that was examined in BSTEM. Through discussions with the U.S. Geological Survey (USGS) in NH and VT it was noted that ice typically does not cause erosion if the ice simply melts in place without significant break-up and if ice floes moving down river causing ice jams and impacting banks do not occur. This is consistent with the findings of the historic analysis conducted and with observations made during field monitoring which occurred during the 2014/2015 winter when much of the TFI was frozen over but the ice simply melted in place during the later winter, early spring of 2015. If, on the other hand, there is significant break-up, ice floes moving down river with the potential for ice jams that are pushed against and scrape along the banks; then such an event could potentially cause erosion and damage to the riverbanks.

Analysis of historic ice information and observations made in the TFI, upstream impoundments (Vernon, Bellows Falls, and Wilder), and other river systems (both impounded and un-impounded) provided valuable insights into what could potentially occur in the TFI in the future as ice formation becomes more likely due to the closure of Vermont Yankee (VY). Analysis of historic data found that ice has caused severe erosion under the right climatic and hydrologic conditions (i.e., severe break-up, ice floes, and ice jams) and has contributed to bank instability which can eventually lead to erosion. In addition to directly causing erosion these processes can also greatly effect riverbank vegetation thus also impacting the stability of the bank. Ice formation and accompanying freeze-thaw cycles may also weaken the soil matrix by developing cracks and spalling of the soil surface; however, the process of break-up plays a more significant role in erosion processes.

Although a quantitative analysis of the impact of ice as a cause of erosion was not possible given weather conditions during the monitoring period and available historic data, the results of the analysis which was conducted indicate that ice has the potential to be a naturally occurring dominant cause of erosion in the TFI in the future if the right climatic and hydrologic conditions persist. Available information and observations indicate that Project operations do not cause an ice break-up event to occur, as ice break-up events occur as a result of climatic and hydrologic conditions (i.e. moderate to high flows, rapid melting, and rainfall) which are independent of Project operations.

Analysis of the contributing primary causes of erosion, found that the majority of riverbank segments in the TFI did not have a contributing primary cause (i.e., a cause contributing 5-50% of erosion). Natural high flows were such a dominant factor in erosion processes that no other contributing primary causes were identified at the majority of riverbank segments. At riverbanks segments that did have contributing primary causes of erosion, boat waves were found to be the most common followed by naturally occurring moderate flows, natural high flows, and Northfield Mountain operations. Turners Falls or Vernon operations were not found to be a contributing primary cause of erosion at any riverbank segment in the TFI. Riverbank segments that exhibited contributing causes of erosion were limited to the Upper (high flows); Northfield Mountain (moderate flows, Northfield Mountain operations, and boats); and Lower (moderate flows and boats) hydraulic reaches. No contributing primary causes of erosion were observed in the Middle hydraulic reach. Secondary causes of erosion (i.e., animals, wind waves, seepage and piping, or freeze-thaw) were not found to be a contributing cause of erosion at any riverbank segment.

Contributing Primary Causes of Erosion	% of Total Riverbank Length[4]	Total length[5]
None	68%	153,400 ft. (29 mi.)
Boats	16%	36,000 ft. (7 mi.)
Natural Moderate Flows	10%	23,200 ft. (4 mi.)
Natural High Flows	9%	20,200 ft. (4 mi.)
Northfield Mountain Operations	4%	8,600 ft. (1.5 mi.)
Vernon Operations	0%	0 ft.
Turners Falls Operations	0%	0 ft.
Ice	I	I

I = Indeterminate

Land-use or land management practices were found to be a potential contributing cause of erosion at 44% of the TFI riverbanks (101,000 ft. or 19 mi.). These segments were localized to areas where the land-use adjacent to the riverbank was classified as Developed or Agriculture and the riparian buffer was 50 ft. or less.

As demonstrated in the tables and discussion above, natural high flows are responsible for the vast majority of erosion in the TFI with hydroelectric operations playing a very limited role, if any. Northfield Mountain or Turners Falls Project operations were not found to be a dominant primary cause of erosion at any riverbank segment in the TFI. Northfield Mountain operations were found to be a contributing primary cause of erosion at only 4% of all riverbanks or 8,600 ft. (1.5 mi.) out of a potential 227,000 ft. (43 mi.). Furthermore, the riverbank segments where Northfield Mountain operations were found to be a contributing cause of erosion are limited to the Northfield Mountain hydraulic reach (reach 2).

[4] Note that since moderate flows and boat waves are contributing causes of erosion at a number of the same riverbank segments, the total percentage for contributing causes does not equal 100%. In other words, given that a riverbank segment can have more than one contributing cause of erosion, the percentages do not add to 100%.

[5] Rounded to the nearest 100 ft. or 0.5 mi.

SUMMARY REPORT

FirstLight Hydro Generating Company (FirstLight), has initiated the process of relicensing the Turners Falls Hydroelectric Project (FERC No. 1889) and the Northfield Mountain Pumped Storage Project (FERC No. 2485) with the Federal Energy Regulatory Commission (FERC or the Commission) using FERC's Integrated Licensing Process (ILP). The current licenses for the Turners Falls and Northfield Mountain Projects were issued on May 4, 1968 and May 5, 1980, respectively, with both set to expire on April 30, 2018. As part of the relicensing process, FirstLight filed a Revised Study Plan (RSP) with FERC on August 14, 2013. Included in the RSP was Study No. 3.1.2 *Northfield Mountain/Turners Falls Operations Impact on Existing Erosion and Potential Bank Instability* (Study No. 3.1.2 or the Causation Study). The methodology and scope for Study No. 3.1.2 were approved with modifications by the Commission in its September 12, 2013 Study Plan Determination Letter (SPDL). Approximately one year after FERC issued its SPDL, FirstLight filed an addendum to the RSP with FERC on September 15, 2014 which detailed protocols for increased investigation of ice as a cause of erosion due to the closure of the Vermont Yankee Nuclear Power Plant (VY) located upstream in the Vernon Hydroelectric Project (Vernon) impoundment.

Study Overview

The goals of Study No. 3.1.2, as stated in the RSP, were to evaluate and identify the causes of erosion in the TFI and to determine to what extent they are related to Northfield Mountain and Turners Falls Project operations. In order to accomplish these goals the RSP (p. 3-25) included the following tasks:

- Conduct a thorough data gathering and literature review effort of existing relevant data to identify data gaps;
- Conduct field investigations and field data collection to fill data gaps. Gather the field data required to conduct detailed analyses of the causes of erosion and the forces that control them;
- Develop an understanding of the historic and modern geomorphology of the Connecticut River. A historic geomorphic assessment will be conducted to provide context for analyzing the modern geomorphology of the Connecticut River;
- Identify the causes of erosion present in the TFI, the forces associated with them, and their relative importance at a particular location. Conduct various data analyses to gain a better understanding of these causes and forces;
- Identify and establish fixed riverbank transects that will be representative of the range of riverbank features, characteristics, and conditions present in the TFI;
- Conduct detailed studies and analyses of erosion processes at the fixed riverbank transects;
- Evaluate the causes of erosion using field collected data and the results of the proposed data analyses. This evaluation will include quantifying and ranking all causes present at each fixed riverbank transect as well as in the TFI in general; and
- Develop a final report that will summarize the findings of this study and the methods used.

During development of the RSP, and continuing after issuance of FERC's September 2013 SPDL, FirstLight conducted an in-depth literature review and data gathering effort which provided the foundation for this study and allowed for the identification of potential data gaps (RSP Task 1). During development of the RSP, FirstLight developed a list of the potential causes of erosion which may be present in the TFI. The preliminary list of potential causes presented in the RSP included (in no particular order):

- Hydraulic shear stress due to flowing water;
- Water level fluctuations due to hydropower operations;
- Boat waves;
- Wind waves;
- Land management practices and anthropogenic influences to the riparian zone;
- Animals;
- Seepage and piping;
- Freeze-thaw; and
- Ice or debris

Based on past experience conducting geomorphic assessments on the Connecticut River and other alluvial rivers, as well as from information gleaned from the preliminary investigation of existing documents and the FRR, the preliminary list of potential causes of erosion was then reviewed and divided in the RSP (p. 3-44) into two categories: 1) potential primary causes of erosion, and 2) potential secondary causes of erosion. From this, the following classifications were developed (in no particular order):

Potential Primary Causes of Erosion

- Hydraulic shear stress due to flowing water
- Water level fluctuations due to hydropower operations
- Boat waves
- Land management practices and anthropogenic influences
- Ice[6]

Potential Secondary Causes of Erosion

- Animals
- Wind waves
- Seepage and piping
- Freeze-thaw

The causes of erosion listed above formed the basis for the field studies and data collection efforts conducted as part of this study as well as the data analysis and evaluation of causes conducted in accordance with the RSP. While all of these potential causes of erosion were investigated, special emphasis was placed on the potential primary causes of erosion (RSP Task 3). The potential primary causes of erosion, and the forces associated with them, were evaluated at 25 detailed study sites located at fixed riverbank transects throughout the geographic extent of the TFI (RSP Task 4).

[6] Ice was originally classified in the RSP as a potential secondary cause of erosion, however, due to the closure of VY and the potential for the increased presence of ice in the TFI, and in accordance with the 2014 Addendum to Study 3.1.2 required by the SPDL, it was elevated to a potential primary cause of erosion in 2014.

The fixed riverbank transects where the potential primary causes of erosion were investigated (also referred to as detailed study sites) were selected in collaboration with stakeholders and were presented in the report titled *Study No. 3.1.2 Northfield Mountain/Turners Falls Operations Impact on Existing Erosion and Bank Instability – Selection of Detailed Study Sites – September 2014* (FirstLight, 2014b).[7] Stakeholders consulted during development of the final set of detailed study sites included: the Connecticut River Streambank Erosion Committee (CRSEC), Connecticut River Watershed Council (CRWC), Franklin Regional Council of Governments (FRCOG), Landowners and Concerned Citizens for License Compliance (LCCLC), National Marine Fisheries Service (NMFS), Massachusetts Riverways, and the Franklin Conservation District (FCD) as well as the Massachusetts Department of Environmental Protection (MADEP) and FERC.

The final set of detailed study sites included 25 locations throughout the geographic extent of the TFI. Detailed study sites encompassed a representative range of riverbank features, characteristics, and erosion conditions and included several sites that had been previously restored as a result of FirstLight's Erosion Control Plan (ECP). Sites were selected at existing, permanent transects (which have been surveyed annually since the 1990's) and at newly identified supplemental detailed study points. Supplemental detailed study points were proposed based on the results of the detailed geomorphic and geotechnical assessments conducted during the 2013 Full River Reconnaissance (FRR, Relicensing Study No. 3.1.1) land-based survey as well as the results of the 2013 FRR boat-based survey. Although the newly identified supplemental representative detailed study points were selected at only one bank, full cross-section surveys were collected at each location.

Detailed study sites were classified as either Calibration or Representative Sites. *Calibration sites* were defined as sites which were established at an existing, permanent transect location where data collection would be used to calibrate the Bank Stability and Toe Erosion Model (BSTEM). Establishing these sites at the existing, permanent transects provided the opportunity to calibrate BSTEM with actual erosion amounts or changes in bank geometry as it has occurred over a period of historic flows and water level data. *Representative sites* were defined as sites established throughout the TFI at locations that exhibit a range of representative features, characteristics, and erosion conditions. These sites did not have repetitive surveys for calibration of BSTEM. Calibration sites could only exist at existing, permanent transects while representative sites can exist anywhere in the TFI. Of the 25 detailed study sites, 16 were classified as representative (of which 7 are both calibration and representative), and 9 were classified as calibration sites. In other words, 16 detailed study sites are located at existing, permanent transects (established in the 1990's) while 9 were established at new locations identified as a result of the 2013 FRR. Figure 1 depicts the locations of the detailed study sites and transects located throughout the TFI.

[7] The *Selection of Detailed Study Sites* report was filed with FERC as part of the *Relicensing Study 3.1.2 Initial Study Report Summary* on September 15, 2014.

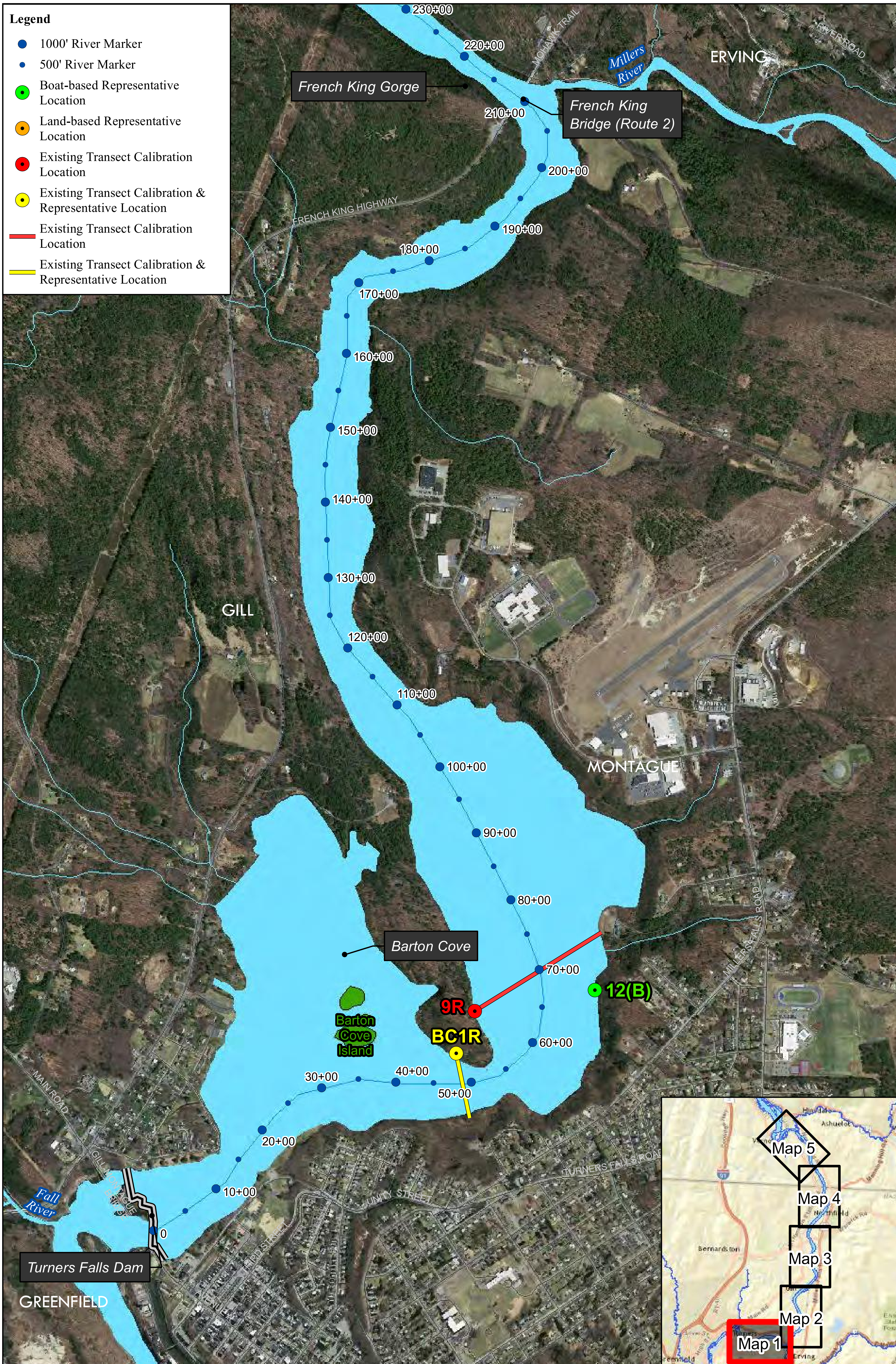

FIRSTLIGHT HYDRO GENERATING COMPANY
Northfield Mountain Pumped Storage Project No. 2485
Turners Falls Hydroelectric Project No. 1889

STUDY 3.1.2

0 625 1,250 2,500 Feet

Figure 1:
Detailed Study Sites
in the Turners Falls Impoundment
Map 1

Service Layer Credits: Sources: Esri, HERE, DeLorme, USGS, Intermap, increment P Corp., NRCAN, Esri Japan, METI, Esri China (Hong Kong), Esri (Thailand), MapmyIndia, © OpenStreetMap contributors, and the GIS User Community

Path: W:\gis\studies\3_1_2\maps\final_report\figure-1.mxd

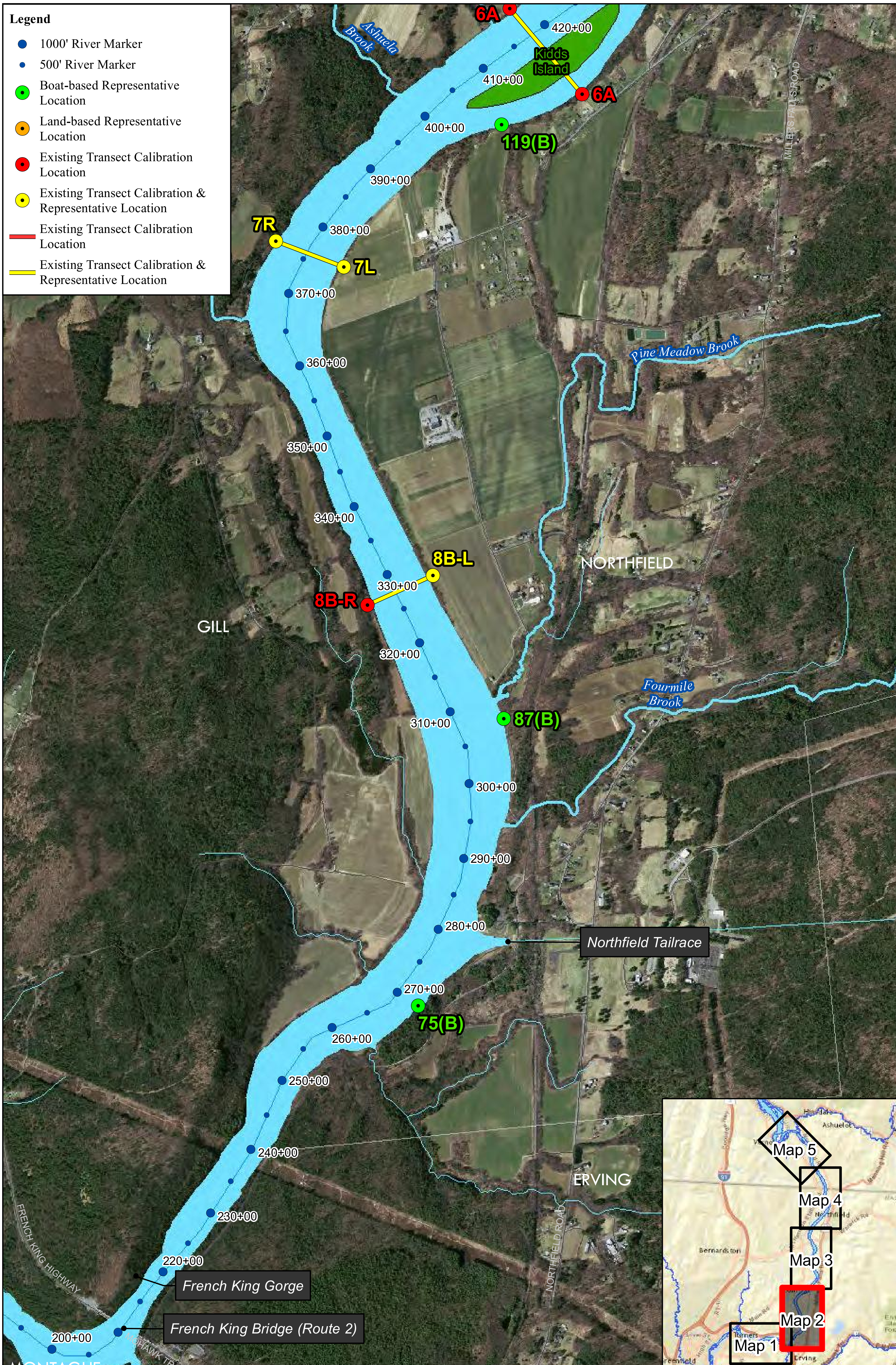

FirstLight Power Resources

FIRSTLIGHT HYDRO GENERATING COMPANY
Northfield Mountain Pumped Storage Project No. 2485
Turners Falls Hydroelectric Project No. 1889

STUDY 3.1.2

N

0 625 1,250 2,500 Feet

Figure 1:
Detailed Study Sites
in the Turners Falls Impoundment
Map 2

Service Layer Credits: Sources: Esri, HERE, DeLorme, USGS, Intermap, increment P Corp., NRCAN, Esri Japan, METI, Esri China (Hong Kong), Esri (Thailand), MapmyIndia, © OpenStreetMap contributors, and the GIS User Community

Path: W:\gis\studies\3_1_2\maps\final_report\figure-1.mxd

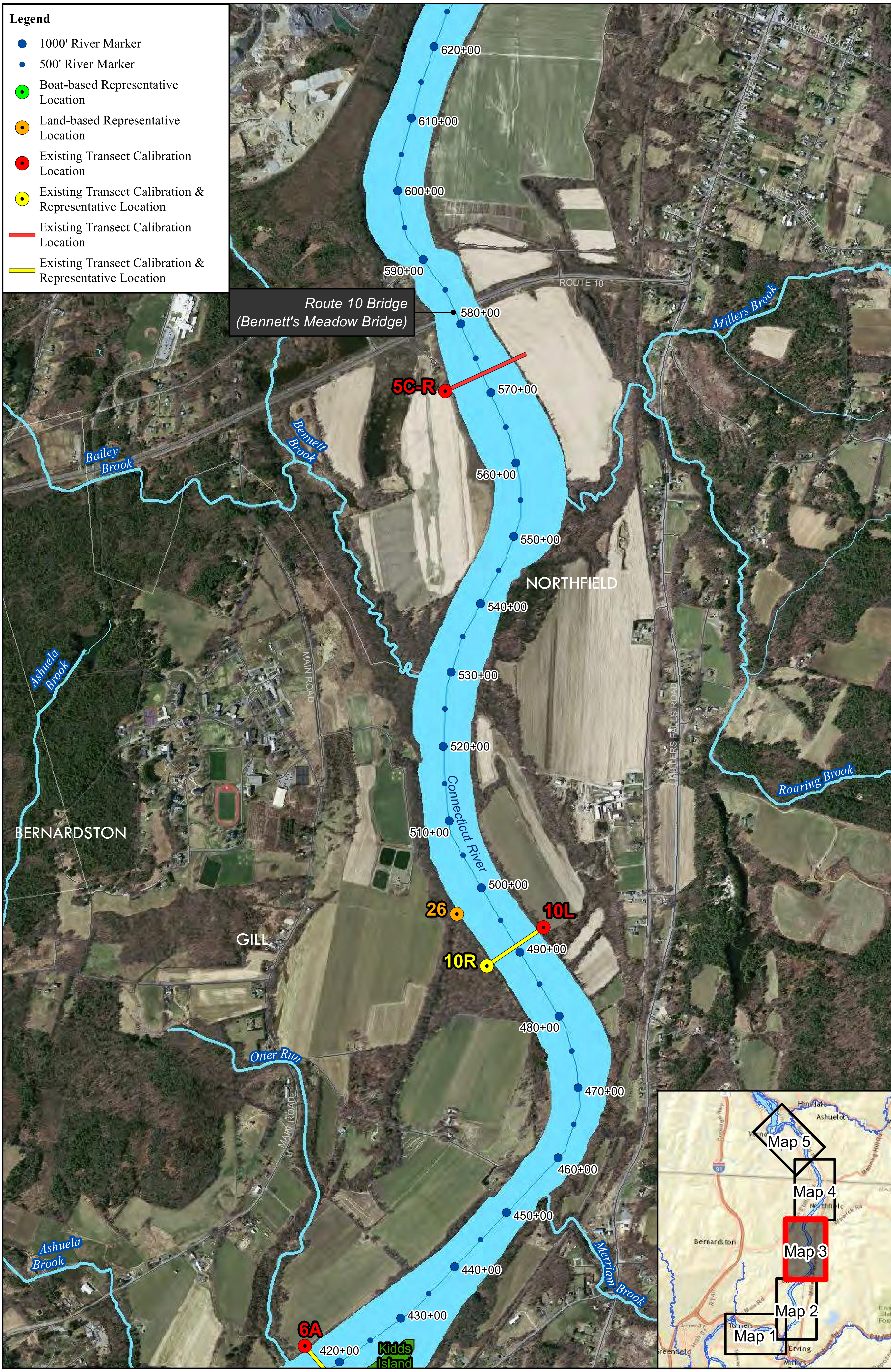

FIRSTLIGHT HYDRO GENERATING COMPANY
Northfield Mountain Pumped Storage Project No. 2485
Turners Falls Hydroelectric Project No. 1889

STUDY 3.1.2

FirstLight Power Resources

N

0 625 1,250 2,500 Feet

Figure 1:
Detailed Study Sites
in the Turners Falls Impoundment
Map 3

Service Layer Credits: Sources: Esri, HERE, DeLorme, USGS, Intermap, increment P Corp., NRCAN, Esri Japan, METI, Esri China (Hong Kong), Esri (Thailand), MapmyIndia, © OpenStreetMap contributors, and the GIS User Community

Path: W:\gis\studies\3_1_2\maps\final_report\figure-1.mxd

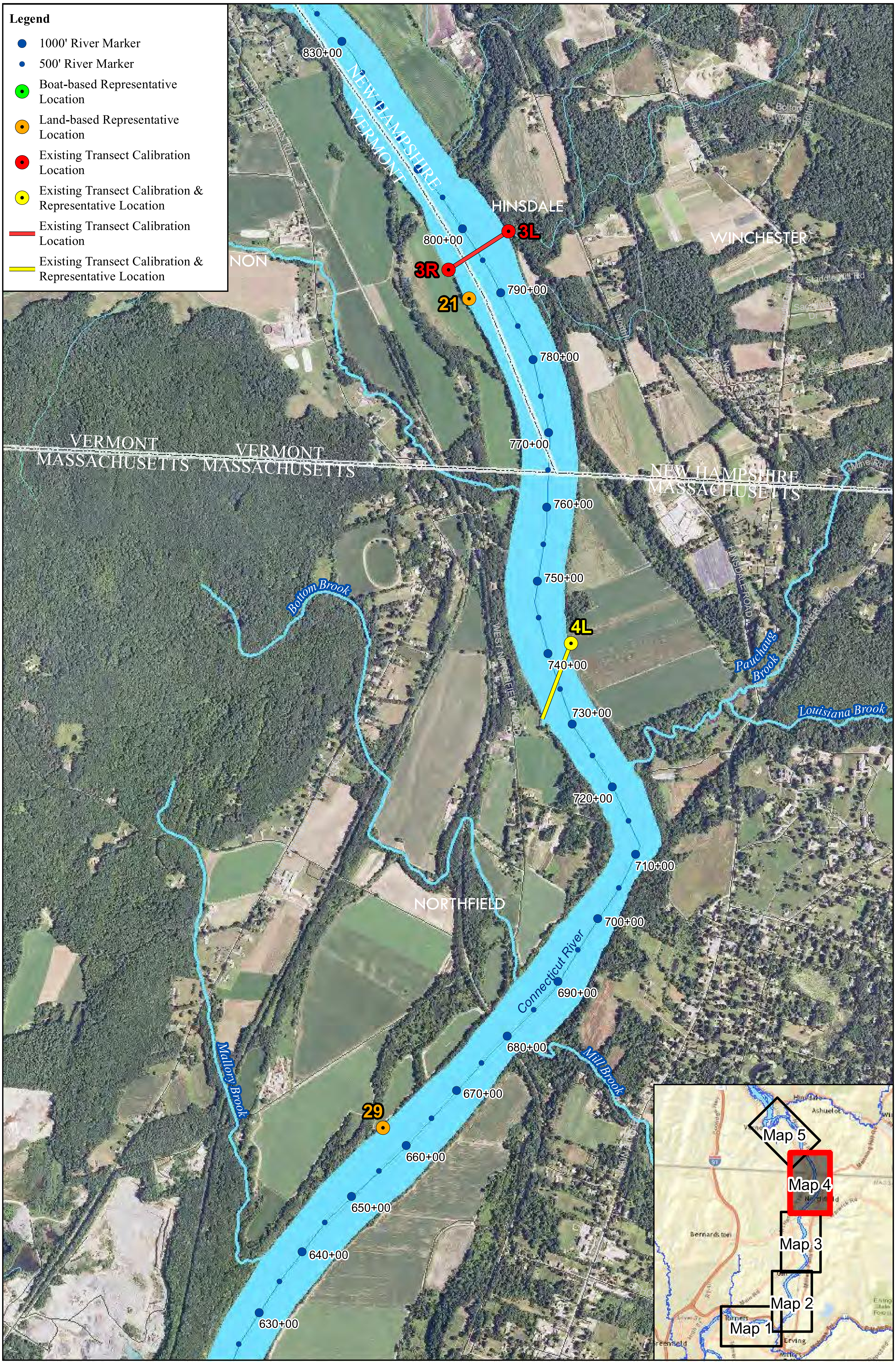

FIRSTLIGHT HYDRO GENERATING COMPANY
Northfield Mountain Pumped Storage Project No. 2485
Turners Falls Hydroelectric Project No. 1889

STUDY 3.1.2

0 625 1,250 2,500 Feet

N

FirstLight Power Resources

Figure 1:
Detailed Study Sites
in the Turners Falls Impoundment
Map 4

Service Layer Credits: Sources: Esri, HERE, DeLorme, USGS, Intermap, increment P Corp., NRCAN, Esri Japan, METI, Esri China (Hong Kong), Esri (Thailand), MapmyIndia, © OpenStreetMap contributors, and the GIS User Community

Path: W:\gis\studies\3_1_2\maps\final_report\figure-1.mxd

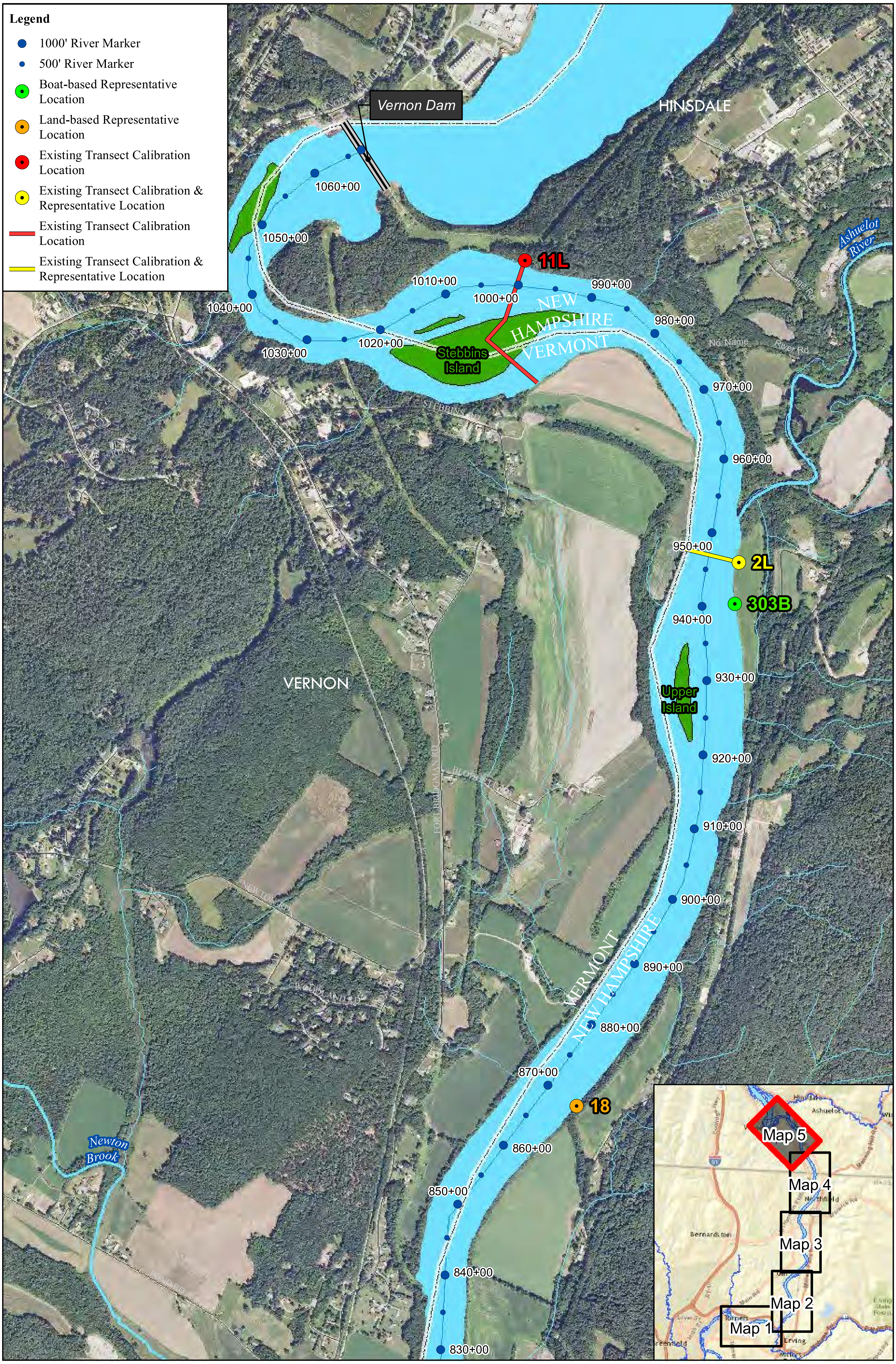

FIRSTLIGHT HYDRO GENERATING COMPANY
Northfield Mountain Pumped Storage Project No. 2485
Turners Falls Hydroelectric Project No. 1889

STUDY 3.1.2

0 625 1,250 2,500 Feet

FirstLight Power Resources

Figure 1:
Detailed Study Sites
in the Turners Falls Impoundment
Map 5

Service Layer Credits: Sources: Esri, HERE, DeLorme, USGS, Intermap, increment P Corp., NRCAN, Esri Japan, METI, Esri China (Hong Kong), Esri (Thailand), MapmyIndia, © OpenStreetMap contributors, and the GIS User Community

Path: W:\gis\studies\3_1_2\maps\final_report\figure-1.mxd

Once the final set of detailed study sites was established, field data collection efforts were carried out during 2014 with supplemental field work also conducted in 2015 and 2016 (ice monitoring). Field activities were conducted in accordance with Task 4 of the RSP as well as the Addendum to the RSP filed with FERC in September 2014. Field data that were collected (either as part of this study or other studies) included:

- TFI water level, flow, and Project operations data (Study No. 3.2.2);
- Bathymetric surveys of the TFI to support development of hydraulic models (Study No. 3.2.2);
- Riverbank features, characteristics, and erosion conditions as observed during the 2013 FRR (Study No. 3.1.1);
- Annual cross-section surveys at the existing, permanent transects and newly identified supplemental detailed study sites;
- BSTEM input parameters including: surface erodibility (critical shear stress), geotechnical strength (effective cohesion and friction angle), bulk unit weight, riverbank sediment particle-size distribution, maximum rooting depth of vegetation, and riparian species distribution;
- Vegetative parameters of five species including root density, distribution and root tensile-strength data;
- Boat-wave data and boat statistics for input into the BSTEM boat-wave algorithm;
- Suspended sediment concentration data (Study No. 3.1.3); and
- Ice monitoring photos

In addition, historical groundwater and boat wave data collected in the 1990's were examined as part of this study. The methodologies for all field data collection efforts are discussed in greater detail in the main report (Volume II) and appendices (Volume III). Field data were post processed and prepared for analysis or inclusion in various models throughout late 2014 and into 2015. Following the completion of the various field studies and data collection efforts, as well as completion of all post processing and quality assurance (QA), the field collected data were analyzed and model runs were executed throughout 2015 and into 2016 (RSP Tasks 5 and 6).

The data analyses conducted for this study consisted of a mix of qualitative and quantitative methods based on RSP Tasks 2, 5, and 6 as well as RSP Table 3.1.2-3. Data analyses followed a three-level approach consisting of:

1. **Qualitative geomorphic analysis:**

   The qualitative geomorphic analysis included developing a geomorphic understanding of the Connecticut River and TFI (RSP Task 2), including: (a) geomorphology of alluvial rivers; (b) geomorphic history of the Connecticut River; (c) analysis of historic datasets; (d) geomorphic analysis of tributaries and upland erosion features; and (e) erosion comparison of the TFI and Connecticut River.

2. **Quantitative engineering and geomorphic analysis:**

   The quantitative engineering and geomorphic analysis included (RSP Task 5 and 6, RSP Table 3.1.2-3): (a) analysis of the hydrologic and hydraulic characteristics of the TFI based on field collected data and hydraulic model results; (b) sediment transport analysis; (c) analysis of hydraulic shear stress, water level fluctuations, boat waves, and ice as potential primary causes of erosion; and (d) analysis of land-use and land management practices via geospatial analysis.

3. **Computer modeling:**

   To better understand the complex hydrologic, hydraulic, and geotechnical dynamics of the TFI three models were utilized, including: a one-dimensional unsteady Hydraulic Engineering Center-River Analysis System (HEC-RAS) model, a two-dimensional River2D model, and BSTEM (RSP Task 5 and 6, RSP Table 3.1.2-3).

   As part of Study No. 3.2.2 *Hydraulic Study of Turners Falls Impoundment, Bypass Reach and below Cabot Station* (Study No. 3.2.2), a fully-calibrated unsteady HEC-RAS model of the TFI was developed for the period 2000 to 2014. The HEC-RAS model generated historic water levels and water surface slopes on an hourly basis through the TFI and at the 25 detailed study sites for inclusion into BSTEM. Historic upstream inflows at Vernon, major tributaries (i.e., the Ashuelot and Millers Rivers), Northfield Mountain operations, and historic water levels at the Turners Falls Dam were utilized during these runs. An additional scenario (Scenario 1 – Northfield Mountain idle) was then developed and run through HEC-RAS to provide hourly water levels for BSTEM at the 25 detailed study sites to determine erosion associated with this modeling scenario.

   A River2D model of the TFI was developed to better understand the complex hydraulics of the TFI and to enhance the understanding gleaned from the HEC-RAS model. The River2D model provided information pertaining to the velocities and shear stresses in the near bank environment. The model was calibrated and then verified with three separate flow events which represented the full range of available observed flows. Once verified, six production runs were performed to investigate changes in velocity and shear stress in the near bank area at the 25 detailed study sites and at areas where unique hydraulic conditions were observed (e.g., eddying).

   BSTEM was used to better understand and evaluate erosion processes, and the forces associated with them, at each of the 25 detailed study sites for the period 2000 to 2014. BSTEM is a state-of-the-science deterministic model that simulates the hydraulic and geotechnical processes responsible for bank erosion, including the effects of vegetation, pore-water pressure, and the confining forces due to flow in the channel. BSTEM was the principal tool used to evaluate the potential primary causes of erosion including hydraulic shear stress due to flowing water, water level fluctuations, and boat waves.

The three-level approach ensures a proper understanding of the physical processes governing bank processes along the reach through the hydraulic action, transport of sediment, river form and response, interaction with infrastructure and/or biologic aspects of riverine morphology or habitat. The three-level approach allows for cumulatively supportive, scientifically justifiable results to be obtained. Each subsequent level of analysis builds on the understanding developed by the previous level.

Based on the results of the analyses discussed above, FirstLight evaluated the causes of erosion in the TFI, including the magnitude, location, and duration of the forces associated with erosion, to identify the dominant and contributing primary causes of erosion at each detailed study site. Secondary causes of erosion were also evaluated to the extent that they were found to be present at a given site. Evaluation of the causes of erosion was consistent with the approach laid out in Task 6 of the RSP. The BSTEM results from each detailed study site, combined with the results of the supplemental engineering and geomorphic analyses conducted as part of the three-level approach, were extrapolated across the TFI such that each riverbank segment identified during the 2013 FRR was assigned a cause(s) of erosion. The extrapolation process was a multi-step process that included analysis of the riverbank features, characteristics, and erosion conditions at each segment, the variability of hydraulic forces throughout the TFI, and the adjacent land-use. The end result of the extrapolation process was the quantification (based on relative percentages), of the dominant and contributing primary cause(s) of erosion at each detailed study site and the TFI overall.

Geomorphic Understanding of the Connecticut River

The Connecticut River, which has a very small portion of its drainage area in Quebec, flows in a southerly direction from the Connecticut Lakes in northern New Hampshire, through western Massachusetts and central Connecticut, and into Long Island Sound. The river forms the border between New Hampshire and Vermont prior to it entering western Massachusetts. On its journey through New England, the river is impounded by 15 dams, some of which are equipped with hydropower facilities. A few of these dams create impoundments large enough to seasonally re-regulate[8] river flows. The majority of hydropower dams are low-head facilities forming narrow impoundments that experience generally lower water velocities at low flows due to raised water levels and velocities that approach near free-flowing conditions at high flows.

The reach of river extending approximately 20 miles from the Turners Falls Dam in Montague, MA to the Vernon Dam in Vernon, VT is also known as the TFI. FirstLight owns and operates the Turners Falls Hydroelectric Project while TransCanada owns and operates the Vernon Hydroelectric Project. The Turners Falls Dam, or a dam of different vintage, has been present at its current location since approximately 1798. The Turners Falls Dam was raised approximately six feet in 1970 during construction of the Northfield Mountain Project to accommodate additional storage volume for the operation of the Project without any significant increase of river flow in the Connecticut River downstream of the dam.

Geomorphic History

During the most recent ice age (approximately 20,000 years ago), the Connecticut River Valley was covered by the Laurentide ice sheet. As the most recent ice age ended, the melting ice was trapped behind a natural dam which consisted of rock and soil that had been pushed up by the ice as it had advanced. The formation of a natural dam combined with the melting glacial water formed what is known as Lake Hitchcock. Lake Hitchcock extended from about the middle of what is now the state of Connecticut (Rocky Hill, CT), through Massachusetts, northward through about 80% of Vermont and New Hampshire to St. Johnsbury, VT; a distance of approximately 200 miles ("Glacial Lake Hitchcock" by Tammy Marie Rittenour). The Lake's water surface in the TFI area was likely more than 150 feet higher than the current level of the Connecticut River, while the bottom of the Lake was likely over 75 feet higher (Field, 2007). Glacial melt from the northern extent of the Lake combined with inflow from various tributaries resulted in the transport of significant quantities of sediment. Approximately 14,000 years ago the natural "dam" holding back Lake Hitchcock was broken and the Lake began to drain. The draining and downcutting of Lake Hitchcock formed what is now the Connecticut River. While some of the deposited lake sediment was likely eroded and transported downstream with the now flowing river, some of the relatively fine deposited sediment (clay, silt, and sand) was left behind in the existing Connecticut River valley.

Over time the watershed became forested and "normal" riverine dynamic processes took over. This history affects the current geomorphology and sediments that are found along the bed and banks of the river and is important to understand in order to provide context for the complex hydraulic and geotechnical processes

[8] Dams having sufficient storage capacity to store water during periods of high flow thereby reducing flood peaks for release during the low flow season.

which occur throughout the Connecticut River today. With the exception of rare segments (such as the French King Gorge located in the TFI), the Connecticut River is an alluvial river. As the previous and more dramatic changes faded into the past, geomorphic changes slowed and became less dramatic, however, typical alluvial river dynamics have and will continue. These dynamics are most pronounced in the previously deposited fine sediments (clay, silt, and sand) that are erodible under normal riverine processes. The fine sediments left behind by Lake Hitchcock are prevalent not only along the majority of the Connecticut River's banks but also throughout the TFI. As noted by Field (2007), most of the riverbank sediments in the TFI are naturally susceptible to erosion because, although they are fine grained, they do not contain much silt and clay which would impart additional resistance through cohesive strength into the materials. The sands and sandy loams are relatively erodible. Field (2007) further noted that natural stability is further compromised by past channel incision through older terrace and floodplain surfaces, leading to greater flow energy expended on the banks rather than having the ability to spread out across broad floodplains (Field, 2007).

As stated above, the Connecticut River is an alluvial river. As discussed in Leopold, et al. (Leopold, Wolman & Miller, 1964), alluvial river systems experience a continual adjustment by processes of aggradation, degradation, scour, deposition, lateral migration, and bank erosion. Even the concept of a river in equilibrium does not mean that a river, so classified, is static and un-changing but instead means that an equilibrium between erosion and deposition is achieved. Based on this concept, the form of the cross-section may not be constant over time and the position of the channel may change, albeit at slow rates. The processes of erosion and deposition can be characteristics of an alluvial stream in equilibrium so long as the changes do not represent large, systematic adjustments over time and space. Changing position, even while retaining overall average channel geometry, necessarily means riverbank erosion occurs even in such channels that are considered to be in equilibrium. This is also the case on the Connecticut River and, more specifically, the TFI.

In recent centuries, with the expansion of development in the region, the Connecticut River has been used as a means of transporting goods, water supply, waste disposal, recreation, and power generation. As part of this development a number of dams were constructed on the Connecticut River for the primary purposes of hydropower production or flood control. Most of the hydropower dams, with the exception of the Murphy, Moore, and Comerford Dams, are less than 60 feet high and form relatively narrow, shallow impoundments upstream of the structures. Flood control dams were constructed by the USACE mostly following the 1936 flood to reduce widespread damage throughout the Connecticut River valley. The intent of the flood control dams is to reduce flood damages that have occurred historically by reducing peak flows to the Connecticut River. Since their construction, the flood control dams have reduced the historic impacts of flood events in parts of the Connecticut River watershed.

Analysis of Historic Datasets

The geomorphic condition of the Connecticut River in general, and TFI specifically, can be further understood by examining historically available maps, aerial photographs, surveys, and reports. Aerial photographs covering the TFI are available over a period of time extending from 1929 to 2014. These photographs provide an important historic perspective over this 80+ year period. Included in this time period were photographs taken along the TFI before and after the construction of the Northfield Mountain Project and associated raising of the Turners Falls Dam.[9] In addition to aerial photographs, historic maps going back over 100 years up through recent LiDAR (Light Detection and Ranging) mapping provide insight as to the recent and existing geomorphology of this section of the river. In reviewing the results of these historic comparisons one must take into account the various accuracy limitations of using such old datasets of varying quality. Limitations associated with these comparisons are discussed at length in the

[9] Construction of the Northfield Mountain Project, including raising the Turners Falls Dam, occurred in the late 1960's and early 1970's. Commercial operation of the Northfield Mountain Project began in 1972.

main report (Volume II). While definitive conclusions or quantitative estimates cannot be drawn from these comparisons, they are still relevant to the analysis.

Analysis of historic datasets and reports which examined erosion processes from the late 1800's to the early 1900's found that significant erosion (several hundred feet in some areas) was found to occur throughout the Connecticut River watershed during this time (Reid, 1990). Comparisons made by Reid (1990) of riverbank position in the vicinity of Otter Run (located in the TFI) using maps surveyed in 1887, 1936, and 1944 found that the banks of the TFI had retreated some 400 feet between 1887 and 1944 in this area. Northrop, Devine, and Tarbell (NDT) also examined the possibility of comparing historic maps to evaluate changes in the position of the river over time (NDT, 1991). As part of this effort, NDT also observed several hundred feet of changes in riverbank position at various locations prior to 1944; however, significant changes (beyond the accuracy limits of the dataset) were not observed in recent decades (i.e. since the 1940's). Both Reid (1990) and NDT (1991) documented much smaller amounts of change in the decades since the 1940's. These relatively small changes in recent decades have been confirmed by annual transect surveys at various locations throughout the TFI which have occurred since the 1990's. Based on this analysis, it is clear that significant erosion occurred at various locations along the Connecticut River over time and prior to the 1940's. While erosion has continued throughout the watershed since the 1940's, it appears to have been reduced to much lower rates, including in the TFI as shown by the annual transect surveys.

When reviewing the historic geomorphology of the Connecticut River, three primary factors are identified as causing the reduction in erosion rates after the 1940's, including: (1) the relative lack of floods in recent decades of the magnitude of those which occurred prior to the 1940's and resulted in substantial erosion and damage (including the flood of 1936); (2) construction of flood control projects throughout the Connecticut River watershed following the flood of 1936; and (3) construction or raising of mainstem Connecticut River dams which reduced river velocities and shear stresses. In the report entitled "Connecticut River Streambank Erosion Study Massachusetts, New Hampshire and Vermont," US Army Corps of Engineers (USACE, 1979), the Corps compared reaches of the river not affected by the dams (i.e., un-impounded reaches) to those where dams formed narrow pools. The report found that dams deepened the water and slowed velocities such that bank erosion due to flowing water was reduced on the order of 34% compared to the natural river (UASCE, 1979).

Specific to the TFI, a number of historic datasets were analyzed in order to better understand changes in riverbank conditions since the 1940's. Originally, FirstLight attempted to compare the riverbank position of the TFI from the 1970's Exhibit K drawings to more recent aerial ortho-photos (as required by FERC's SPDL); however, this was not possible due to the fact that the Exhibit K drawings did not contain any information that could be used to determine the edge-of-water, top of bank, or toe of bank. Focus then shifted to analyzing historic aerial photographs from 1952 and 1961 to evaluate the condition of the 20 most severely eroded sites identified in the ECP (1999) prior to the Turners Falls Dam being raised and the Northfield Mountain Project going online. Based on the results of this analysis it was observed that of the 20 erosion sites identified in the ECP, 14 appear to be eroded prior to the raising of the Turners Falls Dam and construction/operation of the Northfield Mountain Project. Of the 6 remaining sites, one was potentially eroded prior to the raising of the dam (Urgiel Upstream - #4), while riverbank conditions are unclear based on the quality of the aerial photographs at the other five sites. A summary of the findings of this analysis is presented in Table 1.

Table 1: 1952 and 1961 Status of the 20 Erosion Sites identified in the ECP (1999)

Site #	Site Name	Current Status (2014)	Pre-Northfield Mtn. Status
1	Vernon Dam	Not selected for stabilization due to extreme hydraulic conditions associated with Vernon spillway	Eroded: Erosion evident in 1952 with continuing erosion through 2008-2010 ortho-photos.
2	Turners Falls Rod & Gun Club	Stabilized in 2004	Condition changed considerably due to raised water level and construction of club.
3	Bennett Meadow	Stabilized in 2005	Condition unknown based on aerial photos.
4	Urgiel Upstream	Stabilized in 2001	Potentially eroded: sparse riparian vegetation in 1952 photo.
5	Route 10 Bridge	Not selected for stabilization due to unique hydraulic conditions in the vicinity of the Route 10 Bridge	Eroded: Photos used in this analysis as well as earlier photos from analysis associated with Route 10 bridge show ongoing erosion.
6	Skalski	Stabilized in 2004	Condition unknown based on aerial photos: The left bank of the river in the vicinity of Kidds Island has a band of riparian vegetation in the 1952, 1961 and 1990s aerial photos. While not apparent in the aerial photos, erosion had been occurring along this bank and was identified in the ECP and stabilized in 2004 as the Skalski site.
7	Flagg	Stabilized 1999-2000	Eroded: The right bank across from Kidds Island was sparsely vegetated in 1952 and 1961 with ongoing erosion in the 1990s.
8	Un-named	Not selected for stabilization – opposite great meadow	Condition unknown based on aerial photos.
9	Kendall	Stabilized in 2007	Eroded: In 1952 there is some riparian vegetation on the right bank but by the 1961 photograph erosion is evident with no riparian vegetation remaining.
10	River Road	Stabilized in 2003	Eroded: On the inside of the bend along the left bank erosion has occurred over time with the bank moving landward compared to the project boundary line as noted in changes in the bank from the 1952 to 1961 and subsequent aerial photos.
11	Urgiel Downstream	Stabilized in 2005	Eroded: At a bend in the river upstream of Kidds Island the 1952 aerial photo shows a reach with some riparian vegetation. The 1961 aerial photo shows erosion and associated decrease in riparian vegetation.
12	Durkee Point	Stabilized in 2003	Eroded: 1952 and 1961 aerial photos show erosion and lack of riparian vegetation.
13	Split River	Stabilized in 2009 (Lower Split River) and 2010 and 2011 (Upper Split River)	Eroded: 1952 and 1961 aerial photos show erosion and lack of riparian vegetation.
14	Country Road	Stabilized in 2006 (includes site #20)	Eroded: The 1961 aerial photo shows erosion and a significant reduction in riparian vegetation.

Site #	Site Name	Current Status (2014)	Pre-Northfield Mtn. Status
15	Stebbins Island	Not selected for stabilization	Eroded: Downstream end of island has narrowed through erosion from 1952 to 2008-2010.
16	Kaufhold (split into two sites and re-named as "Bathory-Gallagher" and "Wallace-Watson")	Upper Split River stabilized in 2010, Bathory-Gallagher and Wallace-Watson stabilized in 2012 and 2013	Eroded: Bathory-Gallagher and Wallace Watson – Upstream of the tailrace along both banks there was a band of riparian vegetation in the 1952 aerial photo. By the 1961 aerial photo the riparian zone appear to have decreased and erosion is evident. Eroded: Upper Split River – 1952 and 1961 aerial photos show erosion and lack of riparian vegetation.
17	Montague	Stabilized by preventative maintenance in 2008	Eroded: Erosion evident in 1961 photograph.
18	Campground Point	Stabilized by preventative maintenance in 2008	Eroded: Some erosion is evident in the earlier aerial photos such as 1952 continuing through the 2008 ortho-photo.
19	Right Bank Downstream of Davenport or Upper Island	Not selected for stabilization	Condition unknown based on aerial photos (incomplete imagery available).
20	Country Road	Stabilized in 2006 (included as part of site # 14)	Eroded: The 1961 aerial photo shows erosion and a significant reduction in riparian vegetation.

Erosion Comparison of the Turners Falls Impoundment and Connecticut River

One of the priority recommendations identified in Field (2007) was to study patterns of erosion in other reaches of the Connecticut River as a means of comparison to the conditions of the TFI. In response to this recommendation, Simons and Associates (S&A) conducted a study in 2012 comparing bank erosion along the extent of the Connecticut River from Holyoke Dam (Holyoke, MA), upstream through various hydropower impoundments (including Turners Falls, Vernon, Bellows Falls, and Wilder), and continuing to the un-impounded, free-flowing reach from Pittsburg, NH to Gilman Dam (S&A, 2012b). The study reach was approximately 240 miles long.

The study found that riverbank features and characteristics vary considerably along the length of the river. While portions of the river consist of bedrock outcrops that are very stable, much of the riverbanks consist of hillsides or alluvial material that are formed primarily of silt to sand sized material. There are areas that consist of gravel to cobble sized material that are generally less erodible but still are alluvial or transportable by fluvial processes. Much of the riverbanks are quite well vegetated, which generally adds to riverbank stability, although there are segments where a range of erosion and mass-wasting processes remove or damage vegetation and associated riparian land. Riverbank erosion was compared among various reaches to the extent feasible with available data as well as through photographs taken over the years at erosion sites. Key conclusions from this report found that (S&A, 2012b):

- The segment of river with the greatest extent of eroding riverbanks is the un-impounded northern reach (Pittsburg, NH down to Gilman Dam). At the time of the available study, 48.4% of the riverbanks were experiencing moderate or more significant erosion (Field, 2004). Riverbanks that had been rip-rapped covered 17.1% of the length of the river.

- Several erosion sites were identified and photographed in the Bellows Falls, Vernon, Turners Falls, and Holyoke Impoundments in 1997, and again in 2008. All of the erosion sites in 1997 in the Bellows Falls and Holyoke Impoundments and all but one of the 1997 erosion sites in the Vernon Impoundment remained in essentially the same state of erosion when photographed in 2008. Many of these sites were significant in both size and severity. In contrast, most of the erosion sites identified in the TFI in 1998 have been stabilized and were no longer eroding as of 2008.

- In addition to direct stabilization of many of the erosion sites in the TFI that were identified in the 1998 ECP, there is evidence of some natural stabilization processes including increased upper bank vegetation and areas of dense low bank aquatic vegetation that are helping provide a degree of additional stability in some areas.

- Despite the fact that similar percentages of riverbank have been stabilized in the northern, free-flowing reach as in the TFI; the percentage of erosion in the TFI is only about one-third the extent of erosion that is occurring in the northern, free-flowing reach of the Connecticut River (16.7% compared to 48.4%).

- Because riverbank erosion in the TFI is significantly less than in the northern free-flowing reach, erosion sites in other impoundments (Bellows Falls, Vernon, and Holyoke) continued eroding from 1997 to 2008, and many erosion sites have been stabilized in the TFI (including evidence of natural stabilization processes) it can be concluded that the riverbanks in the TFI are in the best condition (more stable and less eroding) than in any other part of the Connecticut River that was examined as part of the 2012 study.

- The TFI, which experiences water level fluctuations due to a combination of run of river/peaking power and pumped-storage hydropower operations, has less riverbank erosion than the other impoundments (Wilder, Bellows Falls, Vernon, and Holyoke) which only experience water level fluctuations resulting from run of river and peaking power operations and do not experience additional fluctuations due to pumped-storage operations. The TFI also experiences significantly less erosion than the northern, free-flowing reach which has no hydropower operations and associated water level fluctuations.

Hydrologic and Hydraulic Characteristics of the TFI

The results of the BSTEM and hydraulic modeling found that the hydrology and hydraulics of the TFI played just as important of a role, if not more so, in erosion processes as riverbank features and characteristics do. Before analyzing and evaluating the causes of erosion it is important to understand the complex hydrologic and hydraulic characteristics of the TFI. As such, this section provides an overview of: (1) the hydrologic setting; (2) hydropower project operations and their impact on flow and water level fluctuations on an hourly basis; (3) hydrologic influences and flow thresholds present in the TFI; and (4) the location and duration of hydraulic forces. The analyses presented in this section are consistent with the approach laid out in the RSP as noted in Tasks 5 and 6 as well as RSP Table 3.1.2-3.

Hydrologic Setting

Analysis of available mean daily flow data as recorded by the U.S. Geological Survey (USGS) at the Montague, MA gage for the period 1904 to 2014 demonstrates that the Connecticut River follows a fairly typical seasonal hydrograph. During this period, mean daily flow in January through most of February averages just over 10,000 cubic feet per second (cfs), in late February to early March the mean flow rises due to spring runoff or freshet peaking to about 40,000 cfs, while the lowest flows (slightly over 5,000 cfs) occur during the late summer to early fall.

The flow on the Connecticut River on a mean daily basis over an annual cycle is unsteady and highly variable. Examination of annual hydrographs demonstrate significant variability in flow over time with changes in flow ranging from a few thousand cfs to several tens of thousands cfs occurring over relatively short periods. The Connecticut River, especially the TFI, experiences significant intraday flow and water level variability which requires examination of the data on an hourly basis. Intraday variability is typically a result of peaking hydroelectric operations and/or pumped-storage operations during periods of low to moderate flow.

Most of the analysis for this study, including BSTEM, were based on hourly hydrologic data from January 1, 2000 to December 31, 2014. This 15-year time period was used for two primary reasons: (1) it was representative of post flood control Connecticut River conditions, and (2) it marked the period of time when the most data (including repetitive cross sections) were available.

Hydropower Operations

When inflow conditions are below the hydraulic capacity of the hydroelectric projects, the facilities often store water in their impoundments on a daily cycle to allow for additional electricity generation during parts of the day when the power demand and market prices increase. When inflow exceeds the hydraulic capacity of the Vernon and Turners Falls Hydroelectric Projects, the facilities are operated in a run-of-river mode where inflow equals outflow on an instantaneous basis. Table 2 provides an overview of the hydraulic capacities of the Vernon, Northfield Mountain, and Turners Falls Hydroelectric Projects.

Table 2: Hydraulic Capacities of the Vernon, Northfield Mountain, and Turners Falls Hydroelectric Projects

Project Name	Hydraulic Capacity (cfs)
Vernon	17,130
Northfield Mountain (Pumping)	15,200
Northfield Mountain (Generating)	20,000
Turners Falls	15,938

The main source of inflow into the TFI is TransCanada's Vernon Hydroelectric Project, which normally acts as a peaking facility when inflows are low. In addition to inflow from Vernon, the TFI also has two major tributaries – the Ashuelot and Millers Rivers. The Northfield Mountain Project also uses the TFI as its lower reservoir. Northfield Mountain has four reversible pump/turbines that at maximum, can pump at 15,200 cfs or can discharge at 20,000 cfs. The Upper Reservoir currently has a FERC maximum usable storage capacity of 12,318 acre-ft. Given this, the Project can pump at maximum capacity for 9.8 hours and generate at maximum capacity for 7.5 hours; however, in reality, the Project rarely pumps or generates at its maximum capacity or utilizes all of the Upper Reservoir volume in a single day.

FirstLight's current FERC license allows the TFI water level to be fluctuated within a 9-foot band between a minimum water surface elevation of 176 and a maximum of 185 ft. NGVD 1929, as measured at the Turners Falls Dam. This 9-foot water level fluctuation provides about 16,150 acre-ft. of storage, if fully utilized; however, FirstLight rarely fluctuates the TFI by more than four feet in a day even though the TFI acts as the lower reservoir for Northfield Mountain and the headpond for the Turners Falls Project power canal (which leads to the generation facilities at Station No. 1 and Cabot Station). As discussed in the March 2015 report for Study No. 3.2.2, at higher flows (i.e. greater than 30,000 cfs) the natural constriction at the French King Gorge becomes a hydraulic control affecting water levels in the mid and upper sections of the TFI. Therefore at higher flows, the effects of water-level management at the Turners Falls Dam by FirstLight becomes much less of a controlling influence of the water surface elevations in the middle and upper parts of the TFI.

During moderate to high flow events hydroelectric generation operations shift from a peaking power operation mode to a run-of-river mode as the flow exceeds the hydraulic capacity of the power plants at Vernon and Turners Falls (17,130 cfs at Vernon and 15,938 cfs at Turners Falls). Flows in excess of the generating capacity are discharged over each dam to the river downstream of the dams. During high flow periods in excess of 30,000 cfs, per an agreement with the USACE, FirstLight lowers the water level at the Turners Falls Dam (but not below El. 176) to limit high water in the Barton Cove area and to a lesser extent, the middle section of the TFI. At flows above 65,000 cfs, as per an agreement with the USACE, if Northfield Mountain is operating, the combined usable volume of the Upper Reservoir and the TFI is required to be kept constant in order to limit discharges from Northfield Mountain adding to the outflow from Turners Falls Dam. As a result of this agreement, if Northfield Mountain is operating during such high flows the hydrologic effect in the TFI is minor.

Hydropower operations at Vernon and Turners Falls are relatively straightforward: below their hydraulic capacities they operate as peaking plants[10], above their hydraulic capacities they operate as run-of-river. During periods of low to moderate flows when peaking operations are occurring, Vernon can impact flow

[10] In the case of the Turners Falls Project, Station No. 1 is generally partially on, fully on, or fully off. FirstLight does not operate Station No. 1 as a peaking facility. Station No. 1 may at times also be operated to pass the required minimum flow.

and water levels downstream to the Turners Falls Dam while water level management at the Turners Falls Dam and Northfield Mountain Project operation can impact flows and water levels upstream to the Vernon Dam. Unlike Vernon and Turners Falls which operate as run-of-river above their hydraulic capacities, Northfield Mountain can operate at flows far greater than 17,130 cfs (i.e., the hydraulic capacity of Vernon). To understand the effect Northfield Mountain operations have on flow and water level fluctuations in the TFI a number of historic time periods and modeled operational scenarios were analyzed. From this analysis, it was observed that during low flows (i.e., flows <18,000 cfs[11]) Northfield Mountain operations accounted for a 2 ft. fluctuation at the five detailed study sites[12] which were examined as part of this analysis.

During moderate to high flows (i.e., flows greater than 18,000 cfs), the effect of Turners Falls Dam operations on water surface elevation fluctuations decreases until eventually the French King Gorge constriction becomes the dominant influence on water surface elevations in the mid and upper TFI. Based on the results of the hydraulic modeling, this typically occurs at flows equal to or greater than 30,000 cfs. The hydrologic analysis conducted during moderate to high flows found that, for the time period examined, when inflow from Vernon exceeds 30,000 cfs and Northfield Mountain operates with 2-3 units the greatest difference in water surface elevations were observed at, or near, the Northfield Mountain tailrace with progressively smaller differences observed in the upstream direction. Specifically, the analysis demonstrated:

- **Site 75BL** *(near the Northfield Mountain tailrace)*: Observed difference in water surface elevation = 1.2 feet;

- **Site 5CR** *(near the Rt. 10 Bridge)*: Observed difference in water surface elevation = 0.9 feet;

- **Site 4L** *(near Pauchaug Boat Launch)*: Observed difference in water surface elevation = 0.7 feet; and

- **Site 303BL** *(downstream of Stebbins Island)*: Observed difference in water surface elevation = 0.5 feet.

Hydrologic Influences and Flow Thresholds

Based on the results of the hydraulic modeling a number of flow thresholds of importance were established. In the upper reach of the TFI (from Vernon Dam to upstream of the NH/MA border – hydraulic reach 4, discussed in the next section) due to the hydraulic capacity of Vernon, flows below 17,130 cfs are controlled by Vernon project operations while flows greater than 17,130 cfs are naturally occurring. As such, in the upper reach of the TFI, the natural high flow threshold was found to be 17,130 cfs. This value was chosen as it represents the point at which Vernon operates in run-of-river mode (i.e. outflow equals inflow), Turners Falls or Northfield Mountain operations have limited to no hydrologic or hydraulic impact, and the upper reach of the TFI is more riverine than the downstream reaches.

For the remaining reaches (from upstream of the NH/MA border to Turners Falls Dam), three flow thresholds were identified: (1) <17,130 cfs; (2) 17,130 – 37,000 cfs; and (3) >37,000 cfs. At flows less than 17,130 cfs (the hydraulic capacity of Vernon) hydropower peaking operations are the dominant hydrologic influence at all locations in the TFI. For flows between 17,130 and 37,000 cfs the dominant hydrologic influence depends on the location in the TFI and can include a combination of Vernon, Northfield Mountain,

[11] 18,000 cfs was chosen as the threshold for this analysis as it is slightly higher than the hydraulic capacity of Vernon (17,130 cfs) in order to account for tributary inflow.
[12] Detailed study sites examined for the hydrologic analysis included: BC1-R, 75BL, 5CR, 4L, and 3030BL. These sites were selected because they spanned the geographic extent of the TFI and were representative of the other sites in their proximity.

and Turners Falls operations, natural hydraulic constrictions (e.g., Stebbins Island, French King Gorge), and/or naturally occurring moderate flows. At flows greater than 37,000 cfs the dominant hydrologic influence is natural high flows.

The natural high flow threshold for the downstream reaches (37,000 cfs) was established for four main reasons: (1) it exceeds the flows at which the French King Gorge becomes the hydraulic control for the mid and upper portion of the TFI; (2) it exceeds the hydraulic capacity of Vernon; (3) it exceeds the maximum combined hydraulic capacity for Vernon and Northfield Mountain at a given location; and (4) although Northfield Mountain may still operate at flows greater than 37,000 cfs, historical operating records indicate this is less frequent than at lower flows.

To determine how often Northfield Mountain operated during periods when flows exceeded 37,000 cfs, FirstLight reviewed the available Project operating data for the period 2000-2014. Based on the results of this analysis it was observed that the Project operated as follows:

- Generation with 1 or more units occurred 2.6% of the time;
- Generation with 2 or more units occurred 0.82% of the time;
- Generation with 3 or more units occurred 0.14% of the time; and
- Generation with 4 units occurred 0.025% of the time

This equates to approximately 9, 3, 0.5, and 0.1 days per year, respectively. Pumping operations when flows exceeded 37,000 cfs were found to follow a similar pattern. Given how infrequently Northfield Mountain historically operated when flows exceeded 37,000 cfs it was determined that 37,000 cfs was an appropriate value for the natural high flow threshold.

Hydraulic Model Results

In support of the BSTEM modeling efforts associated with this study, and in accordance with Task 5 of the RSP, the HEC-RAS model was utilized to generate historic (i.e., Baseline Condition) water levels and Energy Grade Line (EGL) slopes[13] on an hourly basis at the 25 detailed study sites. The Baseline Condition modeling scenario utilized historic upstream inflows at Vernon and tributaries (Ashuelot and Millers Rivers), Northfield Mountain generation and pumping flows, and historic water levels at the Turners Falls Dam. In addition to the Baseline Condition, an additional scenario was developed (Scenario 1 – Northfield Mountain idle) when Northfield Mountain was "turned off" to provide water level and EGL slope data for the BSTEM modeling at the 25 detailed study sites. The HEC-RAS scenarios used the January 1, 2000 to December 31, 2014 period and historic tributary inflows. Input variables for each modeling scenario are shown in Table 3.

[13] The Energy Grade Line is the elevation of the energy head of the water in the river and is the hydraulic grade line plus the velocity head between each model transect. Generally, a greater slope of the energy grade line indicates a higher water velocity and a higher potential for hydraulic erosion. The Energy Grade Line is an important component in the hydraulic-erosion sub-model of BSTEM as it forms the basis for calculating boundary shear stress for nodes along the wetted perimeter along with the hydraulic radius of the segmented flow and the unit weight of water.

Table 3: Operational Conditions and Associated Hydraulic Data for each of the Modeled Scenarios

Model Scenario	Time step	Vernon Operations (flow)	NFM Operations (flow)	TFD Operations (elevation)
Baseline	Hourly	Historic	Historic	Historic
S 1	Hourly	Historic	Idle	Historic

Based on the distribution of the EGL slope derived from the HEC-RAS model runs described above, four distinct hydraulic reaches were identified (Figures 2 and 3). These hydraulic reaches included the Upper (Reach 4), Middle (Reach 3), Northfield Mountain (Reach 2), and Lower (Reach 1) reaches. The median (50th percentile) energy slope for each site is represented by the gray line with 50% of the slopes over the modeling period greater than this value and 50% less. The blue and orange lines represent the 95th and 75th percentiles for each site, respectively. The steepest slopes occur in the "upper" part of the TFI (Reach 4) just downstream from Vernon Dam and extending downstream to about station 80,000. Slopes for the "middle" reach, denoted as Reach 3 (downstream to station 42,000), are generally about an order of magnitude lower. Energy slopes for the Northfield Mountain Reach (Reach 2) are somewhat greater than for both Reaches 3 and the "lower" reach (Reach 1), the latter being the section just above Turners Falls Dam. Table 4 provides an overview of the detailed study sites found in each reach.

Table 4: Detailed Study Sites found in each Hydraulic Reach

Hydraulic Reach	Detailed Study Sites
4 (Upper)	11L, 2L*, 303BL, 18L, 3L, 3R*, 21R
3 (Middle)	4L, 29R, 5CR, 26R, 10L, 10R*, 6AL*, 6AR*
2 (NFM)	119BL, 7L, 7R, 8BL, 8BR*, 87BL, 75BL
1 (Lower)	9R*, 12BL, BC1-R

** Designates a site restored as part of the ECP*

EGL slope was used to identify the variability of hydraulic forces throughout the TFI and to determine the geographic extent where a hydropower project could potentially have an impact on riverbank erosion. Given the clear delineation and characteristics of each hydraulic reach it is unlikely that a hydropower project can have an impact on erosion processes outside of the hydraulic reach in which it is located. While a hydropower project can impact water level fluctuations and flow outside of its hydraulic reach, the magnitude of those impacts are so minor that they do not affect the EGL slope outside of their given reach. For example, even though Northfield Mountain operations can impact the water surface elevation in reaches 3 and 4 at flows which exceed the erosion flow threshold at the detailed study sites, the impacts are so negligible that corresponding changes to the EGL slope do not occur. Thus, given the hydraulic characteristics of each reach it is unlikely that Northfield Mountain operations can impact erosion processes outside of reach 2.

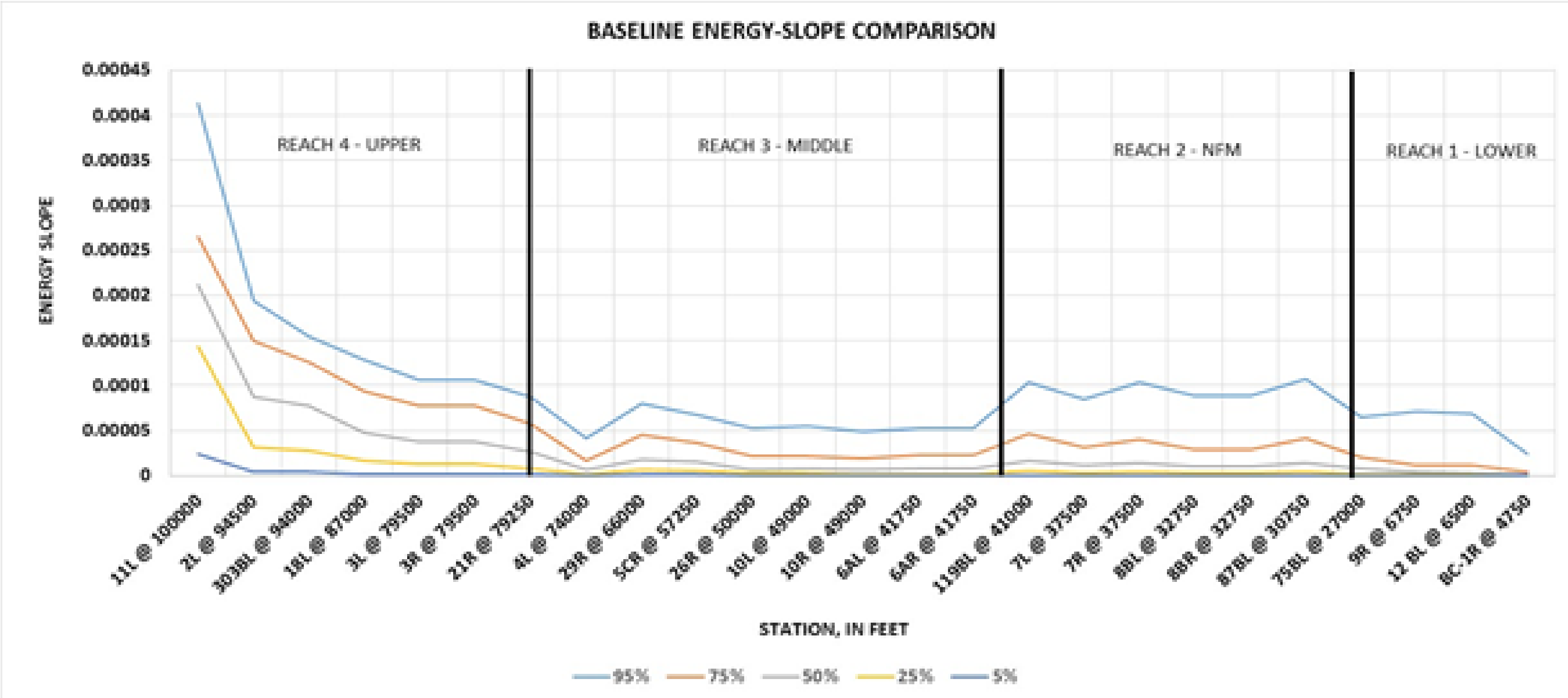

Figure 2: Distribution of Energy Grade Slope Lines throughout the Turners Falls Impoundment

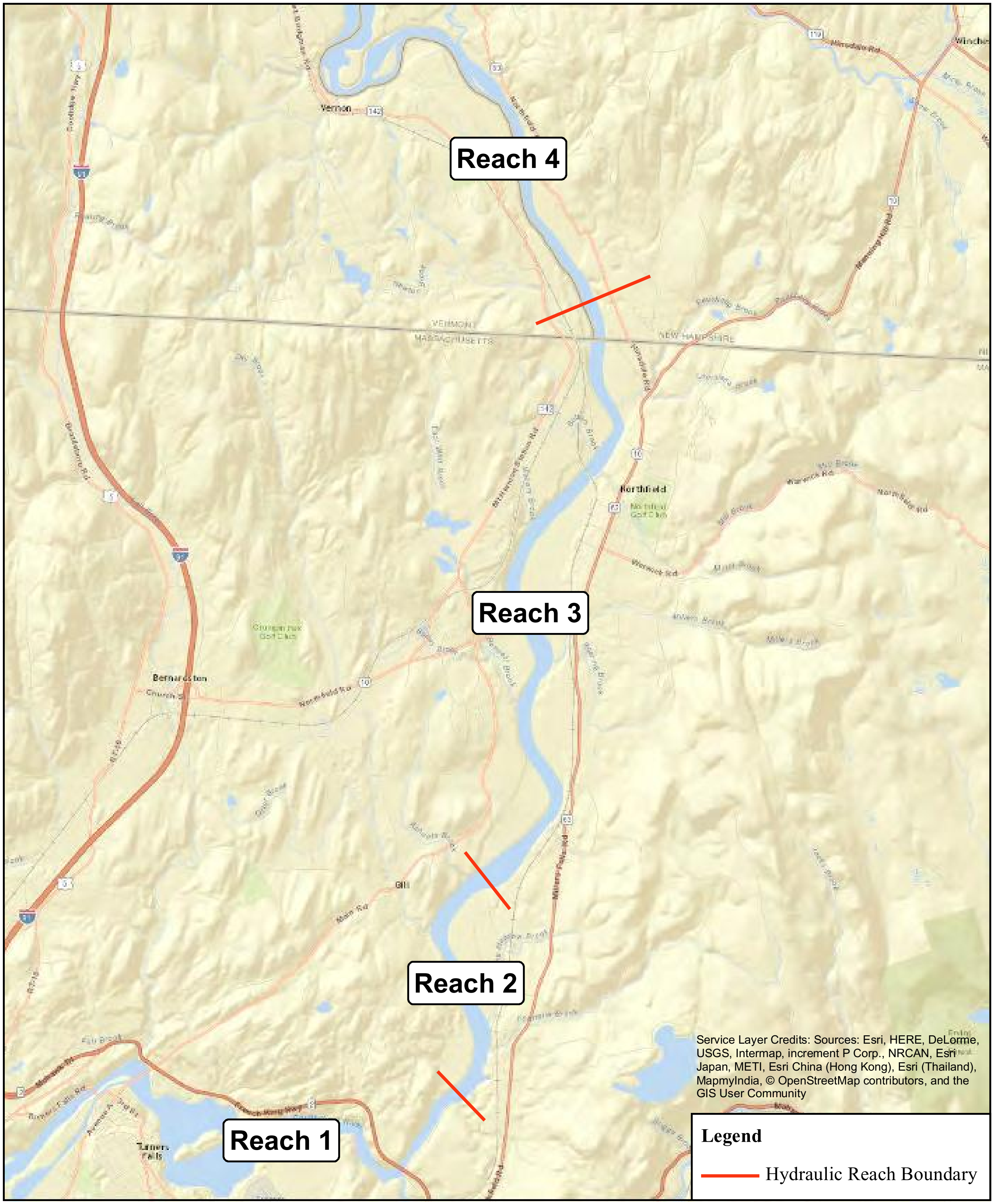

FirstLight Power Resources

FIRSTLIGHT HYDRO GENERATING COMPANY
Northfield Mountain Pumped Storage Project No. 2485
Turners Falls Hydroelectric Project No. 1889

STUDY 3.1.2

Figure 3:
Geographic Distribution
of Hydraulic Reaches

N

0 0.75 1.5 3 Miles

Path: W:\gis\studies\3_1_2\maps\final_report\figure-3.mxd

Location and Duration of Hydraulic Forces

When analyzing and evaluating the causes of erosion in the TFI, it is important to first understand the magnitude, location, and duration of forces associated with each cause. As such, the magnitude, location and duration of forces were analyzed in-depth as part of the hydraulic modeling, BSTEM, and supplemental analyses as noted in Table 3.1.2-3 of the RSP. Results of the BSTEM modeling and supplemental analyses discussed in later sections take into account these factors. For the purpose of this section, discussion focuses on the location and duration of hydraulic forces, or more specifically, on the duration at which various water surface elevations are equaled or exceeded and the corresponding location of the water surface relative to bank position.

As noted in USACE (1979), the forces acting on the bank can be broken into two categories: (1) those acting near the surface of the flow, and (2) those acting with the greatest intensity nearer the bottom of the submerged banks. Given that erosion processes associated with (1) hydraulic shear stress due to flowing water; (2) water level fluctuations due to hydropower operations; (3) boat waves; and (4) ice occur at and/or below the water surface it is vital to understand where on the riverbank the water surface rests and for what duration.

TFI riverbanks are typically characterized by a lower and upper riverbank. The lower bank is typically a flat, beach-like feature that is submerged or experiences daily water level fluctuations during low to moderate flows as a result of hydropower peaking operations. Depending on its location in the TFI, the lower bank may or may not be vegetated. As one moves away from the normal edge-of-water, the lower bank transitions to an upper bank; the toe of which is clearly identifiable on most cross-section plots. The upper bank is typically steep, has some degree of vegetation, and is usually above the water surface except during high flows.

The distinction between the lower bank and the upper bank is an important one as the vast majority of erosion occurs only once the water surface reaches the upper bank. Although peaking hydropower operations can result in water level fluctuations up to 4 feet at a given location over the course of a day, during low to moderate flow periods the water surface in the TFI typically rests on the lower bank. As observed from the BSTEM modeling results and other supplemental analyses, it is not until the water surface reaches the upper bank that erosion processes can potentially commence and even then the flow threshold to initiate erosion processes was found to be greater than 37,000 cfs at the majority of detailed study sites.

In order to determine the amount of time the TFI water surface rests on the lower bank vs. the upper bank a water level duration analysis was conducted at a subset of the 25 detailed study sites[14]. To further understand the location and duration of hydraulic forces on the bank, stage-discharge relationships were then developed at the same sites in order to determine at what flow the water surface reaches the upper bank. TFI flow duration curves for the individual locations based on hourly data for the period 2000-2014 were then analyzed to determine the percent of time flows of that magnitude occur in the TFI. The final step in this analysis was to compare the upper bank flow and water level analysis against the erosion flow threshold found from the BSTEM modeling results at the subset of detailed study sites. The erosion flow threshold for each site was then compared against the flow duration curve to determine the amount of time that flow may be equaled or exceeded. To provide context, the corresponding water surface elevation for the erosion threshold was compared against the elevation of the toe of the upper bank as derived from the annual cross-section surveys. The results of this analysis are summarized in Table 5.

[14] Sites used for this analysis were the same sites chosen for the hydrology analysis previously discussed: BC1-R, 75BL, 5CR, 4L, and 303BL. These sites were chosen as they spanned the geographic extent of the TFI and were found to be representative of the other sites in proximity to them.

Table 5 Hydrologic Analysis at a Subset of Detailed Study Sites located throughout the TFI

Detailed Study Site	Hydraulic Reach	Toe of Upper Bank – El.*	Water Level Duration		Flow to Reach Upper Bank (cfs)	% Time Flow is Exceeded	95% Erosion Flow Threshold (cfs, from BSTEM)	% Time Threshold Flow is Exceeded	Corresponding Threshold WSEL
			% Time on Lower Bank	% Time on Upper Bank					
BC-1R	1 (lower)	184	99%	1%	NA	NA	I	NA	NA
75BL	2 (NFM)	184	90%	10%	32,000	10%	33,822	7%	184
5CR	3 (middle)	184	82%	18%	23,000	18%	47,867	4%	188
4L	3 (middle)	184	78%	22%	17,000	22%	6,991	60%	181
303BL	4 (upper)	185	79%	21%	17,500	21%	53,194	3%	192

**NGVD29, Feet I = Indeterminate*

As observed in the table, the water level rests of the lower bank the vast majority of the time (79-99%). The period of time in which the water surface rests on the lower bank also coincides with the periods when Vernon, Northfield Mountain, and/or Turners Falls are typically operating in a peaking mode (i.e. low and moderate flow periods). This is significant given that the majority of erosion in the TFI only occurs once the water level reaches the upper bank. The 95% erosion flow threshold (i.e., the flow above which 95% of erosion occurs in the TFI at a given location) provides further insight into this. At sites 75BL, 5CR, and 303BL the 95% erosion flow threshold is near or exceeds the natural high flow threshold (37,000 cfs at sites 75BL and 5CR, 17,130 cfs at site 303BL) indicating that 95% of all erosion does not occur until flows beyond the influence of hydropower operations are equaled or exceeded. As observed in the table, these flows occur only 3-7% of the time. In other words, the potential for 95% of all erosion to occur exists only 3-7% at these sites. This finding was consistent at the majority of sites throughout the TFI.

The exception to this is Site 4L where the 95% flow threshold is 6,991 cfs. Further examination of this site indicates that the average rate of annual erosion is 0.017 ft^3/ft/yr., making it the third lowest rate of erosion of all sites in the TFI. Although the 95% flow threshold at this site is very low, it is a product of how little erosion is actually occurring. By contrast, the 50% erosion flow threshold at this site was found to be 83,527 cfs which equates to a water surface elevation of El. 195, exceeded <1% of the time. It should also be noted that the erosion flow threshold at site BC-1R could not be established given that a reliable relationship between stage and discharge could not be developed in the Barton Cove area.

The results from this analysis clearly indicate: (1) the importance of the water surface elevation and its corresponding location on the bank; (2) the importance of the duration of those water surface elevations; and (3) that the window for the majority of erosion to occur is quite small and well beyond the flows at which hydropower operations have an impact on flow or water level.

The hydrology and hydraulic information presented above, combined with the riverbank features, characteristics and erosion conditions identified during the 2013 FRR, provided the foundation for the analysis and evaluation of the causes of erosion and the forces associated with them.

Analysis of the Causes of Erosion

Analysis in this section focuses on the primary causes of erosion as determined by the BSTEM modeling runs and various supplemental analyses which were conducted as part of this study. Primary Causes of erosion discussed below include hydraulic shear stress due to flowing water, water level fluctuation associated with hydropower operations, boat waves, land-use and land management practices, and ice. Results of the analysis of secondary causes of erosion including wind waves, seepage and piping, freeze-thaw, and animals are also discussed below. The analyses and modeling presented in this section were conducted in accordance with Tasks 5 and 6 of the RSP as well as RSP Table 3.1.2-3.

Potential Primary Causes of Erosion – Water level fluctuations associated with hydropower operations, Hydraulic shear stress, and Boat waves: BSTEM Simulation Results

BSTEM simulations were conducted at the 25 detailed study sites for the period 2000-2014. For those sites where stabilization has occurred as part of the ECP, simulations were conducted for the pre- and post-restoration conditions; resulting in a total of 30 simulations per modeling scenario. Three modeling scenarios were executed in order to better understand the role Northfield Mountain operations have on erosion processes. These scenarios included: (1) Baseline Condition (waves on); (2) Baseline Condition (waves off); and (3) Scenario 1 (Northfield Mountain idle). Results of the BSTEM simulations were analyzed to determine the amount of erosion that occurred over the range of discharges under the Baseline Condition. Referred to as the high-flow analysis, these calculations elucidated the role of high flows on bank-erosion rates. The combination of these model scenarios and analyses allowed for a comprehensive evaluation of the potential primary causes of erosion including: (1) water level fluctuations due to hydropower operations; (2) hydraulic shear stress due to flowing water; and (3) boat waves.

The first set of BSTEM simulations were those for the Baseline Condition (waves on) so that the calibration parameters could then be used for subsequent model scenarios. As previously discussed, the Baseline Condition was designed to represent existing conditions during the model period (2000-2014). The results of the Baseline Condition run served as a means of comparison against the other model scenarios (i.e., Scenario 1). Due to the fact that simulation periods at the detailed study sites were not all of equal duration, the results from all of the sites were normalized by dividing the total erosion over the period (in ft^3/ft of channel length) by the number of years of simulation. These values (reported in units of ft^3/ft/yr.) are then readily comparable to interpret relative degrees of bank instability along the TFI.

For the Baseline Condition (wave on), simulated rates of bank erosion along the reach range from very close to 0 ft^3/ft/ yr. to 15.4 ft^3/ft/ yr. at site 3R under pre-restoration conditions. Other sites with bank-erosion rates higher than the 75^{th} percentile for the non-restored sites include 5CR (8.6 ft^3/ft/ yr.), 8BR-pre-restoration (7.4 ft^3/ft/ yr.), 3L (6.1 ft^3/ft/ yr.), 119 BL (5.9 ft^3/ft/yr.) and 9R pre-restoration (5.4 ft^3/ft/ yr.). Of these six highest rates, three of the sites have been restored. Restoration measures have been very effective in reducing bank-erosion rates by about an order of magnitude throughout the TFI, with an average reduction of 93%. Median bank-erosion rates for the non-restored and restored sites are 1.9 and 0.21 ft^3/ft/ yr., respectively. Figure 4 depicts the spatial distribution of erosion rates for all sites under the Baseline Condition.

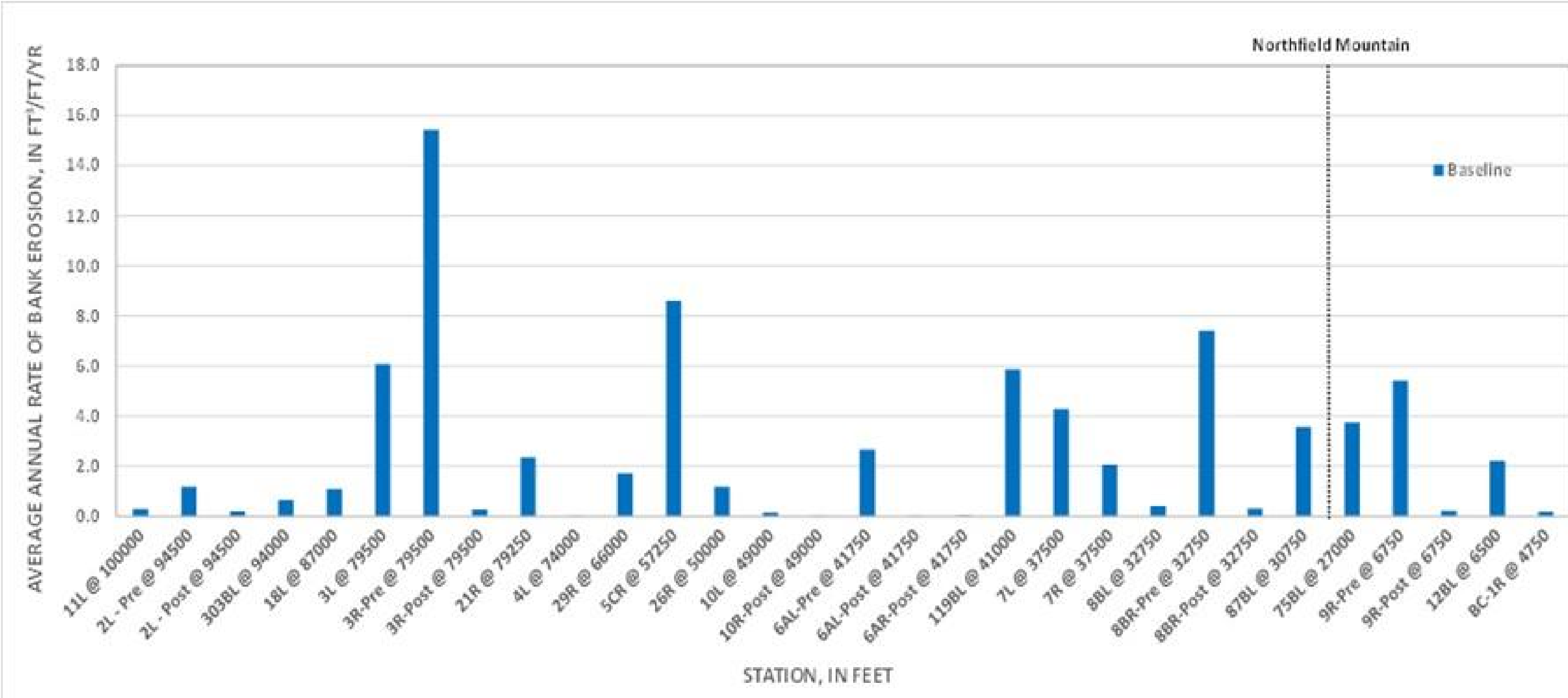

Figure 4: Spatial Distribution of Bank Erosion Rates for all Sites under the Baseline Condition (wave on)

Following completion of the Baseline Condition (wave on) scenario the Baseline Condition was repeated but this time with waves off. The BSTEM wave sub-model has the ability to be turned on or off for a given model run allowing for model results to be compared where the only difference between scenarios is wave activity. Differences between the Baseline Condition with and without waves provided a convenient way to determine the role of boat-generated waves on bank erosion. Comparison of the wave on and wave off scenarios indicated that boat waves had a significant impact on erosion processes in hydraulic reach 1 (lower TFI), minimal impact in hydraulic reach 2 (Northfield Mountain), and no impact in hydraulic reaches 3 (middle TFI) or 4 (upper TFI). The impact of waves in reach 1 can be attributed to the general lake-like conditions found in the lower TFI where water surface elevations vary across a narrow range. The narrow band of water surface elevation fluctuations focuses wave impacts in the zone where the beach/toe intersect the lower-most part of the upper bank. Table 6 demonstrates the impact boat waves have on erosion processes at the detailed study sites in the lower TFI.

Table 6: Summary of Bank Erosion Rates for Sites in the Lower TFI Demonstrating the Impact of Boat Waves

Site/Condition	Station	Dates		Baseline (Waves on)	Baseline (Waves off)	S1 (Waves on)	S1 (Waves off)
	ft	Start	End	$ft^3/ft/yr$	$ft^3/ft/yr$	$ft^3/ft/yr$	$ft^3/ft/yr$
75BL (Reach 2)	27,000	01/01/00	08/27/14	3.76	3.47	3.93	3.72
9R-Pre (Reach 1)	6,750	06/02/00	06/30/08	5.43	0.97	5.19	0.77
9R-Post (Reach 1)	6,750	07/01/08	08/26/14	0.23	0.00	0.22	0.00
12BL (Reach 1)	6,500	01/01/00	08/27/14	2.22	0.24	2.15	0.19
BC-1R (Reach 1)	4,750	06/05/00	08/26/14	0.19	0.00	0.19	0.00

To isolate the impacts of Northfield Mountain Project operations on bank erosion BSTEM Scenario 1 (S1) was executed where Northfield Mountain operations were set to an idle state. The bank erosion rates predicted for S1were subtracted from the erosion rates predicted for the Baseline Condition (wave on). The operational difference between the two scenarios was determine to identify the change in erosion rates resulting from operations at Northfield Mountain. The results of this analysis showed very small effects at every detailed study site indicating that Northfield Mountain Project operations are not a dominant cause of erosion at any location. The exception to this appears to be site 8BR pre-restoration where the model predicted 7.415 $ft^3/ft/yr$. of erosion under the Baseline Condition (wave on) largely attributable to Northfield Mountain Project operations. Current erosion rates at this site, however, reflect the effect of restoration activities in 2012 that greatly reduced erosion rates from 7.415 $ft^3/ft/yr$. to about 0.3 $ft^3/ft/yr$.

The only other locations/conditions that show even a minor impact (> 0.1 $ft^3/ft/yr$) from Northfield Mountain Project operations are sites 7L at station 37,500 (0.17 $ft^3/ft/yr$) and perhaps 119BL at station 41,000 (0.09 $ft^3/ft/yr$). These are all very low erosion rates and if considered in the context of average, annual-erosion rates for non-restoration sites under the Baseline Condition, these contributions fall at or below the 10^{th} percentile of erosion rates. At site 7L bank erosion due to Northfield Mountain Project operations (Baseline minus S1) accounts for about 4% of the erosion under Baseline Conditions while 95% of the erosion occurs at flows greater than 47,700 cfs. At site 119BL the contribution from Northfield

Mountain Project operations is about 1.5%. Table 7 presents a summary of BSTEM results for the various operational scenarios.

Table 7: Summary of BSTEM Results for the Various Operational Scenarios

Site/Condition	Hydraulic Reach	Station	Dates		Baseline (Waves On)	Baseline (Waves off)	S1
		(ft)	Start	End	($ft^3/ft/yr.$)	($ft^3/ft/yr.$)	($ft^3/ft/yr.$)
11L	4 (Upper)	100000	7/15/2005	9/10/2014	0.297	0.296	0.303
2L-Pre		94500	6/20/2000	6/30/2012	1.197	1.184	1.194
2L-Post		94500	7/1/2012	8/28/2014	0.214	0.204	0.213
303BL		94000	1/1/2000	8/27/2014	0.647	0.645	0.674
18L		87000	1/1/2000	8/27/2014	1.092	1.092	1.080
3L		79500	1/1/2000	8/28/2014	6.086	6.090	6.042
3R-Pre		79500	1/1/2000	6/30/2006	15.425	15.407	15.458
3R-Post		79500	7/1/2006	8/28/2014	0.285	0.281	0.282
21R		79250	1/1/2000	8/27/2014	2.359	2.291	2.355
4L	3 (Middle)	74000	1/1/2000	8/28/2014	0.017	0.014	0.017
29R		66000	1/1/2000	8/27/2014	1.718	1.709	1.718
5CR		57250	7/8/2002	9/3/2014	8.606	8.500	8.566
26R		50000	1/1/2000	8/27/2014	1.194	1.145	1.196
10L		49000	1/1/2000	8/27/2014	0.160	0.158	0.158
10R-Post		49000	7/1/2001	8/27/2014	0.000	0.000	0.000
6AL-Pre		41750	1/1/2000	6/30/2004	2.668	2.635	2.736
6AL-Post		41750	7/1/2004	8/27/2014	0.000	0.000	0.000
6AR-Post		41750	6/21/2000	8/27/2014	0.021	0.000	0.020
119BL	2 (NFM)	41000	1/1/2000	8/27/2014	5.876	5.722	5.789
7L		37500	1/1/2000	8/26/2014	4.291	4.242	4.125
7R		37500	1/1/2000	8/26/2014	2.058	2.037	2.047
8BL		32750	6/2/2000	8/26/2014	0.427	0.427	0.399
8BR-Pre		32750	6/2/2000	6/30/2012	7.415	7.394	1.954
8BR-Post		32750	7/1/2012	8/26/2014	0.312	0.312	0.248
87BL		30750	1/1/2000	8/27/2014	3.568	3.607	3.595
75BL		27000	1/1/2000	8/27/2014	3.755	3.475	3.927
9R-Pre	1 (Lower)	6750	6/2/2000	6/30/2008	5.426	0.967	5.192*
9R-Post		6750	7/1/2008	8/26/2014	0.227	0.002	0.224*
12BL		6500	1/1/2000	8/27/2014	2.221	0.239	2.150*
BC-1R		4750	6/5/2000	8/26/2014	0.190	0.000	0.189*

** % in this reach also includes wave influences*

The role of high flows on bank-erosion rates was investigated by analyzing the hourly outputs from each time step in BSTEM. The output data were sorted by the amount of bank erosion during each time step to determine what water elevations and discharges were responsible for bank erosion along the reach. The water elevation data were converted to discharge by developing polynomial regression relations using data from HEC-RAS. Erosion data for each site were thus sorted into 10,000 cfs discharge classes to determine how much erosion had occurred in each discharge class without biasing the classes because of different sizes. Data from each class were then summed to develop a cumulative frequency distribution for each model run. The resulting database of erosion totals provides an opportunity to investigate the relative amounts of erosion that occur at different discharges.

Flows above which 5%, 50%, and 95% of all erosion occurs were then identified for each site (also referred to as erosion flow thresholds). Erosion flow thresholds were then compared against the flow thresholds discussed in the previous section (Upper Reach: below or above 17,130 cfs, remaining reaches: <17,130 cfs, 17,130 – 37,000 cfs, and >37,000 cfs) to identify sites where natural or moderate high flows were the dominant cause of erosion and as a way to confirm the Baseline-S1 analysis. Based on the results of this analysis, the dominant cause of erosion at the vast majority of sites in the TFI was found to be natural high flows. Table 8 presents the distribution of discharges responsible for 5%, 50%, and 95% of bank erosion at the 25 detailed study sites. As previously discussed, Northfield Mountain Project operations can only have a potential impact on erosion in hydraulic reach 2 due to the hydraulic characteristics of the TFI. As shown in Table 8, the erosion flow threshold at which the majority of erosion occurs (i.e., the 50% threshold) is higher than the natural high flow threshold (37,000 cfs) at all sites in reach 2. In other words, the majority of erosion in this reach occurs at flows beyond the influence of Northfield Mountain Project operations.

In regard to Turners Falls operations, a modified extrapolation approach was employed in Reach 1 to determine to what extent, if any, Turners Falls Project operations were a cause of erosion. When compared to the rest of the TFI, Reach 1 has unique and varied geomorphic characteristics. The upper portion of the reach includes the French King Gorge which is very narrow, lined with bedrock, and serves as the hydraulic control for the mid and upper portion of the TFI at high flows. Just downstream of the French King Gorge is the confluence of the Millers River. From this point, the middle portion of the reach is more riverine before transitioning to a wider, more lake-like section upstream of the entrance to Barton Cove and continuing to the Turners Falls Dam. Given the unique geomorphic characteristics of this reach, combined with there being detailed study sites only in the lake-like portion and not the more riverine portion, the modified extrapolation approach was required in order to determine the contributions, if any, of Turners Falls Project operations on erosion.

Based on a combination of BSTEM and hydraulic model results combined with supplemental geomorphic and hydraulic analyses it was determined that in the upper portion of the reach the causes of erosion are similar to those found at Site 75BL where high flows are the dominant cause of erosion with moderate flows and boats as contributing causes. In the middle, riverine portion of the reach high flows are the dominant cause of erosion with boats as a contributing cause. While in the lower, lake-like portion of the reach boats were the dominant cause of erosion with no contributing causes. Based on the results of this analysis, it was determined that Turners Falls Project operations are not a dominant or even contributing cause of erosion in the TFI. This approach is discussed in more detail in later sections as well as in the main report (Volume II).

Table 8: Distribution of Discharges Responsible for 5%, 50%, and 95% of the Bank Erosion in at the 25 Detailed Study Sites

Site	Hydraulic Reach	Station	Total Erosion Under Baseline, $ft^3/ft/yr$	Baseline Scenario Discharge, cfs		
				5% of erosion occurs at flows greater than	50% of erosion occurs at flows greater than	95% of erosion occurs at flows greater than
11L	4 (Upper)	100,000	0.297	56,869	4,985	500
2L - Pre		94,500	1.197	89,294	64,854	49,906
2L - Post		94,500	0.214	71,465	65,195	51,924
303BL		94,000	0.647	79,881	64,684	53,194
18L		87,000	1.092	73,352	54,485	17,824
3L		79,500	6.086	98,234	78,682	37,098
3R-Pre		79,500	15.425	73,365	61,470	39,229
3R-Post		79,500	0.285	87,760	54,420	36,411
21R		79,250	2.359	63,852	46,345	22,928
4L	3 (Middle)	74,000	0.017	95,042	83,527	6,991
29R*		66,000	1.718	11,968	11,968	11,923
5CR		57,250	8.606	76,391	76,391	47,867
26R		50,000	1.194	80,503	60,282	43,294
10L		49,000	0.160	98,882	79,003	58,922
10R-Post		49,000	0.000	49,015	48,156	46,944
6AL-Pre		41,750	2.668	77,664	65,442	56,264
6AL-Post		41,750	0.000	65,167	63,310	62,287
6AR-Post		41,750	0.021	29,662	11,191	7,051
119BL	2 (NFM)	41,000	5.876	70,557	53,969	24,796
7L		37,500	4.291	98,753	65,338	47,731
7R		37,500	2.058	98,463	65,880	53,614
8BL		32,750	0.427	84,451	84,138	77,997
8BR-Pre		32,750	7.415	99,458	99,458	64,443
8BR-Post		32,750	0.312	72,009	69,312	66,504
87BL		30,750	3.568	63,968	42,875	17,849
75BL		27,000	3.755	71,586	48,054	33,822
9R-Pre	1 (Lower)	6,750	5.426	I	I	I
9R-Post		6,750	0.227	I	I	I
12BL		6,500	2.221	I	I	I
BC-1R		4,750	0.190	I	I	I

Note: "I" = indeterminate because a reliable stage-discharge relationship could not be developed

Potential Primary Causes of Erosion - Ice

When initially developing the causes of erosion for the RSP, ice was listed as a potential secondary cause of erosion. For decades ice had not been a significant factor affecting erosion in the TFI due largely to the operation of Vermont Yankee Nuclear Plant (VY) located immediately upstream in the Vernon Impoundment. When in operation, the plant used water from the Connecticut River for cooling after which heated water was discharged back to the river. As a result, the TFI would rarely ice over completely during the winter months.

In 2013, when Entergy announced the closing of VY by December 29, 2014, FERC issued an Interim ILP schedule for Study Plan Determination. During this period, FirstLight elevated ice from a potential secondary cause of erosion to a potential primary cause of erosion to account for the fact that ice may play a more significant role in riverbank erosion processes in the future. FirstLight filed an addendum to the RSP for Study No. 3.1.2 with FERC in September 2014 which highlighted the methodology to be used to more thoroughly examine ice as a potential primary cause of erosion.

Photographs were taken at a number of predetermined locations throughout the TFI to monitor ice conditions during the 2014/2015 winter (partial set of photos) and 2015/2016 winter (full set of photos), including:

- Vernon Dam;
- Confluence of Ashuelot River;
- Pauchaug Boat Launch;
- Route 10 Bridge;
- Northfield Tailrace;
- French King Bridge;
- Confluence of Millers River; and
- Turners Falls Dam

These sites were selected for two primary reasons: (1) they were easily and safely accessible during winter conditions, and (2) they covered the geographic extent of the TFI. In preparation for the 2015-2016 ice season, some photographs were taken of ice conditions that occurred the preceding winter (2014-2015) when conditions were more conducive to the formation of ice. During the 2014/2015 winter much of the TFI was covered with ice. In the later winter/early spring of 2015 ice break-up was uneventful as the ice simply melted in place. No significant riverbank damage or erosion was observed as a result of the ice formation or break-up. Although no erosion was observed, valuable insights were still gained as to the conditions that could potentially lead to ice related erosion.

During the course of the 2015/2016 winter, photos were taken on eight separate occasions starting December 15, 2015 and ending on March 8, 2016. Photos were generally taken every 1-2 weeks. The intent of the photos was to observe: (1) when sheet ice developed; (2) during formation of sheet ice; (3) during ice break-up; and (4) after ice break-up occurred. While ice development was observed during the monitoring period, due to an unseasonably mild winter the TFI never completely iced over.

In discussions with the USGS in Vermont and New Hampshire, they observed that ice typically does not cause erosion if the ice simply melts in place without significant break-up and if ice floes moving down river causing ice jams and impacting the banks do not occur. This is consistent with the observations made following the 2014/2015 winter. If, on the other hand, there is significant break-up, ice floes moving down river with the potential for ice jams that are pushed against and scrape along the banks; then such an event could potentially cause erosion and damage to the riverbanks. Not only is ice formation a necessary component of erosion caused by ice, but so is how the ice breaks up in determining the potential for erosion caused by ice.

In addition to observations made during winter monitoring in 2014, 2015, and 2016 and discussion with the USGS, the analysis of ice as a primary cause of erosion focused on historic observations made in the TFI, upstream impoundments (i.e., Vernon, Bellows Falls, and Wilder), and other river systems (including un-impounded rivers). Ice dynamics in the upper impoundments provided insight into what could potentially occur in the TFI in the future as ice formation becomes more likely due to the closure of VY. Analysis of historic data from the upstream impoundments, and other river systems (including un-impounded rivers), found that, given the right climatic and hydrologic conditions (i.e. high flows), ice has caused severe erosion and has contributed to bank instability and damage to riparian vegetation or limitation of the establishment and growth of vegetation, which can eventually lead to erosion. The results of this analysis found that ice has caused significant erosion and contributed to bank instability in both impounded and un-impounded rivers.

The results of the ice analysis found that ice can have the greatest potential impact on erosion if significant break-up occurs and if ice floes moving down river create ice jams or scrape along the banks. In addition to directly causing erosion these processes can also greatly effect riverbank vegetation thus also impacting the stability of the bank. If on the other hand, the ice simply melts in place and no significant break-up occurs it is unlikely that the ice would cause significant erosion. Ice formation and accompanying freeze-thaw cycles may also weaken the soil matrix by developing cracks and spalling of the soil surface; however, the process of break-up plays a more significant role in erosion processes.

Based on (1) the results of the ice analysis conducted as part of this study; (2) observations made during the 2014/2015 winter when ice formed over much of the TFI; and (3) the results of the various hydrologic analyses previously discussed it appears unlikely that Project operations will exacerbate the impact of ice on erosion processes. The most significant erosion associated with ice is due to ice break-up, floes, and jams and the corresponding damage which occurs as the ice scrapes along the bank while moving downstream. Based on analysis of historic information, these processes occur as a result of moderate to high flows which typically exceed the high flow threshold previously discussed (i.e. 37,000 cfs). At flows greater than 37,000 cfs (or 17,130 cfs in the upper reach) hydropower operations typically have minimal hydrologic impact in the TFI. While ice is the ultimate cause of erosion in these instances, it is not until sufficiently high flows persist for damage to the riverbanks to occur. This is a naturally occurring process independent of hydropower operations.

Sheet ice can also impact riverbank stability by scraping along the bank when water levels fluctuate. As previously demonstrated from the results of the various hydrologic analyses, for the vast majority of the time the water surface (and therefore the ice) rests on the lower riverbank. In the TFI, the lower bank is typically a flat, beach like feature with minimal to no vegetation or erosion. It is not until the water surface (and therefore the ice) reaches the upper bank that erosion could potentially occur. It is typically not until flows approach or exceed the natural high flow threshold that the water level reaches the upper bank. As such, based on the results of the hydrologic analyses conducted, it is unlikely that water level fluctuations associated with typical hydropower operations could result in ice damage to the banks.

These processes were observed during the winter/spring of 2014/2015 when ice formed over much of the TFI; during which time Northfield Mountain operated in a typical manner. Water levels at the Northfield Mountain Tailrace fluctuated approximately 1 to 4 feet on a daily basis, with an average of about 2 feet, and about 5 feet over a week's time through the winter and early spring, however, for the vast majority of the time the water level rested, and fluctuated, on the lower bank. Based on observations of ice through this period, these fluctuations did not cause ice break-up or floes as the ice persisted into March. There was no significant ice break-up event and ice primarily melted in place, probably partly due to inflow from Vernon not exceeding 17,130 cfs until April 4th. Observations of the riverbank later in the year did not exhibit damage due to ice erosion and young riparian vegetation (seedlings and saplings) that had been established prior to the winter of 2014/2015 were observed at various locations in the TFI. Typical Project operations and associated water level fluctuations did not appear to cause or exacerbate ice related erosion or damage.

Although a quantitative analysis of the impact of ice as a cause of erosion was not possible given weather conditions during the monitoring period and available historic data, the results of the analysis which was conducted indicate that ice has the potential to be a naturally occurring dominant cause of erosion in the TFI in the future if the right climatic and hydrologic conditions persist. Available information and observations indicate that Project operations do not cause an ice break-up event to occur, as ice break-up events occur as a result of climatic and hydrologic conditions (i.e. moderate to high flows, rapid melting, and rainfall) which are independent of Project operations.

Potential Primary Causes of Erosion –Land Management Practices and Anthropogenic Influences

Analysis of the potential impact of land management practices and anthropogenic influences on erosion processes in the TFI focused on a number of factors in the area adjacent to the riverbank, including: (1) land-use; (2) width of riparian buffer; (3) agricultural practices; and (4) animal activity (discussed in the next section). As defined in RSP Task 5 and RSP Table 3.1.2-3, analysis of land management practices and anthropogenic influences focused on various geospatial analyses, including GIS and aerial imagery analysis. Special emphasis was placed on riverbank segments where the adjacent land-use was classified as Agriculture or Developed and the width of riparian buffer was less than 50 ft.

As part of the 2013 FRR, the land-use and width of riparian buffer within 200 ft. of adjacent riverbanks throughout the TFI were identified and classified through a combination of desktop GIS analysis and field investigation/validation. Land-use classifications identified during this effort are summarized in Table 9 while width of riparian buffers are summarized in Table 10.

Table 9: Summary of Turners Falls Impoundment Land-use (200 ft. Buffer)

Land-use	Acres	Percentage of Total
Cropland	275	26
Pasture	15	1.5
Barren	1	0.1
Developed	86	8.2
Transportation	22	2.1
Forest	631	60.3
Non-forested wetland	4	0.4
Restored	11	1.1

Table 10: Forested Riparian Buffer Widths (within 500 ft.)

Width (ft.)	Length (mi)	Percentage of Total
0-25	14	31
25-50	3	7
50-100	5	11
100-200	7	15
200-500	16	36

Various types and degrees of erosion found in the TFI can be observed at locations with a wide variety of adjacent land-uses. The strongest correlation between land-use and erosion has been observed in agricultural areas. Agriculture along the river typically is located on relatively flat floodplain terraces with only a narrow or virtually non-existent zone of riparian vegetation. Riparian vegetation along a river corridor plays a significant role in riverbank stability as it damps out or attenuates hydraulic forces of flowing water or waves, provides structure to bind soils together through its fine-root system and provides root reinforcement. To the extent that riparian vegetation is adversely affected, riverbank stability is likewise adversely affected.

As observed in the tables above, 27.5% of TFI riverbanks were classified as either cropland or pasture with 38% of riverbanks exhibiting a riparian buffer less than 50 ft. Frequently riverbanks in areas with narrow or non-existent riparian buffers consist of steep to overhanging banks consisting of silty/sandy soils that are easily erodible unless sufficient vegetation is present to reinforce the soil and provide some buffering of hydraulic forces.

Agricultural irrigation practices can also impact riverbank processes. In relatively recent years, irrigation has been increasingly utilized on a number of agricultural fields adjacent to the Connecticut River. Some irrigation water comes from groundwater pumping and some comes directly from the river. Water is applied on relatively flat terraces adjacent to the river where agricultural fields have been developed. Irrigation water is used to supplement rainfall which adds to wetter soil conditions. Some of the irrigation water provides water to crops and, in this process, a portion of the water goes to evapo-transpiration while some of it infiltrates deeper into the soil and flows back towards the river. Irrigation therefore increases soil moisture and the quantity of water that may seep through the banks which could adversely affect riverbank stability in these localized areas. Additionally, when significant rainfall occurs, water may pond on relatively flat agricultural fields and infiltrate into the ground which also adds to soil saturation (compared to hillslopes where more rainfall tends to occur as runoff and less infiltration into the soil). A greater degree of saturation in these soils would then result in additional seepage through the riverbank and back to the river.

In addition to agriculture, erosion has also been observed in areas where houses and other associated development are located in close proximity to the river. In several instances throughout the TFI where development has occurred in close proximity to the bank, undercutting, overhanging banks, and exposed roots have been observed. It has also been observed that riparian vegetation has also been cleared in these areas, which can adversely affect riverbank stability.

Many of the eroded sites where stabilization has occurred in accordance with the ECP are found at locations where the adjacent land-use is classified as either agricultural or some other type of development thus indicating the adverse effect land-use and land management practices can have on riverbank stability. As a result of the correlation observed between adjacent land-use and bank stability any riverbank segment where the adjacent land-use was classified as Agriculture or Developed and the riparian buffer width was 50 feet or less was classified as having land-use or land management practices as a potential contributing cause of erosion. This equated to approximately 101,000 feet (19 mi.) or 44% of all riverbank segments in the TFI.

Furthermore, riparian vegetation provides a stabilizing influence to riverbanks damping out hydraulic forces and providing soil stability through its supporting root structure. Where land-use removes or reduces vegetation in the riparian corridor, riverbank stability is generally decreased. A riparian buffer zone between land-use such as agriculture and a river provides an important component that adds to riverbank stability. The Connecticut River Joint Commissions (CRJC), in a brochure entitled "Introduction to Riparian Buffers," state

> *Riparian buffer vegetation helps stabilize streambanks and reduce erosion. Roots hold bank soil together, and stems protect banks by deflecting the cutting action of waves, ice, boat wakes, and storm runoff.*

They warn that *"Natural riparian buffers have been lost in many places over the years,"* and recommend a minimum width of riparian buffer of *"at least 50 feet"* to stabilize eroding riverbanks. They further state that *"Riparian buffers are the single most effective protection for our water resources in Vermont and New Hampshire,"* and that restoring riparian buffers will be *"an important step forward"* regarding riverbank stability.

Erosion rates were computed at several detailed study sites both before restoration and after. This provides a direct comparison at a set of sites where hydraulic conditions are similar since they are at the same location in the river with the only change potentially being different flow conditions over time from pre- to post-restoration. Typically a component of restoration included planting of riparian vegetation. Table 11 compares computed pre- and post-restoration erosion rates from BSTEM, along with the changes in vegetation and other characteristics. The post-restoration rates are significantly lower than pre-restoration rates, with reductions in erosion rate ranging from 82% to 100%. Upper riverbank vegetation for post-restoration sites is typically 'Heavy' compared to 'Little' to 'Very Sparse' for pre-restoration conditions. While restoration at some sites includes a rock toe, gravel, woody debris or lower riverbank vegetation; there typically is a significant increase in upper riverbank vegetation. Given that 44% of the length of riverbanks in the TFI are characterized as being affected by development or agriculture with associated narrow to non-existent riparian vegetation zones and given a large reduction in erosion rates for a well vegetated riverbank (82 to 100%), the potential effect of this length of riverbank lacking in riparian vegetation represents a significant adverse condition regarding erosion and riverbank stability.

Table 11. Erosion rate comparison: pre- to post-restoration

Site	Erosion Rate Pre-Restoration (ft^3/ft/yr)	Upper Riverbank Vegetation Pre-Restoration	Erosion Rate Post-Restoration (ft^3/ft/yr)	Upper Riverbank Vegetation Post-Restoration	Other Restoration Components	Percentage Reduction in Erosion Rate
2L	1.2	Very Sparse	0.214	Heavy	none	82%
3R	15.4	Sparse	0.285	Heavy	Rock toe	98%
6AL	2.67	Little	5.5E-05	Heavy	Rock toe	100%
8BR	7.42	Sparse	0.312	Heavy	Gravel, woody debris, lower riverbank vegetation	96%
9R	5.43	Sparse	0.227	Heavy	Coir log	82%

Potential Secondary Causes of Erosion

During study plan development it was believed that potential secondary causes of erosion such as animals, wind waves, seepage and piping, and freeze-thaw could be present at specific locations in the TFI. Based on the geomorphic understanding of the study area, these potential causes of erosion were likely to have minimal to no influence on erosion in the TFI (other than in any localized locations where they may exist). Given this, these potential causes of erosion were analyzed sufficiently to determine their relative contribution to erosion but not to the level of detail and specificity as the potential primary causes of erosion discussed above (RSP Task 3).

While evidence of some secondary causes of erosion were observed at limited, localized segments in the TFI the majority of the secondary causes were found to be insignificant. Analysis of the potential secondary causes of erosion found that:

- As noted in the RSP, **Animals** can be both a potential primary and/or secondary cause of erosion. Cattle grazing to the river's edge or the removal or trampling of vegetation resulting from animal trails leading to the river are potential land management or anthropogenic factors which were evaluated as potential primary causes of erosion. These activities can lead to runoff issues, gullying, and damage to the soil matrix which all contribute to bank instability. Wild animals and birds (potential secondary cause) can also contribute to bank instability and erosion; an example of which are animals that burrow into riverbanks which may lead to concentrated points of seepage or direct damage to the bank.

  The impacts of animal activity, both from an anthropogenic and natural perspective, in reducing riparian vegetation are typically limited to a number of localized areas throughout the TFI. Observed animal pathways are typically on the order of a couple feet wide or narrower and may exist at a spacing of every few hundred feet along agricultural fields. The contributions of anthropogenic influences were taken into consideration in the analysis of land-use and land management practices previously discussed. Sensitive receptors, such as burrows, were identified during the 2013 FRR and were found to be scattered throughout the TFI at a number of localized areas. While animal activity, both anthropogenic and naturally occurring, may potentially contribute to erosion processes at limited, localized areas (e.g., riverbanks adjacent to agricultural fields with narrow riparian buffers) it was not found to be a significant factor in erosion processes throughout the TFI.

- **Wind waves** on the Connecticut River are relatively small and typically do not form breaking waves since the wind cannot act over a significant length of water (called fetch) because the river lies at the bottom of a valley protected on both sides by mountains. This is particularly true of winds that blow in the west to east direction, across the river that primarily flows north to south. Fetch is also relatively short for winds that blow in the north-south direction because the river flows around bends thereby limiting the length over which wind can build waves. Given this, wind waves were generally not found to be a factor in erosion processes throughout the TFI.

- In the lower bank area, a few limited, localized areas of **seepage** were identified flowing over the lower bank or beach in the TFI. The observed lower bank seepage did not appear to cause significant erosion or sloughing in the adjacent upper riverbank areas. Limited seepage and piping were also observed in localized areas of upland erosion that are unrelated to riverbank processes. In these areas, limited riverbank erosion may occur where such features carve through the upper riverbank and eventually reach the river; however, evidence of this was not prominent at the detailed study sites. Given this, seepage and piping were not found to be a significant factor in erosion processes throughout the TFI.

- **Freeze-thaw** activity was analyzed based on historic information obtained from TransCanada as well as research conducted on other rivers. Freeze-thaw can potentially contribute to bank instability and erosion if the right conditions are present. Based on the research conducted as part of this study it was determined that while freeze-thaw has the potential to contribute to bank instability, it is not believed that freeze-thaw would be a significant factor in erosion processes in the TFI.

Summary Evaluation of the Causes of Erosion

In accordance with Task 6 of the RSP, a summary evaluation of the findings discussed in the previous section is presented below. Given that the secondary causes of erosion were found to be insignificant in contributing to erosion (other than at the localized areas where they may exist), this section focuses on the evaluation of the primary causes of erosion. This summary evaluation is the culmination of the findings of the hydraulic modeling, BSTEM, and independent supplemental analyses as noted in Table 3.1.2-3 of the RSP. Discussion in this section is broken into two sub-sections, (1) the causes of erosion at each detailed study site, and (2) the extrapolation of the causes of erosion to each riverbank segment identified during the 2013 FRR.

Hydraulic Shear Stress due to Flowing Water, Water Level Fluctuations due to Hydropower Operations, and Boat Waves: Site specific summary

The results of the BSTEM modeling runs were used to analyze and evaluate primary causes of erosion, including: (1) hydraulic shear stress due to flowing water; (2) water level fluctuations due to hydropower operations; and (3) boat waves. From this analysis dominant and contributing primary causes of erosion were identified and bank erosion rates were calculated at the 25 detailed study sites. For those sites that were restored during the modeling period as part of the ECP, the causes of erosion were determined for both the pre- and post-restoration periods.

To interpret causes and contributing factors to bank erosion, detailed study sites that have had measureable/significant rates of bank erosion were first identified. In order to be classified as having measurable/significant rates of bank erosion, the rate of erosion at a given site must be greater than the erosion rate that represents the lowest 5% of all rates or 0.163 $ft^3/ft/yr$. Table 12 provides a summary of the distribution of mean annual erosion rates by site.

Table 12: Distribution of Mean Annual Erosion Rates by Site

Mean Annual Erosion Rate Classes	Corresponding Erosion Rate ($ft^3/ft/yr.$)	Number of Detailed Study Sites	Detailed Study Sites
0-5%	<0.163	5	4L, 10L, 10R, 6AL, 6AR
6-25%	0.164 – 0.87	8	11L, 2L, 303BL, 3R, 8BL, 8BR, 9R, BC-1R
26-50%	0.88 – 2.22	5	18L, 29R, 26R, 7R, 12BL
51-75%	2.23 – 4.86	4	21R, 7L, 87BL, 75BL
76-95%	4.87 – 8.49	2	3L, 119BL
96-100%	>8.49	1	5CR

As observed in the table, current condition erosion rates (i.e., not including pre-restoration conditions) at five sites fell below the 5% threshold value (0.163 $ft^3/ft/yr.$). Of those five sites, only two (4L and 10L) represented non-restored conditions. Overall, values of current conditions ranged from 0.0 $ft^3/ft/yr.$ at two post-restoration sites (10R and 6AL) to 8.61 $ft^3/ft/yr.$ at Site 5CR, with a median value of 2.22 $ft^3/ft/yr.$

Based on the BSTEM results and using current erosion rates, a matrix of dominant and contributing primary causes, contributing factors, and contributing processes was developed for the detailed study sites (Table 13). The results of this matrix were then overlaid on aerial imagery to geographically show the dominant and contributing primary causes of erosion, contributing factors, and contributing processes found at each site throughout the TFI (Figures 5 and 6). In addition to identifying the causes, factors, and processes associated with erosion at each detailed study site the figures also include color coded symbols for the six classes of current, average-annual erosion rates. When reviewing the matrix and figures it should be noted that dominant and contributing causes attributed to Northfield Mountain or Vernon operations include both hydraulic shear stress due to flowing water and water level fluctuations due to hydropower operations. Similarly, causes attributed to high or moderate flows include hydraulic shear stress due to flowing water and naturally occurring water level fluctuations, while causes attributed to boats include boat waves.

Table 13: Matrix of Causes of Bank Erosion and Contributing Factors at the 25 Detailed Study Sites

Site	Station	Dominant Causes				Contributing Causes				Contributing Factors				Contributing Processes		
		NFM Project Operations	High Flows	Vernon Operations	Boats	NFM Project Operations	High Flows	Moderate Flows	Boats	High, Steep Bank	Minimal Vegetation	Land Use	Seepage/Piping	Hydraulic Erosion	Geotechnical Erosion	Wave Erosion
11L	100000			X			X			X				X		
2L - Pre	94500		X								X	X		X	X	
2L - Post	94500		X									X		X		
303BL	94000		X							X	X			X		
18L	87000		X							X	X			X	X	
3L	79500		X											X	X	
3R-Pre	79500		X							X	X			X	X	
3R-Post	79500		X											X		
21R	79250		X							X	X		X	X		
4L	74000	-	-	-	-	-	-	-	-					X		
29R*	66000	Failure occurs at first time step, cannot determine primary cause								X	X				X	
5CR	57250		X							X	X	X**		X	X	
26R	50000		X							X	X		X	X		
10L	49000	-	-	-	-	-	-	-	-					X		
10R-Post	49000	-	-	-	-	-	-	-	-							
6AL-Pre	41750		X							X	X			X		
6AL-Post	41750	-	-	-	-	-	-	-	-	X						
6AR-Post	41750	-	-	-	-	-	-	-	-	X		X		X		
119BL	41000		X					X		X	X			X	X	
7L	37500		X							X	X			X	X	
7R	37500		X							X				X		
8BL	32750		X			X				X				X		
8BR-Pre	32750	X					X			X	X			X	X	
8BR-Post	32750		X			X				X				X		
87BL	30750		X					X		X				X	X	
75BL	27000		X					X	X	X	X			X	X	X
9R-Pre	6750				X		I			X	X			X		X
9R-Post	6750				X		I			X				X		X
12BL	6500				X		I			X				X	X	X
BC-1R	4750				X		I			X				X		X

* Imminent failure ** Issues with hydraulics caused by the Rt. 10 Bridge I = Indeterminate

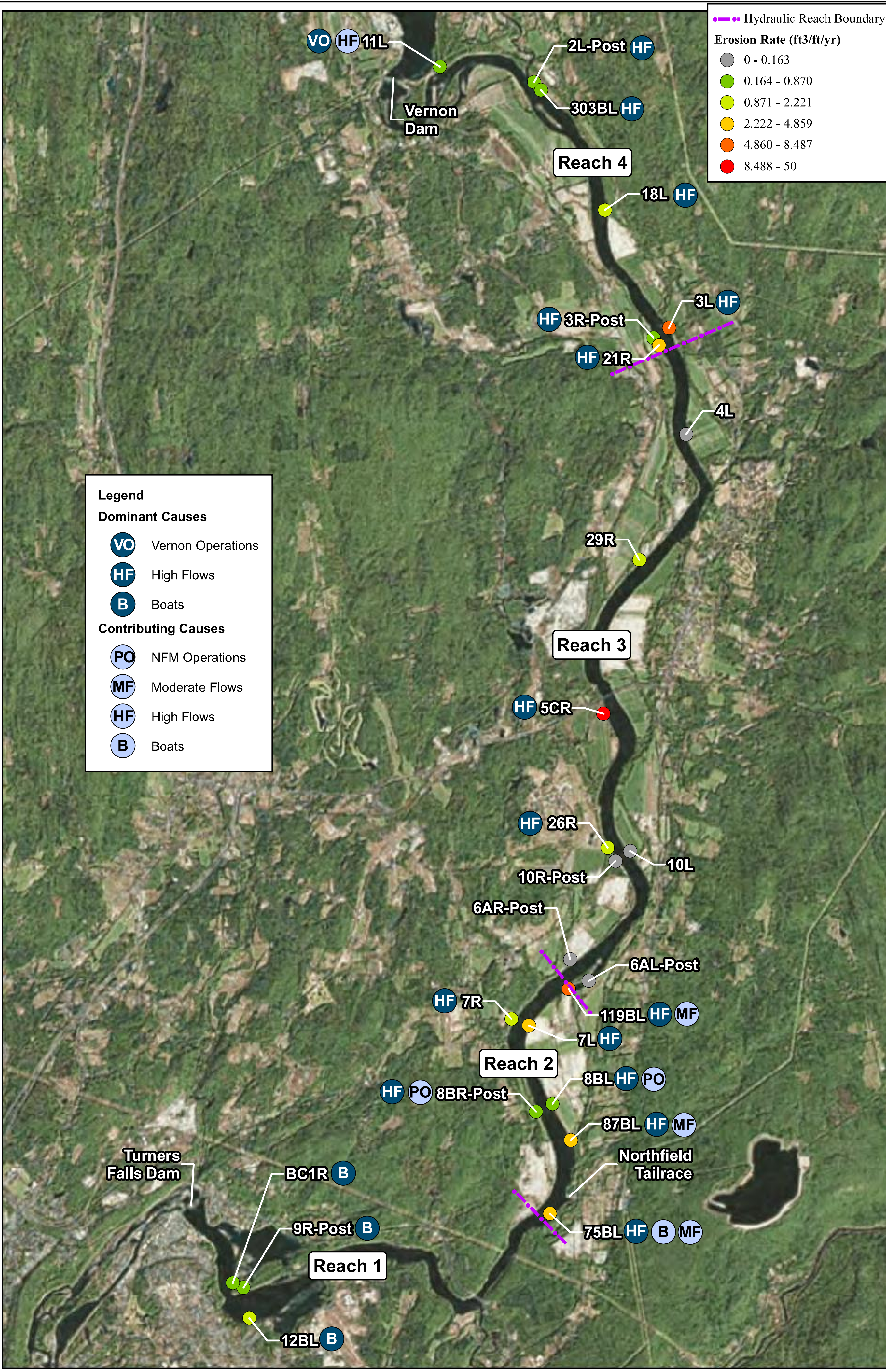

FIRSTLIGHT HYDRO GENERATING COMPANY
Northfield Mountain Pumped Storage Project No. 2485
Turners Falls Hydroelectric Project No. 1889

STUDY 3.1.2

FirstLight Power Resources

N

0 0.625 1.25 2.5 Miles

Figure 5:
Dominant and Contributing Causes of Erosion at each Detailed Study Site

Service Layer Credits: Source: Esri, DigitalGlobe, GeoEye, Earthstar Geographics, CNES/Airbus DS, USDA, USGS, AEX, Getmapping, Aerogrid, IGN, IGP, swisstopo, and the GIS User Community

Path: W:\gis\studies\3_1_2\maps\final_report\figure-5.mxd

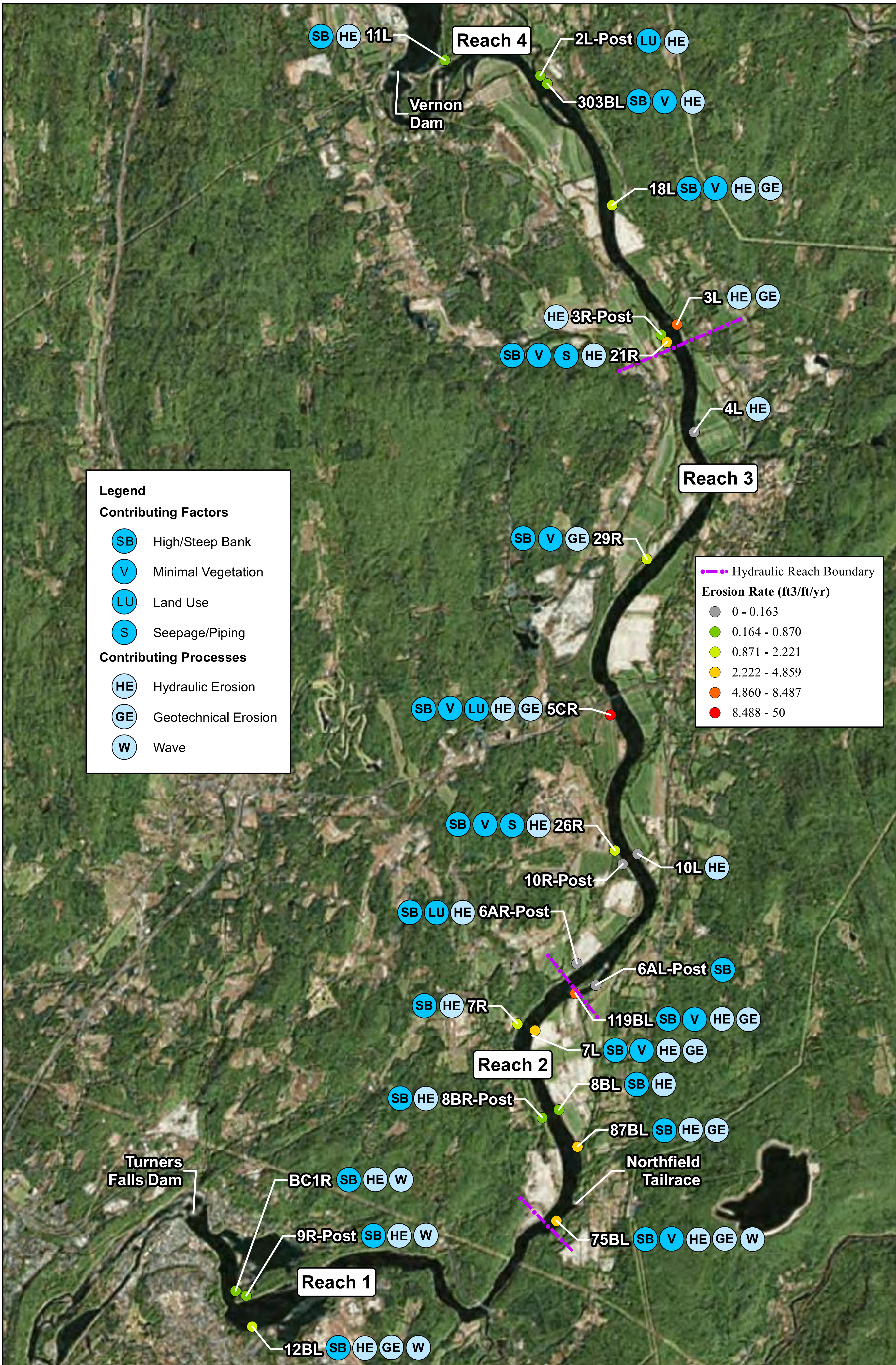

FirstLight
Power Resources

N

FIRSTLIGHT HYDRO GENERATING COMPANY
Northfield Mountain Pumped Storage Project No. 2485
Turners Falls Hydroelectric Project No. 1889

STUDY 3.1.2

0 0.625 1.25 2.5 Miles

Figure 6:
Contributing Erosion Factors and Processes at each Detailed Study Site

Service Layer Credits: Source: Esri, DigitalGlobe, GeoEye, Earthstar Geographics, CNES/Airbus DS, USDA, USGS, AEX, Getmapping, Aerogrid, IGN, IGP, swisstopo, and the GIS User Community

Path: W:\gis\studies\3_1_2\maps\final_report\figure-6.mxd

As demonstrated in the matrix and figures, four different causes of erosion are listed that have specific effects on hydrologic and hydraulic conditions that affect bank processes. These include both "natural" and human-induced effects, including:

- High flows;
- Boats;
- Vernon operations; and
- Northfield Mountain Project operations

To be consistent with the terminology for the primary causes of erosion defined in the RSP, sites classified as having High Flows as a cause of erosion refer to hydraulic shear stresses and naturally occurring water level fluctuations at flows in excess of the hydraulic capacity of Vernon Dam (17,130 cfs in reach 4) and in excess of 37,000 cfs in reaches 3, 2, and 1. Sites classified as having Boats as a cause of erosion indicate the impact of boat waves on bank erosion. Although not included in the list above, land management practices (i.e. riverbank vegetative conditions) were analyzed as contributing factors in BSTEM via the RipRoot sub-model.

To justify the selection of a particular cause and factor for a given site and condition, a quantitative rule set was developed that was based on analysis of the BSTEM results. Most importantly, for a cause to be considered as 'Dominant', it needs to have been responsible for at least 50% of the erosion at the site. This information is obtained directly from the modeling results. For example, for High Flows to be a Dominant cause, more than 50% of the erosion would have to occur at flow rates greater than 17,000 cfs for reach 4 and 37,000 cfs for reaches 3 and 2 as determined from the high-flow analysis[15]. For Northfield Mountain Project Operations to be listed as a Dominant cause, the S1 minus Baseline erosion rate would need to make up at least 50% of the Baseline erosion rate. The same procedure is used as a criterion for waves but in this case the comparison is between the "Waves On" and "Waves Off" scenarios under the Baseline Condition. For a cause to be considered as Contributing, the effect had to be responsible for at least 5% of the bank-erosion rate. This is similar to the justification discussed at the beginning of this section to determine the minimum threshold by which to consider causes of bank erosion.

Selection of contributing factors is based on empirical evidence and observations of conditions at each of the sites along with interpretation of the results of the modeling runs. Assigning Contributing Processes is based on: (1) analysis of BSTEM output which provides for individual erosion volumes by the hydraulic-erosion sub model and by the geotechnical sub-model, and (2) in the case of waves, comparison between "Waves On" and "Waves Off" erosion rates.

As previously noted, there are seven (7) detailed study sites that lie within the Northfield Mountain Reach (reach 2), located between stations 27,000 and 41,000. Sites within the Northfield Mountain Reach include:

- 119BL
- 8BL
- 7L
- 8BR
- 75BL
- 7R
- 87BL

[15] Due to the fact that reliable stage-discharge relationships were not able to be developed in Reach 1 a high flow analysis was not possible in this area.

Although technically not included in this reach because of its generally flatter EGL slopes, Sites 6AL and 6AR at station 41,750 are in the vicinity of the reach. The effects of Northfield Mountain Project operations on bank erosion would, therefore, be expected to show at the sites in closest proximity to the tailrace. Based on the criteria defined above for selection of the causes of bank erosion, Project operations are not a Dominant cause of current bank erosion at any of the sites (Table 12). Project operations are, however, a Contributing cause at Sites 8BL and 8BR, represented by existing and post-restoration conditions, respectively. For conditions prior to restoration at Site 8BR, Project operations were deemed a Dominant cause of bank erosion at this location, but this has been limited by the subsequent restoration work there. Site 8BL with its greater vegetative cover and flatter bank slope was more resilient. At none of the other detailed study sites are Northfield Mountain Project operations deemed to be even a Contributing cause.

Results show that a small amount of erosion at site 7L (station 37,500) can be attributed to Northfield Mountain operations but this amount (3.9%) falls below the threshold value of 5% to be considered a Contributing cause. Site 7R has less than half the erosion rate as 7L and the Dominant cause is High Flows. The difference between sites 7R and 7L can be attributed to the fact that Site 7L has banks that are taller and steeper. The same goes for Site 119BL, approximately 13,000 feet upstream of Northfield Mountain, where about 1.5% of the bank erosion can be attributed to Project operations while the Dominant cause is High Flows. No adverse effect is seen at sites 87BL and 75BL.

With the exception of the sites in the lower TFI (9R, 12BL and BC-1R) where boat waves are the Dominant cause of bank erosion and the uppermost site (11L) just downstream from Vernon Dam where Vernon Operations control bank erosion, the Dominant cause of bank erosion at the remainder of the detailed study sites is High Flows (Table 12).

Hydraulic Shear Stress due to Flowing Water, Water Level Fluctuations due to Hydropower Operations, Boat Waves, and Land Management Practices: Extrapolation of Results

After determining the dominant and contributing primary cause(s) of erosion at each detailed study site the BSTEM results, combined with the results of the supplemental analyses, were extrapolated across the TFI. The purpose of this extrapolation was to determine the cause(s) of erosion at each riverbank segment identified in the 2013 FRR. The extrapolation process was a multi-step process that included analysis of the riverbank features, characteristics, and erosion conditions at each segment, the variability of hydraulic forces throughout the TFI, and the adjacent land-use. The end result of this task was the quantification, based on relative percentages, of the dominant and contributing primary cause(s) of erosion at each fixed riverbank transect and the TFI overall.

The extrapolation methodology utilized in this study was consistent with that which was laid out in the RSP and the regulatory goals of MADEP to "*determine through accurate, repeatable, scientifically based mapping and supportive data collection what fraction of the "banks" of the Turners Falls Impoundment (TFI) are susceptible to or experiencing erosion due to repeated wetting and drying of the soil column. In the process, eliminate all other "banks" within the TFI from further study in regards to this issue, including areas in which bedrock predominates; soils/substrates are presently stable; and hardscape stabilization has previously been installed* (October 17, 2013 correspondence)."

The extrapolation approach consisted of seven main steps, including:

1. Analyze the variability of hydraulic forces throughout the TFI;
2. Analyze and review the site specific BSTEM results;
3. Analyze riverbank features, characteristics, and erosion conditions – which included the following sub-steps:

   a. Identify the detailed study sites where hydropower operations (i.e., Vernon, Northfield Mountain, or Turners Falls) were the dominant or contributing cause of erosion;
   b. Identify the riverbank features, characteristics, and erosion conditions at those sites based on the results of the 2013 FRR;
   c. Identify other segments in hydraulic reach 4 (Vernon) or 2 (Northfield Mountain) that have the same features and characteristics. Map the locations of those segments in ArcGIS.
   d. Compare the locations of those segments identified in Step 3c against (1) the results of the nearest detailed study site, and (2) the hydraulic and geomorphic conditions at that location to determine if the riverbank features and characteristics or hydraulics/geomorphology are the likely factors influencing erosion;
4. Assign each riverbank segment identified in the 2013 FRR dominant and contributing causes of erosion – which included the following sub-steps:
   a. Identify sites where hydropower operations from Northfield Mountain or Vernon were found to potentially be a dominant or contributing cause of erosion based on the results from Steps 3c and 3d;
   b. Extrapolate the results from a given detailed study site, halfway upstream and halfway downstream to the nearest detailed study site. For example, the causes of erosion identified at Site 119BL were extrapolated and assigned to all riverbank segments up to the halfway point upstream to Site 6A and halfway point downstream to Site 7;
5. Conduct supplemental hydraulic and geomorphic analyses in Reach 1 to determine the impact, if any, of Turners Falls Project operations;
6. Analyze land-use and width of riparian buffers adjacent to the riverbanks;
7. Create a map identifying the causes of erosion for each riverbank segment; and
8. Finalize the map and calculate summary statistics

<u>Step 1: Analyze the variability of hydraulic forces throughout the TFI</u>

The variability of hydraulic forces throughout the TFI was analyzed as part of the hydrologic and hydraulic analysis previously discussed. The results of those analyses confirmed that the hydraulic reaches established via the EGL slope accurately represented the geographic extent of which a hydropower project could have a potential impact on riverbank erosion processes. Based on these findings, Vernon operations can only have a potential impact on erosion in reach 4, Northfield Mountain in reach 2, and Turners Falls in reach 1.

<u>Step 2: Analyze and review the site specific BSTEM results</u>

Focus then turned to analyzing the site specific BSTEM results for the 25 detailed study sites. For those sites where restoration had previously occurred, both the pre- and post-restoration results were reviewed. Causal determinations for the extrapolation process followed the same criteria discussed earlier. That is, for a cause to be considered dominant it needs to have been responsible for at least 50% of the erosion at the detailed study site. For a cause to be considered contributing, it had to contribute to >5% of the erosion at a site. Table 14 presents a summary of the BSTEM results used for the extrapolation process.

Table 14: Causes of erosion at detailed study sites summarized from BSTEM

Site	Hydraulic Reach	Station	Dominant Primary Causes					Contributing Primary Causes			
			Project Operations	High Flows	Vernon Operations	Qe_{95} (cfs)	Boats	Project Operations	High Flows	Moderate Flows	Boats
11L		100,000			X	500			X		
2L - Pre		94,500		X		49,906					
2L - Post		94,500		X		51,924					
303BL		94,000		X		53,194					
18L	4 - Upper	87,000		X		17,824					
3L		79,500		X		37,098					
3R-Pre		79,500		X		39,229					
3R-Post		79,500		X		36,411					
21R		79,250		X		22,928					
4L		74,000	-	-	-	6,991	-	-	-	-	-
29R*		66,000	Failure occurs at first time step, cannot determine primary cause(s)								
5CR		57,250		X		47,867					
26R		50,000		X		43,294					
10L	3 - Middle	49,000	-	-	-	58,922	-	-	-	-	-
10R-Post		49,000	-	-	-	46,944	-	-	-	-	-
6AL-Pre		41,750		X		56,264					
6AL-Post		41,750	-	-	-	62,287	-	-	-	-	-
6AR-Post		41,750	-	-	-	7,051	-	-	-	-	-
119BL		41,000		X		24,796				X	
7L		37,500		X		47,731					
7R		37,500		X		53,614					
8BL	2 - NFM	32,750		X		77,997		X			
8BR-Pre		32,750	X			64,443			X		
8BR-Post		32,750		X		66,504		X			
87BL		30,750		X		17,849				X	
75BL		27,000		X		33,822				X	X
9R-Pre		6,750				I	X		I		
9R-Post	1 - Lower	6,750				I	X		I		
12BL		6,500				I	X		I		
BC-1R		4,750				I	X		I		

As shown in the table an "X" indicates the cause(s) of erosion, a "-" indicates that erosion was insignificant, and an "I" means indeterminate. The term Qe_{95} is the flow above which 95% of erosion occurred as determined from the BSTEM results. Since there is no definable stage-discharge relationship in the lower portion of the TFI, Qe_{95} was not determined in that reach (as indicated with an "I" in the table).

Step 3: Analyze the Riverbank Features, Characteristics, and Erosion Conditions

As observed in the Table 14, only one site (8BR-Pre) was identified as having Northfield Mountain operations be the dominant cause of erosion while two sites (8BL and 8BR-Post) were identified as having Northfield Mountain operations be a contributing cause. Similarly, only one site (11L) was identified as having Vernon operations be the dominant cause of erosion; no sites were found to have Vernon operations be a contributing cause. Based on these results, the corresponding 2013 FRR riverbank segments and their features, characteristics, and erosion conditions for each site mentioned above were identified and summarized. The riverbank features, characteristics, and erosion conditions associated with Site 11L were then compared against all segments in reach 4 in order to identify segments with common features and characteristics. Given that the features and characteristics found at Site 11L are relatively common of riverbanks in the TFI, 25 segments were identified in reach 4 with common features and characteristics to those found at Site 11L.

A similar analysis was then conducted for Site 8BR-Pre. Due to the fact that 8BR is a restoration site, the riverbank features and characteristics as observed during the 1998 FRR were compared against the features and characteristics identified during the 2013 FRR for all riverbank segments found in reach 2 to determine if similarities exist at other locations within the reach. No riverbank segments were found in reach 2 with the same characteristics as were observed at Site 8BR in 1998. Although no riverbank segments were found to be an exact match, three FRR segments were identified as having very similar characteristics – 75, 87, and 109. The only difference between these segments and Site 8BR (1998) was in regard to upper riverbank vegetation where 8BR (1998) was classified as having None to Very Sparse vegetation and FRR segments 75, 87, and 109 were classified as having Sparse vegetation. These three segments total 276 ft. in length, or 0.12% of the total length of TFI riverbanks.

Finally, the same comparison was then conducted for the features and characteristics at Sites 8BL and 8BR-Post. Based on the results of this comparison, eight FRR segments in reach 2 were identified as having the same features and characteristics as Sites 8BL and 8BR-Post.

Step 4: Assign each riverbank segment dominant and contributing causes of erosion

The location of the FRR segments identified above were then analyzed to determine what the likely driving erosion factor would be at each site (i.e. riverbank features and characteristics, hydraulics, geomorphology, or geography) and were compared against the causes of erosion identified at the nearest detailed study site. If based on this analysis, it was determined that the features and characteristics were the likely driving factor in erosion processes the site would be assigned Northfield Mountain or Vernon operations as the dominant or contributing cause of erosion. If, however, it was determined that hydraulics or geomorphology were the driving factor then the site was assigned the cause(s) of the nearest detailed study site (which in some cases was hydropower operations).

For those segments in reach 4 that were located between Vernon Dam and Site 11L, it was determined that Vernon operations was the dominant cause of erosion due to the hydraulics, geomorphology, and BSTEM results at Site 11L. For those segments that were located downstream of Site 11L it was determined that, although the features and characteristics were the same as Site 11L, the causes of erosion would be determined by the results of the nearest detailed study site (which in this case was always high flows with no contributing causes). This determination was made based on the hydraulics, geomorphology, and consistency of BSTEM results across all detailed study sites in reach 4 downstream of Site 11L.

A similar analysis was then conducted for the segments located in reach 2. FRR segments 75 and 109 are approximately 33 and 36 ft. in length and are surrounded by detailed study sites which indicate that high flows are the dominant cause of erosion. Given this, FRR segments 75 and 109 were classified as having the same causes of erosion as the nearest detailed study site. FRR segment 87 is located at detailed study site 87BL and therefore was assigned the causes of erosion observed at that site as determined by BSTEM. Similar to the rationale for segments 75 and 109, FRR segments 78 and 116 were assigned the causes of erosion found at the nearest detailed study site. All remaining segments were classified as Northfield Mountain being a contributing cause of erosion.

Once the analysis of common riverbank features and characteristics was completed, the remaining riverbank segments identified during the FRR were assigned dominant and contributing causes of erosion based on the results of the nearest detailed study site. The results of the nearest detailed study site were extrapolated halfway upstream and downstream to its neighboring study site. For example, the results found at detailed study site 8BL were extrapolated to all riverbank segments which were located from that site halfway upstream to site 7 and halfway downstream to site 87B such that Site 8BL would be in the middle of all segments which were assigned the same causes as were found at that site. This is demonstrated in later figures.

<u>Step 5: Conduct supplemental hydraulic and geomorphic analyses in Reach 1 to determine the impact, if any, of Turners Falls Project operations</u>

As previously discussed, Turners Falls Project operations can only be a potential cause of erosion in hydraulic reach 1 (lower) due to the hydraulic characteristics of the TFI. Detailed study sites in the lower reach only exist in the vicinity of Barton Cove (12BL) with the nearest upstream study sites located at the Northfield Mountain tailrace (75BL, upstream of the French King Gorge). The geomorphic characteristics of the TFI between the Barton Cove and Northfield Mountain sites vary significantly. Given this, it is not appropriate to do a straight extrapolation from site 75BL to Site 12BL. As such, a modified extrapolation approach was used to determine the causes of erosion in the area between these study sites. The modified approach utilized a combination of BSTEM results, geomorphic assessment, and hydraulic model analysis.

For the upstream and downstream portions of reach 1, the causes of erosion at the nearest detailed study sites were extrapolated to the riverbank segments in these areas. In the upstream portion of the reach, this included the area from just downstream of detailed study site 75BL to the French King Bridge. Given that this area is upstream of, or includes, the French King Gorge, and is composed mainly of bedrock, the hydraulic conditions are the same, or similar, as those found at detailed study site 75BL thus making the extrapolation of the causes found at that site appropriate.

The downstream portion of the reach, from Turners Falls Dam to upstream of the entrance to Barton Cove before the river narrows, is lake-like, has unique geomorphic characteristics when compared to the other portions of the reach, and includes three detailed study sites. The results at the three detailed study sites demonstrate how dominant the effect of boat waves are in causing erosion in this area. As a result of these findings, combined with the unique geomorphic characteristics of this area and that water level fluctuations are limited to a very narrow band, the results of the detailed study sites were extrapolated to the riverbank segments in the downstream portion of the reach. The results of this extrapolation classified all riverbank segments in this area as having boat waves as the dominant cause of erosion with no contributing causes.

In the middle portion of this reach (i.e., from where the river narrows upstream of Barton Cove to the French King Gorge) the results of the hydraulic modeling, combined with the findings of the 2013 FRR, were used to analyze the potential for Turners Falls Project operations to cause erosion. In this section of the TFI, the water surface elevation is normally largely a function of the gate setting by FirstLight at the Turners Falls Dam. The slope of the WSEL is generally flat to the lower part of French King Gorge under most flow conditions. In addition to the flows released to the power canal, FirstLight can release over 130,000 cfs via the bascule and taintor gates at the Turners Falls Dam at the long term median WSEL of 181.3. As a result, there is a not a stage discharge relationship in this part of the TFI as there is upstream of French King Gorge (especially at higher flows). While a reliable stage discharge relationship could not be developed, analysis of water level data during a representative year (2011) was completed to determine the impacts, if any, of Turners Falls operations on erosion.

Based on an extensive set of time-stamped photos collected in associated with the 2013 FRR and corresponding water surface elevation data FirstLight was able to determine the elevation of the lower bank -upper bank transition. Once this elevation was determined, FirstLight could then determine the amount of time that water levels exceeded the top of the lower bank and rested on the silt/sand upper bank as well as the flows at which that occurred. The transition from the lower bank to the upper bank is significant given that, in this area, the lower bank sediment is classified as bedrock or boulders with upper bank sediment classified as silt/sand. The results of the hydraulic model were then used to determine the percentage of time during the modeling period that the water level equaled or exceeded this elevation and at what flow.

This analysis found that for the vast majority of the time the water level rests, or fluctuates, on the bedrock/boulders where erosion due to hydraulic forces is inconsequential. In the event that the water level does rest, or fluctuate, on the silt composed upper bank flows typically exceed the natural high flow threshold (37,000 cfs). In other words, the only time the water level is higher than the bedrock-silt interface, and therefore the only time when erosion could potentially occur, is during naturally occurring high flows. Review of the data during the analysis period (2011) found that only those flows which occurred during Hurricane Irene resulted in water surface elevations exceeding the top of the lower bank. As such, the dominant cause of erosion in this area was classified as high flows. Given that boat waves were found to be the dominant cause of erosion at the downstream study sites and a contributing cause of erosion at Site 75BL, boat waves were also classified as a contributing cause of erosion in this area.

As described above, the results of the modified extrapolation approach employed in Reach 1 indicate that Turners Falls Project operations are not a dominant or even contributing cause of erosion at any riverbank segment in the lower reach. Furthermore, during high flow events water level management at the Turners Falls Dam may actually aid in the prevention of erosion as water levels in the impoundment are typically drawn down to prevent unnecessary spilling.

Step 6: Analyze land-use and width of riparian buffers

Once each riverbank segment was classified with the appropriate erosion cause(s), land-use, land management practices, and anthropogenic influences were evaluated to determine their potential impact as a contributing primary cause of erosion. In order to determine this, land-use and width of riparian buffer datasets developed as part of the 2013 FRR were analyzed to identify segments where the adjacent land-use was classified as either Agriculture or Developed and the width of riparian buffer was 50 ft. or less. Based on the results of this analysis, it was found that 252 segments (101,000 ft. or 19 mi.) were identified where land management practices, anthropogenic influences, and/or land-use are a potential contributing cause of erosion (Figure 7).

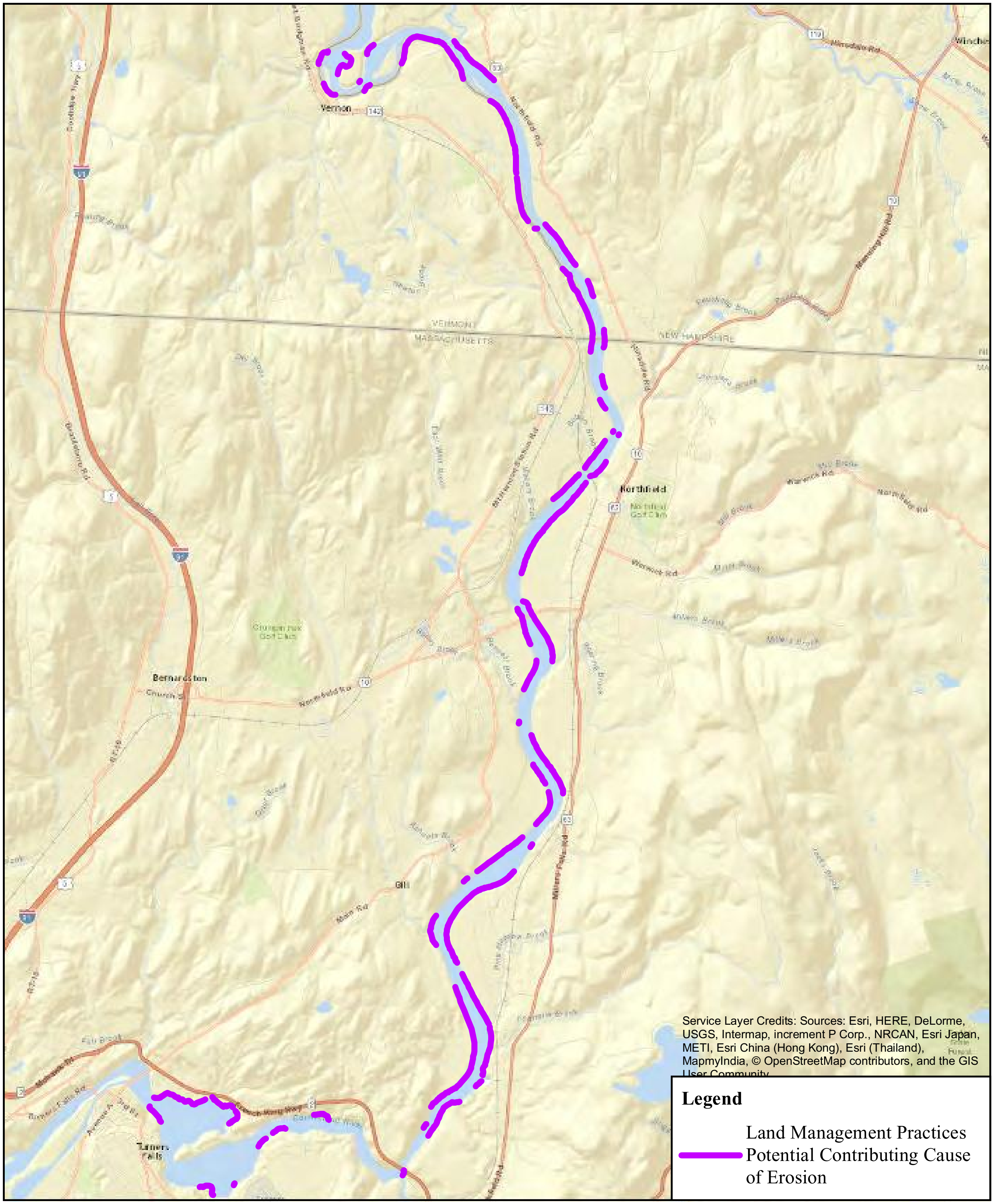

Service Layer Credits: Sources: Esri, HERE, DeLorme, USGS, Intermap, increment P Corp., NRCAN, Esri Japan, METI, Esri China (Hong Kong), Esri (Thailand), MapmyIndia, © OpenStreetMap contributors, and the GIS User Community

FIRSTLIGHT HYDRO GENERATING COMPANY
Northfield Mountain Pumped Storage Project No. 2485
Turners Falls Hydroelectric Project No. 1889

STUDY 3.1.2

N

0 0.75 1.5 3 Miles

Figure 7:
Location of Turners Falls Impoundment Riverbank Segments where Land Management Practices are a Potential Contributing Cause of Erosion

Path: W:\gis\studies\3_1_2\maps\final_report\figure-7.mxd

Steps 7 and 8: Create a map identifying the causes of erosion and calculate summary statistics

The extrapolation process resulted in a clear classification of the dominant primary causes of erosion throughout the TFI such that Vernon operations were found to be the dominant cause of erosion from Vernon Dam to downstream of Site 11L. From downstream of Site 11L until upstream of the entrance to Barton Cove high flows were found to be the dominant cause of erosion, while from upstream of the entrance to Barton Cove to the Turners Falls Dam boat waves were identified as the dominant primary cause.

Based on the results of the BSTEM analysis, high flows were found to be such a dominant cause of erosion throughout the TFI that the majority of riverbank segments did not have any contributing causes of erosion assigned to them. The relatively limited areas where contributing causes were found included: (1) the area from Vernon Dam to downstream of Site 11L where high flows were a contributing cause; (2) one area in reach 3 where moderate flows were a contributing cause; (3) a few areas in reach 2 where Northfield Mountain operations were a contributing cause; (4) a few areas around the Northfield Mountain tailrace extending to below the French King Gorge where moderate flows and boats were contributing causes; and (5) the riverine section in reach 1from the French King Bridge to upstream of the entrance to Barton Cove where boat waves were a contributing cause.

Once all extrapolation steps were completed, the dominant and contributing primary causes of erosion were quantified based on the total number of FRR segments, the total length of those segments (in both feet and miles), and the % of total TFI riverbank length for each primary cause (excluding ice). These results are presented in Tables 15 and 16.

Table 15: Quantification of the Dominant Primary Causes of Erosion in the Turners Falls Impoundment

Dominant Primary Cause of Erosion	No. FRR Segments	Total Length (ft.)	Total Length (mi.)	% of Total Riverbank Length
Natural High Flows	474	175,900	33	78%
Boat waves	60	30,800	6	13%
Vernon Operations	59	20,200	4	9%
Northfield Mountain Operations	0	0	0	0%
Turners Falls Operations	0	0	0	0%

Table 16: Quantification of the Contributing Causes of Erosion in the Turners Falls Impoundment

Contributing Primary Cause of Erosion	No. FRR Segments	Total Length (ft.)	Total Length (mi.)	% of Total Riverbank Length[16]
None	401	153,400	29	68%
Boats	96	36,000	7	16%
Natural Moderate Flows	53	23,200	4	10%
Natural High Flows	59	20,200	4	9%
Northfield Mountain Operations	20	8,600	1.5	4%
Vernon Operations	0	0	0	0%
Turners Falls Operations	0	0	0	0%
Land Management Practices *(potential contributing cause)*	249	101,000	19	44%

As shown in the tables, the dominant and contributing primary causes of erosion were quantified using relative percentages for every TFI riverbank segment identified during the 2013 FRR (excluding islands). Based on the results of this analysis:

- Natural High Flows were found to be the dominant primary cause of erosion in the TFI at 78% of all riverbanks, followed by Boat Waves (13%), and Vernon Operations (9%); and
- Northfield Mountain operations were not found to be a dominant cause of erosion at any riverbank segment in the TFI.

In regard to contributing primary causes of erosion:

- The majority of the riverbank segments in the TFI (68%) did not have a contributing cause of erosion;
- Boats were a contributing cause at 16% of all riverbank segments followed by moderate flows (10%), High Flows (9%), and Northfield Mountain operations (4%);

[16] Note that since moderate flows and boat waves are contributing causes of erosion at a number of the same riverbank segments, the total percentage for contributing causes does not equal 100%. In other words, given that a riverbank segment can have more than one contributing cause of erosion, the percentages do not add to 100%.

- Vernon operations were not found to be a contributing cause of erosion at any riverbank segments; and
- Land management practices were found to be a potential contributing cause of erosion at 44% of all TFI riverbanks.

The spatial distribution of the causes of erosion throughout the TFI are shown in Figure 8.

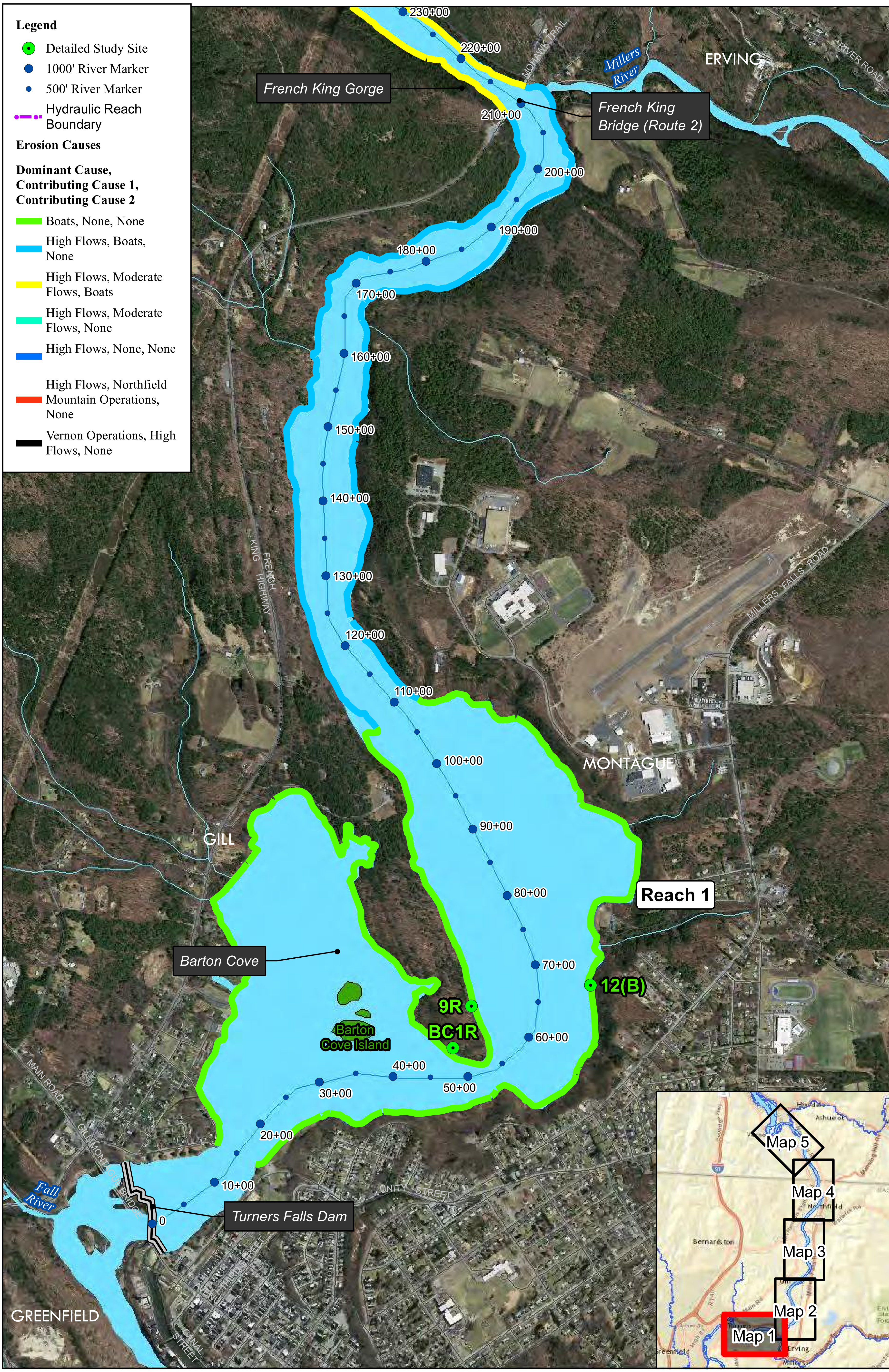

FirstLight Power Resources

FIRSTLIGHT HYDRO GENERATING COMPANY
Northfield Mountain Pumped Storage Project No. 2485
Turners Falls Hydroelectric Project No. 1889

STUDY 3.1.2

0 625 1,250 2,500 Feet

Figure 8:
Final Extrapolation of the Causes of Erosion for each Riverbank Segment in Turners Falls Impoundment
Map 1

Service Layer Credits: Sources: Esri, HERE, DeLorme, USGS, Intermap, increment P Corp., NRCAN, Esri Japan, METI, Esri China (Hong Kong), Esri (Thailand), MapmyIndia, © OpenStreetMap contributors, and the GIS User Community

Path: W:\gis\studies\3_1_2\maps\final_report\figure-8.mxd

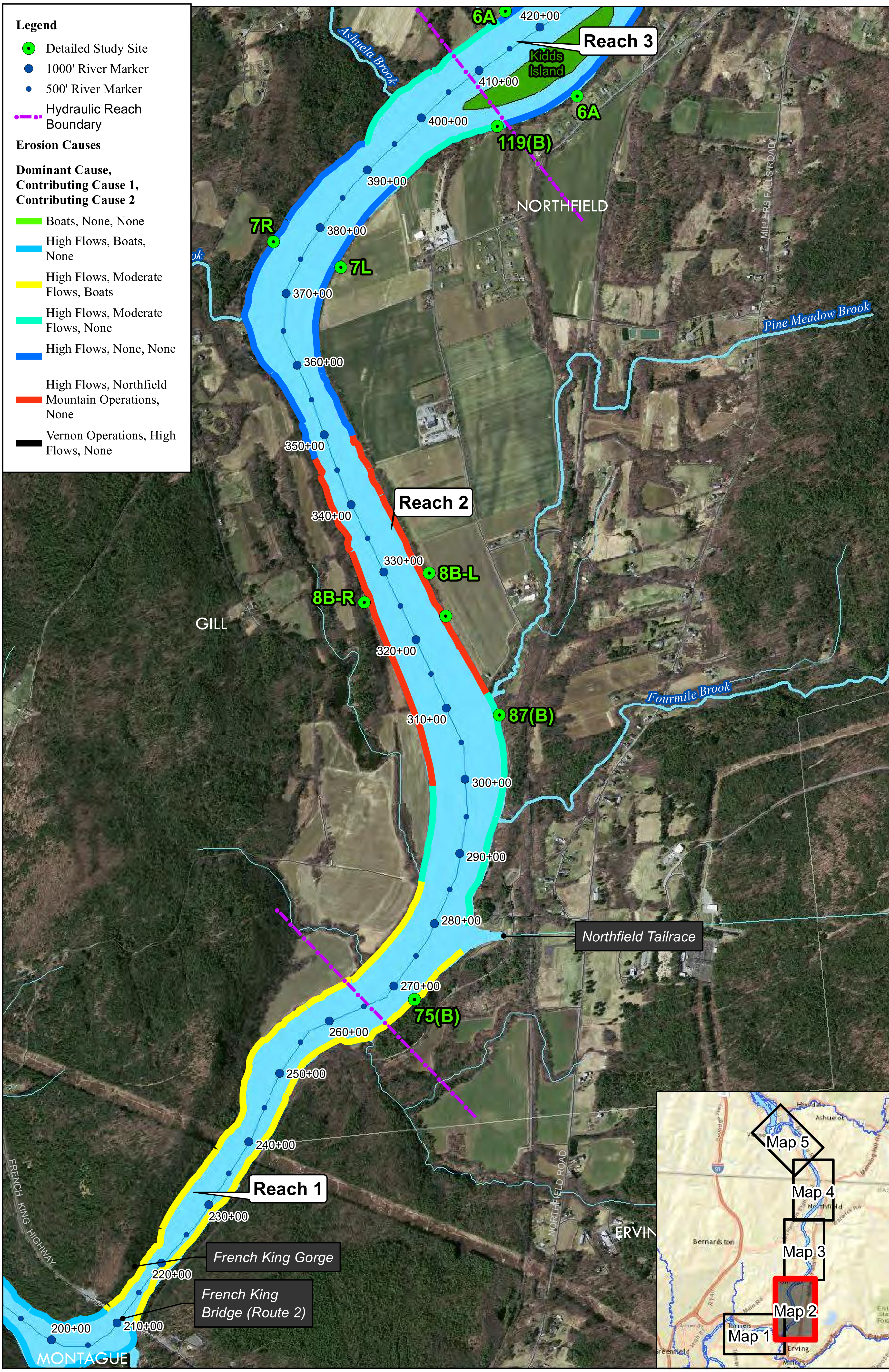

FIRSTLIGHT HYDRO GENERATING COMPANY
Northfield Mountain Pumped Storage Project No. 2485
Turners Falls Hydroelectric Project No. 1889

STUDY 3.1.2

0 625 1,250 2,500 Feet

N

FirstLight Power Resources

Figure 8:
Final Extrapolation of the Causes of Erosion for each Riverbank Segment in Turners Falls Impoundment
Map 2

Service Layer Credits: Sources: Esri, HERE, DeLorme, USGS, Intermap, increment P Corp., NRCAN, Esri Japan, METI, Esri China (Hong Kong), Esri (Thailand), MapmyIndia, © OpenStreetMap contributors, and the GIS User Community

Path: W:\gis\studies\3_1_2\maps\final_report\figure-8.mxd

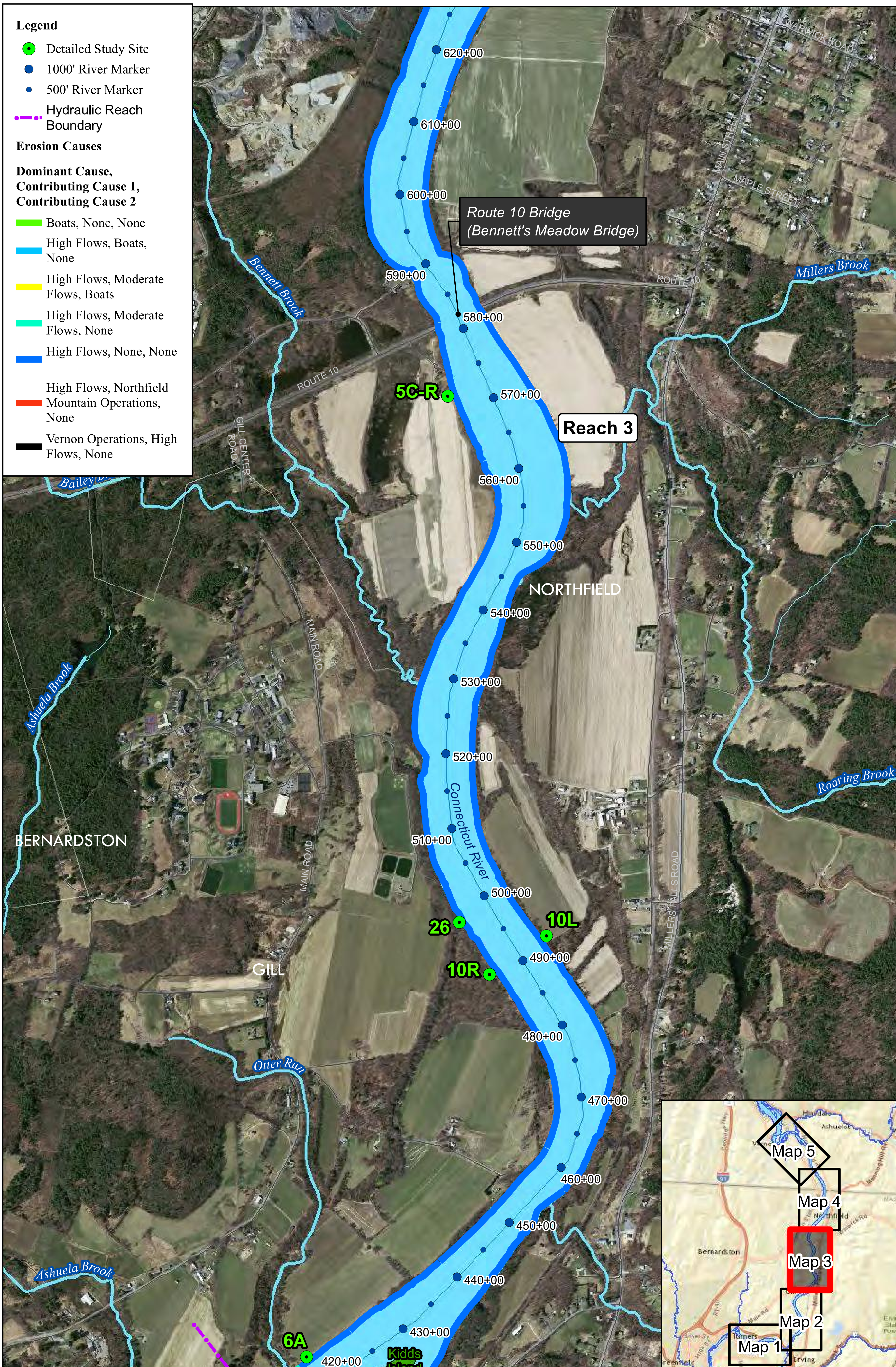

FIRSTLIGHT HYDRO GENERATING COMPANY
Northfield Mountain Pumped Storage Project No. 2485
Turners Falls Hydroelectric Project No. 1889

STUDY 3.1.2

FirstLight Power Resources

N

0 625 1,250 2,500 Feet

Figure 8:
Final Extrapolation of the Causes of Erosion for each Riverbank Segment in Turners Falls Impoundment
Map 3

Service Layer Credits: Sources: Esri, HERE, DeLorme, USGS, Intermap, increment P Corp., NRCAN, Esri Japan, METI, Esri China (Hong Kong), Esri (Thailand), MapmyIndia, © OpenStreetMap contributors, and the GIS User Community

Path: W:\gis\studies\3_1_2\maps\final_report\figure-8.mxd

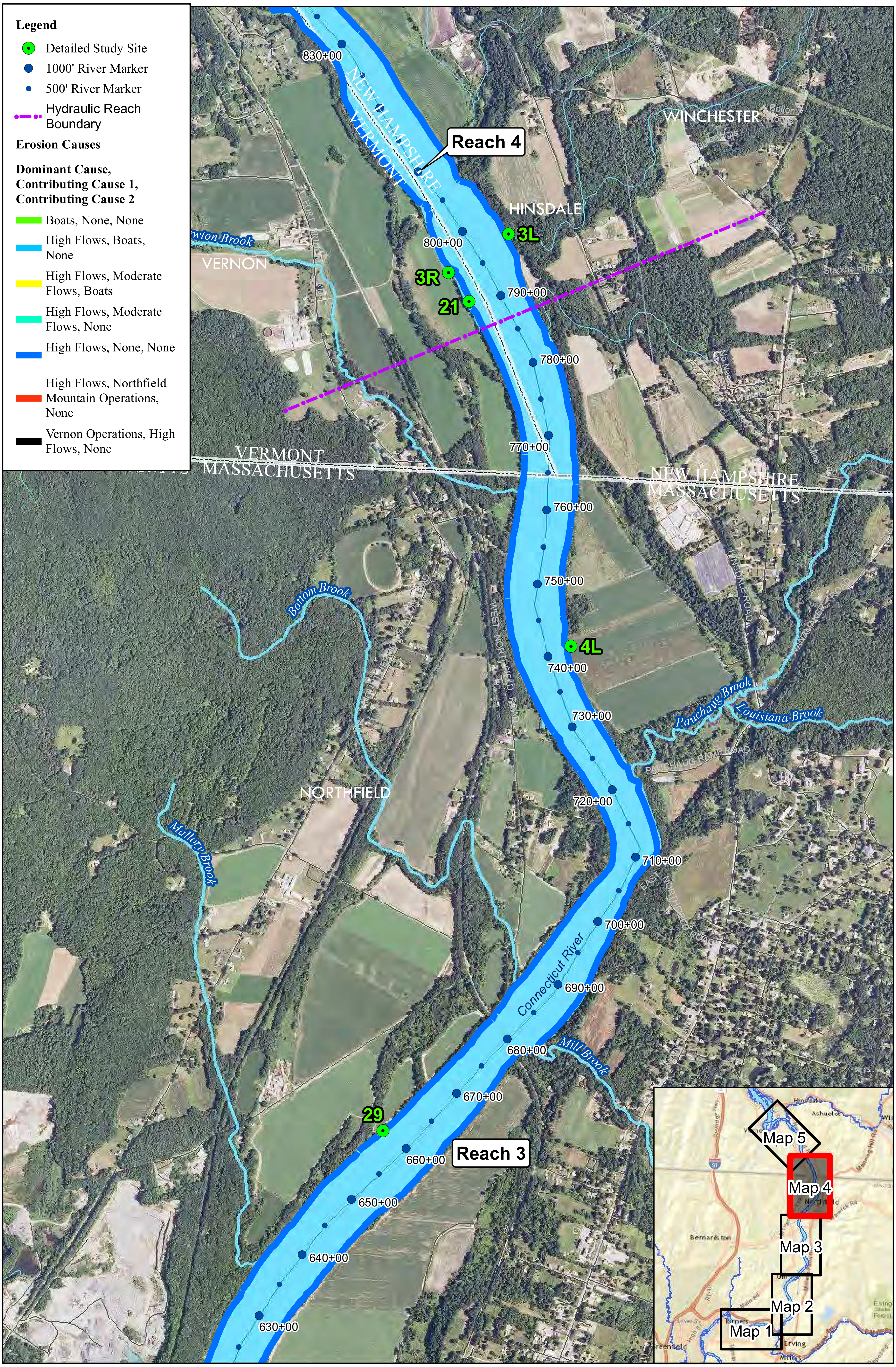

FIRSTLIGHT HYDRO GENERATING COMPANY
Northfield Mountain Pumped Storage Project No. 2485
Turners Falls Hydroelectric Project No. 1889

STUDY 3.1.2

FirstLight Power Resources

N

0 625 1,250 2,500 Feet

Figure 8:
Final Extrapolation of the Causes of Erosion for each Riverbank Segment in Turners Falls Impoundment
Map 4

Service Layer Credits: Sources: Esri, HERE, DeLorme, USGS, Intermap, increment P Corp., NRCAN, Esri Japan, METI, Esri China (Hong Kong), Esri (Thailand), MapmyIndia, © OpenStreetMap contributors, and the GIS User Community

Path: W:\gis\studies\3_1_2\maps\final_report\figure-8.mxd

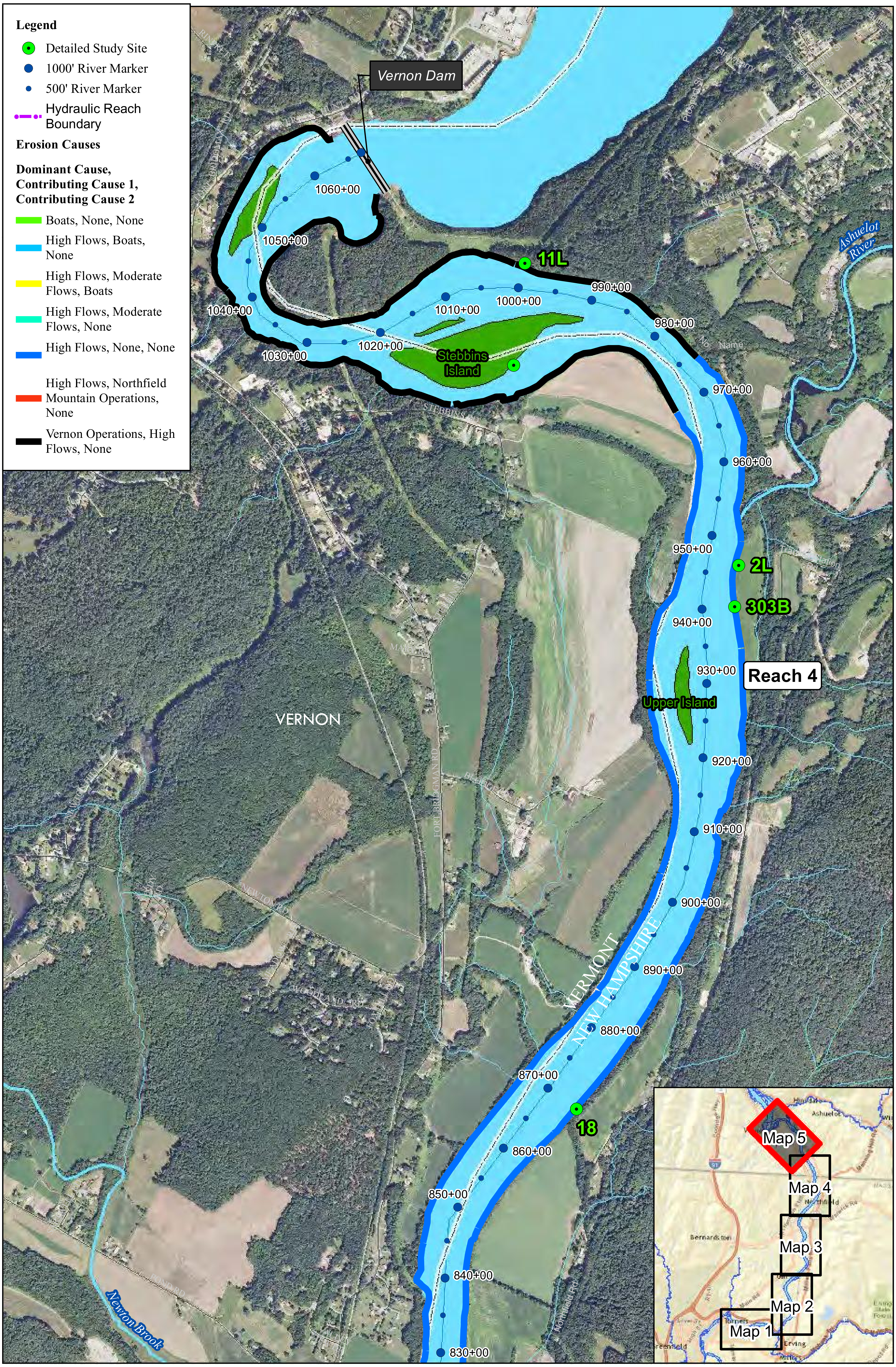

FIRSTLIGHT HYDRO GENERATING COMPANY
Northfield Mountain Pumped Storage Project No. 2485
Turners Falls Hydroelectric Project No. 1889

STUDY 3.1.2

0 625 1,250 2,500 Feet

Figure 8:
Final Extrapolation of the Causes of Erosion for each Riverbank Segment in Turners Falls Impoundment
Map 5

Service Layer Credits: Sources: Esri, HERE, DeLorme, USGS, Intermap, increment P Corp., NRCAN, Esri Japan, METI, Esri China (Hong Kong), Esri (Thailand), MapmyIndia, © OpenStreetMap contributors, and the GIS User Community

Path: W:\gis\studies\3_1_2\maps\final_report\figure-8.mxd

Conclusions

The causes of erosion in the TFI were identified via state-of-the-science modeling and supplemental engineering analyses at 25 detailed study sites located throughout the study area. The detailed study sites spanned the longitudinal extent of the TFI and were representative of the riverbank features, characteristics, and erosion conditions found throughout the study area. The results from the 25 detailed study sites were then extrapolated throughout the TFI such that each riverbank segment identified during the 2013 FRR had a dominant and, in some cases, contributing cause(s) of erosion assigned to it. The complex hydrologic and hydraulic characteristics of the TFI were also examined in-depth and accounted for during this process and were found to be just as important, if not more so, to erosion processes than riverbank features and characteristics were.

In summary, Study No. 3.1.2 found the following:

- Naturally occurring moderate and high flows have the greatest impact on erosion in the TFI. Natural high flows are the dominant cause of erosion at 78% of all riverbank segments in the TFI and a contributing cause of erosion at 9% of all segments. Moderate flows are a contributing cause of erosion at 10% of all riverbank segments;

- Hydropower operations have limited to no impact on bank erosion in the TFI:

    - Northfield Mountain Project operations are not a dominant cause of erosion at any riverbank segment in the TFI. They are a contributing cause of erosion at 4% of the total riverbank segments (8,600 ft.);

    - Turners Falls Project operations are not a dominant or contributing cause of erosion at any riverbank segment in the TFI; and

    - Vernon Project operations are a dominant cause of erosion at 9% of all riverbank segments in the TFI (20,200 ft.). They are not a contributing cause of erosion at any riverbank segment

- Boats are a dominant cause of erosion at 13% of all riverbank segments in the TFI (30,800 ft.), all of which are located in the lower reach (reach 1). They are a contributing cause of erosion at 16% of all riverbank segments (36,000 ft.);

- Based on analysis of historic information from the Connecticut River, as well as other river systems, ice has the potential to be a naturally occurring dominant cause of erosion in the TFI in the future given the right climatic and hydrologic conditions. Due to the hydrologic and hydraulic characteristics of the TFI, it is anticipated that hydropower operations will have limited to no impact on ice as related to bank erosion;

- Land management practices and anthropogenic influences are a potential contributing primary cause of erosion at 44% of all riverbank segments in the TFI (101,000 ft.); and

- Potential secondary causes of erosion such as wind waves, animals, seepage and piping, and freeze-thaw were found to be insignificant in causing erosion in the TFI beyond the limited, localized areas where they may exist.

Study No. 3.1.2 was conducted in accordance with the FERC and MADEP approved RSP using a robust dataset which spanned a 15-year period, proven analysis methods, and state-of-the-science modeling platforms. The results of this study were based on the analysis of a wide variety of datasets including hydrologic, hydraulic, geotechnical, and geomorphic data, analysis of both empirical and modeled data (including both 1-D and 2-D hydraulic models and BSTEM), and review of a wealth of historic information. The findings of this study represent the most thorough understanding of erosion dynamics in the TFI to date.

Relicensing Study 3.1.2

Northfield Mountain / Turners Falls Operations Impact on Existing Erosion and Potential Bank Instability Study Report

Volume II – Main Report

Northfield Mountain Pumped Storage Project (No. 2485) and Turners Falls Hydroelectric Project (No. 1889)

Prepared for:

FirstLight Power Resources

Prepared by:

Simons & associates

Cardno Shaping the Future

Gomez and Sullivan Engineers

Kit Choi, PhD, PE

OCTOBER 2016

TABLE OF CONTENTS

LIST OF TABLES

LIST OF FIGURES

LIST OF ABBREVIATIONS

BST	borehole shear-test
BSTEM	Bank Stability and Toe Erosion Model
c	Effective cohesion
ca	Apparent cohesion
cfs	cubic feet per second
cm	centimeter
CO_2	Carbon dioxide
Corps, The	US Army Corps of Engineers
CT	State of Connecticut
CRREL	Cold Regions Research and Engineering Laboratory
CRSEC	Connecticut River Streambank Erosion Committee
CRWC	Connecticut River Watershed Council
D	root diameter, in mm
DBH	diameter at breast height
d_{50}	median particle diameter
ECP	Erosion Control Plan
FCD	Franklin Conservation District
FEMA	Federal Emergency Management Agency
FERC	Federal Energy Regulatory Commission
FirstLight	FirstLight Hydro Generating Company
FIS	Flood Insurance Study
FOV	Field of View concept
FRCOG	Franklin Regional Council of Governments
FRR	Full River Reconnaissance
Fs	Factor of Safety
ft	feet
g	gram
GB	gigabyte
GIS	Geographic Information System
GPS	Global Positioning System
Gomez and Sullivan	Gomez and Sullivan Engineers, DPC
HEC	Hydraulic Engineering Center
HEC-RAS	Hydraulic Engineering Center- River Analysis System
(HYDROs	Laser In-situ Scattering Transmissometry HYDRO unit
Hz	hertz
ILP	Integrated Licensing Process
in	Inch

ISO-NE	Independent System Operator New England
k	erodibility coefficient
kPa	kilopascal
LCCLC	Landowners and Concerned Citizens for License Compliance
LiDAR	Light Detection and Ranging
LISST	Laser In-situ Scattering Transmissometry
m	meter
MA	State of Massachusetts
MADEP	Massachusetts Department of Environmental Protection
MassGIS	Massachusetts Geographic Information Systems Center
mi	mile
mm	milimeter
MPa	Megapascals
MTWT	Monday Tuesday Wednesday Thursday
MWH	megawatt hours
N	Newton
NAD	North American Datum
ND	Non-Detect
NDT	Northrop, Devine, and Tarbell
NEE	New England Environmental
NFM	Northfield Mountain Pumped Storage Project
NGVD	National Geodetic Vertical Datum
NH	State of New Hampshire
NHDES	New Hampshire Department of Environmental Services
NH GRANIT	New Hampshire Geographically Referenced Analysis and Information Transfer System
NMFS	National Marine Fisheries Service
NRCS	Natural Resources Conservation Service
OHWM	Ordinary High Water Mark
PAD	Pre-Application Document
PSP	Proposed Study Plan
QA	Quality Assurance
RMS	Root mean squared
RSP	Revised Study Plan
RTK	Real Time Kinematics
s	second
S&A	Simons and Associates
SD1	Scoping Document

SD2	Scoping Document 2
SPDL	Study Plan Determination Letter
SSC	Suspended Sediment Concentration
StreamSide	Laser In-situ Scattering Transmissometry StreamSide unit.
τ_c	critical shear stress
TFI	Turners Falls Impoundment
T_r	Root tensile strength
TSV	Total Survey Variance
USACE	US Army Corps of Engineers
USDA-ARS	U.S. Department of Agriculture - Agricultural Research Service
USGS	U.S. Geological Survey
WLOG	Wave logger
VT	State of Vermont
VY	Vermont Yankee Nuclear Power Plant
y	year

1 INTRODUCTION

FirstLight Hydro Generating Company (FirstLight) is the current licensee of the Northfield Mountain Pumped Storage Project (FERC No. 2485) and the Turners Falls Hydroelectric Project (FERC No. 1889). FirstLight has initiated the process of relicensing the two Projects with the Federal Energy Regulatory Commission (FERC, the Commission) using FERC's Integrated Licensing Process (ILP). The current licenses for Northfield Mountain and Turners Falls Projects were issued on May 14, 1968 and May 5, 1980, respectively, with both set to expire on April 30, 2018.

As part of the ILP, FERC conducted a public scoping process during which various resource issues were identified. On October 31, 2012, FirstLight filed its Pre-Application Document (PAD) and Notice of Intent with FERC. The PAD included FirstLight's preliminary list of proposed studies. On December 21, 2012, FERC issued Scoping Document 1 (SD1) and preliminarily identified resource issues and concerns. On January 30 and 31, 2013, FERC held scoping meetings for the two Projects. FERC issued Scoping Document 2 (SD2) on April 15, 2013.

FirstLight filed its Proposed Study Plan (PSP) on April 15, 2013 and, per the Commission regulations, held a PSP meeting at the Northfield Visitors Center on May 14, 2013. Thereafter, FirstLight held ten resource-specific study plan meetings to allow for more detailed discussions on each PSP and on studies not being proposed. On June 28, 2013, FirstLight filed with the Commission an Updated PSP to reflect further changes to the PSP based on comments received at the meetings. On or before July 15, 2013, stakeholders filed written comments on the Updated PSP. FirstLight filed a Revised Study Plan (RSP) on August 14, 2013 with FERC addressing stakeholder comments. Included in the RSP was Study No. 3.1.2 *Northfield Mountain/Turners Falls Operations Impacts on Existing Erosion and Potential Bank Instability* (Study No. 3.1.2 or Causation Study). The methodology and scope for Study No. 3.1.2 were approved with modifications by the Commission in its September 13, 2013 Study Plan Determination Letter (SPDL) (FERC, 2013). Those modifications included:

- FirstLight should include analysis of operational changes through the period 1999 to 2013 to identify any correlation between operational changes and observed changes in erosion rates;
- FirstLight should perform its historic geomorphic assessment using available mapping such as 1970 vintage ground survey of the impoundment;
- FirstLight should consult with stakeholders on transect site selection, and;
- FirstLight should employ the RIPROOT module of BSTEM to describe the erodibility of soils and banks;

On August 27, 2013, Entergy Corp. announced that the Vermont Yankee Nuclear Power Plant (VY), located on the downstream end of the Vernon Impoundment on the Connecticut River and upstream of the two Projects, would be closing no later than December 29, 2014. With the closure of VY, it was anticipated that certain environmental baseline conditions would change during the relicensing study period. In their September 13, 2013 SPDL, FERC approved many of the studies or approved them with FERC modification; however, due to the impending closure of VY, FERC did not act on 19 proposed or requested studies pertaining to aquatic resources. The SPDL for these 19 studies was deferred until after FERC held a technical meeting with stakeholders on November 25, 2013 regarding any necessary adjustments to the proposed and requested study designs and/or schedules due to the impending VY closure. FERC issued its second SPDL on the remaining 19 studies on February 21, 2014, approving the RSP with certain modifications. In addition, due to VY's closure and the resulting potential for the increased presence of ice in the Turners Falls Impoundment (TFI) (because of the change in thermal regime with VY closing), FirstLight filed an addendum to the RSP for Study No. 3.1.2 on September 15, 2014 which detailed protocols for increased investigation of ice as a cause of erosion.

As stated in the RSP, the goals of Study No. 3.1.2 were to evaluate and identify the causes of erosion in the TFI and to determine to what extent they are related to Northfield Mountain and Turners Falls Project operations. In order to accomplish these goals the RSP (p. 3-25) included the following objectives:

- Conduct a thorough data gathering and literature review effort of existing relevant data to identify data gaps;
- Conduct field investigations and field data collection to fill data gaps. Gather the field data required to conduct detailed analyses of the causes of erosion and the forces that control them;
- Develop an understanding of the historic and modern geomorphology of the Connecticut River. A historic geomorphic assessment will be conducted to provide context for analyzing the modern geomorphology of the Connecticut River;
- Identify the causes of erosion present in the TFI, the forces associated with them, and their relative importance at a particular location. Conduct various data analyses to gain a better understanding of these causes and forces;
- Identify and establish fixed riverbank transects that will be representative of the range of riverbank features, characteristics, and conditions present in the TFI;
- Conduct detailed studies and analyses of erosion processes at the fixed riverbank transects;
- Evaluate the causes of erosion using field collected data and the results of the proposed data analyses. This evaluation will include quantifying and ranking all causes present at each fixed riverbank transect as well as in the TFI in general; and
- Develop a final report that will summarize the findings of this study and the methods used.

In order to achieve these objectives, the study methodology was divided into seven tasks:

- Task 1: Data Gathering and Literature Review;
- Task 2: Geomorphic Understanding of the Connecticut River;
- Task 3: Causes of Erosion;
- Task 4: Field Studies and Data Collection;
- Task 5: Data Analyses;
- Task 6: Evaluation of the Causes of Erosion; and
- Task 7: Report and Deliverables

In order to accomplish the goals and objectives of this study, FirstLight assembled a team of technical experts with global experience in the fields of geomorphology, hydrology and hydraulics, geotechnical engineering, water resources engineering, and environmental science. The team of experts included personnel from: Simons & Associates (S&A), Cardno, The National Center for Computational Hydroscience at the University of Mississippi, and Gomez and Sullivan Engineers, DPC (Gomez and Sullivan). Field support was also provided by New England Environmental (NEE). Key team members included:

- Robert Simons, PhD, PE (S&A, Fluvial Geomorphologist and Hydraulic Engineer);
- Andrew Simon, PhD (Cardno, Fluvial Geomorphologist);
- Yavuz Ozeren, PhD, PE (National Center for Computational Hydroscience and Engineering at the University of Mississippi, Research Scientist);
- Kit Choi, PhD, PE (Geotechnical Engineer);
- Jennifer Hammond (Cardno, Project Engineer);
- Nick Danis, PE (Cardno, Project Engineer);
- Timothy Sullivan, GISP (Gomez and Sullivan, Regulatory Specialist); and
- John Hart (Gomez and Sullivan, Water Resources Engineer)

Thomas Sullivan, PE and Mark Wamser, PE (Gomez and Sullivan, Water Resources Engineers) also provided technical support. The team of professionals were approved by the Massachusetts Department of Environmental Protection (MADEP) in advance of the study commencing. Key personnel listed above have decades of experience on complex river systems around the world. In addition, Andrew Simon, along with his colleagues at the U.S. Department of Agriculture - Agricultural Research Service (USDA-ARS), was the original developer of the Bank Stability and Toe Erosion Model (BSTEM) used as part of this study. Bios for each key team member can be found in Volume III (Appendix A).

In accordance with RSP Task 1, during development of the RSP, and continuing after issuance of FERC's September 2013 SPDL, FirstLight conducted an in-depth literature review and data gathering effort which provided the foundation for this study and allowed for the identification of potential data gaps. Based on the literature and datasets gathered FirstLight was able to conduct a qualitative historic geomorphic assessment of the Connecticut River and TFI (RSP Task 2). The results of the historic assessment provided important context to the study as well as a better understanding of the various hydrologic, hydraulic, geotechnical, and geomorphic dynamics at play in the study reach. Additionally, as part of the initial data gathering and review effort, as well as during development of the RSP, FirstLight developed a list of the potential causes of erosion which may be present in the TFI (RSP Task 3). The preliminary list of potential causes presented in the RSP included (in no particular order):

- Hydraulic shear stress due to flowing water;
- Water level fluctuations due to hydropower operations;
- Boat waves;
- Wind waves;
- Land management practices and anthropogenic influences to the riparian zone;
- Animals;
- Seepage and piping;
- Freeze-thaw; and
- Ice or debris

Based on past experience conducting geomorphic assessments on the Connecticut River and other alluvial rivers, as well as from information gleaned from the preliminary investigation of existing documents and the FRR, the preliminary list of potential causes of erosion was then reviewed and divided in the RSP (p. 3-44) into two categories: 1) potential primary causes of erosion, and 2) potential secondary causes of erosion. From this, the following classifications were developed:

Potential Primary Causes of Erosion

- Hydraulic shear stress due to flowing water
- Water level fluctuations due to hydropower operations
- Boat waves
- Land management practices and anthropogenic influences
- Ice[1]

Potential Secondary Causes of Erosion

- Animals
- Wind waves
- Seepage and piping
- Freeze-thaw

The causes of erosion listed above formed the basis for RSP Tasks 4 (Field Studies and Data Collection), 5 (Data Analyses), and 6 (Evaluation of the Causes of Erosion). While all of these potential causes of erosion were investigated, special emphasis was placed on the potential primary causes of erosion, as discussed in the RSP. The potential primary causes of erosion, and the forces associated with them, were evaluated at a number of fixed riverbank transects located throughout the geographic extent of the TFI.

In accordance with the requirements of the RSP and FERC's SPDL, the fixed riverbank transects where the potential primary causes of erosion were investigated (also referred to as detailed study sites) were selected in collaboration with stakeholders and were presented in the report titled *Study No. 3.1.2 Northfield Mountain/Turners Falls Operations Impact on Existing Erosion and Bank Instability – Selection of Detailed Study Sites – September 2014* (FirstLight, 2014b).[2] Discussion pertaining to the final number of sites and their locations is also included later in this report. Stakeholders consulted during development of the final set of detailed study sites included: the Connecticut River Streambank Erosion Committee (CRSEC), Connecticut River Watershed Council (CRWC), Franklin Regional Council of Governments (FRCOG), Landowners and Concerned Citizens for License Compliance (LCCLC), National Marine Fisheries Service (NMFS), Massachusetts Riverways, and the Franklin Conservation District (FCD) as well as the Massachusetts Department of Environmental Protection (MADEP) and FERC.

Once the final list of detailed study sites was determined, various field data collection efforts were carried out during 2014, with supplemental field work conducted in 2015 and 2016 (ice monitoring). Field activities were conducted in accordance with Task 4 of the RSP as well as the Addendum to the RSP filed with FERC in September 2014.[3] Field data collection efforts are discussed in greater detail in Section 4 of this report. Field data were post processed and prepared for analysis or inclusion in various models throughout late 2014 and into 2015. Following the completion of the various field studies and data collection efforts, as well as completion of all post processing and QA, the field collected data were analyzed and model runs were executed throughout 2015 and into 2016 in accordance with RSP Tasks 5 and 6.

[1] Ice was originally classified in the RSP as a potential secondary cause of erosion, however, due to the closure of VY and the potential for the increased presence of ice in the TFI, and in accordance with the 2014 Addendum to Study 3.1.2 required by the SPDL, it was elevated to a potential primary cause of erosion in 2014.
[2] The *Selection of Detailed Study Sites* report was filed with FERC as part of the *Relicensing Study 3.1.2 Initial Study Report Summary* on September 15, 2014.
[3] The addendum to the RSP, or Ice Addendum, was filed with FERC as part of the *Relicensing Study 3.1.2 – Initial Study Report Summary* on September 15, 2014

The data analyses conducted for this study consisted of a mix of qualitative and quantitative methods based on RSP Tasks 2, 5, and 6 as well as RSP Table 3.1.2-3. Overall, data analyses followed a three-level approach consisting of:

1. Qualitative geomorphic analysis;
2. Quantitative engineering and geomorphic analysis; and
3. Computer modeling

This approach ensures a proper understanding of the physical processes governing bank processes along the reach through the hydraulic action, transport of sediment, river form and response, interaction with infrastructure and/or biologic aspects of riverine morphology or habitat. The three-level approach allows for cumulatively supportive, scientifically justifiable results to be obtained. Each subsequent level of analysis builds on the understanding developed by the previous level. The results of the various analyses discussed in Section 5 were then used to determine the cause(s) of erosion at each detailed study site. These results were then extrapolated throughout the study area resulting in detailed maps identifying the cause, or causes, of erosion at each riverbank segment within the TFI.

Each of the previously mentioned tasks which were identified in the RSP are discussed in greater detail in the ensuing sections and appendices of this report. This includes discussion of: the Geomorphic History of the Connecticut River (Section 2); the Potential Causes of Erosion (Section 3); Field Studies and Data Collection (Section 4); Data Analyses and Evaluation of the Causes of Erosion (Section 5); and a Summary Evaluation of the Causes of Erosion in the TFI (Section 6).

2 GEOMORPHIC UNDERSTANDING OF THE CONNECTICUT RIVER

RSP Task 2 calls for FirstLight to develop a geomorphic understanding of the Connecticut River to fully understand the various processes at work in the TFI. The RSP calls for this task to entail summarizing the historic and modern geomorphology of the Connecticut River, providing background information on the dynamic nature of alluvial rivers, discussing general characteristics of the drainage basin, and comparing the present state of various reaches of the Connecticut River, and/or tributaries, within the TFI. The RSP also requires that analysis and discussion of the historic geomorphology of the Connecticut River be conducted through the review of historic aerial imagery, topographic maps, photographs, surveys, plans, and/or archival studies and literature. Furthermore, in its September 13, 2013 SPDL, FERC recommended that FirstLight perform its historic geomorphic assessment using available mapping such as the 1970 vintage ground survey of the TFI as a base map, comparing it against more recent aerial imagery and available survey data to analyze trends in bank position within the TFI. The goal of the historic assessment was to provide context when discussing the modern geomorphology of the river.

The Connecticut River, which has a very small portion of its drainage area in Quebec, flows in a southerly direction from the Connecticut Lakes in northern New Hampshire, through western Massachusetts and central Connecticut, and into Long Island Sound (Figure 2-1). The river forms the border between New Hampshire and Vermont prior to it entering western Massachusetts. On its journey through New England, the river is impounded by 15 dams, some of which are equipped with hydropower facilities. A few of these dams create impoundments large enough to seasonally re-regulate[4] river flows. The majority of hydropower dams are low-head facilities forming narrow impoundments that experience generally lower water velocities at low flows due to raised water levels and velocities that approach near free-flowing conditions at high flows.

The Connecticut River was once a lake (Lake Hitchcock), formed after the ice melted at the end of the most recent ice age. This history affects current geomorphology and sediments that are found along the bed and banks of the river and is important to understand. The numerous flat terraces found along the Connecticut River were once deposits of fine sediment that settled in the bed of Lake Hitchcock. With the exception of rare segments (such as the French King Gorge located in the TFI), the Connecticut River is an alluvial river. Alluvial rivers consist of banks and bed materials that the river itself transports, deposits, or erodes. As such, alluvial rivers, by definition, are dynamic; thus various riverbank segments along the length of the Connecticut River are eroding as a result of its alluvial nature.

The reach of river extending approximately 20 miles from the Turners Falls Dam in Montague, MA to the Vernon Dam in Vernon, VT is also known as the TFI (Figure 2-2). FirstLight owns and operates the Turners Falls Hydroelectric Project while TransCanada owns and operates the Vernon Hydroelectric Project. The Turners Falls Dam, or a dam of different vintage, has been present at its current location since approximately 1798. The Turners Falls Dam was raised approximately six feet in 1970 during construction of the Northfield Mountain Project to accommodate additional storage volume for the operation of the Project without any significant increase of river flow in the Connecticut River downstream of the dam.

While this study specifically focuses on the TFI, for context it is important to understand the history and geomorphology of the entire Connecticut River, particularly the role of Vernon Dam which forms the upstream boundary of the TFI when discussing the dynamics of the TFI. Riverbank erosion has been a long-standing concern along the Connecticut River due to the proximity of infrastructure, farmland, property, and other valuable resources within the river corridor. Varying degrees of erosion in both free-flowing and

[4] Dams having sufficient storage capacity to store water during periods of high flow thereby reducing flood peaks for release during the low flow season.

impounded reaches of the Connecticut River have been documented over time. To provide context and a better understanding of the dynamics of both the Connecticut River and TFI, this section includes the following discussions:

- Geomorphology of Alluvial Rivers (Section 2.1);
- Geomorphic history of the Connecticut River (Section 2.2);
- Analysis of historic datasets (Section 2.3);
- Geomorphic analysis of tributaries and upland erosion features (Section 2.4);
- Erosion comparison of the TFI and Connecticut River (Section 2.5); and
- Summary of the Geomorphology of the Connecticut River (Section 2.6)

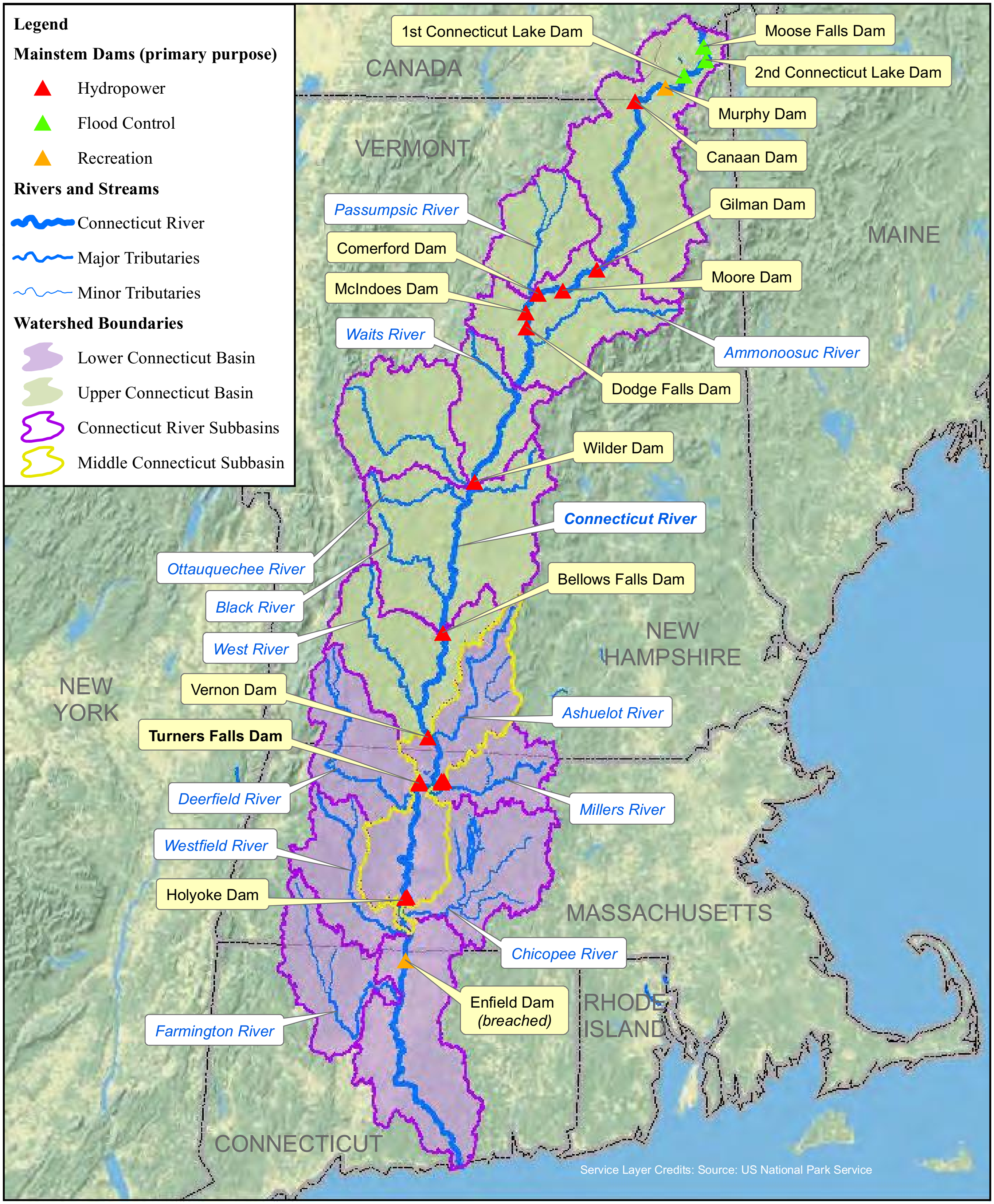

FIRSTLIGHT HYDRO GENERATING COMPANY
Northfield Mountain Pumped Storage Project No. 2485
Turners Falls Hydroelectric Project No. 1889

STUDY 3.1.2

Figure 2-1
Connecticut River Watershed

Path: W:\gis\studies\3_1_2\maps\final_report\figure_2-1.mxd

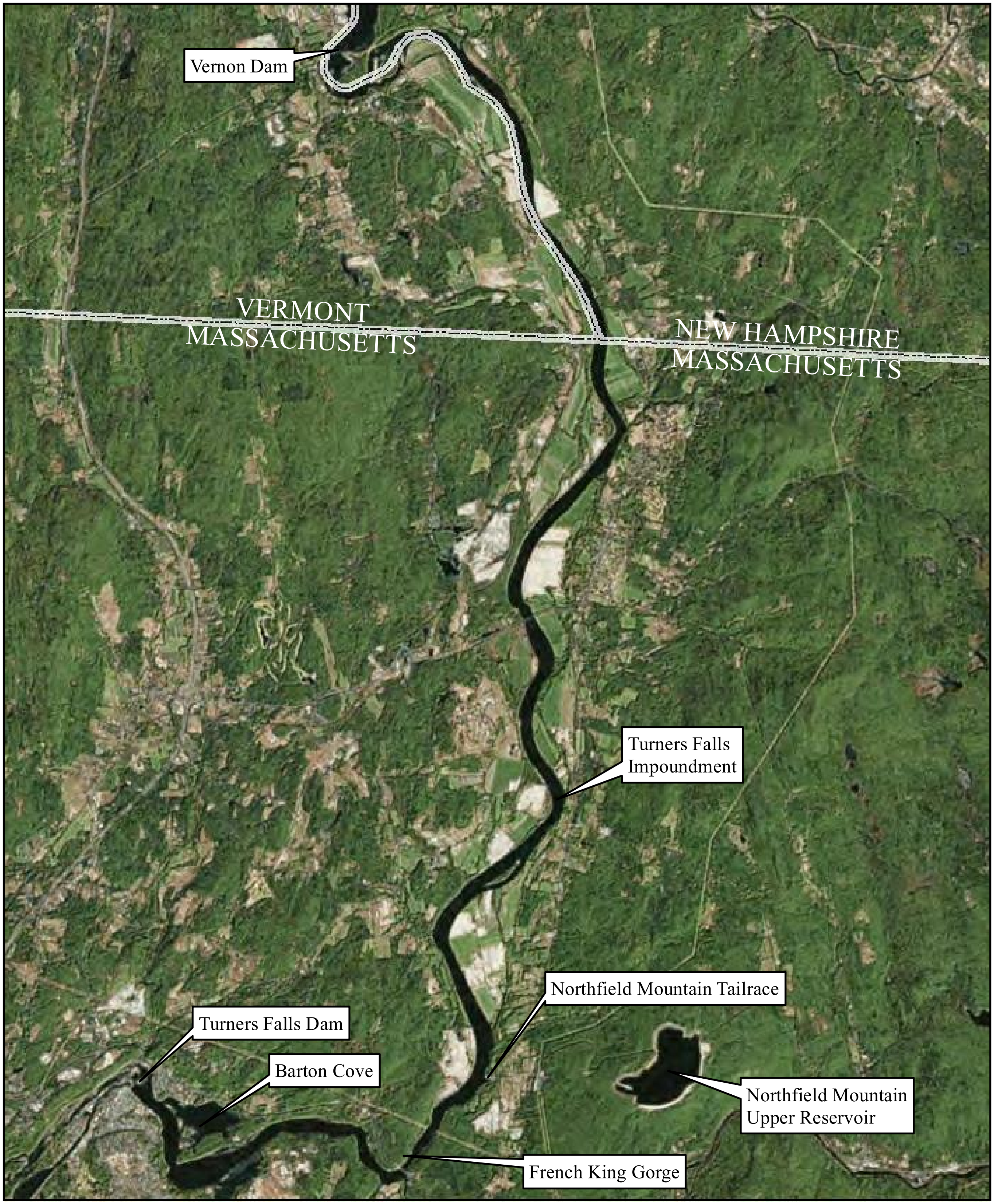

FIRSTLIGHT HYDRO GENERATING COMPANY
Northfield Mountain Pumped Storage Project No. 2485
Turners Falls Hydroelectric Project No. 1889

STUDY 3.1.2

N

0 0.75 1.5 3 Miles

Figure 2-2:
Turners Falls Impoundment

Service Layer Credits: Source: Esri, DigitalGlobe, GeoEye, Earthstar Geographics, CNES/Airbus DS, USDA, USGS, AEX, Getmapping, Aerogrid, IGN, IGP, swisstopo, and the GIS User Community

Path: W:\gis\studies\3_1_2\maps\final_report\figure_2-2.mxd

2.1 Geomorphology of Alluvial Rivers

The Connecticut River, with the exception of rare segments, is an alluvial river that was formed following the last ice age. Prior to developing a geomorphic understanding of the river it is important to first understand the nature and geomorphology of alluvial rivers in general. The dynamic nature of alluvial rivers is described in one of the foremost and well-known textbooks, Fluvial Processes in Geomorphology (Leopold *et al*., 1964). Leopold, *et al*. discussed the continual adjustment of river systems by processes of aggradation, degradation, scour, deposition, lateral migration and bank erosion. Even the concept of a river in equilibrium does not mean that a river, so classified, is static and un-changing.

As noted by Leopold, *et al*., the concept of equilibrium in an idealized channel is based on the premise that a natural channel operates in a balance between its ability to transport sediment and the sediment delivered to it from upstream. The former is based on hydraulic characteristics such as stream power or flow energy that determine sediment-transport competence (a measure of the largest size that can be transported) and sediment-transport capacity (the amount of sediment that can be transported for a given flow). This implies that an alluvial stream not only carries sediment but also may entrain and deposit sediment depending on hydraulic characteristics of the flow and the boundary characteristics (shape and resistance) of the channel. If an alluvial stream has excess stream power relative to its sediment load, it will entrain (erode) sediment from its boundary. If it is transporting more sediment than the capacity for a given flow, it will deposit sediment. Erosion may be vertical or lateral and erosion of one bank may be accompanied by deposition on the other side of the channel, maintaining, on average, a relatively constant channel cross-section. Equilibrium does not mean that no erosion occurs but rather that an equilibrium between erosion and deposition is achieved. Based on this concept of equilibrium, the form of the cross-section may not be constant over time and the position of the channel may change, albeit at slow rates. Thus, the processes of erosion and deposition can be characteristics of an alluvial stream in equilibrium so long as the changes do not represent large, systematic adjustments over time and space. Changing position, even while retaining overall average channel geometry, necessarily means riverbank erosion occurs even in such channels that are considered to be in equilibrium.

The concept of the dynamic nature of rivers is confirmed in The Fluvial System (Schumm, 1977), which notes that while it would be convenient if a river were unchanging, an alluvial river generally is changing its position as a consequence of hydraulic forces acting on its bed and banks. Schumm further noted that archaeological, botanical, geological, and geomorphic evidence supports the conclusion that most rivers are subject to constant changes as a normal part of their morphologic evolution (Schumm, 1977; Simon, 1989). These adjustments occur over a variety of temporal and spatial scales ranging from a reach where a single flood hydrograph where scour may occur on the rising limb and deposition may occur on the receding limb, to long periods of time representing the evolution of a channel system.

In summary, as noted by some of the most renowned fluvial geomorphologists, even those river reaches considered to be in "equilibrium" can be expected to move laterally and adjust through processes that include riverbank erosion. Erosion is a natural process, even in channels in equilibrium that cannot and should not be totally controlled.

Examples of natural river dynamics can be found by looking at rivers in the National Parks where no significant development or regulation of rivers for hydropower, agriculture, water supply, navigation, or recreational powerboat use is typically found. Figures 2.1-1 through 2.1-3 show the effect of natural channel dynamics resulting in riverbank erosion on the Yellowstone River in Yellowstone National Park and the Middle Fork of the Flathead River in Glacier National Park. Numerous other examples can be found at National Parks throughout the U.S. It is clear that rivers without significant development and commercial or boat use, and which are protected from such uses, are not exempt from natural geomorphic processes including riverbank erosion. In fact, these rivers can display significant, dynamic geomorphic processes resulting in riverbank erosion. Geomorphic processes include erosion, accretion, lateral migration, avulsion and shifting of meander bends. All of these natural processes occur in alluvial rivers of all types and sizes, regardless of whether they are found in completely natural settings without external influences or if they are affected by development and anthropogenic uses of various types.

Figure 2.1-1: Yellowstone River – Yellowstone National Park (a)

Figure 2.1-2: Yellowstone River – Yellowstone National Park (b)

Figure 2.1-3: Middle Fork of the Flathead River – Glacier National Park

2.2 Geomorphic History of the Connecticut River

The geomorphic history of the Connecticut River can be divided into two main periods, 1) the recent[5] geomorphic history, and 2) the modern geomorphology. The recent geomorphic history includes the major geomorphic events and processes which occurred approximately 20,000 years ago during and following the last ice age when the river was formed. The modern geomorphology encompasses the processes of the past several centuries when development began expanding throughout the watershed. Various geomorphic processes and events occurred during each of these time periods which continue to impact the Connecticut River watershed today. The geomorphic events and processes associated with these time periods are discussed in greater detail below.

2.2.1 Recent Geomorphic History of the Connecticut River

The Connecticut River has experienced significant changes over the last 20,000 years. During the most recent ice age (approximately 20,000 years ago), the Connecticut River valley was covered by the Laurentide Ice sheet. As the ice progressed to the south, it scraped and pushed rock and soil away from some areas and into mounds in other locations. Thus, the ice redistributed rock and soils throughout the area as well as compressing the underlying rock and soil. As the most recent ice age ended, the melting ice was trapped behind a natural dam which consisted of rock and soil that had been pushed up by the ice as it had advanced. The formation of a natural dam combined with the melting glacial water formed what is known as Lake Hitchcock (Figure 2.2.1-1).

Lake Hitchcock extended from about the middle of what is now the state of Connecticut (Rocky Hill, CT), through Massachusetts, northward through about 80% of Vermont and New Hampshire to St. Johnsbury, VT; a distance of about 200 miles ("Glacial Lake Hitchcock" by Tammy Marie Rittenour). The lateral margins of the lake were confined by the Green Mountains on the west and the White Mountains on the east. As the ice progressively melted northward, water in the lake rose over time creating a large pool of relatively quiescent water. The lake's water surface in the TFI area was likely more than 150 ft. higher than the current level of the Connecticut River; while the lake bottom was likely over 75 ft. higher (Field, 2007).

Glacial melt from the northern extent of the lake combined with inflow from various tributaries resulted in the transport of significant quantities of sediment. As this sediment reached the quieter downstream waters of the lake, velocities rapidly decreased along with sediment transport capacity. This resulted in sediment deposition along the bottom and sides of the lake. Coarser sediment would drop out first with progressively finer sediment making it somewhat further into the lake. Numerous deltas developed along the sides of the lake as well as a somewhat general deposit of finer materials along the bottom. As a result of these processes, the Connecticut River valley bottom is composed of a series of terraces stepping up from the river. As noted in Field, 2007, an example of these type of terrace surfaces is Moose Plain which is located in the vicinity of the TFI (Figure 2.2.1-2). While Moose Plain demonstrates the various terraces neatly along one transect, in most instances this is not the case.

Approximately 14,000 years ago the natural "dam" holding back Lake Hitchcock was broken and the lake began to drain ("Geologic History of the Connecticut River Valley near Greenfield, MA," Richard D. Little). The break was likely the result of instabilities in the natural dam combined with increasing pressure on the dam material. Once the lake began draining it likely eroded through the soil and loose rock until it reached more solid and less erodible rock below. The draining and downcutting of Lake Hitchcock formed what is now the Connecticut River. While some of the deposited lake sediment was probably eroded and transported downstream with the now flowing water, some of the relatively fine deposited sediment (clay, silt and sand) was left behind in the existing Connecticut River valley. Additional erosion and downcutting

[5] The term "recent" is being used in a long-term geomorphic context going back to the last ice age. This is considered recent compared to the numerous geologic ages that preceded this period of time over the life span of the earth.

occurred as the ground beneath the ice and water rebounded vertically from the decreasing load that no longer existed.

Through time the watershed became forested and "normal" riverine dynamic processes took over. As these previous and more dramatic changes faded into the past, geomorphic changes slowed and became less dramatic, however, typical alluvial river dynamics have and will continue. These dynamics are most pronounced in the previously deposited fine sediments that are erodible under normal riverine processes. The fine sediments (clay, silt, and sand) left behind by Lake Hitchcock are prevalent not only along the majority of the Connecticut River's banks but also throughout the TFI. As noted by Field (2007), most of the riverbank sediments in the TFI are naturally susceptible to erosion because, although they are fine grained, they do not contain much silt and clay which would impart additional resistance through cohesive strength into the materials. The sands and sandy loams are relatively erodible. Field (2007) further noted that natural stability is further compromised by past channel incision through older terrace and floodplain surfaces, leading to greater flow energy expended on the banks rather than having the ability to spread out across broad floodplains (Field, 2007).

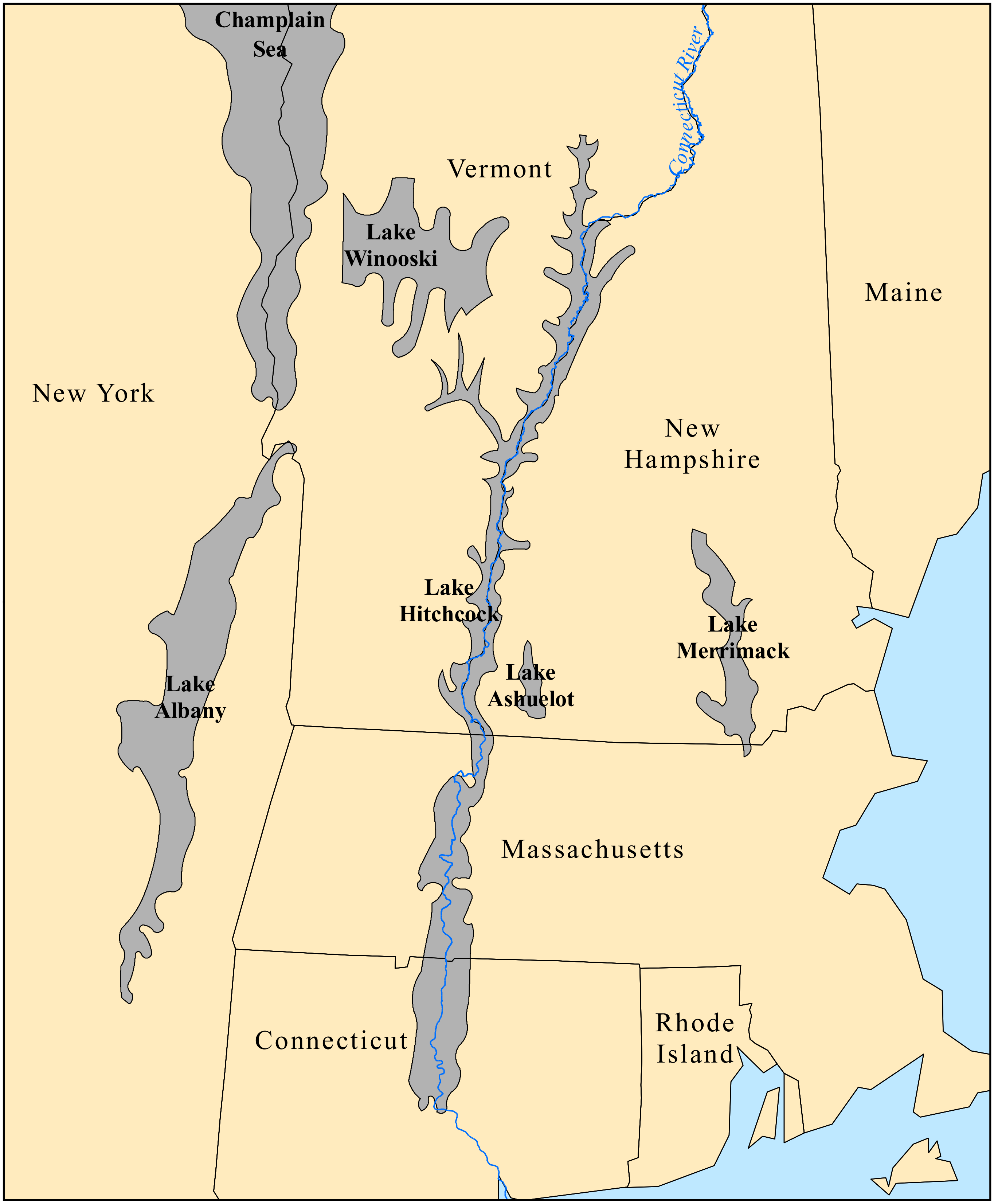

FIRSTLIGHT HYDRO GENERATING COMPANY
Northfield Mountain Pumped Storage Project No. 2485
Turners Falls Hydroelectric Project No. 1889

STUDY 3.1.2

Figure 2.2.1-1:
Lake Hitchcock

FirstLight Power Resources

Path: W:\gis\studies\3_1_2\maps\final_report\figure_2_2_1-1.mxd

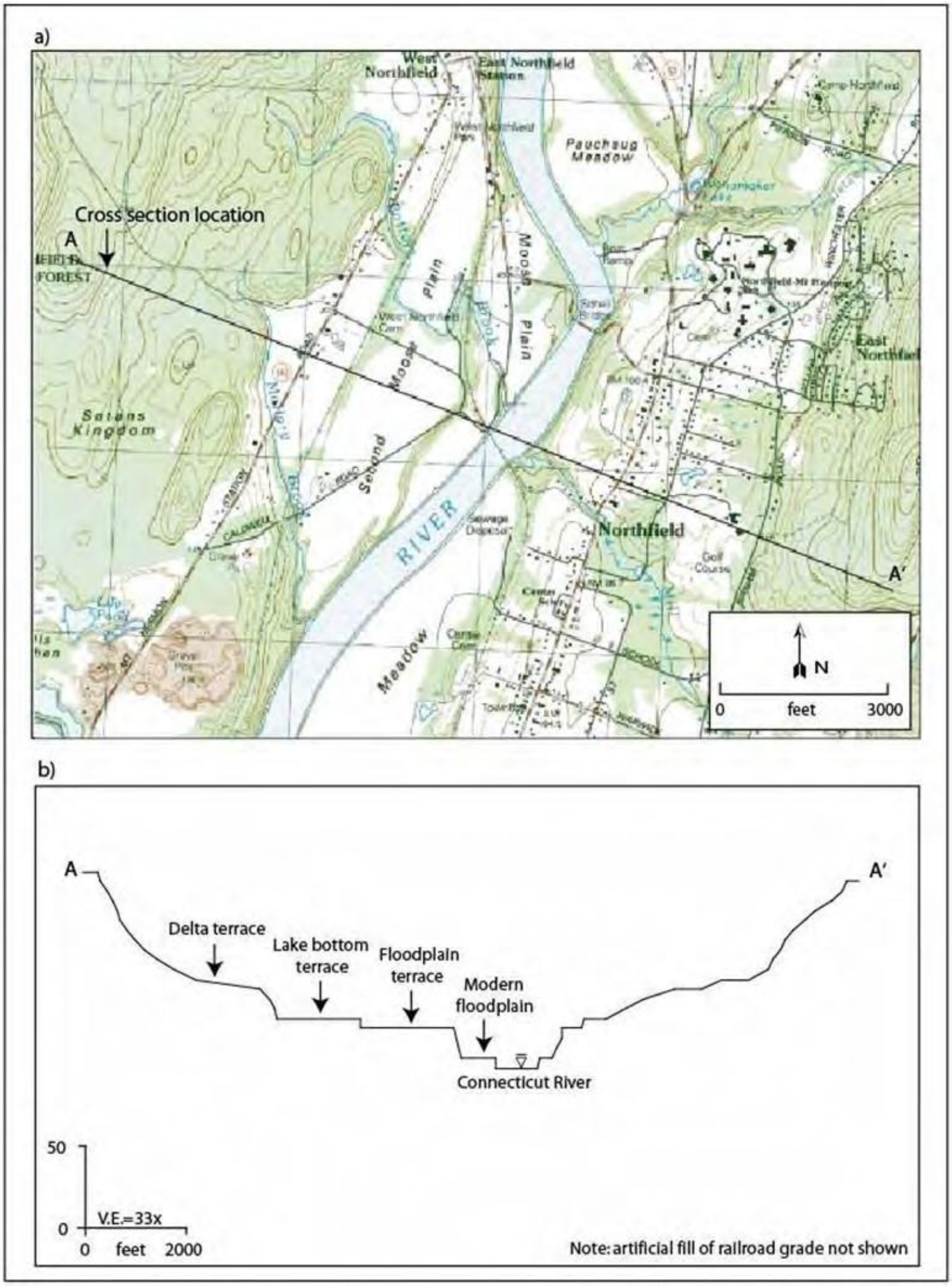

Figure 2.2.1-2: Moose Plain Terraces (Field, 2007)

2.2.2 Modern Geomorphology

In recent centuries, with the expansion of development in the region, the Connecticut River has been used as a means of transporting goods, water supply, waste disposal, recreation, and power generation. As part of this development, several dams were constructed on the Connecticut River for the primary purpose of hydropower production. Table 2.2.2-1 provides a list of the dams located on the Connecticut River. Most of these dams, with the exception of Murphy, Moore and Comerford Dams, are less than 60 feet in height and form relatively narrow, shallow impoundments upstream of the structures. The mainstem dams, and all dams in general, typically reduce the river velocity and trap sediment, the magnitude of which depends on the sediment transport capacity through the impoundment compared to the upstream sediment supply which determines the sediment trapping efficiency.

In addition to the mainstem dams, several United States Army Corps of Engineers (Corps or USACE) flood control dams have been constructed on larger tributaries to the Connecticut River. These facilities were constructed to reduce flood damages that had occurred historically (e.g., damages from the 1936 flood) by reducing peak flows to the Connecticut River and therefore reducing potential flood related damages. Since their construction, the flood control dams have generally been successful in reducing the historic impacts of flood events throughout the Connecticut River watershed, including reducing (but not eliminating) the erosive effects of peak flow events on riverbanks.

The modern geomorphology of the Connecticut River is typical of an alluvial river and is consistent with that described in Section 2.1. As expected of any alluvial river, the Connecticut River has continued to adjust over time through processes of aggradation, degradation, scour, deposition, lateral migration, and bank erosion. Episodic sediment deposition events have been known to occur in the river, such as was observed following Tropical Storm Irene in August 2011. Some sediment deposition also occurs as a result of the spring freshet or other similar high flow events. After such events, while some sediment remains, the river typically erodes some of this deposited material. Since the deposited sediment typically consists of suspended sediment which is fine material (clay, silt and sand), the Connecticut River has the ability to occasionally erode and transport some of this deposited sediment provided by upstream sources or tributaries, such that the overall trend of the river may appear to be more of erosion than deposition. The dynamic nature of the Connecticut River is evident by the fact that riverbank erosion occurs to one degree or another throughout its length in both free-flowing and impounded reaches. While there has been a very long-term tendency towards erosion along the river as the river incised through old lake deposits, it has essentially reached a state of dynamic equilibrium with base level controlled by areas of bedrock or armoring as well as dams along the mainstem.

Over the last several decades numerous studies have been conducted examining riverbank dynamics throughout the Connecticut River watershed as well as the TFI. These studies have ranged from historic analyses and comparisons and geomorphic assessments to hydraulic modeling and riverbank erosion surveys. To understand the modern geomorphology of the Connecticut River and TFI, several of these studies were reviewed and additional analyses were conducted when developing this report. The findings of these analyses are discussed in greater detail throughout the following sections of this report.

Table 2.2.2-1: Connecticut River Dams

Connecticut River Dam *(Upstream to Downstream)*	**Height (ft)**
Moose Falls Flowage	10
Second Connecticut Lake Dam	28
First Connecticut Lake Dam	56
Murphy Dam (Lake Francis)	106
Canaan Dam	27
Lyman Falls Dam	Breached
Wyoming Dam	Breached
Gilman Dam	40
Moore Dam	178
Comerford Dam	170
McIndoe Falls Dam	25
Dodge Falls Dam	28
Wilder Dam	39
Bellows Falls Dam	57
Vernon Dam	60
Turners Falls Dam	35
Holyoke Dam	30
Enfield Dam	Breached

2.3 Analysis of historic datasets

The geomorphic condition of the Connecticut River in general, and TFI specifically, can be further understood by examining available historic maps, aerial photographs, and surveys. Aerial photographs covering the TFI are available over a period of time extending from 1929 to 2014. These photographs provide an important historic perspective over this 80+ year period. Included in this time period were photographs taken along the TFI before and after the construction of the Northfield Mountain Project and associated raising of the Turners Falls Dam.[6] In addition to aerial photographs, historic maps going back over 100 years up through recent LiDAR (Light Detection and Ranging) mapping provide insight as to the recent and existing geomorphology of this section of the river.

Discussion, evaluation, and analysis of these sources of information is presented throughout this section. The purpose of this qualitative assessment is to provide context and important insight as to the condition of the Connecticut River and TFI historically and over recent decades. As such, this section includes the following discussions:

- Historic aerial photographs and maps – limitations (Section 2.3.1)
- Analysis of historic datasets – Connecticut River (Section 2.3.2)
- Analysis of historic datasets – Turners Falls Impoundment (Section 2.3.3)
- Analysis of the 20 erosion sites identified in the Erosion Control Plan (Section 2.3.4)

2.3.1 Historic aerial photographs and maps – limitations

While historic datasets such as aerial photographs and maps provide important historic context, valuable insights, and a better understanding of the geomorphic processes which have occurred over time, there are several significant limitations to comparing historic aerial photographs and maps to present ortho-photos which should be noted.

When mapping or taking aerial photographs over relatively large areas, it is recognized that the surface of the earth is curved while maps are a flat or plane representation of a curved surface. In addition, aerial photographs are taken from the lens of a camera that is vertically above one point on the ground or one small area of each of the photographs that are taken. As such, distortions are often present in the areas of the photograph that are taken farther away from that area that is directly below the camera. This is particularly true around the edges of the photograph depending on any tilt or angle of the line of view of the camera compared to vertical.

A georeferencing process is often utilized to adjust for some of these potential distortions and to bring all sources of information into a common datum. It is well understood that georeferencing or overlaying one mapping dataset onto another can be fraught with issues if not managed properly. One needs to understand how the datasets were compiled, what the resulting accuracies were and what the intended goal of the mapping was to successfully combine them and understand the limitations of the process. Even then the georeferencing process is subject to its own set of errors and accuracy limitations. Historic maps and aerial photographs are often georeferenced to survey data and common features found on more recent ortho-photos.

By their definition, ortho-photos have been reduced to a flat surface, provide a uniform map scale throughout their extent for a given accuracy, and provide a current, truly visual map source over a large

[6] Construction of the Northfield Mountain Project, including raising the Turners Falls Dam, occurred in the late 1960's and early 1970's. Commercial operation of the Northfield Mountain Project began in 1972.

extent. Ortho-photos used for this study typically had an accuracy of 6-10 feet (2-3 meters referenced in the source). When the overlaid dataset also happens to be reduced to a flat surface one can typically find a suitable translation, rotation and scale factor to overlay the mapping. Historic aerial photographs are often more problematic in that it is typically unclear as to how they were generated. Unlike the 2009 or 2014 State of Massachusetts Geographic Information Systems Center (MassGIS) ortho-photos, historic aerials have more than likely not had any rectification performed to correct distortions caused by camera orientation or terrain relief. The transformation of a simple aerial photograph is not as predictable and can be greatly assisted by other factors that confirm the transformation. In the case of the Connecticut River over the last 40 years, several large rock/boulder/bedrock shorelines exist where minimal movement is expected and therefore can be used to confirm the transformation. The results of georeferencing efforts conducted by FirstLight as part of this study typically yielded root-mean-squared (RMS) values less than +/-15 ft.

Other factors to consider when comparing datasets from different vintages is that the top of the riverbank may or may not be well defined and may be difficult to discern from aerial or ortho-photos. At some locations, the top of bank may be a flat terrace whereas the riverbank is steeply sloping so there is an abrupt break in topography. At other locations, a riverbank may just be part of a hillslope that continues sloping upwards, well beyond any limit of high water without any break in topography. In addition, many riverbank areas are densely vegetated so both visibility and topographic accuracy is limited. As a result, determining the historic location of the river often focuses on identifying the edge of the river/water interface.

Although determining the historic position of the river by identifying the edge-of-water is easier than identifying the top of bank, it is not without its own accuracy limitations. Without knowing the specific time and date when each image is taken, the water levels and river conditions are often unknown. Due to varying water levels the question arises as to whether any measured change in river position is due to an actual change in the bank or simply due to the difference in water level. Water levels may change from day to day or even hour to hour while the aerial photographs are being taken; thus, water level conditions may not be consistent within a single set of images. Furthermore, when comparing aerial photographs or edge-of-water datasets from before and after the Turners Falls Dam was raised in 1970, the approximately 6 foot rise in TFI water level would have to be accounted for. Given this, comparing edge-of-water locations from year to year or decade to decade would likely not yield useful or accurate results.

Due to these considerations, if observed changes in river position are within the accuracy limits of the dataset quantitative determinations are not meaningful. To determine if significant changes in riverbank position have actually occurred, the observed change (whether real or perceived) must be of a significant magnitude greater than the accuracy limits of the data. Given that the accuracy limits of the data can be 30 to 40 feet or more depending on their quality, it is often only appropriate to conduct qualitative geomorphic comparison's using historic aerial photographs or maps to provide context or to determine general trends.

As a result of the limitations discussed above, the analysis of historic aerial photographs and maps discussed throughout this report will be limited to a qualitative assessment focused on general geomorphic trends and observations throughout the Connecticut River watershed and TFI. The results of this qualitative assessment provide context in regard to the modern geomorphology of the study area.

2.3.2 Analysis of historic datasets – Connecticut River

In *"Riverbank Erosion on the Connecticut River at Gill, Massachusetts: its Causes and its Timing"* (Reid, 1990) historic maps and datasets from the late 1800's and early to mid-1900's were analyzed to determine geomorphic changes over time. Specifically, this analysis compared historic maps and aerial photographs at several locations along the river.

In the vicinity of Northampton, MA an 1831 map was compared to a 1958 aerial photograph which demonstrated the growth of Elwell Island and a "large amount of retreat of the Hadley (east) bank" (Figure

2.3.2-1) (Reid, 1990). Changes in the bank line were on the order of several hundred feet based on visual comparisons with the overall river width. Comparisons were also made using maps that were surveyed in 1887, 1936, and 1977 (Figure 2.3.2-2). The results of these comparisons showed that the riverbank in the vicinity of Otter Run in the TFI (a tributary to the river in the vicinity of Kidds Island) had retreated some 400 feet between 1887 and 1977. Finally, a comparison of an 1880 map to a 1977 map showed significant erosion progressing over time in a zone of "active erosion" (near the town of Northfield) as well as other locations where the river had moved approximately one river width or on the order of several hundred feet (Figure 2.3.2-3).

Northrop, Devine, and Tarbell (NDT) also examined the possibility of comparing historic maps to evaluate changes in the position of the river over time (NDT, 1991). As part of this effort NDT reviewed work conducted by Reid (1990) and accuracy information from the U.S. Geological Survey (USGS). Several hundred feet of changes in riverbank position were observed at various locations by both NDT and Reid prior to 1944; however, significant changes (beyond the accuracy limits of the datasets) were not observed in the decades since the 1940's. Both Reid and NDT documented much smaller amounts of change in the more recent decades. The observed relatively small changes in recent decades have been confirmed by annual transect surveys at various locations throughout the TFI which have occurred since the 1990's.

As discussed in the previous section, in reviewing the results of these historic comparisons one must take into account the various accuracy limitations of using such old datasets of varying quality. While definitive conclusions or quantitative estimates cannot be drawn from these comparisons, they are still relevant to the analysis. As such, it is clear that significant erosion occurred at various locations along the Connecticut River over time and prior to the 1940's. While erosion continued throughout the watershed following the 1940's it appears to have been reduced to much lower rates, as is discussed in later sections of this report.

When reviewing the historic geomorphology of the Connecticut River, three primary factors are identified as causing the reduction in erosion rates after the 1940's, including: (1) the relative lack of floods in recent decades of the magnitude of those which occurred prior to the 1940's which resulted in substantial erosion and damage (including the flood of 1936); (2) construction of flood control projects throughout the Connecticut River watershed following the flood of 1936; and (3) construction or raising of mainstem Connecticut River dams which reduced river velocities and shear stresses. Each of these potential factors is discussed in more detail below.

The devastating flood of 1936 caused significant damage, erosion, and channel changes to occur throughout New England and, more specifically, the Connecticut River watershed. During a two week period in March of 1936 New England was impacted by a combination of rainfall and snowmelt that totaled over 10 inches. The rainfall and snowmelt, combined with ice jams at certain locations in the river, resulted in the most severe flooding that has ever occurred. The flood of 1936 continues to be the flood of record and also resulted in new flow records from Hartford, CT all the way up to northern New Hampshire which still stand today (Grover, 1937).

Specific to the TFI, the flood of 1936 caused significant erosion and channel change at several locations. As noted in Field (2007), the flood of 1936 spread across the floodplain with enough force that a new channel 20 ft. deep across was cut across Moose Plain and around Schell Bridge. Similar avulsion channels were also observed immediately north of Munns Ferry, across Bennett Meadow near the Rt. 10 Bridge, and on Pine Meadow downstream of Kidds Island; however, only the channel north of Munns Ferry is believed to have formed as a result of the 1936 flood, the others may have been the result of earlier floods (Field, 2007).

Examples of erosion and channel change that occurred during the 1936 flood can be seen by comparing the 1929 to 1939 aerial photographs. As described by Field (2007), an avulsion channel formed behind the Schell Bridge as a result of the flood. Access to this new channel would later be blocked with riprap placed by government works projects in an effort to close the avulsion and maintain the existing channel. Even decades after the 1936 flood, remnants of the avulsion channel can be seen (Figures 2.3.2-4 – 2.3.2-7) (Field, 2007). Another example of erosion and change resulting from the 1936 flood can be seen by comparing 1929 to 1939 photographs in the vicinity of Stebbins Island down to the confluence with the Ashuelot River (Figures 2.3.2-8 – 2.3.2-9).

In addition to the flood of 1936 there were numerous other historic floods which have been noted, including: 1763, 1854, 1857, 1862, 1869, and 1870 (Hemenway, 1891) as well as 1639 (Kinnison *et al.*, 1938), 1896 (Bain, no date), 1866 (Scott, 2005) and 1824. The 1824 flood was noted to have "washed out the South Hadley Dam, Turners Falls Dam, and the small dam built below the confluence of the Millers River (Pressey, 1910)." Floods of these magnitudes have not occurred since the late 1930's.

As a result of the severe damage associated with the 1936 flood, a series of flood control projects were constructed in the Connecticut River watershed by the USACE. Examination of instantaneous water year flood peaks at the Montague USGS gage show that peak flows have declined in recent decades (Figure 2.3.2-10). While some of this decline in peak flows could be due to natural long-term hydrologic cycles, a significant part of the decline may be attributed to the success of the numerous flood control projects in the watershed. In addition to showing the instantaneous water year peak flow from 1904-2014, Figure 2.3.2-10 also depicts the average peak flow for four time periods as a means of comparison; these time periods include:

- 1904-2014 (representing the entire period of record other than 2015);
- 1904-1960 (pre-flood control through flood control development);
- 1961-2014 (post-flood control period); and
- 2000-2014 (Study 3.1.2 investigation period)

Finally, as mainstem dams were constructed or raised at various locations along the river, the velocities and shear stresses decreased. In a report entitled "Connecticut River Streambank Erosion Study Massachusetts, New Hampshire and Vermont," US Army Corps of Engineers (USACE, 1979), the effect of dams along the mainstem of the river was explained as follows, *"Dams deepened the water and slowed velocities such that bank erosion due to the flowing water was reduced."*

The 1979 study also compared reaches of the river not affected by the dams to those where dams formed narrow pools. An analysis of forces was conducted from a theoretical perspective. Based on this analysis the report found that theoretically the natural river is roughly 1.34 times more susceptible to major bank erosion than impoundments created by dams (USACE, 1979). The Corps then compared the number of erosion sites per mile for the natural segments of the river compared to those impounded by hydropower dams. The results of this analysis found that the number of erosion sites per mile for the natural river was 0.92 while for impounded areas it was 0.68 indicating that the natural river is 1.35 times more susceptible to bank erosion than impoundments (USACE, 1979). The Corps went on to conclude in its report that the presence of impoundments reduces bank erosion on the order of 34% compared to the natural river (USACE, 1979).

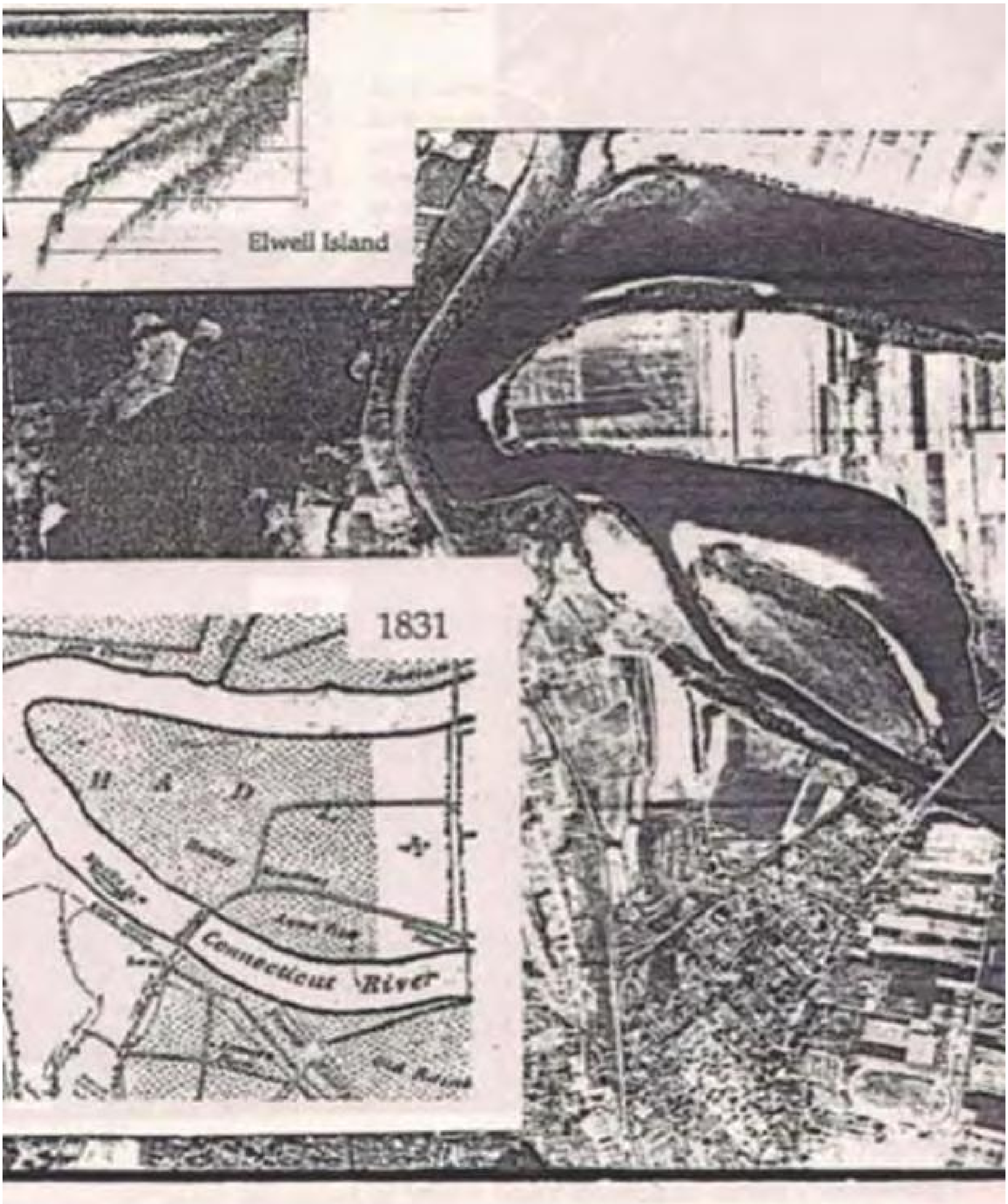

Figure 2.3.2-1 Riverbank Comparison 1831 to 1958 (Reid, 1990)

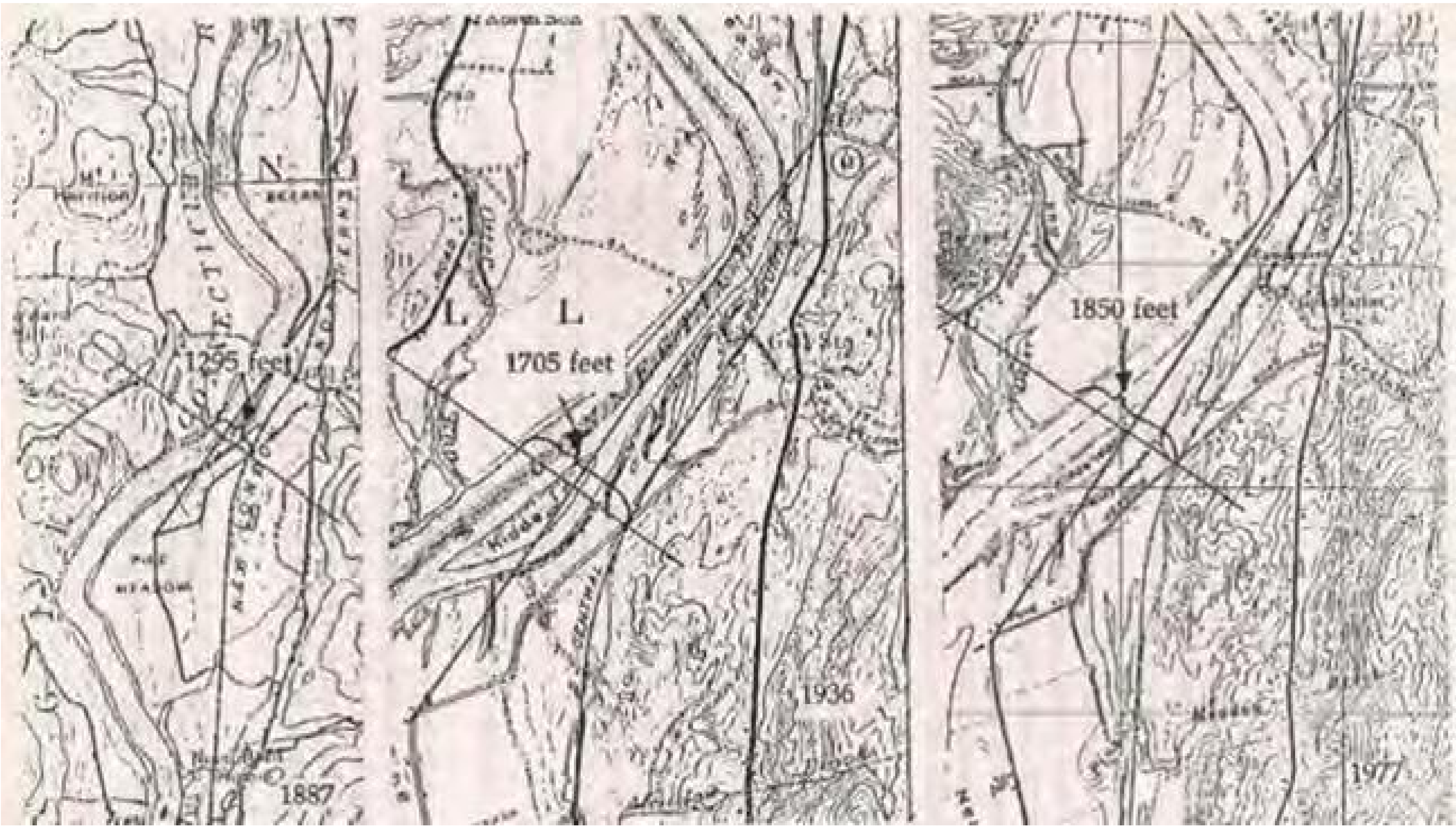

Figure 2.3.2-2 Riverbank Comparison 1887, 1936, and 1977 (Reid, 1990)

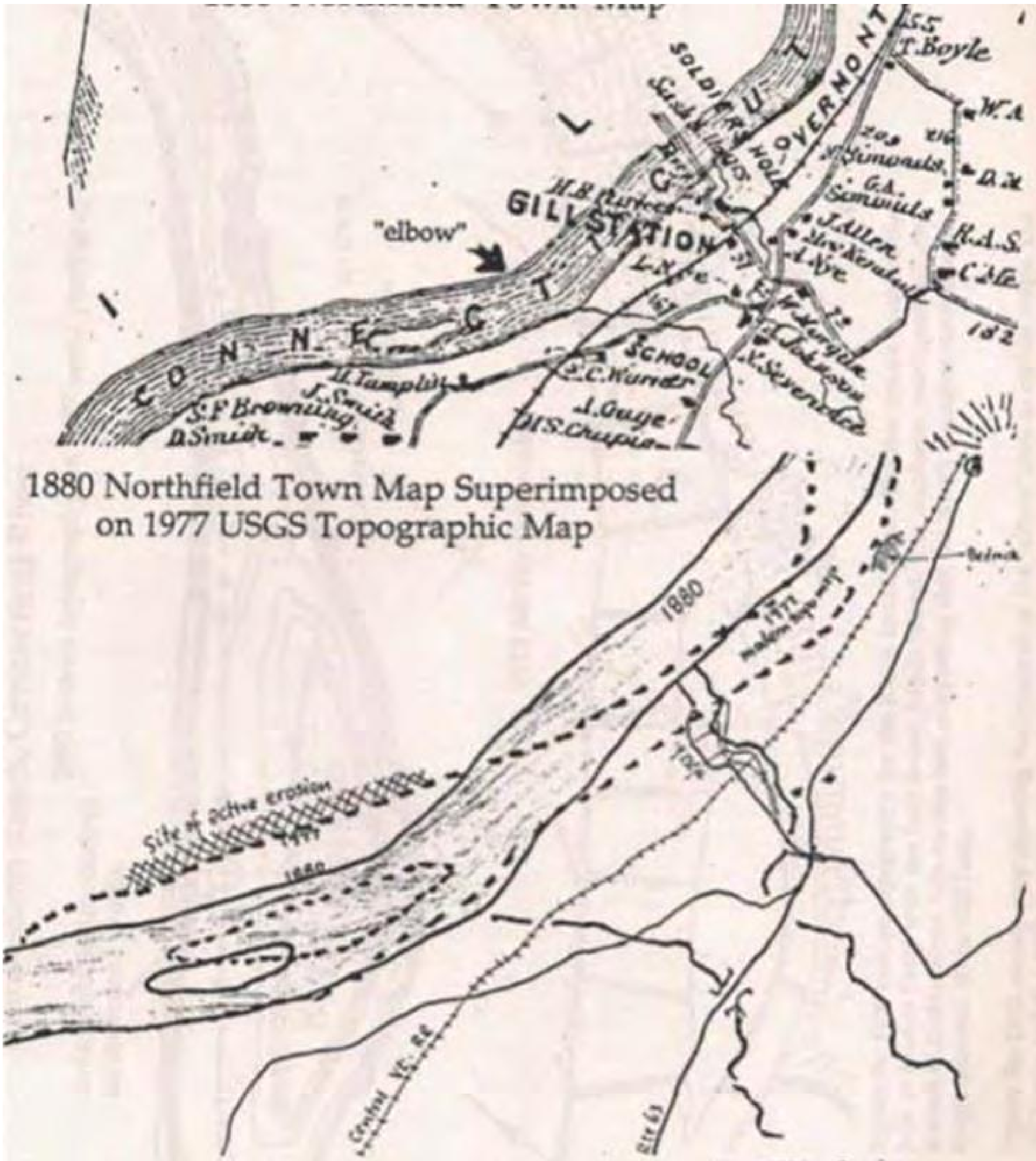

Figure 2.3.2-3 Riverbank Comparison 1880 to 1977 (Reid, 1990)

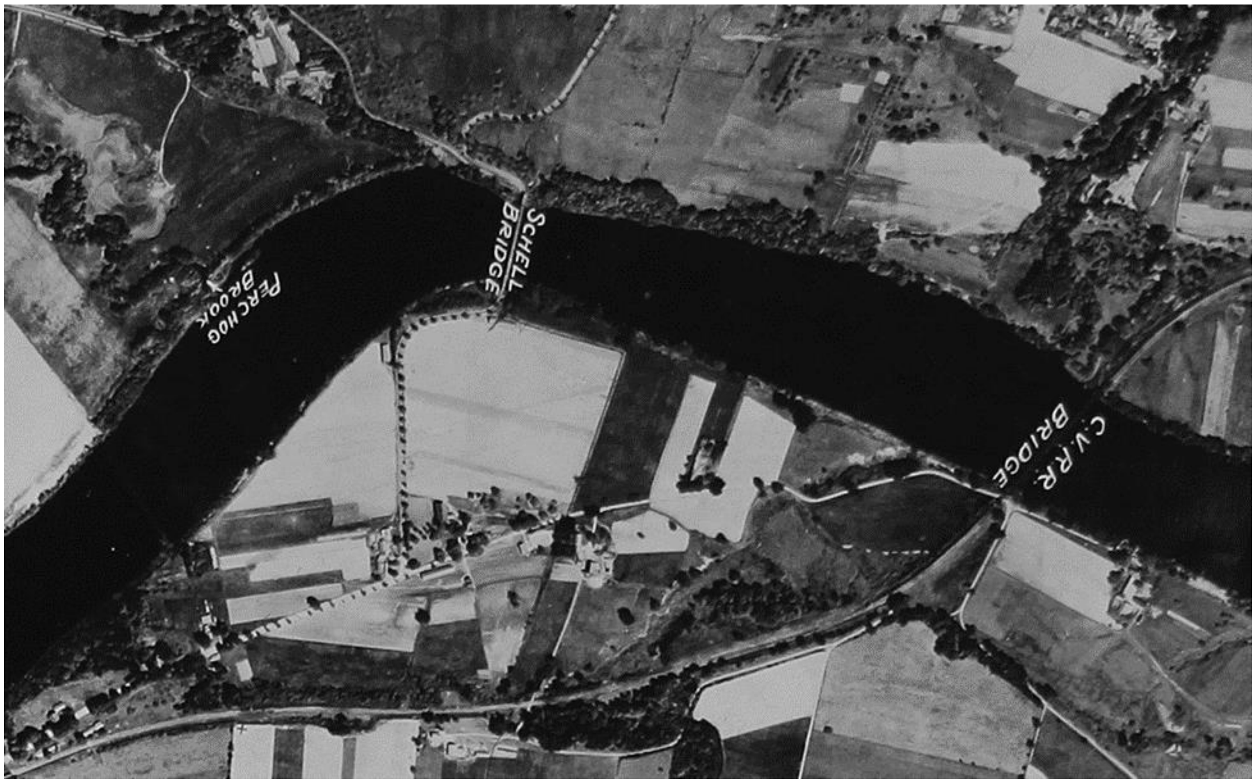

Figure 2.3.2-4 Connecticut River in the vicinity of Schell Bridge, 1929 (a)

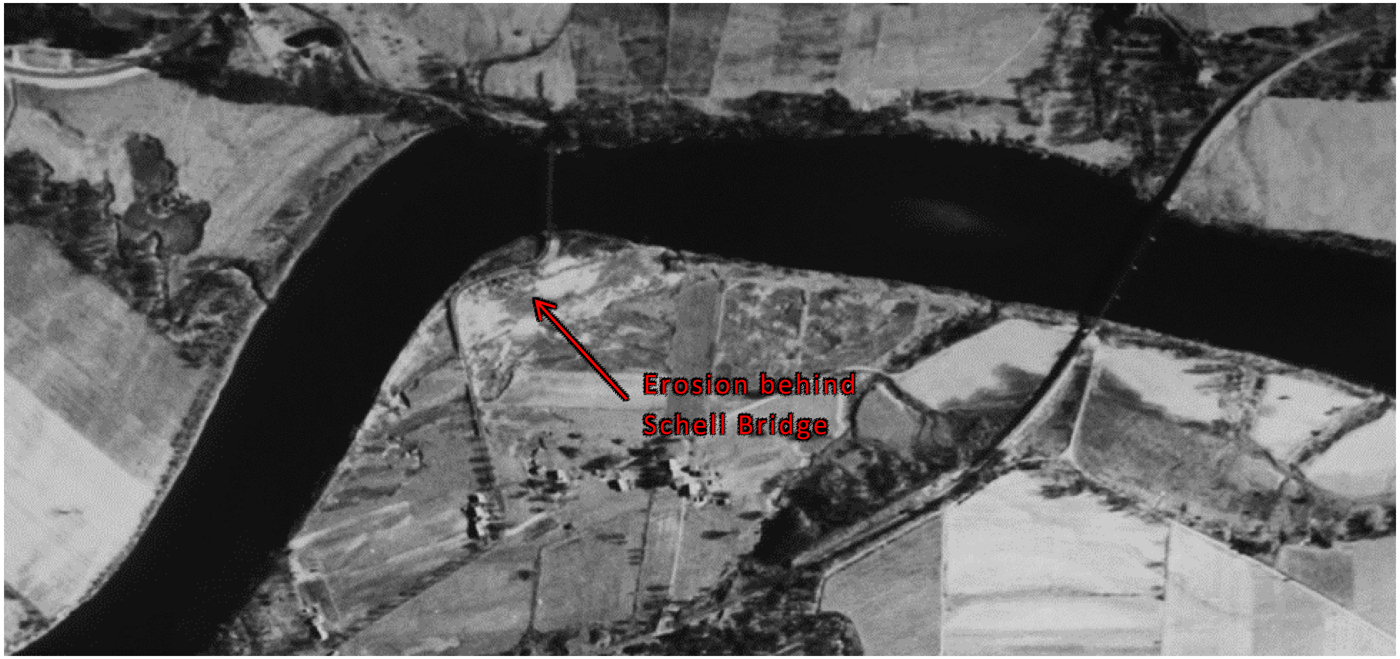

Figure 2.3.2-5 Connecticut River in the vicinity of Schell Bridge, 1939 (b)

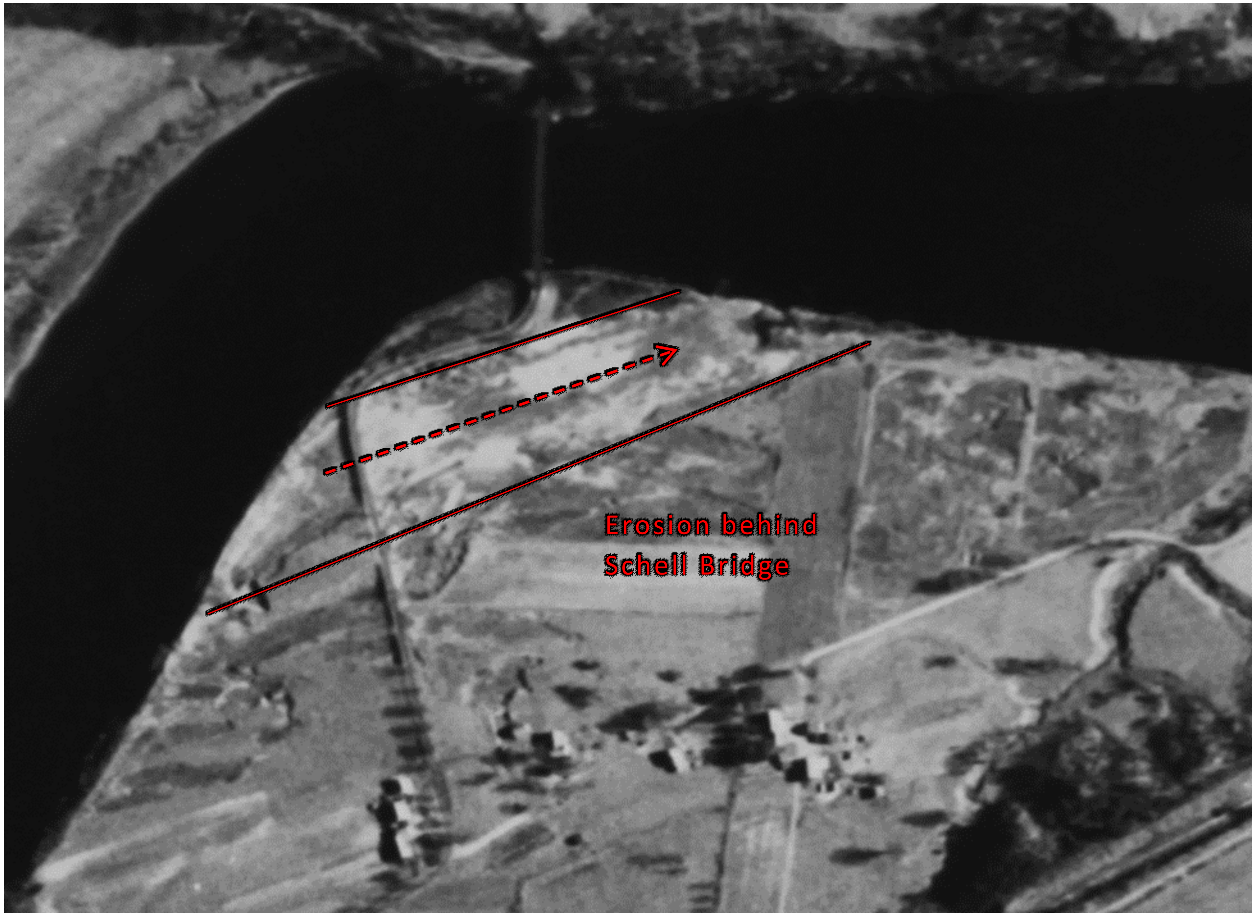

Figure 2.3.2-6 Erosion behind Schell Bridge, 1939 (c)

Figure 2.3.2-7 Abandoned avulsion channel behind Schell Bridge (d) (Field, 2007)

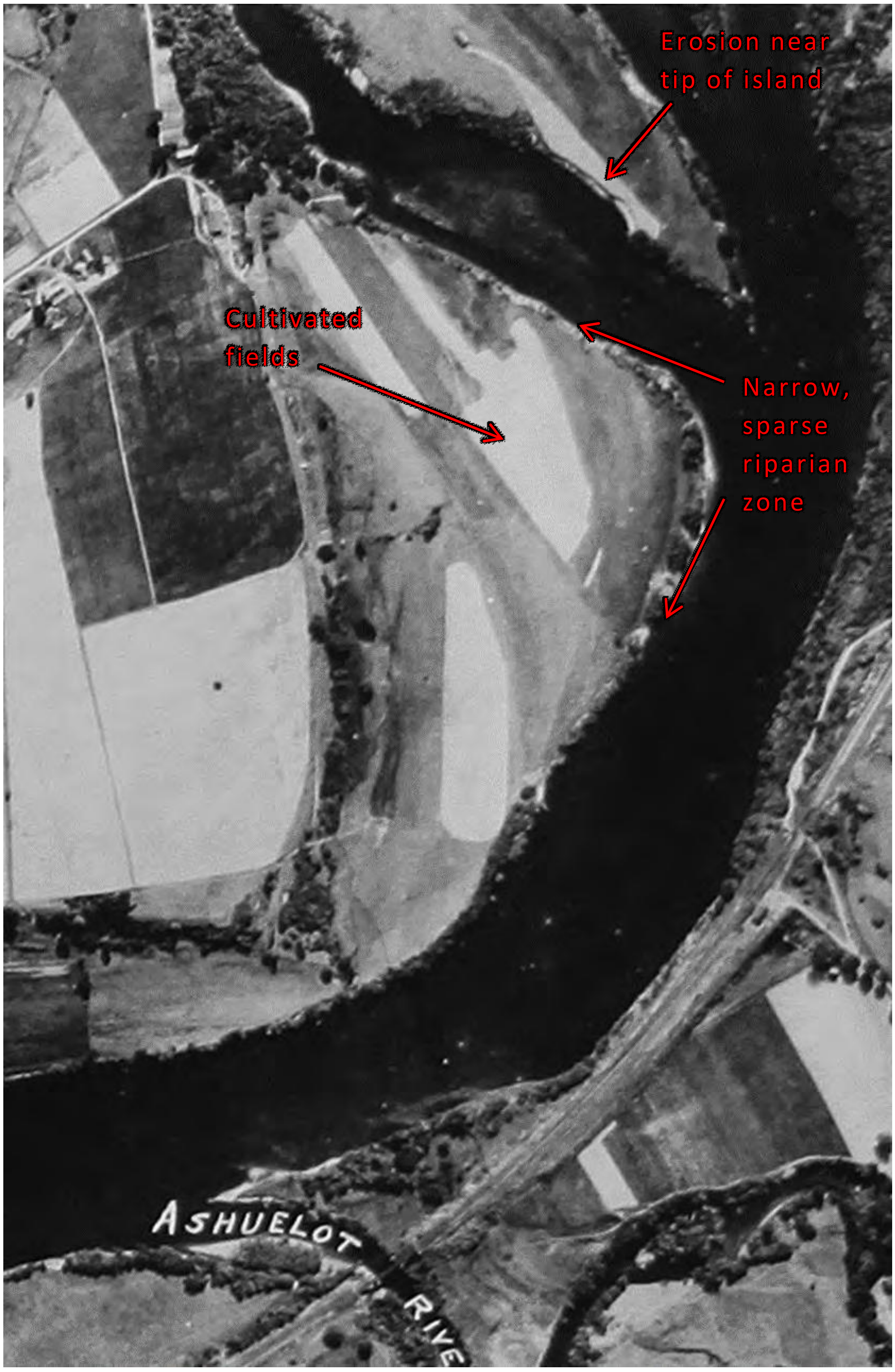

Figure 2.3.2-8 Stebbins Island – Ashuelot River, 1929 (a)

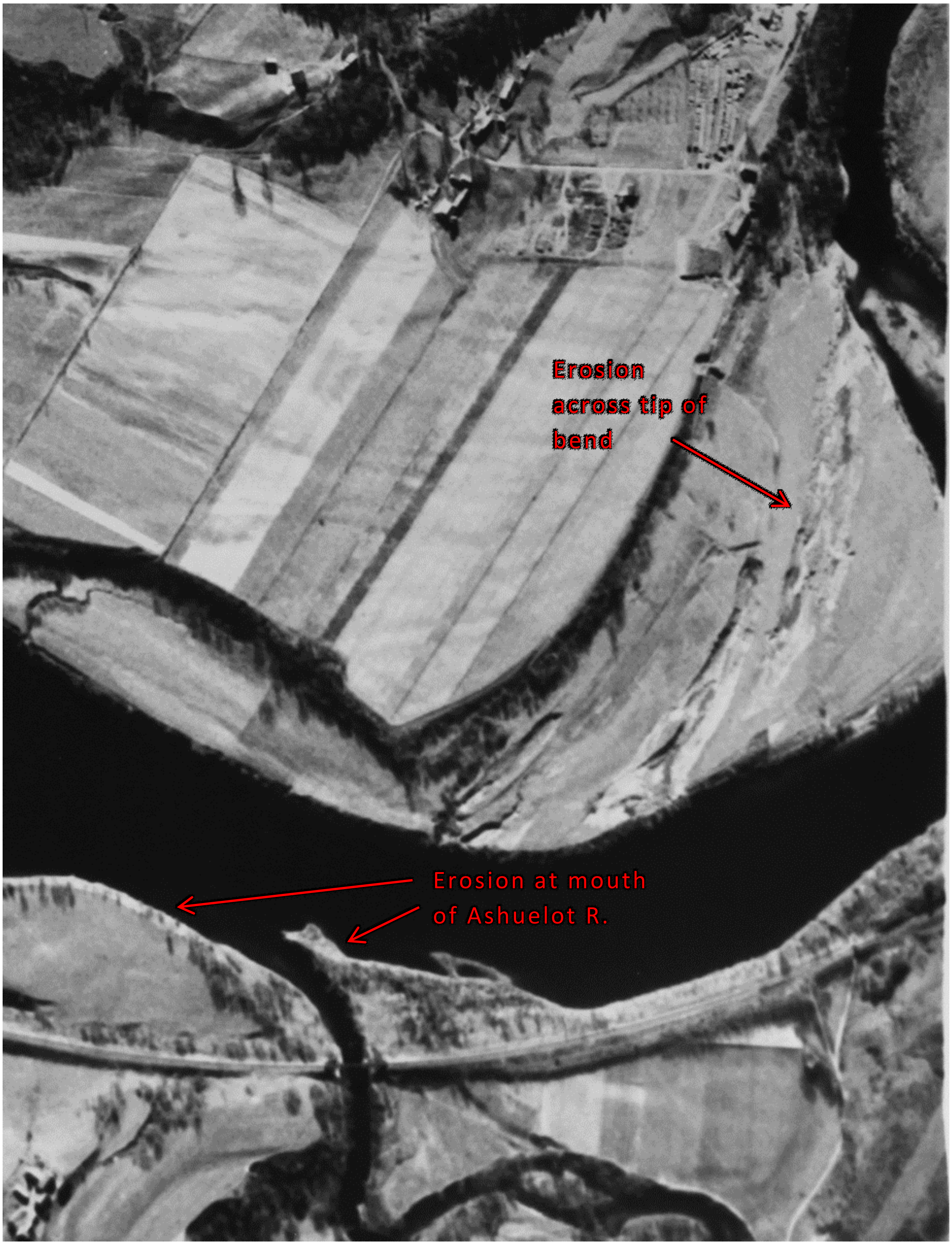

Figure 2.3.2-9 Stebbins Island – Ashuelot River, 1939 (b)

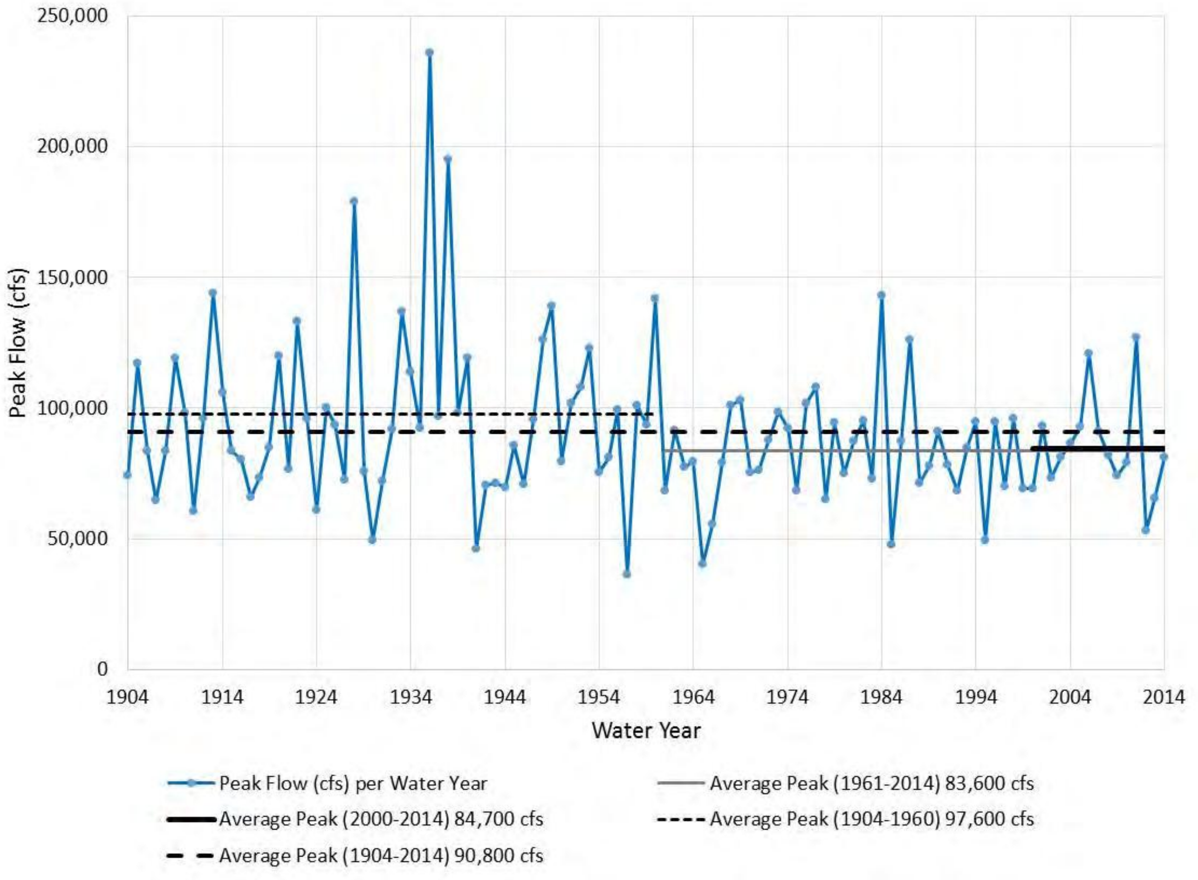

Figure 2.3.2-10 Annual Peak Streamflow – Montague, MA 1904-2014 (USGS)

2.3.3 Analysis of historic datasets – Turner Falls Impoundment

In addition to the historic analysis of the Connecticut River described in the previous section, FirstLight also attempted to conduct a historic geomorphic assessment specific to the TFI. As discussed in the RSP, the goal of this assessment was to provide context when discussing the modern geomorphology of the TFI through the use of available aerial photographs and ortho-photos, historic survey information, and other historic datasets. FERC's September 13, 2013 SPDL further recommended that FirstLight perform the historic geomorphic assessment using available mapping such as the 1970 vintage ground survey data (i.e. the Exhibit K drawings) to analyze trends in bank position within the TFI. In accordance with the RSP and FERC SPDL, FirstLight attempted to use the following datasets when conducting this assessment: 1952, 1961, and 1970 aerial photos, the 1971 Exhibit K drawings, and 2014 ortho-photos obtained from MassGIS and New Hampshire Geographically Referenced Analysis and Information Transfer System (NH GRANIT). Comparison of these datasets were plagued by numerous challenges and limitations which prevented this comparison from yielding any meaningful results.

The first challenge that was encountered when conducting this assessment was relative to the Exhibit K drawings. The original Exhibit K drawings were developed in the late 1960's and early 1970's by Gordon Ainsworth Associates through a combination of aerial imagery, photogrammetry, and ground surveys. The original Exhibit K drawings contained information pertaining to the project boundary, minimum and maximum flow lines, ownership rights, topography, and miscellaneous facility details. National Map Accuracy Standards suggest that this mapping should have been compiled to an accuracy of 1/40th of an inch, which translates to $\pm$10 feet. The original drawings were hand drawn and existed in hard copy format only. FirstLight scanned the hard copy drawings, imported them into ArcGIS, and georeferenced them using coordinates given on the maps in NAD27 Massachusetts State Plane coordinate system.

Upon preliminary review of the drawings, it appeared that the Minimum Flow Line depicted the edge-of-water, however, as the drawings were reviewed more closely that did not appear to be the case. Furthermore, it is unclear how the location of the Minimum Flow Line was identified and what mapping methods were used to develop the original maps. FirstLight also explored the possibility of developing correlations between the Minimum Flow Line depicted on the original Exhibit K drawings and existing surveyed cross-sections of the river to determine the location of the edge-of-water at the time the original drawings were developed, however, that effort proved unsuccessful. The location of the Maximum Flow Line was also reviewed to determine if it could be used to conduct the analysis FERC recommended. Upon review of the drawings it became clear that the Maximum Flow Line would not be an accurate representation of the edge-of-water given that its location extends into the floodplain a far distance from the actual river channel in a number of locations.

Given that the Exhibit K drawings did not contain any information that could be used to determine the edge-of-water, top of bank, or toe of bank they were not useful in conducting a historic geomorphic assessment of the TFI and therefore were not used.

Focus then turned to comparing the 1952, 1961, and 1970 aerial photos with more recent ortho-photos. While the historic aerial photographs were useful for general or site specific observations of the TFI geomorphology at that time, direct comparison of the edge-of-water or riverbank position of the historic photographs with the more recent ortho-photos did not yield useful results given that the historic aerial photographs were taken before the Turners Falls Dams was raised[7] (1952 and 1961) or during construction modifications to the dam (1970). When comparing the 1952 and 1961 historic photos with the more recent ortho-photos it was unclear if changes in the position of the edge-of-water were the result of changes in riverbank position or simply the result of changes in water level due to the raising of the dam. Comparisons

[7] The Turners Falls Dam was raised approximately 6 feet in 1970 as part of the construction of the Northfield Mountain Project.

of the edge-of-water from the 1970 aerial photographs with the more recent ortho-photos also proved to not be useful since the water levels in the TFI were drawn down significantly at the time the 1970 photos were captured to accommodate the construction modifications of the dam.

Due to the limitations discussed above and in Section 2.3.1, a historic geomorphic assessment via comparison of edge-of-water or riverbank position over time was not possible with the available data. While such a comparison did not yield useful results, the historic aerial photographs still provided valuable insights into geomorphic trends when used to examine and compare the condition of specific sites over time. The results of these site specific evaluations and comparisons are discussed in the following section.

2.3.4 Analysis of the 20 Erosion Sites Identified in the Erosion Control Plan

In 1998 a FRR survey was conducted to document riverbank features, characteristics, and conditions throughout the TFI. From this, the Erosion Control Plan (ECP) was developed which identified the 20 most severely eroding sites in the TFI (S&A, 1999). The location of the 20 sites is shown in Figure 2.3.4-1. As part of the historic geomorphic assessment discussed in this section, historic aerial photographs were utilized to evaluate riverbank conditions at the 20 sites identified in the ECP. Table 2.3.4-1 includes a summary of these sites and a comparison of their current status relative to their condition prior to the Turners Falls Dam being raised and the Northfield Mountain Project commencing operation.

Historic aerial photographs from the 1952 and 1961 were analyzed to identify riverbank conditions at each of the 20 most severely eroded sites noted in the ECP. Aerial photographs from these time periods were selected for two main reasons including: (1) they represented conditions in the TFI prior to the raising of the Turners Falls Dam and commencement of Northfield Mountain operations, and (2) they represented riverbank conditions before the shoreline stabilization projects were constructed as part of the ECP. Volume III (Appendix B) contains a full set of figures depicting the conditions at each of the 20 sites identified in the ECP as they appeared in the 1952 and/or 1961.

Based on the results of this analysis it is observed that of the 20 erosion sites identified in the ECP, 14 appear to be eroded prior to raising the Turners Falls Dam and construction/operation of the Northfield Mountain Project. Sites which appear to exhibit erosion in the 1950's and 1960's include:

- Vernon Dam (Site #1)
- Route 10 Bridge (Site #5)
- Flagg (Site #7)
- Kendall (Site #9)
- River Road (Site #10)
- Urgiel Downstream (Site #11)
- Durkee Point (Site #12)
- Split River (Site #13)
- Country Road (Site #14 and #20)
- Stebbins Island (Site #15)
- Kaufhold (Site #16)
- Montague (Site #17)
- Campground Point (Site #18)

Of the 6 remaining sites, one was potentially eroded prior to the Project (Urgiel Upstream - #4), while at the five other sites riverbank conditions are unclear based on the quality of the aerial photographs. Sites where riverbank conditions are unclear include:

- Turners Falls Rod & Gun Club (Site #2)
- Bennett Meadow (Site #3)
- Skalski (Site #6)
- Un-named site (Site #8)
- Davenport or Upper Island (Site #19)

It is significant that a vast majority of the most severely eroded sites identified as part of the 1998 ECP were eroded in the 1952 and 1961 aerial images, prior to raising the Turners Falls Dam and construction of the Northfield Mountain Project.

In addition to the 20 erosion sites identified in the ECP, analysis of the historical aerial photographs revealed several other sites in the TFI that were eroding prior to the raising of the Turners Falls Dam and construction/operation of Northfield Mountain. These additional sites included: the right bank near the downstream end of Stebbins Island, the right bank across from the Ashuelot River confluence, the left bank across from Rock Island, the left bank across from the Mt. Hermon School, the left bank across from Bennett Meadow, and the right bank across from the future location of the Northfield Mountain tailrace. It is instructive to follow what has occurred at these eroded sites over time based on aerial photos, FRRs or other available observations:

- Right bank near downstream end of Stebbins Island: Recent aerial photos and FRR observations show that a narrow zone of riparian vegetation has developed on this previously eroded area indicating natural stabilization is occurring;

- Right bank across from Ashuelot River confluence: A narrow zone of riparian vegetation has become established on this previously eroded bank based on aerial photos and FRR observations;

- Left bank across from Rock Island: Eroded riverbank shown in the 1952 and 1961 aerial photographs now supports a narrow band of riparian vegetation based on recent aerial photographs;

- Left bank across from the Mt. Hermon School: The 1952 and 1961 photographs show eroded conditions with virtually no riparian vegetation. A zone of riparian vegetation becomes established and grows as seen on the 1990’s and more recent aerial photographs and confirmed by FRR observations;

- Left bank across from Bennett Meadow: Experimental riverbank protection was placed along this segment of bank by the USACE in the 1970’s including articulated blocks on fabric and tires placed in various configurations; and

- Right bank across from Northfield Mountain Tailrace: Rock from the construction of Northfield Mountain was placed at the toe of this eroded riverbank. Vegetation has become established on the upper bank as shown in the series of aerial photographs and FRR observations.

Volume III (Appendix B) includes images of historical aerial photographs depicting erosion in 1952 and 1961 in these areas.

Table 2.3.4-1: Status of the 20 Erosion Sites Identified in the ECP

Site #	Site Name	Current Status (2014)	Pre-Northfield Mtn. Status
1	Vernon Dam	Not selected for stabilization due to extreme hydraulic conditions associated with Vernon spillway	Eroded: Erosion evident in 1952 with continuing erosion through 2008-2010 photos.
2	Turners Falls Rod & Gun Club	Stabilized in 2004	Condition changed considerably due to raised water level and construction of club.
3	Bennett Meadow	Stabilized in 2005	Condition unknown based on aerial photos.
4	Urgiel Upstream	Stabilized in 2001	Potentially eroded: sparse riparian vegetation in 1952 photo.
5	Route 10 Bridge	Not selected for stabilization due to unique hydraulic conditions in the vicinity of the Route 10 Bridge	Eroded: Photos used in this analysis as well as earlier photos from analysis associated with Route 10 bridge show ongoing erosion.
6	Skalski	Stabilized in 2004	Condition unknown based on aerial photos: The left bank of the river in the vicinity of Kidds Island has a band of riparian vegetation in the 1952, 1961 and 1990s photographs. While not apparent in the photographs, erosion had been occurring along this bank and was identified in the ECP and stabilized in 2004 as the Skalski site.
7	Flagg	Stabilized 1999-2000	Eroded: The right bank across from Kidds Island was sparsely vegetated in 1952 and 1961 with ongoing erosion in the 1990s.
8	Un-named	Not selected for stabilization – opposite great meadow	Condition unclear based on aerial photos.
9	Kendall	Stabilized in 2007	Eroded: In 1952 there is some riparian vegetation on the right bank but by the 1961 photograph erosion is evident with no riparian vegetation remaining.
10	River Road	Stabilized in 2003	Eroded: On the inside of the bend along the left bank erosion has occurred over time with the bank moving landward compared to the project boundary line as noted in changes in the bank from the 1952 to 1961 and subsequent photographs.
11	Urgiel Downstream	Stabilized in 2005	Eroded: At a bend in the river upstream of Kidds Island the 1952 photograph shows a reach with some riparian vegetation. The 1961 photograph shows erosion and associated decrease in riparian vegetation.
12	Durkee Point	Stabilized in 2003	Eroded: 1952 and 1961 photographs show erosion and lack of riparian vegetation.
13	Split River	Stabilized in 2009 (Lower Split River) and 2010 (Upper Split River)	Eroded: 1952 and 1961 photographs show erosion and lack of riparian vegetation.
14	Country Road	Stabilized in 2006 (includes site #20)	Eroded: The 1961 photograph shows erosion and a significant reduction in riparian vegetation.

Site #	Site Name	Current Status (2014)	Pre-Northfield Mtn. Status
15	Stebbins Island	Not selected for stabilization	Eroded: Downstream end of island has narrowed through erosion from 1952 to 2008-2010.
16	Kaufhold	Upper Split River stabilized 2010, Bathory-Gallagher stabilized 2012-2013	Eroded: Bathory-Gallagher – Upstream of the tailrace along both banks there was a band of riparian vegetation in the 1952 photograph. By the 1961 photograph the riparian zone appear to have decreased and erosion is evident. Eroded: Upper Split River – 1952 and 1961 photographs show erosion and lack of riparian vegetation.
17	Montague	Stabilized by preventative maintenance in 2008	Eroded: Erosion evident in 1961 photograph.
18	Campground Point	Stabilized by preventative maintenance in 2008	Eroded: Some erosion is evident in the earlier photographs such as 1952 continuing through the 2008 aerial photo
19	Davenport or Upper Island	Not selected for stabilization	Condition unknown based on aerial photos (incomplete imagery available).
20	Country Road	850 ft stabilized in 2006 (included as part of site # 14)	Eroded: The 1961 photograph shows erosion and a significant reduction in riparian vegetation.

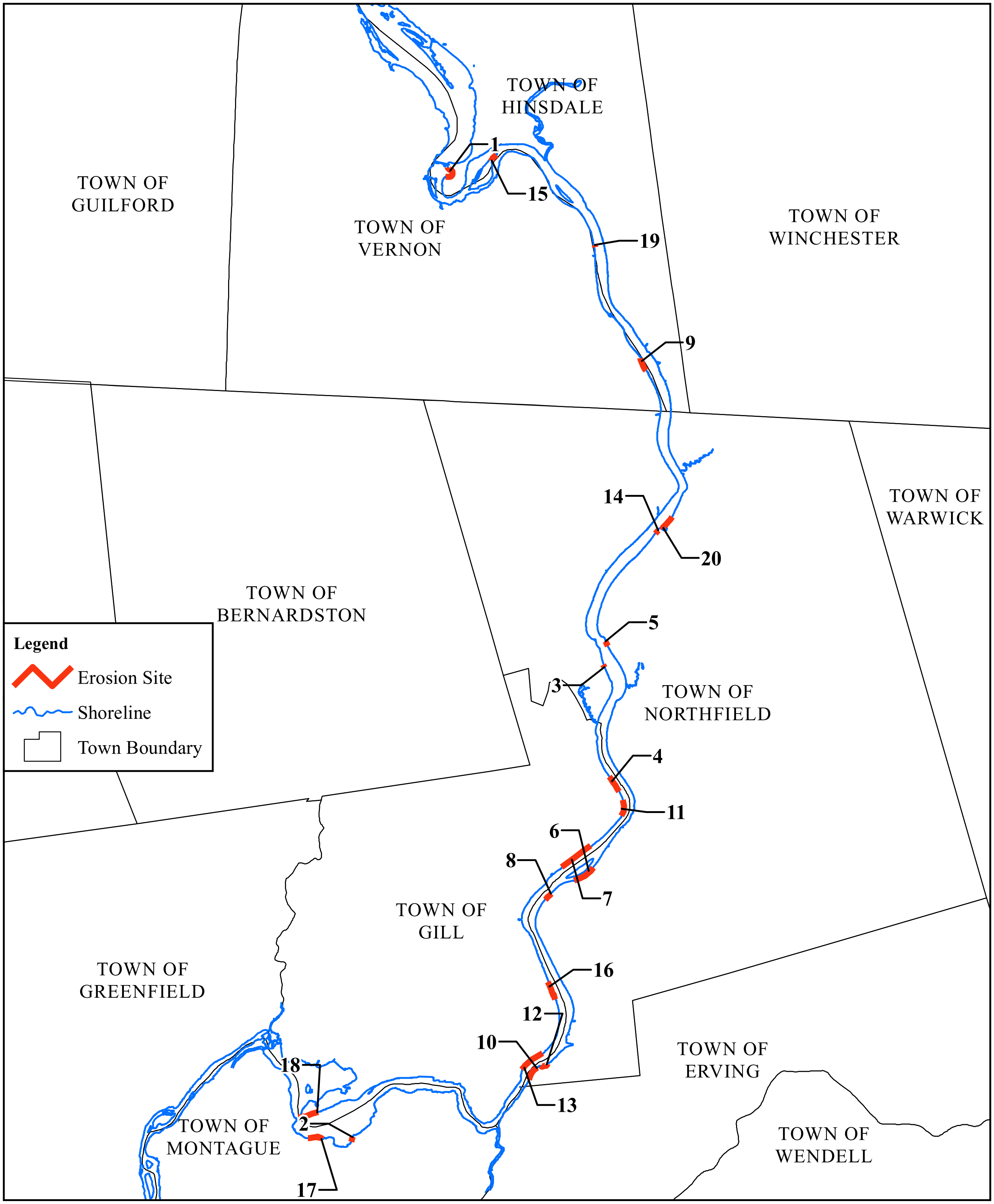

FIRSTLIGHT HYDRO GENERATING COMPANY
Northfield Mountain Pumped Storage Project No. 2485
Turners Falls Hydroelectric Project No. 1889

STUDY 3.1.2

Figure 2.3.4-1:
Twenty Sites with Highest Erosion Rank (ECP 1998)

FirstLight Power Resources

N

0 0.875 1.75 3.5 Miles

Path: W:\gis\studies\3_1_2\maps\final_report\figure_2_3_4-1.mxd

2.4 Geomorphic Analysis of Tributaries and Upland Erosion Features

Tributaries also play an important role in the geomorphology of the Connecticut River and TFI. The energy associated with water flowing from the higher elevations of the surrounding hillsides and mountain ridges tends to erode sediment from the tributary watersheds which is then transported to the mainstem. Inflow and sediment loads from the tributaries can result in both deposition and erosion in the mainstem. For example, during Tropical Storm Irene several inches to a foot or more of sediment was deposited at various locations along the banks of the TFI due to severe erosion farther upstream, particularly from tributaries. Conversely, erosion has been known to occur in the vicinity of various tributary confluences throughout the TFI based on observations of the river at confluences with tributaries and aerial photographs.

The tributaries draining into the TFI have a wide range watershed sizes. The drainage area at the Vernon and Turners Falls Dams are 6,266 mi^2 and 7,163 mi^2, respectively, a difference of 897 mi^2. The two main tributaries to the TFI are the Millers and Ashuelot Rivers which have drainage areas of 390 mi^2 and 420 mi^2 at the confluence with the Connecticut River (combined 810 mi^2) respectively. The combined drainage area of the two tributaries accounts for 88% of the drainage between the Vernon and Turners Falls Dam's. Figure 2.4-1 to Figure 2.4-4 depict these tributaries. The Millers and Ashuelot Rivers have eroded down to stable beds consisting of rock such that little additional erosion of the beds of these two tributaries is possible. Other tributaries are quite steep with beds consisting of gravel, sand or finer material which are erodible and are in the process of erosion, incision, and channel widening. The other TFI tributaries include 16 named and 20 unnamed tributaries which account for the remaining 87 mi^2. The 16 named TFI tributaries include:

- Ashuelot River
- Newton Brook
- Pauchaug Brook
- Bottom Brook
- Mill Brook
- Mallory Brook
- Millers Brook
- Roaring Brook
- Bennett Brook
- Merriam Brook
- Otter Run
- Ashuela Brook
- Dry Brook
- Pine Meadow Brook
- Fourmile Brook
- Millers River

Figure 2.4-5 denotes the tributaries of the TFI. Erosion is often the dominant process at the confluence of tributaries and the Connecticut River/TFI as channels are often cut through the riverbanks as the tributary flows into the mainstem. To the extent tributaries are eroding, incising and expanding; the tributary erosion evolution as it interacts with riverbanks of the mainstem at the confluence may extend the tributary erosion processes to the mainstem in localized areas. As a tributary enters the main river, flow in the tributary can attack the side of the riverbank through which it flows. As a result the main riverbank can be attacked from the main river on the front side of the bank as well as on the side from the tributary. When a tributary meanders as it approaches the main river, flow in the tributary can also attack the back side of the main riverbank.

In addition to tributaries, upland erosion features have also been observed to contribute to riverbank erosion in the TFI. Upland erosion features, if they connect to the main river act as small tributaries. In such cases an upland erosion feature can attack the side or back of the main riverbank as does a tributary. Analysis of LiDAR data and USGS maps indicate that several upland erosion features are present throughout the study area. These upland erosion features have been observed to form drainage patterns that also contribute inflow to the TFI. To more closely examine the potential impact these upland erosion features and drainage patterns may have on the geomorphology of the TFI, contours derived from LiDAR data[8] of the study area were overlaid on current ortho-photos. Observations made from the LiDAR data were compared against photos collected in the field during the 2013 FRR and subsequent field work associated with this study. Volume III (Appendix C) contains examples of the upland erosion features identified during this analysis.

Further observations of the locations of tributaries and upland erosion features in the TFI finds that a number of the 20 most severely eroded sites identified in the ECP, as well as some erosion sites selected for stabilization in recent years, are located in the immediate vicinity of these features. Table 2.4-1 examines the 20 sites identified in the ECP plus 5 sites recently recommended for stabilization. Of these 25 sites, 16 are directly adjacent to tributaries or upland erosion features. At the 9 remaining sites other factors adversely affect riverbank stability. Two have unusual and extreme hydraulic conditions (S&A, 2012a), four have a very narrow riparian zone adjacent to agricultural activity, one is located at a very narrow tip of an island, while the remaining two have other factors contributing to erosion.

Table 2.4-1: Review of Erosion Sites Identified in the ECP Compared to their Proximity to Tributaries or Upland Erosion Features

Site #/ Name	Presence of tributaries /upland erosion features	Observations
Vernon Dam	No	While there are no tributaries/upland erosion feature, erosion is caused by the rapid current, turbulence and eddying caused by the Vernon Dam gates that release water from the left side of the structure near the bank.
Rod & Gun Club	Yes	Topography shows ravine and alluvial fan shaped feature along with disturbance due to development (road, boat dock).
Bennett Meadow	No	Agricultural terrace with little to no riparian zone (see ECP, site 3).
Urgiel upstream	Yes	Topography modified by stabilization but upstream and downstream upland erosion/damage features can be seen and aerial photo and field observations indicate such features. Seepage through area was observed. Linear erosion feature extends through part of site and extends upstream several hundred feet (unknown cause but downslope from ponds.
Route 10 Bridge	No	Extreme hydraulic conditions with eddying and strong currents from rocky point across river between old and new bridges. One upland erosion/drainage feature. Adjacent to agricultural field with narrow riparian zone.
Skalski	Yes	Next to tributary.
Flagg	Yes	Tributary (Otter Run Brook) splits two sections of stabilization.

[8] LiDAR data of the Connecticut River was collected by US Imaging from April 26-28, 2013 (leaf off) during normal river flows. The data was collected using an Optech M-300 Orion LiDAR Sensor and Integrated CS-10000 Digital CameraAircraft– Cessna T210N – N6258YQA. The LiDAR data was checked against the independently obtained QA/QC points throughout the project area and was found to have a Root Mean Square Error (RMSE) for the sample (RMSEz) of 6.1cm (vertical). The digital imagery was checked against more than 60 photo targets and Photo ID points along the project corridor and was found to have better than 12 cm horizontal standard deviation.

Site #/ Name	Presence of tributaries /upland erosion features	Observations
ECP Site #8	Yes	Tributary and several upland erosion features in the vicinity. Adjacent to gravel pit/quarry and downgradient from Sawyer Ponds.
Kendall	No	Agricultural field, adjacent to abandoned railroad bridge with failed concrete pier which fell into the river and directs current towards riverbank.
River Road	Yes	Site of gully activity
Urgiel downstream	Yes	Modified topography from stabilization changed landscape but observations indicate drainage paths and wetlands uplands from site exist as does seepage through area.
Durkee Point	Yes	Adjacent to tributary.
ECP Site #13	Yes	Transition between ag, hillside, drainage and trail to river.
Country Road	Yes	Tributary flows around from behind stabilized section and joins river on the downstream end of stabilization.
Stebbins Island	No	Narrow, downstream tip of island.
Bathory/Gallagher Upper Split River	No	Agricultural terrace with narrow riparian zone.
Montague	Yes	Numerous upland erosion features.
Campground Point	No	Steep slope with road above and topographic irregularities which could be associated with upland erosion features.
ECP Site #19 (Right bank d/s Upper or Davenport Island)	No	Agricultural terrace with narrow riparian zone.
Country Road	Yes	Tributary flows around from behind stabilized section and joins on the downstream end of stabilization.
Bonnette Farm	Yes	Adjacent to Ashuelot River.
Segment 12 (2013 FRR)	Yes	Numerous upland erosion features.
Segment 75 (2013 FRR)	Yes	Adjacent to tributary
Segment 87 (2013 FRR)	Yes	Adjacent to tributary
Shearer	Yes	Adjacent to tributary

Figure 2.4-1: Ashuelot River – Hinsdale, NH (September 2015)

FirstLight Power Resources

N

FIRSTLIGHT HYDRO GENERATING COMPANY
Northfield Mountain Pumped Storage Project No. 2485
Turners Falls Hydroelectric Project No. 1889

STUDY 3.1.2

0 500 1,000 2,000 Feet

Figure 2.4-2: Aerial View of the Ashuelot River Flowing into the Connecticut River

Path: W:\gis\studies\3_1_2\maps\final_report\figure_2_4_2.mxd

Figure 2.4-3: Millers River Confluence with Connecticut River (during Tropical Storm Irene)

FirstLight Power Resources

FIRSTLIGHT HYDRO GENERATING COMPANY
Northfield Mountain Pumped Storage Project No. 2485
Turners Falls Hydroelectric Project No. 1889

STUDY 3.1.2

Figure 2.4-4: Aerial View of the Millers River Flowing into the Connecticut River

Path: W:\gis\studies\3_1_2\maps\final_report\figure_2_4_4.mxd

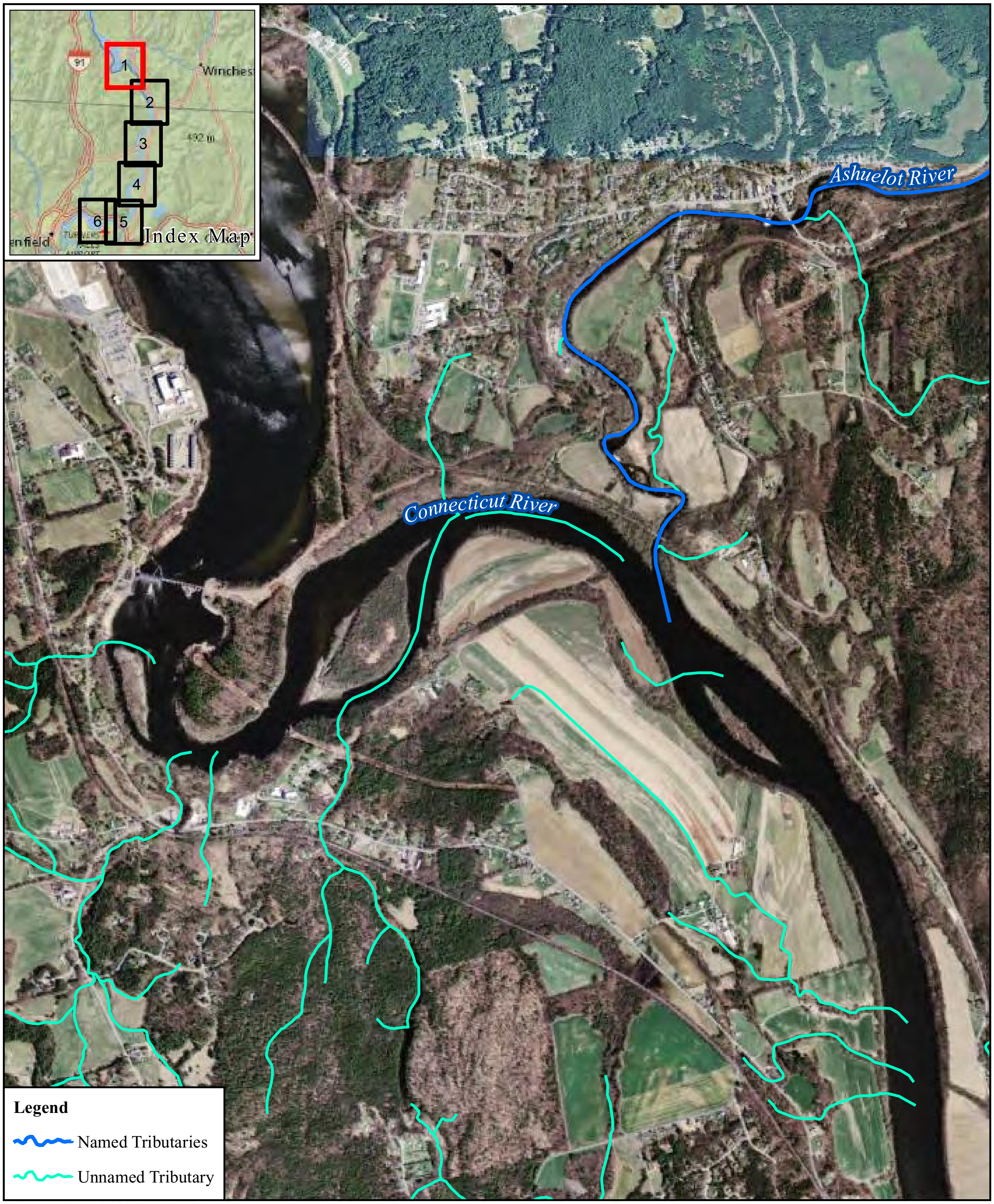

FIRSTLIGHT HYDRO GENERATING COMPANY
Northfield Mountain Pumped Storage Project No. 2485
Turners Falls Hydroelectric Project No. 1889

STUDY 3.1.2

Figure 2.4-5: Turners Falls Impoundment Tributaries Map 1

N

0 1,000 2,000 4,000 Feet

Path: W:\gis\studies\3_1_2\maps\final_report\figure_2_4_5.mxd

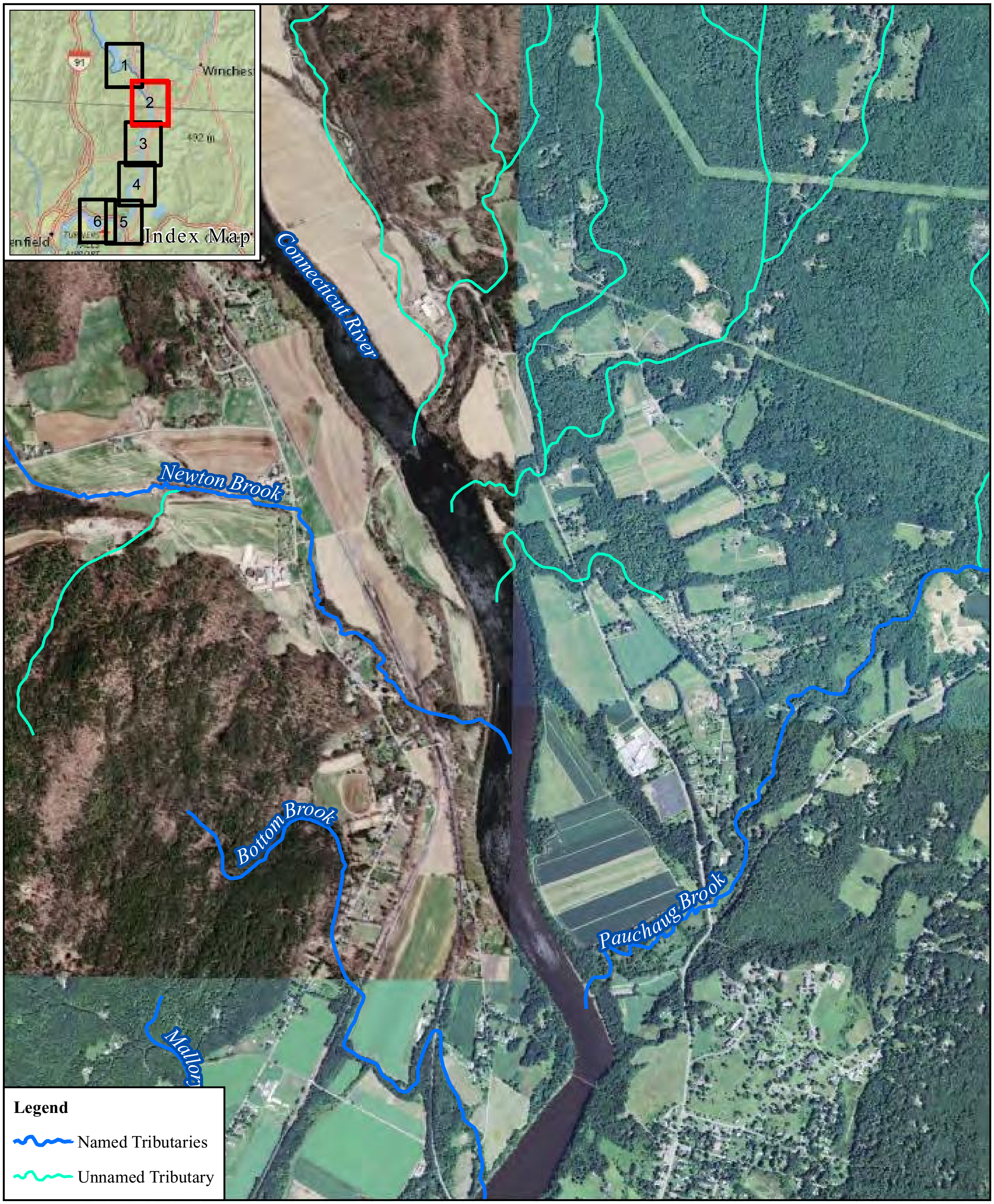

FIRSTLIGHT HYDRO GENERATING COMPANY
Northfield Mountain Pumped Storage Project No. 2485
Turners Falls Hydroelectric Project No. 1889

STUDY 3.1.2

Figure 2.4-5: Turners Falls Impoundment Tributaries Map 2

FirstLight Power Resources

N

0 1,000 2,000 4,000 Feet

Path: W:\gis\studies\3_1_2\maps\final_report\figure_2_4_5.mxd

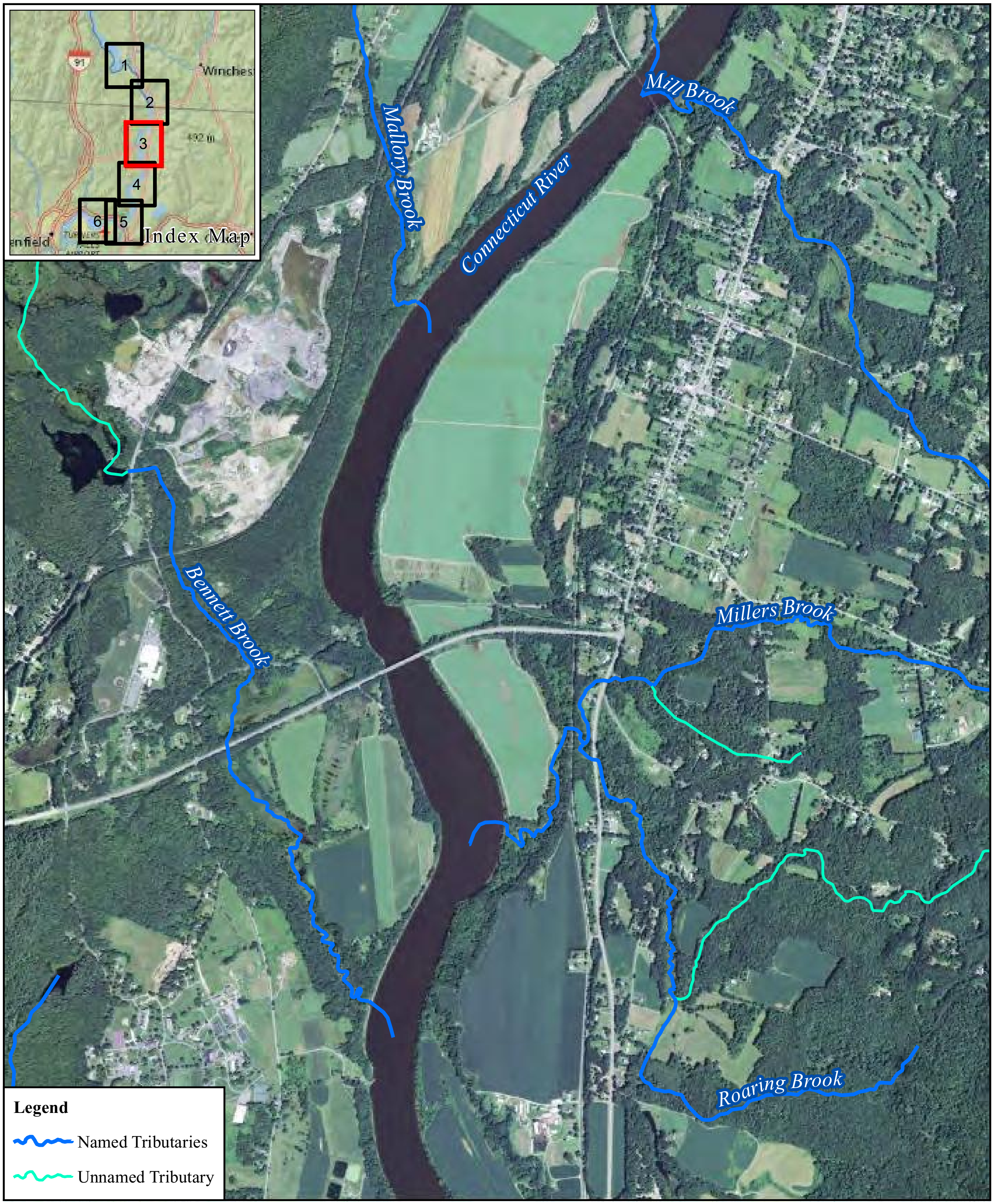

FIRSTLIGHT HYDRO GENERATING COMPANY
Northfield Mountain Pumped Storage Project No. 2485
Turners Falls Hydroelectric Project No. 1889

STUDY 3.1.2

Figure 2.4-5: Turners Falls Impoundment Tributaries Map 3

FirstLight Power Resources

N

0 1,000 2,000 4,000 Feet

Path: W:\gis\studies\3_1_2\maps\final_report\figure_2_4_5.mxd

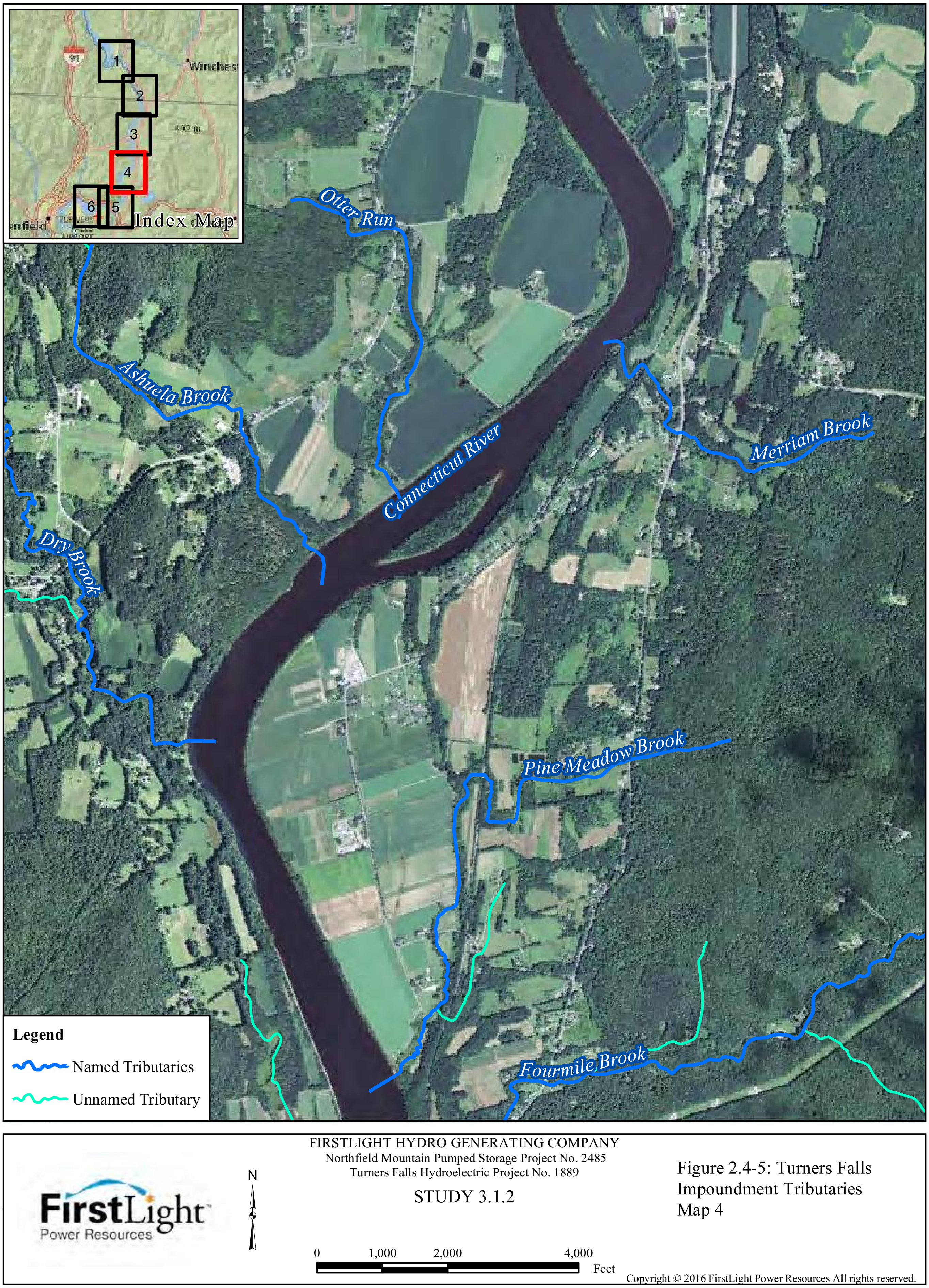

FIRSTLIGHT HYDRO GENERATING COMPANY
Northfield Mountain Pumped Storage Project No. 2485
Turners Falls Hydroelectric Project No. 1889

STUDY 3.1.2

Figure 2.4-5: Turners Falls Impoundment Tributaries Map 4

Path: W:\gis\studies\3_1_2\maps\final_report\figure_2_4_5.mxd

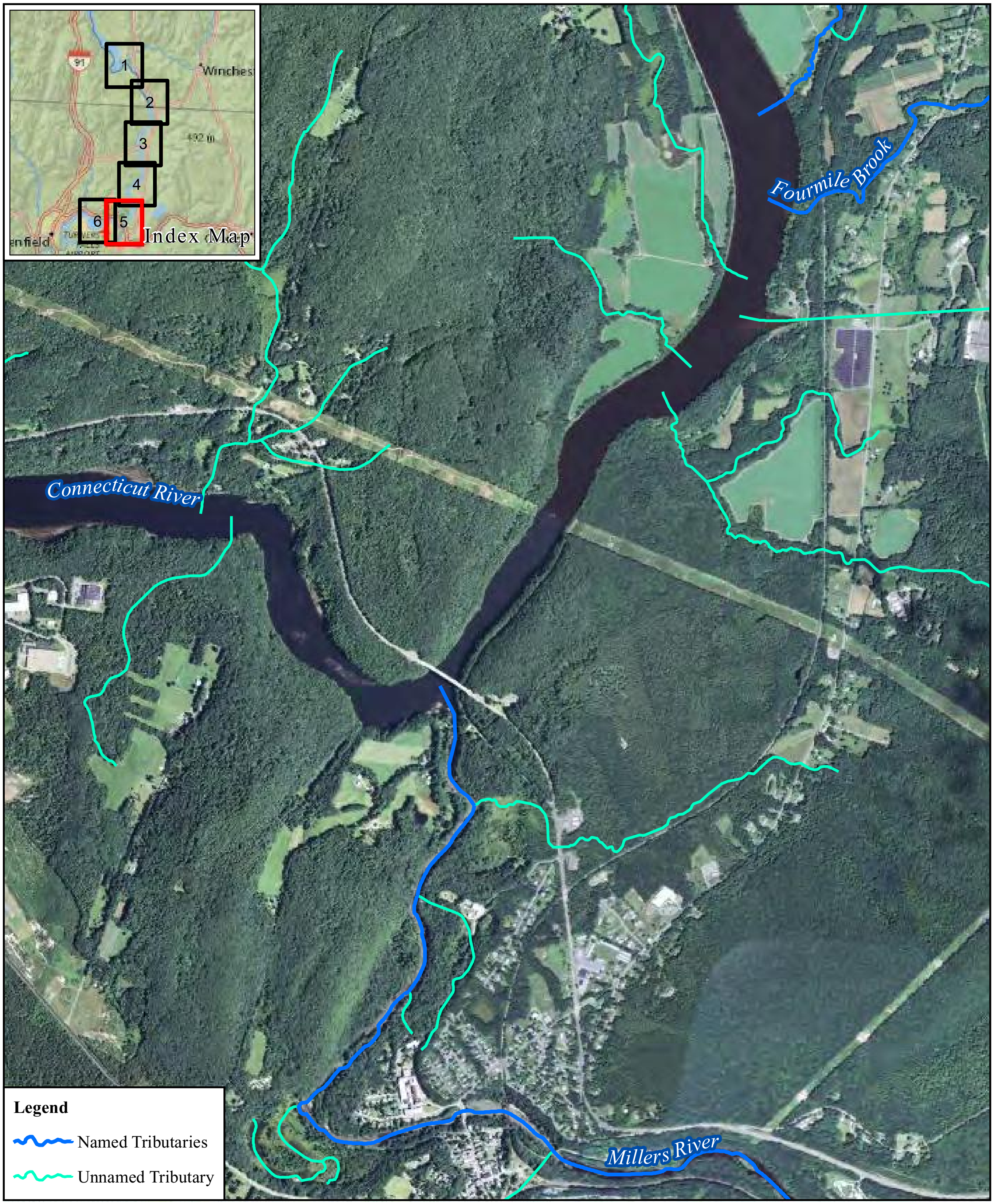

FIRSTLIGHT HYDRO GENERATING COMPANY
Northfield Mountain Pumped Storage Project No. 2485
Turners Falls Hydroelectric Project No. 1889

STUDY 3.1.2

FirstLight Power Resources

N

0 1,000 2,000 4,000 Feet

Figure 2.4-5: Turners Falls Impoundment Tributaries Map 5

Path: W:\gis\studies\3_1_2\maps\final_report\figure_2_4_5.mxd

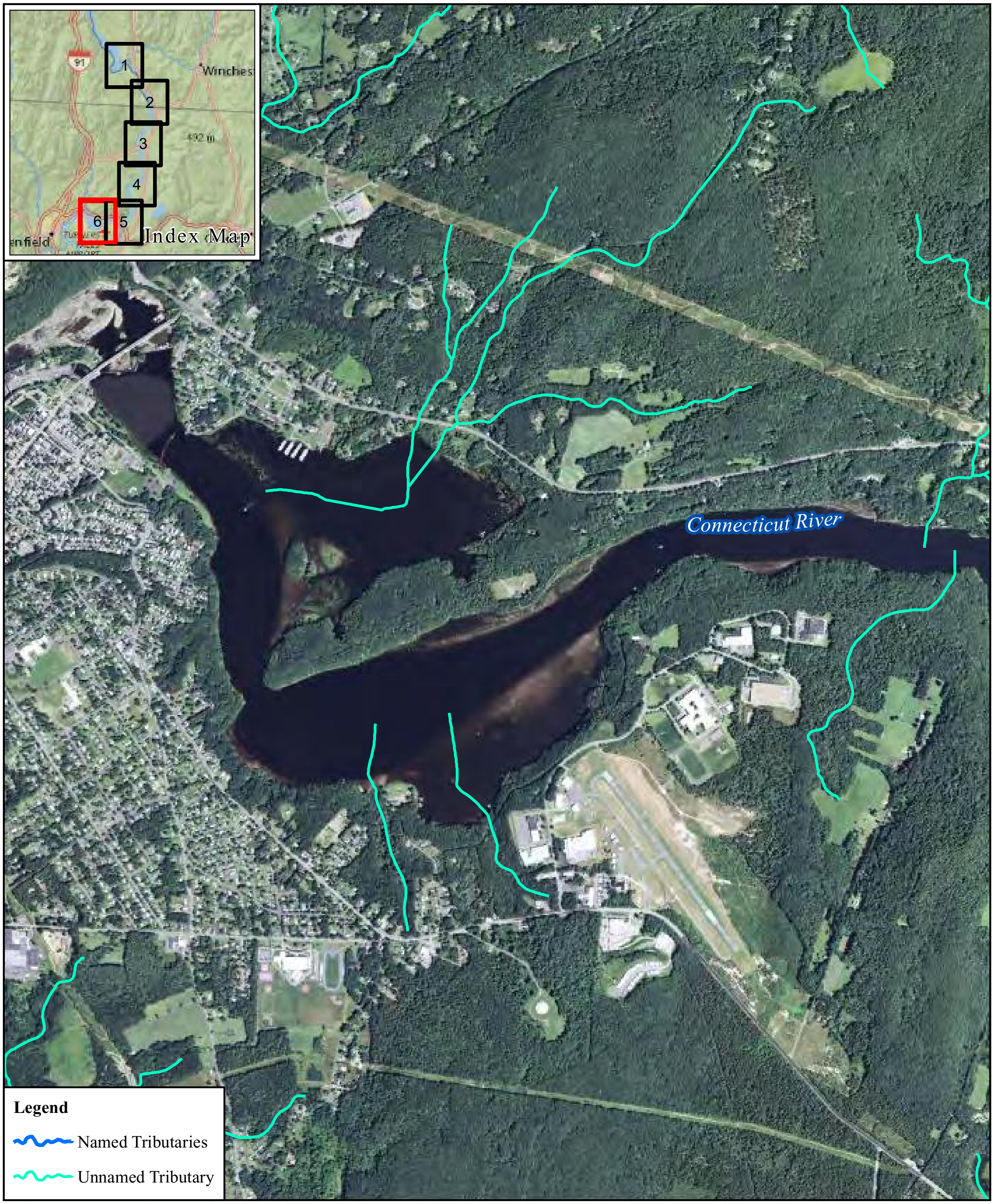

FIRSTLIGHT HYDRO GENERATING COMPANY
Northfield Mountain Pumped Storage Project No. 2485
Turners Falls Hydroelectric Project No. 1889

STUDY 3.1.2

Figure 2.4-5: Turners Falls Impoundment Tributaries Map 6

N

0 1,000 2,000 4,000 Feet

Path: W:\gis\studies\3_1_2\maps\final_report\figure_2_4_5.mxd

2.5 Erosion comparison of the Turners Falls Impoundment and Connecticut River

S&A conducted a study which compared erosion along the extent of the Connecticut River from Holyoke Dam (Holyoke, MA), upstream through various hydropower impoundments (including Turners Falls, Vernon, Bellows Falls, and Wilder), and continuing to the un-impounded, free-flowing reach from Gilman Dam to Pittsburg, NH (S&A, 2012b). The study reach was approximately 240 miles long. The study was conducted partially in response to recommendations made in Field (2007) which presented a list of "highest priority recommendations." One of the priority recommendations identified by Field (2007) was to study the patterns of erosion in other reaches of the Connecticut River for comparative purposes.

The study found that riverbank features and characteristics vary considerably along the length of the river. While portions of the river consist of bedrock outcrops that are very stable, much of the riverbanks consist of hillsides or alluvial material that are formed primarily of silt to sand sized material. There are areas that consist of gravel to cobble sized material that are generally less erodible but still are alluvial or transportable by fluvial processes. Much of the riverbanks are quite well vegetated, which generally adds to riverbank stability, although there are segments where a range of erosion and mass-wasting processes remove or damage vegetation and associated riparian land. Riverbank erosion was compared among various reaches to the extent feasible with available data as well as through photographs taken over the years at erosion sites. Key conclusions from this report found that (S&A, 2012b):

- The segment of river with the greatest extent of eroding riverbanks is the un-impounded northern reach (Pittsburg, NH down to Gilman Dam). At the time of the available study, 48.4% of the riverbanks were experiencing moderate or more significant erosion (Field, 2004). Riverbanks that had been rip-rapped covered 17.1% of the length of the river.

- Several erosion sites were identified and photographed in the Bellows Falls, Vernon, Turners Falls, and Holyoke Impoundments in 1997, and again in 2008. All of the erosion sites in 1997 in the Bellows Falls and Holyoke Impoundments and all but one of the 1997 erosion sites in the Vernon Impoundment remained in essentially the same state of erosion when photographed in 2008. Many of these sites were significant in both size and severity. In contrast, most of the erosion sites identified in the TFI in 1998 have been stabilized and were no longer eroding as of 2008.

- In addition to direct stabilization of many of the erosion sites in the TFI that were identified in the 1998 ECP, there is evidence of some natural stabilization processes including increased upper bank vegetation and areas of dense low bank aquatic vegetation that are helping provide a degree of additional stability in some areas.

- Despite the fact that similar percentages of riverbank have been stabilized in the northern, free-flowing reach as in the TFI; the percentage of erosion in the TFI is only about one-third the extent of erosion that is occurring in the northern, free-flowing reach of the Connecticut River (16.7% compared to 48.4%).

- Because riverbank erosion in the TFI is significantly less than in the northern free-flowing reach, erosion sites in other impoundments (Bellows Falls, Vernon, and Holyoke) continued eroding from 1997 to 2008, and many erosion sites have been stabilized in the TFI (including evidence of natural stabilization processes) it can be concluded that the riverbanks in the TFI are in the best condition (more stable and less eroding) than in any other part of the Connecticut River that was examined as part of the 2012 study.

- The TFI, which experiences water level fluctuations due to a combination of run of river/peaking power and pumped-storage hydropower operations, has less riverbank erosion than the other impoundments (Wilder, Bellows Falls, Vernon, and Holyoke) which only experience water level fluctuations resulting from run of river and peaking power operations and do not experience additional fluctuations due to pumped-storage operations. The TFI also experiences significantly less erosion than the northern, free-flowing reach which has no hydropower operations and associated water level fluctuations.

Significant erosion has been occurring and is ongoing in the un-impounded (free-flowing) reaches of the Connecticut River as well as in the impoundments other than the TFI as documented in the comparison report. Examples of erosion in these reaches of river are shown photographically in Figures 2.5-1 through 2.5-10. Figure 2.5-1 shows large-scale and severe erosion in a free-flowing reach of the river. An example of some of the erosion sites located in 1997 in the Bellows Falls Impoundment is shown in Figure 2.5-2, while other erosion examples in the Vernon and Holyoke Impoundments are shown in Figures 2.5-3 and 2.5-4.

The erosion sites identified in 1997 were revisited in 2008 to photographically document any changes that might have occurred since 1997. Sets of photographs showing 1997 and 2008 images at the same sites are presented in Figures 2.5-5 and 2.5-6 for the Bellows Falls Impoundment; Vernon – Figures 2.5-7 and 2.5-8; and Holyoke – Figures 2.5-9 and 2.5-10. For these three impoundments, erosion sites in 1997 were observed to be in the same eroding condition in 2008.

Note: Near Brunswick Springs, VT

Figure 2.5-1: Erosion of Glacial Outwash Deposits in Un-impounded Reach of Connecticut River (Field, 2004)

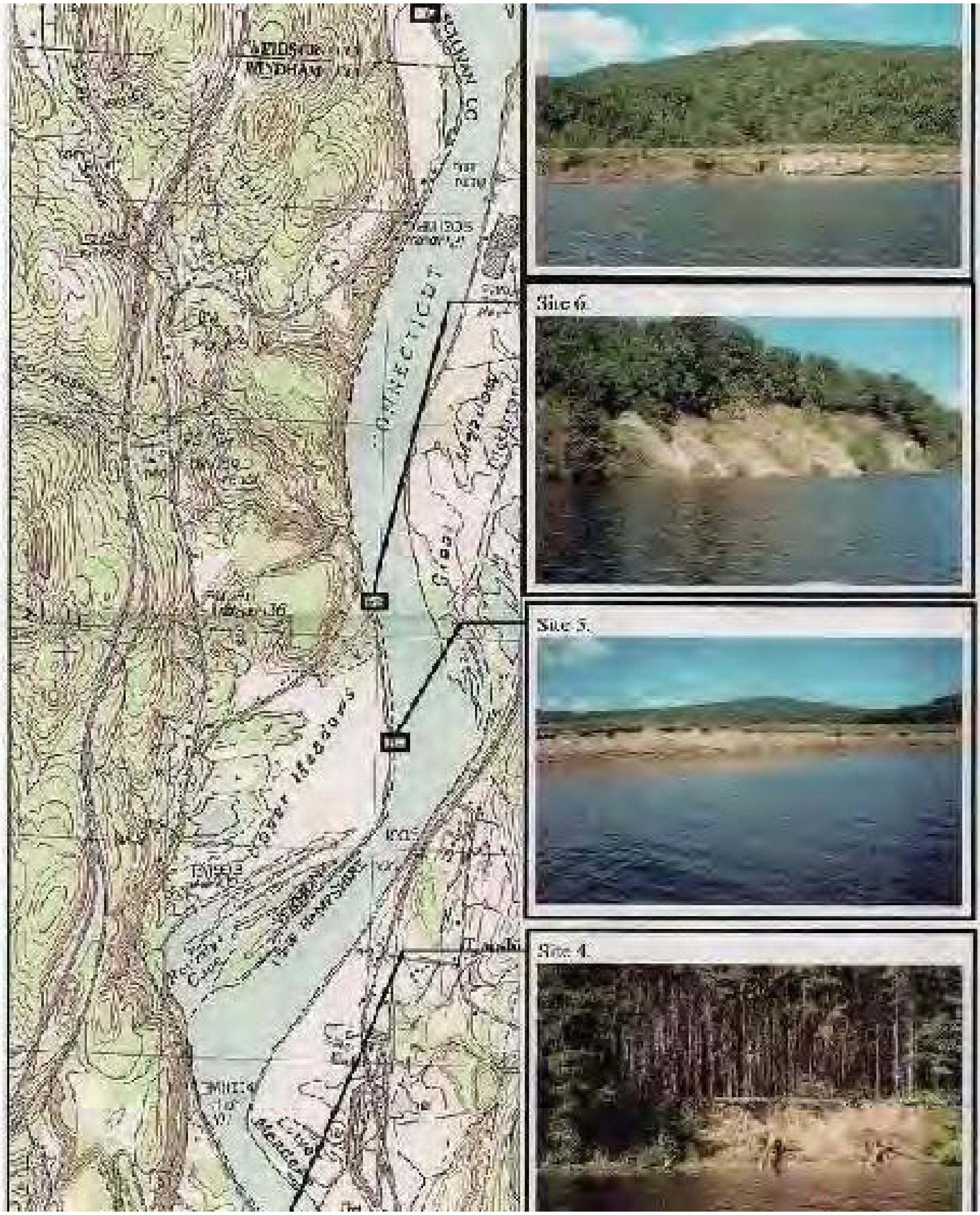

Figure 2.5-2: Erosion sites 4-7, Bellows Falls Impoundment (1997)

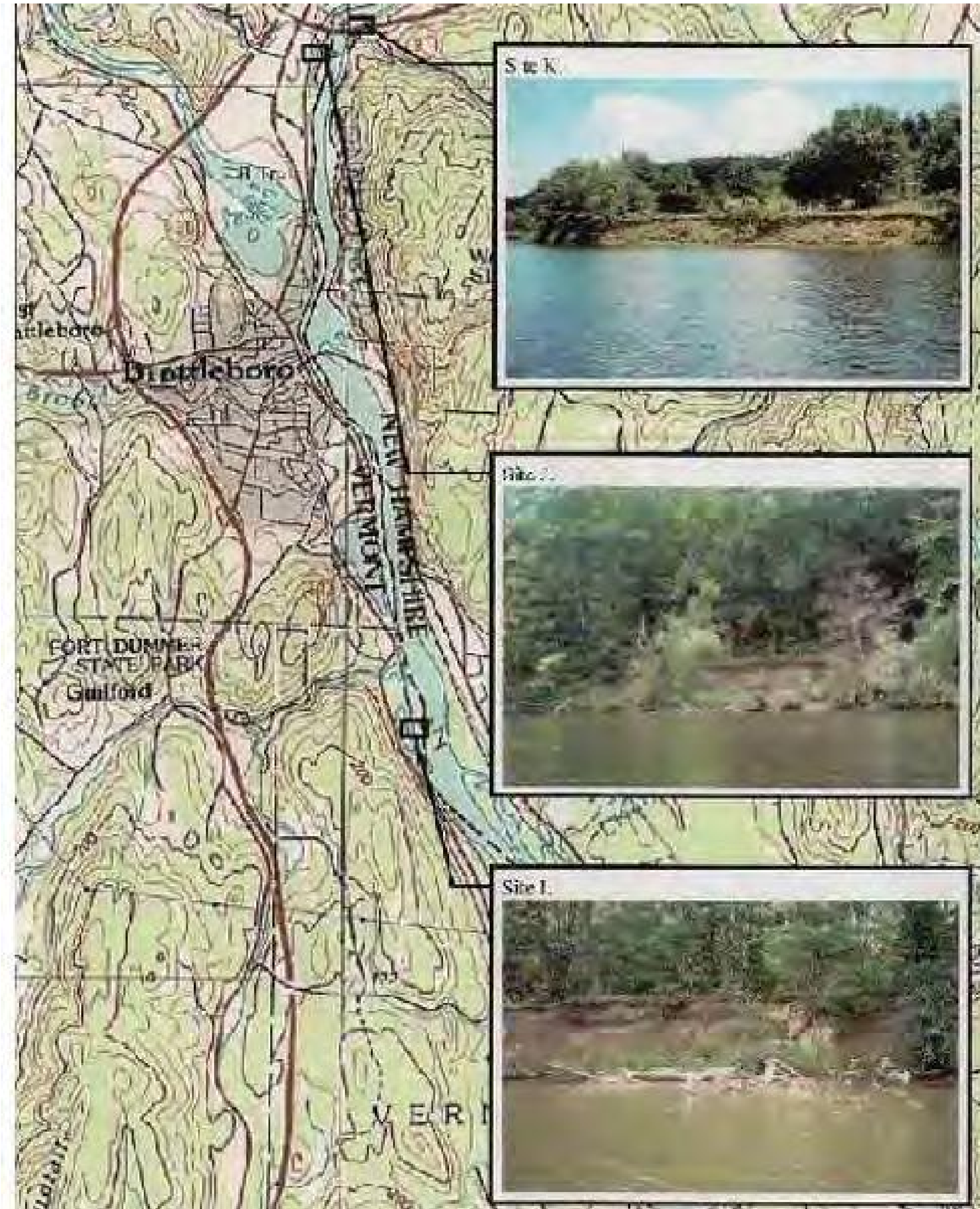

Figure 2.5-3: Erosion sites I-K, Vernon Impoundment (1997)

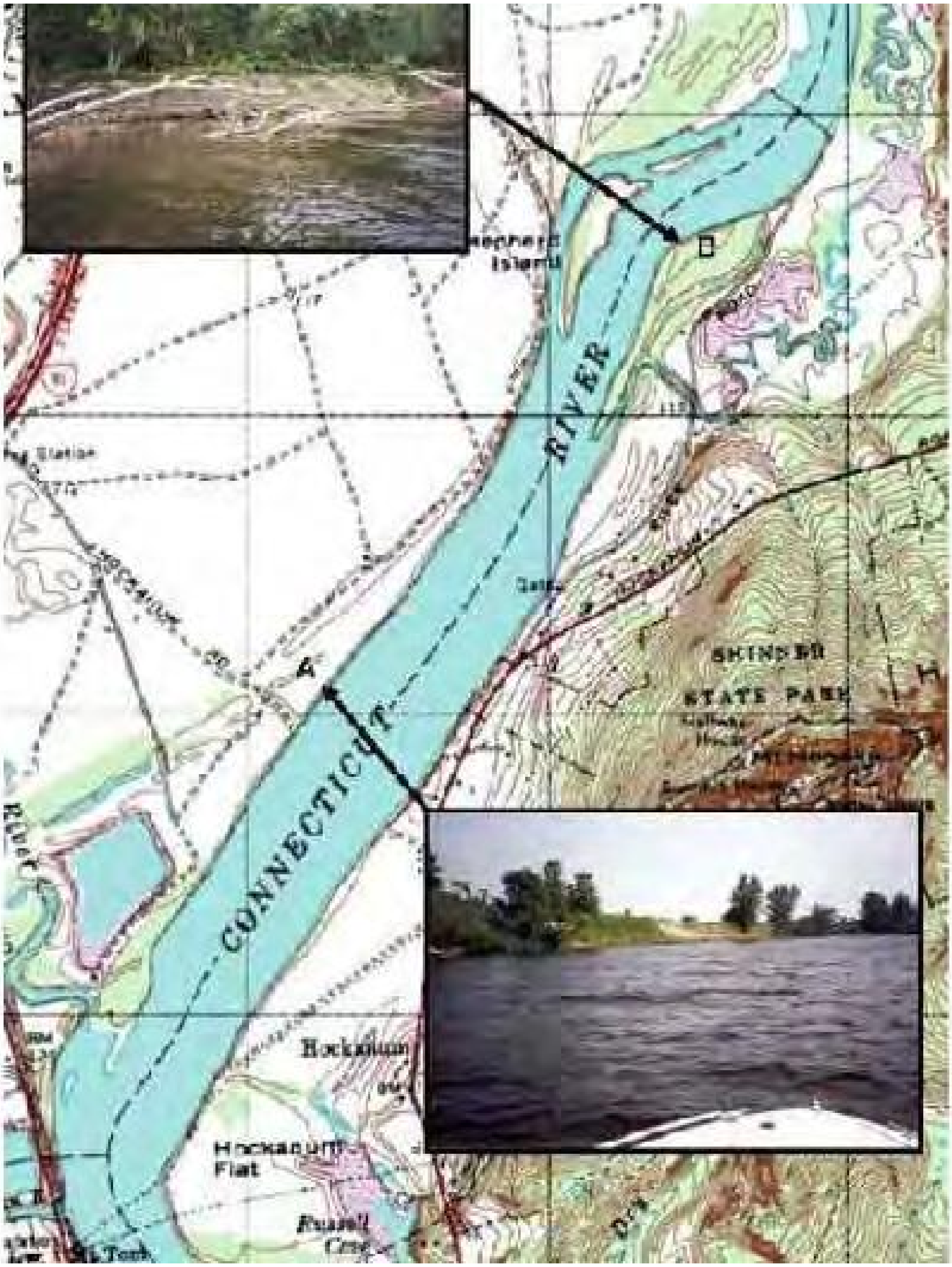

Figure 2.5-4 Erosion sites A and B, Holyoke Impoundment (1997)

Figure 2.5-5: Bellows Falls Impoundment – Location 8 (1997)

Figure 2.5-6: Bellows Falls Impoundment – Location 8 (2008)

Figure 2.5-7: Vernon Impoundment – Location I (1997)

Figure 2.5-8: Vernon Impoundment – Location I (2008)

Figure 2.5-9: Holyoke Impoundment – Location D (1997)

Figure 2.5-10: Holyoke Impoundment – Location D (2008)

2.6 Summary Discussion of the Geomorphology of the Connecticut River

Recent geomorphic history[9] suggests that the Connecticut River was formed by the retreat of a large glacial lake (Lake Hitchcock) following the last ice age. As the Connecticut River formed it cut down through sediment that had been deposited in Lake Hitchcock, changing from a depositional to erosional geomorphic feature. The Connecticut River, with the exception of rare bedrock lined sections such as the French King Gorge, is an alluvial river. Alluvial rivers by definition continue to adjust over time through processes of aggradation, degradation, scour, deposition, lateral migration, and bank erosion. Given this, although the river has reached a state of dynamic equilibrium over time, some degree of erosion is expected to continue. According to Leopold *et al*. (Leopold *et al*., 1964), an ideal natural channel in equilibrium essentially means that the channel size generally retains an overall unchanging average size, with erosion in one place balanced by deposition in another, resulting in a channel changing its position over time. That is, the form of the cross-section is stable, but the position of the channel is not.

Various groups have evaluated and analyzed erosion over time by examining historic maps, aerial photographs, and other datasets ranging from the 1700's to present day. Historic geomorphic comparisons and analyses, while limited by their accuracy, provide valuable context and insights into the modern geomorphology of the Connecticut River. Historic observations (prior to the 1940's) found that the Connecticut River, in some locations, changed hundreds of feet up to approximately 1,000 feet. In recent decades, comparisons of river change using aerial photographs found that measured riverbank changes were typically within the accuracy of the analysis. The observation that the Connecticut River changed more significantly prior to the 1940's than later is believed to be due to three main reasons: (1) historic floods which occurred prior to the 1940's have not occurred of the same magnitude since (e.g., the flood of 1936); (2) construction of flood control projects throughout the Connecticut River watershed following the flood of 1936 have resulted in reduced flood peaks; and (3) construction or raising of mainstem Connecticut River dams have reduced river velocities and shear stresses. Due to these factors, and others, the potential for erosion was higher prior to the 1940's than compared to recent decades.

In addition to the historic geomorphology of the Connecticut River it is also important to understand the modern geomorphology and topography when evaluating causes of erosion. Available USGS maps indicate that 36 named and un-named tributaries enter the TFI while analysis of available LiDAR derived contour information demonstrates that numerous upland erosion features have formed in the land surface in the vicinity of the river. These tributaries and upland erosion features were formed via erosion processes and result in additional inflow to the TFI. When evaluating the 20 most severely eroded sites identified in the ECP (S&A, 1999), as well as several sites recently recommended for stabilization, it was found that the majority of the sites were located at tributaries and upland erosion features. Additionally, through comparisons of historic aerial photographs from 1952 and 1961 it is observed that the majority of these sites were eroded prior to the raising of the Turners Falls Dam and operation of the Northfield Mountain Project.

The dynamic nature of the Connecticut River is evident by how riverbank erosion occurs to one degree or another throughout its length in both free-flowing and impounded reaches. Simons & Associates (2012b) conducted a comparison study to evaluate the varying erosion conditions throughout the Connecticut River from Holyoke Dam (Holyoke, MA) to Pittsburg, NH (240 mile long reach), which included both free flowing and impounded reaches. The study found that the segment of river with the greatest extent of eroding riverbanks was actually the un-impounded northern reach (Pittsburg, NH down to Gilman Dam), further illustrating the alluvial nature of the Connecticut River. This is consistent with the findings of the

[9] Recent geomorphic history is considered as beginning at the end of the last ice age when the Connecticut River formed as Lake Hitchcock drained. Modern or current geomorphology is considered as being the time period over the past few hundred years as development occurred in the watershed.

USACE who noted in their 1979 erosion study that: (1) erosion in free flowing, un-impounded reaches was 1.35 times more likely to occur than in impounded reaches, and (2) the presence of impoundments reduces bank erosion on the order of 34% (USACE, 1979).

3 POTENTIAL CAUSES OF EROSION

One of the main objectives of this study was to evaluate and identify the causes of erosion, and the forces associated with them, throughout the TFI. Erosion occurs when the forces that act on a riverbank exceed the forces that resist movement of riverbank material. Forces acting on a riverbank that may cause erosion range from flowing water against the riverbank to rapid water level fluctuations, ice, boat waves, or land-use, to a name a few. While there are multiple causes of erosion there are also multiple riverbank characteristics and phenomena that resist the forces that can lead to erosion. These could include, among others, the size or size distribution of soil particles that form the riverbank, the cohesion and frictional properties of the soil particles, vegetation, and bank geometry. Riverbank erosion or stability is the result of a complex interaction between riverbank features and characteristics, the forces that cause erosion, and the resistance to erosion that the riverbank provides.

While there are many different forces which can lead to erosion, actual riverbank erosion generally falls into two primary process categories: 1) particle by particle erosion of surficial materials, or 2) mass wasting. Mass wasting is defined as the process where riverbanks experience movement of blocks or other large pieces of bank material downslope under the influence of gravity. Further complicating the riverbank erosion process is that several processes of erosion may be occurring either simultaneously or in sequence at one or more positions vertically or laterally in a segment of riverbank. For example, the river current may gradually erode the lower portion or toe of the riverbank in a particle by particle process undercutting and removing support for the upper riverbank. The upper bank may then collapse, rotate, or slide in a mass-wasting event. The upper bank mass-wasting event could be caused by a number of factors, or combination of factors, including a high flow event, wave action, seepage and positive pore-water pressure.

This section presents discussion of the causes of erosion, and the forces associated with them, which are present throughout the TFI and which were the basis for this study.

3.1 Identification of Causes of Erosion

When initially developing the methodology for this study a list of potential causes of erosion present in the TFI was developed and included in the RSP. This list was developed based on the geomorphic history of the study area as well as past experience conducting FRR's and other geomorphic evaluations of the Connecticut River. The list of potential, contributing causes of erosion presented in the RSP included (in no particular order):

- Hydraulic shear stress due to flowing water;
- Water level fluctuations due to hydropower operations;
- Boat waves;
- Wind waves;
- Land management practices and anthropogenic influences to the riparian zone (e.g., removal of riparian vegetation, cattle grazing to the river's edge, heavily traveled recreation trails, etc.);
- Animals;
- Seepage and piping;
- Freeze-thaw; and

- Ice or debris

This potential list was then finalized and divided in the RSP into two classifications: 1) potential primary causes of erosion, and 2) potential secondary causes of erosion. Potential primary causes of erosion were those which were thought to be most prevalent throughout the TFI based on past experience conducting geomorphic assessments on the Connecticut River, and other alluvial rivers, as well as from a preliminary investigation of existing documentation. In accordance with the RSP, these causes were studied in great detail at a number of detailed study sites throughout the geographic extent of the TFI. In addition to encompassing the geographic extent of the TFI, the detailed study sites also exhibited the full range of riverbank features and characteristics as observed during the 2013 FRR. The results from the various field investigations which occurred at each site were then incorporated into BSTEM or were used for independent, supplemental analyses as described in Section 5. Potential primary causes of erosion included (in no particular order):

- Hydraulic shear stress due to flowing water;
- Water level fluctuations due to hydropower operations;
- Boat waves;
- Land management practices and anthropogenic influences to the riparian zone; and
- Ice

During study plan development it was anticipated that potential secondary causes of erosion such as animals, wind waves, seepage and piping, and freeze-thaw could be present at specific locations in the TFI. Based on the geomorphic understanding of the study area it was anticipated that these potential secondary causes of erosion were likely to have minimal to no influence on erosion in the TFI (other than in any specific locations where they may exist). Accordingly, these causes of erosion were analyzed sufficiently to determine their relative contribution to erosion but not to the level of detail and specificity as the potential primary causes of erosion mentioned above.

When the RSP was filed with FERC (August 14, 2013), ice was initially classified as a secondary cause of erosion. Following the announced closure of VY in 2014 it was anticipated that Connecticut River water temperatures would decrease which could potentially result in the increased presence of ice in the TFI during the winter months. As a result of this potential change to the baseline conditions of the study, ice was elevated from a potential secondary cause of erosion to a potential primary cause and studied in greater detail during the winter of 2015-2016 in accordance with the methodology laid out in the addendum to the RSP.

Each of the potential primary causes of erosion which were found to exist in the TFI, as well as the potential secondary causes of erosion which were observed, are discussed in more detail below.

3.2 Erosion Processes

This section presents a more detailed discussion of the potential primary and secondary causes of erosion, and the forces associated with them, which were found to be present in the TFI based on the results of the analyses conducted as part of this study. Information pertaining to the methods, field studies, and data collection pertaining to each cause can be found in Section 4 while details pertaining to the analysis of each cause, and the forces associated with them, can be found in Section 5. Maps and information classifying the cause(s) of erosion at each riverbank segment throughout the TFI can be found in Section 6.

3.2.1 Hydraulic Shear Stress due to Flowing Water

As water flows downstream along a riverbank it exerts a force, often referred to as shear stress or tractive force. Shear stress can be related to the velocity of flowing water. Shear stress increases with increasing velocity or water surface slope of the flowing water. This force tries to remove soil particles whenever the shear stress exceeds what is called the critical shear stress. For non-cohesive sediment particles (such as sand, gravel, cobbles, and boulders), the critical shear stress depends on the size or weight of the particle. Smaller, lighter particles are easier to move and transport than larger, heavier particles. As the velocity or shear stress increases, the sizes of sediment particles that may be removed and transported increases, as does the quantity of sediment that is transported. Thus, higher flows with higher velocities induce greater stresses on riverbanks causing greater erosion and sediment transport. For cohesive soils (clay and to some degree, silt) electro-chemical bonds cause sediment particles to be bound together such that erosion occurs when hydraulic forces exceed the strength of these bonds. A critical shear stress or permissible velocity may be used to describe the relationship between hydraulic forces (boundary shear stress) and whether or not erosion of cohesive sediments may occur.

In addition to the simple concept of hydraulic shear stress exerted by the flow on riverbanks, there are several natural tendencies of rivers that cause erosion. Irregularities in riverbank alignment and other non-uniform flow conditions may cause the formation of eddies. An eddy is a circular pattern of flow that separates or breaks away from the main direction of flow and is directed towards the riverbank, then upstream along the bank, before completing a circular pattern returning again to a downstream direction farther away from the bank. Eddies may cause riverbank erosion by increasing the velocity of flow adjacent to the bank which may then induce further mass-movement of riverbank material.

Rivers do not flow in a straight path, they meander. Meandering is evident along the Connecticut River as it bends and curves from side to side as it generally flows north to south. Meander bends tend to migrate slowly downstream over time. These bends also become over-extended or compressed resulting in the formation of cutoffs of bends and oxbow lakes. All of these processes result in migration of the river via the ongoing erosion and deposition process.

Geomorphic processes of meandering and hydraulic processes of eddy formation tend to cause riverbank erosion and movement of riverbanks through lateral migration and even avulsion. These processes were considered in the analysis of riverbank erosion in the TFI.

3.2.2 Water Level Fluctuations

The water level in the TFI varies over time as a result of a number of factors including seasonal and other hydrological flow variations and hydropower operations. Water level variations due to hydrological flow variations can include snowmelt and rainfall runoff from the watershed which can vary on a daily (or shorter) basis to seasonally. Water level variations due to hydrologic events take hours, days or weeks and range from a few feet up to as many as 10 feet or more in magnitude in major runoff events. Storm events or snow melt, from the upstream watershed or tributaries, drive these major flow variations.

Water levels in the TFI also vary due to hydropower operations from three projects that effect flow and water level, including the Vernon Hydroelectric Project at the upstream end of the TFI, Northfield Mountain (upstream of the French King Gorge), and Turners Falls Hydroelectric Project at the downstream end of the TFI at Turners Falls Dam. Fluctuations due to the various hydropower operations occur on an hourly basis with a magnitude on the order of 3 to 5 feet over a daily cycle; the FERC license permits a 9 foot fluctuation as measured as the Turners Falls Dam.

As water rises, it infiltrates into the riverbank and, if sustained over a sufficient period of time, the high water levels can saturate the soil to a certain depth. Water in the pore spaces within the riverbank material increases the weight of the soil resulting in increased gravitational forces. The added weight can, in some instances, overcome forces resisting movement of riverbank material to the point where pieces of material break loose and fall or slide down the riverbank when the water level recedes. As the water level falls, water levels in the bank drop. Some may seep back out of the bank through processes of seepage and piping (see Section 3.2.7). Seepage and piping can induce hydraulic forces that by themselves may cause erosion.

3.2.3 Boat Waves

Boat or wind waves can result in water surface fluctuations of relatively small amplitude (on the order of a few inches up to about 1 foot) and short frequency (on the order of seconds or less).

Wind waves on the Connecticut River are relatively small and typically do not form breaking waves since the wind cannot act over a significant length of water (called fetch) because the river lies at the bottom of a valley protected on both sides by mountains. This is particularly true of winds that blow in the west to east direction, across the river that primarily flows north to south. Fetch is also relatively short for winds that blow in the north-south direction because the river flows around bends thereby limiting the length over which wind can build waves. Given this, wind waves were generally not found to be a factor in erosion processes throughout the TFI and are not discussed further in this report.

While boat and wind waves have some similarities, boat waves, particularly those that are formed close to the shore, can cause an impact and greater disturbance than just a simple fluctuation. Boat waves tend to be larger in amplitude than wind waves and were observed to travel across the water surface impacting the riverbanks in the TFI. Wave energy is converted to a shear stress acting as a vector sum with the shear stress due to flow. The repeated crashing of boat waves against the riverbank can result in repeated particle by particle erosion until, eventually, a mass wasting event occurs due to the undermined bank. This can be especially true when water levels are elevated and/or the boat waves are repeatedly crashing against the same elevation of the bank for extended periods of time. This is particularly true when the waves impact the toe of the upper bank (or higher) as opposed to the flat lower bank (beach).

3.2.4 Land Management Practices and Anthropogenic Influences to the Riparian Zone

Land-use or management practices may affect the stability of riverbanks. A healthy riparian zone including vegetation that dampens the velocity and effective stress acting on the bank material, and attenuates waves near the riverbank that can significantly reduce erosion. In addition, the fine-root structure helps bind the soil particles together; further increasing the resistance to hydraulic forces. Increased shear strength is also provided by root reinforcement within the upper bank. To the extent that riparian vegetation is impacted by land-use, land management practices, or anthropogenic influences the erosion resistance from vegetation may be likewise reduced. Vegetation may be cleared for agriculture, housing or other types of development. On the other hand, erosion protection or riverbank stabilization may prevent or minimize erosion in segments of the river. It is also recognized that erosion protection at a given location along a river may adversely affect adjacent riverbank areas in the vicinity of where erosion protection has been developed.

3.2.5 Ice

Ice may cause erosion or damage to riparian vegetation which can cause erosion. Sheet ice may increase the velocity or flow of water in the area below the ice and adjacent to the riverbank. With changing water levels, it may pull or scrape vegetation. If ice floes form during ice breakup, moving blocks of ice can again scrape, damage, or even shear off vegetation. Ice floes may also impact directly against the bank moving or breaking off blocks of soil. Through damage or removal of vegetation or direct displacement of the soil itself, ice has the capacity to erode riverbanks.

In addition, water is found in at least some of the pore spaces between soil particles in riverbanks. During sufficiently cold weather (in terms of temperature and duration), some of the water in riverbanks can freeze. As water freezes it expands thereby loosening soil particles or causing an expansion of the space between particles or causing cracks in the soil matrix. Additional water can find its way into larger spaces and with additional freeze-thaw cycles more disruption of the soil matrix can occur. This freeze-thaw process is a common cause of damage to pavement on roads. In cold climates, freeze-thaw can adversely affect riverbank stability allowing flow-related forces or gravity to have an enhanced erosive effect on riverbanks.

3.2.6 Animals

As noted in the RSP, animals can be both a potential primary and/or secondary cause of erosion. Cattle grazing to the river's edge or the removal or trampling of vegetation resulting from animal trails leading to the river are potential land management or anthropogenic factors which were evaluated as potential primary causes of erosion. These activities can lead to runoff issues, gullying, and damage to the soil matrix which all contribute to bank instability. Wild animals and birds (potential secondary cause) can also contribute to bank instability and erosion; an example of which are animals that burrow into riverbanks which may lead to concentrated points of seepage or direct damage to the bank.

3.2.7 Seepage and Piping

When the flow and water level is higher than the water level in the ground, water can infiltrate laterally into the riverbank. Either when high water recedes or when the ground-water table is higher than the river, a hydraulic gradient drives water from the surrounding ground towards the river. Water moves through the soil but may not drain as quickly as the water level. The pressure gradient can weaken or act against the standing riverbanks causing blocks of sediment to loosen, drop, or slide. During periods of declining stage, seepage of water occurs towards the river and out of the riverbanks. This water may find a layer of coarser sediment, with greater hydraulic conductivity, where seepage flows with greater velocity through the riverbank. Seepage of water through the soil in general, or piping through confined layers or concentrated areas of flow, can move soil particles causing internal erosion or weakening. This can lead to the development of undercuts and to greater movement of blocks of soil acted on by gravity.

While a few limited areas of seepage were identified flowing over the lower bank or beach in the TFI, these areas did not exhibit significant erosion or sloughing due to seepage related erosion on the upper riverbank areas. As such, seepage and piping were not found to be a significant factor in erosion processes throughout the TFI at the detailed study sites and are not discussed further in this report. Groundwater data collected from monitoring wells adjacent to the river are discussed in Section 5.5.2.1 as it pertains to the impact of water level fluctuations in the TFI.

4 FIELD STUDIES, DATA COLLECTION, AND MODELING BACKGROUND

Various geomorphic, geotechnical, hydraulic, and hydrologic datasets were developed in the TFI during the 1990's and 2000's which provided a valuable foundation for this study. While the existing datasets proved useful, data gaps were identified during the data gathering and literature review conducted as part of RSP Task 1. Based on these data gaps, additional field studies and data collection efforts were identified and completed in order to satisfy the objectives established in the RSP. Additional field studies and data collection efforts were a combination of investigations associated with other relicensing studies (e.g., Study No. 3.1.1, 3.2.2, etc.) and those unique to this study (e.g., BSTEM input parameters). Field studies and data collection efforts which were conducted in accordance with RSP Task 4 included:

- Compilation of Project operations and USGS data (water surface elevation, flow, etc.) for the period 2000-2014;
- 2013 Full River Reconnaissance Survey (Study No. 3.1.1) which characterized the riverbank features, characteristics, and erosion conditions throughout the TFI;
- Bathymetric surveys of the TFI to support development of the hydraulic models (Study No. 3.2.2)
- Development of a HEC-RAS model of the TFI (Study No. 3.2.2);
- Development of a River2D model of the TFI;
- Compilation of annual historic cross-section surveys and development of new cross-section surveys for the long-term fixed riverbank transects (2000-2014)[10] and newly identified detailed study sites (2014 and 2015);
- Various input datasets for BSTEM;
- Suspended sediment monitoring and sampling (Study No. 3.1.3); and
- Investigation of ice and its potential impact on riverbank processes

Each of these field studies or data collection efforts are discussed in greater detail in the following sections. The data yielded from these efforts, combined with the considerable amount of existing information, provided the geomorphic, geotechnical, hydraulic, and hydrologic data needed to satisfy the goals and objectives of this study, including determining the impact of Project operations on erosion and bank instability. As discussed in Section 5, these datasets were used for a range of analyses as part of the three-level analysis approach previously discussed.

Field studies and data collection efforts conducted as part of this study occurred at a number of detailed study sites located throughout the geographic extent of the TFI.[11] Detailed study sites were identified in 2014 in consultation with stakeholders, FERC, and MADEP in accordance with FERC's SPDL. The

[10] While some long-term fixed riverbank transects have been surveyed as far back as the 1990's, only the survey data from 2000-2014 was utilized for this study as this was the period modeled in BSTEM.
[11] Due to accessibility issues, ice monitoring and boat wake data collection occurred at locations other than the detailed study sites.

detailed study site selection process was presented in the 2014 report titled *Study No. 3.1.2 Northfield Mountain/Turners Falls Operations Impact on Existing Erosion and Bank Instability – Selection of Detailed Study Sites – September 2014* (FirstLight, 2014b). A summary of this process is presented in the following section.

4.1 Selection of Detailed Study Sites

To gain a thorough understanding of the causes of erosion, the forces associated with them, and their relative importance at a particular location, FirstLight developed a methodology to identify and select a number of detailed study sites where investigation and analyses would occur as part of this study. Data collected at each of the detailed study sites were used as input parameters for BSTEM as well as other analyses associated with the three-level approach. In-depth investigation at the detailed study sites was typically limited to the potential primary causes of erosion, and the forces associated with them, although observations of any potential secondary causes of erosion were made if such causes were present. The final set of detailed study sites represented both existing permanent transects and newly identified sites. The study sites spanned the geographic extent of the TFI and encompassed the full range of riverbank features, characteristics, and erosion conditions observed during the 2013 FRR.

The final set of detailed study sites were selected based on a four step methodology:

1. Evaluate Existing, Permanent Transects and Identify Calibration and/or Representative Locations for Detailed Study;

2. Identify Supplemental Representative Locations for Detailed Study;

3. Evaluate the Range of Riverbank Features and Characteristics of the Representative Locations Selected for Detailed Study; and

4. Evaluate the Geographic Distribution of the Representative Locations Selected for Detailed Study

An existing, permanent transect is a permanently established cross-section that has been surveyed from one bank, across the river, to the other bank. These transects were established in areas where erosion had been known to occur dating back to the 1990's and have generally been surveyed annually. Typically a benchmark with a known vertical and horizontal datum is placed on the endpoints such that future surveys can be compared. Due to varying hydraulic and geomorphic conditions found along a river, riverbank features, characteristics, and erosion conditions can vary from one bank to the other at a given transect. As such, each transect represented two potential detailed study points. For the purposes of this study, a detailed study point was defined as the specific location (i.e. right or left bank) where detailed investigation, field data collection, and analysis occurred.

Existing permanent, transects were evaluated and compared against the results of the 2013 FRR at which time they were classified as: (1) calibration only sites; (2) both calibration and representative sites; or (3) eliminated from consideration. *Calibration sites* were defined as detailed study sites established at an existing, permanent transect location where data collection would be used to calibrate BSTEM. Establishing these sites at the existing, permanent transects provided the opportunity to calibrate BSTEM with actual erosion amounts or changes in bank geometry as it has occurred over a period of historic flows and water level data. *Representative sites* were defined as detailed study sites established throughout the TFI at locations that exhibit a range of representative features, characteristics, and erosion conditions. These sites did not have repetitive surveys for calibration of BSTEM. Calibration sites could only exist at existing, permanent transects while representative sites can exist anywhere in the TFI. The selected existing, permanent transects were then compared against a table of riverbank characteristics of interest to identify potential gaps.

Riverbank features and characteristics identified during this gap analysis were then supplemented with additional representative detailed study points. Supplemental representative detailed study points were proposed based on the results of the detailed geomorphic and geotechnical assessments conducted during the 2013 FRR land-based survey as well as the results of the 2013 FRR boat-based survey. The newly identified supplemental representative detailed study points were selected at only one bank, however, full cross-section surveys were collected at each location. The combination of representative existing, permanent transects and supplemental representative detailed study points resulted in a comprehensive set of locations which were representative of the riverbank features and characteristics of interest found throughout the TFI.

Once the list of representative locations selected for detailed study was selected the range of riverbank features and characteristics of those locations were evaluated to ensure they were representative of conditions found throughout the TFI. In order to be considered representative, the detailed study sites must have exhibited the range of riverbank characteristics of interest and met the following criteria:

- Locations where riverbanks are stable (including at least one site where bank stabilization has occurred as a result of the ECP and at least one site that is naturally stable with no bank stabilization work present);
- Locations where the potential for future erosion is low;
- Locations where the potential for future erosion is high; and
- Locations where active erosion is occurring

Following the completion of the representativeness assessment, the geographic distribution of the representative locations selected for detailed study was evaluated to ensure they were appropriately distributed throughout the TFI.

After completing this four step methodology FirstLight presented a list of proposed representative and calibration study sites to MADEP, CRWC, FRCOG, CRSEC, and the New Hampshire Department of Environmental Services (NHDES) for review and comment as per FERC's SPDL (FERC, 2013). After receiving written comments and meeting with the MADEP and Stakeholders, FirstLight updated and finalized the location of detailed study sites based on the feedback received.[12] After filing the final set of detailed study site locations with FERC, no further comments were received from MADEP or the Commission.

The final list of detailed study sites established for this study included 25 locations throughout the geographic extent of the TFI which encompassed a representative range of riverbank features, characteristics, and erosion conditions. Of the 25 detailed study sites, 16 were classified as representative (of which 7 are both calibration and representative), and 9 were classified as calibration sites. In other words, 16 detailed study sites are located at existing, permanent transects while 9 were established at new locations identified as a result of the 2013 FRR. Table 4.1-1 demonstrates the riverbank features and characteristics of interest and which detailed study site(s) exhibits those traits while Table 4.1-2 and 4.1-3 provide additional details about each site. The location of the detailed study sites is depicted in Figures 4.1-1 and 4.1-2.

[12] Meetings were held on June 4, 2014 at MADEP offices in Springfield, MA and June 24, 2014 and August 4, 2014 at the Northfield Mountain Visitors Center.

As illustrated in Table 4.1-1, the selected representative sites have a balanced distribution over the various Stages of Erosion and Extents of Current Erosion found throughout the TFI. In regard to the Stage of Erosion, of the 16 representative sites, two are located where Potential Future Erosion exists, five at Actively Eroding sites, four at Eroded sites, and five at Stable sites.[13] In regard to the Extent of Erosion, six representative sites are located where None/Little Erosion exists, five where Some Erosion exists, three where Some to Extensive Erosion exists, and two where Extensive Erosion exists. In addition, a broad range of significant upper and lower riverbank features including vegetation, slope, sediment, and bank height are well represented. Finally, as demonstrated in Figures 4.1-1 and 4.1-2 the final list of detailed study sites adequately covers the geographic extent of the TFI.

A discussion of how the detailed study sites were selected and the full results of this process are found in, *"Relicensing Study 3.1.2 Northfield Mountain/Turners Falls Operations Impact on Existing Erosion and Potential Bank Instability Selection of Detailed Study Sites – September 2014"* (FirstLight, 2014b). Field efforts associated with Study No. 3.1.2 began in July 2014 and continued through September 2014. Data collection was completed in the summer of 2015. Data collection efforts are discussed in detail in the ensuing sections. Detailed site sketches of each detailed study site developed by Kit Choi (geotechnical engineer) are found in Volume III (Appendix D).

[13] Sites classified as Stable represent locations that were Stable at the time of observation.

Table 4.1-1: Summary of Riverbank Features and Characteristics – Representative Locations for Detailed Study

FEATURES	CHARACTERISTICS[14]					
Upper Riverbank Slope	**Overhanging** 26, 87(B)	**Vertical** 2L, 21, 29, 75(B)	**Steep** 7L, 8B-L, 12(B), 21, 26, 29, 119(B)	**Moderate** 4L, 7R, 10R, 18, 303B, BC-1R	Flat	
Upper Riverbank Height	Low	**Medium** 4L, 303B	**High** 2L, 7L, 7R, 8B-L, 10R, 12(B), 18, 21, 26, 29, 75(B), 87(B), 119(B), BC-1R			
Upper Riverbank Sediment[15]	Clay	**Silt/Sand** 2L, 4L, 7L, 7R, 8B-L, 10R, 12(B), 18, 21, 26, 29, 75(B), 87(B), 119(B), 303B, BC-1R	Gravel	Cobbles	Boulders	Bedrock
Upper Riverbank Vegetation	**None to Very Sparse**	**Sparse** 12(B), 75(B), 87(B), 119(B)	**Moderate** 2L, 8B-L, 21	**Heavy** 4L, 7L, 7R, 10R, 18, 26, 29, 303B, BC-1R		
Lower Riverbank Slope[16]	Vertical	Steep	**Moderate** 7R, 10R	**Flat/Beach** 2L, 4L, 7L, 8B-L, 12(B), 18, 21, 26, 29, 75(B), 87(B), 119(B), 303B, BC-1R		

[14] Categories that are highlighted in yellow were identified as characteristics that are indicative of areas where active erosion is most likely to occur or the potential for future erosion is high. Highlighted categories were identified based on review of historic geomorphic data and the results of the 2013 FRR. Transects and detailed study points that will be used for investigation and analyses associated with Study No. 3.1.2 are based on the highlighted categories.
[15] While clay, gravel, cobble, boulder, and bedrock upper riverbank sediments may exist in some locations throughout the Impoundment, these locations are rare and therefore are not representative of riverbank features and characteristics found in the study area. As such, these characteristics are not of interest to the objectives of this study.
[16] Vertical and Steep lower riverbank slopes are typically indicative or areas where active erosion is occurring or the potential for future erosion is high and therefore would normally be highlighted in yellow. These categories are not highlighted, however, as these specific riverbank conditions do not exist in the Impoundment.

FEATURES	CHARACTERISTICS[14]					
Lower Riverbank Sediment	Clay	**Silt/Sand** 2L, 4L, 7L, 8B-L, 12(B), 18, 26, 29, 75(B), 87(B), 119(B), 303B, BC-1R	**Gravel** 21	**Cobbles** 10R	**Boulders** 7R	Bedrock
Lower Riverbank Vegetation	**None to Very Sparse** 2L, 4L, 7L, 7R, 8B-L, 12(B), 18, 21, 26, 29, 75(B), 87(B), 119(B), BC-1R	**Sparse** 10R	**Moderate**	**Heavy** 303B		
Stage of Erosion	**Potential Future Erosion** 7L, 8B-L	**Active Erosion** 12(B), 21, 26, 29, 75(B)	**Eroded** 18, 2L*, 87(B), 119(B)	Stable 4L, 7R, 10R, 303B, BC-1R		
Extent of Current Erosion	**None/Little** 4L, 7L, 7R, 10-R, 303B, BC-1R	**Some** 2L, 8B-L, 18, 26, 29	**Some to Extensive** 21, 87(B), 119(B)	**Extensive** 12(B), 75(B)		

Table 4.1-2: Overview of Representative and Calibration Locations for Detailed Study

Location ID	Source	Bank[17]	Representative or Calibration Site	Comments
BC-1R	Existing, Permanent Transect	Right Bank	Both	Surveyed transect at the entrance to Barton Cove
2L	Existing, Permanent Transect	Left Bank	Both	Surveyed transect just downstream of major tributary (Ashuelot River), erosion with recent stabilization using vegetation only.
3L	Existing, Permanent Transect	Left Bank	Calibration	Surveyed transect, right bank – stabilized (2007, Kendall site), left bank – located downstream of Kendall with multiple types of erosion and indicators of potential erosion. Both banks of the surveyed transect includes an area with erosion occurring prior to stabilization in 2007 and stabilization since then with the opposite bank experiencing several types of erosion and potential erosion indicators with concurrent survey data.
3R	Existing, Permanent Transect	Right Bank	Calibration	
4L	Existing, Permanent Transect	Left Bank	Both	Surveyed transect – cross-section shows some change and left bank exhibits potential erosion indicators and erosion (right bank stable with limited potential indicators of future erosion)
5CR	Existing, Permanent Transect	Right Bank	Calibration	Surveyed transect with right bank showing erosion and multiple types of potential erosion, left bank previously stabilized by COE experimental techniques (tires).
6AL	Existing, Permanent Transect	Left Bank	Calibration	Surveyed transect at a location of erosion and heavy boat use in the past with both banks stabilized (Flagg, 2000 and Skalski, 2004). An island bank that is not stabilized is also included to be studied.
6AR	Existing, Permanent Transect	Right Bank	Calibration	
7L	Existing, Permanent Transect	Left Bank	Both	Surveyed transect with one forested high bank and the other a farmed terrace with indicators of potential future erosion.
7R	Existing, Permanent Transect	Right Bank	Both	
8BL	Existing, Permanent Transect	Left Bank	Both	Surveyed transect with one bank with erosion and indicators of potential future erosion and other bank with erosion that is in the process of being stabilized with current techniques of large woody debris, built-up toe and vegetation (Wallace, Bathory/Gallagher, 2012). Detailed study will occur at both banks of the transect.
8BR	Existing, Permanent Transect	Right Bank	Calibration	
9R	Existing, Permanent Transect	Right Bank	Calibration	Surveyed transect with right bank that had eroded but stabilized with preventative maintenance measures (Campground Point, 2008)
10L	Existing, Permanent Transect	Left Bank	Calibration	Surveyed transect with erosion occurring before stabilization in 2001-2002 on right bank (Urgiel upstream), stable left bank. A recent vertical shift in the bank has developed both through the stabilized site and upstream which is of interest in understanding and monitoring.
10R	Existing, Permanent Transect	Right Bank	Both	
11L	Existing, Permanent Transect	Left Bank	Calibration	Surveyed transect through island, left bank and bank of island exhibits erosion and potential erosion indicators
18	FRR Land-based Survey	Left Bank	Representative	Land-based point located between surveyed Transects 2 and 3, multiple indicators of potential erosion
21	FRR Land-based Survey	Right Bank	Representative	The land-based point is experiencing more than one type of erosion and multiple indicators of potential erosion and may be considered for some type of future stabilization
26	FRR Land-based Survey	Right Bank	Representative	Land-based site exhibits various types of erosion and potential future erosion and may represent bank conditions prior to stabilization of transect 10 - right bank.
29	FRR Land-based Survey	Right Bank	Representative	Located between transects 4 and 5A, erosion and multiple indicators of potential erosion
12B	FRR Boat-based Survey	Left Bank	Representative	Boat-based segment with extensive, active erosion and limited vegetation; located downstream of French King Gorge and just upstream of Barton Cove
75B	FRR Boat-based Survey	Left Bank	Representative	Boat-based segment with extensive, active erosion just downstream of the Northfield Mountain Tailrace.

[17] Defined as looking downstream

Location ID	Source	Bank[17]	Representative or Calibration Site	Comments
87B	FRR Boat-based Survey	Left Bank	Representative	Boat-based segment exhibits eroded conditions and several indicators of potential future erosion; located upstream of Northfield Mountain Tailrace and a short distance downstream of Shearer stabilization site
119B	FRR Boat-based Survey	Left Bank	Representative	Boat-based segment exhibits eroded conditions and several indicators of potential future erosion; located near the downstream end of Kidds Island
303B	FRR Boat-based Survey	Left Bank	Representative	Boat-based segment located downstream of the Ashuelot River confluence. Segment exhibits Heavy lower riverbank vegetation and Medium upper riverbank height.
9	*Supplemental sites selected based on the results of the 2013 FRR*			
7	*Existing, permanent transect sites that will be used as both representative and calibration locations*			
9	*Existing, permanent transect sites that will be used as supplemental calibration locations*			
25				

Table 4.1-3: Summary of Riverbank Features and Characteristics – Representative and Calibration Locations for Detailed Study

Location ID	Bank	Source	Representative or Calibration	UPPER RIVERBANK				LOWER RIVERBANK			Type of Erosion	Indicator(s) of Potential Erosion	Stage of Erosion	Extent of Current Erosion
				Slope	Height	Sediment	Vegetation	Slope	Sediment	Vegetation				
BC-1R	Right Bank	Existing, Permanent Transect	Both	Moderate	High	Silt/Sand	Heavy	Flat/Beach	Silt/Sand	None/Very Sparse	Undercut	Creep/Leaning Trees	Stable	None/Little
2L	Left Bank	Existing, Permanent Transect	Both	Vertical	High	Silt/Sand	Moderate	Flat/Beach	Silt/Sand	None to Very Sparse	Rotational Slump	Creep/Leaning Trees, Overhanging	Eroded	Some
3L	Left Bank	Existing, Permanent Transect	Calibration	Moderate	Low	Silt/Sand	Heavy	Flat/Beach	Silt/Sand	None to Very Sparse	Undercut, Rotational Slump	Creep/Leaning Trees, Overhanging	Eroded	Some
3R	Right Bank	Existing, Permanent Transect	Calibration	Moderate	High	Silt/Sand	Heavy	Moderate	Gravel	None to Very Sparse	-	-	Stable	None/Little
4L	Left Bank	Existing, Permanent Transect	Both	Moderate	Medium	Silt/Sand	Heavy	Flat/Beach	Silt/Sand	None to Very Sparse	-	Creep/Leaning Trees	Stable	None/Little
5CR	Right Bank	Existing, Permanent Transect	Calibration	Steep	High	Silt/Sand	Moderate	Flat/Beach	Silt/Sand	None to Very Sparse	Slide or Flow	Overhanging Bank, Exposed Roots, Creep/Leaning Trees	Eroded	Some
6AL	Left Bank	Existing, Permanent Transect	Calibration	Moderate	High	Silt/Sand	Heavy	Moderate	Cobbles	None to Very Sparse	-	-	Stable	None/Little
6AR	Right Bank	Existing, Permanent Transect	Calibration	Steep	High	Silt/Sand	Heavy	Flat/Beach	Silt/Sand	Heavy	-	-	Stable	None/Little
7L	Left Bank	Existing, Permanent Transect	Both	Steep	High	Silt/Sand	Heavy	Flat/Beach	Silt/Sand	None to Very Sparse	Undercut	Creep/Leaning Trees	Potential Future Erosion	None/Little
7R	Right Bank	Existing, Permanent Transect	Both	Moderate	High	Silt/Sand	Heavy	Moderate	Boulders	None to Very Sparse	-	-	Stable	None/Little
8BL	Left Bank	Existing, Permanent Transect	Both	Steep	High	Silt/Sand	Moderate	Flat/Beach	Silt/Sand	None to Very Sparse	Undercut	Creep/Leaning Trees, Exposed Roots, Overhanging Bank	Potential Future Erosion	Some
8BR	Right Bank	Existing, Permanent Transect	Calibration	Steep/Overhanging	High	Silt/Sand	Heavy	Flat/Beach	Gravel	None to Very Sparse	-	Overhanging	In process of stabilization	None/Little
9R	Right Bank	Existing, Permanent Transect	Calibration	Moderate	High	Silt/Sand	Moderate	Flat/Beach	Silt/Sand	None to Very Sparse	-	Creep/Leaning Trees	Stable	None/Little
10L	Left Bank	Existing, Permanent Transect	Calibration	Moderate	High	Silt/Sand	Heavy	Flat/Beach	Silt/Sand	None to Very Sparse	-	-	Stable	None/Little
10R	Right Bank	Existing, Permanent Transect	Both	Moderate	High	Silt/Sand	Heavy	Moderate	Cobbles	Sparse	-	-	Stable	None/Little
11L	Left Bank	Existing, Permanent Transect	Calibration	Moderate	High	Silt/Sand	Heavy	Flat/Beach	Silt/Sand	None to Very Sparse	Undercut	Undercut, Creep/Leaning trees	Stable	None/Little

Location ID	Bank	Source	Representative or Calibration	UPPER RIVERBANK				LOWER RIVERBANK			Type of Erosion	Indicator(s) of Potential Erosion	Stage of Erosion	Extent of Current Erosion
				Slope	Height	Sediment	Vegetation	Slope	Sediment	Vegetation				
18	Left Bank	FRR Land-based Survey	Representative	Moderate	High	Silt/Sand	Heavy	Flat/Beach	Silt/Sand	None/Very Sparse	Undercut	Undercut, Exposed Roots, Creep/Leaning Trees	Eroded	Some
21	Right Bank	FRR Land-based Survey	Representative	Steep (some vertical)	High	Silt/Sand	Moderate	Flat/Beach	Gravel, Silt/Sand	None/Very Sparse	Rotational Slump, Undercut	Undercut, Exposed Roots, Creep/Leaning Trees	Active	Some to extensive
26	Right Bank	FRR Land-based Survey	Representative	Steep/Overhanging	High	Silt/Sand	Heavy	Flat/Beach	Silt/Sand	None/Very Sparse	Rotational Slump, Undercut	Undercut, Exposed Roots, Creep/Leaning Trees	Active	Some
29	Right Bank	FRR Land-based Survey	Representative	Steep (near vertical)	High	Silt/Sand	Heavy	Flat/Beach	Silt/Sand	None/Very Sparse	Rotational Slump, Undercut	Undercut, Exposed Roots, Creep/Leaning Trees	Active	Some
12B	Left Bank	FRR Boat-based Survey	Representative	Steep	High	Silt/Sand	Sparse	Flat/Beach	Silt/Sand	None to Very Sparse	Undercut	Exposed Roots, Overhanging Bank	Active	Extensive
75B	Left Bank	FRR Boat-based Survey	Representative	Vertical	High	Silt/Sand	Sparse	Flat/Beach	Silt/Sand	None to Very Sparse	Topple, Overhanging Bank	Creep/Leaning Trees, Overhanging Bank	Active	Extensive
87B	Left Bank	FRR Boat-based Survey	Representative	Overhanging	High	Silt/Sand	Sparse	Flat/Beach	Silt/Sand	None to Very Sparse	Undercut, Rotational Slump	Exposed Roots, Creep/Leaning Trees, Overhanging Bank	Eroded	Some to Extensive
119B	Left Bank	FRR Boat-based Survey	Representative	Steep	High	Silt/Sand	Sparse	Flat/Beach	Silt/Sand	None to Very Sparse	Slide or Flow	Exposed Roots, Creep/Leaning Trees, Overhanging Bank	Eroded	Some to Extensive
303B	Left Bank	FRR Boat-based Survey	Representative	Moderate	Medium	Silt/Sand	Heavy	Flat/Beach	Silt/Sand	Heavy	-	-	Stable	None/Little

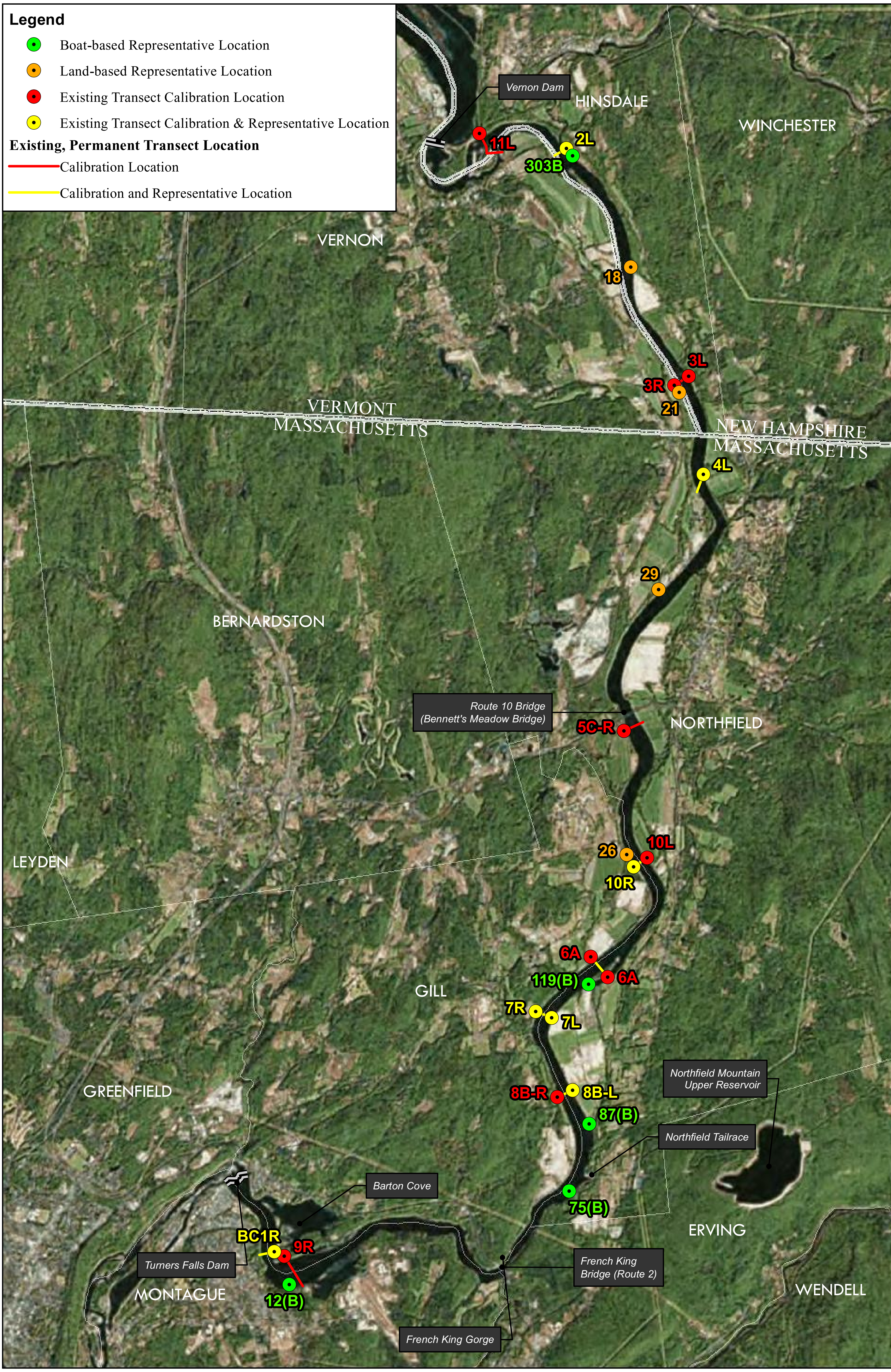

FirstLight Power Resources

FIRSTLIGHT HYDRO GENERATING COMPANY
Northfield Mountain Pumped Storage Project No. 2485
Turners Falls Hydroelectric Project No. 1889

STUDY 3.1.2

Figure 4.1-1 :
Detailed Study Sites
Turners Falls Impoundment

Service Layer Credits: Source: Esri, DigitalGlobe, GeoEye, Earthstar Geographics, CNES/Airbus DS, USDA, USGS, AEX, Getmapping, Aerogrid, IGN, IGP, swisstopo, and the GIS User Community

Path: W:\gis\studies\3_1_2\maps\final_report\figure_4_1-1.mxd

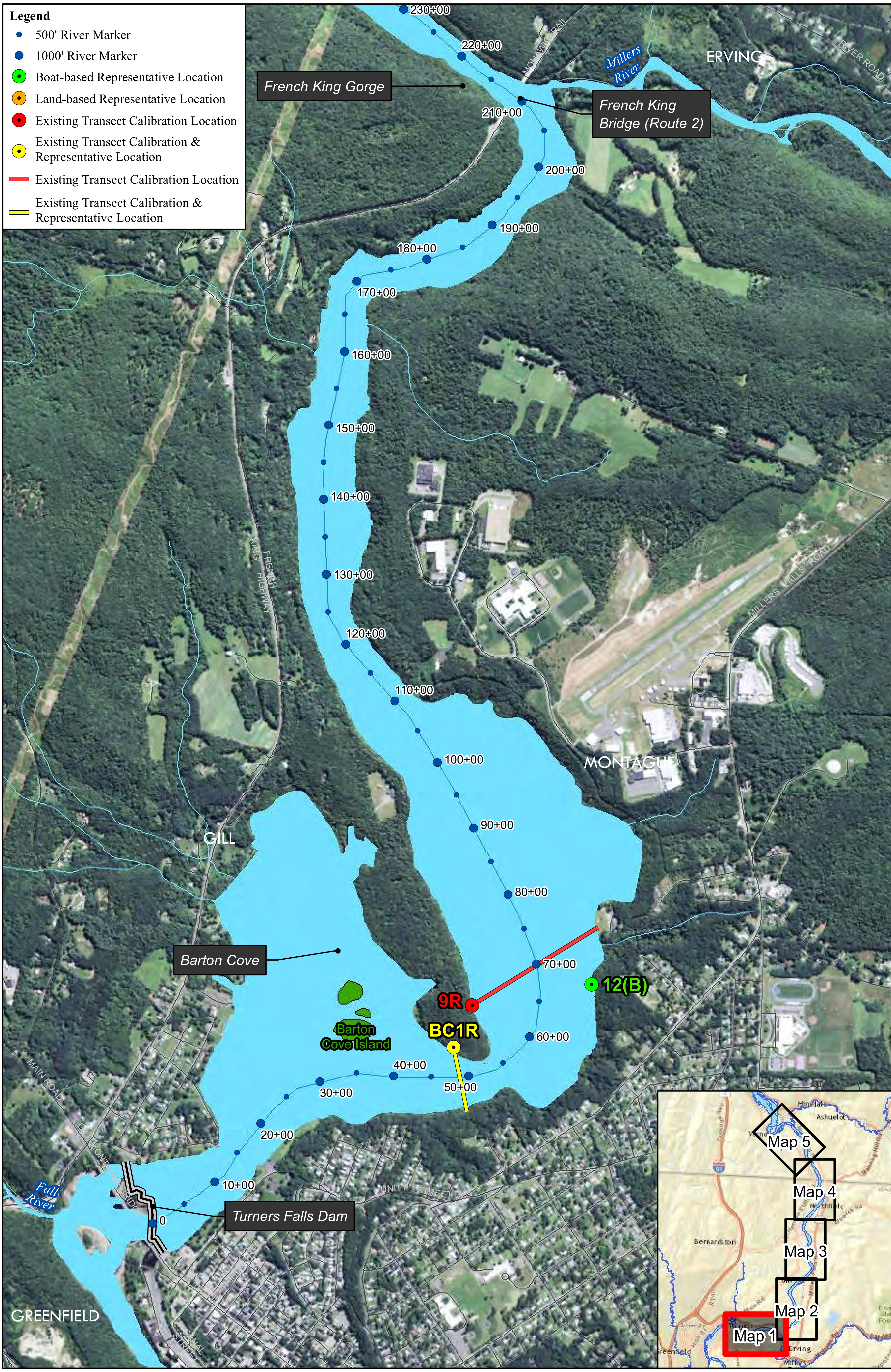

FIRSTLIGHT HYDRO GENERATING COMPANY
Northfield Mountain Pumped Storage Project No. 2485
Turners Falls Hydroelectric Project No. 1889

STUDY 3.1.2

0 625 1,250 2,500 Feet

Figure 4.1-2:
Representative & Calibration Locations for Detailed Study
Map 1

Service Layer Credits: Sources: Esri, HERE, DeLorme, USGS, Intermap, increment P Corp., NRCAN, Esri Japan, METI, Esri China (Hong Kong), Esri (Thailand), MapmyIndia, © OpenStreetMap contributors, and the GIS User Community

Path: W:\gis\studies\3_1_2\maps\final_report\figure_4_1-2.mxd

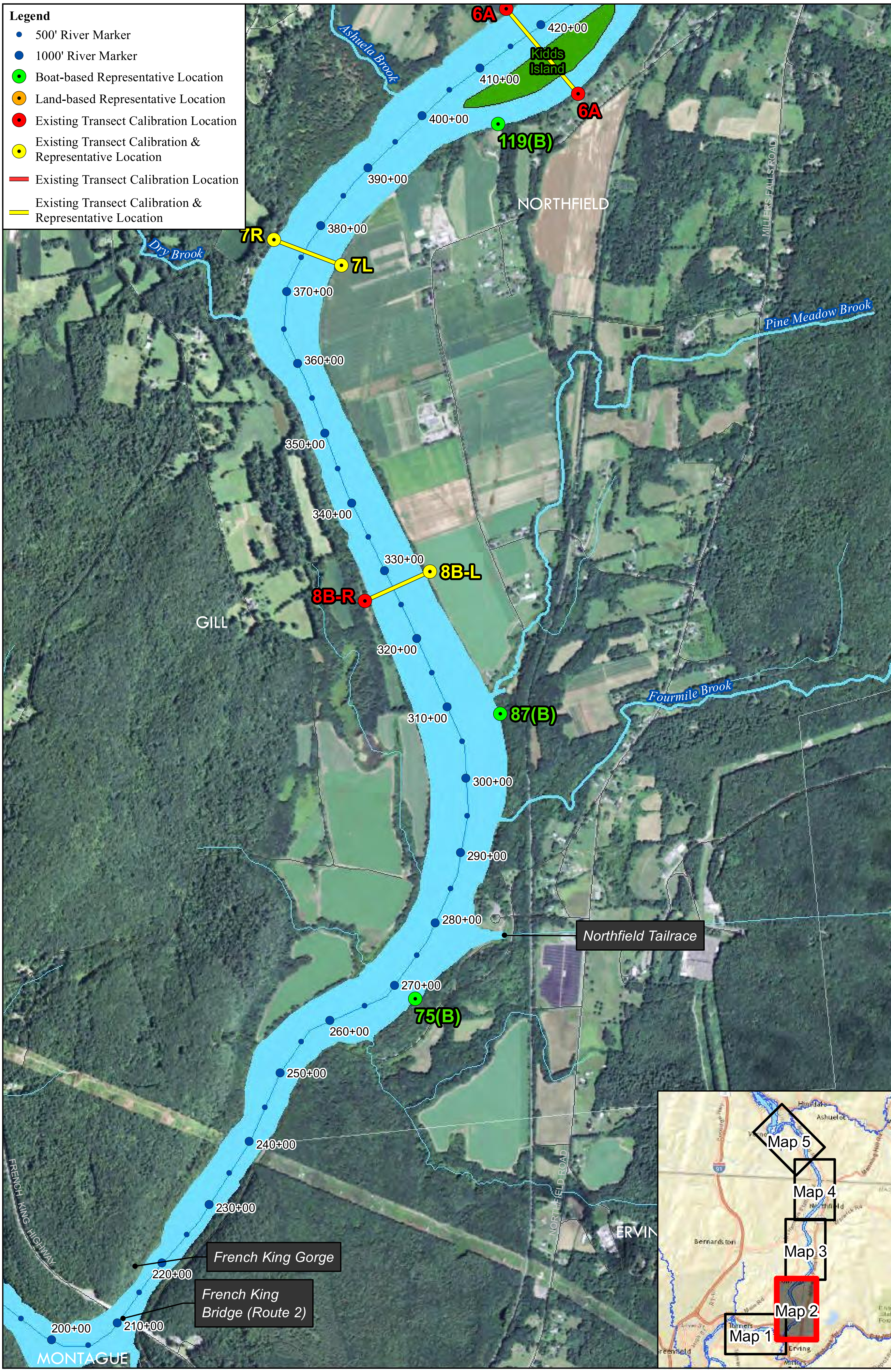

FIRSTLIGHT HYDRO GENERATING COMPANY
Northfield Mountain Pumped Storage Project No. 2485
Turners Falls Hydroelectric Project No. 1889

STUDY 3.1.2

FirstLight Power Resources

N

0 625 1,250 2,500 Feet

Figure 4.1-2:
Representative & Calibration Locations for Detailed Study
Map 2

Service Layer Credits: Sources: Esri, HERE, DeLorme, USGS, Intermap, increment P Corp., NRCAN, Esri Japan, METI, Esri China (Hong Kong), Esri (Thailand), MapmyIndia, © OpenStreetMap contributors, and the GIS User Community

Path: W:\gis\studies\3_1_2\maps\final_report\figure_4_1-2.mxd

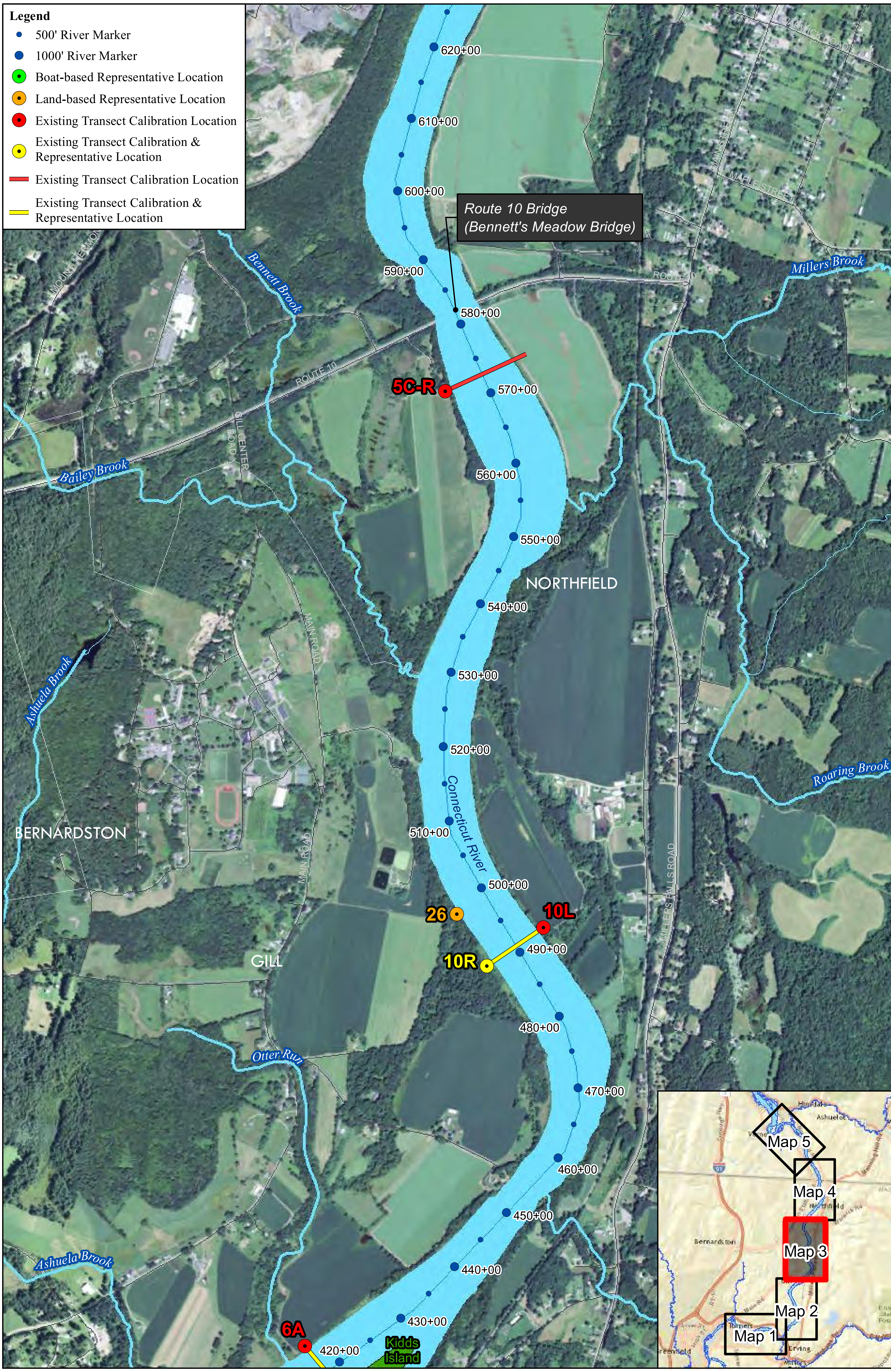

FIRSTLIGHT HYDRO GENERATING COMPANY
Northfield Mountain Pumped Storage Project No. 2485
Turners Falls Hydroelectric Project No. 1889

STUDY 3.1.2

N

0 625 1,250 2,500 Feet

Figure 4.1-2:
Representative & Calibration Locations for Detailed Study
Map 3

Service Layer Credits: Sources: Esri, HERE, DeLorme, USGS, Intermap, increment P Corp., NRCAN, Esri Japan, METI, Esri China (Hong Kong), Esri (Thailand), MapmyIndia, © OpenStreetMap contributors, and the GIS User Community

Path: W:\gis\studies\3_1_2\maps\final_report\figure_4_1-2.mxd

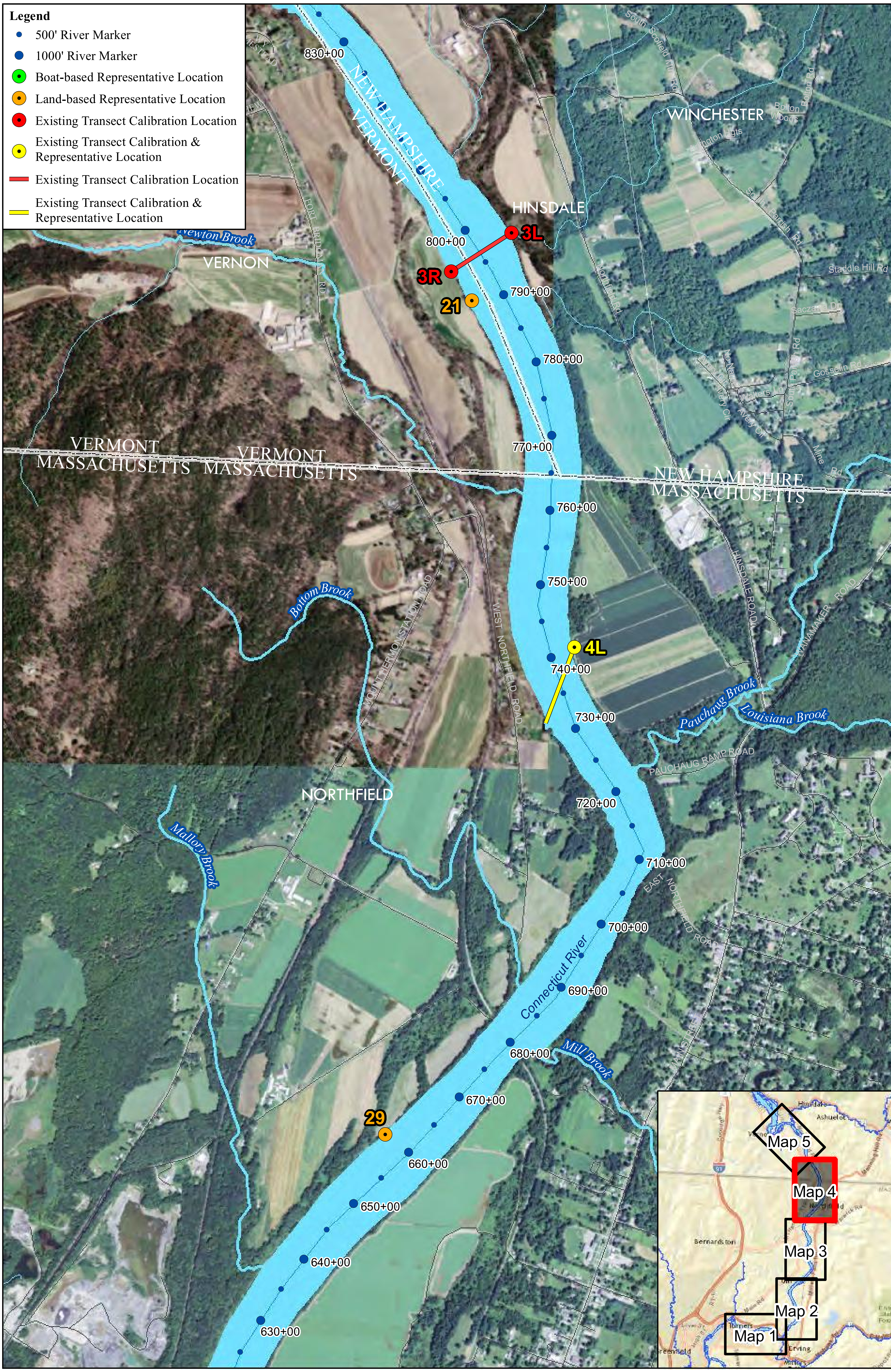

FIRSTLIGHT HYDRO GENERATING COMPANY
Northfield Mountain Pumped Storage Project No. 2485
Turners Falls Hydroelectric Project No. 1889

STUDY 3.1.2

N

0 625 1,250 2,500 Feet

Figure 4.1-2:
Representative & Calibration Locations for Detailed Study
Map 4

Service Layer Credits: Sources: Esri, HERE, DeLorme, USGS, Intermap, increment P Corp., NRCAN, Esri Japan, METI, Esri China (Hong Kong), Esri (Thailand), MapmyIndia, © OpenStreetMap contributors, and the GIS User Community

Path: W:\gis\studies\3_1_2\maps\final_report\figure_4_1-2.mxd

FIRSTLIGHT HYDRO GENERATING COMPANY
Northfield Mountain Pumped Storage Project No. 2485
Turners Falls Hydroelectric Project No. 1889

STUDY 3.1.2

0 625 1,250 2,500 Feet

Figure 4.1-2:
Representative & Calibration Locations for Detailed Study
Map 5

Service Layer Credits: Sources: Esri, HERE, DeLorme, USGS, Intermap, increment P Corp., NRCAN, Esri Japan, METI, Esri China (Hong Kong), Esri (Thailand), MapmyIndia, © OpenStreetMap contributors, and the GIS User Community

FirstLight Power Resources

Path: W:\gis\studies\3_1_2\maps\final_report\figure_4_1-2.mxd

4.2 Field Data Collection Methodology

Study No. 3.1.2 included the collection of a considerable amount of field data upon which a range of analyses and computer modeling were conducted. Field data collection efforts conducted in support of the analyses discussed in Section 5 are presented in-depth throughout this section, including:

- Project operations and water level data – Section 4.2.1
- 2013 Full River Reconnaissance Survey (Study No. 3.1.1) – Section 4.2.2
- Hydraulic modeling (HEC-RAS (Study No. 3.2.2) and River2D) – Section 4.2.3
- Cross-section surveys – Section 4.2.4
- Riverbank sediment particle size distribution, erodibility, geotechnical, and vegetation root density and strength data for BSTEM – Sections 4.2.5 – 4.2.7
- Boat wave data – Section 4.2.8
- Sediment transport (Study No. 3.1.3) – Section 4.2.9
- Groundwater data – Section 4.2.10
- Ice – Section 4.2.11

4.2.1 Project Operations and Water Level Data

At several key locations throughout the TFI, FirstLight has collected and recorded various data to support the operation and management of the Turners Falls and Northfield Mountain Projects. These data include such information as upstream flow released from Vernon Dam and water level, water level at the Northfield Mountain tailrace, water level and storage volume in the Northfield Mountain Upper Reservoir, water levels in the vicinity of Turners Falls Dam and power canal, and flow through the power canal to Cabot Station. These data, along with other information, are recorded on an hourly basis on Hydraulic Computation Data Sheets by FirstLight. Data from the handwritten sheets were digitized for the time period 2000-2014. The digitized data have been utilized in a variety of ways to show variations in water level and flow over time and to understand important relationships between flow and water level.

In support of various relicensing studies FirstLight also installed temporary water level loggers at various locations throughout the TFI from approximately August 1 to November 19, 2013 and from late March to November 7, 2014. The temporary water level loggers were typically deployed in the spring once flows receded and were left in place until late fall at which time they were removed for the winter. Data was typically collected on a 15 or 30 minute time step. The data collected via the seasonal water level loggers provided additional data coverage throughout the geographic extent of the TFI.

In addition to the data collected and recorded by FirstLight, tributary inflow data was obtained from USGS gages located on the Ashuelot (USGS Gage No. 01161000) and Millers Rivers (USGS Gage No. 01166500). Data recorded at these gages, and obtained for this study, included both flow and water level. The USGS also operates a gage on the Connecticut River downstream of the Turners Falls Project in Montague, MA[18] (USGS Gage No. 01170500) which provides flow and water level data.

---

[18] Note the Montague USGS Gage includes flow contribution from the Deerfield River.

Figure 4.2.1-1 provides the locations where permanent and temporary data collection occurs as well as the locations of the USGS gages previously mentioned.

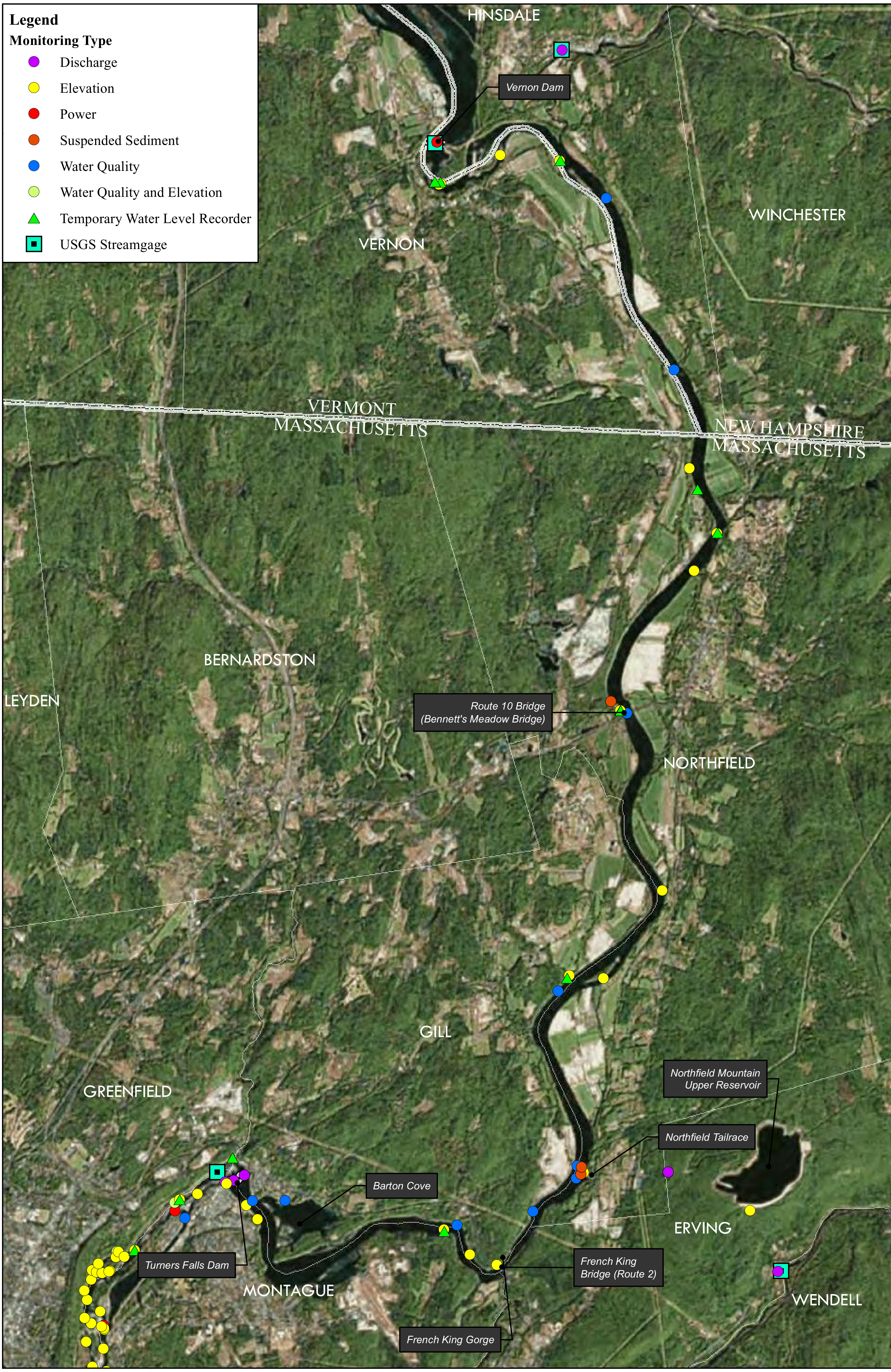

FIRSTLIGHT HYDRO GENERATING COMPANY
Northfield Mountain Pumped Storage Project No. 2485
Turners Falls Hydroelectric Project No. 1889

STUDY 3.1.2

Figure 4.2.1-1:
TFI Water Level and
Flow Equipment Locations

Service Layer Credits: Source: Esri, DigitalGlobe, GeoEye, Earthstar Geographics, CNES/Airbus DS, USDA, USGS, AEX, Getmapping, Aerogrid, IGN, IGP, swisstopo, and the GIS User Community

Path: W:\gis\studies\3_1_2\maps\final_report\figure_4_2_1-1.mxd

4.2.2 2013 Full River Reconnaissance Survey

Relicensing Study No. 3.1.1 – *2013 Full River Reconnaissance* was conducted in 2013[19] with a goal of documenting riverbank features, characteristics, and erosion conditions throughout the TFI from Vernon to the Turners Falls Dam. The main field components of the FRR included: (1) land-use mapping; (2) sensitive receptor mapping; (3) evaluation of past bank stabilization projects; (4) land-based survey; and (5) boat-based survey. An evaluation of the existing, permanent transects located throughout the TFI was also conducted as part of the land- and boat-based surveys. Georeferenced video and geo-tagged photographs were captured at each riverbank segment in order to document riverbank conditions as they were in November 2013. In addition riverbank features and characteristics, land-use, sensitive receptors, and stabilization projects observed during the 2013 FRR were developed into maps in ArcGIS. A final report was filed with FERC on September 15, 2014[20] with an addendum to the report filed with FERC on February 24, 2015.

The boat-based survey identified and recorded the coordinates of the start and end points of riverbank segments based on common riverbank features, characteristics, and erosion conditions as defined in the RSP for Study No. 3.1.1 (FirstLight, 2014a). All riverbanks throughout the TFI, including islands, were assessed during the survey. The boat-based survey provided the best vantage point and perspective of the entire riverbank (i.e. upper and lower bank) the findings of the boat-based survey were used as the primary data source when establishing riverbank segments and developing summary statistics.

The 2013 boat-based survey resulted in delineation of 641 total riverbank segments, including islands. Of the 641 segments, 596 segments totaling 228,009 ft. were located on riverbanks with an additional 45 segments on islands. Segment lengths ranged from 13 ft. to 3,330 ft. with an average river segment length of 383 ft. The minimum and maximum segment lengths for previous FRR's ranged from 20 to over 4,000 ft. with segment lengths ranging from 480 to 1,267. The segment lengths for the 2013 FRR are shorter than all previous FRRs by a significant percentage in all statistical categories resulting in more detailed spatial data.

The land-based survey, conducted simultaneously with the boat-based survey as per MADEP request, identified and defined indicators of potential erosion and bank instability as well as erosion features that may not have been visible from a boat. Land-based segments were delineated and defined based on features and characteristics observed while traversing the top of the bank throughout the entire TFI, including islands. The land-based survey included all riverbanks and islands in the TFI except in areas where: (1) access was not possible or the area was deemed impassible; (2) access was unsafe; or (3) bank conditions did not warrant assessment (e.g. bedrock areas). Detailed geotechnical and geomorphic assessments, including field notes, sketches, and photographs, were also conducted at areas of interest as noted by the fluvial geomorphologist and geotechnical engineer. Overall a total of 38 detailed assessments were conducted. Observations made during the land-based survey were used to complement the findings of the boat-based survey and provide supplemental information and perspective to the overall assessment of TFI riverbanks.

The results of the 2013 FRR indicated that the majority of the upper riverbanks in the TFI were found to have moderate or steep slopes, heights greater than 12 ft., be comprised of silt/sand, and have heavy vegetation. The majority of the lower riverbanks were found to have flat/beach to moderate slopes, be comprised of silt/sand, and have none to very sparse vegetation. Erosion conditions in the TFI were found to be generally stable with None/Little current erosion occurring through much of this reach. As noted in the report, 84.8% of the total length of the TFI riverbanks were found to have None/Little erosion, 14.1%

[19] The majority of the field work associated with the FRR was conducted in the fall of 2013 with supplemental field work occurring in the spring and summer of 2014.
[20] *Relicensing Study No. 3.1.1 2013 Full River Reconnaissance Northfield Mountain Pumped Storage Project (No. 2485) and Turners Falls Hydroelectric Project (No. 1889)*

Some erosion, 0.5% Some to Extensive erosion, and 0.6% Extensive erosion. Furthermore, 5.5% of the total length of TFI riverbanks were found to have Potential Future Erosion, 0.6% Active Erosion, 9.1% Eroded, 83.5% Stable, and 1.3% in the Process of Stabilization. Table's 4.2.2-1 and 4.2.2-2 provide riverbank classification criteria and classification definitions which were used during the 2013 FRR. Table 4.2.2-3 includes summary statistics for TFI riverbank features and characteristics. Figure 4.2.2-1 depicts the extent of erosion throughout the TFI as observed during the 2013 FRR.

The findings of the 2013 FRR were used to inform the selection of detailed study sites and, combined with the annual cross-section surveys, in support of various analyses and modeling discussed in Section 5. A more in-depth discussion of the 2013 FRR, including all related figures and tables, can be found in the final study report issued in September 2014 (FirstLight, 2014a).

Table 4.2.2-1: Turners Falls Impoundment Riverbank Classifications for the 2013 FRR Boat-based survey (FirstLight, 2014a)

UPPER RIVERBANK CHARACTERISTICS[21]						
Upper Riverbank Slope	Overhanging *>90°*	Vertical *90°*	Steep *(>2:1)*	Moderate *(4:1-2:1)*	Flat *(<4:1)*	
Upper Riverbank Height *(total height above normal river level)*	Low *(<8 ft.)*	Medium *(8-12 ft.)*	High *(>12 ft.)*			
Upper Riverbank Sediment	Clay *(.001-.062mm)*	Silt/Sand *(.062-2 mm)*	Gravel *(2-64mm)*	Cobbles *(64-256mm)*	Boulders *(256-2048mm)*	Bedrock
Upper Riverbank Vegetation	None to Very Sparse *(<10%)*	Sparse *(10%-25%)*	Moderate *(25%-50%)*	Heavy *(>50%)*		
Sensitive Receptors	*Important wildlife habitat located at or near the riverbank*					
LOWER RIVERBANK CHARACTERISTICS						
Lower Riverbank Slope	Vertical *90°*	Steep *(>2:1)*	Moderate *(4:1-2:1)*	Flat / Beaches *(<4:1)*		
Lower Riverbank Sediment	Clay *(.001-.062mm)*	Silt/Sand *(.062-2 mm)*	Gravel *(2-64mm)*	Cobbles *(64-256mm)*	Boulders *(256-2048mm)*	Bedrock
Lower Riverbank Vegetation	None to Very Sparse *(<10%)*	Sparse *(10%-25%)*	Moderate *(25%-50%)*	Heavy *(>50%)*		
Sensitive Receptors	*Important wildlife habitat located at or near the riverbank*					
EROSION CLASSIFICATION						
Type(s) of Erosion	Falls – Undercut	Falls – Gullies	Topples	Slide or Flow	*Planar Slip* *Rotational Slump* *Flow*	
Indicators of Potential Erosion	Tension Cracks	Exposed Roots	Creep/ Leaning Trees	Overhanging bank	Notching	Other
Stage(s) of Erosion	Potential Future Erosion	Active Erosion	Eroded	Stable		
Extent of Current Erosion	None/Little *(<10%)*	Some *(10%-40%)*	Some to Extensive *(40%-70%)*	Extensive *(>70%)*		

[21] All quantitative classification criteria (e.g. slope, height, vegetation, extent, etc.) were based on approximate estimates made during field observations of riverbanks. The FRR was a reconnaissance level survey that did not include quantitative field measurements of characteristics.

Table 4.2.2-2: 2013 FRR Riverbank Classification Definitions (FirstLight, 2014a)

RIVERBANK CHARACTERISTICS *(Upper and Lower)*[22]	
Riverbank Slope	**Overhanging** – any slope greater than 90º
	Vertical – slopes that are approximately 90º
	Steep – exhibiting a slope ratio greater than 2 to 1
	Moderate – ranging between a slope ratio of 4 to 1 and 2 to 1
	Flat – exhibiting a slope ratio less than 4 to 1[23]
Riverbank Height	**Low –** height less than 8 ft above normal river level[24]
	Medium – height between 8 and 12 ft above normal river level
	High – height greater than 12 ft above normal river level
Riverbank Sediment	**Clay –** any sediment with a diameter between .001 mm and 2 mm
	Silt / Sand – any sediment with a diameter between .062 mm and 2 mm
	Gravel – any sediment with a diameter between 2 mm and 64 mm
	Cobbles – any sediment with a diameter between 64 mm and 256 mm
	Boulders – any sediment with a diameter between 256 mm and 2048 mm
	Bedrock – unbroken, solid rock
Riverbank Vegetation	**None to Very Sparse –** less than 10% of the total riverbank segment is composed of vegetative cover
	Sparse – 10-25% of the total riverbank segment is composed of vegetative cover
	Moderate – 25-50% of the total riverbank segment is composed of vegetative cover
	Heavy – 50 % or greater of the total riverbank segment is composed of vegetative cover
Sensitive Receptors	Important wildlife habitat located at or near the riverbank.
EROSION CLASSIFICATIONS	
Type(s) of Erosion[25]	**Falls –** Material mass detached from a steep slope and descends through the air to the base of the slope. Includes erosion resulting from transport of individual particles by water.
	Topples – Large blocks of the slope undergo a forward rotation about a pivot point due to the force of gravity. Large trees undermined at the base enhance formation.
	Slides – Sediments move downslope under the force of gravity along one or several discrete surfaces. Can include planar slips or rotational slumps.
	Flows – Sediment/water mixtures that are continuously deforming without distinct slip surfaces.
Indicators of Potential Erosion	**Tension Cracks –** a crack formed at the top edge of a bank potentially leading to topples or slides (FGS, 2007)
	Exposed Roots – trees located on riverbanks with root structures exposed, overhanging.
	Creep – defined as an extremely slow flow process (inches per year or less) indicated by the presence of tree trunks curved downslope near their base (FGS, 2007)
	Overhanging Bank – any slope greater than 90º
	Notching – similar to an undercut, defined as an area which leaves a vertical stepped face presumably after small undercut areas have failed.

[22] All quantitative classification criteria (e.g. slope, height, vegetation, extent, etc.) were based on approximate estimates made during field observations of riverbanks. The FRR was a reconnaissance level survey that does not include quantitative analysis.
[23] Beaches are defined as a lower riverbank segment with a flat slope
[24] For the purpose of this study, Normal Water Level was defined as water levels within typical pool fluctuation levels, but below 186 ft.
[25] FGS, 2007

	Other – Indicators of potential erosion that do not fit into one of the four categories listed above will be noted by the field crew.[26]
Stage(s) of Erosion	**Potential Future Erosion –** riverbank segment exhibits multiple or extensive indicators of potential erosion
	Active Erosion – riverbank segment exhibits one or more types of erosion as well as evidence of recent erosion activity
	Eroded – riverbank segment exhibits indicators that erosion has occurred (e.g. lack of vegetation, etc.), however, recent erosion activity is not observed. A segment classified as Eroded would typically be between Active Erosion and Stable on the temporal scale of erosion.
	Stable – riverbank segment does not exhibit types or indicators of erosion
Extent of Current Erosion	**None/Little[27] –** generally stable bank where the total surface area of the bank segment has approximately less than 10% active erosion present.
	Some – riverbank segment where the total surface area of the bank segment has approximately 10-40% active erosion present
	Some to Extensive – riverbank segment where the total surface area of the bank segment has approximately 40-70% active erosion present
	Extensive – riverbank segment where the total surface area of the bank segment has approximately more than 70% active erosion present

[26] Segments with features classified as "Other" exhibited various erosion processes that did not fit in one of the existing classification categories.

[27] Riverbanks consist of an irregular surface and include a range of natural materials (silt/sand, gravel, cobbles, boulders, rock, and clay), above ground vegetation (from grasses to trees), and below ground roots of different densities and sizes. Due to these characteristics, there are small areas of disturbance which often occur at interfaces between materials, particularly in the vicinity of the water surface. These small disturbed areas can be considered as erosion, or sometimes can result from deposition or even eroded deposition. No natural riverbank exists which does not have at least some relatively small degree of disturbance or erosion associated with the natural combination of sediment types/sizes and vegetation. As such, the extent of erosion for generally stable riverbanks that include these relatively small disturbed areas is characterized as little/none.

Table 4.2.2-3: Summary statistics of Turners Falls Impoundment riverbank features and characteristics – 2013 FRR (FirstLight, 2014a)

Riverbank Features	Characteristics					
Upper Riverbank Slope	Overhanging 1.8%	Vertical 1.6%	Steep 28.0%	Moderate 59.8%	Flat 8.8%	
Upper Riverbank Height	Low 15.5%	Medium 5.7%	High 78.8%			
Upper Riverbank Sediment	Clay -	Silt/Sand 95.6%	Gravel -	Cobbles -	Boulders 0.9%	Bedrock 3.5%
Upper Riverbank Vegetation	None to Very Sparse 1.9%	Sparse 1.3%	Moderate 17.1%	Heavy 79.7%		
Lower Riverbank Slope	Vertical 0.8%	Steep 2.3%	Moderate 27.5%	Flat/Beach 69.4%		
Lower Riverbank Sediment	Clay <0.1%[28]	Silt/Sand 59.6%	Gravel 7.9%	Cobbles 8.7%	Boulders 11.9%	Bedrock 11.9%
Lower Riverbank Vegetation	None to Very Sparse 88.3%	Sparse 3.5%	Moderate 3.2%	Heavy 5.0%		
Type of Erosion	Falls-Undercut 43.4%	Falls-Gullies 0.03%	Topples 1.1%	Slide or Flow 6.2%	Planar Slip 1.1%	Rotational Slump 1.5%
Potential Indicators of Erosion	Tension Cracks <0.10[29]%	Exposed Roots 38.1%	Creep/Leaning Trees 62.7%	Overhanging Bank 12.7%	Notch 5.0%	Other 1.1%

[28] Clay was found in few segments of the river but where some clay was found the sediment was dominated by another type of sediment either vertically or horizontally within a segment. When this occurred the segment was classified using the dominant sediment type. For example, some clay was observed in segment 342 (just downstream of Vernon Dam on the left bank) but the segment was classified using the dominant sediment type.
[29] Tension cracks can only be observed from land-based observations. Some tension cracks were observed during the land-based survey and are reported at those sites as indicated in the notes for the land-based work. Tension cracks were not observed to be significant in the more general top of bank observations when walking along the length of the TFI.

Riverbank Features	Characteristics					
Stage of Erosion	Potential Future Erosion 5.5%	Active Erosion 0.6%	Eroded 9.1%	Stable 83.5%	In Process of Stabilization 1.3%[30]	
Extent of Current Erosion	None/Little 84.8%	Some 14.1%	Some to Extensive 0.5%	Extensive 0.6%		

[30] While originally not one of the RSP erosion condition classifications, one riverbank segment was classified as being "In the Process of Stabilization" due to the fact that riverbank stabilization work was being constructed at this particular segment (421, Bathory/Gallagher 2013) during the 2013 FRR. A gravel beach at the top of the lower riverbank had been placed along with large woody debris. Vegetation is then being planted to provide additional stabilization on the gravel beach as well as extending other vegetation onto portions of the upper riverbank.

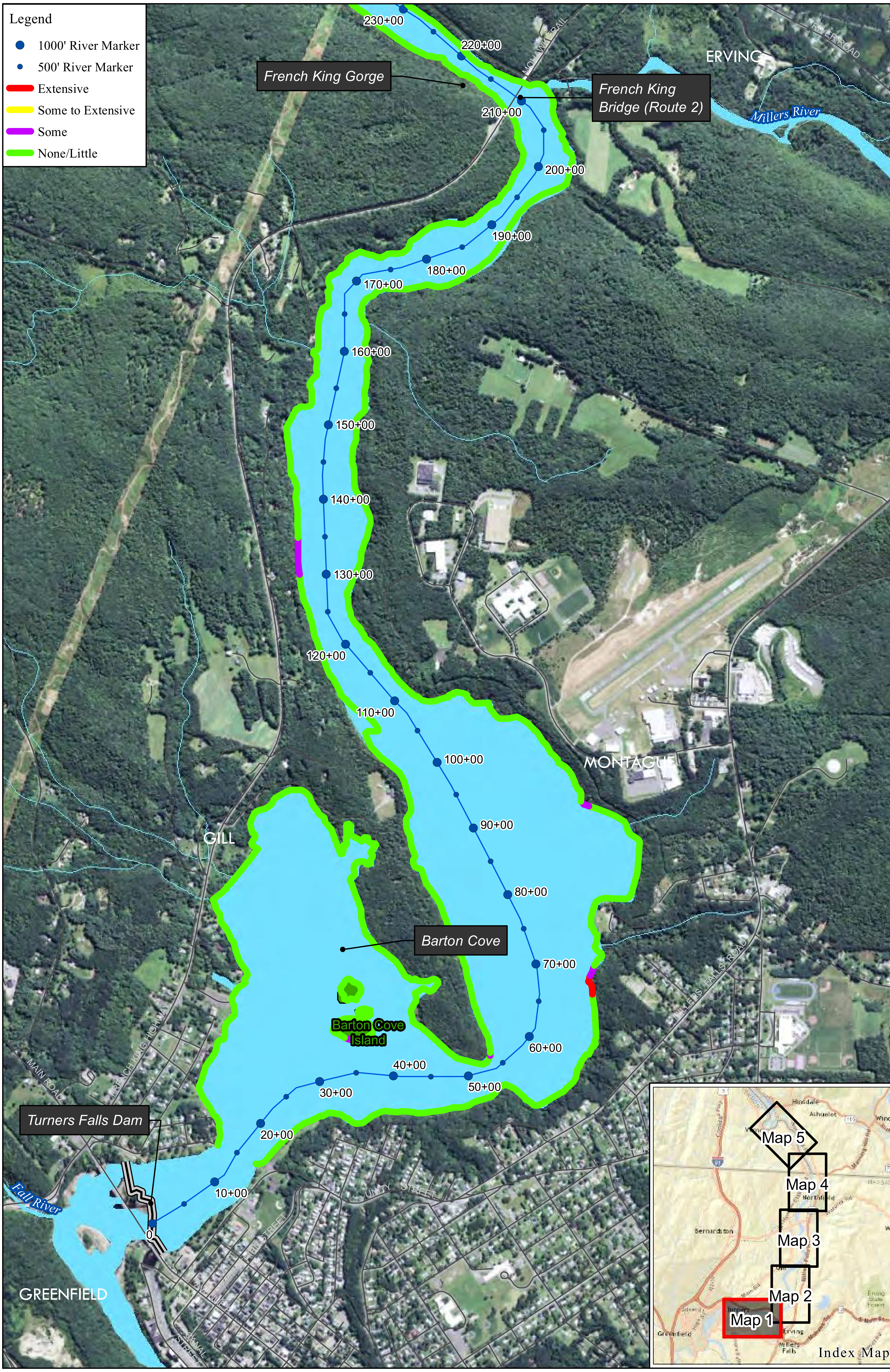

FIRSTLIGHT HYDRO GENERATING COMPANY
Northfield Mountain Pumped Storage Project No. 2485
Turners Falls Hydroelectric Project No. 1889

STUDY 3.1.2

0 650 1,300 2,600 Feet

Figure 4.2.2-1:
Extent of Current Erosion
Map 1

Service Layer Credits: Sources: Esri, HERE, DeLorme, USGS, Intermap, increment P Corp., NRCAN, Esri Japan, METI, Esri China (Hong Kong), Esri (Thailand), MapmyIndia, © OpenStreetMap contributors, and the GIS User Community
Source: Esri, DigitalGlobe, GeoEye, Earthstar Geographics, CNES/Airbus DS, USDA, USGS, AEX, Getmapping, Aerogrid, IGN, IGP, swisstopo, and the GIS User Community

Path: W:\gis\studies\3_1_2\maps\final_report\figure_4_2_2-1.mxd

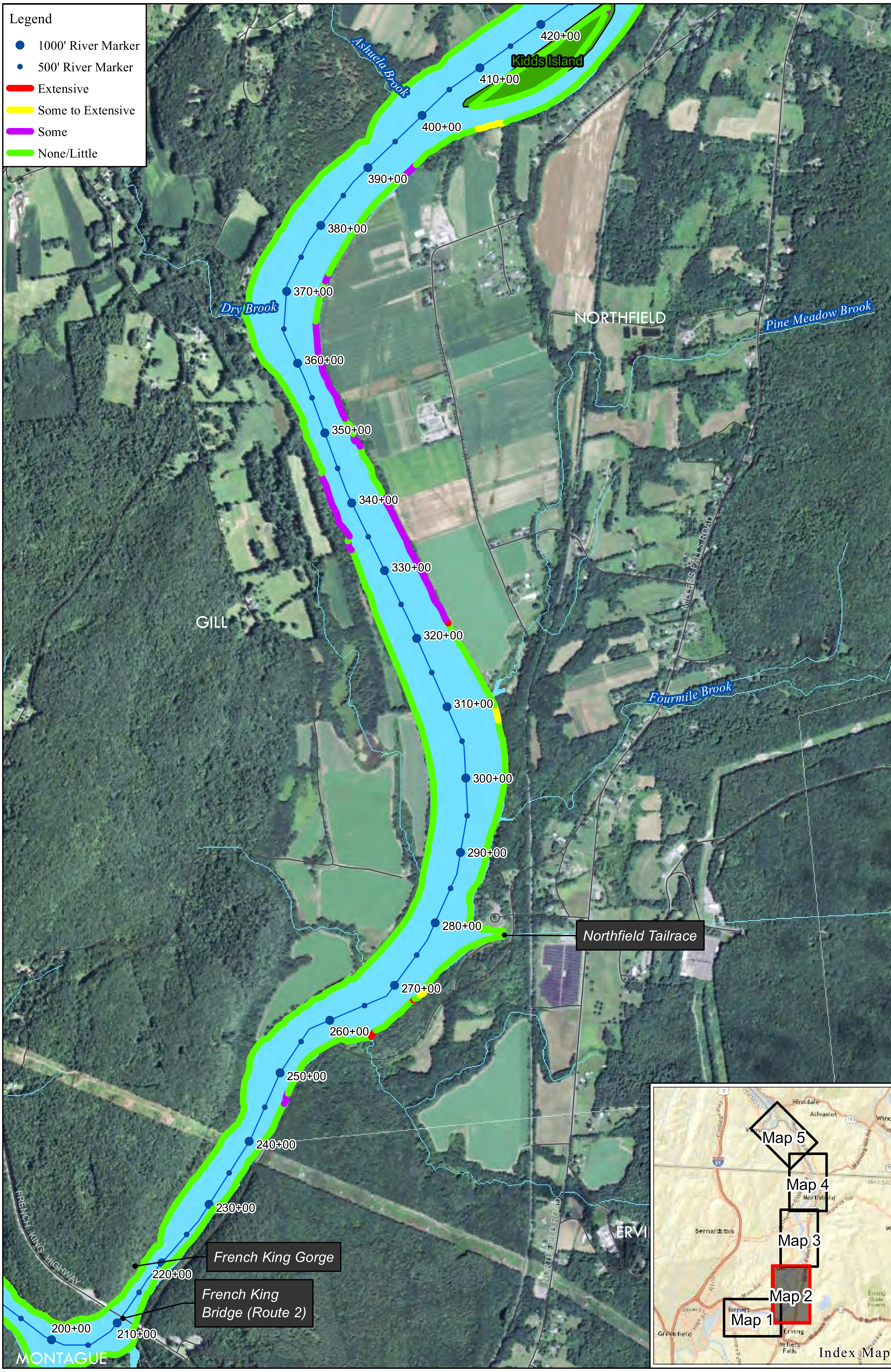

FIRSTLIGHT HYDRO GENERATING COMPANY
Northfield Mountain Pumped Storage Project No. 2485
Turners Falls Hydroelectric Project No. 1889

STUDY 3.1.2

Figure 4.2.2-1:
Extent of Current Erosion
Map 2

FirstLight Power Resources

N

0 650 1,300 2,600 Feet

Service Layer Credits: Sources: Esri, HERE, DeLorme, USGS, Intermap, increment P Corp., NRCAN, Esri Japan, METI, Esri China (Hong Kong), Esri (Thailand), MapmyIndia, © OpenStreetMap contributors, and the GIS User Community
Source: Esri, DigitalGlobe, GeoEye, Earthstar Geographics, CNES/Airbus DS, USDA, USGS, AEX, Getmapping, Aerogrid, IGN, IGP, swisstopo, and the GIS User Community

Path: W:\gis\studies\3_1_2\maps\final_report\figure_4_2_2-1.mxd

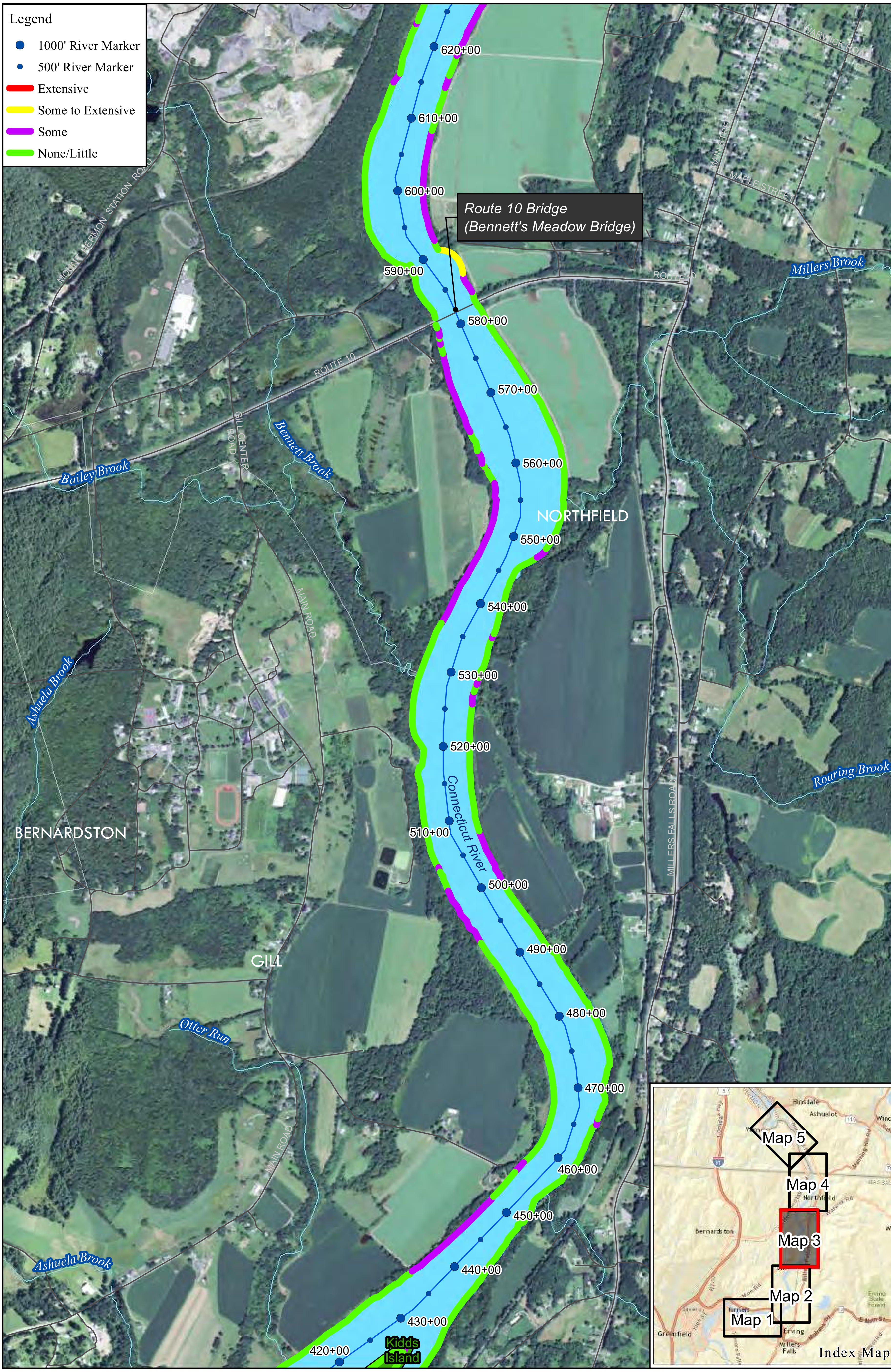

FIRSTLIGHT HYDRO GENERATING COMPANY
Northfield Mountain Pumped Storage Project No. 2485
Turners Falls Hydroelectric Project No. 1889

STUDY 3.1.2

N

0 650 1,300 2,600 Feet

Figure 4.2.2-1:
Extent of Current Erosion
Map 3

Service Layer Credits: Sources: Esri, HERE, DeLorme, USGS, Intermap, increment P Corp., NRCAN, Esri Japan, METI, Esri China (Hong Kong), Esri (Thailand), MapmyIndia, © OpenStreetMap contributors, and the GIS User Community
Source: Esri, DigitalGlobe, GeoEye, Earthstar Geographics, CNES/Airbus DS, USDA, USGS, AEX, Getmapping, Aerogrid, IGN, IGP, swisstopo, and the GIS User Community

Path: W:\gis\studies\3_1_2\maps\final_report\figure_4_2_2-1.mxd

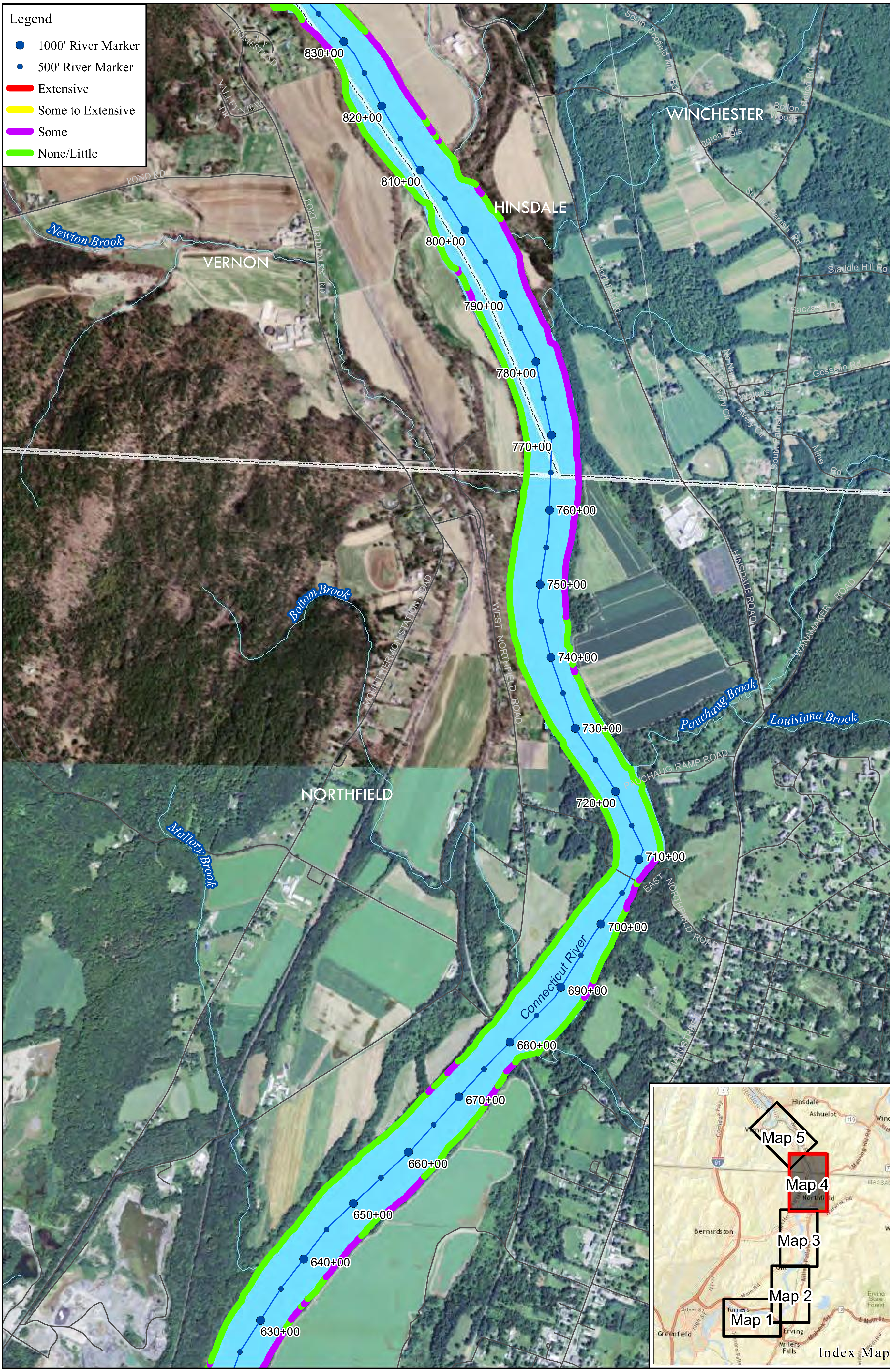

FIRSTLIGHT HYDRO GENERATING COMPANY
Northfield Mountain Pumped Storage Project No. 2485
Turners Falls Hydroelectric Project No. 1889

STUDY 3.1.2

FirstLight Power Resources

N

0 650 1,300 2,600 Feet

Figure 4.2.2-1:
Extent of Current Erosion
Map 4

Service Layer Credits: Sources: Esri, HERE, DeLorme, USGS, Intermap, increment P Corp., NRCAN, Esri Japan, METI, Esri China (Hong Kong), Esri (Thailand), MapmyIndia, © OpenStreetMap contributors, and the GIS User Community
Source: Esri, DigitalGlobe, GeoEye, Earthstar Geographics, CNES/Airbus DS, USDA, USGS, AEX, Getmapping, Aerogrid, IGN, IGP, swisstopo, and the GIS User Community

Path: W:\gis\studies\3_1_2\maps\final_report\figure_4_2_2-1.mxd

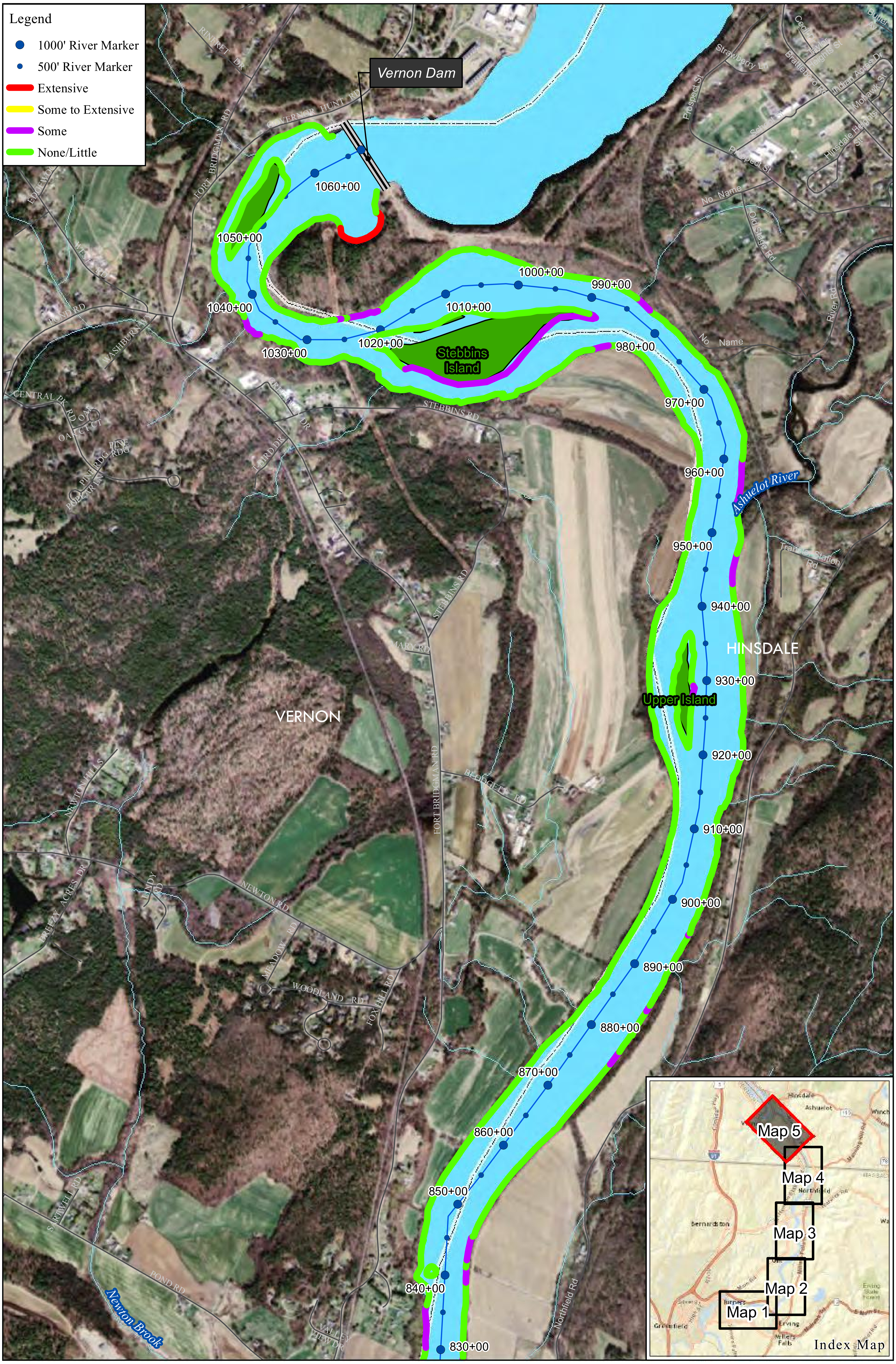

FIRSTLIGHT HYDRO GENERATING COMPANY
Northfield Mountain Pumped Storage Project No. 2485
Turners Falls Hydroelectric Project No. 1889

STUDY 3.1.2

0 650 1,300 2,600 Feet

Figure 4.2.2-1:
Extent of Current Erosion
Map 5

Service Layer Credits: Sources: Esri, HERE, DeLorme, USGS, Intermap, increment P Corp., NRCAN, Esri Japan, METI, Esri China (Hong Kong), Esri (Thailand), MapmyIndia, © OpenStreetMap contributors, and the GIS User Community
Source: Esri, DigitalGlobe, GeoEye, Earthstar Geographics, CNES/Airbus DS, USDA, USGS, AEX, Getmapping, Aerogrid, IGN, IGP, swisstopo, and the GIS User Community

Path: W:\gis\studies\3_1_2\maps\final_report\figure_4_2_2-1.mxd

4.2.3 Hydraulic Modeling

Hydraulic modeling was conducted as an integral part of this study in support of the analysis of: (1) water levels and how they change over time, and (2) the hydraulic forces that flowing water impose on riverbanks. Two hydraulic models were utilized for this effort: HEC-RAS and River2D. The HEC-RAS model was developed as part of Study No. 3.2.2 *Hydraulic Study,* while the River2D model was created specifically for the Causation Study. Both models encompassed the geographic extent of the TFI from Vernon Dam to the Turners Falls Dam and relied on similar input and calibration datasets. Input datasets used for these models included historic and updated (2014) TFI bathymetric data, water level data derived from the permanent FirstLight monitoring equipment and seasonal water level loggers, and flow data derived from FirstLight and/or USGS data.

The HEC-RAS model was integral in support of the BSTEM runs and analyses discussed in Section 5. After the HEC-RAS model was calibrated, it was utilized to generate historic water levels and water surface slopes on an hourly basis through the TFI and at the 25 Detailed Study Sites utilizing historic upstream inflows at Vernon and tributaries (Ashuelot and Millers Rivers), Northfield Mountain operations (flows used for pumping and generating), and historic water levels at the Turners Falls Dam. Another scenario (Scenario 1 – Northfield Mountain idle) was then developed and run through HEC-RAS to provide hourly water levels for BSTEM at the 25 Detailed Study Sites to determine erosion associated with this modeling scenario.

The results of the two-dimensional River2D model were used to better understand velocities and shear stresses in the near bank environment. The model was calibrated and then verified with three separate flow events. The verification events represented the full range of available observed flows. Once verified, six production runs were performed in order to investigate changes in velocity and shear stress in the near bank area at the 25 detailed study sites and at areas where unique hydraulic conditions were observed (e.g., eddying).

The HEC-RAS and River2D models are discussed further in Section 5.2.

4.2.4 Cross-section Surveys

Following completion of the first FRR in 1998 and development of the subsequent ECP, 22 permanent transects were established in the TFI for continued monitoring. The 22 transects were selected for two primary reasons: (1) they were relatively evenly spaced throughout the geographic extent of the TFI, and (2) most were located at sites where erosion had been observed. The 22 transects have been surveyed annually since 1999 to monitor any changes in riverbank or channel geometry. Transect surveys typically entailed surveying the complete cross-section starting at one riverbank, across the channel bed, and up the other riverbank. Permanent markers are typically placed on both banks denoting the start/end points of the cross-section survey to allow for direct comparison of past and future surveys.

In addition to the 22 permanent transects established in 1998, FirstLight identified 9 supplemental transects during the detailed study site selection process discussed in Section 4.1. Although the supplemental detailed study sites were only located on one riverbank, full cross-section surveys have been conducted annually at each of these locations since 2014. Figure 4.2.4-1 shows the location of both the permanent and supplemental transects.

Cross-section survey data were used to calibrate BSTEM and for analysis of changes in cross-section geometry over time. Cross-section plots have been created comparing the results of each annual survey. These plots have also been updated to include the Ordinary High Water Mark (OHWM). Discussion pertaining to how the OHWM was identified can be found in Section 4.2.4-1.

Figure 4.2.4-2 provides an example of a cross-section plot. Cross-section plots for all transects are located in Volume III (Appendix E).

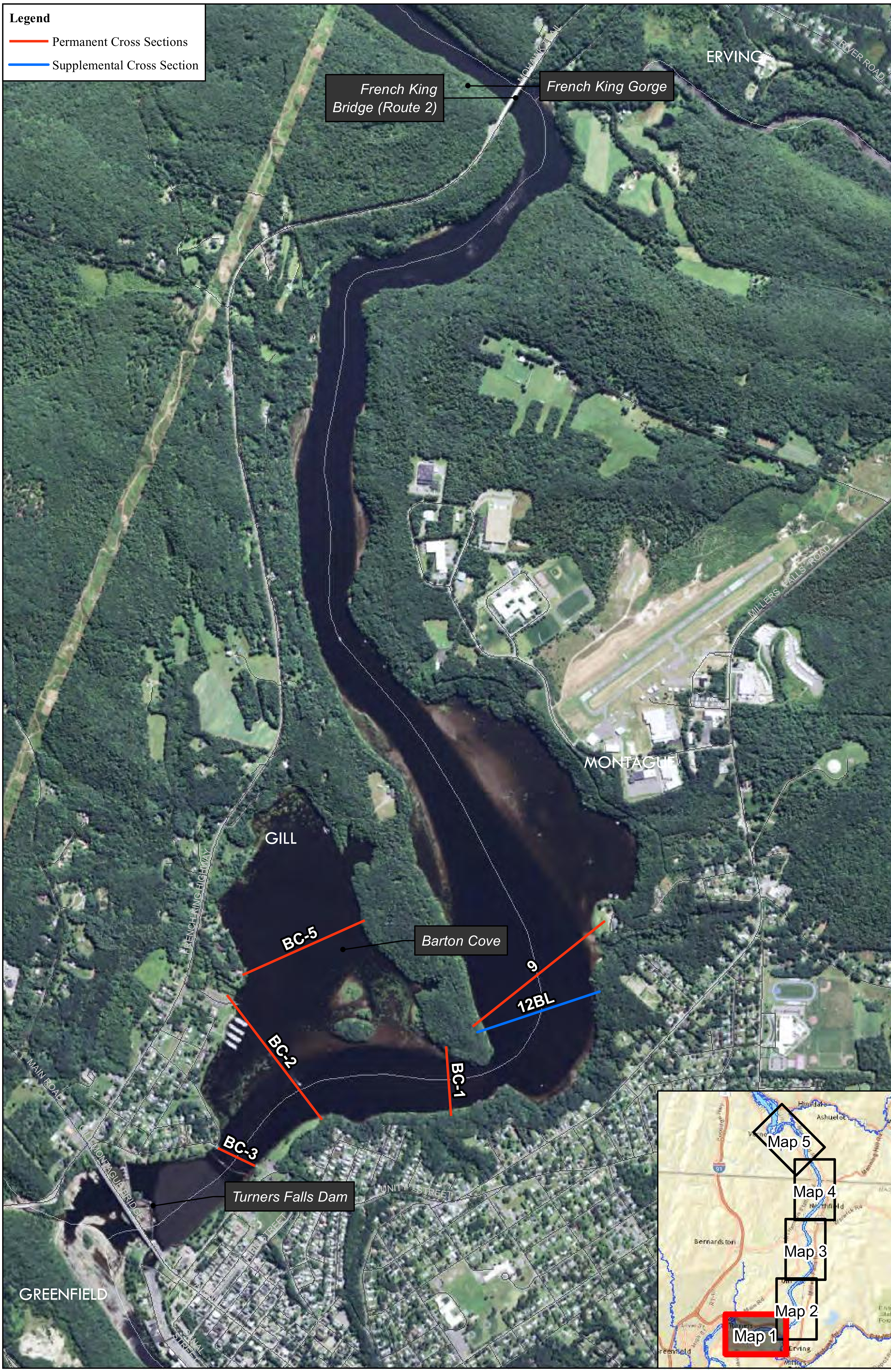

FIRSTLIGHT HYDRO GENERATING COMPANY
Northfield Mountain Pumped Storage Project No. 2485
Turners Falls Hydroelectric Project No. 1889

STUDY 3.1.2

0 625 1,250 2,500 Feet

FirstLight Power Resources

Figure 4.2.4-1:
Turners Falls Impoundment
Cross-section

Service Layer Credits: Sources: Esri, HERE, DeLorme, USGS, Intermap, increment P Corp., NRCAN, Esri Japan, METI, Esri China (Hong Kong), Esri (Thailand), MapmyIndia, © OpenStreetMap contributors, and the GIS User Community

Path: W:\gis\studies\3_1_2\maps\final_report\figure_4_2_4-1.mxd

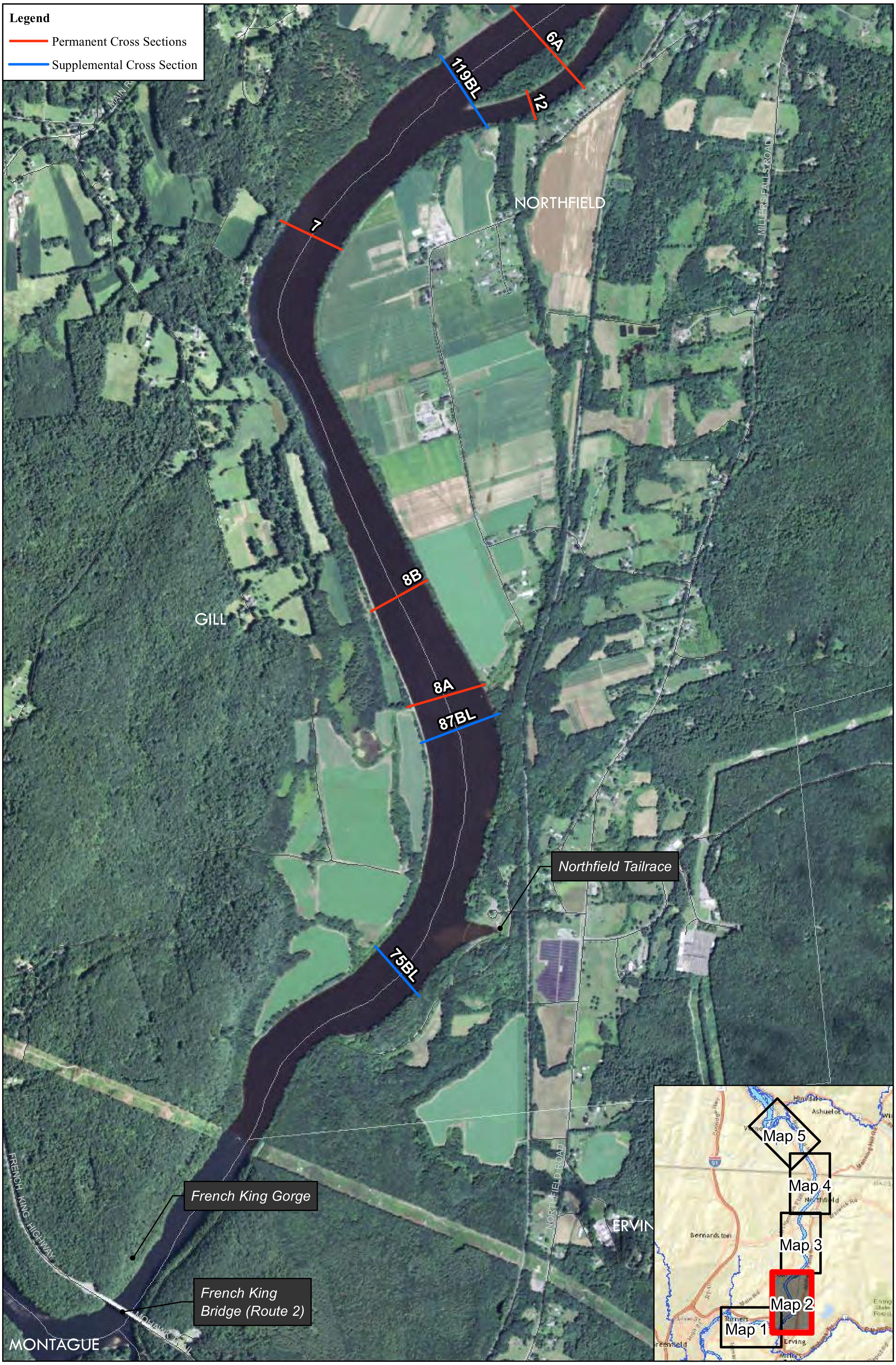

FIRSTLIGHT HYDRO GENERATING COMPANY
Northfield Mountain Pumped Storage Project No. 2485
Turners Falls Hydroelectric Project No. 1889

STUDY 3.1.2

0 625 1,250 2,500 Feet

Figure 4.2.4-1:
Turners Falls Impoundment
Cross-section

Service Layer Credits: Sources: Esri, HERE, DeLorme, USGS, Intermap, increment P Corp., NRCAN, Esri Japan, METI, Esri China (Hong Kong), Esri (Thailand), MapmyIndia, © OpenStreetMap contributors, and the GIS User Community

Path: W:\gis\studies\3_1_2\maps\final_report\figure_4_2_4-1.mxd

FIRSTLIGHT HYDRO GENERATING COMPANY
Northfield Mountain Pumped Storage Project No. 2485
Turners Falls Hydroelectric Project No. 1889

STUDY 3.1.2

N

0 625 1,250 2,500 Feet

Figure 4.2.4-1:
Turners Falls Impoundment
Cross-section

Service Layer Credits: Sources: Esri, HERE, DeLorme, USGS, Intermap, increment P Corp., NRCAN, Esri Japan, METI, Esri China (Hong Kong), Esri (Thailand), MapmyIndia, © OpenStreetMap contributors, and the GIS User Community

Path: W:\gis\studies\3_1_2\maps\final_report\figure_4_2_4-1.mxd

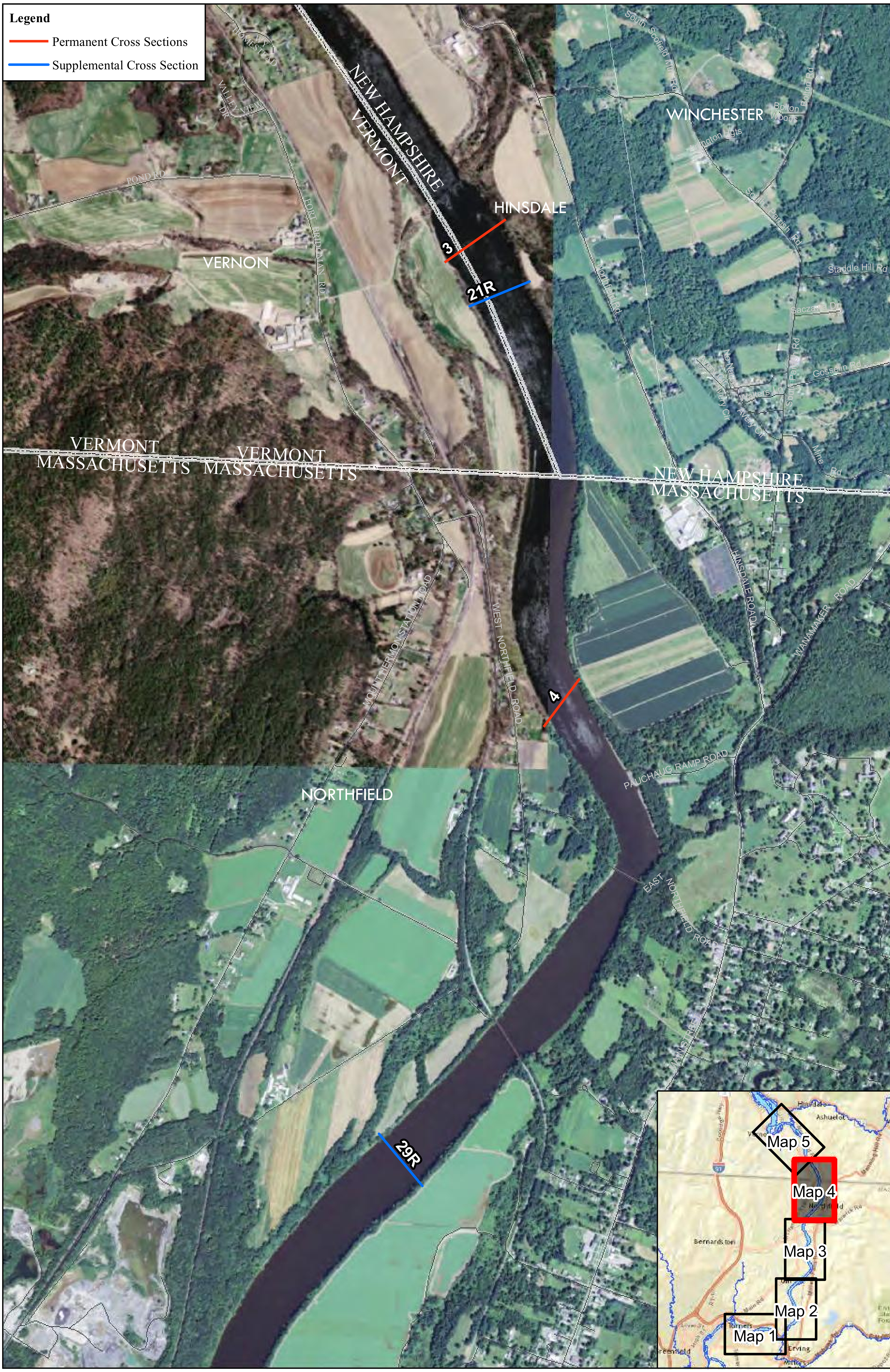

FIRSTLIGHT HYDRO GENERATING COMPANY
Northfield Mountain Pumped Storage Project No. 2485
Turners Falls Hydroelectric Project No. 1889

STUDY 3.1.2

0 625 1,250 2,500 Feet

Figure 4.2.4-1:
Turners Falls Impoundment
Cross-section

Service Layer Credits: Sources: Esri, HERE, DeLorme, USGS, Intermap, increment P Corp., NRCAN, Esri Japan, METI, Esri China (Hong Kong), Esri (Thailand), MapmyIndia, © OpenStreetMap contributors, and the GIS User Community

Path: W:\gis\studies\3_1_2\maps\final_report\figure_4_2_4-1.mxd

FIRSTLIGHT HYDRO GENERATING COMPANY
Northfield Mountain Pumped Storage Project No. 2485
Turners Falls Hydroelectric Project No. 1889

STUDY 3.1.2

0 625 1,250 2,500 Feet

Figure 4.2.4-1:
Turners Falls Impoundment
Cross-section

Service Layer Credits: Sources: Esri, HERE, DeLorme, USGS, Intermap, increment P Corp., NRCAN, Esri Japan, METI, Esri China (Hong Kong), Esri (Thailand), MapmyIndia, © OpenStreetMap contributors, and the GIS User Community

Path: W:\gis\studies\3_1_2\maps\final_report\figure_4_2_4-1.mxd

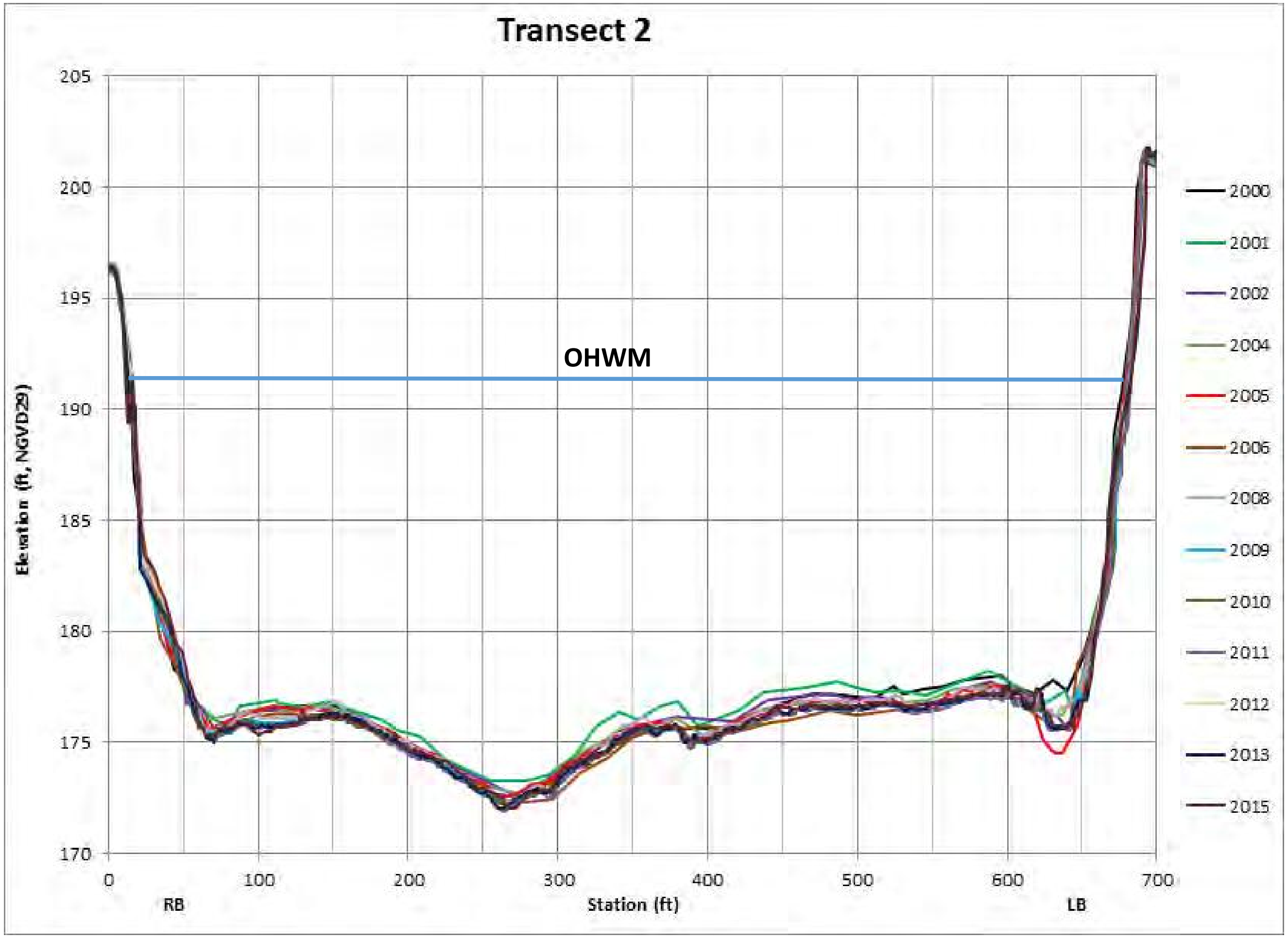

Figure 4.2.4-2 Example cross-section plot

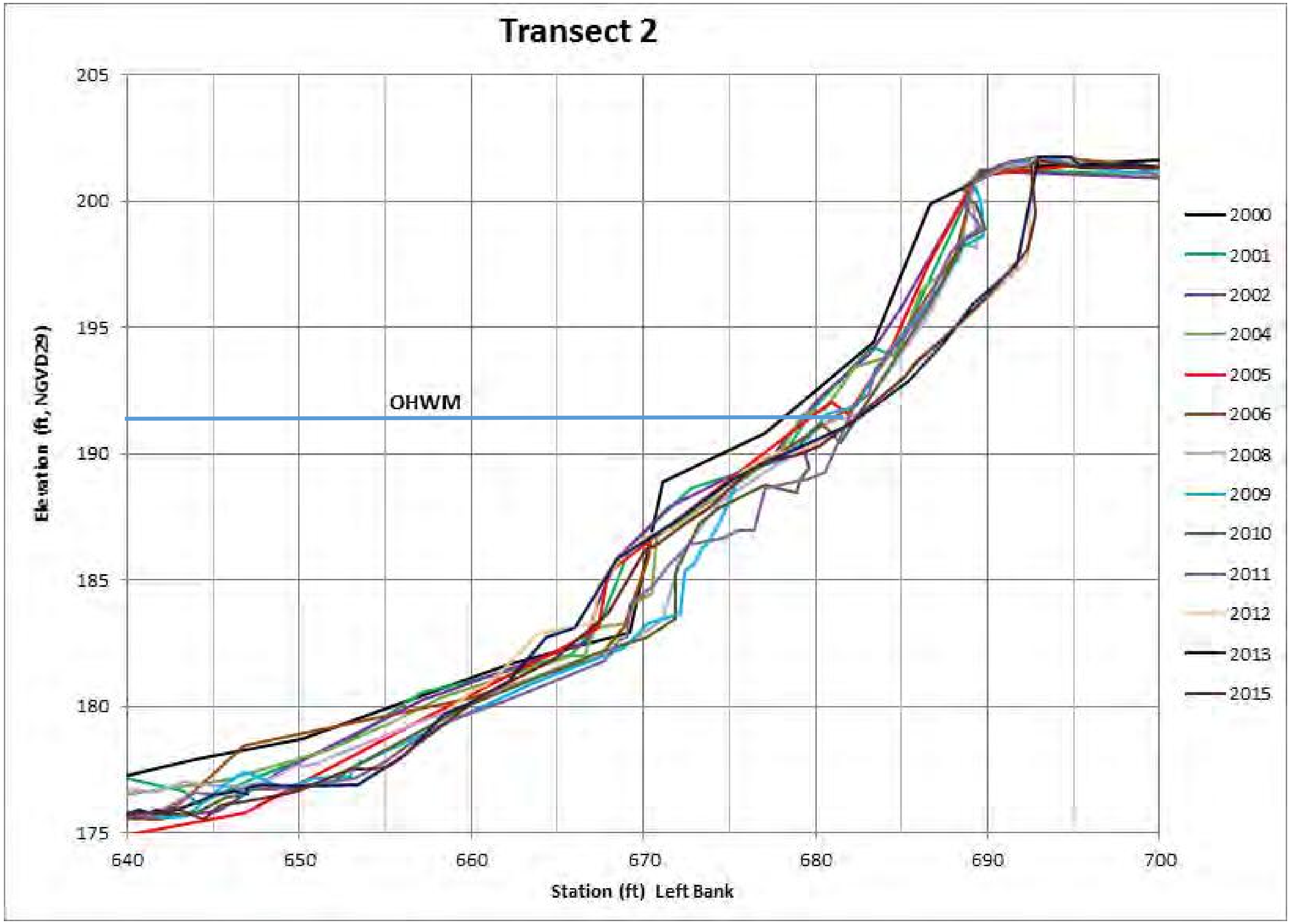

Figure 4.2.4-2 Example cross-section plot

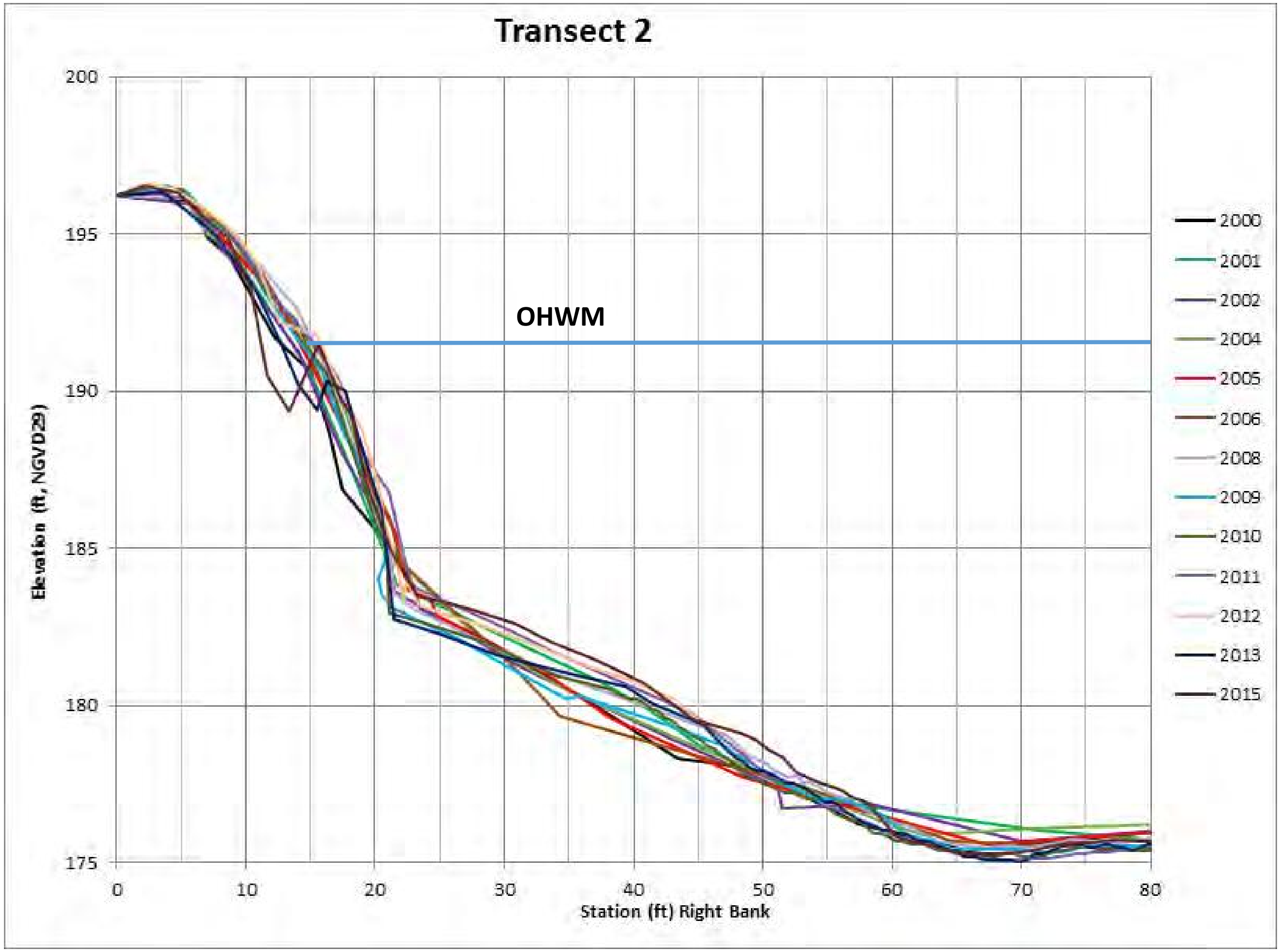

Figure 4.2.4-2 Example cross-section plot

4.2.4.1 Ordinary High Water Mark

On November 5, 2013, following the issuance of FERC's first SPDL, FirstLight met with representatives of MADEP to review the RSP and discuss, among other things, the methodology for Relicensing Study No. 3.1.2. During this meeting MADEP requested that FirstLight identify the OHWM in the TFI as part of the Causation Study. Based on this request, the attendees agreed that FirstLight would develop a methodology to determine the OHWM and, once developed, consult with MADEP for its approval. In the subsequent months following that meeting FirstLight developed a methodology to identify the OHWM in the TFI. FirstLight presented this approach to MADEP on May 27, 2016; receiving approval from the Department on June 1, 2016. The methodology, discussed in more detail below, combined statistical analysis using the available HEC-RAS model and field evaluation based on the USACE OHWM determination criteria.

OHWM Definition and Criteria

Ordinary High Water Mark is defined in Title 33: Navigation and Navigable Waters, CHAPTER II: CORPS OF ENGINEERS, DEPARTMENT OF THE ARMY, DEPARTMENT OF DEFENSE PART 328: DEFINITION OF WATERS OF THE UNITED STATES 328.3 – Definitions:

> *(e) The term ordinary high water mark means that line on the shore established by the fluctuations of water and indicated by physical characteristics such as clear, natural line impressed on the bank, shelving, changes in the character of soil, destruction of terrestrial vegetation, the presence of litter and debris, or other appropriate means that consider the characteristics of the surrounding areas.*

Physical characteristics to consider in determining the Ordinary High Water Line are described in REGULATORY GUIDANCE LETTER No. 05-05 Date: 7 December 2005 SUBJECT: Ordinary High Water Mark Identification

> *b. The following physical characteristics should be considered when making an OHWM determination, to the extent that they can be identified and are deemed reasonably reliable:*

- Natural line impressed on the bank
- Shelving
- Changes in the character of soil
- Destruction of terrestrial vegetation
- Presence of litter and debris
- Wracking
- Vegetation matted down, bent, or absent
- Sediment sorting
- Leaf litter disturbed or washed away
- Scour
- Deposition
- Multiple observed flow events
- Bed and banks
- Water staining
- Change in plant community

Further guidance regarding determination of OHWM was provided by the USACE when they noted that the: *"list of OHWM characteristics is not exhaustive. Physical characteristics that correspond to the line on the shore established by the fluctuations of water may vary depending on the type of water body and conditions of the area. There are no "required" physical characteristics that must be present to make an OHWM determination. However, if physical evidence alone will be used for the determination, districts* *should generally try to identify two or more characteristics, unless there is particularly strong evidence of one."*

The USACE recognized the difficulties in determining OHWM by field investigation stating that *"where the physical characteristics are inconclusive, misleading, unreliable, or otherwise not evident, districts may determine the OHWM by using other appropriate means that consider the characteristics of the surrounding areas, provided those other means are reliable. Such other reliable methods that may be indicative of the OHWM include, but are not limited to, lake and stream gage data, elevation data, spillway height, flood predictions, historic records of water flow, and statistical evidence."*

Methodology

The determination of the elevation defining the OHWM combined field observations and statistical analysis at surveyed transects upstream of the French King Gorge.[31] A statistical analysis of the water level data from the calibrated HEC-RAS model for 2000-2014 was conducted to determine an appropriate, statistically-based OHWM elevation. The range of water levels examined during the statistical analysis were then field verified at a number of the permanent transects located upstream of the French King Gorge based on the physical characteristics described by the USACE. Based on the results of the field evaluation and the statistical analysis, the water surface elevation associated with the 2% exceedance was selected as the OHWM. This elevation was found to be reasonably conservative based on the results of the statistical analysis while also often being well above (i.e. at a higher elevation) the majority of the physical characteristics defined by the USACE. This approach follows guidance provided by the USACE in the available literature. The methodology used to determine the OHWM in the TFI is summarized below:

1. Conduct statistical analysis of water level data from the calibrated HEC-RAS model for 2000-2014, including: peak annual water levels and associated statistics (minimum, maximum, average, median), water level duration analysis, and average water level

2. Using a range of water level durations, mark and photograph, riverbanks at a number of detailed study sites so that assessments can be made of physical characteristics related to OHWM

3. Based on assessment of field data, select appropriate statistical definitions of OHWM

4. Develop cross-sections / maps of OHWM

<u>Statistical Analysis</u>

At the detailed study sites, water levels were computed on an hourly basis using the historic discharge at Vernon Dam as the upstream boundary condition, tributary inflow, the operation of the Northfield Mountain Pumped Storage Project, and historic water levels at Turners Falls Dam as the downstream boundary condition. This hydraulic modeling analysis produced hourly water levels for the time period from 2000 through 2014, consisting of a set of approximately 131,400 numbers. Two types of statistical analyses were conducted using these sets of data: peak annual water level, minimum peak annual water level, averages and medians of annual peak water levels, and a water level-duration analysis. The peak annual water level analysis results in a set of numbers at the detailed study sites while the water-level duration analysis results

---

[31] Sites located below French King Gorge were not evaluated in the field due to the fact that the water surface elevation differences between the modeled scenarios (i.e. 0.27%, 0.5%, 1%, and 2%) were minimal as a result of the relatively flat nature of this portion of the TFI and since the water level is largely determined by the operation of the Turners Falls Dam. Water surface elevation differences between the various exceedances were found to be greater upstream of the hydraulic constriction at the French King Gorge.

in a graph showing the percentage of time that given water levels are equaled or exceeded. Figure 4.2.4.1-1 provides an example of the water-level duration analysis conducted at Site 8BR.

To provide a range of water levels for comparison, water levels at several percentage durations were determined from the water level-duration curves (0.27%, 0.5%, 1%, 2%, 5%). These percentage durations represent the corresponding lengths of time in days (on an annualized basis): 1, 1.83, 3.65, 7.3 and 18.3. In other words, a 0.5% duration represents a water level which is exceeded the equivalent of 1.83 days per year over the 2000-2014 time period (or 27.4 days over 15 years). The results of these statistical analyses are condensed into Table 4.2.4.1-1 and compared against the average, median, maximum and minimum peak water levels achieved over that period.

Table 4.2.4.1-1: Statistical Summary of Peak Annual Water Levels and Water Level Duration Analysis (2000-2014)

Yearly Peaks	BC-1R*	9R*	12BL*	75BL	87BL	8BR	8BL	7R	7L	119BL	6AR	6AL	10L
Average	184.57	184.57	184.57	189.42	189.80	189.94	189.94	190.48	190.48	190.75	190.81	190.81	191.07
Median	184.40	184.41	184.41	189.5	189.88	190.03	190.03	190.61	190.61	190.90	190.97	190.97	191.24
Maximum	185.50	185.50	185.50	193.61	194.08	194.24	194.24	195.02	195.02	195.41	195.52	195.51	195.84
Minimum	184.07	184.07	184.07	186.59	186.89	187.05	187.05	187.54	187.54	187.74	187.79	187.79	187.99
Exceedances													
5%	183.31	183.32	183.32	184.84	185.06	185.22	185.22	185.62	185.62	185.83	185.89	185.89	186.14
2%	183.70	183.70	183.70	186.69	187.02	187.20	187.20	187.74	187.74	188.03	188.09	188.09	188.36
1%	183.90	183.89	183.89	187.81	188.17	188.36	188.36	188.94	188.94	189.23	189.30	189.30	189.59
0.50%	184.01	184.01	184.01	188.58	188.96	189.14	189.14	189.74	189.74	190.06	190.13	190.13	190.41
0.27%	184.20	184.20	184.21	189.15	189.53	189.72	189.72	190.36	190.36	190.68	190.75	190.75	191.05

Yearly Peaks	10R	26R	5CR	29R	4L	21R	3L	18L	303BL	2L	11R	11L
Average	191.10	191.13	191.52	191.95	192.59	192.94	193.03	193.76	194.48	194.42	195.52	195.54
Median	191.28	191.3	191.71	192.15	192.62	192.97	193.07	193.79	194.51	194.45	195.55	195.57
Maximum	195.88	195.91	196.43	197.03	200.17	200.49	200.58	201.15	201.80	201.69	202.57	202.59
Minimum	188.01	188.04	188.41	188.85	189.33	189.70	189.80	190.55	191.25	191.23	192.32	192.34
Exceedances												
5%	186.16	186.18	186.52	186.89	187.29	187.58	187.66	188.33	189.01	189.02	190.02	190.03
2%	188.39	188.41	188.80	189.23	189.70	190.04	190.12	190.85	191.58	191.55	192.63	192.65
1%	189.62	189.65	190.05	190.49	190.97	191.32	191.41	192.17	192.90	192.86	193.96	193.98
0.50%	190.44	190.47	190.91	191.38	191.86	192.23	192.33	193.10	193.85	193.8	194.92	194.94
0.27%	191.08	191.11	191.54	192.00	192.50	192.87	192.97	193.74	194.47	194.42	195.51	195.53

Notes:
* Denotes location below French King Gorge
Average peak = Average of the peak 1 hour annual water level in each year from 2000-2014
Median peak = Median of the peak 1 hour annual water levels in each year from 2000-2014
Maximum peak = Highest single 1 hour annual peak water level during period 2000-2014 (which was in 2011)
Minimum peak = Lowest single 1 hour annual peak water level during period 2000-2014

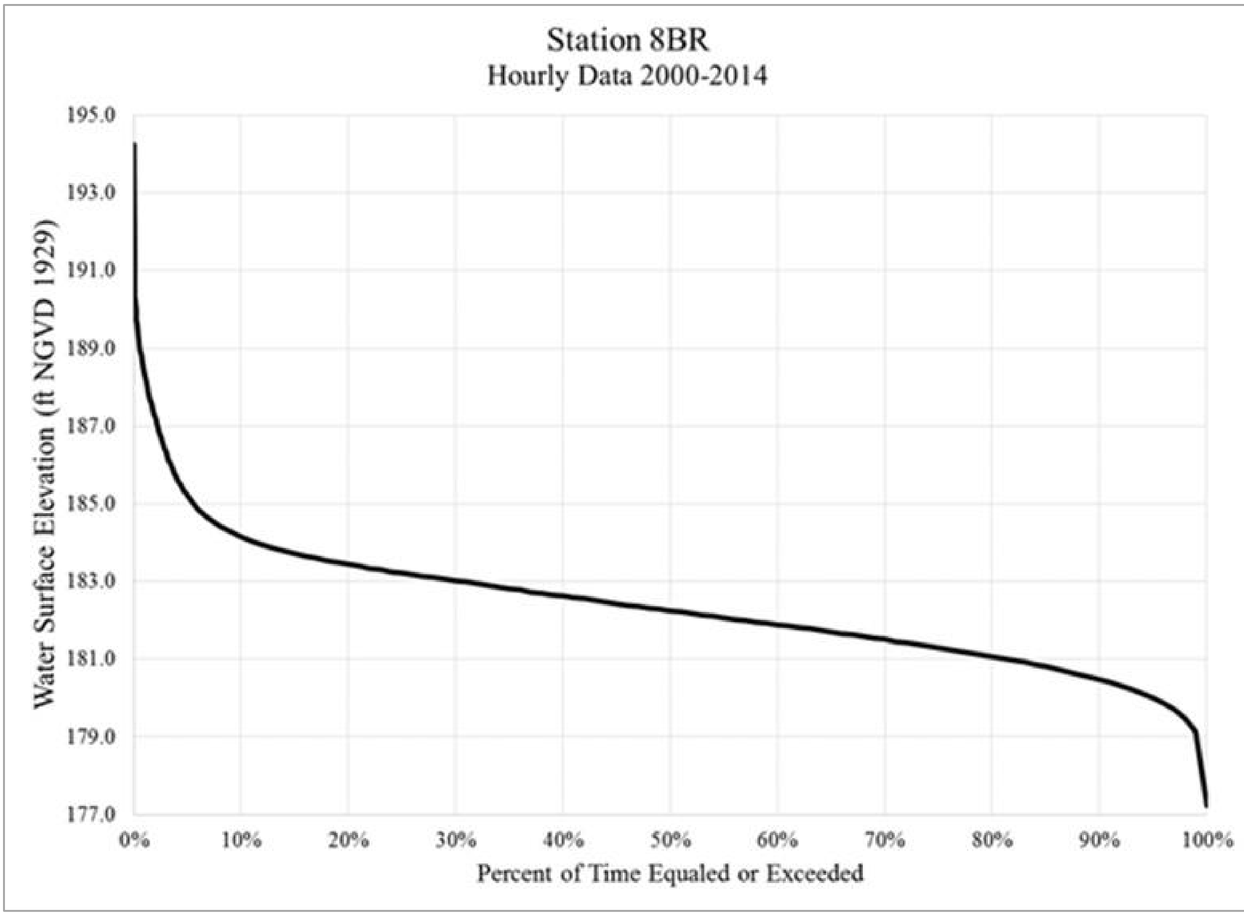

Figure 4.2.4.1-1. Water level-duration curve at Site 8BR

Field Analysis

The field analysis was conducted by surveying a range of water levels at eleven detailed study sites along the length of the TFI upstream of the French King Gorge. Water levels selected for survey during the field component included 0.27%, .5%, 1% and 2% which, as described previously, represent from 1 to 7.3 days per year. Figures were developed showing these water levels on a photograph of the riverbanks. The photographs were then analyzed in order to identify the various physical characteristics noted by the USACE, and discussed earlier in this section, which were present.

Photographs of the riverbanks at a number of sites along the TFI were then labeled with observed physical characteristics as well as a range of water levels from the water level-duration analysis to help determine which statistical measure should be used to define an appropriate water level to represent the ordinary high water mark (Figures 4.2.4.1-2 through 4.2.4.1-8). These figures show the OHWM which is marked as a horizontal yellow line, with physical characteristics labeled above and below the OHWM as observed at each site. At many of these sites there are multiple physical characteristics that identify the OHWM, while at some there are none visible since they are below water.

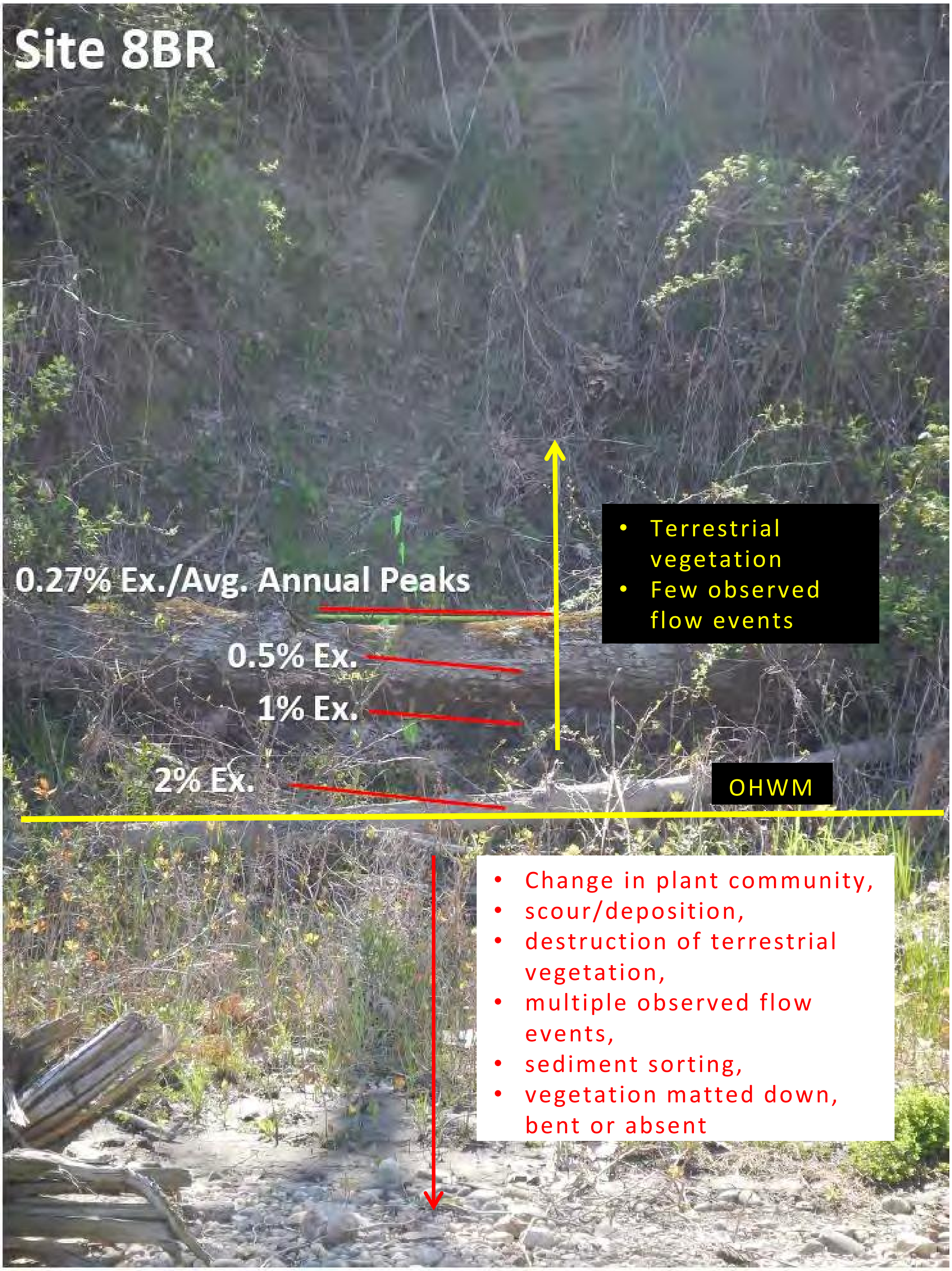

Figure 4.2.4.1-2. Physical characteristics of OHWM at Site 8BR

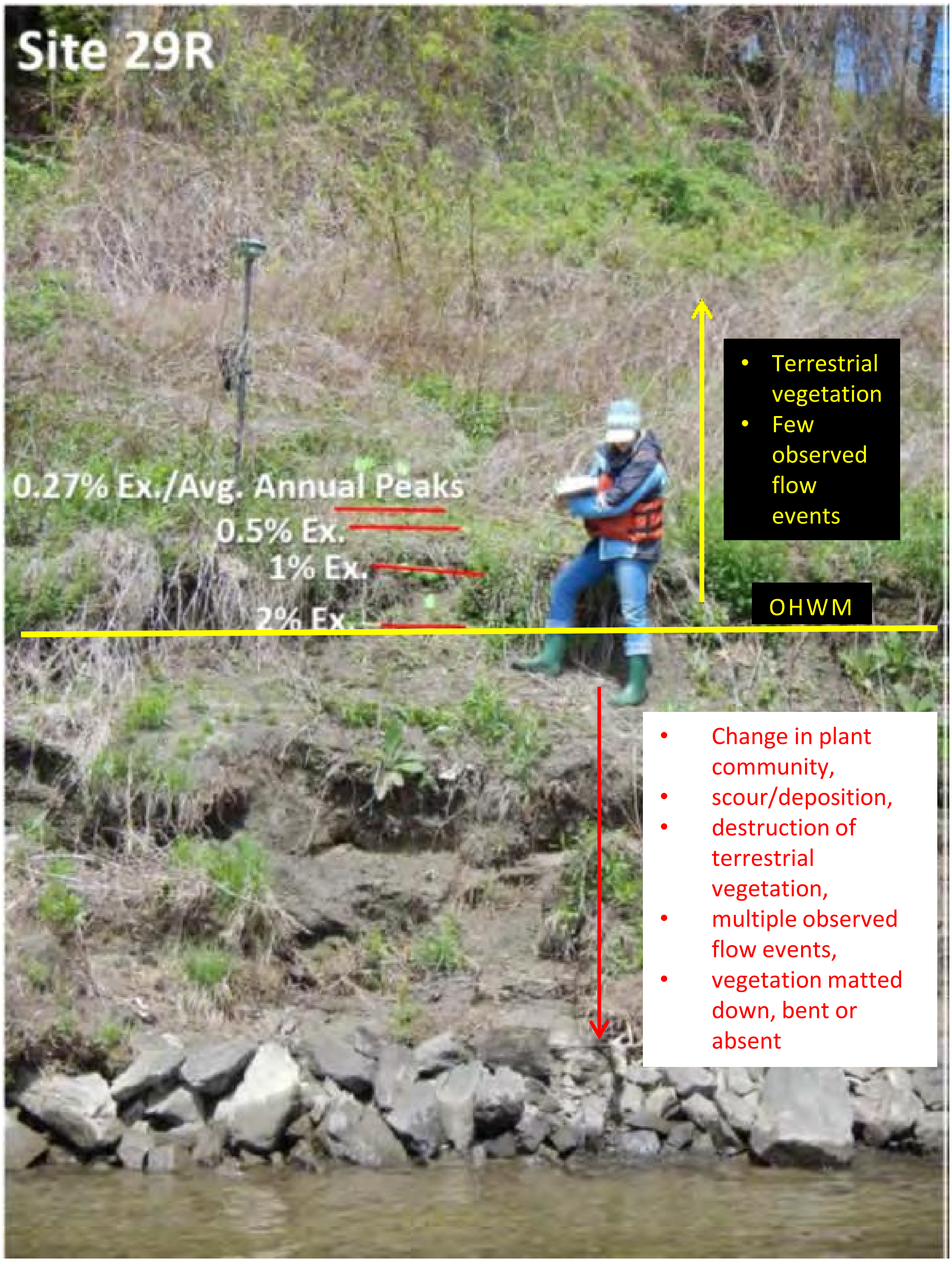

Figure 4.2.4.1-3. Physical characteristics of OHWM at Site 29R

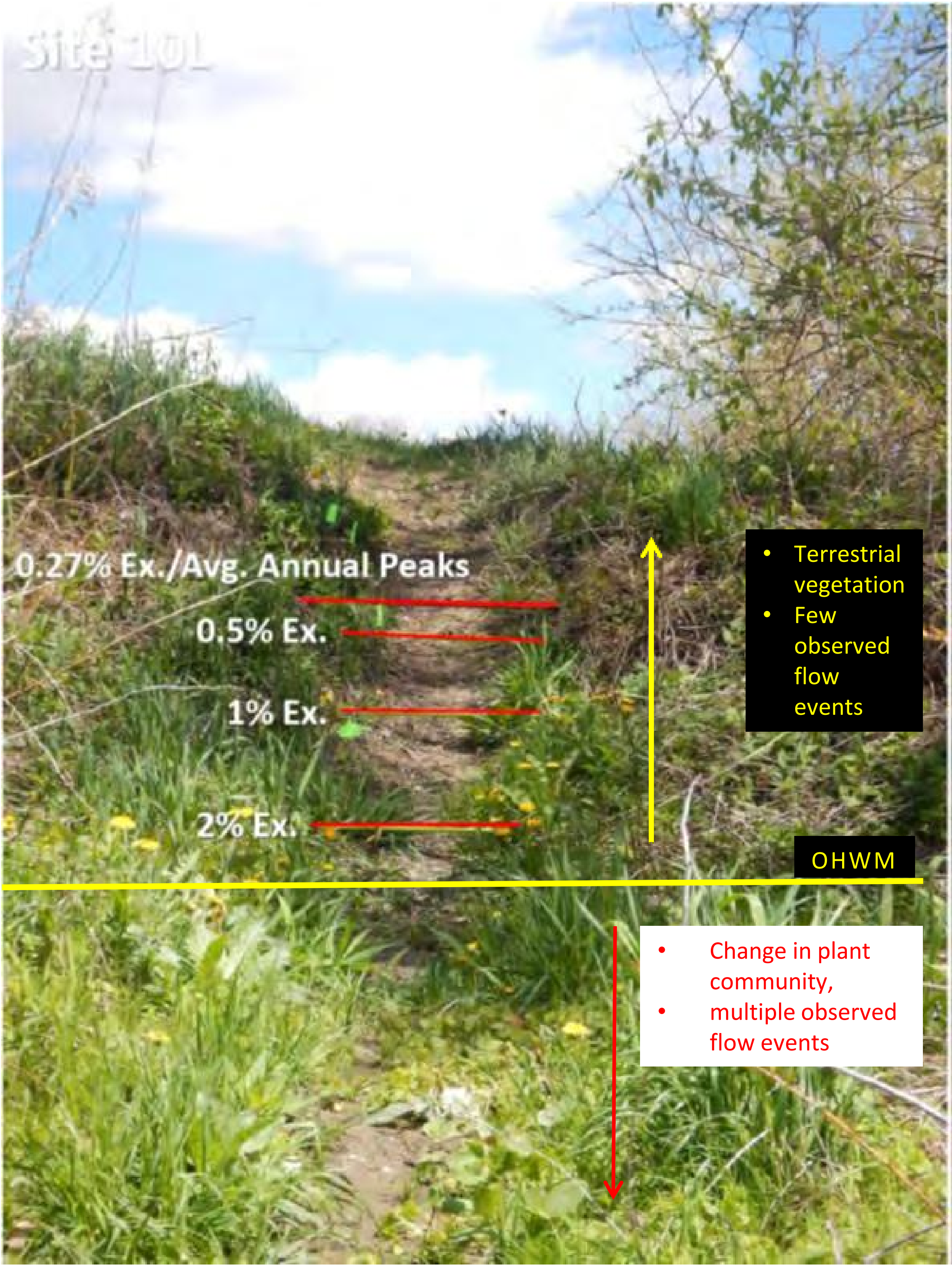

Figure 4.2.4.1-4. Physical characteristics of OHWM at Site 10L

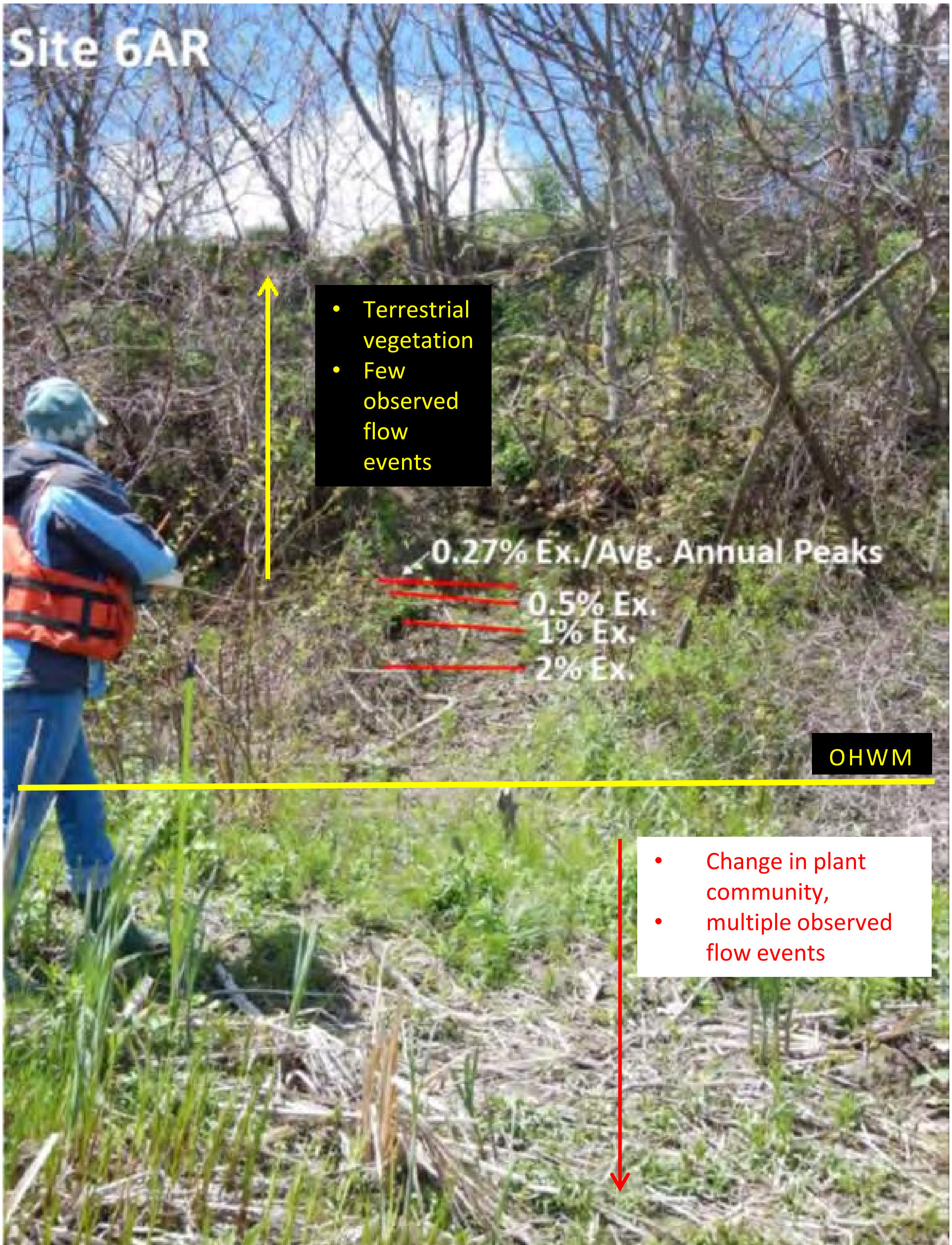

Figure 4.2.4.1-5. Physical characteristics of OHWM at Site 6AR

Figure 4.2.4.1-6 Physical characteristics of OHWM at Site 10R

Figure 4.2.4.1-7 Physical characteristics of OHWM at Site 11L

Figure 4.2.4.1-8 Physical characteristics of OHWM at Site 2L

Determination of OHWM

The determination of OHWM consisted of a field survey/observation component and statistical analysis of water levels. At a number of sites, there were a number of physical characteristics that indicated the location of the OHWM. Where such physical characteristics were observed, they were linked to water level via the water level-duration analysis. At some locations there were no readily observed physical characteristics of the OHWM for the region of the bank below the OHWM due to the water level at the time of the field survey. Table 4.2.4.1-2 summarizes the results of the combination of field observations and statistical analysis of water level.

Some locations exhibited physical characteristics indicating the OHWM at a water level associated with the statitistical analysis, some locations below this level, and others where field observations were inconclusive (below OHWM characteristics not observed due to water level at the time of the survey), the guidelines from the USACE were followed. This approach considers physical characteristics used to characterize the OHWM and also follows the Regulatory Guidance Letter, No. 05-05, December 7, 2005 (USACE) regarding the concept where *"physical characteristics are inconclusive, misleading, unreliable, or otherwise not evident,"* in cases where *"water levels or flows may be manipulated by human intervention for power generation or water supply"* by applying *"elevation data," "historical records of water flow, and statistical evidence."*

In order to develop a conservatively high elevation for the OHWM in the TFI, the highest water level where numerous OHWM physical characteristics were observed was selected. At four locations, the 2% exceedance water level was the highest elevation of the OHWM observed at sites investigated. At five locations, observations indicate that the OHWM was lower than the 2% exceedance water level, and at two locations, physical characteristics indicative of conditions below the OHWM were submerged below the water level at the time of the field work meaning that the OHWM was below the elevation of the 2% exceedance. This approach results in an OHWM that is conservatively high in that at some locations, the actual OHWM could be lower, but at no locations is there indication of a higher OHWM. The 2% level represents an upper limit of what the OHWM is; and to be consistent, the 2% level was then applied at all locations through the TFI.

Based on the statistical analysis of water levels, the ordinary high water mark as indicated by the 2% level was plotted on cross-sections at detailed study sites upstream of the French King Gorge. Other water levels were also plotted to put the results of the OHWM into perspective, these included the 0.27% (which is close to the average and median 1 hour peak annual flow), 5%, and the overall average flow for 2000-2014. An example of a set of such graphs is provided below for Site 8B (Figures 4.2.4.1-9 through 4.2.4.1-11). Cross-section plots depicting the OHWM at each transect are included in Volume III (Appendix E).

Table 4.2.4.1-2: OHWM Elevation at Field Investigated Sites

Site	OHWM elevation
11L	Physical characteristics above OHWM observed above water level, <2%
2L	Physical characteristics above OHWM observed above water level, <2%
29R	2%
26R	2%
10L	<2%
10R	<2%
6AL	<2%
6AR	2%
7L	<2%
8BR	2%
75BL	<2%

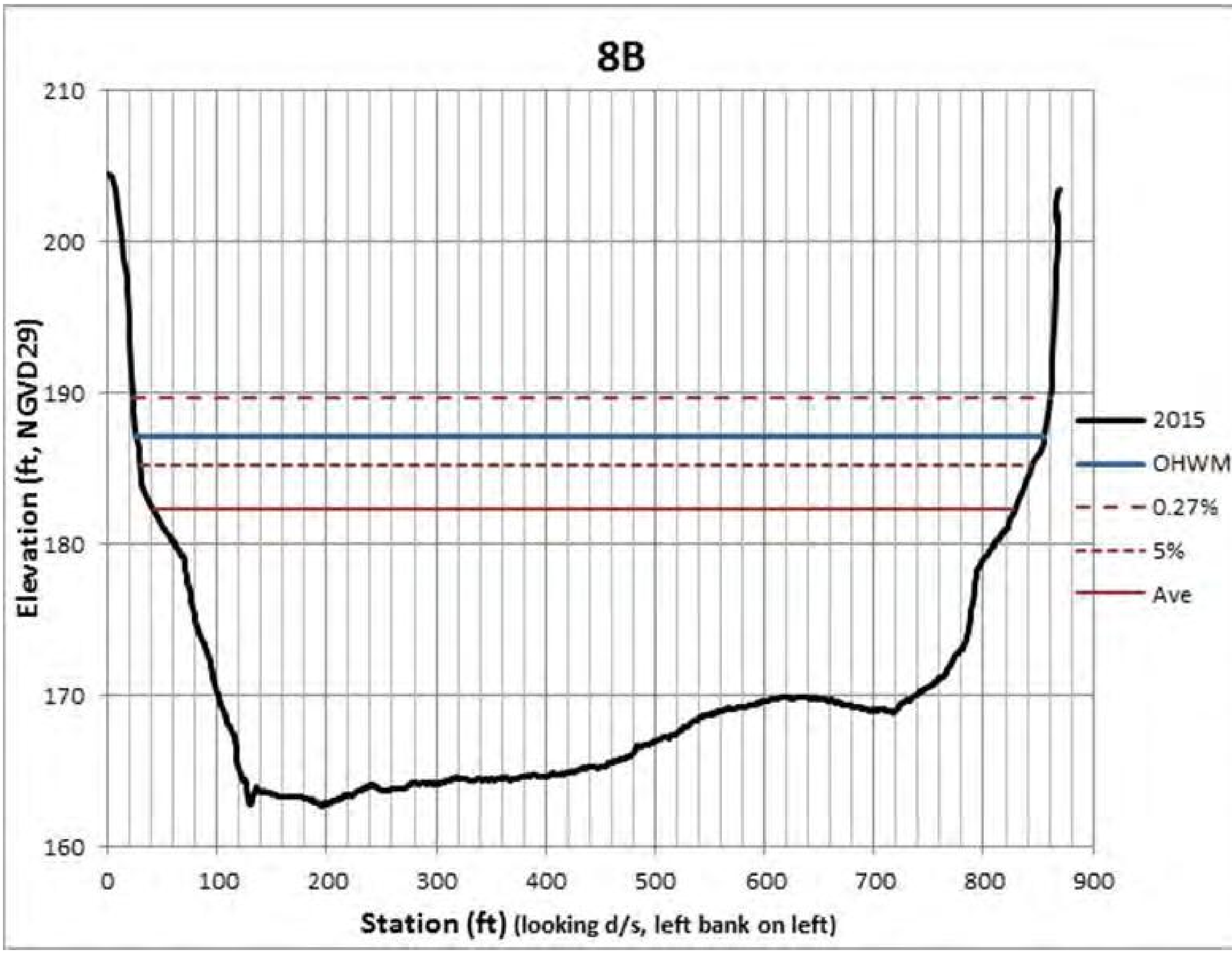

Figure 4.2.4.1-9. OHWM at Site 8B, complete cross-section

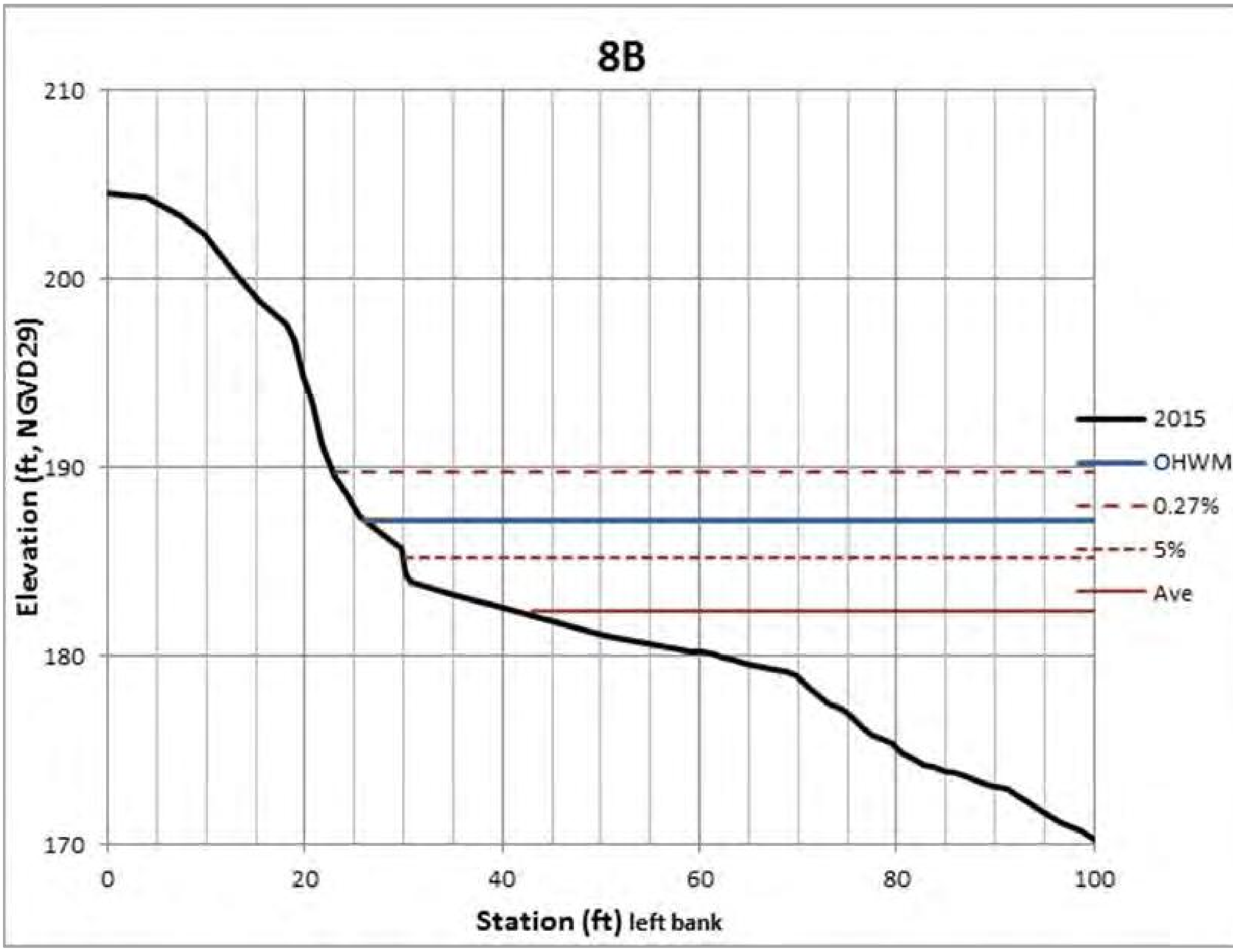

Figure 4.2.4.1-10. OHWM at Site 8B, left bank

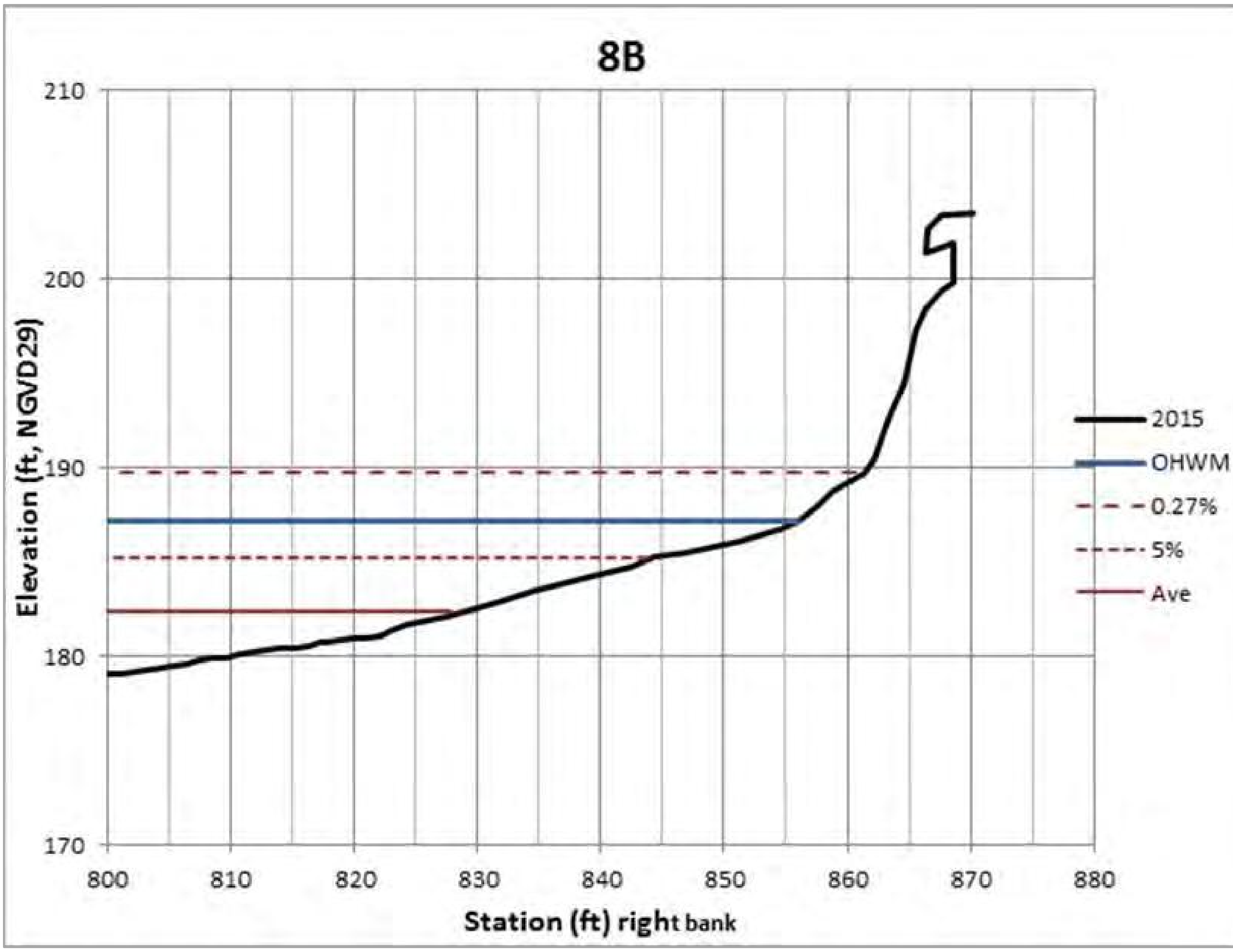

Figure 4.2.4.1-11. OHWM at Site 8B, right bank

4.2.5 Bank Stability and Toe Erosion Model (BSTEM)

BSTEM is a mechanistic bank-stability model specifically designed for alluvial channels. It is programmed in Visual Basic and exists in the Microsoft Excel environment as a simple spreadsheet tool. Data input, along with the various sub-routines are included in different worksheets. The user is able to move freely between worksheets according to their needs at various points of model application. The static version of BSTEM is available to the public free of charge at:

http://www.ars.usda.gov/Research/docs.htm?docid=5044

More details regarding the technical background of BSTEM, and its subroutines (streambank stability, toe erosion and RipRoot), are contained within Volume III (Appendix F). The technical background regarding the newly added wave algorithm is contained within Volume III (Appendix G).

4.2.5.1 General Model Capabilities

The original model, developed by Simon and Curini (Simon & Curini, 1998) Simon *et al.* (Simon, Curini, Darby, & Langendoen, 1999; 2000) is a Limit Equilibrium analysis in which the Mohr-Coulomb failure criterion is used for the saturated part of the streambank, and the Fredlund *et al.* (Fredlund, Morgenstern, Widger, 1978) criterion is used for the unsaturated part. The latter criterion indicates that apparent cohesion changes with matric suction (negative) pore-water pressure, while effective cohesion remains constant. In addition to accounting for positive and negative pore-water pressures, the model incorporates complex geometries, up to five user-definable layers, changes in soil unit weight based on water content, and external confining pressure from streamflow. Current versions combine three limit equilibrium-method models that calculate Factor of Safety (Fs) for multi-layer streambanks. The methods simulated are horizontal layers (Simon *et al.*, 1999; 2000), vertical slices with tension crack (Morgenstern & Price, 1965) and cantilever failures (Thorne & Tovey, 1981). The model can easily be adapted to incorporate the effects of vegetation, geotextiles or other bank-stabilization measures that affect soil strength.

The version of BSTEM described in Simon *et al.*, (Simon, Pollen-Bankhead & Thomas, 2011) and available (Ver. 5.4) includes a sub-model to predict bank-toe and bank-surface erosion, and undercutting by hydraulic shear. This is based on an excess shear-stress approach that is linked to the geotechnical algorithms. Complex geometries resulting from simulated bank-toe erosion are used as the new input geometry for the geotechnical part of the bank-stability model. The geometry of the potential failure plane can be determined automatically by an iterative search routine that locates the most critical failure-plane geometry. In the Static version, if a failure is simulated, the resulting bank geometry can be exported back into either sub-model to simulate conditions over time by running the sub-models iteratively with different flow and water-table conditions. In the Dynamic version, this is done automatically by the model.

The mechanical, reinforcing effects of riparian vegetation (Simon & Collison, 2002; Micheli & Kirchner, 2002) can be included in model simulations. This is accomplished with the RipRoot model (Pollen & Simon, 2005) that is based on fiber-bundle theory and included in the Bank Vegetation and Protection worksheet. The current static version of BSTEM (Ver. 5.4) also includes new features that can account for enhanced hydraulic stresses on the outside of meander bends as well as reduced, effective hydraulic stress operating on fine-grained materials in a reach characterized by a rougher boundary.

The bank-modeling work included in Simon and Curini (1998), Simon *et al.* (2000) and Simon and Collison (2002) utilized a research version of BSTEM that includes the same fundamental algorithms as the Static version but also allows for input of an unsteady flow series (i.e. stage can vary at each time step). This version was called BSTEM-Dynamic 1.0. To more accurately simulate bank-erosion processes, BSTEM-Dynamic Ver. 2.0 includes a near-bank groundwater sub-model that permits dynamic adjustment of pore-water pressures over extended hydrographs. This version has been used by scientists at the U.S. Department of Agriculture - Agricultural Research Service (USDA-ARS) National Sedimentation Laboratory and at Cardno to simulate bank-erosion processes and to predict bank-erosion rates over time periods of up to 100 years (Simon & Klimetz, 2012). BSTEM-Dynamic has been applied successfully in diverse environments across the globe including Australia, New Zealand, Taiwan, China, England, California, Mississippi, Vermont, South Dakota, Washington, and now along the Connecticut River. This dynamic version of BSTEM will be made available to the public in the future at the discretion of the USDA-ARS, National Sedimentation Laboratory.

In this study we used BSTEM Dynamic Ver. 2.3 which was further modified (from Ver. 2.0) to include variable roughness by layer, and the effect of boat waves in each modeled time step.

4.2.5.2 Bank Toe Erosion Sub-Model

The Bank-Toe Erosion sub-model is used to estimate erosion of bank and bank-toe materials by hydraulic shear stresses. The effects of toe protection are incorporated into the analysis by changing the characteristics of the toe material in the model. The model calculates an average boundary shear stress from channel geometry and flow parameters, defined by flow depth and the duration of the time step (steady, uniform flow). The assumption of steady, uniform flow is not critical insomuch as the model does not attempt to route flow and sediment and is used only to establish the boundary shear stress for a specified duration (the period of the time step) along the bank surface. The model also allows for different critical shear stress and erodibility of separate zones with potentially different materials at the bank and bank toe. The bed elevation is fixed because the model does not incorporate the simulation of bed sediment transport. Toe erosion by hydraulic shear is calculated using an excess shear approach. Modifications made to BSTEM Dynamic Ver. 2.0 for this study allow the toe erosion sub-model to account for variations in water-surface slope in each time step.

4.2.5.3 Bank Stability Sub-Model

The bank stability sub-model simulates planar failure types in steep banks, and shear failure in banks that have been undercut by preferential erosion of an erodible basal layer (Figure 4.2.5.3-1). These are shear-type failures that occur when the driving force (stress) exceeds the resisting force (strength). The model combines two limit-equilibrium methods that estimate the Factor of Safety (F_s) of multi-layer streambanks. F_s is the ratio between the resisting and driving forces acting on a potential failure block. A value of unity indicates that the driving forces are equal to the resisting forces and that failure is imminent (F_s = 1). Instability exists under any condition where the driving forces exceed the resisting forces (F_s < 1), conditional stability is indicated by F_s values between 1 and 1.3, with stable bank conditions having a F_s >1.3.

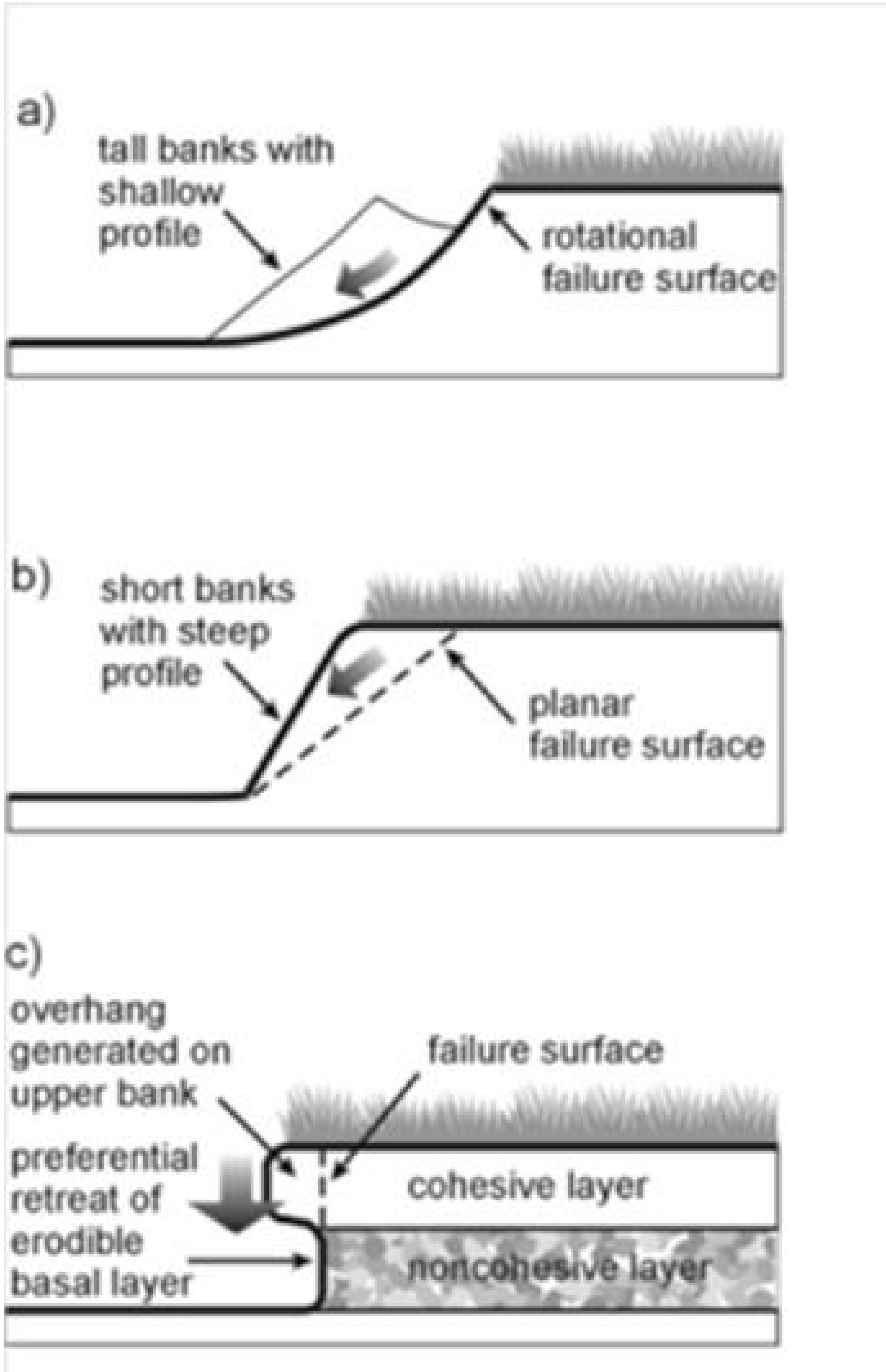

Figure 4.2.5.3-1: Streambank Failure Mechanisms

4.2.5.4 Root Reinforcement Sub-Model (RipRoot)

Vegetation can have a number of positive and negative effects on streambank stability. Of these effects, one of the most important to account for in stability calculations is the effect of root-reinforcement on soil shear strength. Soil is generally strong in compression, but weak in tension. The fibrous roots of trees and herbaceous species are strong in tension but weak in compression. Root-permeated soil, therefore, makes up a composite material that has enhanced strength (Thorne, 1990). Many studies have found an inverse power relationship between ultimate tensile strength, T_r, and root diameter, d (examples include but are not limited to: Waldron & Dakessian, 1981; Gray and Sotir, 1996; Abernethy and Rutherfurd, 2001; Simon & Collison, 2002; Pollen & Simon, 2005), and have shown that root-reinforcement can affect the shear-strength of the bank materials, and locations of shear failure surfaces within the banks.

In the RipRoot model currently embedded in BSTEM, a vegetation assemblage can be created by accessing the species database contained in the sub model; the user enters species, approximate vegetation ages, and approximate percent cover of each species at each site to estimate root density. Root-reinforcement values are then calculated automatically using RipRoot's progressive breaking algorithm. The database of species contained within RipRoot includes tests performed across the United States and has been expanded as part of this study to include five of the most common species found along the Turner Falls reach of the Connecticut River.

4.2.5.5 BSTEM Data Requirements

As BSTEM is a mechanistic model, the data required to operate the model are all related to quantifying the driving and resisting forces that control the hydraulic and geotechnical processes that operate on and along a streambank. Input-parameter values can all be obtained directly from field surveying and testing. If this is not possible, the model provides default values by material type for many parameters.

Data required for BSTEM fall into three broad categories: (1) bank geometry and stratigraphy, (2) hydraulic data, and (3) geotechnical data. A summary of the required input parameters is provided in Table 4.2.5.5-1. The default geotechnical values that are included in the model are provided in Table 4.2.5.5-2 (Simon *et al.*, 2011).

Table 4.2.5.5-1: Required User-Input Parameters for BSTEM

Hydraulic Processes: Bank Surface					
Driving Forces			**Resisting Forces**		
Parameter	**Purpose**	**Source**	**Parameter**	**Purpose**	**Source**
Channel Slope (*S*)	Boundary shear stress (τ_o)	Field survey or design plan	Particle diameter (*D*) (*cohesionless*)	Critical shear stress (τ_c)	Bulk sample particle size (*cohesionless*); Default values in model
			Critical shear stress (τ_c) (*cohesive*)	Critical shear stress (τ_c)	Jet test (*cohesive*); Default values in model
Flow depth (*h*)	Boundary shear stress (τ_o)	Field survey, gage information, design plan	Particle diameter (*D*) (*cohesionless*)	Erodibility coefficient (*k*)	Bulk sample particle size (*cohesionless*); Default values in model
			Critical shear stress (τ_c) (*cohesive*)	Erodibility coefficient (*k*)	Jet test (*cohesive*); Default values in model
Unit weight of water (γ_w)	Boundary shear stress (τ_o)	Considered constant, 9810 N/m^3			
Geotechnical Processes: Bank Mass					
Parameter	**Purpose**	**Source**	**Parameter**	**Purpose**	**Source**
Unit weight of sediment (γ_s)	Weight (*W*), Normal force (σ)	Core sample in bank unit; Default values in model	Unit weight of sediment (γ_s)	Weight (*W*), Normal force (σ)	Core sample in bank unit; Default values in model
Bank height (*H*)	Shear stress	Field survey or design plan	Effective cohesion (*c'*)	Shear strength (τ_f)	Borehole shear, direct shear, triaxial shear; Default values in model
Bank angle (α)	Shear stress	Field survey or design plan	Effective angle (φ')	Shear strength (τ_f)	
			Pore-water pressure (μ_w)	Shear strength (τ_f)	Interpolated from water table

Table 4.2.5.5-2: Default Values in BSTEM (bold) for Geotechnical Properties

Soil Type	Statistic	*c'* (kPa)	Φ' (degrees)	γ_{sat} (kN/m^3)
Gravel (uniform)*		0.0	36.0	20.0
Sand and Gravel*		0.0	47.0	21.0
Sand	75th percentile	1.0	32.3	19.1
	Median	**0.4**	**30.3**	**18.5**
	25th percentile	0.0	25.7	17.9
Loam	75th percentile	8.3	29.9	19.2
	Median	**4.3**	**26.6**	**18.0**
	25th percentile	2.2	16.7	17.4
Clay	75th percentile	12.6	26.4	18.3
	Median	**8.2**	**21.1**	**17.7**
	25th percentile	3.7	11.4	16.9

Data derived from more than 800 *in situ* direct-shear tests with the Iowa Borehole Shear Tester except where indicated (From Hoek and Bray (1977) as cited by Simon *et al.*, 2011).

4.2.5.6 General Model Limitations

BSTEM can simulate the most common types of bank failures that typically occur along alluvial channels. Once failure is simulated, the failed material is assumed to enter the flow. The model does not simulate rotational failures that generally occur in very high banks of homogeneous, fine-grained materials characterized by low bank angles. Although potentially damaging with regards to the amount of land loss, these failures are not common along the reach. Evidence of historical rotational failures was observed only on high-terrace surfaces, far removed from the active channel. Bank undercutting by seepage erosion is similarly not included in the version described herein. This is not considered a problem along the Turners Falls reach as evidence of seepage processes were observed at only a few sites by field crews. Finally, the hydrologic effects of riparian vegetation, including interception, evapo-transpiration and the accelerated delivery of water along roots and macro pores cannot be simulated at this time.

4.2.5.7 BSTEM Summary

BSTEM Dynamic contains both geotechnical-stability and hydraulic-erosion algorithms, thereby allowing for deterministic analysis of bank stability over time. As such, flow stage at each time step is read into the model, and the amount and location of hydraulic erosion is calculated. The resulting new bank geometry for that time step is then used in the geotechnical algorithm to determine the stability of the bank by calculating the bank's Factor of Safety (<1.0 = unstable) at that time step. If a geotechnical failure is predicted, the geometry is updated again to account for the failure before the next flow-stage value is read in at the next time step. In this way BSTEM Dynamic 2.3 can predict the retreat of a streambank for flow series ranging in length from hours to decades. In addition to being able to take into account both hydraulic and geotechnical processes, the model has a groundwater component that contributes to the geotechnical strength algorithm, and can account for the effects of root-reinforcement provided by riparian vegetation, through the RipRoot sub-model (Pollen & Simon, 2005; Pollen, 2007; Thomas & Bankhead, 2010).

4.2.6 BSTEM Input Data Collection

To determine the erosion resistance of the 25 detailed study sites throughout the TFI (as previously shown in Figure 4.1-1 and 4.1-2), Cardno staff, with assistance of staff from NEE, performed field tests to quantify the geotechnical and hydraulic resistance of the bank and bank-toe materials at each site. The locations of these sites were discussed in Section 4.1, are representative of the range of conditions present along the reach and are spaced relatively evenly. Rough surveys of the tested banks were also carried out at each site with a tape and Brunton compass to provide bank heights, angles, and stratigraphic layering for the tested bank. The data collected in the field were used by Cardno to populate BSTEM-Dynamic 2.3.

4.2.6.1 Geotechnical Data Collection: Borehole Shear Tests

To properly determine the resistance of bank materials to erosion by mass movement, data must be acquired on those characteristics that control shear strength; that is cohesion, angle of internal friction, pore-water pressure, and bulk unit weight. Cohesion and friction angle data can be obtained from standard laboratory testing (triaxial shear or unconfined compression tests), or by in-situ testing with a borehole shear-test (BST) device (Lohnes & Handy 1968; Thorne, Murphey & Little, 1981; Lutenegger & Hallberg, 1981; Little, Thorne & Murphy, 1982). To gather data on the internal shear-strength properties of the banks, in-situ tests with the Iowa Borehole Shear Tester (BST) were used (Figure 4.2.6.1-1 - Figure 4.2.6.1-2).

The BST provides direct, drained shear-strength tests on the walls of a borehole. To use the BST, a 0.069 m (2.75 in) diameter hole is bored using an auger, from the floodplain or other flat surface into a particular bank layer to be tested. Under a known initial pressure, the shear head is then placed in the borehole to the desired depth and expanded to the walls of the borehole, using CO_2 gas connected to the Normal Stress console. After initial consolidation, the pulling assembly is used to apply an axial stress to the shear head, measured on the shear gauge, until failure beyond the walls of the borehole occurs. The axial stress is released, and the normal pressure is raised typically in increments of about 10-20 kPa, and an additional 5-30 minutes of consolidation is provided, depending on the soil type and moisture content.

The shearing process is repeated to generate a series of data points representing the material's shear stress at failure at each associated normal stress applied to the walls of the borehole. The data points are then plotted, with normal stress on the x-axis and shear stress on the y-axis (Figure 4.2.6.1-3). The gradient of the resulting linear relation represents the friction angle of the soil layer tested and the y-intercept represents the apparent cohesion (ca) of the soil layer. Effective cohesion (c') is then calculated by subtracting a measure of the soil suction (negative pore-water pressure; asymptote in Figure 4.2.6.1-4) from the value of apparent cohesion (y-intercept in Figure 4.2.6.1-3). This is done by solving for c', substituting the asymptotic suction value from Figure 4.2.6.1-4, and assuming a value of ϕ^b. We generally use a value of 10^o based on field tests in alluvial materials (Simon *et al.*, 2000).

The friction angle can be thought of as being similar to the angle of repose; this is the steepest angle that a cohesionless slope can maintain without losing its stability. When a slope or streambank possesses this angle, its shear strength perfectly counterbalances the force of gravity acting upon it, and remains stable unless other driving forces are also present (for example water). Pore-water pressure at the time of sampling is obtained using a digital tensiometer inserted into a core that has been retrieved from the test depth.

Advantages of the BST include:

1. The test is performed *in situ* and testing is, therefore, performed on undisturbed material;

2. Cohesion and friction angle are evaluated separately. The cohesion value represents apparent cohesion (ca). Effective cohesion (c') is then obtained by adjusting ca according to measured pore-water pressure and ϕ^b (rate of increase in strength with increasing matric suction);

3. A number of separate trials are run at the same sample depth to produce single values of cohesion and friction angle based on a standard Mohr-Coulomb failure envelope;

4. Data and results obtained from the instrument are plotted and calculated on site, allowing for repetition if results are unreasonable; and

5. Tests can be carried out at various depths in the bank to locate weak strata (Thorne *et al*. 1981).

At each testing depth, a small core of known volume was removed and sealed to be returned to the laboratory. The samples were weighed, dried and weighed again to obtain values of moisture content and bulk density, the latter required for analysis of streambank stability. In addition, bulk samples were obtained at each testing depth for particle-size analysis.

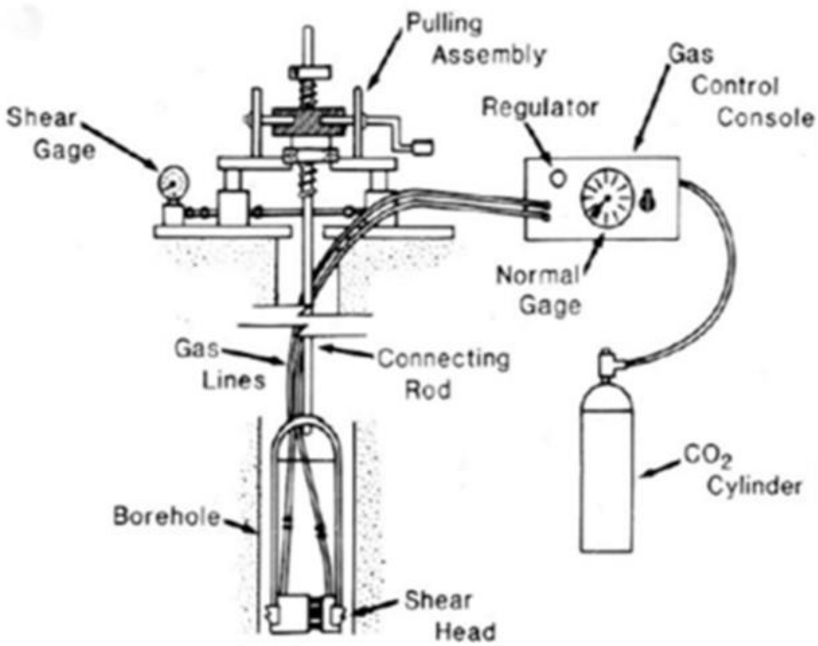

Figure 4.2.6.1-1: Schematic Representation of Borehole Shear Tester (BST)

Figure 4.2.6.1-2: Conducting a Borehole Shear Test (BST)

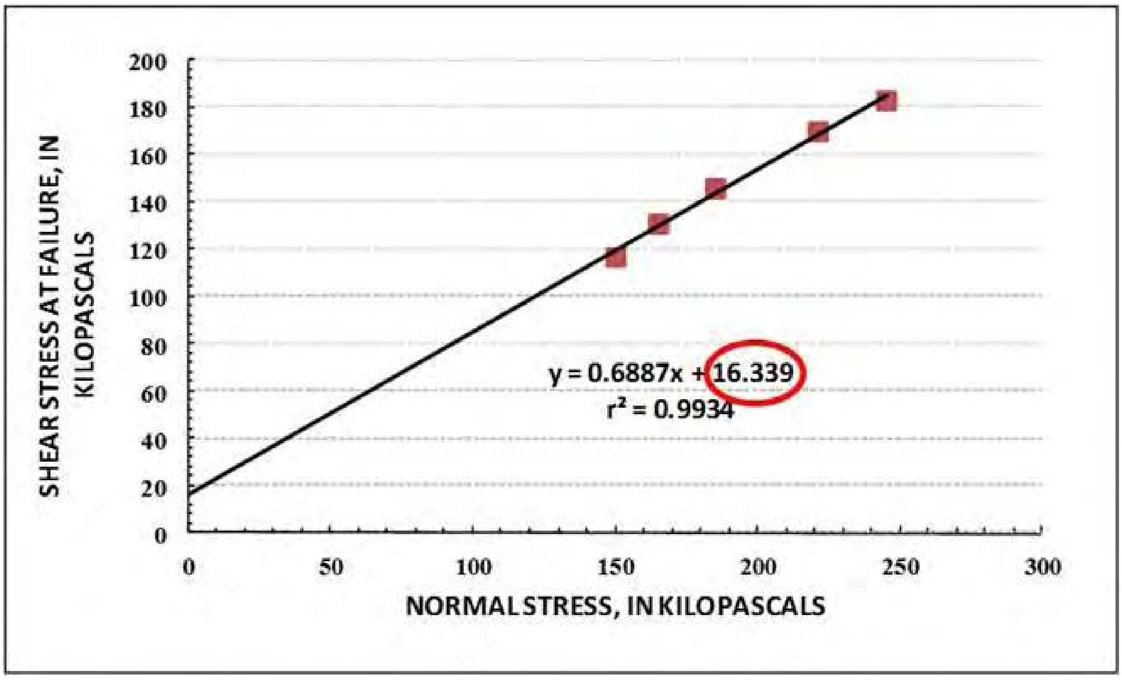

Figure 4.2.6.1-3: Example of a Borehole Shear Test (BST)

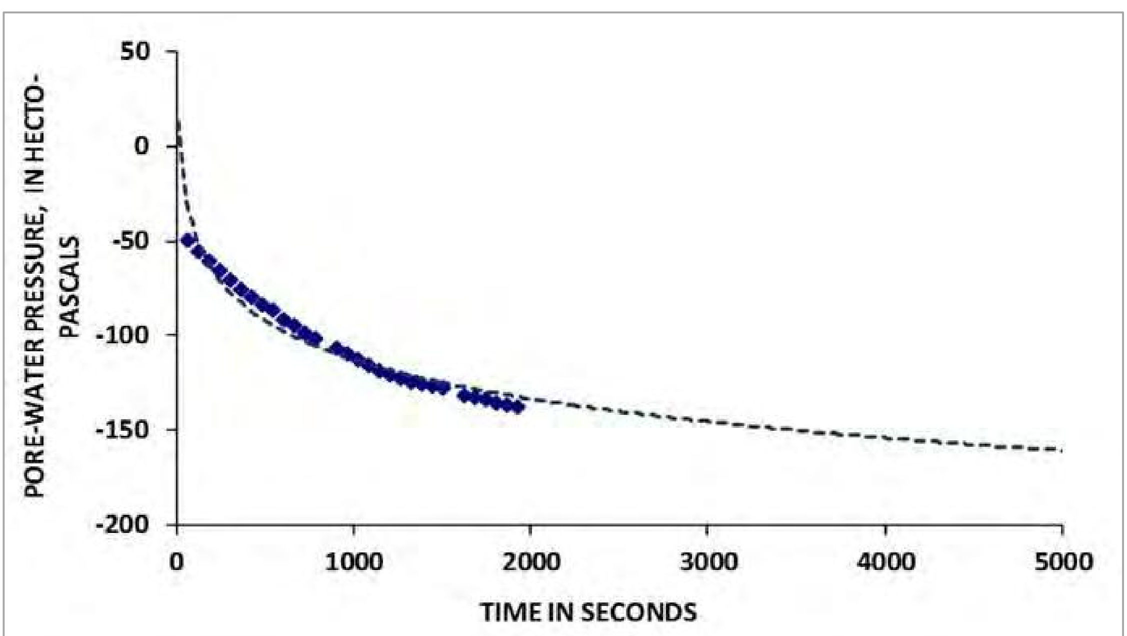

Figure 4.2.6.1-4: Typical Pore-Water Pressure Data Obtained from a Core using a Digital Tensiometer

4.2.6.2 Hydraulic-Resistance Data Collection: Submerged Jet Tests

Hydraulic-resistance of the bank-toe and bank face are important for predicting scour and undercutting of the channel banks within BSTEM. Where materials are non-cohesive, resistance is due to particle size and weight, therefore, a bulk particle-size or particle count is sufficient to describe resistance properties. However, cohesive materials are not entrained into the water column predictably due to particle size and weight but due to the electro-chemical bonds between particles. To test *in situ* erodibility of cohesive materials, a submerged jet test was developed by the USDA-ARS (Figure 4.2.6.2-1; Hanson, 1990; ASTM, 1995). This device was developed based on knowledge of the hydraulic characteristics of a submerged jet and the characteristics of soil-material erodibility.

The Mini-Jet used throughout this project is a scaled-down version of the original instrument. Side-by-side testing of the mini-jet and the standard submerged jet are reported in Simon *et al.,* (2010; 2011) and Al-Madhhachi *et al.*, 2013 (Figure 4.2.6.2-2). The method provided by Al-Madhhachi *et al.*, (2013) to scale mini-jet results to the full-size jet was adopted in this work.

Depth-of-scour is measured manually using a point gauge at known increments over time. As the scour depth increases with time, the applied shear stress decreases, due to increasing dissipation of jet energy within the plunge pool. Detachment rate is initially high and asymptotically approaches zero as applied shear stress approaches the critical shear stress of the material (Figure 4.2.6.2-3). A difficulty in determining equilibrium scour depth is that the length of time required to reach equilibrium can be large. Fitting time-series scour data to the logarithmic-hyperbolic method described in Hanson and Cook (Hanson & Cook, 1997), however, provides the critical shear stress, (τ_c) and the erodibility coefficient, (k). Essentially, k is the slope of the scour vs. time curve, expressing the volume of material eroded per unit force (Newtons) and per unit time (seconds) (Figure 4.2.6.2-3). Hence, k is expressed as cm^3/N-s. As part of the field program, bulk samples were also taken of the surficial bank sediments to be tested for particle-size distribution.

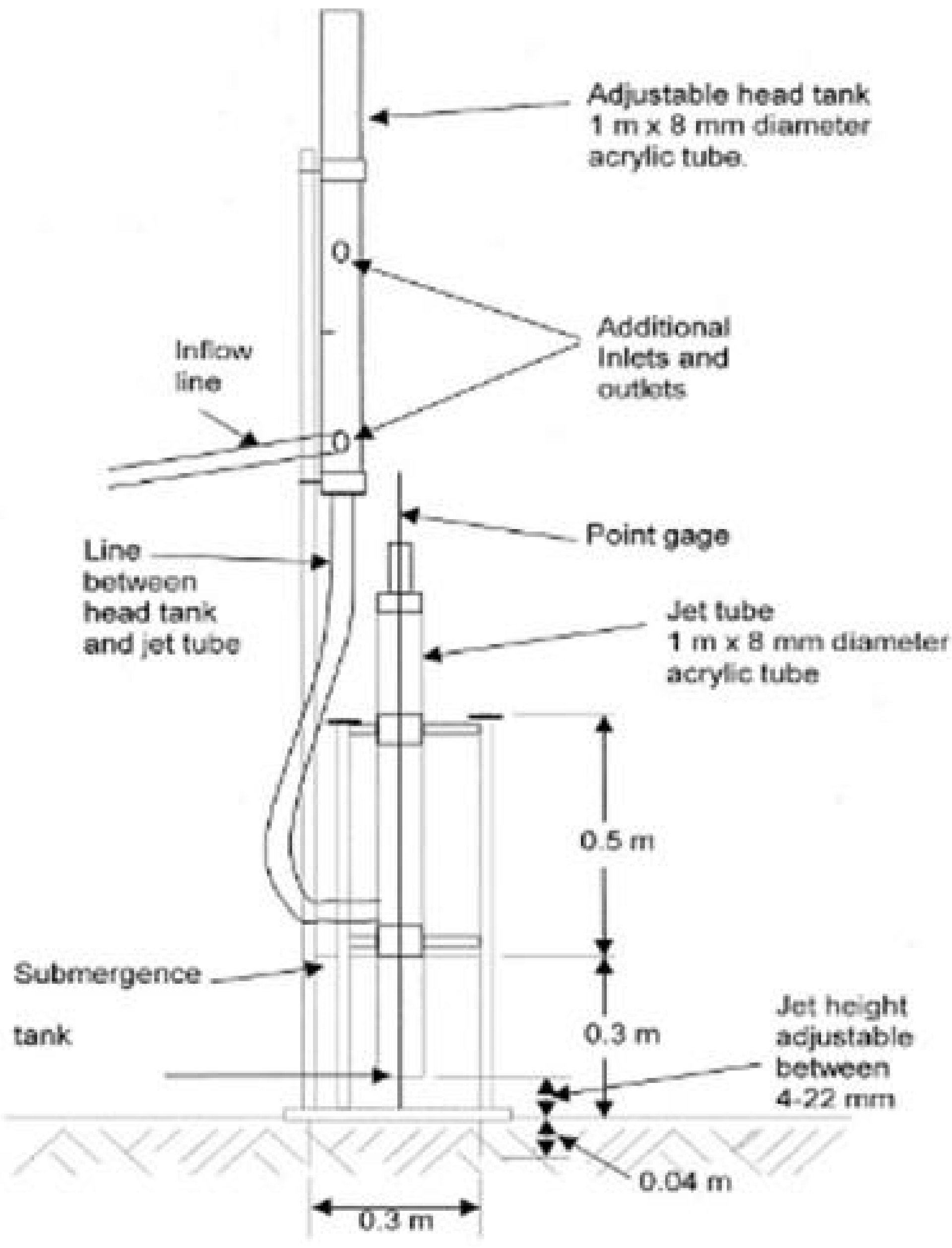

Figure 4.2.6.2-1: Schematic of Original Jet-Test Device

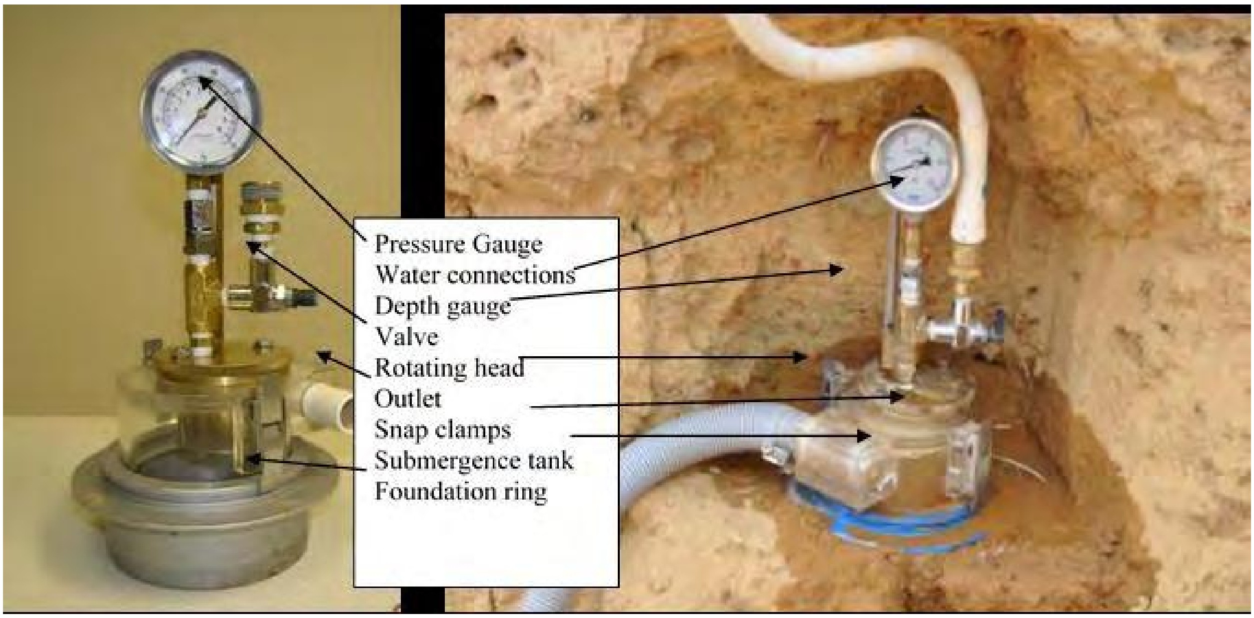

Figure 4.2.6.2-2: Photographs of Scaled-down “Mini-jet”

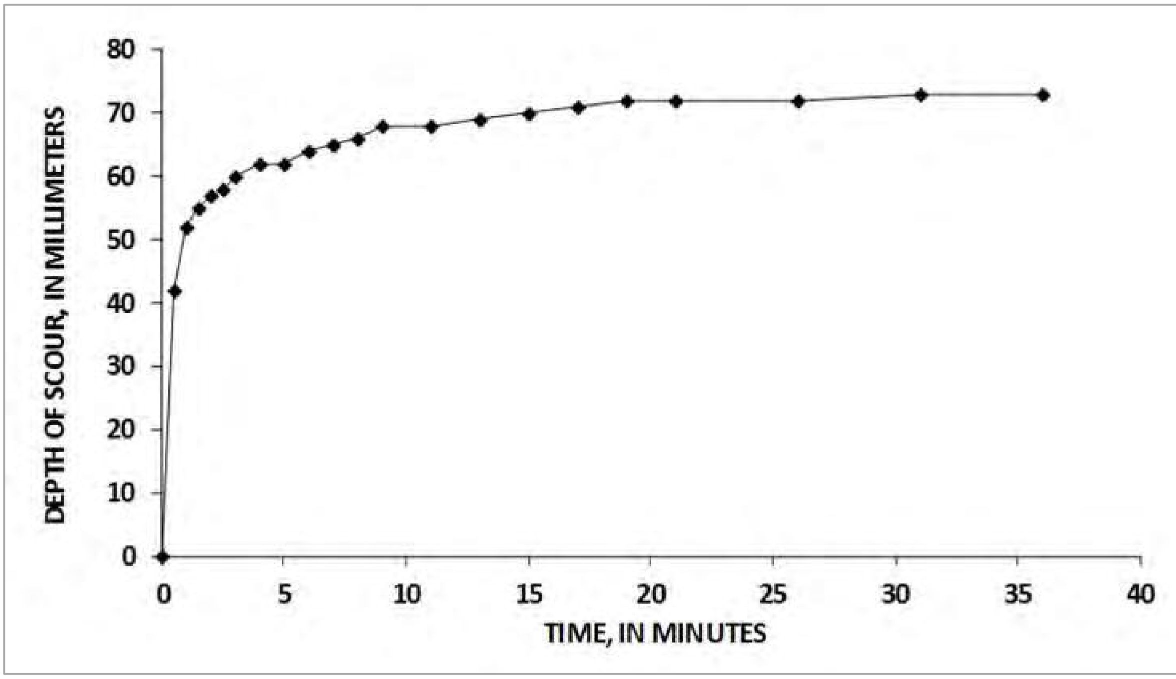

Figure 4.2.6.2-3: Example Scour Plot From Mini-jet Test

4.2.6.3 Particle Size of Bank Sediments

Bulk bank-material samples were taken at each location tested by the BST and the submerged jet test device. In addition, if coarse-grained materials were present (gravels and cobbles) measurements of 100 particles were conducted to determine the size distribution. These data were then combined with the bulk-sample particle-size analysis to determine an overall distribution of sizes. These data were collected to associate test results with general material types, and to provide information on entrainment thresholds for non-cohesive materials. The laboratory used a particle size of 0.063 mm as the break point between sand and silt. Thus, reference to fine-grained materials is defined as that proportion of the sample finer than 0.063 mm. A total of 126 bulk and particle-count samples of bank face, bank toe (beach) and internal bank materials were collected and analyzed. Results from an example analysis are shown in Figure 4.2.6.3-1.

Bank materials at the test locations are, for the most part, a combination of sands and silts in varying proportions (Table 4.2.6.3-1 and Figure 4.2.6.3-2). The median composition of the bank materials is 0% gravel, 51.5% sand, 41.8% silt and 3.8% clay. This is not to say that gravel is not present at some of the sites. Particle counts were conducted at 10 sites along the reach owing to the presence of some gravel and cobbles along the beach- bank toe regions. In some cases, their presence was due to placement as part of restoration works. Full distributions by particle-size class are shown in Figure 4.2.6.3-2.

The majority of the materials (72%) can be classified as either sandy or silt loams Table 4.2.6.3-2. This and the general lack of clays in the bank strata should limit the magnitude of permeability differences in the banks that would relate to issues with perched groundwater and seepage. Values used for saturated hydraulic conductivity (according to textural class) were obtained from the Natural Resources Conservation Service (NRCS) website (NRCS, 2015). These are also shown in Table 4.2.6.3-2.

Sorting the samples into distinct sampling locations of beach-toe, bank face, and internal bank materials provides further insights into the nature of the bank materials. The low-bank surfaces most susceptible to hydraulic erosion are those that are impacted most frequently by flows, the "beach" and "bank-toe" locations. The materials at these locations generally contain more sand (about 79%) than the bank face (43% sand) or internal bank materials (56% sand) (Table 4.2.6.3-3). Also note the general lack of fines (about 16% silts and clays) in the beach and bank-toe materials. The general lack of cohesive clays in the bank materials, particularly on the bank-toe and beach surfaces can make them relatively susceptible to erosion by hydraulic forces and wave action. Those sites with gravel along the beach and bank toe are, however, less susceptible to erosion by hydraulic forces because of the increased resistance provided by the larger clasts. The median diameter (d_{50}) of the gravel materials ranges from 7 mm at site 8B-L to 57.5 mm at site 10R. This latter size is characteristic of two other sites (57 mm at site 6A-L and 55.5 mm at site 3R) where restoration measures, including gravel toe protection have been implemented

Some of the distinct similarities and differences in the composition of the three types of sampling locations become evident in comparing the longitudinal distribution of the materials (Figure 4.2.6.3-3). Equal ranges of sand and silt, with zero gravel mark the bank face and internal-bank sediment distributions. This is not surprising given that they both represent in situ bank materials. The striking difference in the beach-toe distributions along with the locations of the predominantly gravel sites can be clearly seen in Figure 4.2.6.3-3 (Bottom). It is those sites containing gravel at the beach-toe locations that are much less susceptible to hydraulic erosion because of shear stresses that are generally less than critical shear stress required for entrainment.

A list of the results for all sites and locations, along with the average values by site are summarized in Table 4.2.6.3-4. Those sites that show some gravel proportion are indicative of gravels along the beach-bank toe region as none were observed within the bank mass.

Table 4.2.6.3-1: Textural Classes of Bank-material Sediments along the Study Reach

Percentile	% Gravel	% Sand	% Silt	% Clay	% Fines
75^{th}	0.0	69.5	57.2	6.0	64.2
50^{th}	0.0	51.5	41.8	3.8	46.9
25^{th}	0.0	33.0	23.7	1.9	25.2

Table 4.2.6.3-2: Classification of Bank Materials in the Study Reach and Associated Saturated Hydraulic Conductivity (K_{sat}) Obtained from NRCS (2015)

Material Type	Number	Percent of total	K_{sat} (m/s)
Loam	2	1.7	9.15E-06
Loamy sand	16	13.2	9.17E-05
Sand	15	12.4	1.41E-04
Sandy loam	45	37.2	2.82E-05
Silt loam	42	34.7	9.15E-06
Silty clay loam	1	0.8	2.82E-06

Table 4.2.6.3-3: Median Composition of Bank-material Sediments from Different Sampling Locations

Location	Number	% Gravel	% Sand	% Silt	% Clay	% ML+CL
Internal	62	0.0	56.2	40.0	3.6	43.8
Beach-Toe	25	0.0/77.5	69.5	13.7	1.6	16.3
Bank Face	39	0.0	42.0	52.4	5.7	58.0

Table 4.2.6.3-4: Particle-size Data of the Bank Materials along the Turners Falls Impoundment

Site	Type	Station	% Gravel	% Sand	% Silt	% Clay	% ML+CL	d_{50}	Texture	Site Average				
										% Gravel	% Sand	% Silt	% Clay	% ML+CL
10L	Bank Face	49000	0	16.9	72.8	10.3	83.1		silt loam	0.0	54.6	39.7	5.7	45.4
10L	Bank Face	49000	0	20.9	67.1	12.0	79.1		silt loam					
10L	Beach-Toe	49000	0	64.3	32.3	3.5	35.7		sandy loam					
10L	Internal	49000	0	89.9	9.3	0.8	10.1		sand					
10L	Internal	49000	0	66.0	30.1	3.9	34.0		sandy loam					
10L	Internal	49000	0	69.7	26.6	3.6	30.3		sandy loam					
10R	Bank Face	49000	0	31.6	62.4	6.0	68.4		silt loam	25.0	36.9	35.8	2.3	38.1
10R	Beach-Toe	49000	100	0.0	0.0	0.0	0.0	57.5	gravel					
10R	Internal	49000	0	51.3	47.1	1.6	48.7		sandy loam					
10R	Internal	49000	0	64.8	33.6	1.6	35.2		sandy loam					
119BL	Bank Face	41000	0	25.1	68.9	6.0	74.9		silt loam	0.0	38.1	59.0	3.8	61.9
119BL	Bank Face	41000	0	42.0	54.4	3.7	58.0		silt loam					
119BL	Beach-Toe	41000	0	53.4	45.0	1.6	46.6		sandy loam					
119BL	Internal	41000	0	49.8	46.7	3.5	50.2		sandy loam					
119BL	Internal	41000	0	35.3	59.0	5.7	64.7		silt loam					
119BL	Internal	41000	0	40.6	56.6	2.8	59.4		silt loam					
119BL	Internal	41000	0	20.8	75.7	3.5	79.2		silt loam					
11L	Bank Face	100000	0	54.7	38.7	6.6	45.3		sandy loam	0.0	25.4	63.7	10.9	74.6
11L	Internal	100000	0	13.7	73.4	12.9	86.3		silt loam					
11L	Internal	100000	0	7.8	79.1	13.1	92.2		silt loam					
12BL	Bank Face	6750	0	78.7	21.6	0.3	21.9		loamy sand	0.0	89.4	10.3	0.4	10.7
12BL	Beach-Toe	6750	0	89.1	10.2	0.8	10.9		sand					

Site	Type	Station	% Gravel	% Sand	% Silt	% Clay	% ML+CL	d_{50}	Texture	Site Average				
										% Gravel	% Sand	% Silt	% Clay	% ML+CL
12BL	Internal	6750	0	84.9	15.1	0.0	15.1		loamy sand					
12BL	Internal	6750	0	96.1	3.1	0.8	3.9		sand					
12BL	Internal	6750	0	98.4	1.6	0.0	1.6		sand					
18L	Bank Face	87000	0	62.4	64.0	3.6	37.6		sandy loam	0.0	62.6	33.2	4.2	37.4
18L	Bank-Face	87000	0	25.0	66.4	8.6	75.0		silt loam					
18L	Beach-Toe	87000	0	94.6	4.9	0.5	5.4		sand					
18L	Internal	87000	0	68.4	27.6	3.9	31.6		sandy loam					
21R	Bank Face	79250	0	46.7	48.9	4.5	53.3		sandy loam	0.0	55.6	40.3	4.1	44.4
21R	Bank Face	79250	0	66.0	30.5	3.5	34.0		sandy loam					
21R	Beach-Toe	79250	0	74.7	24.4	0.8	25.3		loamy sand					
21R	Internal	79250	0	56.7	38.7	4.6	43.3		sandy loam					
21R	Internal	79250	0	49.1	45.6	5.3	50.9		sandy loam					
21R	Internal	79250	0	40.4	53.9	5.8	59.6		silt loam					
26R	Bank Face	79250	0	16.8	72.9	10.3	83.2		silt loam	7.6	43.0	44.8	4.6	49.4
26R	Bank Face	50000	0	20.8	81.0	8.2	79.2		silt loam					
26R	Beach-Toe	50000	38	51.9	9.6	0.6	10.2		gravelly sand					
26R	Internal	50000	0	82.2	16.2	1.6	17.8		loamy sand					
26R	Internal	50000	0	43.5	54.5	2.0	56.5		silt loam					
29R	Bank Face	66000	0	51.9	44.2	3.9	48.1		sandy loam	0.0	56.5	39.6	3.9	43.5
29R	Back Face	66000	0	31.2	61.9	6.9	68.8		silt loam					
29R	Beach-Toe	66000	0	78.2	20.2	1.7	21.8		loamy sand					
29R	Internal	66000	0	71.2	26.3	2.5	28.8		sandy loam					
29R	Internal	66000	0	50.0	45.5	4.5	50.0		sandy loam					

Site	Type	Station	% Gravel	% Sand	% Silt	% Clay	% ML+CL	d_{50}	Texture	Site Average				
										% Gravel	% Sand	% Silt	% Clay	% ML+CL
2L	Bank Face	94500	0	52.8	41.8	5.4	47.2		sandy loam	0.0	47.5	48.5	4.0	52.5
2L	Bank Face	94500	0	23.7	70.6	5.6	76.3		silt loam					
2L	Beach-Toe	94500	0	74.1	24.0	1.9	25.9		loamy sand					
2L	Internal	94500	0	48.9	47.7	3.4	51.1		sandy loam					
2L	Internal	94500	0	38.2	58.1	3.7	61.8		silt loam					
303BL	Bank Face	94000	0	66.0	30.1	3.8	34.0		sandy loam	0.0	49.2	45.9	4.9	50.8
303BL	Bank Face	94000	0	32.3	62.6	5.1	67.7		silt loam					
303BL	Beach-Toe	94000	0	83.7	13.7	2.6	16.3		loamy sand					
303BL	Internal	94000	0	25.7	66.4	7.9	74.3		silt loam					
303BL	Internal	94000	0	38.5	56.6	5.0	61.5		silt loam					
3L	Bank Face	79500	0	46.4	47.9	5.7	53.6		sandy loam	0.0	59.5	36.7	3.8	40.5
3L	Bank Face	79500	0	54.6	40.9	4.5	45.4		sandy loam					
3L	Beach-Toe	79500	0	79.3	18.0	2.7	20.7		loamy sand					
3L	Internal	79500	0	59.0	37.5	3.5	41.0		sandy loam					
3L	Internal	79500	0	58.2	38.9	2.9	41.8		sandy loam					
3R	Bank Face	79500	0	66.3	29.9	3.8	33.7		sandy loam	20.0	52.6	24.7	2.8	27.4
3R	Bank Face	79500	0	52.7	41.8	5.5	47.3		sandy loam					
3R	Beach-Toe	79500	100	0.0	0.0	0.0	0.0	55.5	gravel					
3R	Internal	79500	0	76.0	22.4	1.6	24.0		loamy sand					
3R	Internal	79500	0	67.9	29.2	2.9	32.1		sandy loam					
4L	Bank Face	74000	0	44.8	49.6	5.6	55.2		sandy loam	0.0	55.6	39.9	4.5	44.4
4L	Bank Face	74000	0	47.0	47.0	6.0	53.0		sandy loam					
4L	Beach-Toe	74000	0	69.5	28.8	1.7	30.5		sandy loam					

Site	Type	Station	% Gravel	% Sand	% Silt	% Clay	% ML+CL	d_{50}	Texture	Site Average				
										% Gravel	% Sand	% Silt	% Clay	% ML+CL
4L	Internal	74000	0	58.2	37.4	4.4	41.8		sandy loam					
4L	Internal	74000	0	58.4	36.9	4.8	41.6		sandy loam					
5CR	Bank Face	57250	0	48.4	45.6	6.0	51.6		sandy loam	0.0	52.7	42.3	5.0	47.3
5CR	Bank Face	57250	0	56.4	39.8	3.8	43.6		sandy loam					
5CR	Bank Face	57250	0	43.2	51.0	5.7	56.8		silt loam					
5CR	Beach-Toe	57250	0	85.6	12.5	1.9	14.4		loamy sand					
5CR	Internal	57250	0	55.8	40.5	3.7	44.2		sandy loam					
5CR	Internal	57250	0	39.1	51.4	8.5	60.9		silt loam					
5CR	Internal	57250	0	40.4	54.3	5.3	59.6		silt loam					
6AL	Bank Face	41750	0	41.6	51.4	6.1	58.4		silt loam	20.0	50.7	25.7	3.6	29.3
6AL	Bank Face	41750	0	34.3	58.5	7.2	65.7		silt loam					
6AL	Beach-Toe	41750	0	0.0	0.0	0.0	0.0	57.0	gravel					
6AL	Internal	41750	0	90.0	6.9	3.1	10.0		sand					
6AL	Internal	41750	0	87.8	10.8	1.4	12.2		sand					
6AR	Beach-Toe	41750	0	44.7	48.3	7.0	55.3		loam	0.0	38.0	54.0	8.0	62.0
6AR	Beach-Toe	41750	0	56.9	38.1	5.1	43.1		sandy loam					
6AR	Internal	41750	0	20.3	69.2	10.5	79.7		silt loam					
6AR	Internal	41750	0	30.1	60.6	9.3	69.9							
75BL	Bank Face	27000	0	63.3	34.3	2.3	36.7			13.0	52.2	31.4	3.5	34.8
75BL	Beach-Toe	27000	78	17.7	4.1	0.2	4.3	28.5	gravel					
75BL	Internal	27000	0	90.0	8.1	1.9	10.0		sand					
75BL	Internal	27000	0	75.1	22.1	2.8	24.9		loamy sand					
75BL	Internal	27000	0	51.6	43.6	4.7	48.4		sandy loam					

Site	Type	Station	% Gravel	% Sand	% Silt	% Clay	% ML+CL	d_{50}	Texture	Site Average				
										% Gravel	% Sand	% Silt	% Clay	% ML+CL
75BL	Internal	27000	0	15.1	76.1	8.8	84.9		silt loam					
7L	Bank Face	37500	0	27.5	64.5	8.0	72.5		silt loam	0.0	59.7	36.4	3.9	40.3
7L	Beach-Toe	37500	0	95.8	4.2	0.0	4.2		sand					
7L	Internal	37500	0	32.6	59.0	8.4	67.4		silt loam					
7L	Internal	37500	0	73.1	25.2	1.7	26.9		loamy sand					
7L	Internal	37500	0	69.4	28.9	1.7	30.6		sandy loam					
7R	Bank Face	37500	0	51.0	44.2	4.9	49.0		sandy loam	0.0	63.3	32.3	4.4	36.7
7R	Bank Face	37500	0	34.7	57.4	7.9	65.3		silt loam					
7R	Beach-Toe	37500	0	75.1	22.8	2.0	24.9		loamy sand					
7R	Internal	37500	0	98.4	1.6	0.0	1.6		sand					
7R	Internal	37500	0	92.8	5.3	1.9	7.2		sand					
7R	Internal	37500	0	27.6	62.6	9.8	72.4		silt loam					
87BL	Bank Face	30750	0	34.3	59.0	6.7	65.7		silt loam	0.0	37.4	56.3	6.4	62.6
87BL	Bank Face	30750	0	19.5	71.0	9.5	80.5		silt loam					
87BL	Beach-Toe	30750	0	42.4	50.6	7.0	57.6		silt loam					
87BL	Internal	30750	0	56.8	39.5	3.8	73.2		sandy loam					
87BL	Internal	30750	0	52.5	45.0	2.5	27.5		sandy loam					
87BL	Internal	30750	0	18.8	72.5	8.7	81.2		silt loam					
8BL	Bank Face	32750	0	36.0	57.1	6.9	64.0		silt loam	18.0	35.5	55.8	6.2	62.1
8BL	Beach-Toe	32750	72.0	28.0	--	--	--	7.0	gravel					
8BL	Internal	32750		45.3	48.5	6.2	54.7		sandy loam					
8BL	Internal	32750		32.6	61.9	5.5	67.4		silt loam					
8BR	Bank Face	32750		35.2	59.8	5.0	64.8		silt loam	19.3	46.1	42.1	4.0	46.2

Site	Type	Station	% Gravel	% Sand	% Silt	% Clay	% ML+CL	d_{50}	Texture	Site Average				
										% Gravel	% Sand	% Silt	% Clay	% ML+CL
8BR	Beach-Toe	32750		23.0	--	--	--	13.0	gravel					
8BR	Internal	32750		66.4	30.1	3.5	33.6		sandy loam					
8BR	Internal	32750		59.9	36.5	3.6	40.1		sandy loam					
9R	Bank Face	6500		8.9	77.9	13.2	91.1		silt loam	0.0	53.9	39.5	6.6	46.1
9R	Beach-Toe	6500		89.4	9.1	1.5	10.6		sand					
9R	Internal	6500		76.2	21.9	1.9	23.8		loamy sand					
9R	Internal	6500		86.0	12.4	1.6	14.0		sand					
9R	Internal	6500		8.9	76.4	14.7	91.1		silt loam					
BC-1R	Beach-Toe	4750	23.0	75.8	1.2	0.0	1.2		gravelly sand	5.8	58.8	25.6	9.9	35.5
BC-1R	Internal	4750		95.2	1.5	3.3	4.8		sand					
BC-1R	Internal	4750		45.3	46.4	8.3	54.7		loam					
BC-1R	Internal	4750		18.9	53.4	27.8	81.1		silty clay loam					

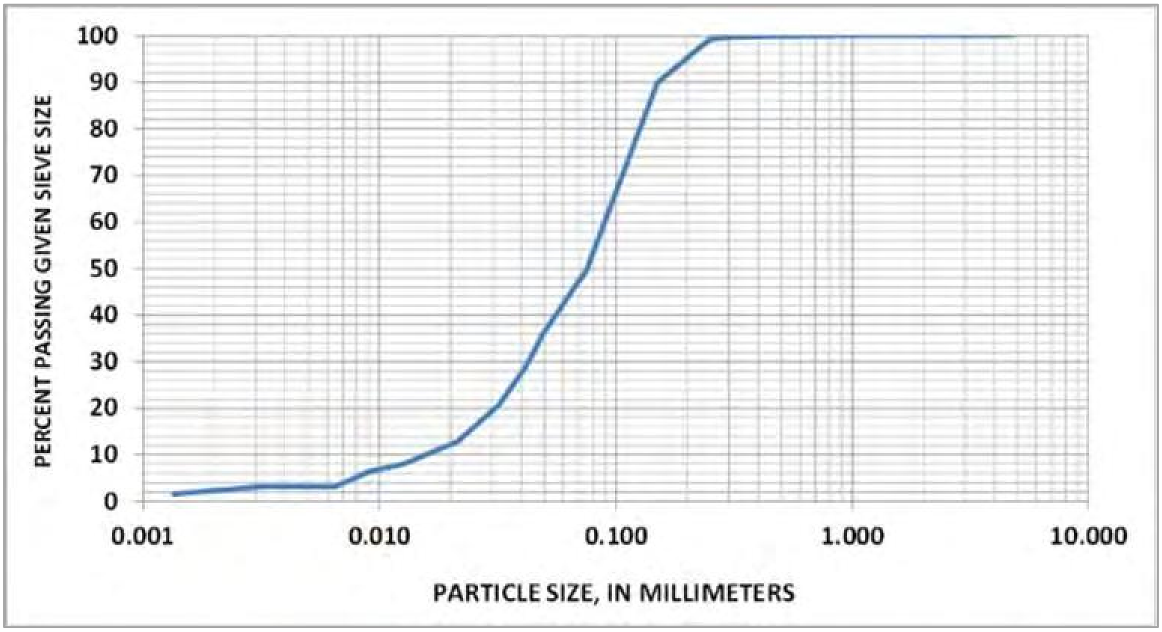

Figure 4.2.6.3-1: Example Results of Particle-size Analysis Showing Composition of Bank

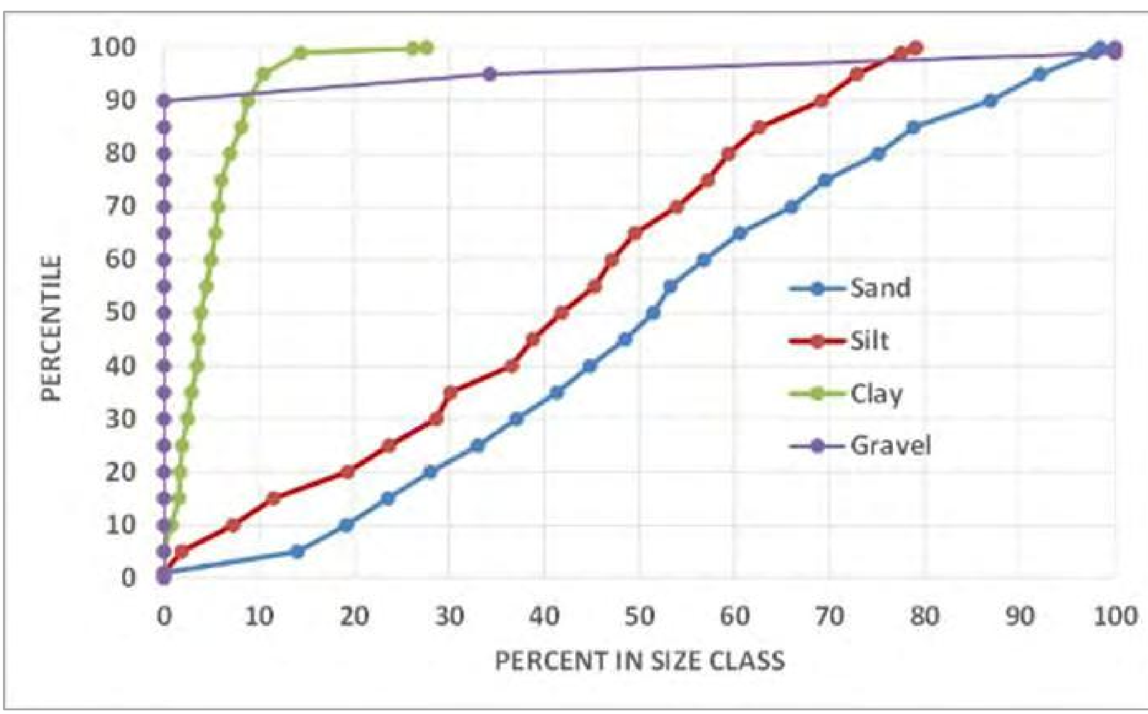

Figure 4.2.6.3-2: Frequency Distribution of the Composition of the Bank Material Sediments for the 25 Study Sites

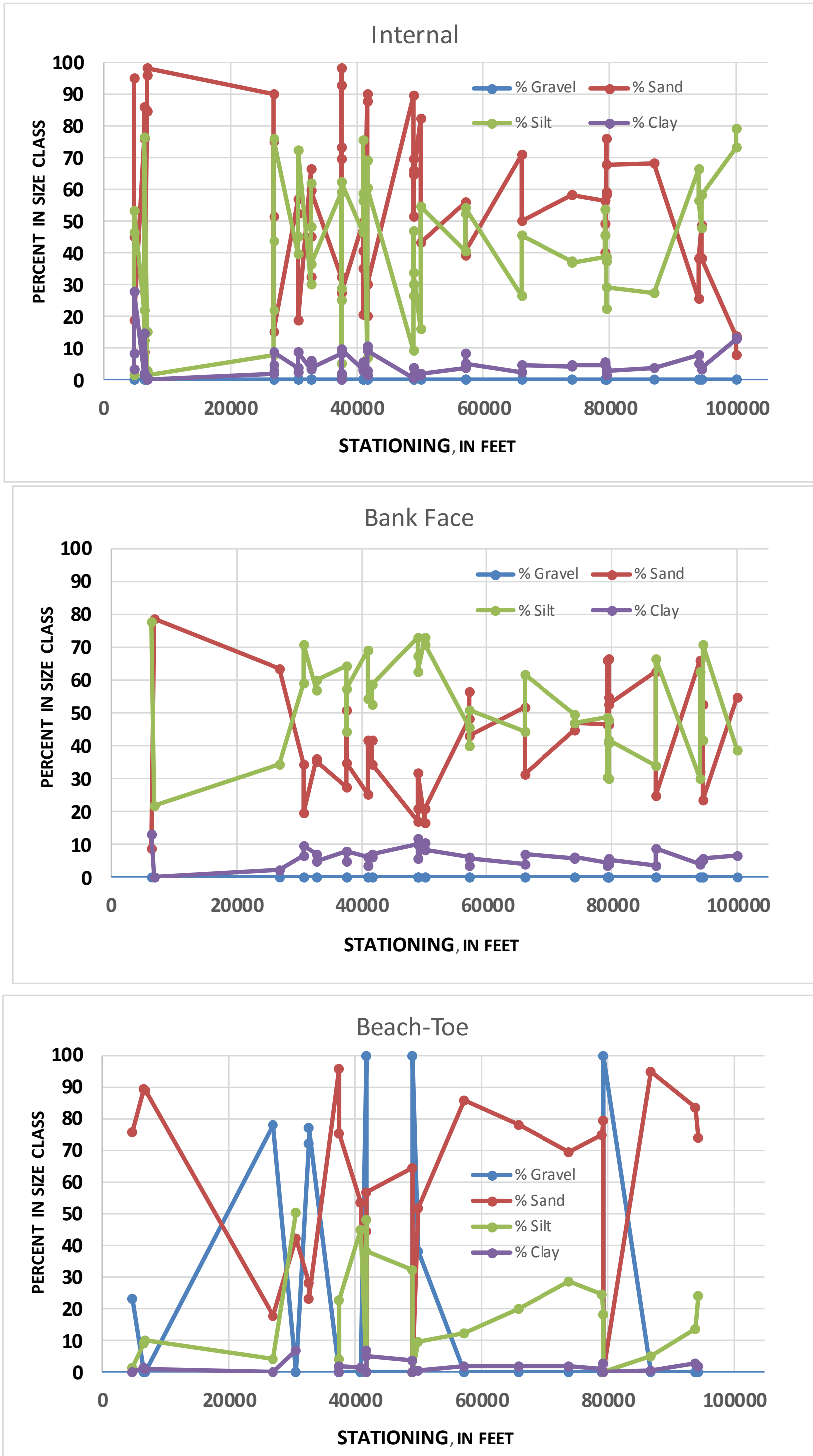

Figure 4.2.6.3-3: Longitudinal Distribution of Bank-material Composition for the Three Types of Sampling Locations – Internal (Top), Bank face (Middle), and Beach-Toe (Bottom)

4.2.6.4 Bulk Density of *In Situ* Bank Sediments

Bulk density is one of the required parameters within BSTEM to calculate both the driving and resisting forces responsible for bank stability. As such, a 2-inch by 2-inch diameter core was extracted from each borehole at the depth of geotechnical testing with the BST. Bulk density tends not to be highly variable, particularly in alluvial settings.

A total of 57 bulk-density samples were obtained at the study sites (Table 4.2.6.4-1). The median value under ambient conditions was 91.9 lbs/ft^3 (1.47 g/cm^3). Table 4.2.6.4-1 also shows values for dry bulk density and moisture content (at the time of testing) with the latter in the range of 8-18% range for most samples. Values of bulk density are adjusted within BSTEM as the water table raises and falls during a simulation.

Table 4.2.6.4-1: Summary of Bulk Density Data Collected at Sites in the Turners Falls Impoundment

Site	Location	Test #	Depth	Dry Bulk Density		Ambient Bulk Density		Ambient moisture content
			(ft)	g/cm^3	lbs/ft^3	g/cm^3	lbs/ft^3	(%)
10L	Left Bank	BST-2	2.6	1.27	79.2	1.55	97.1	18.4
10L	Left Bank	BST-1	3.9	1.29	80.7	1.40	87.6	7.9
10L	Left Bank	BST-3	8.2	1.26	78.7	1.46	91.0	13.5
10R	Right Bank	BST-1	2.6	1.39	86.8	1.66	103.9	16.4
10R	Right Bank	BST-2	4.9	1.33	82.9	1.58	98.4	15.8
119BL	Left Bank	BST-1	2.0	1.49	93.1	1.83	114.1	18.4
119BL	Left Bank	BST-2	3.3	1.22	76.2	1.36	85.1	10.5
119BL	Left Bank	BST-5	4.9	1.31	81.7	1.52	94.8	13.9
119BL	Left Bank	BST-4	9.8	1.36	84.6	1.64	102.5	17.5
11L	Left Bank	BST-1	5.6	1.21	75.7	1.58	98.4	23.1
11L	Left Bank	BST-2	8.9	1.22	76.2	1.55	96.6	21.1
12BL	Left Bank	BST-1	3.3	1.39	87.0	1.47	91.9	5.3
12BL	Left Bank	BST-4	3.3	1.38	86.2	1.44	90.1	4.3
12BL	Left Bank	BST-1	5.6	1.40	87.2	1.47	91.5	4.7
18L	Left Bank	BST-1	2.3	1.32	82.7	1.43	89.4	7.5
21L	Left Bank	BST-3	3.3	1.28	80.1	1.47	92.0	12.9
21L	Left Bank	BST-1	3.6	1.17	73.1	1.45	90.6	19.3
21L	Left Bank	BST-2	9.5	1.33	82.9	1.67	104.4	20.6
26R	Right Bank	BST-1	3.3	1.22	76.3	1.41	88.2	13.5
26R	Right Bank	BST-2	7.2	1.66	103.7	1.75	109.1	5.0
29R	Right Bank	BST-1	4.6	1.39	86.8	1.62	101.4	14.3
29R	Right Bank	BST-2	9.8	1.33	82.9	1.47	91.9	9.7
2L	Left Bank	BST-1	3.3	1.26	78.5	1.44	90.1	12.8

Site	Location	Test #	Depth	Dry Bulk Density		Ambient Bulk Density		Ambient moisture content
			(ft)	g/cm^3	lbs/ft^3	g/cm^3	lbs/ft^3	(%)
2L	Left Bank	BST-2	4.9	1.31	81.9	1.48	92.5	11.5
303BL	Left Bank	BST-1	3.6	1.22	75.9	1.41	88.2	13.9
303BL	Left Bank	BST-2	4.9	1.28	80.1	1.44	89.7	10.6
3L	Left Bank	BST-1	3.6	1.17	73.3	1.33	83.3	12.0
3L	Left Bank	BST-2	5.2	1.34	83.8	1.57	98.3	14.8
3R	Right Bank	BST-2	4.9	1.31	81.9	1.44	89.6	8.6
3R	Right Bank	BST-1	5.2	1.38	86.3	1.55	97.0	11.0
4L	Left Bank	BST-1	3.3	1.19	74.1	1.42	88.9	16.6
4L	Left Bank	BST-2	4.9	1.22	76.0	1.39	86.8	12.5
5CR	Right Bank	BST-1	3.9	1.10	68.9	1.24	77.1	10.7
5CR	Right Bank	BST-3	4.9	1.25	77.7	1.54	96.2	19.2
5CR	Right Bank	BST-2	7.5	1.34	83.9	1.66	103.7	19.1
6AL	Left Bank	BST-1	2.3	1.80	112.2	1.92	119.7	6.2
6AL	Left Bank	BST-2	4.6	1.43	89.5	1.56	97.7	8.4
6AR	Right Bank	BST-1	4.9	1.20	75.0	1.54	95.9	21.8
6AR	Right Bank	BST-2	Low bank	1.25	77.9	1.68	104.9	25.8
75BL	Left Bank	BST-2	2.3	1.39	86.6	1.44	89.6	3.3
75BL	Left Bank	BST-2	3.3	1.22	76.1	1.38	85.9	11.4
75BL	Left Bank	BST-1	4.3	1.31	82.0	1.60	99.9	17.9
7L	Left Bank	BST-1	5.2	1.38	86.0	1.45	90.6	5.1
7L	Left Bank	BST-2	9.8	1.34	83.5	1.46	91.4	8.7
7R	Right Bank	BST-1	4.9	1.41	87.9	1.46	91.1	3.5
7R	Right Bank	BST-2	9.2	1.61	100.7	1.67	104.3	3.4
87BL	Left Bank	BST-2	3.0	1.15	71.8	1.46	91.4	21.4
87BL	Left Bank	BST-1	5.0	1.24	77.2	1.34	83.6	7.7
87BL	Left Bank	BST-3	9.8	1.25	77.8	1.35	84.5	8.0
8BL	Left Bank	BST-1	5.2	1.09	67.9	1.20	74.7	9.1
8BR	Right Bank	BST-1	4.9	1.39	86.5	1.62	101.1	14.5
8BR	Right Bank	BST-2	10.2	1.35	84.4	1.52	94.7	10.9
9R	Right Bank	BST-2	1.3	1.37	85.3	1.79	111.9	23.8
9R	Right Bank	BST-1	3.9	1.51	94.1	1.56	97.2	3.2
9R	Right Bank	BST-3	4.6	1.35	84.0	1.46	91.0	7.7

Site	Location	Test #	Depth	Dry Bulk Density		Ambient Bulk Density		Ambient moisture content
			(ft)	g/cm^3	lbs/ft^3	g/cm^3	lbs/ft^3	(%)
BC-1R	Right Bank	TOB	1.0	1.32	82.6	1.38	86.1	4.1
BC-1R	Right bank	BST-2	1.6	1.25	78.3	1.58	98.4	20.5
75th Percentile				**1.38**	**86.21**	**1.58**	**98.40**	**17.5**
Median				**1.31**	**82.02**	**1.47**	**91.92**	**12.0**
25thPercentile				**1.24**	**77.23**	**1.44**	**89.60**	**7.9**

4.2.6.5 Geotechnical Parameters: Effective Cohesion and Friction Angle

Geotechnical data (cohesion and friction angle) obtained *in situ* with the BST are the fundamental measures of bank strength used to simulate and predict bank stability under a range of moisture conditions. Results of the 61 BST tests show that the cohesive strengths of banks along the TFI are quite variable but generally low (Table 4.2.6.5-1). Average values of effective cohesion and friction angle are 5.2 kPa and 30.5°, respectively. A more reliable measure of the central tendency of the distributions is the median values because outliers have less of an affect. As such, the median values for c' and ϕ' are 1.9 kPa and 31.6°, respectively, indicating that many banks are generally without much cohesive strength. Given the lack of clay-sized materials, this was expected. The frequency distribution for effective cohesion (Figure 4.2.6.5-1) shows that about 30% of the tests were in cohesionless materials while 35% were < 0.5 kPa and 50% were < 2.0kPa. Materials with greater cohesive strengths are evenly distributed across the range. Less than 20% of the tested materials had cohesive strengths greater than 10 kPa. Friction angles show the typical narrow range of values with the central 50% of the distribution ranging from 29.2 to 33.3° (Figure 4.2.6.5-1; Bottom).

The longitudinal distribution of average, effective-cohesion (c') values along the TFI also shows considerable variability (Figure 4.2.6.5-2). Average values are often not a good index of the strength of the bank as these values could be made up of different layers of widely varying strengths. They are shown here along with the individual test results to provide a visual presentation of the range of values over the study reach. Even at sites with some cohesive layers, there are often materials of low to zero cohesion making up the remainder of the bank. A notable exception is site BC-1R at station 4,900 where the tested bank materials displayed significant cohesive strengths.

Table 4.2.6.5-1: Summary of Geotechnical Data Collected in 2014 with the Borehole Shear Tester and a Digital Tensiometer for Sites along the Turners Falls Impoundment

Site	Station (feet)	Test #	Location	Depth	c_a	Suction	c'	ϕ'
				(m)	(kPa)	(kPa)	(kPa)	(degrees)
2L	94700	1	L	1.0	18.3	7.5	**5.4**	**21.8**
2L	94700	2	L	1.6	4.6	17.2	**1.6**	**33.7**
3L	79600	1	L	1.1	20.1	13.6	**17.7**	**26.0**
3L	79600	2	L	1.6	2.3	15.1	**0.0**	**34.4**
3R	79600	1	R	1.6	3.8	9.9	**2.1**	**31.0**
3R	79600	2	R	1.5	3.7	11.1	**1.7**	**30.9**
4L	74000	2	L	1.2	0.0	19.1	**0.0**	**32.3**
4L	74000	combined	L	1.5	0.0	19.1	**0.0**	**33.2**
5CR	57300	1	R	1.5	9.6	21.5	**5.9**	**32.4**
5CR	57300	2	R	1.2	6.3	19.8	**2.9**	**31.0**
5CR	57300	3	R	2.8	6.7	14.1	**4.2**	**31.4**
6AR	41800	1	R	1.2	9.0	27.0	**4.3**	**33.7**
6AR	41800	2	R	0.6	12.2	35.0	**6.1**	**29.5**
6AR	41800	3	R	1.1	4.7	27.0	**0.0**	**32.9**
6AR	41800	5	R	2.9	4.5	50.0	**0.0**	**33.7**
6L	41800	1	L	0.6	10.1	50.0	**8.0**	**29.5**
6L	41800	2	L	1.0	0.4	70.0	**0.0**	**33.2**
7L	37600	1	L	1.6	20.1	25.1	**15.7**	**26.6**
7L	37600	2	L	3.0	0.0	21.0	**0.0**	**35.3**
7R	37600	1	R	1.5	0.0	6.3	**0.0**	**29.7**
7R	37600	2	R	2.8	2.5	4.8	**1.7**	**29.0**
7R	37600	5	R	3.8	6.5	5.0	**5.6**	**31.3**
8BL	32800	1	L	1.6	0.0	19.5	**0.0**	**33.2**
8BR	32800	1	R	1.0	8.7	15.0	**6.1**	**28.1**
8BR	32800	2	R	2.0	7.0	22.0	**3.2**	**33.7**
8BR	32800	3	R	2.8	16.2	16.2	**12.7**	**20.0**
9R	65100	2	R	0.4	15.6	5.1	**14.7**	**28.2**
9R	65100	3	R	1.5	1.3	9.4	**0.0**	**33.1**
10L	49100	1	L	1.2	1.5	9.6	**0.0**	**30.3**
10L	49100	2	L	0.8	0.0	10.6	**0.0**	**33.4**
10L	49100	3	L	2.5	2.8	11.6	**0.8**	**33.3**

Site	Station (feet)	Test #	Location	Depth	c_a	Suction	c'	ϕ'
				(m)	(kPa)	(kPa)	(kPa)	(degrees)
10R	49100	1	R	0.8	15.6	1.8	**15.0**	**25.6**
10R	49100	2	R	1.5	3.3	12.4	**1.2**	**31.0**
11L	100000	1	L	1.0	2.1	10.0	**0.4**	**33.2**
11L	100000	3	L	0.9	3.2	19.0	**0.0**	**31.8**
12BL	6700	2	L	1.0	5.6	4.9	**4.7**	**31.4**
12BL	6700	3	L	1.5	7.7	13.8	**5.3**	**29.2**
12BL	6700	4	L	1.0	5.0	2.9	**4.5**	**25.4**
18L	87000	1	L	0.9	2.0	16.7	**0.0**	**31.0**
21R	79100	1	R	1.1	25.0	23.4	**20.9**	**19.8**
21R	79100	2	R	2.9	3.7	8.7	**2.2**	**32.8**
21R	79100	3	R	1.0	21.5	17.7	**18.4**	**24.2**
21R	79100	4	R	1.0	5.9	23.4	**1.8**	**31.6**
26R	49800	1	R	1.0	0.0	14.8	**0.0**	**31.3**
26R	49800	2	R	2.2	5.6	7.0	**4.4**	**35.4**
26R	49800	3	R	0.9	0.5	14.8	**0.0**	**31.4**
29R	66000	1	R	1.4	11.9	16.1	**9.1**	**31.8**
29R	66000	2	R	3.0	0.0	14.3	**0.0**	**34.1**
75BL	27000	1	L	1.3	0.3	6.4	**0.0**	**33.8**
75BL	27000	4	L	1.0	8.6	38.1	**1.9**	**36.7**
87BL	30700	1	L	1.6	18.7	25.7	**14.2**	**27.3**
87BL	30700	2	L	0.9	13.1	20.9	**9.5**	**32.3**
87BL	30700	3	L	3.0	21.5	19.1	**18.2**	**27.7**
87BL	30700	4	L	0.8	4.7	20.9	**1.1**	**33.9**
119BL	40600	2	L	1.0	5.6	34.9	**0.0**	**35.3**
119BL	40600	4	L	3.0	5.0	12.9	**2.8**	**33.0**
119BL	40600	5	L	1.5	3.1	30.2	**0.0**	**36.2**
303L	94000	1	L	1.1	9.0	41.7	**1.7**	**32.8**
303L	94000	2	L	1.5	2.7	22.8	**0.0**	**36.2**
BC-1R	4900	1	R	0.8	30.0	7.9	**28.6**	**11.3**
BC-1R	4900	2	R	0.5	34.0	7.9	**32.6**	**16.7**

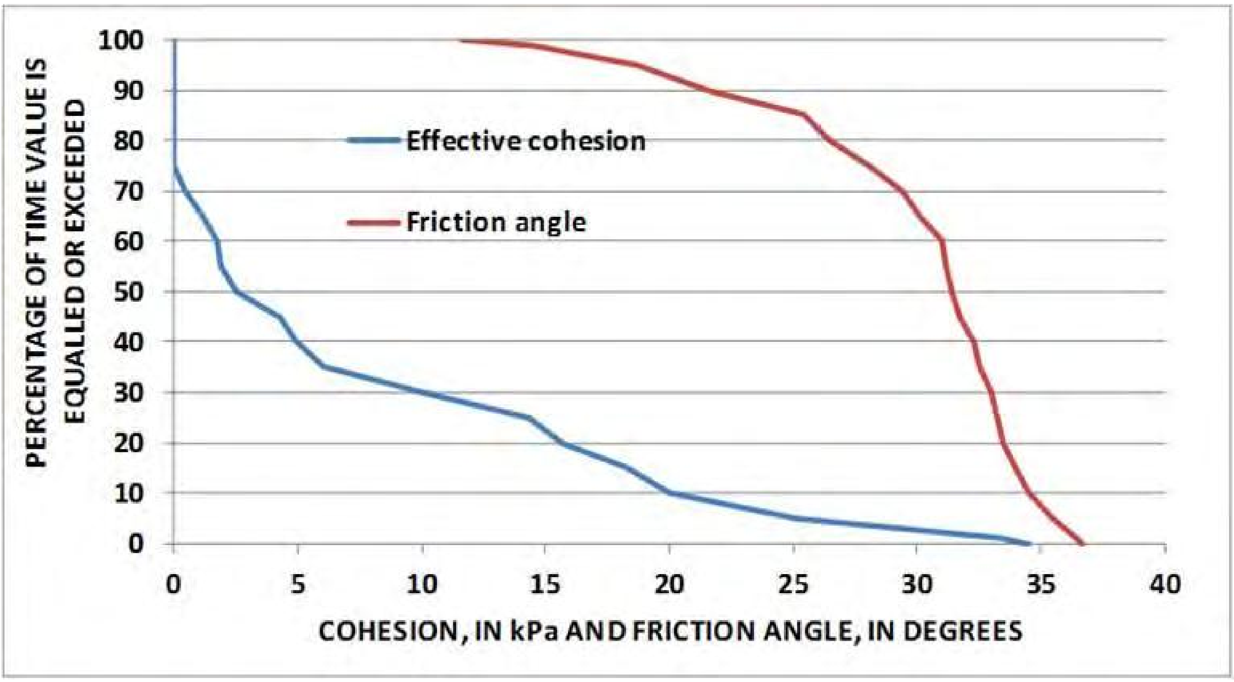

Figure 4.2.6.5-1: Frequency Distribution of Effective Cohesion and Friction Angle for the 60 Geotechnical Tests taken with the BST at the 25 Study Sites along the TFI

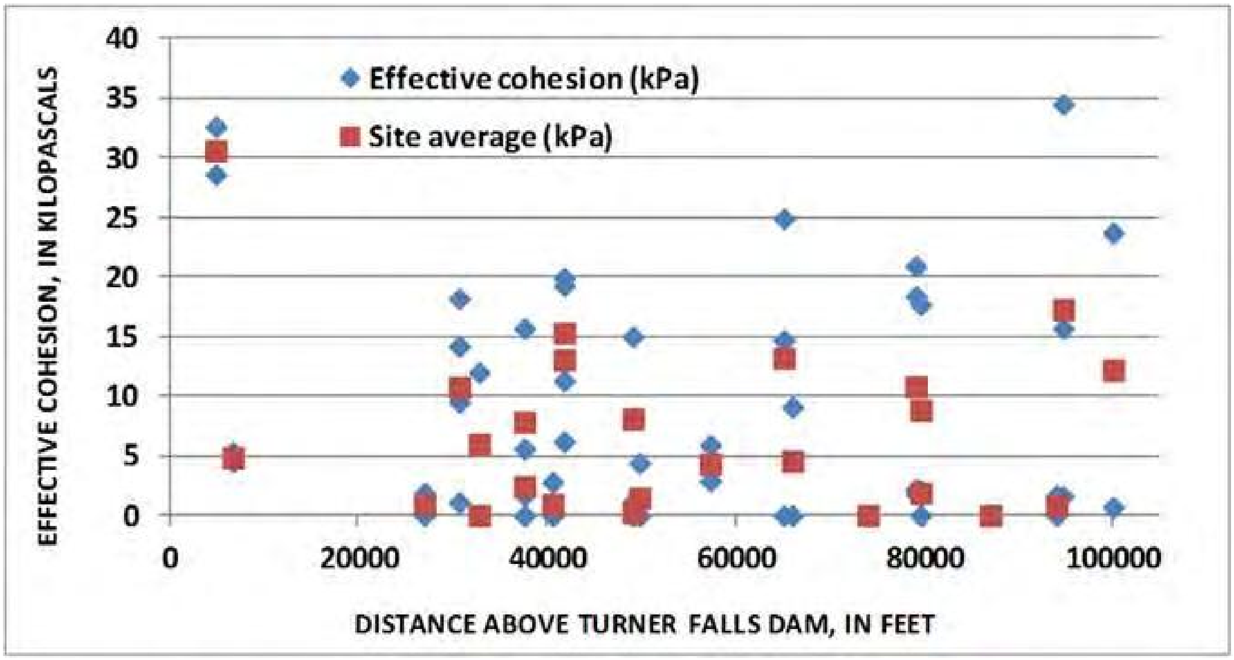

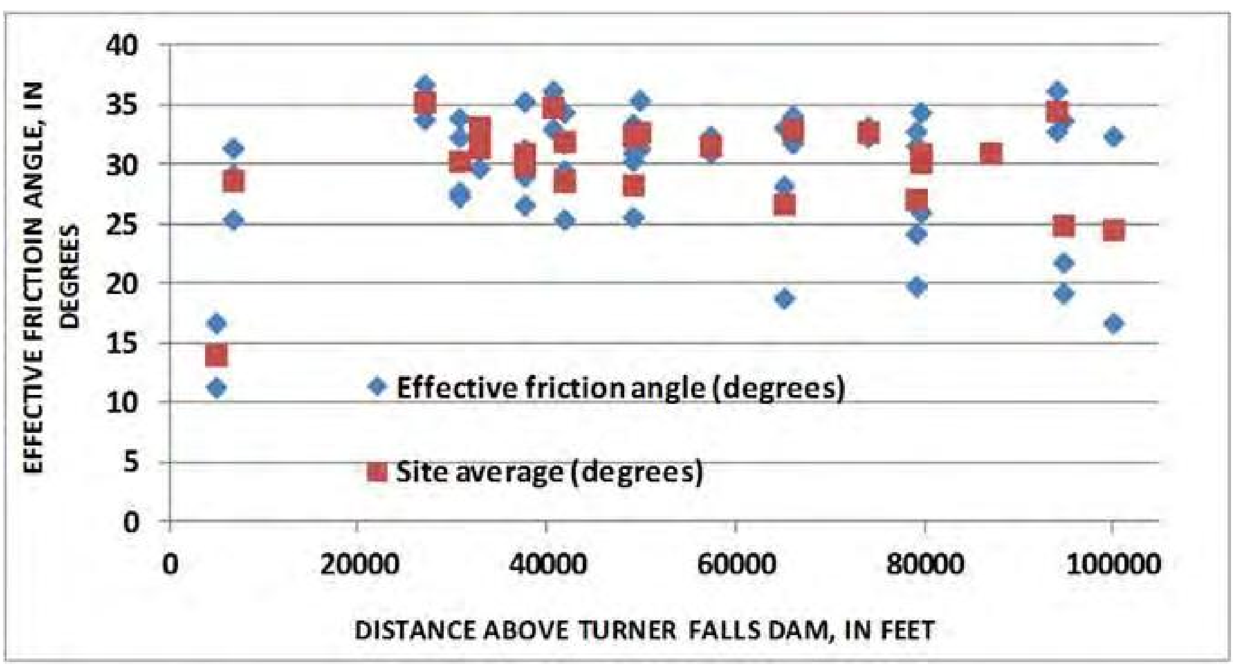

Figure 4.2.6.5-2: Effective Cohesion (Top) and Friction Angle (Bottom) for Sites along the TFI

4.2.6.6 Hydraulic Resistance: Critical Shear Stress and Erodibility

The susceptibility of surficial-bank and bank-toe materials to erosion by hydraulic forces is important to modeling and predicting bank-erosion rates because it is the hydraulic processes (during peak flows and/or from wave action) that can cause undercutting of the bank making it more susceptible to collapse. Results from *in situ* testing with the submerged jet test device and by conducting particle counts of cohesionless sediment show relatively erodible sediment.

Jet tests were carried out at 23 of the 25 sites. Results of these 71 tests are shown in Table 4.2.6.6-1. The exceptions were site BC-1R where a dense matting of moss and roots prevented successful tests, and at 12BL where the surficial materials were composed of sand and could be characterized by bulk particle size. Values of critical shear stress for surficial materials at these two sites were determined from calculations using the Shields criteria and the median particle diameter (d_{50}) as the representative size. Recall that hydraulic resistance of other, larger cohesionless materials was also determined this way based on particle-count data.

Using the rule of thumb that the hydraulic resistance of surficial sediments measured in Pa is generally equivalent to the resistance of cohesionless materials in mm, we can state that in general, the resistance of the surficial materials in the reach is representative of sand-sized materials. The inter-quartile range of critical shear stresses range from about 0.14 Pa to about 2.3 Pa with a median value of 0.54 Pa (Table 4.2.6.6-2). More resistant materials were tested at several sites. Only 5% of the tests had materials with critical shear-stress values greater than 12.2 Pa; 1% with values greater than 18.3 Pa. Some beach/toe locations that contain placed rock such as sites 3R, 6AL, and 10R have the greatest critical shear stresses because of the size and weight of the clasts at these three sites (d_{50} ranges from 55.0 mm to 57.5 mm). The full distribution of jet test values can be seen in Table 4.2.6.6-2 as well as in Figure 4.2.6.6-1. Values of the erodibility coefficient (k) were calculated from the equation published by Hanson and Simon, (Hanson & Simon, 2001):

$$k = 0.2\ \tau_c^{\ -0.5} \tag{1}$$

where τ_c = critical shear stress, in Pa; and k = erodibility coefficient, in $cm^3/N\text{-}s$.

Their frequency distribution is shown in Figure 4.2.6.6-2. The spatial variation in critical shear stress for individual tests and for site medians are shown in Figure 4.2.6.6-3.

Table 4.2.6.6-1: Jet Test Data for Bank Materials of the Turners Falls Impoundment

Site	Test	τ_c	Median τ_c	Calculated *k*	Location
		(Pa)	(Pa)	Cm^3/N-s)	
2L	1	12.0	0.137	0.58	BF
2L	2	0.271		0.384	BF
2L	3	0.0022		4.23	BF
2L	4	0.0003		11.7	BF
3L	1	2.73	0.777	0.121	BF
3L	2	0.777		0.227	BF
3L	4	0.328		0.349	BF
3R	1	0.261	0.639	0.391	BF
3R	3	0.639		0.250	BF
3R	4	0.685		0.242	BF
4L	1	0.0511	0.106	0.885	BF
4L	2	0.200		0.447	BF
4L	3	0.16		0.500	BF
4L	4	0.0051		2.80	BF
5CR	1	1.03	1.03	0.197	BF
5CR	6	0.66		0.246	BF
5CR	7	1.08		0.192	BF
6AL	2	2.900	0.64	0.117	BT
6AL	3	0.236		0.412	BF
6AL	4	0.640		0.250	BF
6AR	1	0.428	0.475	0.306	BF
6AR	6	0.475		0.290	BF
6AR	3	0.669		0.245	BT
7L	1	1.17	0.748	0.185	BF
7L	2	0.326		0.350	BF
7R	1	0.54	7.14	0.272	BT
7R	2	2.37		0.130	BT
7R	3	11.9		0.058	BF
7R	4	17.4		0.048	BF
8BL	1	2.77	3.33	0.120	BF
8BL	2	3.88		0.102	BF
8BR	1	0.336	0.627	0.345	BT
8BR	2	0.918		0.209	BT
9R	1	20.5	10.3	0.044	BF
9R	2	0.0003		11.5	BF
10L	1	0.190	0.585	0.459	BF
10L	2	0.629		0.252	BF
10L	3	0.541		0.272	BF
10L	4	2.23		0.134	BF
10R	1	0.836	3.47	0.219	BF
10R	2	6.1		0.081	BF
11L	1	8.29	2.91	0.069	BT
11L	2	0.181		0.470	BT
11L	3	2.91		0.117	BF
18L	1	3.27	3.27	0.111	BT
18L	2	17.2		0.048	BT
18L	4	2.13		0.137	BF
75BL	2	6.71	3.41	0.077	BF
75BL	3	0.11		0.603	BF

Site	Test	τ_c (Pa)	Median τ_c (Pa)	Calculated *k* Cm^3/N-s)	Location
87BL	1	0.0514	0.082	0.882	BF
87BL	2	0.0917		0.660	BF
87BL	3	0.314		0.357	BF
87BL	4	0.0726		0.742	BF
21R	1	0.00164	0.1945	4.94	BF
21R	2	0.177		0.475	BF
21R	3	1.7		0.153	BF
21R	4	0.212		0.434	BF
26R	1	0.00158	0.024	5.03	BF
26R	3	0.0243		1.28	BF
26R	4	0.0302		1.15	BF
29R	1	2.94	1.51	0.117	BF
29R	2	1.47		0.165	BF
29R	3	0.0795		0.709	BF
29R	4	1.549		0.161	BF
119BL	1	0.00081	0.0025	7.03	BF
119BL	3	0.00246		4.03	BF
119BL	4	0.1015		0.628	BF
303BL	1	4.78	2.49	0.091	BT
303BL	2	12.3		0.057	BT
303BL	3	0.0708		0.752	BF
303BL	4	0.205		0.442	BF

Table 4.2.6.6-2: Frequency Distribution for the 71 Jet Tests Conducted Along the Turners Falls Impoundment

Percentile	Critical shear stress: τ_c		Calculated *k*
	(Pa)	(lbs/ft^2)	(cm^3/N-s)
99.99	205	0.43	11.74
99.9	203	0.42	11.73
99	18.3	0.38	11.6
95	12.2	0.254	4.99
90	6.71	0.140	2.80
85	3.58	0.0747	0.883
80	2.90	0.0606	0.709
75	2.30	0.0480	0.552
70	1.55	0.0324	0.459
65	1.06	0.0220	0.423
60	0.777	0.0162	0.357
55	0.650	0.0136	0.325
50	0.541	0.0113	0.272
45	0.382	0.0080	0.248
40	0.314	0.0066	0.227
35	0.224	0.0047	0.195
30	0.190	0.0040	0.161
25	0.135	0.0028	0.132
20	0.0795	0.0017	0.117
15	0.0513	0.0011	0.106
10	0.0051	0.0001	0.077
5	0.0016	0.00003	0.057
1	0.00030	0.00001	0.047
0.1	0.00029	0.00001	0.0444
0.01	0.0029	0.00001	0.0442

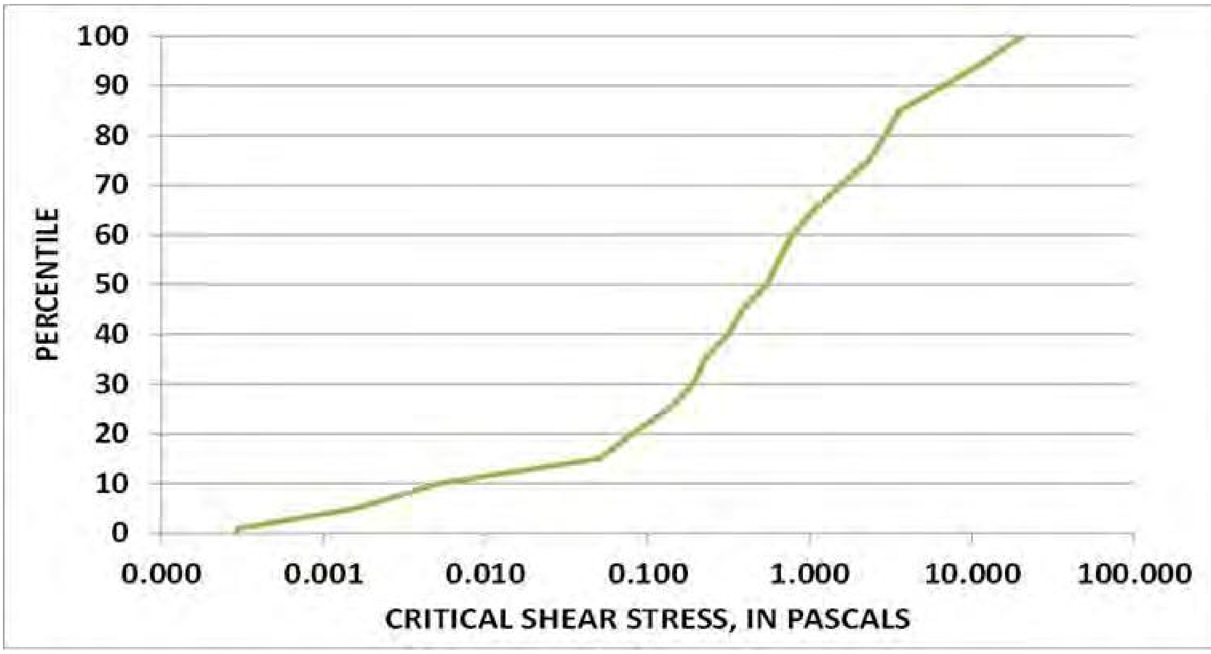

Figure 4.2.6.6-1: Plot of Frequency Distribution of Critical Shear Stress (t_c) from the 71 Jet Tests Conducted along the TFI

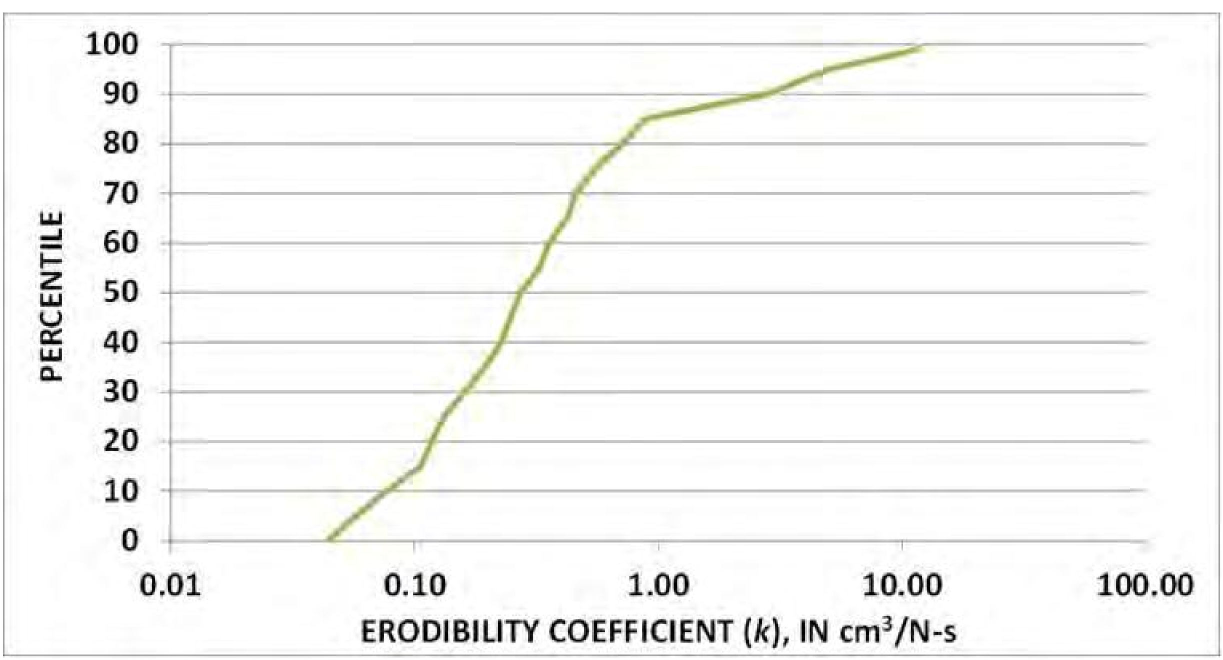

Figure 4.2.6.6-2: Plot of Frequency Distribution of the Erodibility Coefficient (k) for the 71 Jet Tests Conducted along the TFI

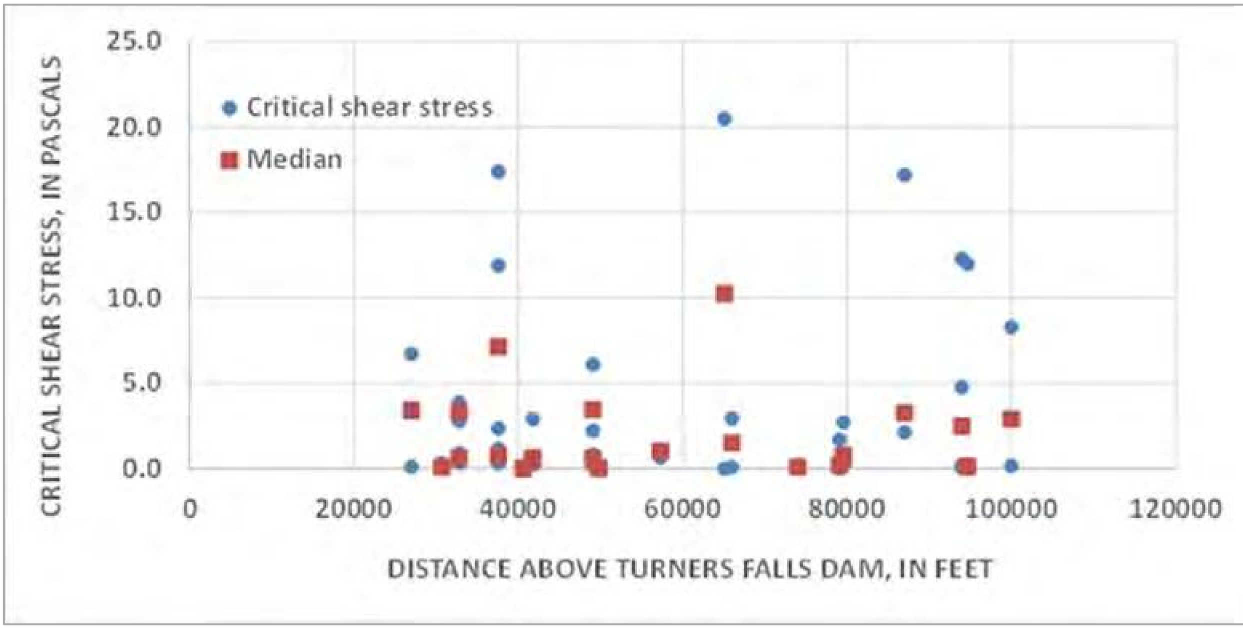

Figure 4.2.6.6-3: Longitudinal Distribution of Measured Critical Shear Stress of Surficial Bank Materials at the Study Sites

4.2.7 Methodology for Quantifying Root-Reinforcement

Vegetation has a number of effects on the geotechnical and hydraulic processes occurring within and at channel margins. Of particular importance is the reinforcement that can be provided to a bank by the roots growing within it. This reinforcement of soil by roots is akin to the reinforcement of concrete by rebar; the soil matrix is strong in compression, and the roots are strong in tension. The combination of the two materials provides a reinforced matrix, the strength of which can be quantified through knowledge of the soil strength alone, and the number, diameters, and tensile strengths of the roots present within the banks. Therefore, to quantify root-reinforcement in the context of bank stability two types of data collection are necessary: 1) root tensile strength data (which varies by species), and 2) the rooting density with associated root diameter distributions at varying depths throughout the banks (which is species and site specific), also known as the root architecture. The latter is obtained through a combination of root mapping of representative species in the reach and applied to specific sites with data on canopy cover of species assemblages.

BSTEM contains a root-reinforcement algorithm, RipRoot that currently contains a database of 25 species, for which root tensile strength and root architecture have previously been collected. The data collection has focused largely on Southeastern, and Western USA riparian species. As part of this study, five species commonly found along the study reach were investigated, to be added to the RipRoot database, and used in BSTEM model simulations of the TFI.

Collection and analysis of root architecture data is time consuming and laborious. To be efficient with this data collection, root architecture data was collected for a range of tree ages for each of the species, and the average distribution of root densities and diameters was calculated for the range of ages. Plant assemblage data (percent cover, species and age) was recorded at each of the BSTEM modeling sites, so that these average root-architecture parameters and species specific root tensile-strength relations could be applied to give a specific root-reinforcement value at each BSTEM modeling site.

4.2.7.1 Testing for Tensile Strength

The five species selected for study along the TFI were: Red oak, Silver maple, American elm, Green ash and Basswood. These species were selected through consultation with the FirstLight study team and were selected because of their dominance throughout the TFI. Root tensile strength measurements for each of the five species were collected at exposed bank faces using a root-puller device (Figure 4.2.7.1-1). This device is comprised of a metal frame and winch, connected to a load cell. Each root was winched until it broke and the peak load before breaking recorded, along with the root diameter at the breaking point, so that each root's tensile strength could be calculated.

For each species at least 48 roots of various diameters (ranging from 0.5 mm to 5 mm) were tested, to allow for the development of species-specific tensile strength–diameter relations that can be used in the RipRoot model, and associated BSTEM simulations. 30 roots is the minimum number of roots necessary to develop a relation where statistics do not have to be adjusted for a low number of trials. Where possible, more roots were tested to strengthen the confidence in the relationship. Roots larger than 5mm were not tested since the tensile strength-diameter relation for roots is a power function that flattens out around this threshold. For each species, locations were selected where exposed roots were visible, attached to living trees, and easily identifiable as being from a tree of known species. The number of trees tested for each species varied according to the number of roots available at the sites located, and the range of root diameters present. The GPS locations and the number of trees and roots tested for each species are shown in Table 4.2.7.1-1.

Table 4.2.7.1-1: List of GPS Locations for Root Tensile Strength Testing and the Number of Trees Tested

	GPS locations			Number of trees tested	Total number of roots tested
Green ash	N 42.69222	N42.69222	-	3	56
	W 72.47222	W72.47222	-		
Red oak	N42.62244	N42.67754	-	2	48
	W72.48399	W72.46957	-		
Silver maple	N42.72319	-	-	15	59
	W72.45639	-	-		
American elm	N42.62756	N42.70070	N42.69539	4	77
	W72.48412	W72.46786	W72.47020		
Basswood	N42.677931	-	-	6	48
	W72.469924	-	-		

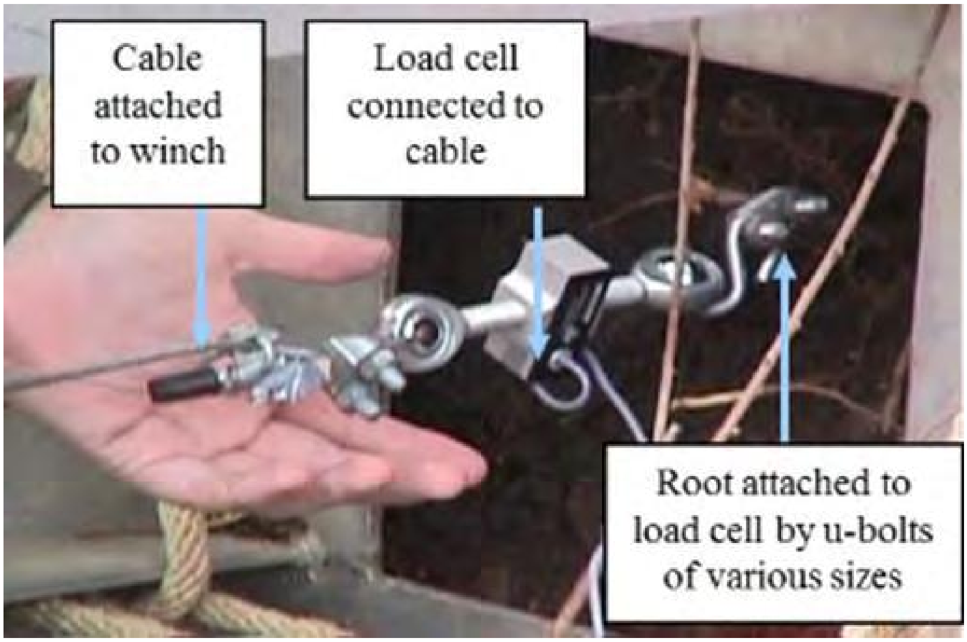

Figure 4.2.7.1-1: Photo Showing a Close-up of the Way that the Load Cell and Roots/Rhizomes are Connected to the Winching Cable of the Root-puller

4.2.7.2 Measurements of Root Densities and Root Diameter Distributions

The RipRoot model also requires knowledge of typical rooting densities, and root diameter distributions throughout the bank (Figure 4.2.7.2-1). Data were collected in the field to provide the typical ranges of these parameters for each of the five selected species so that the RipRoot and BSTEM models can accurately account for vegetation under existing conditions. For each of the five species under investigation, trees of various ages growing at the bank edge were selected. Trees sampled ranged in age from approximately 8 years to over 100 years (sample sizes and ages are shown in Table 4.2.7.2-1). The age of each tree was estimated by developing a diameter at breast height (DBH) to age relation for each species, from tree-ring cores taken in the field. Once a relation had been established for each species, only a DBH measurement was required to estimate the age of subsequent trees.

The collection of root architecture data is laborious. To collect the most data as possible in an efficient manner, a combination of field and photo analysis techniques were used to quantify root density and root diameter distributions. Initially, several trees were measured using both techniques, to verify the number of roots counted using each method, and test that the photo analysis method provided comparable results to the field method. To measure root architecture in the field, a 0.5m x 0.5m grid, marked off into 0.1m x 0.1m squares was attached to the bank face over the exposed roots of each study tree (Figure 4.2.7.2-2). A digital caliper was used to measure the number and diameter of roots in each square and the results recorded so that lateral and vertical patterns and extent could be determined.

In addition, each tree and its roots were photographed using a high resolution camera. In each image a tape measure was made visible, so that each photo could be calibrated with the imaging software SigmaScan. In addition, five roots in each photograph were measured in the field, and then measured in the photo using the image-analysis software to check the calibration for each image. Once the field data and photo-analysis data had been compared in detail for 3 trees, the field crews switched to just taking the digital photos of each tree to be sampled, thus allowing for faster field-data collection, and a larger sample size in the time available. To analyze each image, the field photos were merged so that one image existed for each tree to be investigated (e.g. Figure 4.2.7.2-3).

Next, the tape measure in each image was used to calibrate the "measure" tool in SigmaScan, and the five flagged roots in each image were measured and compared to the field measurements as a check, before starting detailed image analysis. Once the distance calibration had been confirmed, a 0.1m x 0.1m grid was superimposed onto the image (Figure 4.2.7.2-4), and the area of the image to be studied was isolated.

Then, just as was done in the field, the number and diameters of roots in each cell was recorded. The SigmaScan software puts each root measurement into a spreadsheet automatically, which makes this process easier than measuring and recording in the field, and having to enter this data manually later. In both methods, each root is only counted once, at the location where it first emerges from the bank. Thus, a root that is hanging down the face of the bank is not counted in every cell it can be seen in. This is because the object is to quantify the number of roots cutting across the potential failure plane of the bank, in this case, assumed to be the bank face itself. This makes both field measurement, and analysis of the digital photos time consuming, as it is easy to count roots several times if care is not taken.

Root data for each tree was then analyzed according to the standard root diameter size classes used in the RipRoot Model (<1mm, 1-2mm, 2-3mm, 3-5mm, 5-10mm, 10-20mm, and >20mm). Variations between species were investigated, as well as variations within species, over the age ranges tested.

At three locations, measurements were taken in the field, and were then compared to the results of the digital photo analysis, to insure that the results were within acceptable limits of error. An example of the results of one of these comparisons is presented in Figure 4.2.7.2-5 for an American elm tree. The results of this comparison show that for the smallest root classes (<1mm and 1-2mm), the number of roots identified was slightly higher in the field, but in the 2 to 3mm diameter range and above the photo analysis method identified more roots. These results make sense in that the finer roots were easier to see up close, in person.

Data collection pertaining to the larger roots can get confusing to count in the field as each should only be counted once, where it emerges from the bank. It can be hard to keep track of this in the field, and due to the proximity to the river it can be hard to physically step back and take a broader view of the root system. Using the photo analysis method each root can be labeled and counted more easily, and the software can be used to zoom in and out as necessary. For the example presented below, the total number of roots counted in the field was 70, and the number of roots counted using the photo analysis method was 79, a difference of 12.9%, but considering the variability in rooting density even between specimens of the same species and age, this is within an acceptable range of variation. The other two comparisons of the two methods showed similar results, in each case with slightly more roots being recorded in the image analysis compared to in the field. This is likely a result that when performing the image analysis it is easier to zoom in and out, to label the roots you've already counted, and to get a better overview of the root system as a whole. The percent difference between the two methods ranged from 8.5% to the example shown here of 12.9%. The use of the photo analysis method allowed for analysis of a much larger dataset for this project than would have been possible using the field method alone.

In total, the root architecture of 33 trees was recorded and measured. The species, ages, and GIS locations of the trees sampled are shown in Table 4.2.7.2-1. Trees ages ranged from 6 years to approximately 100 years, with the distribution of ages sampled varying between species, as per the prevalence and resulting availability of trees to test at the bank edge.

Table 4.2.7.2-1: Summary of Trees Tested for Root Architecture

SPECIES	Number of trees tested	Tree Age from average field growth rates	GPS location	
			N	W
Red oak	6	9	42.62244	-72.48399
		16	42.62775	-72.48412
		35	42.67754	-72.46957
		102	42.62244	-72.48399
		30	42.62046	-72.48283
		59	42.63864	-72.48854
		88	42.7745	-72.49963
Silver maple	7	17	42.69222	-72.47222
		28	42.71873	-72.45532
		31	42.71873	-72.45532
		33	42.71873	-72.45532
		56	42.71873	-72.45532
		58	42.67169	-72.46969
		67	42.64347	-72.47790
American elm	8	6	42.69539	-72.47020
		26	42.62756	-72.48412
		31	42.66364	-72.46963
		57	42.62756	-72.48412
		49	42.7007	-72.46786
		64	42.70476	-72.46219
		71	42.64381	-72.47780
Green ash	6	8	42.69222	-72.47222
		19	42.62756	-72.48412
		23	42.69222	-72.47222
		35	42.6527	-72.46745
		45	42.66467	-72.47023
		53	42.64966	-72.47131
Basswood	6	7	42.67782	-72.46983
		11	42.64624	-72.47168
		13	42.67782	-72.46983
		13	42.64624	-72.47168
		14	42.63525	-72.48743
		15	42.67782	-72.46983
		18	42.63525	-72.48743
		30	42.64437	-72.47628

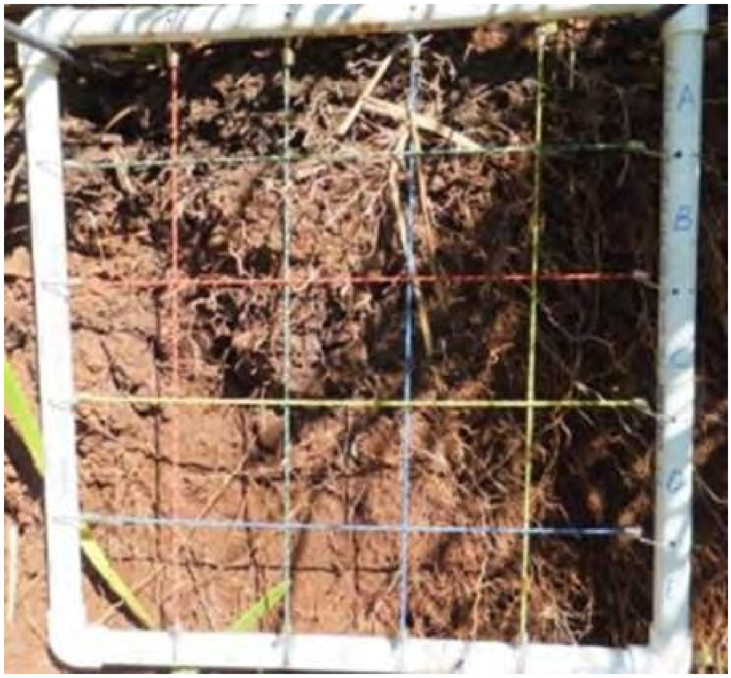

Figure 4.2.7.2-1: Example of Grid Used for Root Diameter and Density Measurements in the Field

Figure 4.2.7.2-2: Merged Image Ready for Analysis in SigmaScan

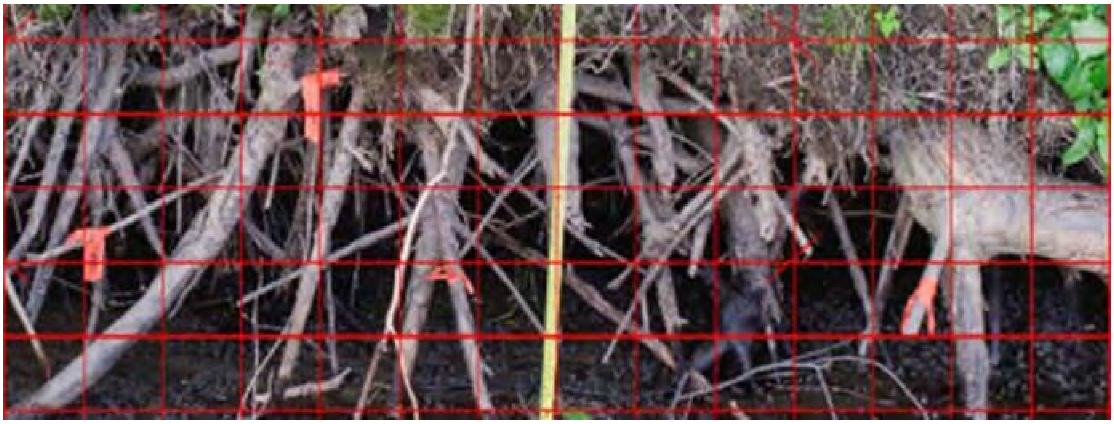

Figure 4.2.7.2-3: Image with 0.1m x 0.1m Grid Superimposed, Ready for Analysis in SigmaScan

Figure 4.2.7.2-4: Zoomed Image with 0.1m x 0.1m Grid Superimposed, Showing Individual Root Diameter Measurements Made in SigmaScan

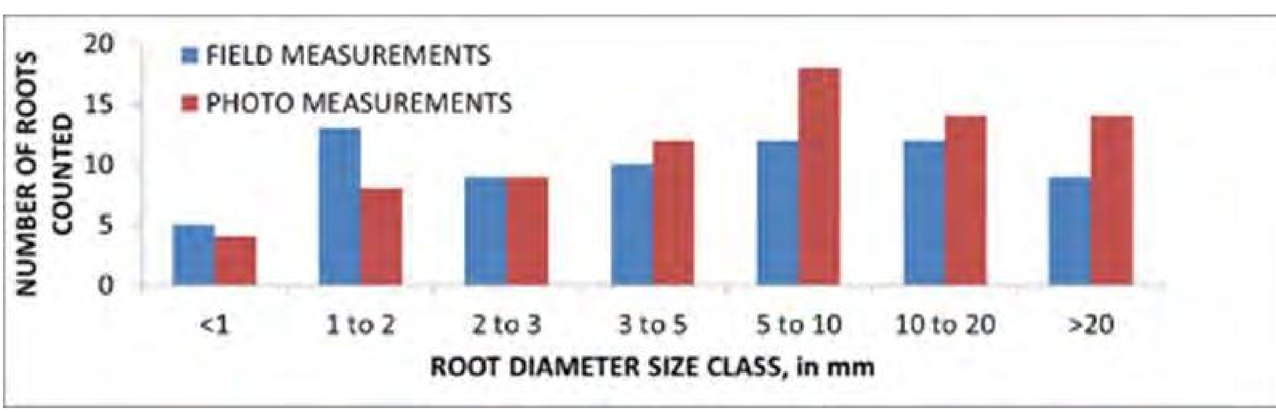

Figure 4.2.7.2-5: Comparison of the Number of Roots Measured for an American Elm Tree – Field vs. Photo Measured

4.2.7.3 Tensile-Strength Relationships

The tensile strength relations for each of the five species are best represented using a non-linear power function that is typical of other species (Simon & Collison, 2002; Pollen-Bankhead & Simon, 2013):

$$T_r = a\,D^{-b} \tag{2}$$

where T_r = root tensile strength in Megapascals (MPa) and D is root diameter, in mm.

The regression parameter a (representing the strength at 1 mm) varied from 28.7 for Red oak to 53.2 for Silver maple. As can be seen from Figure 4.2.7.3-1, however, there is a great deal of overlap between the data sets of the five species, which is a typical finding when comparing data sets between species (Pollen-Bankhead & Simon, 2013). In addition, r^2 values ranged from 0.291 for Silver maple, to 0.613 for American elm, reflecting the natural inherent variability, not only between species, but also within species. The literature around this topic reports that although difference between species does exist, several different factors can add to the scatter in the data. Of these factors, variations in root moisture, and cellulose content (Hales *et al.*, 2009) are the biggest reasons for variations within and between species, as these vary temporally and spatially according to local soils and topography, which are independent of the species tested. The species-specific relations shown below have been added to the BSTEM RipRoot database, so that site specific root-reinforcement values could be calculated for each site modeled with BSTEM.

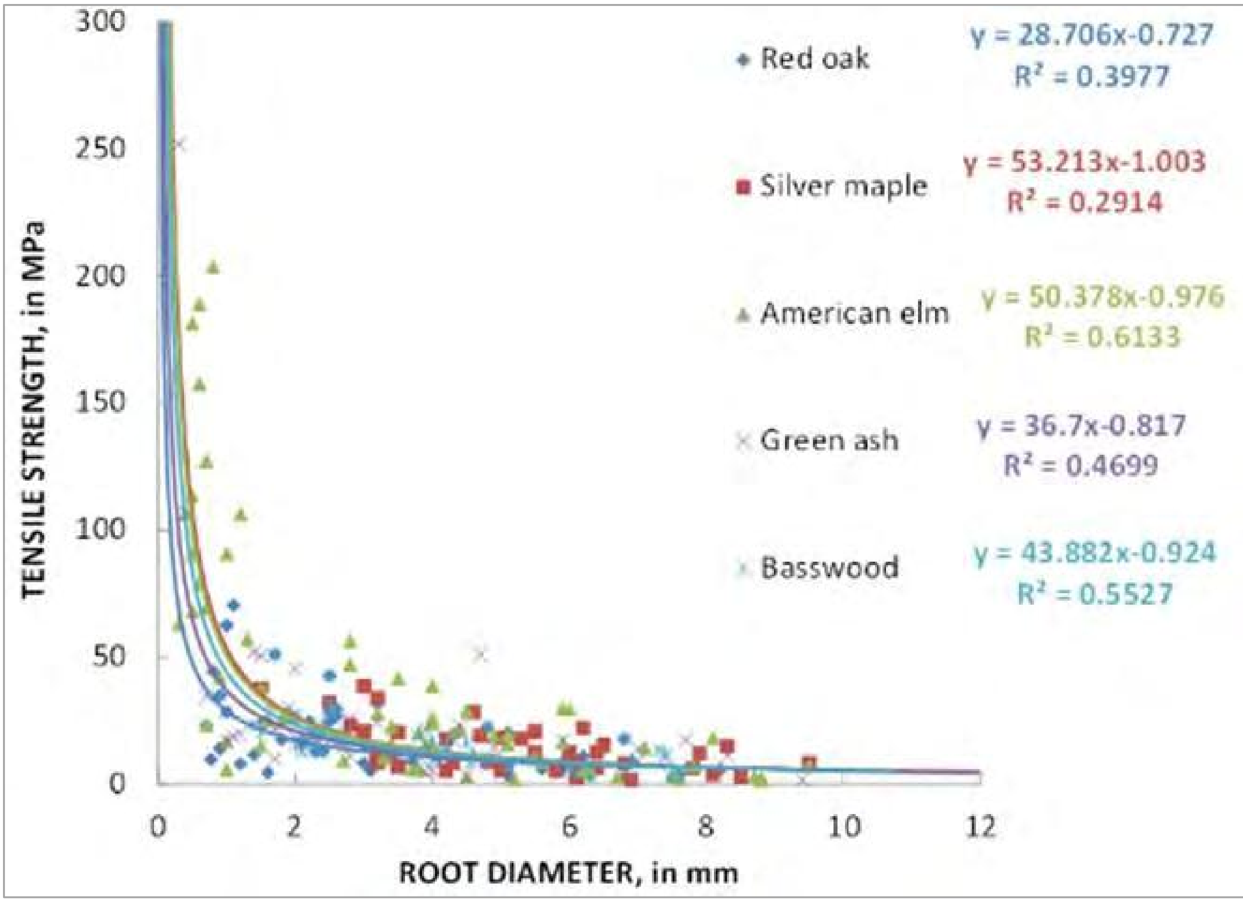

Figure 4.2.7.3-1: Root-diameter Tensile Strength Relations for Each of the Five Species Studied along the TFI

4.2.7.4 Diameter-Age Relations

Diameter–age relations were developed for each species so that the root-architecture data collected here could be applied to each of the 25 modeling sites by simply noting on each field form the dominant species at each site and typical values for DBH. Tree cores were taken for all of the trees sampled for root density and root diameter distribution so that average annual growth rates could be calculated and compared to values found in the literature (Table 4.2.7.4-1). The annual growth rates (mm/y) calculated from the field data matched literature values well, except in the case of Basswood, where the field data suggested a faster annual growth rate than reported in the literature (Burns *et al.*, 1990). The reference cited provides the silvic characteristics of about 200 forest tree species, including the five species from this study. The growth rates reported in this citation are, therefore, based on a broad geographic area encompassing the limits of growth for each species, which could explain the local variation seen here for Basswood trees. The field data suggest that the Basswood trees sampled had the fastest growth rate (13 mm/y) with the other four species ranging from 7-9 mm/y.

Table 4.2.7.4-1: Field Data for Diameter-age Relations and Calculated Average-annual Growth Rates for Each Species based on Field Data and Literature Values

	Diameter (cm)	Rings	Calculated annual growth (mm/y)	Average growth rate from field data (mm/y)	Growth rate reported in literature (mm/y)	
AE1	10	20	5	7	7	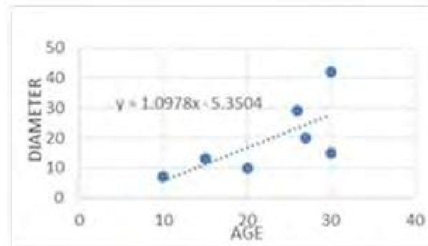
AE2	15	30	5			
AE3	20	27	7			
AE4-1	42	30	Core did not get center			
AE4-2	13	15	9			
AE5	29	26	11			
AE6	7	10	7			
BA1-1	18	-	No core taken	13	4	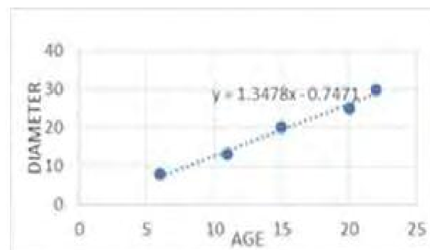
BA1-2	20	15	13			
BA1-3	30	22	14			
BA2-1	13	11	12			
BA2-2	8	6	13			
BA2-3	25	20	13			
GA1	45	41	11	8	7	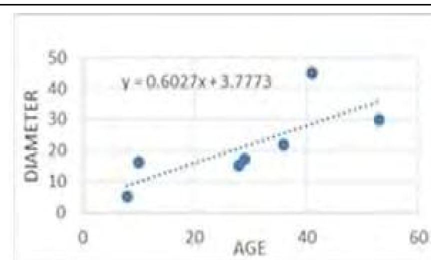
GA2	15	25	5			
GA3	5	8	6			
GA4	17	29	6			
GA5	22	36	6			
GA7	16	10	16			
GA8	30	53	6			
RO-1-1	20	22	9	8	5	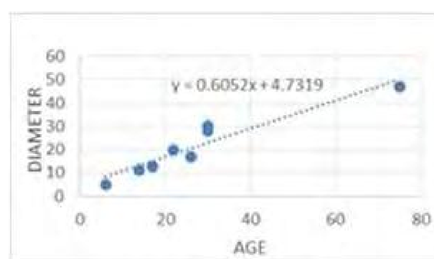
RO-1-2	28	30	9			
RO2	30	30	10			
RO3	11	14	8			
RO4	17	26	7			
RO5	5	6	8			
RO6	47	75	Core did not get center			
RO7	13	17	8			
SIM1-1	11	15	7	9	7 to 25	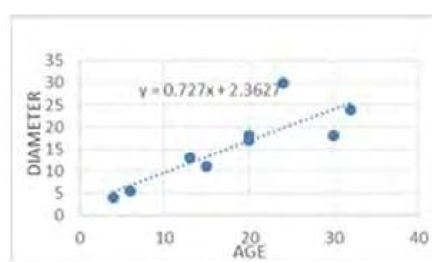
SIM1-2	17	20	9			
SIM1-3	18	30	6			
SIM4-1	30	24	13			
SIM4-2	5.5	6	9			
SIM5-1	13	13	10			
SIM5-2	4	4	10			
SIM6-1	18	20	9			
SIM7	24	32	8			

4.2.7.5 Root-Architecture Data

The root-architecture data collected in the field and processed during the digital photo analysis were collated and summarized by tree age species to look at variations in numbers of roots in each diameter size class. Maximum rooting densities along the TFI recorded as part of this study ranged from 246 roots per m^2 of bank face for Northern red oak to 790 roots per m^2 of bank face for Basswood trees. These densities are within the range of maximum rooting densities for species already coded into RipRoot, which range from 240 roots per m^2 of bank face for Black willow trees to 890 roots per m^2 of bank face for Cottonwood trees.

The data for the five study species show that in terms of the total number of roots present at the bank face there was an increase in rooting density up to the 20-50 year old category for three of the five species studied (Red oak, Silver maple and American elm; Table 4.2.7.5-1). For these three species, trees in the oldest category (>50 years) had less roots overall. It is interesting to note, however, that although the total number of roots recorded decreased beyond the 20-50 year old age group, the size of the roots present tended to increase, showing a coarsening of the root mass in the banks (Figure 4.2.7.5-1 shows an example for Red oak). In the case of the Green ash trees investigated along the study reach, the rooting density continued to increase across all of the age classes covered by the data collected, and similar to the previous three species, there was also a coarsening of the root diameters (Table 4.2.7.5-1). The Basswood trees showed the opposite trend to the Green ash, with rooting density declining as trees matured, but again the percent of roots in each size class shifted towards coarser roots in the oldest age class (Table 4.2.7.5-1).

The variations in rooting densities and the diameter distributions that make up that density for each species and age class have implications for the amount of root-reinforcement that is calculated by the RipRoot model (Table 4.2.7.5-1; Figure 4.2.7.5-2). The root-reinforcement values in Table 4.2.7.5-1 assume a 100% cover of that individual species and age category. Fine roots are stronger per unit area than larger diameter roots, but it takes hundreds if not thousands of these smaller roots to make up the area of one large root. In the case of the rooting densities measured along the study reach, the presence of coarser roots in the >10 mm diameter size class has more effect on the root-reinforcement calculations in RipRoot than the rooting density of the finer roots. This can be seen in the results in Figure 4.2.7.5-2 and Table 4.2.7.5-1 showing how estimated root-reinforcement for each species varies for each age class of trees.

For example, even though the total number of Red Oak roots is lower in the >50 year old category, the estimated root-reinforcement is higher than in the 20-50 year old category. This is because although the total number of roots decreased in the >50 year old category, the number of larger diameter roots increased (Table 4.2.7.5-1; Figure 4.2.7.5-1). The increased area of the larger roots outweighed the decrease in the area of the smaller roots in the 20-50 year category. The same pattern can be seen in the American elm data.

In the case of Basswood where the overall rooting density declined from the youngest to oldest age category, root-reinforcement correspondingly declined from the 0-10 year category to the 10-20 year tree category as root numbers declined. In the oldest category for this species, however, the root-reinforcement then increased again, because although the overall number of roots declined further in this category there was a shift to larger root diameters, the effect of which outweighed the decrease in root numbers when root-reinforcement was calculated.

The previous paragraphs discussed variations in root-reinforcement for varying ages of each species. Variations in root-reinforcement *between* species occur as a result of not only the rooting densities and diameter distributions discussed above, but also the species specific tensile-strength curve parameters. In addition, the vegetation present at each site is an assemblage of several species usually with a range of tree ages present. The way that these species specific rooting densities and tensile strength curve parameters were applied to each site is discussed in the next section.

Rooting depths in the root architecture analyses of the bank top trees, were noted to range from approximately 0.3 to 1.5 m below the top of the bank. Rooting densities generally decline exponentially from the soil surface downwards, with roots being concentrated in the top meter of soil (Pollen-Bankhead

& Simon, 2009). The data collected in this study also showed this to be the case, with the 0.5 to 1.0 meter layers showing the highest density of roots >1mm in diameter. Fine roots were concentrated near the soil surface, some of which may have been tree roots, and some of which may have been associated with understory shrubs and grasses.

Table 4.2.7.5-1: Distribution of Roots within Each Diameter Size Class, Broken Down by Species and Averaged for Each Tree-age Class

Red Oak	**Root Diameter in mm**								**Calculated Root-reinforcement from RipRoot (kPa)**
Age	<1	1 to 2	2 to 3	3 to 5	5 to 10	10 to 20	>20	Total	
0 to 10	3	11	11	6	5	2	1	37	1.78
10 to 20	20	16	16	9	15	4	1	81	2.27
20 to 50	27	66	53	42	33	17	8	246	9.70
50+	19	32	23	25	32	18	12	157	13.2
Silver Maple	**Root Diameter in mm**								**Calculated Root-reinforcement from RipRoot (kPa)**
Age	<1	1 to 2	2 to 3	3 to 5	5 to 10	10 to 20	>20	Total	
0 to 10	-	-	-	-	-	-	-	-	-
10 to 20	0	0	0	0	3	11	24	37	21.7
20 to 50	23	72	50	106	93	45	23	412	26.2
50+	9	18	15	16	22	11	6	97	6.84
American Elm	**Root Diameter in mm**								**Calculated Root-reinforcement from RipRoot (kPa)**
Age	<1	1 to 2	2 to 3	3 to 5	5 to 10	10 to 20	>20	Total	
0 to 10	72	40	8	8	12	8	0	148	2.8
10 to 20	78	112	39	36	26	14	6	311	7.66
20 to 50	84	183	69	65	40	20	13	475	13.6
50+	12	90	46	57	21	16	17	260	15.9
Green Ash	**Root Diameter in mm**								**Calculated Root-reinforcement from RipRoot (kPa)**
Age	<1	1 to 2	2 to 3	3 to 5	5 to 10	10 to 20	>20	Total	
0 to 10	64	32	4	24	8	12	8	152	9.11
10 to 20	75	127	24	35	26	23	22	332	23.3
20 to 50	35	149	62	37	31	26	28	367	29.4
50+	20	103	67	80	130	53	53	507	54.8
Basswood	**Root Diameter in mm**								**Calculated Root-reinforcement from RipRoot (kPa)**
Age	<1	1 to 2	2 to 3	3 to 5	5 to 10	10 to 20	>20	Total	
0 to 10	148	396	96	74	40	28	8	790	12.8
10 to 20	27	42	36	25	21	11	5	467	6.24
20 to 50	2	1	2	2	7	12	15	40	14.4
50+	-	-	-	-	-	-	-	-	-

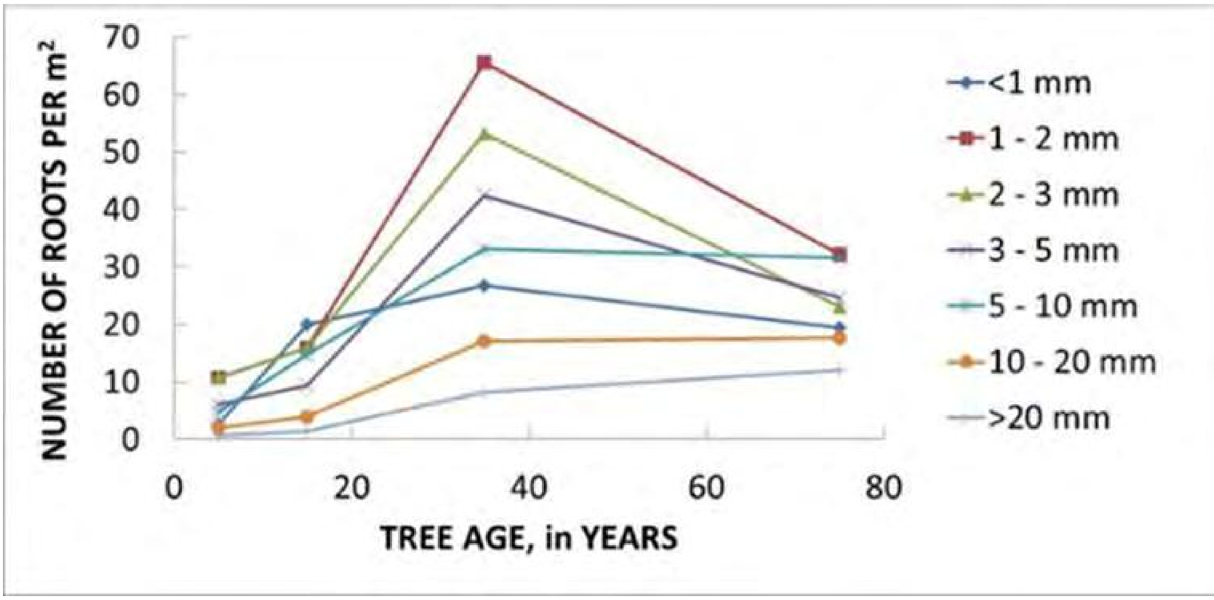

Figure 4.2.7.5-1: Frequency of Red Oak Roots of Different Diameters for Different Age Categories

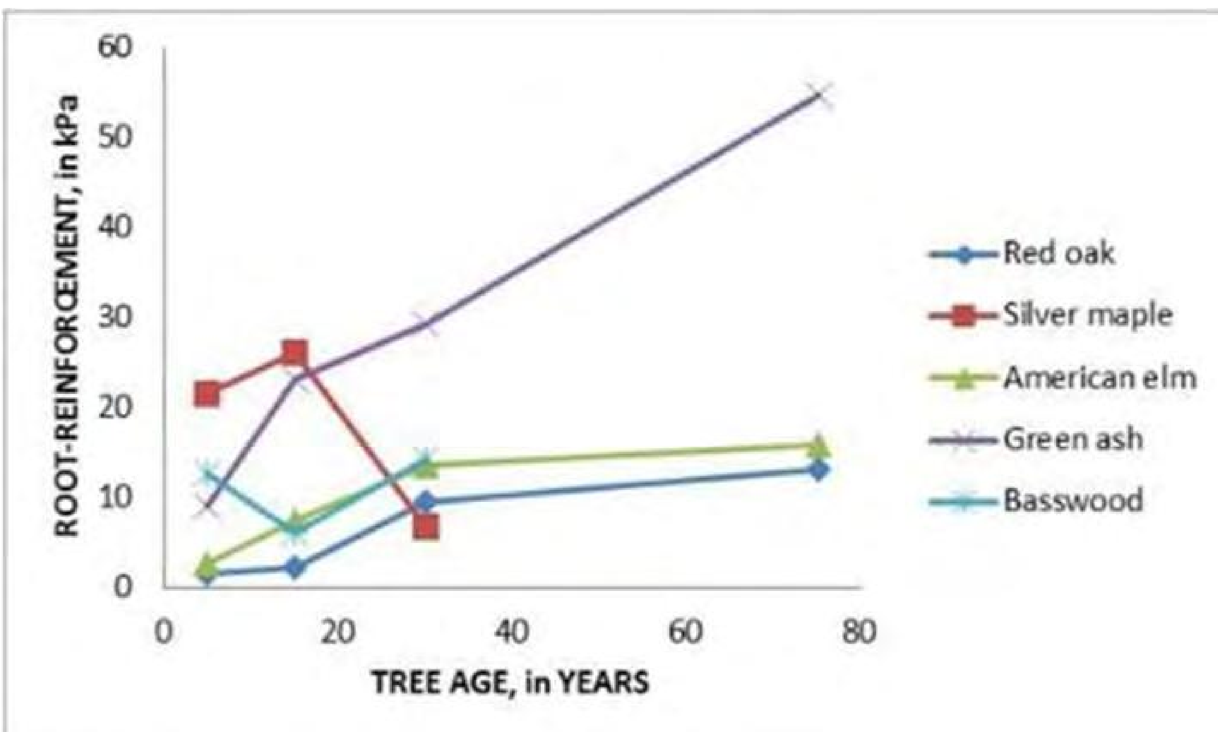

Figure 4.2.7.5-2: RipRoot Root-reinforcement Estimates for Each of the Five Study Species, Assuming 100% Coverage of that Species and Age

4.2.7.6 Calculating Root-Reinforcement at Each Study Site

Vegetation surveys were completed at each of the 25 detailed study sites so that vegetation could be correctly accounted for in the RipRoot algorithm within BSTEM using the species specific rooting densities and tensile strength curve parameters previously discussed. At each site the composition of the vegetation assemblage present was recorded, separating the vegetative cover into bank top, bank face and bank toe. For each part of the bank the percent contribution to vegetative cover from each species and the approximate age of that species was noted. Data were separated into tree cover and understorey cover so that both could be accounted for in root-reinforcement calculations in RipRoot. The percent tree cover and understorey data are summarized in Figures 4.2.7.6-1 – 4.2.7.6-3.

On the bank top, the percent cover of trees varies from 0 to 100% (Figure 4.2.7.6-1), but at all but four of the intensive sites tree cover is 20% or greater. At those sites where few or no trees are present, crops are the dominant land-use at one (Site 3R), and grasses at two others (Sites 119L and 6AR), with a mixture of bare soil, grasses, and herbaceous cover dominating the bank top at Site BC-1R. Where the percent cover of trees is higher, this obviously positively impacts the amount of root-reinforcement that is provided to the upper part of any potential failure surfaces within the streambanks.

On the bank face, the percent tree cover is consistently higher along the study reach than on the bank top, exceeding 40% cover at all but 5 sites. Where trees are more sparse (Figure 4.2.7.6-2; e.g. Site 3R, 6AR) there is still a good cover of shrubs and herbaceous species so there is still some vegetation cover present. This impacts both root-reinforcement of the bank and also bank roughness and the erodibility of the bank to hydraulic shear stresses. It should be noted that although the tree cover is 95% and 70% at sites 75BL and BC-1R respectively, the understorey data at these locations indicates a high percentage (80%) of the soil under the trees is bare. In these cases, although the trees are contributing to root-reinforcement within the banks themselves, there is less surface protection from hydraulic forces.

The percent tree cover at the bank toe (Figure 4.2.7.6-3) is generally lower than both on the bank top and on the bank face. This is unsurprising given the increased magnitude and duration of shear stresses acting at this point on each bank which results in lower occurrences of seedling germination and survival. Trees are still present on many of the bank toes throughout the study reach, but the percent cover did not exceed 65%. The understorey data also shows that even where trees are present there is a very little understorey vegetation, with >80% bare soil being recorded at 15 of the sites at the bank toe. At this point on the bank, tree roots that are present have little to no impact on reinforcement of potential shear surfaces through the bank, but any roots or vegetation present will impact channel roughness and susceptibility of the bank toe region to hydraulic shear stresses.

Figure 4.2.7.6-4 shows the percent cover of each of the five study tree species at each site along the reach, from upstream to downstream (left to right), which was used as input to BSTEM. As can be seen in the figure, at most sites at least one of the five study species was present either on the bank top, face or toe of the banks. Silver maple trees were more commonly found in the upstream half of the reach, whereas Red oaks, while present throughout the study reach, tended to dominate the assemblages in the downstream half of the reach. Green ash trees were found in higher frequencies between sites 21R and 5CR, although they were also found throughout the study reach.

The bank top and bank-face vegetation data were used as input to the RipRoot algorithm as these trees are the ones whose roots are most likely to be growing through potential failure planes within the bank. The percent cover for the bank face and bank toe were taken into consideration when applying roughness (n) values to those corresponding layers. In addition to the five tree species included in this study, any understorey vegetation was noted and included in the RipRoot run for each site. Where tree species other than the five species studied were present at a study site their percent composition was substituted by the most similar tree species from the RipRoot database. Table 4.2.7.6-1 shows an example of the input for Site 8R. RipRoot outputs for the bank top and bank face at the remaining sites are shown in Table 4.2.7.6-2.

The root-reinforcement values derived from RipRoot and utilized in BSTEM ranged from 0.3 to 14.1 kPa, with a median value of 3.75 kPa (Figure 4.2.7.6-5). If we consider these values in the context of the strength of the soil matrix (bank materials) we gain a better perspective of the importance of the root networks for bank stability. The effective cohesion values along the study reach tended to be quite low, which is characteristic of the sandy loam soils that dominate these banks. The median effective cohesion (*c'*) value for the bank materials along the study reach was 1.9 kPa (mean = 5.2 kPa), which is within the effective cohesion range for a loamy sand. BST tests also showed that 30% of the tested bank materials were cohesionless, 35% were less than 0.5 kPa, and only 20% were greater than 10 kPa. A median root-reinforcement value of 3.75 kPa is 97% greater than the median strength of the soil samples tested, meaning that on average, the reinforced soil-root matrix along the reach is 200% stronger than the soil alone. Where roots reinforce a weaker, sandier soil, this percentage increase in strength could be even higher. Conversely, at sites such as BC-1R where effective soil cohesion is very high (28.6 and 32.6 kPa) or where bank slopes are high in the absence of bank-face vegetation, the contribution from roots can be limited.

Table 4.2.7.6-1: Example of RipRoot Input Data for Site 8R

Species	Percent of Assemblage	Approximate Age (years)
Grasses	10	-
Am. basswood	5	7.5
Green ash	10	12.5
Northern red oak	7.5	7.5
Northern red oak	7.5	50

Table 4.2.7.6-2: RipRoot Outputs for Root-reinforcement to be added to the Bank Top and Bank Face Where Applicable in the BSTEM Simulations

Site	RipRoot Output (kPa)		Notes
	Top Bank	Bank Face	
11L	3.43		
2L	2.53	6.22	
303L	3.90		
18L	3.44		
3L	9.40		
3R	0.30		
21R	4.00	3.60	Layer 2 only. From 1.0m depth to 3.6m depth
4L	2.10	5.20	
29R	6.90		
5CR	14.1		
26R	4.54		
10L	4.90	3.5	Layers 2 and 3. All but Toe.
10 R	3.18		
6AL	3.20		
6AR	0.47		
119L	2.17		
7L	11.4		
7R	2.30	10.5	Layers 2 and 3. All but Toe.
8BL	1.94	6.1	Layers 2 and 3. All but Toe.
8BR	4.62	1.7	Layers 2 and 3. All but Toe.
87L	13.9		
75BL	5.90		
9R	3.89	3.6	Layers 2 and 3. All but Toe.
12L	4.59		
BC-1R	3.56	2.5	Layers 2 and 3. All but Toe.

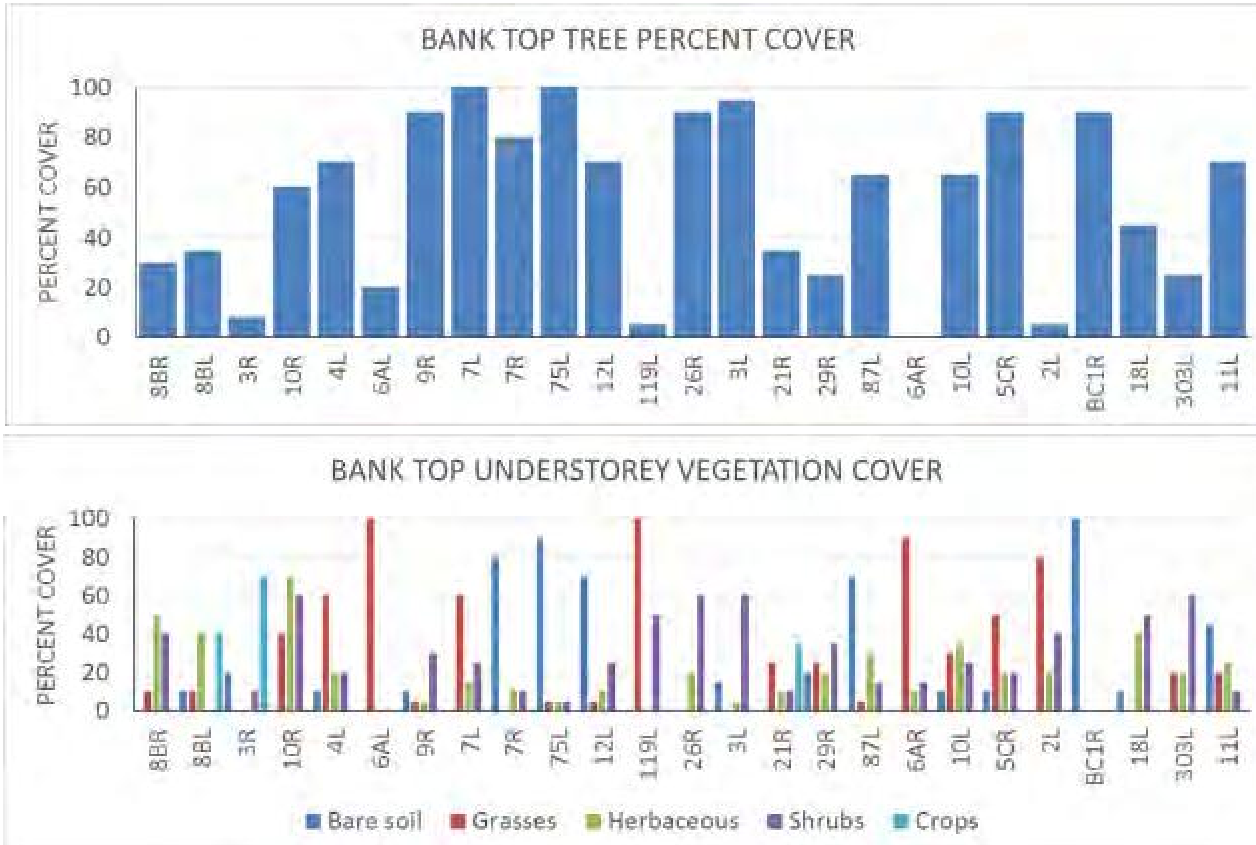

Figure 4.2.7.6-1 Percent cover for tree and understorey vegetation categories on the bank top, at each site

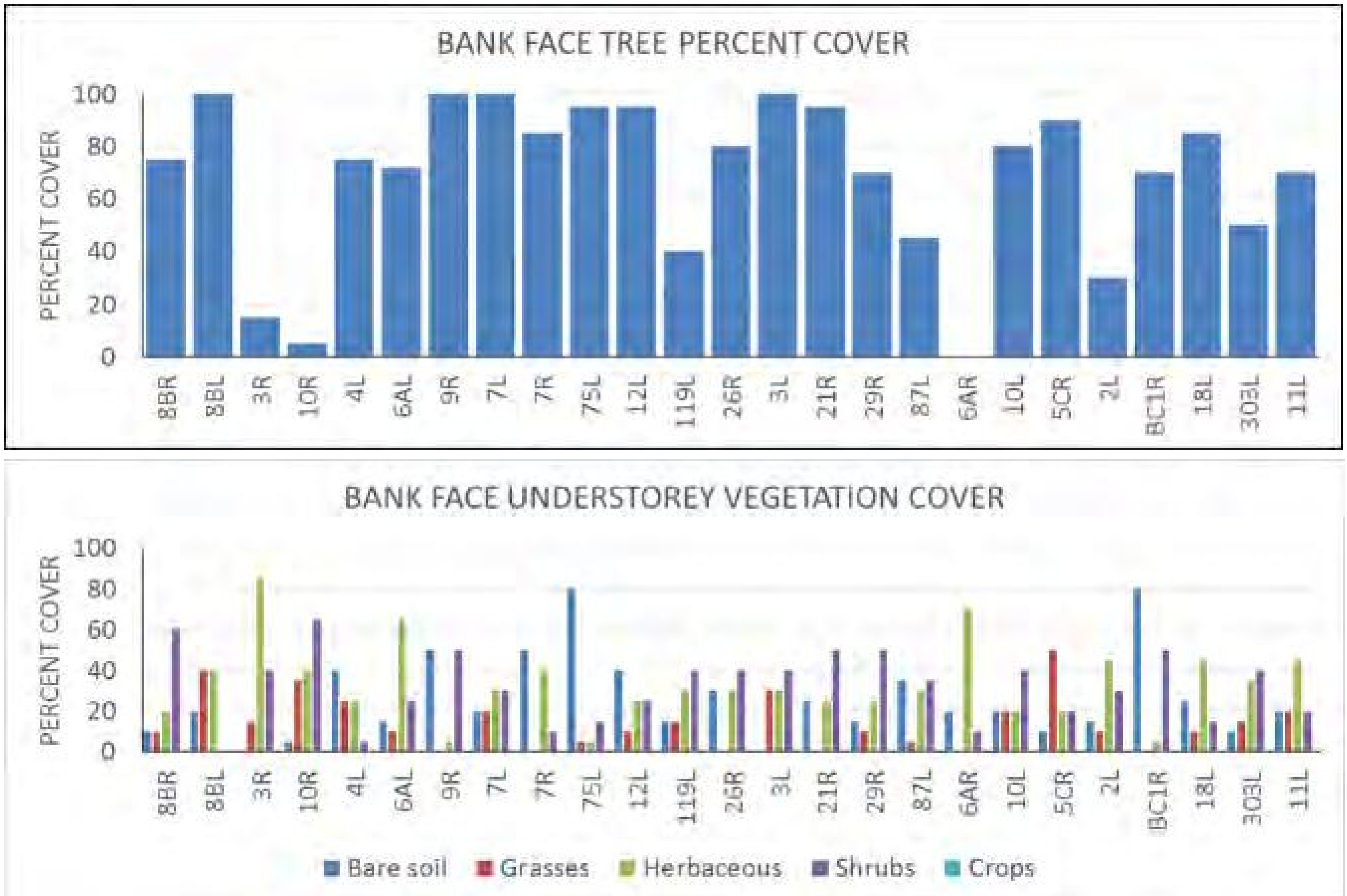

Figure 4.2.7.6-2: Percent Cover for Tree- (Top) and Understory-vegetation (Bottom) Categories on the Bank Face at Each Site

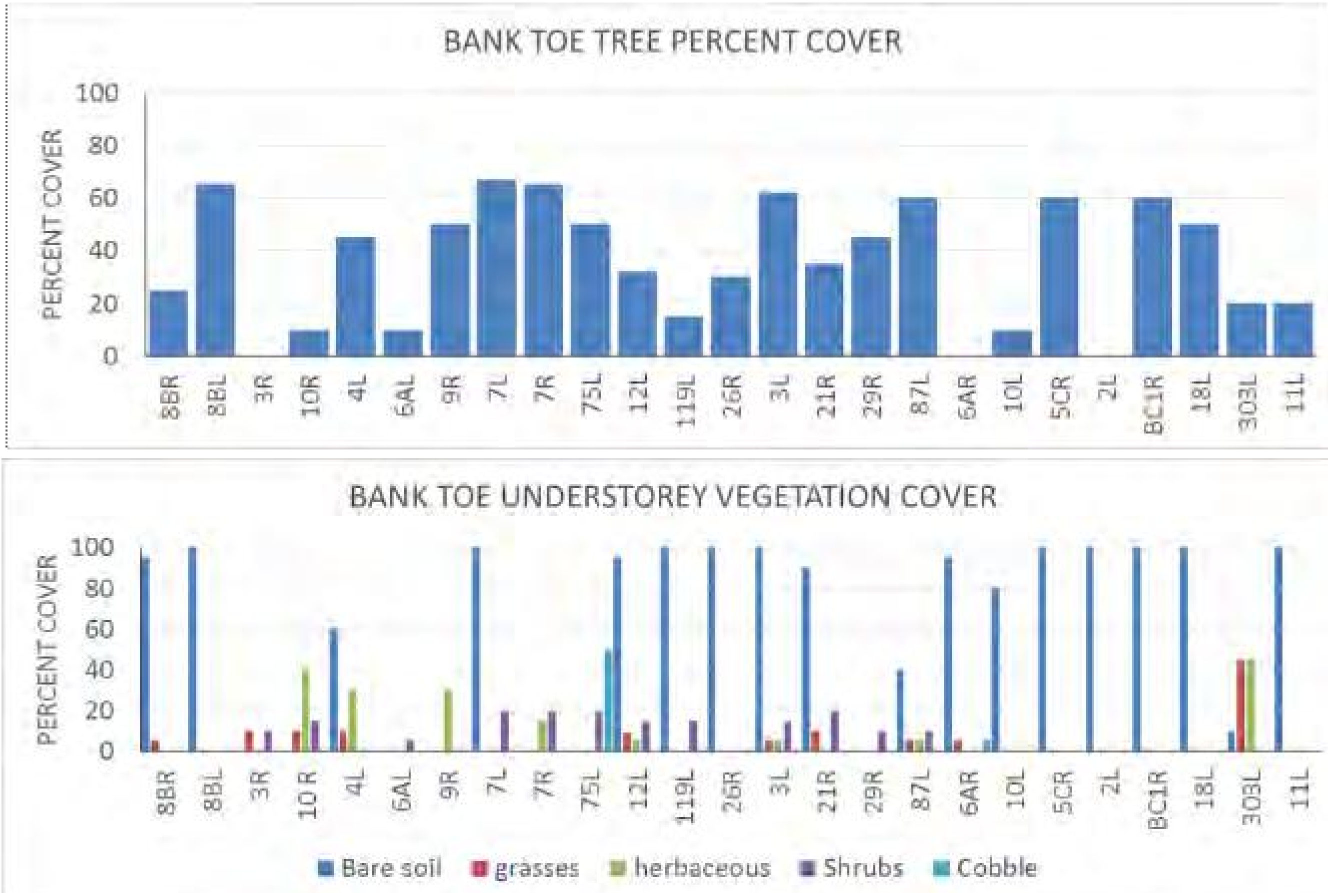

Figure 4.2.7.6-3 Percent cover for tree and understorey vegetation categories at the bank toe, at each site

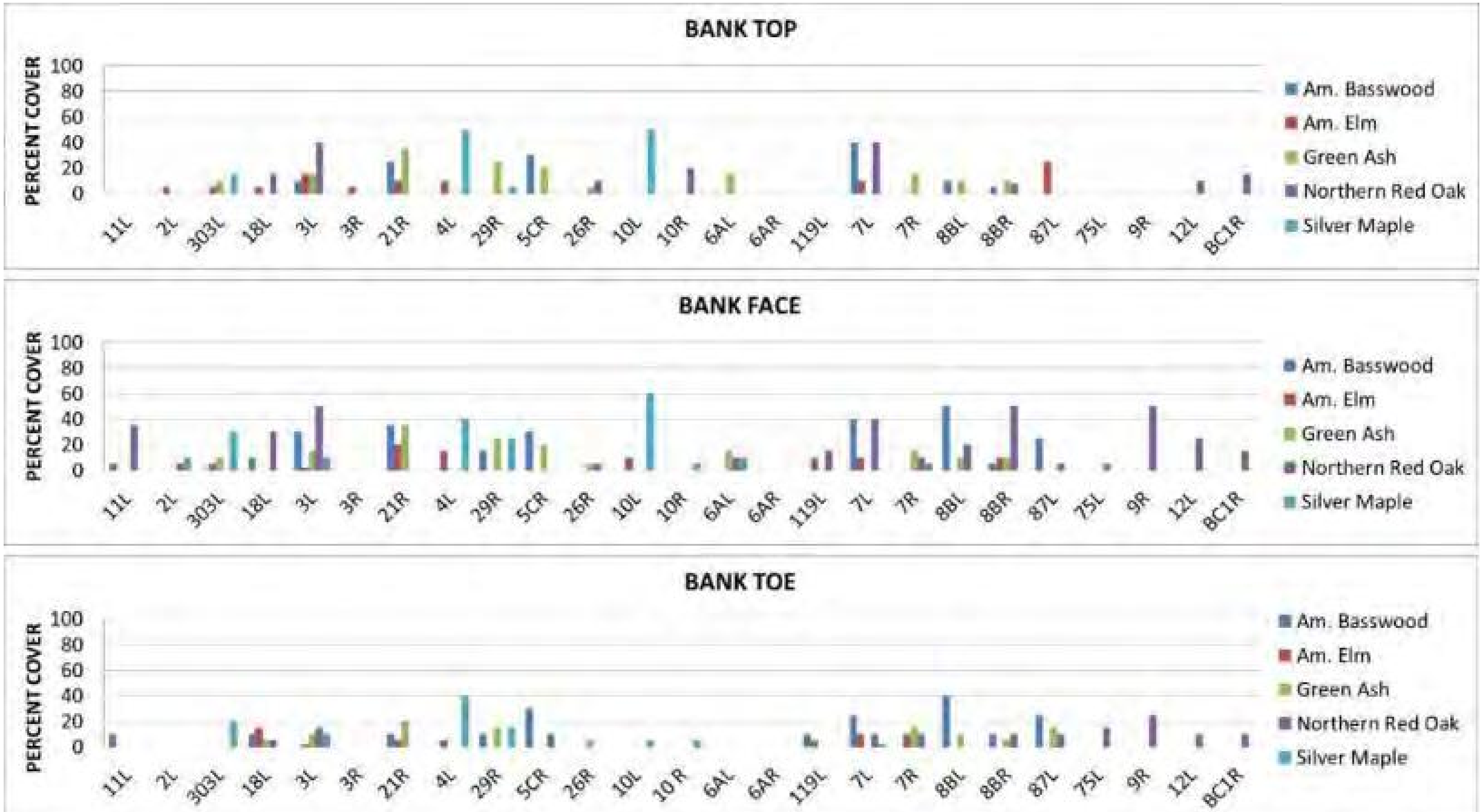

Figure 4.2.7.6-4 Longitudinal distribution of percent cover for the five tree species investigated for root-reinforcement along the study reach

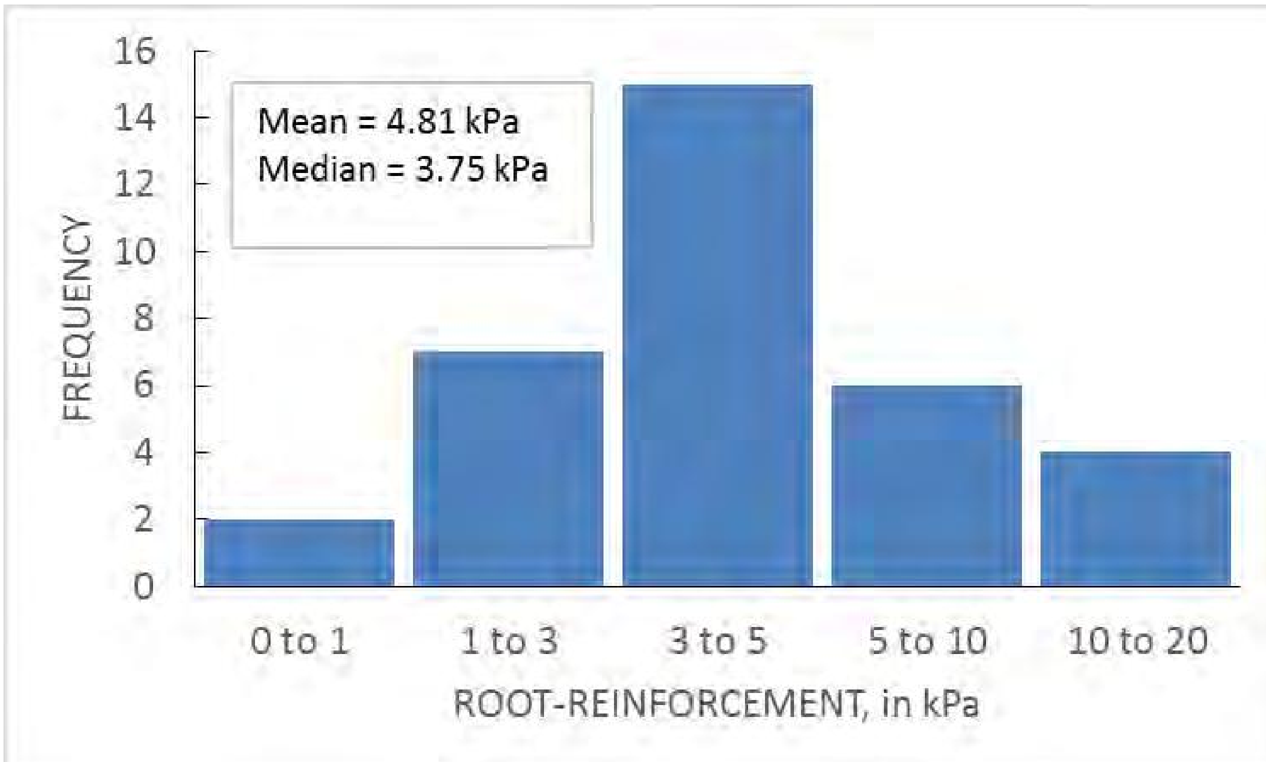

Figure 4.2.7.6-5 Distribution of root-reinforcement values along the Turners Falls Impoundment

4.2.8 Boat-Generated Wave Management on the Connecticut River - BSTEM

Basic relations describing the wave pattern around a moving boat are presented in Volume III (Appendix G). The generated wave system can simply be defined by the wave period (or wavelength), wave height and direction of wave propagation. The total energy carried by the wave train is a function of the wave height, and the wave height depends on many different factors including the velocity of the boat, dimension (length, width, draft) and the shape of the boat and the hull design, total displacement volume, distance of the shoreline from the sailing line, channel width, water depth, and the cross-sectional area. Wave height estimations necessitate more sophisticated methods due to the number of variables involved. Simple empirical methods can provide reasonable approximations of boat-generated wave prediction but the validity of these models are limited by the range of data used in their derivation.

Boat-wave data were collected during several time periods from the late 1990's up through the summer of 2015. The initial data consisted of placing a staff gage in the water near the riverbank and videotaping boat waves. From this, the frequency and magnitude of the wave amplitude as they approached and broke on the riverbank was developed from the video information. Some near-bank suspended sediment samples were also collected when boat waves were breaking. Boat-wave data, as described above, were collected on the following dates: May 8, 1997, July 12-13, 1997, July 26-27, 2008, and during September 2008. Appendix H provides boat wave data collected during these time periods.

A set of boat wave data was specifically collected in 2015 in support of the Causation Study for use in BSTEM. The hydrodynamics of boat waves and the approach to collect detailed boat wave data in 2015 is described below. This section concerns field measurement of boat traffic and boat-generated wave properties at three monitoring locations throughout the TFI. Each measurement station consisted of one or more wave loggers to measure the water-surface displacement and a time-lapse camera to capture the boats as they pass. Wave-logger data analysis procedures, boat statistics and wave properties during the measurement period are presented in the following sections.

4.2.8.1 Boat Wave Monitoring Sites

Boat-monitoring sites were established at three locations throughout the geographic extent of the TFI. Figure 4.2.8.1-1 shows the relative distances between the sites. Figure 4.2.8.1-2 depicts the locations of the wave logger sites and camera installation sites as well as the location of the detailed study sites examined in BSTEM.

The monitoring sites were selected based on the availability of camera installation sites suitable for boat monitoring (i.e. bridges). In order to have the field of view covering an area large enough to resolve the boat activity, the cameras had to be installed sufficiently high and far from the river, yet close enough to have enough spatial resolution. The relations between spatial and temporal resolution, and the target distance for the selected cameras are explained in the following section. Both banks of the river are covered with shrubs and trees, which limited the field of view of the cameras. Moving closer to the river to avoid vegetation limited the field of view and camera height, which made the banks impractical for boat monitoring. The cameras also require frequent maintenance for download and battery replacement; therefore, installing the cameras on the existing bridges along the river was the most viable option due to the ease of access and a sufficiently wide field of view. Six cameras were installed on three bridges, Schell Bridge (Cam-1), Route 10 Bridge (Rt. 10) (Cam-2), and the French King Bridge (Cam-3).

A wave-logger station was constructed near each camera site. The first wave logger (WLOG-1) was located upstream of the Schell Bridge, close to left bank of the river, near site 4L. The second wave logger (WLOG-2) was located downstream of the Rt. 10 Bridge, on the right bank near site 5CR. The remaining two wave loggers (WLOG-3 and WLOG-4) were located upstream of French King Bridge and downstream of site 75BL, on the left bank. These locations were selected based on the site conditions and camera field of view. The objective was to measure the boat-generated waves close to the shore before they shoal and break. Each wave logger was attached to a T-post, which was driven with a sledge hammer into the riverbed near the bank. The length of the T-posts also limited workable water depth and constrained the wave logger site locations. Given these limitations, only a narrow section along the river cross-section was suitable for the placement of wave loggers.

Document Accession #: 20161014-5107   Filed Date: 10/14/2016

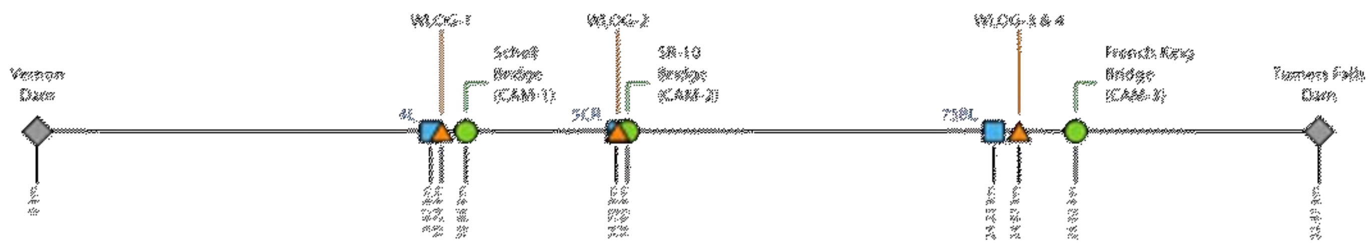

Figure 4.2.8.1-1: Relative Distance between Boat-monitoring Sites

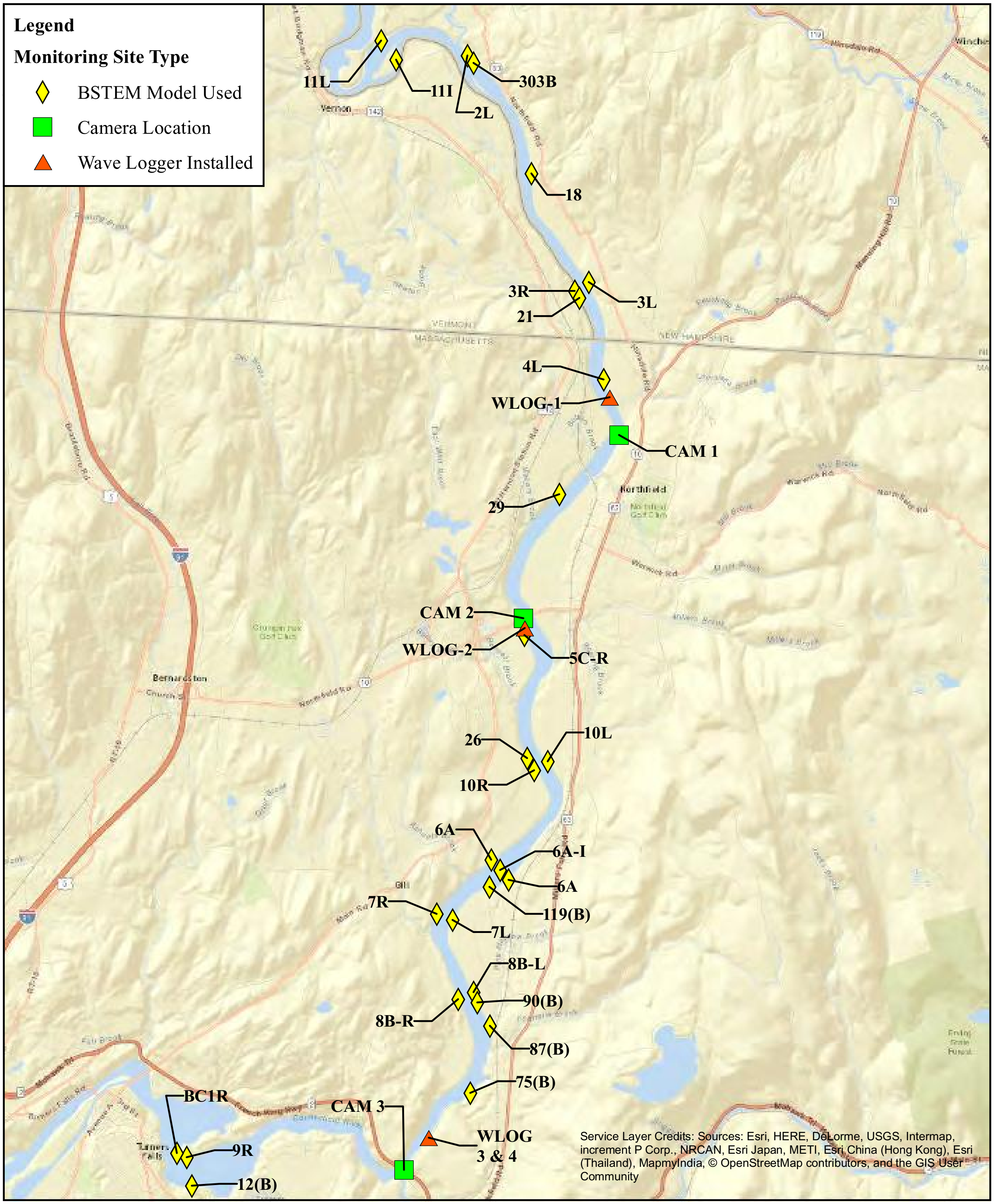

FIRSTLIGHT HYDRO GENERATING COMPANY
Northfield Mountain Pumped Storage Project No. 2485
Turners Falls Hydroelectric Project No. 1889

STUDY 3.1.2

Figure 4.2.8.1-2: Locations of Boat-monitoring Sites

FirstLight Power Resources

Path: W:\gis\studies\3_1_2\maps\final_report\figure_4_2_8_1-2.mxd

4.2.8.2 Instrumentation and Data Collection

Two types of equipment were utilized for the collection of data related to boat-waves – cameras and wave loggers. In-depth discussion pertaining to each type of equipment is presented below.

Cameras

Two different types of consumer-grade cameras were used during the measurements. The specifications of these cameras are listed in Table 4.2.8.2-1. Both cameras were configured to take pictures at 10-second intervals at a pixel resolution of 1280 by 720 during daylight. Each field site was equipped with one of each type of camera. The wide-angle camera (Brinno) served as the primary camera while the other one was used as the backup. Both cameras are rated to run over two weeks with this configuration without replacing the batteries and the memory card.

The primary difference between the two types of cameras was the area each picture covers, described by the Field of View concept (FOV). FOV is the area that is visible to the camera sensor through its optical component. For the same sensor resolution (or pixel resolution) the camera with the wider FOV will provide a larger portion of the outside word at a smaller resolution. This is explained in Figure 4.2.8.2-1. The wide-angle camera (Brinno) (illustrated with the orange line in Figure 4.2.8.2-1) has 115° FOV while the narrow-angle camera (Moutrie) (illustrated with the green line) has 50° FOV. The wide-angle camera covers a relatively larger area but it won't detect smaller objects due to the lowered resolution. A boat will appear smaller on the wider FOV camera and resolved with fewer pixels compared to the one with narrower FOV. However, the boat will stay longer in the wide-angle FOV; therefore, for a given time lapse interval, faster boats can be detected.

The frame interval (time interval between two frames) and the maximum operation time of the cameras with both types of lenses (50° and 115° FOV) based on a boat moving at 20 m/s are shown in Figure 4.2.8.2-1. The boat sailing line is assumed to be perpendicular to the camera direction. The frame interval is reduced when the boats are closer to the camera, increasing the frame rate, which also increases the energy and memory requirements. Pulling the camera back from the target is one solution to this problem, but not practical for this field setup. When the camera is oriented in the streamwise direction, which was adapted in the current study, the vertical FOV becomes more important than the horizontal FOV in terms of positioning the cameras. This is illustrated in Figure 4.2.8.2-2 where the two plots show how pixel resolution changes with distance for various camera heights.

The illustrated geometry on top is plotted for x vs s_h, and x/h_c vs s_h/x_c, where x is the distance from the camera, s_h is the spatial dimension of each pixel and h_c is the height of the camera. The pixel resolution reduces asymptotically in the vertical direction and the rate depends on the height of the camera. In order to have a wider vertical FOV, the camera has to be raised. When the camera is lowered, the vertical resolution is reduced considerably. Streamwise camera orientation is advantageous for capturing high-speed boats, but the camera height limits the precision of the measurements. Figure 4.2.8.2-3 shows example shots from the two types of cameras at the three sites. Each pair of pictures refers to the same time for comparison.

The cameras were held in place on the bridge hardware by hose clamps and zip ties. Data from the cameras were downloaded every two weeks at which time the batteries were also replaced. The Rt. 10 Bridge and French King Bridge cameras were mounted in the middle of the bridge rail, whereas the Schell Bridge camera was close to the left bank to provide a better view angle of the river upstream.

Table 4.2.8.2-1: Comparison of Camera Specifications

	Brinno HDR	Moultrie-1100i
		
Resolution	1280x720 (1.3 MP) HDR	1280 x 720 (1.3 MP) 2304 x 1296 (3 MP) 2688 x 1512 (4MP) 4608 x 2592 (12 MP)
Aperture	F2.0, 19mm (35mm eqv.)	
Time lapse	1s – 24hrs	10s, 30s, 1min – 1day
Field of view (FOV)	112˚	50˚
Memory	32 GB	32 GB
Batteries	4 x AA	8 x AA
Video resolution	720p	720p
No of photos with 32GB memory	77,280 photos	77,280 photos
No of photos with 4AA batteries	80,000 photos	80,000 photos
Other		80 ft infrared Temperature gauge

Figure 4.2.8.2-1 Camera field of view (FOV) comparison

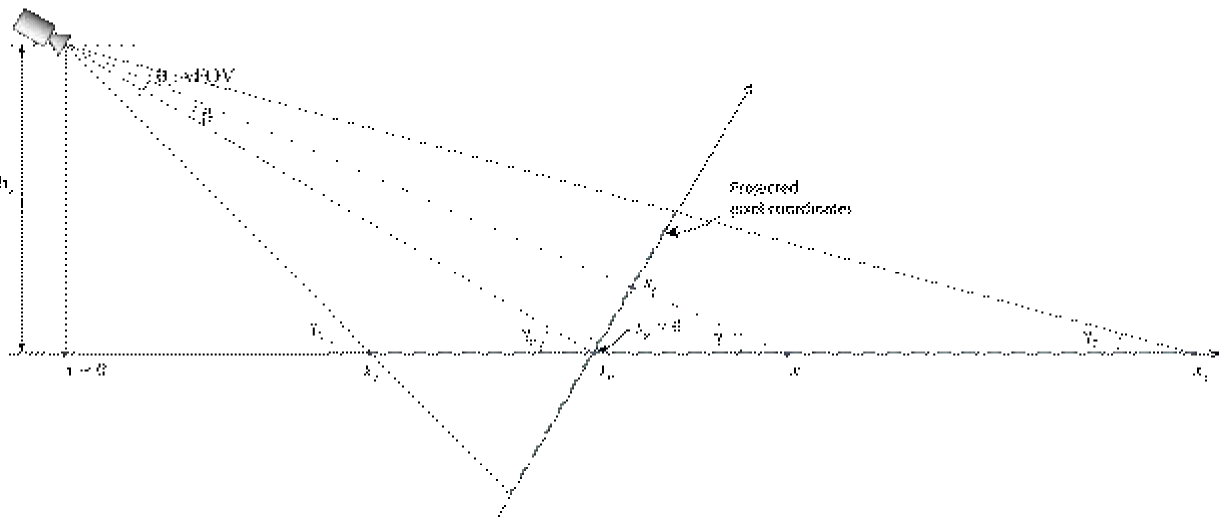

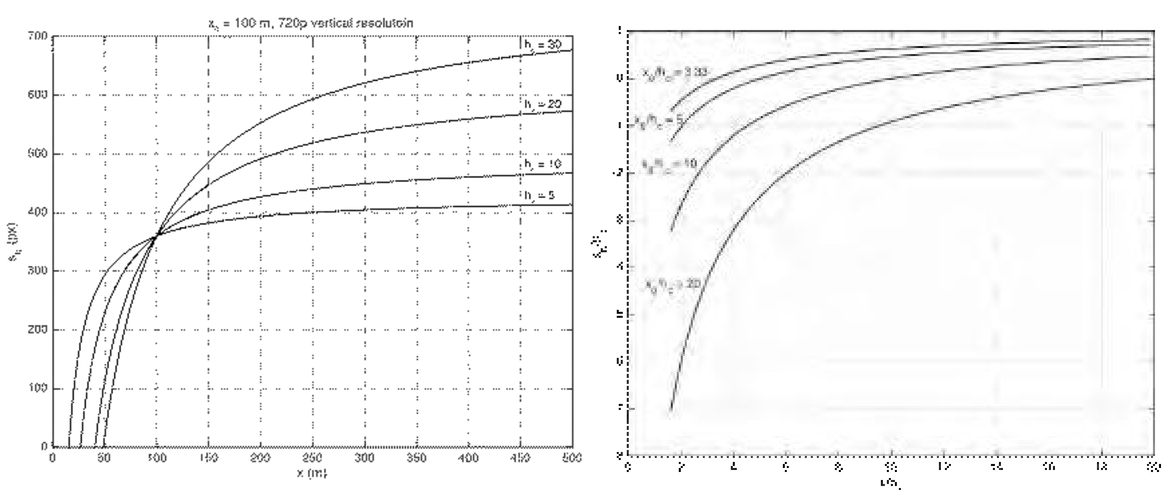

Figure 4.2.8.2-2 Pixel resolution and camera height relations

Schell/M1

Schell/B1

Rt. 10/M2

Rt. 10/B2

French King/M3

French King/B3

Figure 4.2.8.2-3: Example Photographs Recorded at the Monitoring Sites

Wave Loggers

Four wave loggers were used to measure water-surface displacement at three sites in the study area. The wave loggers include a capacitance type wave staff and a battery powered microprocessor that stores the water level. The specifications of the wave loggers are given in Figure 4.2.8.2-4. The loggers were operated continuously (100% burst time/interval time) at 30Hz frequency. Equipped with 2GB flash cards, the expected uninterrupted recording time of the loggers was on the order of months at 30Hz frequency. Nonetheless, the recorded data was downloaded at two-week intervals to avoid unexpected data loss.

The loggers recorded the water-surface displacement at 30Hz frequency and the ambient air temperate at 2.5Hz. Boat- and wind-generated waves in the study area are mostly in a frequency range of 0.2Hz – 2Hz. The 30Hz measurement frequency provided a fairly good temporal resolution, which is 15-readings-per-wave at the high frequency end of this range. Each logger had a 2-m-long staff producing an integer count between 0-4095 depending on the wave level relative to the staff, which is equivalent to a spatial resolution of approximately 0.5 mm.

For the wave loggers to measure the water level, the wave staffs had to be in contact with the water surface at all times. The optimum elevation of the wave loggers that maximized its contact with the water was calculated knowing the stage history. Stage histograms were generated for each site using HEC-RAS simulations of the 15-year long period between 2000 and 2014. The simulation results closest to the wave-logger sites were used for this analysis. Figure 4.2.8.2-5 shows the exceedance probability of the entire water-level dataset, and for the summer months from May through September (MJJAS) at site 4L (near WLOG-1), 5CR (near WLOG-2) and site 75BL (near WLOG 3 & 4). Mean elevations for 12 months and MJJAS, and the minimum and maximum elevations are also shown in these plots. Red lines indicate the stage when the discharge is 20,000 cfs and 40,000 cfs. The mid-height of the wave staffs were determined using the calculated mean values.

Figures 4.2.8.2-6 through 4.2.8.2-8 illustrate the installed elevations of the wave loggers compared to the probability distribution of the stage. Red marks on the staffs indicate the midpoint of the staffs. A maximum measurable water-surface elevation is reached when 90% of the staff is submerged in the water. The stage is above this elevation less the 10% of the time during summer mouths (MJJAS).

Galvanized steel T-posts were installed to support the wave loggers. 8-ft (2.44 m) long T-posts were vertically driven into the riverbed using a sledge hammer (Figure 4.2.8.2-9). Additional sections were bolted on top of the post as it was driven into the bed until 4-5 ft. (1.2 -1.5 m) was under the riverbed. The loggers were bolted to these T-posts and plumbed. Reflectors and flags were attached to increase visibility. Staffs were secured to the T-posts at 2/3 their height to limit its motion. T-posts were then anchored to the bank with flagged nylon ropes.

Table 4.2.8.2-2 summarizes the camera and wave-logger settings used during the field monitoring. Beginning dates of the data recording for each instrument are also listed in this table. Figure 4.2.8.2-10 shows pictures of the cameras and wave loggers after the installation.

Table 4.2.8.2-2: Camera and Wave Logger Configurations

Camera location	Schell Bridge	Rt. 10 Bridge	French King Bridge
Camera type	Moultrie	Moultrie	Moultrie
Frame rate	0.1 fps	0.1 fps	0.1 fps
Interval	7am - 8pm	7am - 7pm	6am - 9pm
Start date	20-May	15-May	15-May
Camera type	Brinno	Brinno	Brinno
Frame rate	0.1 fps	0.1 fps	0.1 fps
Interval	6am - 9pm	6am - 9pm	6am - 9pm
Start date	21-May	15-May	15-May
Logger location	Upstream of 4L	Downstream of 5CR	Upstream of 75BL
Frequency	30Hz	30Hz	30Hz
Start date	20-May	13-May	21-May

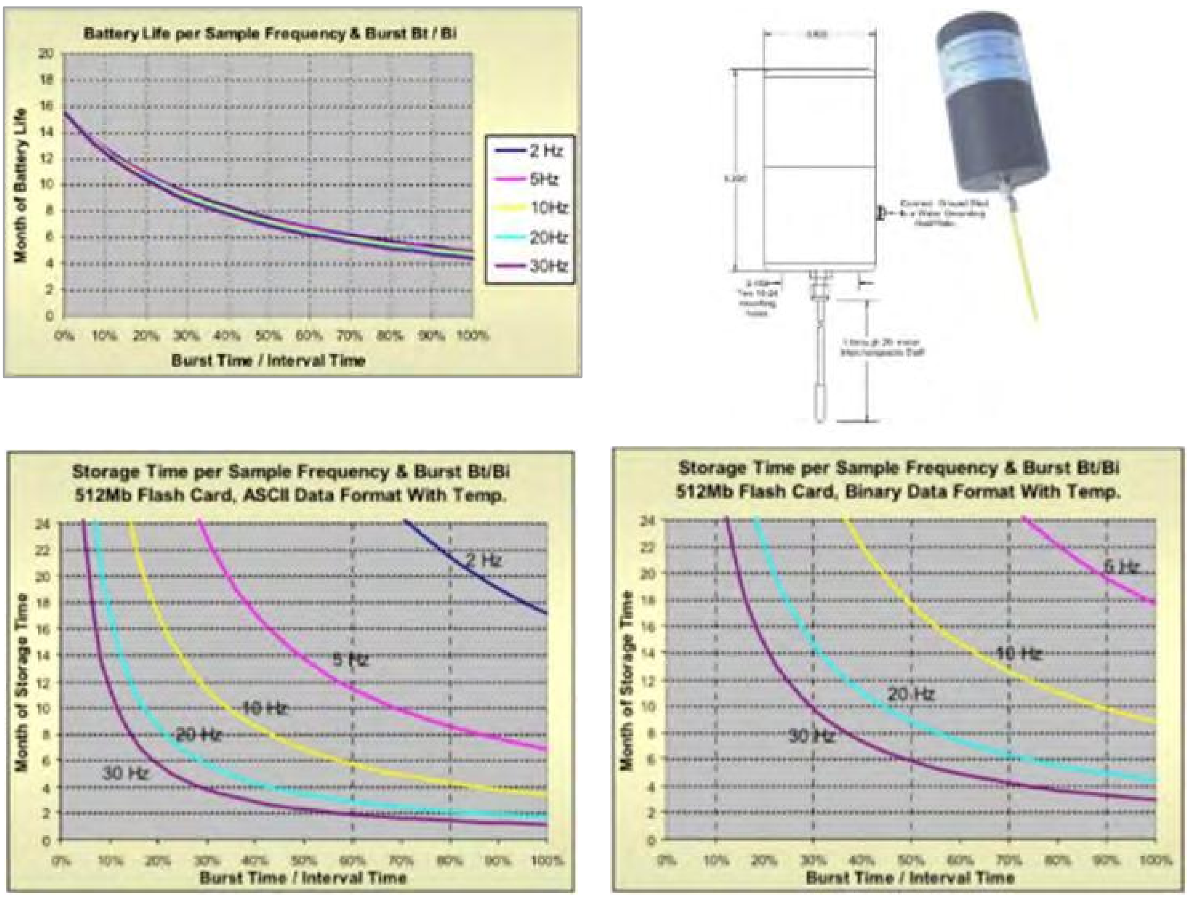

Figure 4.2.8.2-4: Wave Logger Specifications

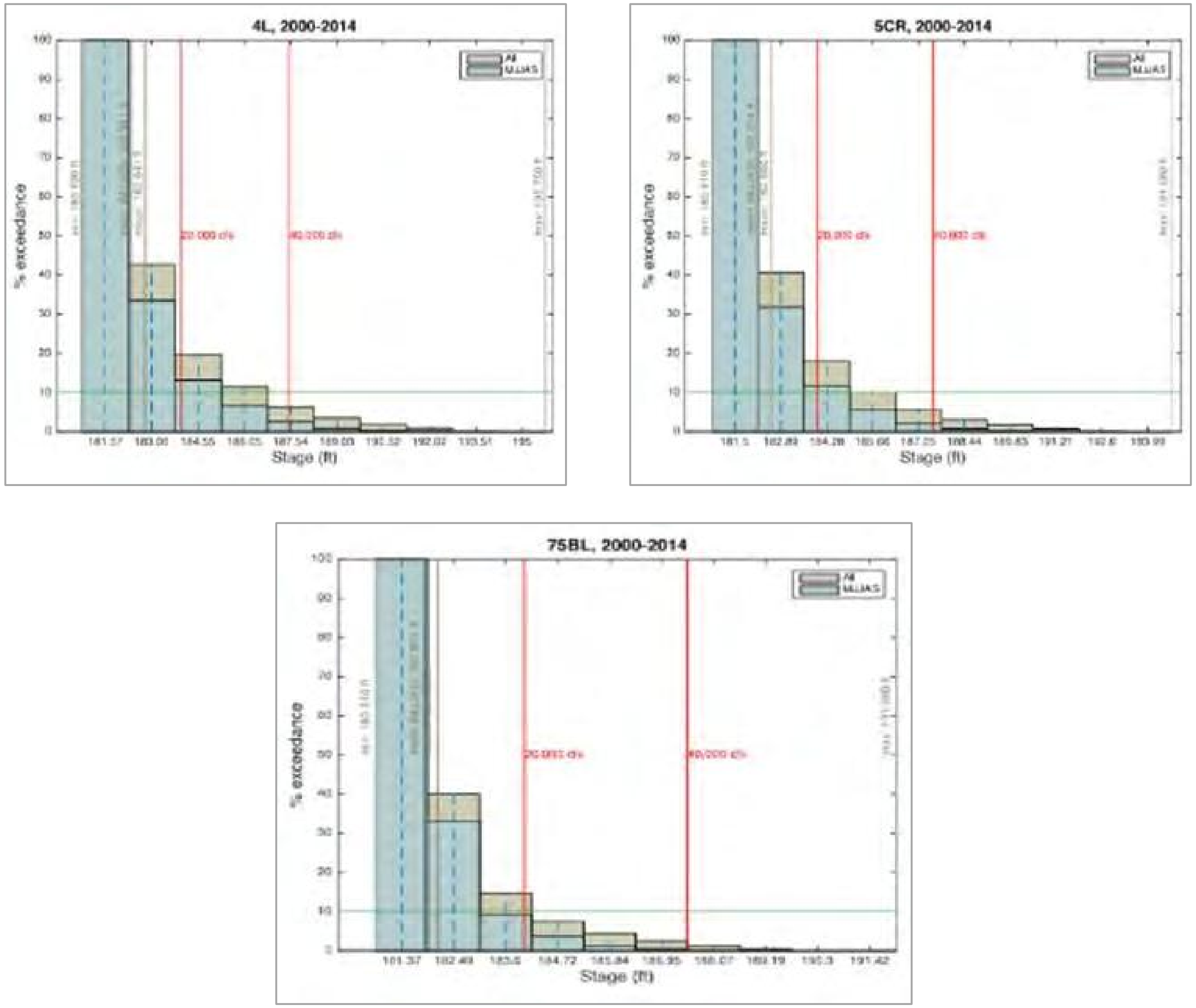

Figure 4.2.8.2-5: Exceedance Probability of the Stage at Sites 4L, 5CR, and 75BL

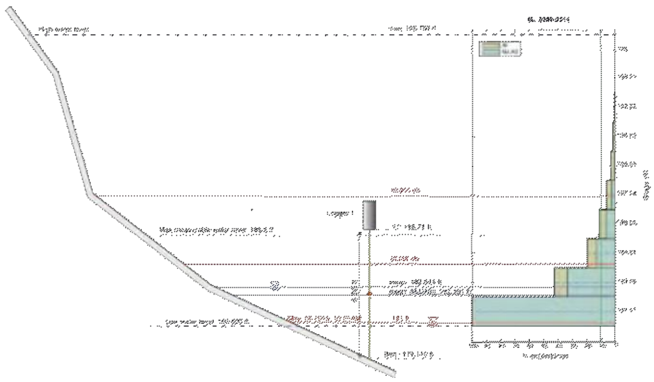

Figure 4.2.8.2-6 WLOG-1 installation elevation

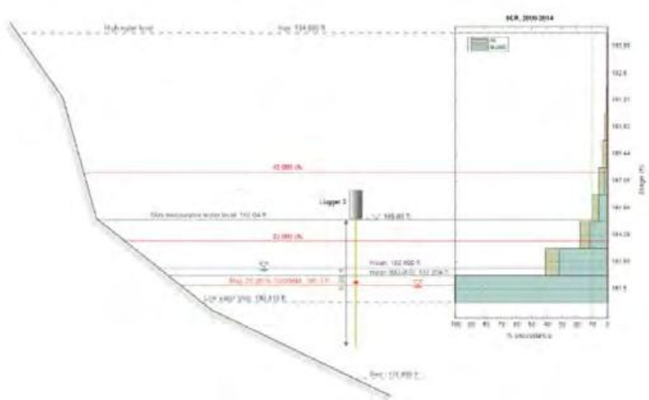

Figure 4.2.8.2-7 WLOG-2 installation elevation

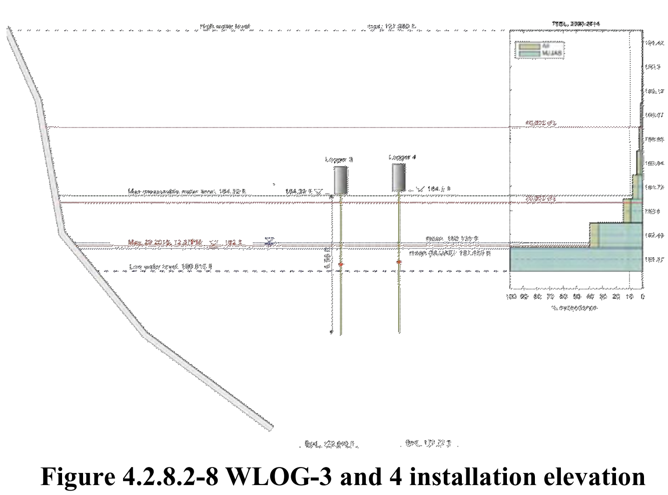

Figure 4.2.8.2-8 WLOG-3 and 4 installation elevation

Figure 4.2.8.2-9: Installation of the T-posts

Figure 4.2.8.2-10: Cameras and Wave Loggers at the Three Installation Sites

4.2.8.3 Data Analysis

Boat waves were recorded continuously at four loggers between May 22, 2015 and September 14, 2015. Quantitative boat-traffic statistical data and boat-generated wave data were obtained mainly from the wave logger data analysis. The time-lapse recordings supported the wave analysis by providing visual information. For instance, the boat signatures in the wave data are validated using the video recordings. Figure 4.2.8.3-1 shows an example time series of the water-surface displacement and its spectrum after two boats passing by WLOG-2. The pictures of the two boats are recorded on CAM-2 as shown in the figure. Pictures clearly indicate that the boat in the top frame (at 2:15 pm) was traveling at supercritical speed (see Volume III - Appendix G) in the downstream direction, and the one in the bottom frame (at 2:17 pm) was traveling at subcritical speed in the upstream direction. Subcritical and supercritical speeds are identical to displacement and planing speeds respectively. This information was used to separate the individual wave envelopes of different boats in the time series data. Rain event information was also acquired from the video recordings.

Raw wave-logger data includes elevation counts (integer between 0 - 4095), which represents the water level relative to the staff length, recorded at 30Hz data rate. Each logger generates a separate file every 24 hours with 2.592 million data points. Counts were converted to actual elevations using a linear calibration, and transformed to a reference datum (NAVD88, US feet) through Real Time Kinematics (RTK) GPS survey of the water-surface elevations at the wave-logger sites (Table 4.2.8.3-1) (obtained from Gomez and Sullivan Engineers). Each measurement was repeated three times to reduce uncertainty (~2-3 cm accuracy).

The time series at the four-wave loggers were analyzed to obtain mean-water level and water-surface displacements during the monitoring period. Daily signals were filtered using a low-pass IRR (internal impulse response) filter of order 10 and with a 10 s cut-off length to remove high frequency components. This process removed the high frequency noise in the data as well as the boat wave, leaving only the gradual changes in the water level throughout the day. The original signal was normalized with the filtered signal to obtain water-surface fluctuations, including the boat waves. The high frequency components were removed using another low-pass filter, of order 10 and cut-off length. A sample of collected wave data can be seen in Figure 4.2.8.3-2. Boat waves at a fixed location appear as short low- to high-frequency "chirps" superimposed into the random wind waves. Boat waves are magnified in Figure 4.2.8.3-2 to show their distinctive shapes.

Boat waves have distinct characteristics that can be used to identify them in the recorded signal. Waves with different frequencies travel with different speeds in water. At a stationary point, the recorded wave signal shows a wave group gradually shifting from low to high frequency, due to frequency dispersion. This transient wave group has a unique oscillatory pattern, and usually much more energetic then irregular wind-generated waves. The amplitude of the wave's increases as the frequencies increase until maximum wave amplitude is reached.

The frequency content and steady oscillatory signal can be found using Fourier transform. Fourier transform converts the time series signal into a spectrum in the frequency domain; hence the resulting spectrum is not time dependent. The time history of the frequencies of a transient signal, similar to boat waves can be found using local time-frequency analysis (i.e. wavelet transform or windowed Fourier transform). Wavelet transform uses inner products to measure the similarity between the time series signal and a wavelet function. The resulting transformation is visually represented by a scalogram. Figure 4.2.8.3-3 shows an example boat-wave group and its scalogram using Morlet wavelet. The vertical axis of the scalogram is frequency and the color indicates the correlation of the signal with the scale for a given frequency. Windowed Fourier transform divides the signal into segments, and each segment is transformed into Fourier space using a window function. The time-series signal is decomposed into its time-frequency-spectral density components, which is visually represented by the spectrogram. The spectrogram is a function of both the frequency and time since the decomposition is local.

Both methods produced similar results in the current study to detect boat waves in the recorded signal. Windowed Fourier transform was faster than the wavelet transform and, therefore, adopted in this study. Figure 4.2.8.3-4 illustrates a typical signal and its spectrogram, which is obtained using windowed Fourier transform. Figure 4.2.8.3-5 shows a 14-hour long signal recoded at WLOG-2 on May 24, 2015, and the spectrogram of the same signal. Horizontal axis is time, vertical axis is frequency and the contours represent the energy level. The spectrogram is obtained using a Hamming windowed Fourier transform, of 512 (number of data points in the 30Hz signal) with 75% overlapping. Each segment of the signal and the spectrogram indicated by a rectangle is magnified to show details. The low frequency to high-frequency "chirp" pattern can be easily identified. The photo in the figure shows the boat that generated the recorded wave group in the final plot.

Using the spectrogram, individual boat passes were identified in the frequency domain. The locations of the maximum wave heights and the wave frequencies associated with those waves were obtained in each boat-wave signal using zero-crossing analysis. The waves are defined between two successive zero down crossings in the normalized signal. The wave height is the difference between the maximum and minimum water-surface displacement in each wave and the wave period is the time length of each wave.

Wind-generated waves are irregular and narrow banded in waters with limited fetch. Neither period nor the heights of the wind-generated waves are constant. The waves are represented in terms of statistical quantities. They are described by spectral quantities rather than individual wave properties. Irregular waves from water-surface recordings can be considered as a combination of a series of regular waves with different periods that are superimposed with a random phase, and a certain amount of energy is transmitted by each component. The distribution of the energy for each wave frequency can be determined by transforming the wave record from the time domain to the frequency domain. The distribution of wave heights closely follows the Rayleigh distribution for wind-generated waves, assuming the random water surface elevation follows a Gaussian distribution. Significant wave height can be approximated by the standard deviation (square root of the variance of the signal) (Longuet-Higgins 1952).

$$H_{mo} = 4.004\sqrt{m_o} \tag{1}$$

where m_o is the zero-th moment of the spectrum. The i-th moment of the continuous spectrum is obtained by,

$$m_i = \int_0^\infty f^i S(f)df \tag{2}$$

where $S(f)$ is the wave energy spectral density and designates the distribution of variance with frequency, f, assuming that the function is continuous in the frequency domain. The spectral definition of the significant wave height, H_{m0} is approximately equal to the average of the highest one-third of the waves in a wave record.

Table 4.2.8.3-1: Water-surface Elevations at the Wave-logger Sites

Point Id	Location	Northing[1]	Easting[1]	Orth. height[2]	Quality pos.	Quality hgt.	Quality pos. + hgt.	Quality pos. + hgt.
BW.US.PAUCH.2	U/S Schell Br. / Pauchaug	3087969.294	399610.9674	181.044	0.0221	0.0389	0.0448	0.0448
BW.US.PAUCH.3	U/S Schell Br. / Pauchaug	3087969.35	399610.9731	181.0357	0.0235	0.0411	0.0474	0.0474
BW.US.PAUCH.4	U/S Schell Br. / Pauchaug	3087969.373	399610.8988	181.0248	0.0343	0.0613	0.0702	0.0702
BW.RT10.1	D/S Rt. 10 Bridge	3074722.91	394885.5408	181.6438	0.0939	0.1505	0.1774	0.1774
BW.RT10.2	D/S Rt. 10 Bridge	3074724.397	394887.1386	181.6687	0.0852	0.1464	0.1694	0.1694
BW.RT10.3	D/S Rt. 10 Bridge	3074726.058	394888.6429	181.7639	0.0712	0.1276	0.1461	0.1461
BW.FK.1	U/S French King Bridge	3047261.858	389916.4445	181.9623	0.0995	0.1821	0.2075	0.2075
BW.FK.2	U/S French King Bridge	3047258.927	389915.7756	182.0804	0.0851	0.1474	0.1702	0.1702
BW.FK.3	U/S French King Bridge	3047255.204	389915.2834	182.0352	0.0781	0.138	0.1586	0.1586

[1] NAD83 Massachusetts State Plane (US Feet) Coordinate System
[2] NAVD88 (US Feet)

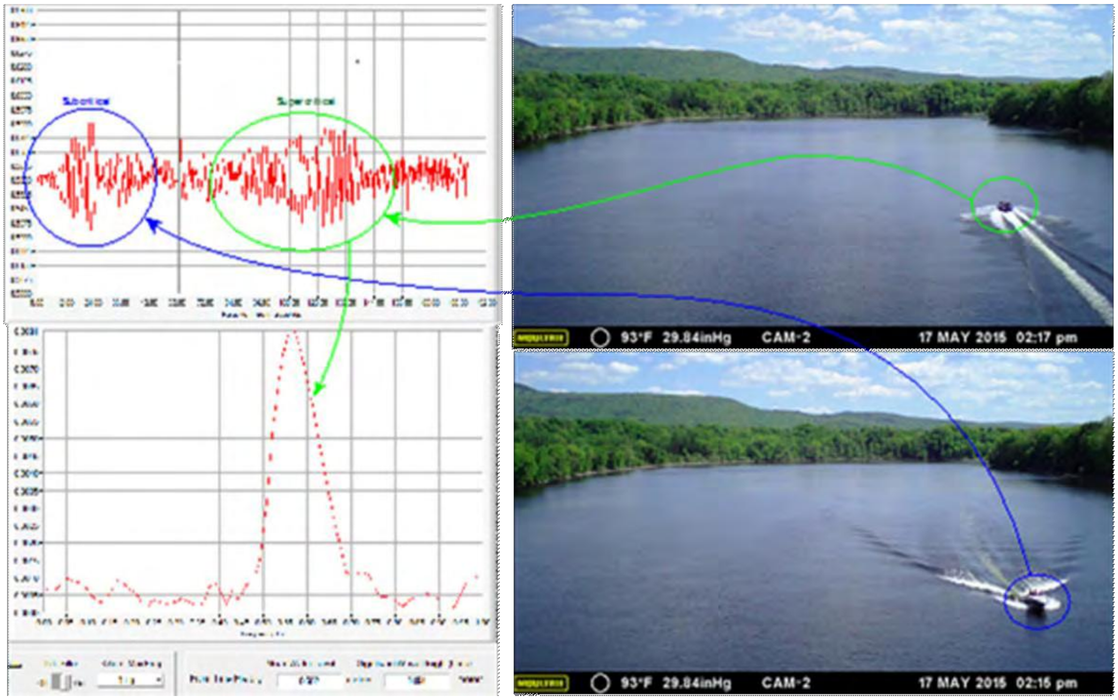

Figure 4.2.8.3-1 An example of collected boat-wave data

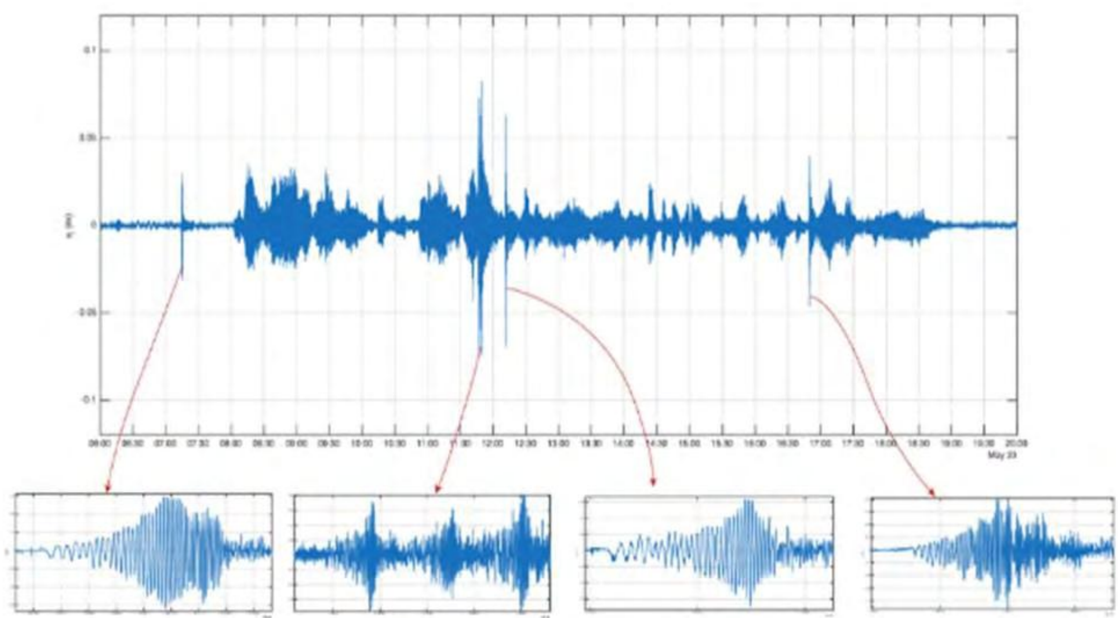

Figure 4.2.8.3-2 An example of water-surface displacement data showing boat waves

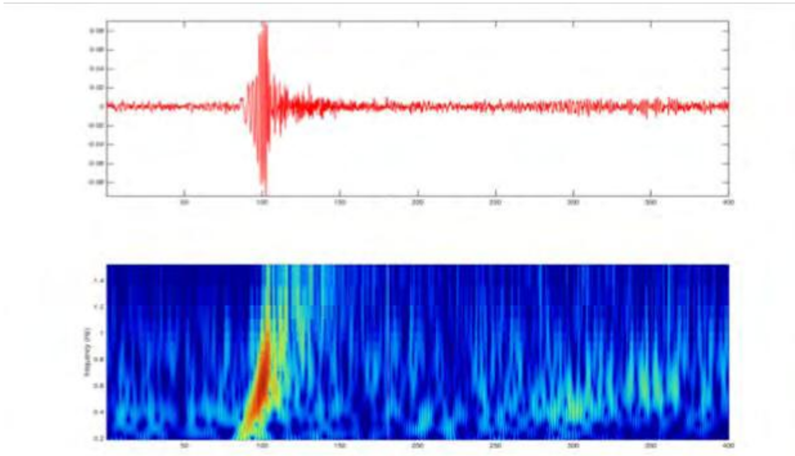

Figure 4.2.8.3-3 A typical boat wave group and its scalogram

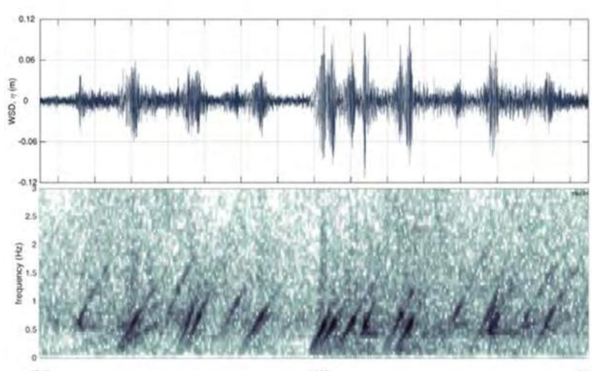

Figure 4.2.8.3-4 Example spectrogram

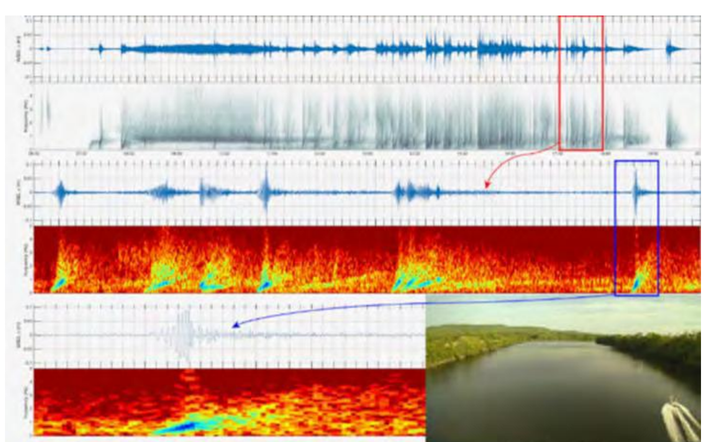

Figure 4.2.8.3-5: A Day-long Recording of the Wave Signal at WLOG-2 and its Spectrogram

4.2.8.4 Summary of Analysis Procedures for the Wave-Logger Data

Important steps of the boat-detection algorithm are summarized below:

- Separate the water-surface fluctuations, $h(t)$, and mean water level, z(t), from the water-level row signal with a low pass IRR filter.
- Apply windowed Fourier transform to find the spectrogram $S(t,f)$ using Hamming window of size 512 and 75% overlap. The windows are 17s long and 4.3s apart, center-to-center.
- Find the mean spectral density, $\bar{S}(t)$, in the low frequency band 0.05Hz-0.8Hz. Most of the wind-generated waves are left on the high-frequency side of this range.
- Remove low-frequency modulations $\bar{S}(t)$ in using a third-order Savitzky-Golay filter.
- Find the peaks and their locations (tpeak) in the filtered $\bar{S}(t)$ time-series. The locations are defined as the window centers.
- Filter the high frequency components in the water-surface fluctuations $h(t)$ with a low pass IRR filter and isolate waves in the frequency range of 0.1Hz - 2.5 Hz,
- Apply zero-crossing analysis and calculate the wave height H(t) and wave period T(t) time series,
- Calculate the spectral estimate for the significant wave height Hm0 using the equations 1 and 2.
- Find the peak zero-crossing wave heights H_{max} and wave periods T_{max}, nearest to tpeak.
- Compare the results with the time-lapse videos and remove the falsely detected boats.

The analysis with the steps summarized above was automated except for the final step in which the detected boat waves were compared with the time-lapse videos. The procedure was applied to the collected data to calculate boat-traffic statistics and the wave properties at each logger. In Figures 4.2.8.4-1 through 4.2.8.4-3, the analytic results are plotted for each site for selected days. Each figure consists of three plots: the one on top is the mean-water depth and water-surface elevation (NAVD88, US Feet) on the secondary axis, the middle plot is the water-surface displacement, significant wave height, the zero-crossing wave amplitude, and the temperature (secondary axis), and the bottom plot is the spectrogram, which shows the spectral energy, frequency and time relationship.

The 24-hour long data in Figure 4.2.8.4-1a was recorded at WLOG1 on June 13, 2015. The identified boats are marked with red on both the water-surface displacement plot and the spectrogram. 56 boat passes were recorded throughout that day. The temperature recorded inside the wave logger housing was usually overestimated during daylight hours, however, it is still included in the figures to show relative change. Darker areas in the spectrogram for frequency >~1.5Hz indicate low-energy, wind-generated waves, smoothly distributed in time and in the high-frequency area of the frequency axis. Figure 4.2.8.4-1b shows the results on June 14, 2015. 50 boats were detected on this day, but no wind waves are visible in the spectrogram. High-energy boat waves are discontinuous and spread across a wide range of frequencies. Wave height for the boat waves were mostly 3-4 times higher than that of the wind generated waves, which translates to an order of magnitude difference in their energies.

Wave data on June 8th (Monday) between 6 am and 9 pm, at WLOG2 is plotted in Figure 4.2.8.4-2a. No boats were recorded throughout the day. The source of waves was the wind, which can be seen in the spectrogram. Due to the sustained wind, the wave spectrogram peaked around 0.5Hz frequency. This was one of the few days that wind waves reach the energy level in the figure, yet the wave height was still around 5 cm - 6 cm. Near the Rt. 10 Bridge, where the WLOG2 site was located, the river widens as much as 300 m and the fetch length can be as long as 800 m depending on the wind direction. Both sides of the river are nearly flat and lack woody vegetation (Figure 4.2.8.4-4). Therefore, among all three wave-monitoring locations, the WLOG2 site is expected to have the highest wind-generated waves. Wave data for another windy day, July 15th (Saturday) near the Rt. 10 Bridge is shown in Figure 4.2.8.4-2b. Boat waves are separated from the wind waves with their relatively high energy content and leading low-frequency wave in the wave group.

Two examples for WLOG3 data near the French King Bridge are plotted in Figure 4.2.8.4-3. The first set of plots (Figure 4.2.8.4-3a) corresponds to June 28th, the second set (Figure 4.2.8.4-3b) corresponds to June 14th. Inspecting the spectrogram for these two days, the number of boats on June 28th was far less than the number of boats on June 14th, and June 28th was relatively windy. Even though both days were Sundays, time-lapse video data reveals that June 28th was a rainy day, which can be seen in Figure 4.2.8.4-5. The significance of rainy days in the analysis of boat-traffic statistics is explained in the following sections.

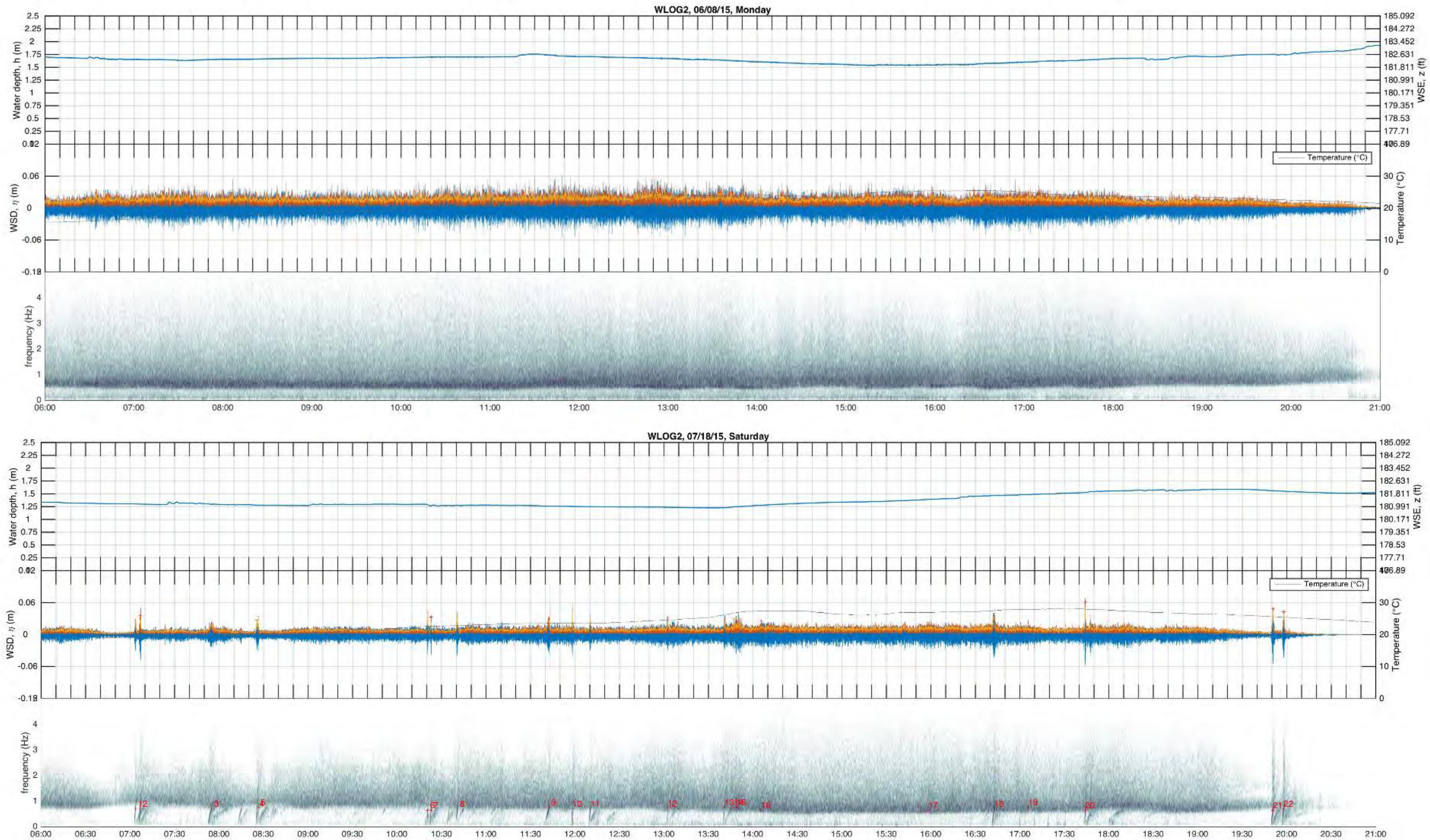

Figure 4.2.8.4-1 Wave data analysis summary for WLOG-1

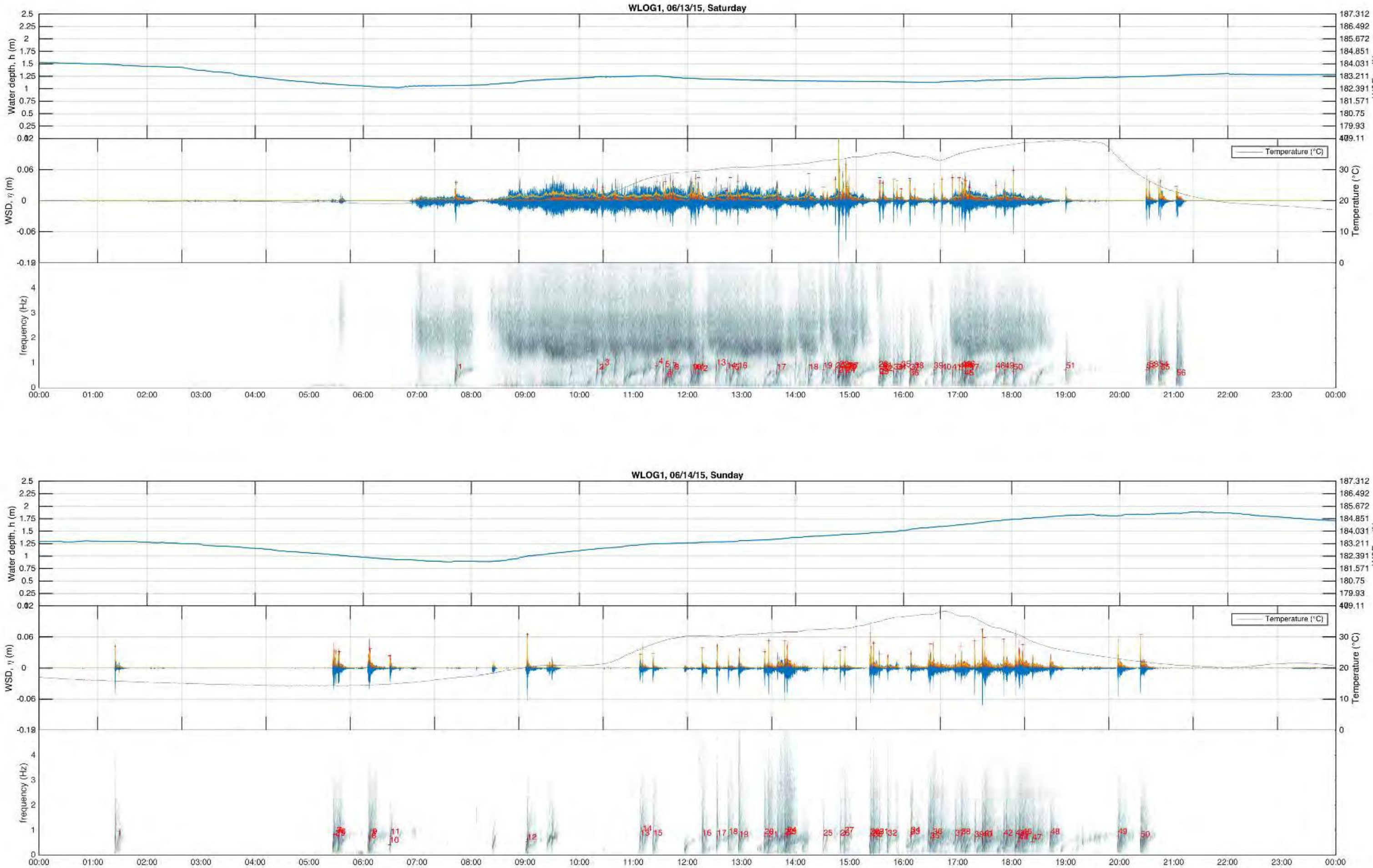

Figure 4.2.8.4-2 Wave data analysis summary for WLOG-2 (a – top group, b – bottom group)

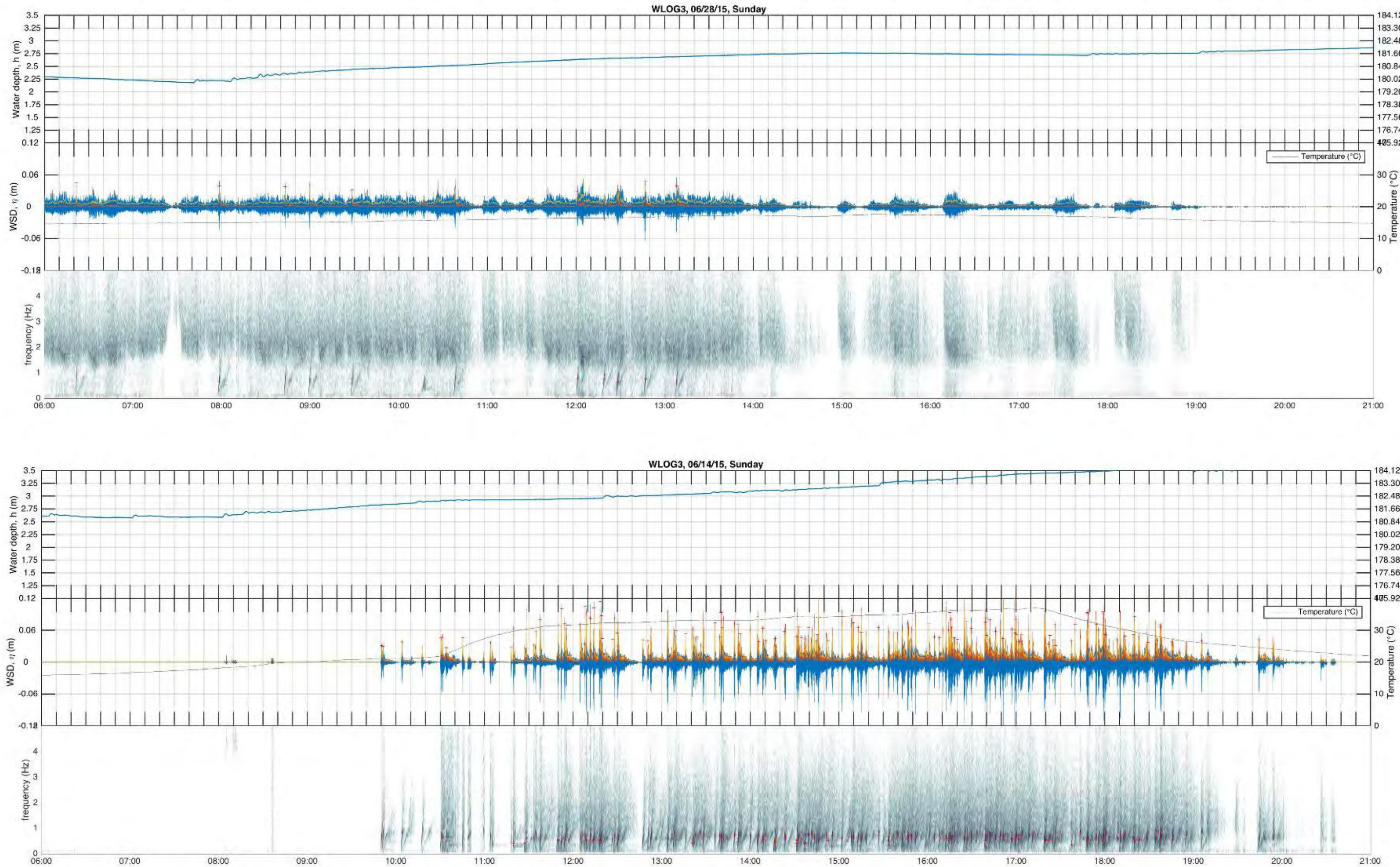

Figure 4.2.8.4-3 Wave data analysis summary for WLOG3 (a – top group, b – bottom group)

Figure 4.2.8.4-4: Rt. 10 Bridge Site CAM2 View and Aerial View (Google)

Figure 4.2.8.4-5: Comparison of Dry and Rainy Sundays: a View from the French King Bridge

4.2.8.5 Results of Boat and Wave Statistics

The total number of boats estimated from the wave-logger data analysis is listed in Table 4.2.8.5-1. 12,148 boating events were recorded at three sites during the 117-days of data collection (WLOG3 and WLOG4 data is averaged). The WLOG3 and WLOG4 site near the French King Bridge had the busiest boat traffic compared to the other two locations. This is possibly because the site is closer to the boat ramps and small marinas around the Turner Falls, MA area. It's also attractive to tourism and recreation for its scenic views.

The daily number of boats (daily traffic) at each wave logger site along with the rainy days (obtained from the recorded videos) are listed in Table 4.2.8.5-2. Figure 4.2.8.5-1 illustrates the daily distribution of the boat traffic during data-collection period. Green bars indicate dry days and blue bars indicate rainy days. Sundays and holidays are highlighted with dark green or blue. Daily- maximum and daily-minimum temperatures are also plotted in the same figures. The analysis results show that the weekend traffic can exceed 200 boats for some days. Weekends, especially Sundays, have significantly higher daily traffic then that of the weekdays. Boat traffic drops drastically during rainy days regardless of the day of the week. There is no noticeable trend between the months; nevertheless, the traffic is relatively low in June, which may be due to relatively frequent rainy days. In summary, the results show that the daily traffic depends primarily on the day of the week, precipitation or weather conditions, and location along the river.

Mean-daily traffic for each day of the week is listed for the entire dataset in Table 4.2.8.5-3, and for only dry days in Table 4.2.8.5-4. Figure 4.2.8.5-2 shows the bar charts for the same data. The highest traffic is on Sunday at all of the sites. The lowest mean traffic flow rate is during the weekdays, Monday to Thursday (MTWT). The traffic flow rate begins increasing on Friday and peaks on Saturday on dry days. The French King Bridge site has the highest mean-daily traffic with up to 180 boats per day on dry Sundays.

Rain dramatically affects the boat traffic flow, regardless of the location. In Figure 4.2.8.5-3 rainy days and dry days are compared for Sunday and weekdays (MTWT). Error bars are the standard deviations. The mean traffic flow can drop as low as 10% if it rains on Sundays and 20% on a weekday. The uncertainty of the average traffic flow is higher on weekdays because of the limited number of boating events. These ratios are similar at all three sites.

Figure 4.2.8.5-4 shows the hour-of-the-day distribution of the average boat traffic. The traffic. The chart is based on the entire dataset. The highest frequency of boats was observed between noon and 8 pm, peaking around 2 pm. Hourly peak-traffic flow rate ranged between 2.5 and 8. The WLOG3 and WLOG4 site shows double peaks, which is because the traffic peaked at different times for each direction of traffic flow. Upstream traffic peaked around 2 pm while downstream traffic peaked around 5 pm.

The distribution of the wave parameters H_{max} and T_{max}, and the water depth, h is shown in Figures 4.2.8.5-5 through 4.2.8.5-7. Various probability-distribution models are fitted to these histograms. The average maximum wave height was around 7 to 8 cm and the average wave period was approximately 1.4 s. Both wave-height and wave-period histograms are skewed to the left. Mean wave height and time-lapse video analysis revealed that the majority of the boat traffic consists of 6 m to 9 m-long high-speed recreational vessels moving at supercritical speeds.

Table 4.2.8.5-1: Total Measured Number of Boats

Wave Logger	Location	Dates	Number of Boats
WLOG-1	Schell Bridge	May 21 – Aug 28	2,133
WLOG-2	Rt. 10 Bridge	May 21 – Sep 14	2,650
WLOG-3	French King Bridge	May 21 – Sep 14	7,365
WLOG-4	French King Bridge	May 21 – Sep 14	7,263

Table 4.2.8.5-2: Number of Boats Recorded for Each Day of the Sampling Period at the Four Wave Loggers

Date	WLOG-1		WLOG-2		WLOG-3		WLOG-4	
	N	Rain	N	Rain	N	Rain	N	Rain
21-May-15	2		3		5		4	
22-May-15	15		12		23		21	
23-May-15	19		7		39		39	
24-May-15	91		77		173		173	
25-May-15	32		26		50		51	
26-May-15	5		6		13		13	
27-May-15	9		3		15		15	
28-May-15	4		3		9		10	
29-May-15	24		24		72		69	
30-May-15	67		41		141		142	
31-May-15	7	1	6	1	17	1	17	1
1-Jun-15	2	1	0	1	2	1	2	1
2-Jun-15	0	1	2	1	6	1	6	1
3-Jun-15	1		1		8		8	
4-Jun-15	6		4		10		10	
5-Jun-15	8		15		37		37	
6-Jun-15	12		16		48		49	
7-Jun-15	38		46		139		142	
8-Jun-15	7		0		1		1	
9-Jun-15	5		4		12		12	
10-Jun-15	30		12		29		29	
11-Jun-15	14		13		29		30	
12-Jun-15	15		17		43		39	
13-Jun-15	56		19		97		100	
14-Jun-15	50		98		190		201	
15-Jun-15	2	1	0	1	0	1	0	1
16-Jun-15	2		1		3		3	
17-Jun-15	22		14		20		20	
18-Jun-15	9		6		17		17	
19-Jun-15	15		18		75		74	
20-Jun-15	30		39		115		113	

Date	WLOG-1		WLOG-2		WLOG-3		WLOG-4	
	N	Rain	N	Rain	N	Rain	N	Rain
21-Jun-15	10	1	6	1	34	1	36	1
22-Jun-15	14		12		45		46	
23-Jun-15	3		0		5		6	
24-Jun-15	0		1		20		15	
25-Jun-15	18		19		32		32	
26-Jun-15	23	1	21	1	48	1	43	1
27-Jun-15	32		36		87		87	
28-Jun-15	0	1	14	1	12	1	13	1
29-Jun-15	5		2		10		10	
30-Jun-15	9	1	4	1	14	1	14	1
1-Jul-15	2	1	0	1	5	1	5	1
2-Jul-15	11		13		37		39	
3-Jul-15	59		46		152		147	
4-Jul-15	12	1	11	1	35	1	34	1
5-Jul-15	80		107		239		235	
6-Jul-15	22		22		72		66	
7-Jul-15	5		6		10		10	
8-Jul-15	1		4		21		23	
9-Jul-15	16		18		37		37	
10-Jul-15	37		37		83		82	
11-Jul-15	59		62		161		165	
12-Jul-15	79		93		226		222	
13-Jul-15	5		9		27		23	
14-Jul-15	7		1		2		2	
15-Jul-15	7		3		23		24	
16-Jul-15	28		13		51		52	
17-Jul-15	29		28		85		84	
18-Jul-15	30		18		51		53	
19-Jul-15	76		94		205		206	
20-Jul-15	24		19		55		50	
21-Jul-15	20		18		42		43	
22-Jul-15	27		23		44		44	

Date	WLOG-1		WLOG-2		WLOG-3		WLOG-4	
	N	Rain	N	Rain	N	Rain	N	Rain
23-Jul-15	22		22		36		40	
24-Jul-15	29		11		56		56	
25-Jul-15	66		56		214		201	
26-Jul-15	69		42		77		72	
27-Jul-15	9		3		13		13	
28-Jul-15	11		17		30		26	
29-Jul-15	32		24		87		84	
30-Jul-15	0	1	3	1	12	1	12	1
31-Jul-15	36		36		96		98	
1-Aug-15	49		78		151		162	
2-Aug-15	94		71		180		181	
3-Aug-15	15		12		54		57	
4-Aug-15	3		4		22		22	
5-Aug-15	13		8		45		44	
6-Aug-15	16		16		46		42	
7-Aug-15	34		14		76		71	
8-Aug-15	25		41		172		170	
9-Aug-15	63		73		185		183	
10-Aug-15	17		15		42		42	
11-Aug-15	1	1	0	1	0	1	0	1
12-Aug-15	1		7		16		17	
13-Aug-15	13	1	14	1	61	1	51	1
14-Aug-15	10		21		76		61	
15-Aug-15	40		49		143		100	
16-Aug-15	67		116		212		207	
17-Aug-15	10		14		65		58	
18-Aug-15	1		13		54		50	
19-Aug-15	4		19		43		44	
20-Aug-15	1		2		21		24	
21-Aug-15	0	1	4	1	18	1	14	1
22-Aug-15	20		31		139		133	
23-Aug-15	1	1	7	1	38	1	35	1

Date	WLOG-1		WLOG-2		WLOG-3		WLOG-4	
	N	Rain	N	Rain	N	Rain	N	Rain
24-Aug-15	4		13		36		36	
25-Aug-15	0	1	0	1	2	1	1	1
26-Aug-15	1		4		25		24	
27-Aug-15	5		6		26		17	
28-Aug-15	2		16		62		64	
29-Aug-15			72		147		143	
30-Aug-15			53		198		204	
31-Aug-15			15		42		45	
1-Sep-15			12		42		47	
2-Sep-15			15		44		43	
3-Sep-15			6		21		21	
4-Sep-15			14		41		51	
5-Sep-15			67		191		192	
6-Sep-15			65		209		203	
7-Sep-15			75		196		202	
8-Sep-15			12		35		36	
9-Sep-15			15		41		46	
10-Sep-15			5		5		5	
11-Sep-15			11		22		21	
12-Sep-15			36		83		86	
13-Sep-15		1	2	1	7	1	8	1
14-Sep-15			0		2		3	
TOTAL	**2,133**		**2,175**		**6,039**		**5,907**	

Table 4.2.8.5-3: Daily Average Number of Boats: Rainy and Dry Days

	Monday	Tuesday	Wednesday	Thursday	Friday	Saturday	Sunday
WLOG-1	12.0	5.1	10.7	11.0	22.4	36.9	51.8
WLOG-2	13.9	6.3	9.6	9.8	20.3	39.9	57.1
WLOG-3	41.9	18.3	30.4	26.8	62.6	118.5	137.7
WLOG-4	41.5	18.2	30.3	26.1	60.7	115.8	137.5

Table 4.2.8.5-4: Daily Average Number of Boats: Dry Days Only

	Monday	Tuesday	Wednesday	Thursday	Friday	Saturday	Sunday
WLOG-1	13.7	6.3	11.4	11.7	24.1	38.8	70.7
WLOG-2	11.6	8.0	10.2	9.9	21.3	41.8	77.9
WLOG-3	36.7	23.4	32.1	25.5	66.6	123.7	186.1
WLOG-4	35.8	23.4	32.0	25.3	65.0	120.9	185.8

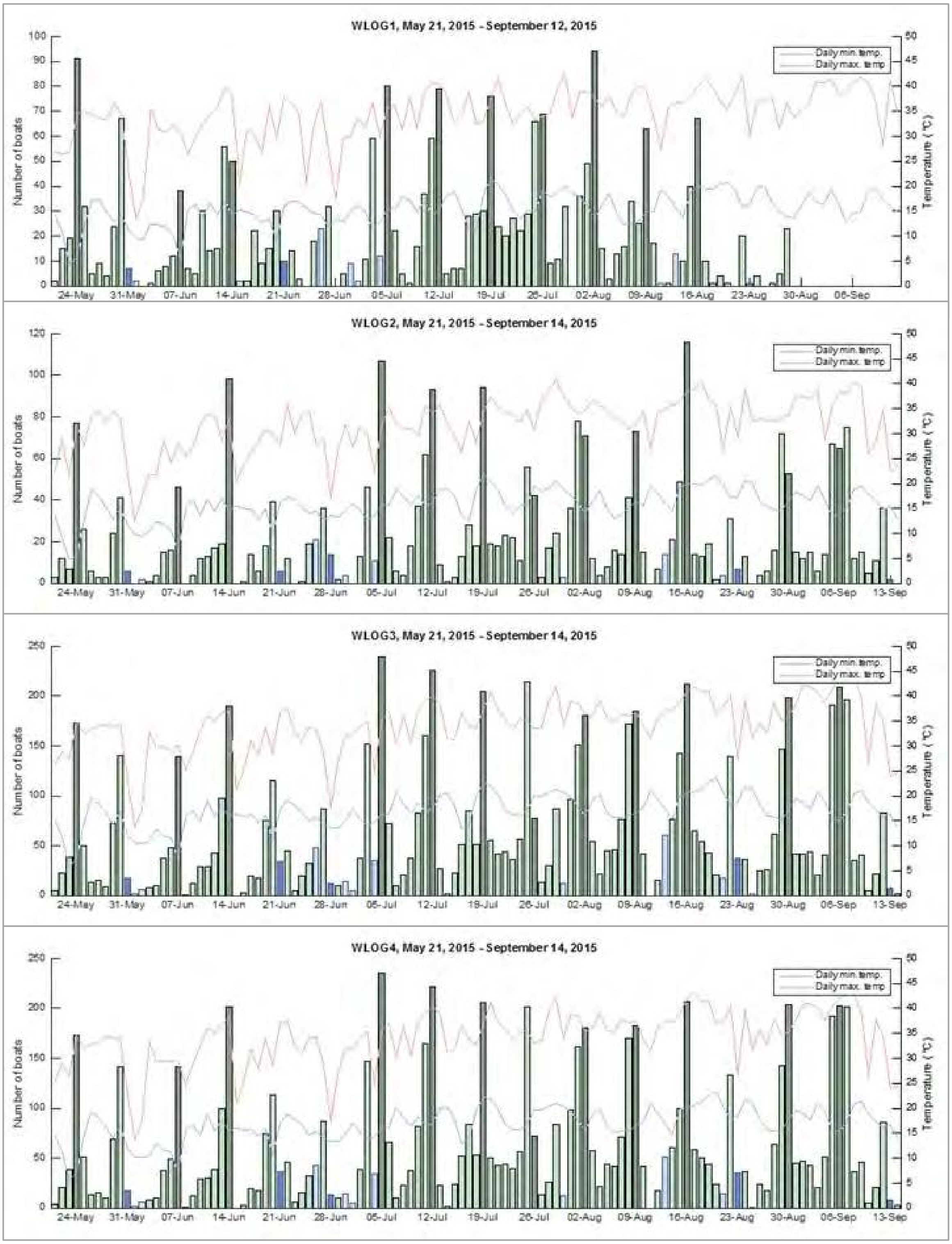

Figure 4.2.8.5-1: Boat Traffic Statistics Between May 21st and Sep 14th

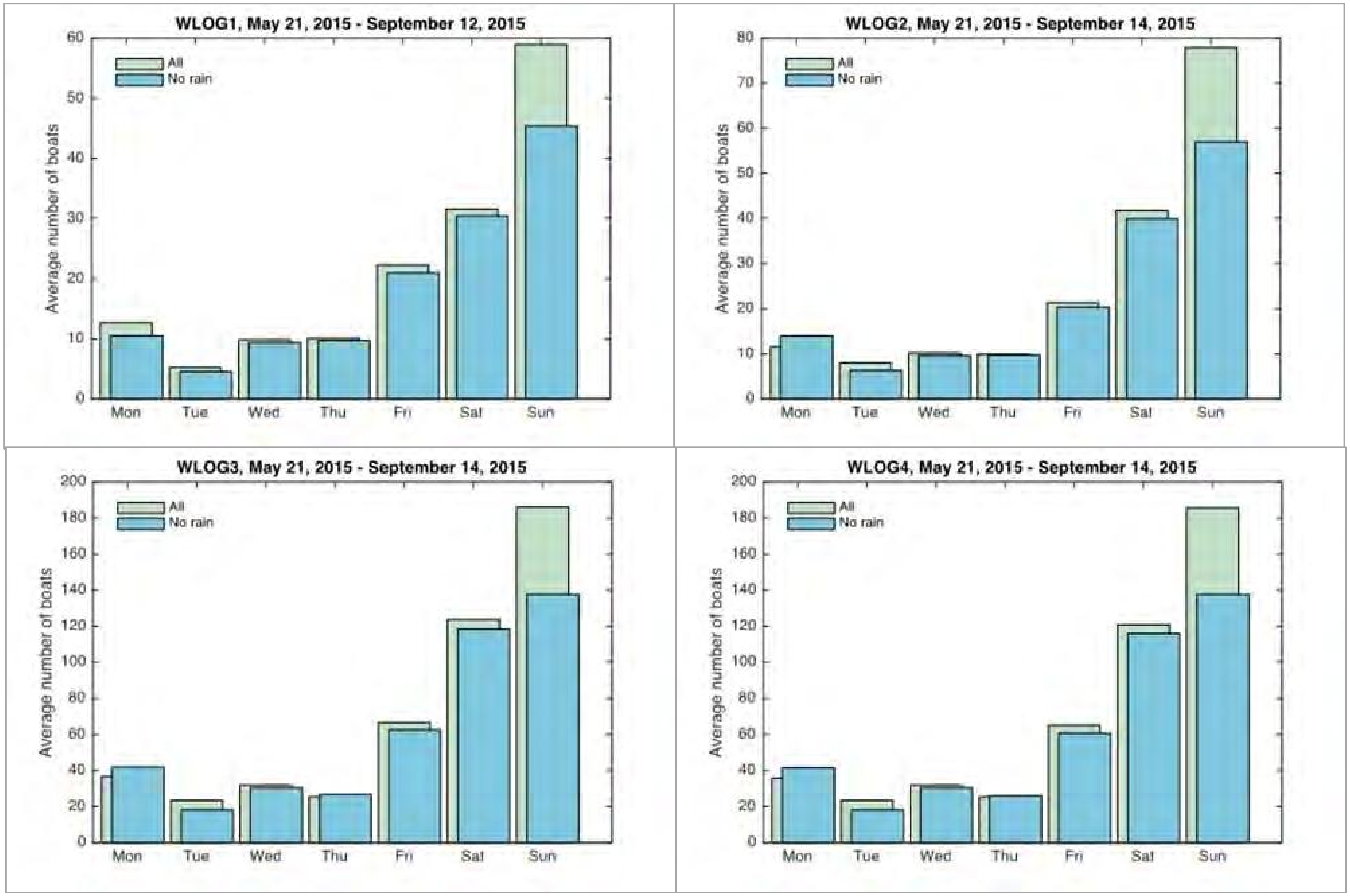

Figure 4.2.8.5-2: Day-of-the-week Boat Traffic Mean Flow: Dry and Rainy Days

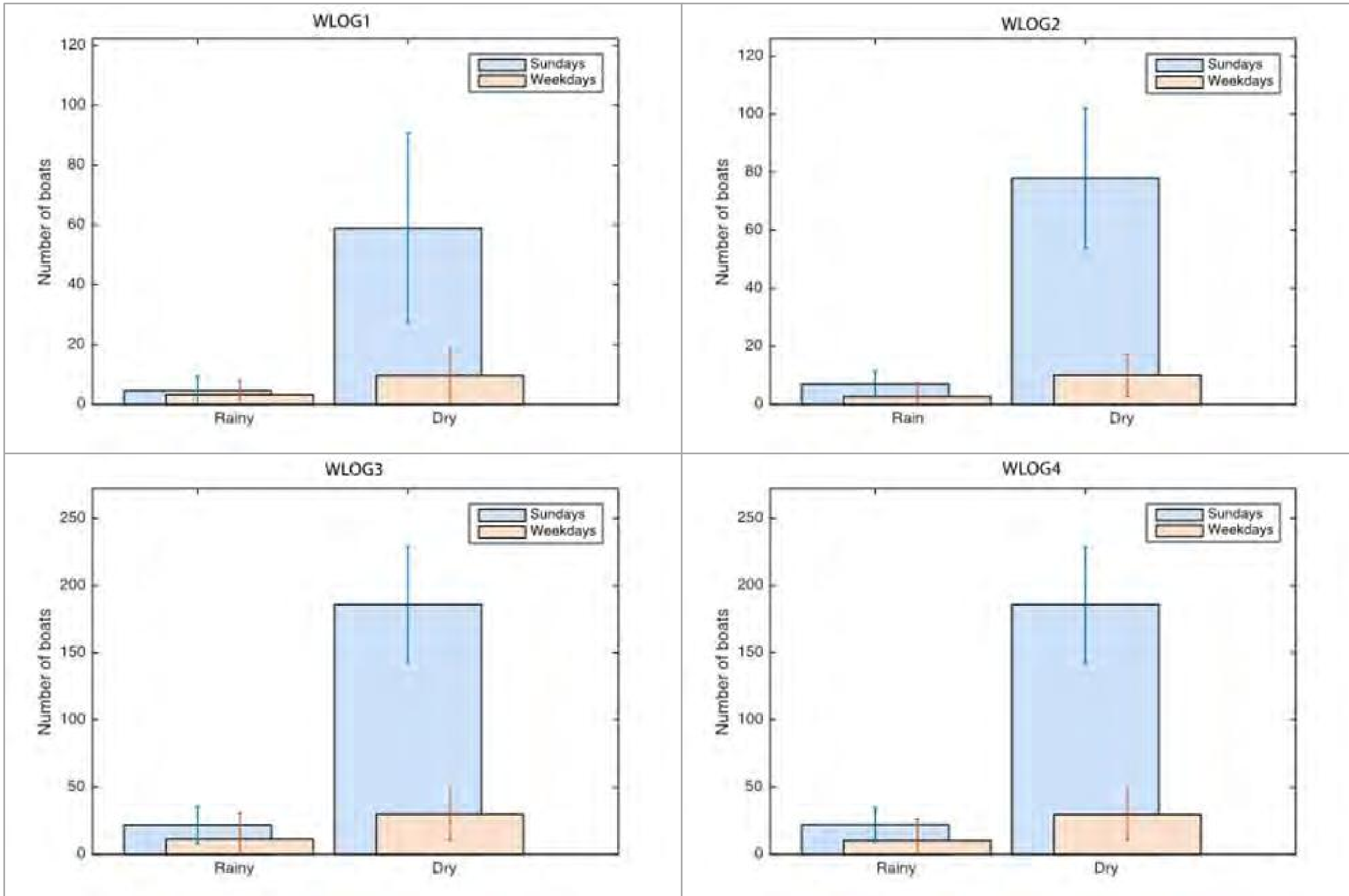

Figure 4.2.8.5-3: Average Rainy and Dry Day Boat Traffic Flow: Sundays and Weekdays

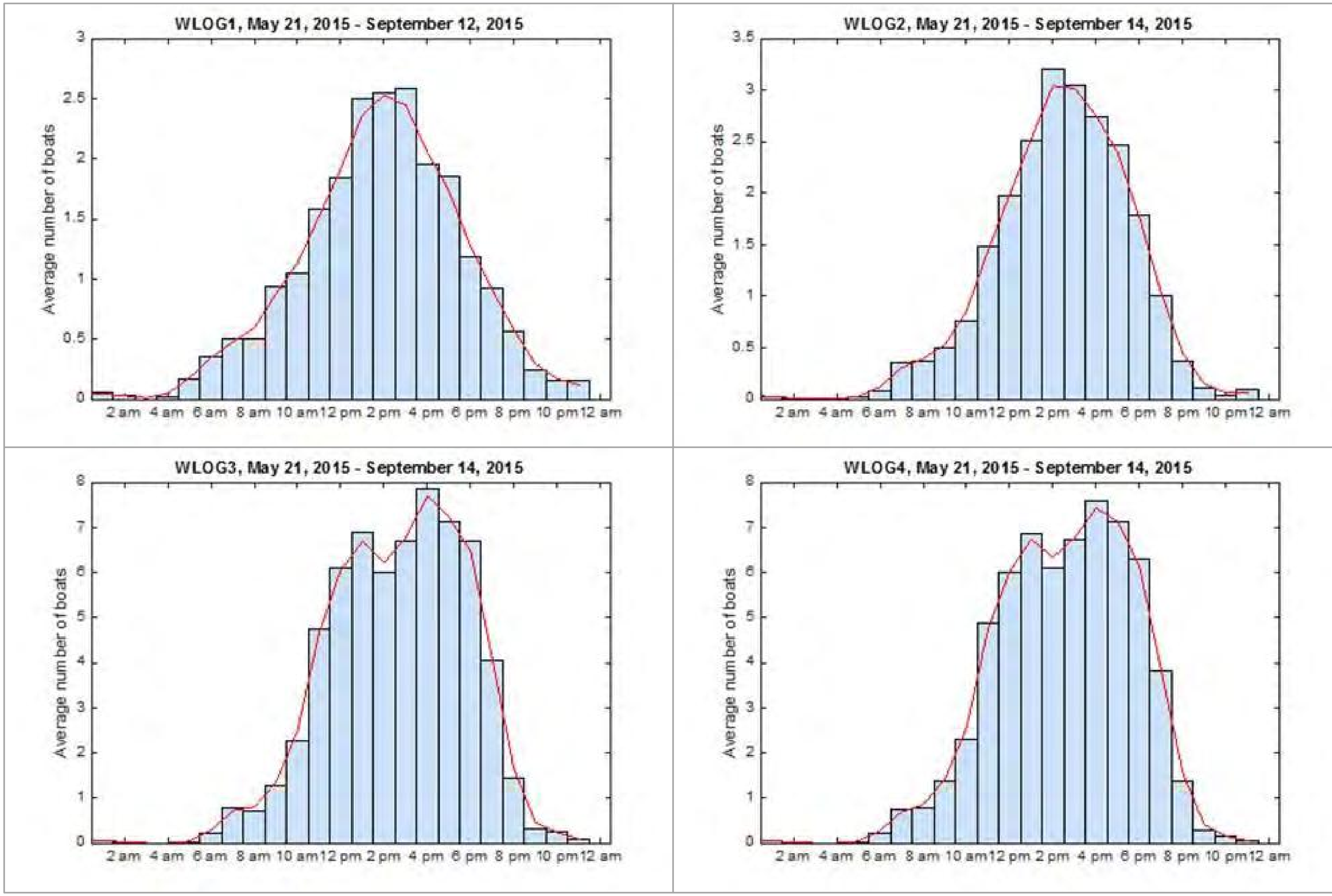

Figure 4.2.8.5-4: Hourly Distribution of the Boat Traffic Flow

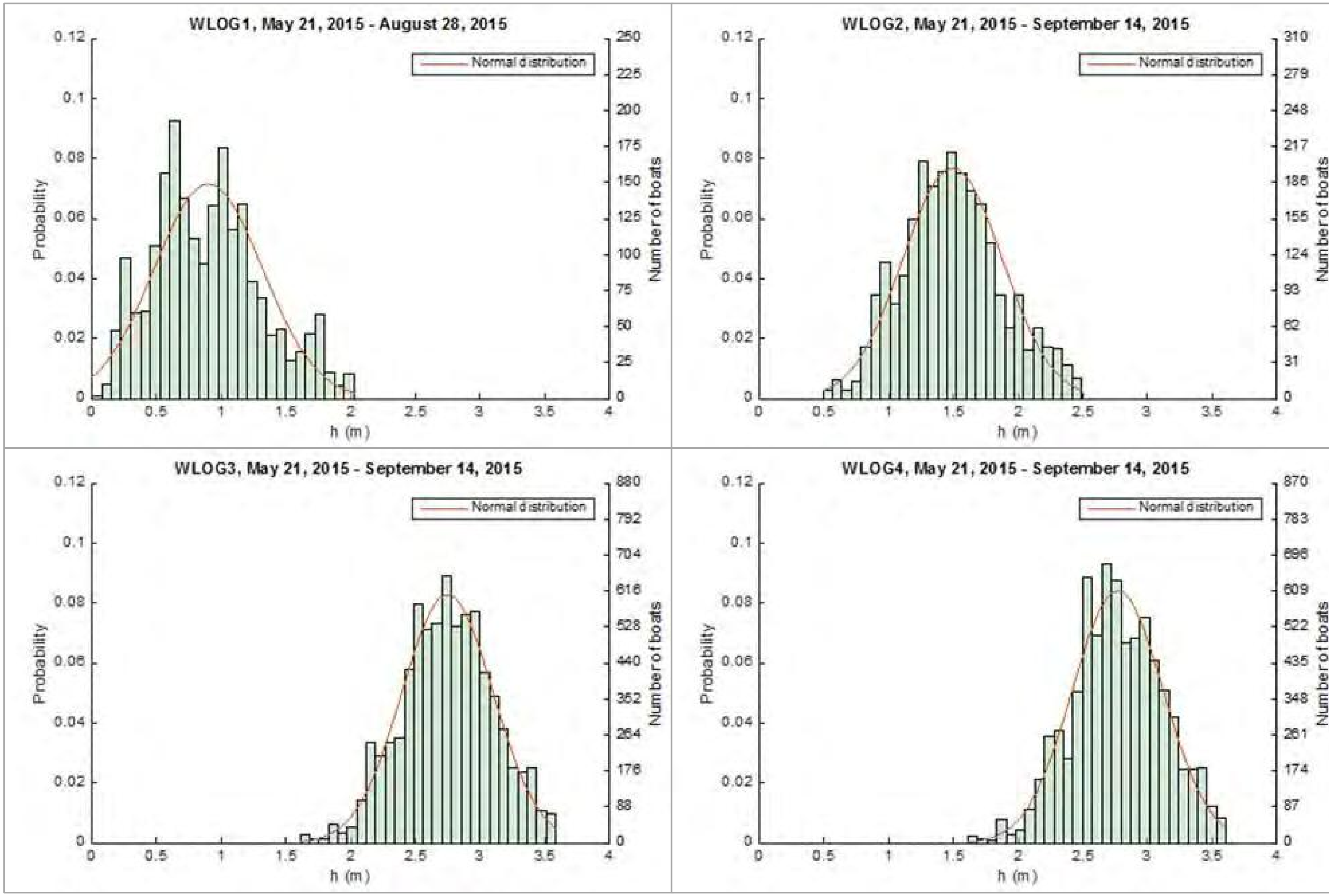

Figure 4.2.8.5-5: Water Depth Distribution

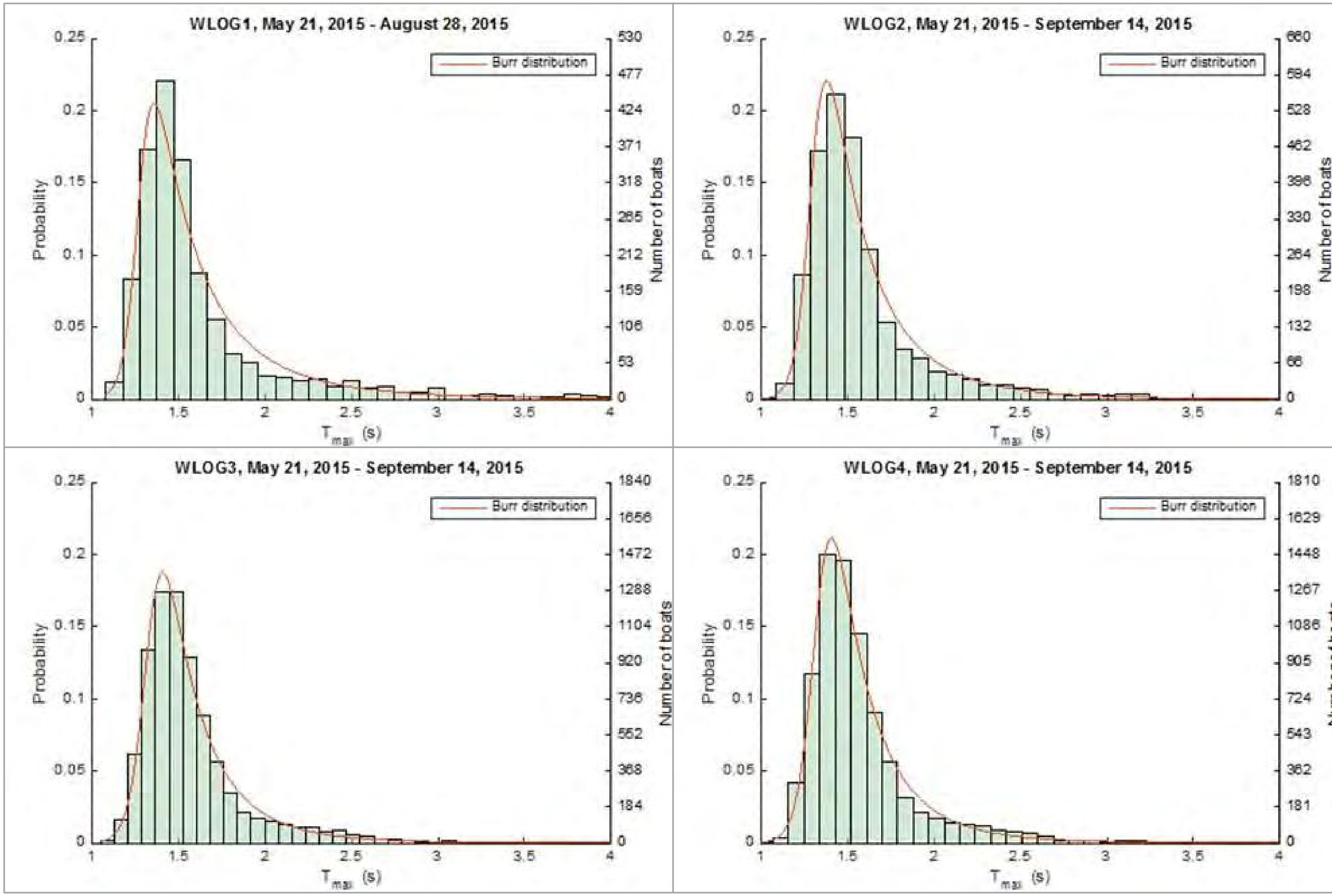

Figure 4.2.8.5-6: Maximum Wave Period Distribution

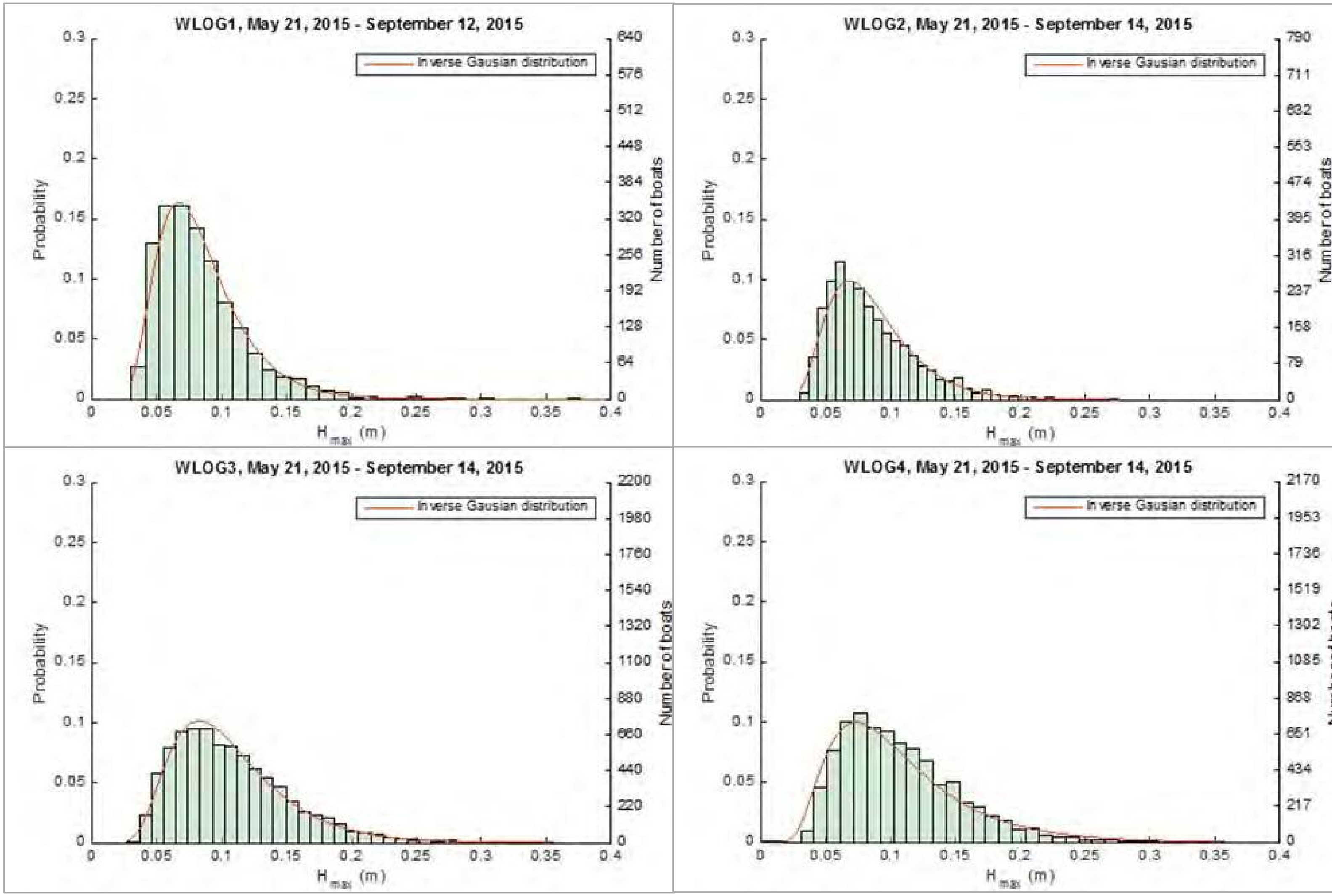

Figure 4.2.8.5-7: Wave Height Distribution

4.2.8.6 Temporal and Spatial Extrapolation of Boat-Traffic Data

Estimation of the relative contribution of boat waves to streambank erosion requires knowledge of the spatial and temporal distribution of instances of boat passage and the properties of the generated waves during each passage. Despite their substantial impact, the availability of historic boat-wave data was extremely limited for hydraulic and bank-erosion modeling. Currently, the BSTEM wave model uses maximum wave height, H_{max} and the wave period, Tmax associated with H_{max} to estimate the hydraulic erosion due to waves. Long-term BSTEM simulations required prediction of wave-traffic statistics and boat-generated wave properties by spatial and temporal extrapolations. The analysis described here includes development of methods to estimate the wave parameters, H_{max} and T_{max} at 20 locations (25 sites – five locations have right and left banks) longitudinally along the river over the 15-year period, and generation of input datasets for BSTEM using these distributions. A 15-year, hourly dataset was developed by combining measured daily and weekly variations of boat traffic, together with information on seasonal variations, boat ownership statistics and historic rainfall data obtained from various sources.

Methods and Results

As part of boat-generated, wave-measurement study, four wave loggers recorded wave data at three sites along the TFI. Boat traffic and boat-generated waves were continuously recorded at 30Hz between May 22, 2015 and September 14, 2015 (sample period). Analysis of the recorded data revealed boat-induced waves and their properties at each site. The generated data was used to extract boat-wave statistics including daily and hourly distribution of the number of boat passes, as well as water level, wave height (H_{max}) and wave period (T_{max}) histograms which can be used as input into the BSTEM boat wave model for boat-generated wave erosion prediction. The available data were used to predict historical boat traffic during the 15-year period between January 1st, 2000 and December 31st 2014.

Temporal Extrapolation

The majority of the boats observed during the field monitoring were recreational boats. Time lapse videos at the three sites indicated that over 90% of the recorded boat passes were recreational boats of sizes less then 25ft long. Consequently, the boat traffic in the area strongly depends on the day of the week as well as the weather conditions. Analysis of the collected data and personal communications with local boat owners in the area supports this conclusion. The results presented in the previous section show that the number of boats per day (daily traffic flow, or daily traffic) observed during a weekday was 10%-20% of the daily flow on a Sunday. Daily flow was reduced to as low as 20% during rainy days. Recreational traffic also varies seasonally mainly due to the weather conditions and restrictions during off-season. Even though the measurement period wasn't long enough to see the long-term trends in the boat traffic, it's still possible to estimate yearly and decadal trends from other sources. The measured boat-wave statistics data were supplemented by historic climate and boat-ownership data to generate a 15-year boat-generated wave data for BSTEM-Dynamic 2.3.

Here, a simple partially deterministic model is used to calculate daily traffic (N) by introducing a series of coefficients that modifies an ideal value for daily traffic (N_0).

$$N = c_1 c_2 c_3 c_4 N_0 \tag{3}$$

Or

$$N = CN_0 \tag{4}$$

where

$$C = c_1 c_2 c_3 c_4 \qquad (5)$$

In this model N_0 is the number of boats per day during an ideal day, which is defined as a dry Sunday during high season. The N_0 value is calculated by averaging the number of boats observed on the 'sunny' Sundays between Memorial Day (May 25th, 2015) and Labor Day (September 7th, 2015). Since each wave logger produced a separate traffic dataset, a unique N_0 value is calculated for each wave logger site. N_0 values for the wave logger sites are listed in Table 4.2.8.6-1.

The coefficients c_1, c_2, c_3 and c_4 are assumed to be independent and their product C for each site is the ratio of the daily boat traffic flow on a given day relative to that of the ideal day. The coefficients are defined as follows:

c_1: Rainy-day coefficient ($0 < c_1 < 1$). Reduces the number of boats by a factor if it is a rainy day. If most of the daytime hours were cloudy and noticeable precipitation was observed during this period, then the day was considered as a "rainy day". Rainy days were manually identified using the time-lapse recording. Each day in the sample period was identified as rainy or dry to assign a value for c_1 of unity (1.0) for dry days whereas it takes different values for weekdays and weekends and for each wave logger (Table 4.2.8.6-2). Daily- rainfall data for Amherst, MA was used to calculate c_1 for the simulation period (source: NOAA National Climatic Data Center Asheville NC).

c_2: Day of the week coefficient ($0 < c_2 < 1$). This coefficient reduces the number of boats for each day of the week based of the weekday distribution during the sample period. Only dry days were used during averaging (Table 4.2.8.6-3).

$$c_2 = N_{day} / N_{Sunday,dry} \qquad (6)$$

c_2 coefficient for holidays (Labor Day, Independence Day etc.) is changed to unity regardless of the day of the week they fall on.

c_3: Month of the year coefficient ($0 < c_3 < 1$). Reduces the number of boats based on the month of the year. Monthly distribution of total boating hours in the United States in 2001-2002 was used to calculate this coefficient (Note – while this is a distribution for the United States it is only being used to determine the coefficient that is being applied to the measured data. The data collected from the TFI is actual use from Memorial Day to Labor Day and it correlates closely with the distribution being applied). Figure 4.2.8.6-1 shows the number of people boating and number of hours in the water in the United States. Rearranging the months, a normal distribution can be obtained in Figure 4.2.8.6-2. c_3 was assumed to be unity (1.0) around the peak, for the months June, July, and August and the remaining moths were calculated based on this distribution.

$$c_3 = \frac{P_{month}}{(P_{June} + P_{July} + P_{August})/3} \quad \text{(P is persons boating)} \qquad (7)$$

c_4: Year coefficient (c4 > 0). The coefficient is calculated for each year between 2000 and 2014 using historic variations in the boat ownership in the United States. It was assumed that the variation in the boat traffic follows the same trend with the boat ownership variations. Based on the trend depicted in Figure 4.2.8.6-3, a linear decline in the boat ownership was used to calculate c_4 for the year between 2000 and 2008. c_4 was assumed to be unity (1.0) for the years 2009 to 2014 (Table 4.2.8.6-4).

Table 4.2.8.6-5 shows a sample list of coefficients and the bar chart in Figure 4.2.8.6-4 shows the complete list of C values for the simulation period. Each day between 1/1/2000 and 12/31/2014 has a C coefficient, which is multiplied by N_0 (for each site) to determine the number of boat passes for a given day (*k*) and at a given site (*j*). The procedure described above is deterministic; hence, the *N* values will be identical for the same *C* coefficients. In reality, daily traffic flow can vary due to various reasons that are not considered in the simulation. These uncertainties are introduced by adding a Gaussian noise in the daily traffic flow of the ideal day.

$$N_{0j}^{*} = N_{0j} + \frac{1}{4} s_s h^k \qquad (8)$$

where N_{0j}^{*k} is the number of boats on an ideal day for site j and s_s is the standard deviation of the observed ideal days during the sampling period. Time series h^k is Gaussian random noise with zero mean and unit standard deviation (unit normal distribution). After adding the uncertainty, N_{0j}^{*k} varies in time and specific for each wave logger site.

Table 4.2.8.6-1: N_0 Values for Each Wave Logger

	Dates	Number of boats	N_0
WLOG-1	May 21 – Aug 28	2,133	70.7
WLOG-2	May 21 – Sep 14	2,650	81.7
WLOG-3	May 21 – Sep 14	7,365	182.6
WLOG-4	May 21 – Sep 14	7,263	182.2

Table 4.2.8.6-2: Rainy Day Coefficients

c_1	WLOG-1	WLOG-2	WLOG-3	WLOG-4
Weekday	0.210	0.130	0.186	0.192
Weekend	0.064	0.101	0.138	0.139

Table 4.2.8.6-3: Weekday Coefficients

c_2	WLOG-1	WLOG-2	WLOG-3	WLOG-4
Monday	0.19	0.15	0.21	0.21
Tuesday	0.08	0.08	0.10	0.10
Wednesday	0.16	0.12	0.17	0.17
Thursday	0.17	0.13	0.16	0.16
Friday	0.32	0.25	0.35	0.34
Saturday	0.55	0.46	0.66	0.64
Sunday	1.00	1.00	1.00	1.00

Table 4.2.8.6-4: Month Coefficient (c_3) and Year Coefficient (c_4)

Month	c_3
January	0.2
February	0.16
March	0.19
April	0.38
May	0.61
June	1.00
July	1.00
August	1.00
September	0.75
October	0.51
November	0.30
December	0.22

Year	c_4
2000	1.183
2001	1.167
2002	1.151
2003	1.135
2004	1.118
2005	1.102
2006	1.086
2007	1.070
2008	1.054
2009	1.000
2010	1.000
2011	1.000
2012	1.000
2013	1.000
2014	1.000

Table 4.2.8.6-5: A Sample Coefficients List

WLOG-4	c_1	c_2	c_3	c_4	C
08/24/06	1.000	0.159	1	1.086	0.172
08/25/06	0.139	0.336	1	1.086	0.051
08/26/06	0.139	0.639	1	1.086	0.096
08/27/06	1.000	1.000	1	1.086	1.086
08/28/06	0.192	0.207	1	1.086	0.043
08/29/06	1.000	0.096	1	1.086	0.104
08/30/06	0.192	0.165	1	1.086	0.034
08/31/06	1.000	0.159	1	1.086	0.172
09/01/06	1.000	0.336	0.75	1.086	0.273
09/02/06	1.000	0.639	0.75	1.086	0.521
09/03/06	0.139	1.000	0.75	1.086	0.113
09/04/06	0.139	1.000	0.75	1.086	0.113

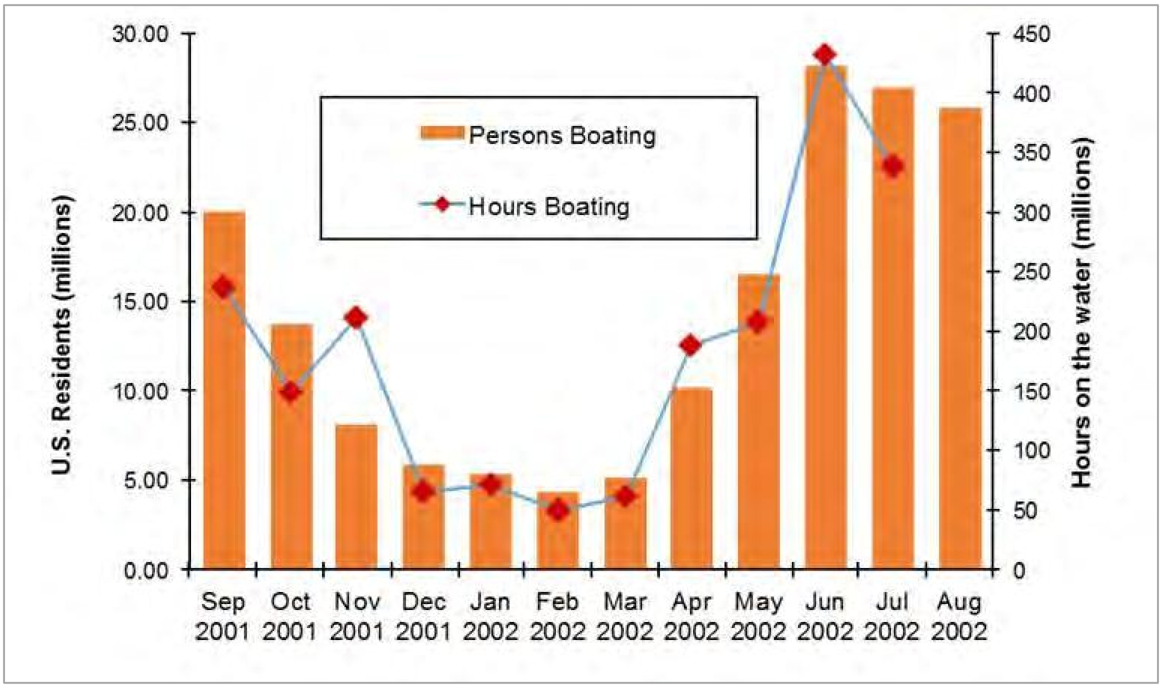

Figure 4.2.8.6-1: Monthly Distribution of Persons Boating and Hours of Boating in the United States

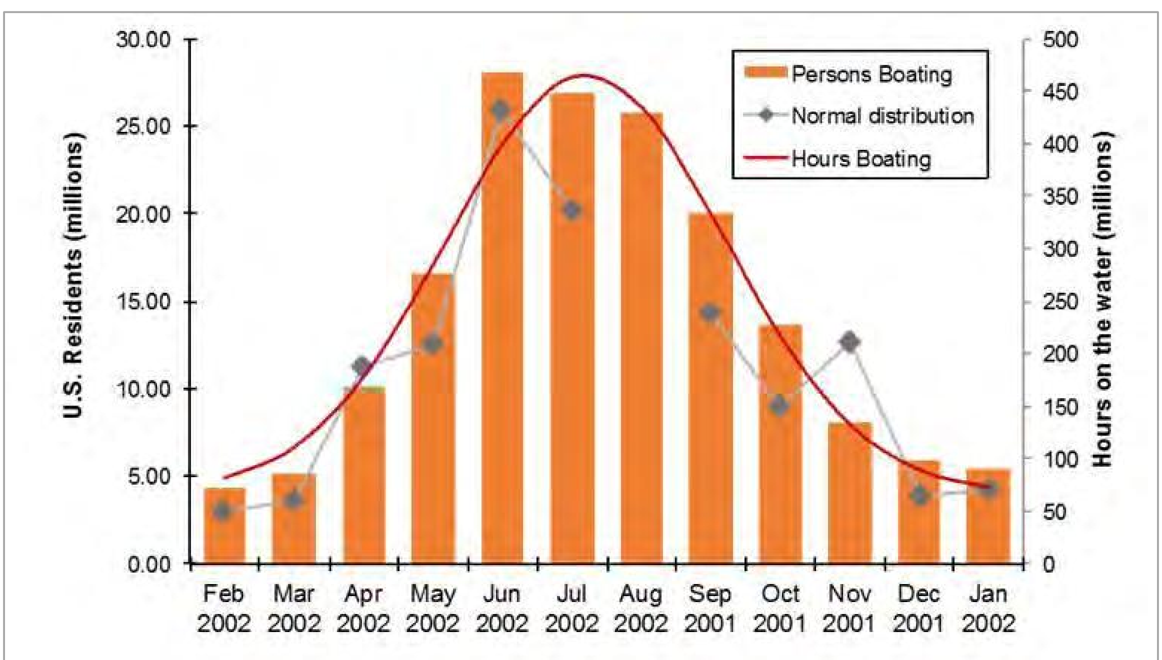

Figure 4.2.8.6-2: Monthly Distribution of Persons Boating and Hours of Boating in the United States; Rearranged

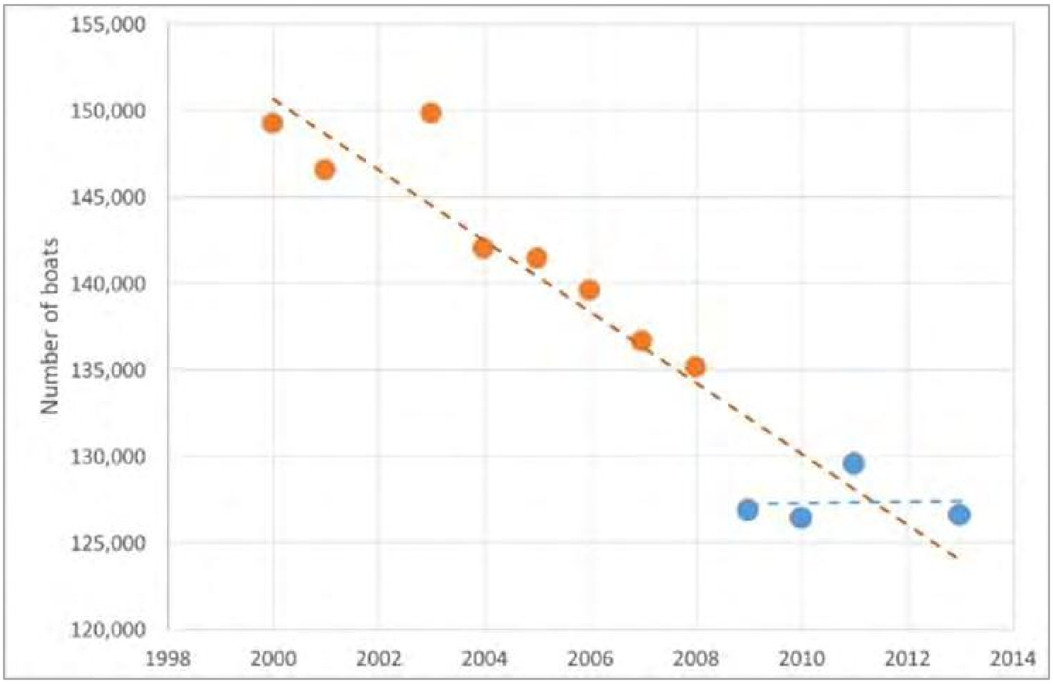

Figure 4.2.8.6-3: Historic Variations in Boat Ownership

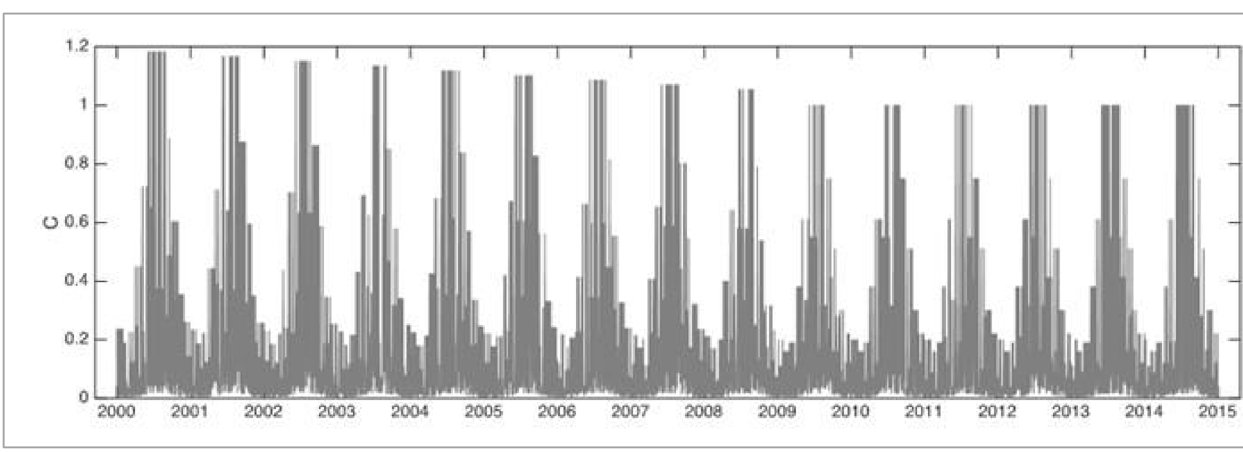

Figure 4.2.8.6-4: WLOG-4, Coefficient "C"

Spatial Interpolation

Boat traffic along the river varied as a function of boat-ramp access, site conditions etc. These differences were observed at the three wave-logger sites during data collection. Ideal-day boat counts (N) at 20 intermediate sites between WLOG-1 and WLOG-3 were interpolated by inverse distance weighting using the two nearest wave-logger sites. Upstream of WLOG-1 and downstream of WLOG-3, N is equal to the nearest wave logger measurement. With this procedure, seven sites upstream of WLOG-1 used the N_{WLOG1} and the three sites downstream of WLOG-3 used N_{WLOG4}. N for the remaining 10 sites was interpolated using the closest two wave-logger measurements. With the two-point interpolation, equation 8 is modified as:

$$N_j^k = round\left(W_A C_A^k N_{0A}^{*k} + W_B C_B^k N_{0B}^{*k}\right) \tag{9}$$

where k is the day index, j is the site index, W_A and W_B are the weights, C_A and C_B are the correction coefficients, and $N_{0\mathrm{A}}$ and N_{0B} are the ideal day daily traffic flow. A and B refer to the two wave-logger sites closes to site j. The weights W_A and W_B, and the wave- logger sites A and B for the interpolated sites, are listed in Table 4.2.8.6-6. The 20 locations (25 sites – five locations have right and left banks) where the 15-year daily simulated boat traffic was interpolated are shown in Figure 4.2.8.6-5 while the actual simulated results are shown in Figure 4.2.8.6-6.

Table 4.2.8.6-6: Inverse Distance Weights for the Simulation Sites

Site	$WLOG_A$	W_A	$WLOG_B$	W_B
11L	1	1	1	0
2L	1	1	1	0
303BL	1	1	1	0
18L	1	1	1	0
3L	1	1	1	0
21R	1	1	1	0
4L	1	0.951	2	0.049
29R	2	0.503	1	0.497
5CR	2	1	2	0
26R	2	0.779	3	0.221
10L	2	0.748	3	0.252
6AL	2	0.527	3	0.473
119BL	2	0.504	3	0.496
7L	3	0.603	2	0.397
8BL	3	0.748	2	0.252
87BL	3	0.809	2	0.191
75BL	3	0.924	2	0.076
12BL	3	1	3	0
9R	3	1	3	0
BC-1R	3	1	3	0

Figure 4.2.8.6-5: Simulation Sites Along the Study Reach

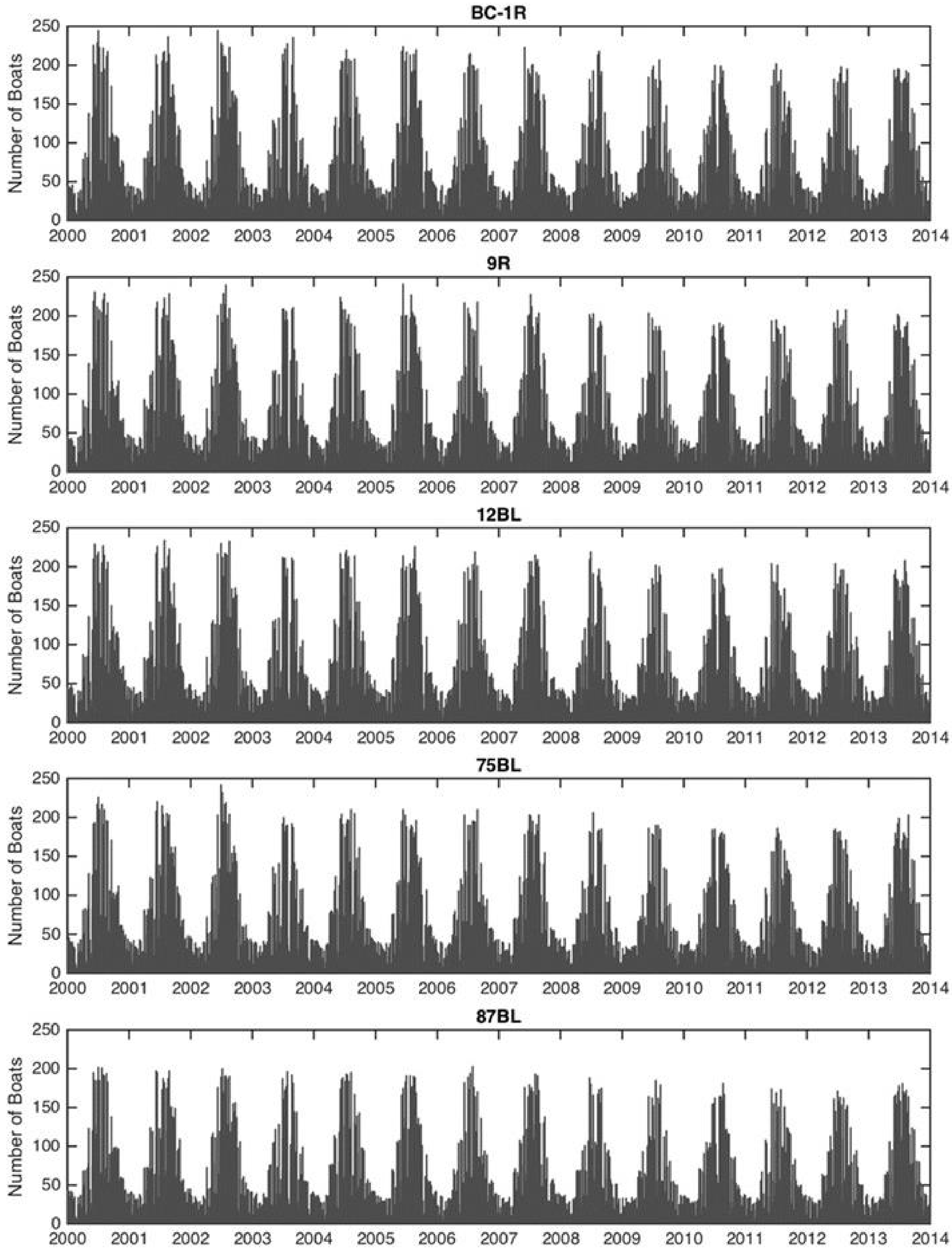

Figure 4.2.8.6-6: Simulated 15-year Daily Boat Traffic

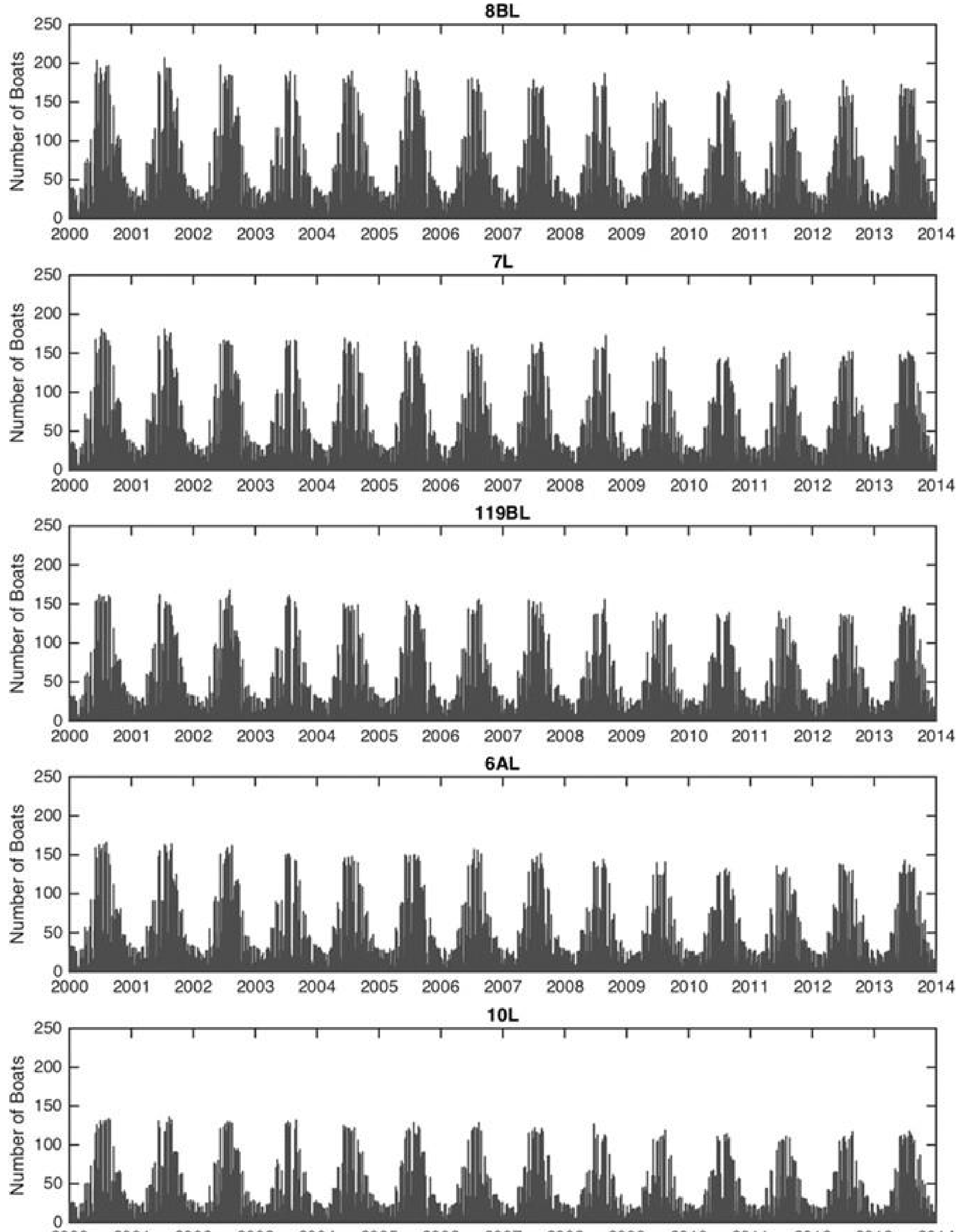

Figure 4.2.8.6-6: Simulated 15-year Daily Boat Traffic (cont.)

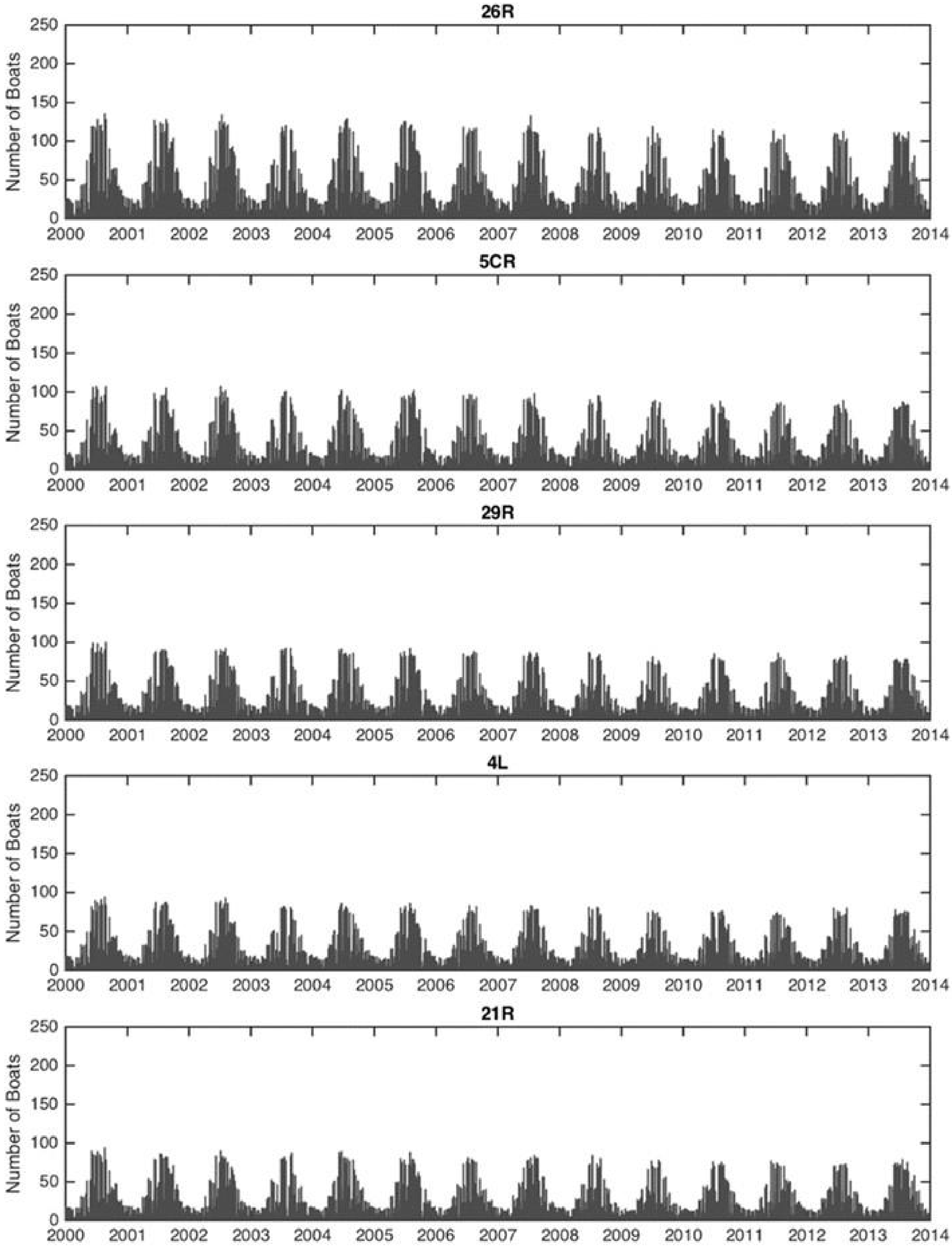

Figure 4.2.8.6-6: Simulated 15-year Daily Boat Traffic (cont.)

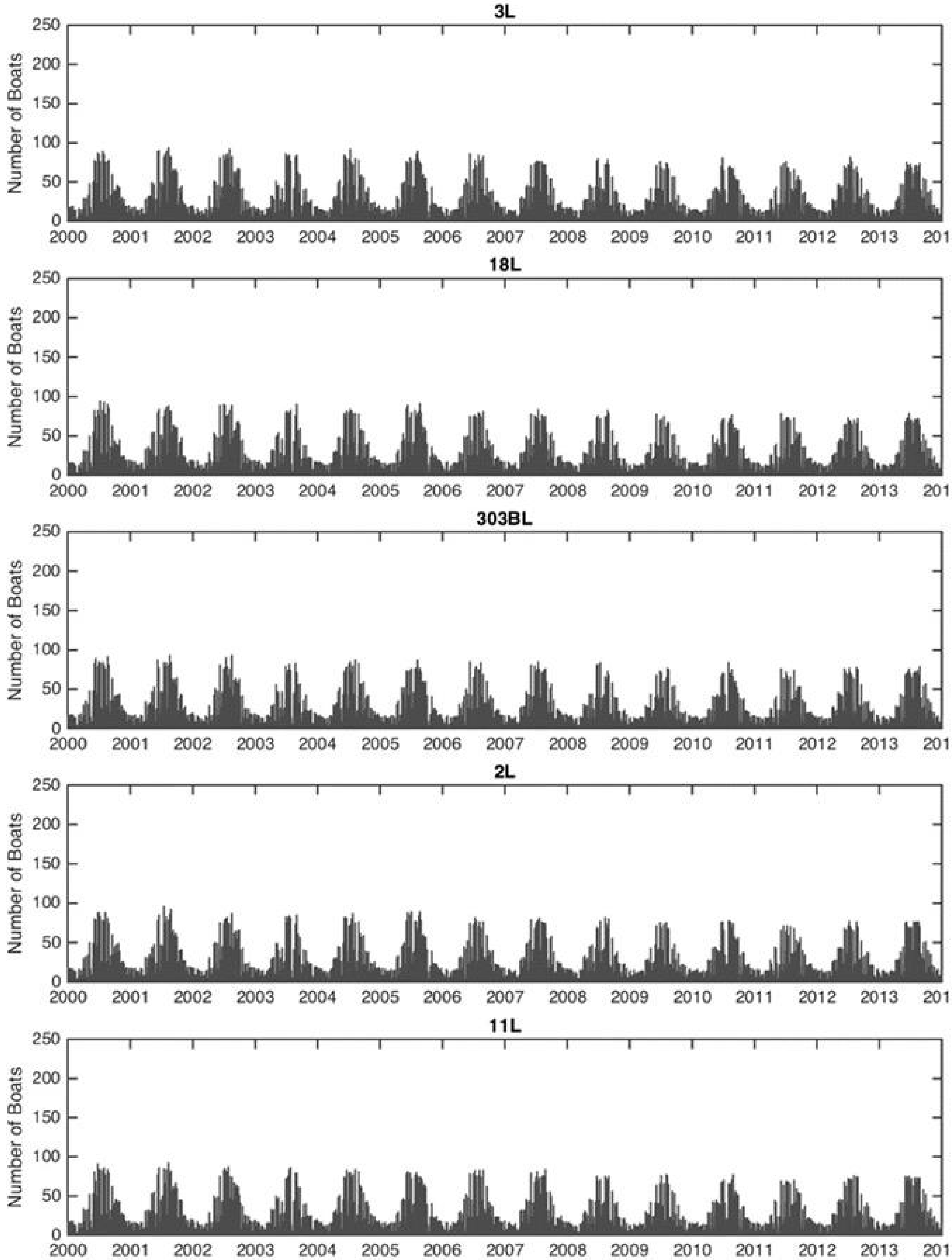

Figure 4.2.8.6-6: Simulated 15-year Daily Boat Traffic (cont.)

4.2.8.7 Distribution of the Daily Traffic

The previous section describes the temporal extrapolation and spatial interpolation methods used to calculate daily boat traffic at 20 locations (25 sites – five locations have right and left banks) for the 15-year simulation period. A table that includes the number of boats per day was obtained for 5,479 days at each site. The next step was to distribute the daily traffic throughout the day, using the measured, hourly volume of boat traffic (boats-per-hour, bph).

First, the hourly volumes of boat traffic at the wave-logger sites were normalized to calculate the average probability-density function (boat traffic hourly probability density function, *bPDF*) of the measured boat traffic. bPDF of the remaining 20 sites ($bPDF_j$) was interpolated using the measured *bPDF*'s ($bPMF_{WLOG}$). The interpolation was carried out using the same inverse distance weights, W_A and W_B, given in the previous section:

$$bPDF_j(t_h) = W_A \times bPDF_A(t_h) + W_B \times bPDF_B(t_h) \tag{10}$$

where, t_h indicates the hour of the day. This procedure is illustrated in Figure 4.2.8.7-1 $bPDF_j$s of the 20 sites are shown in Figure 4.2.8.7-1.

$bPDF_j$ was used as a kernel to distribute the traffic flow, N_j^k (Eq. 9) for each day of the simulation. Hourly volume can be defined simply by:

$$bhv_j(t_h) = round(N_j^k \times bPDF_j(t_h)) \tag{11}$$

However, this relation results in significant leak due to the round-off error in the hourly volume, $bhv_j(t_h)$ Especially for weekdays when daily traffic flow is small (on the order of 10-20 boats/day), Equation 11 can give hourly volume in the order 0.1 to 1 boats/hour, which will lead to a round-off in the order of 50%-100%:

$$\sum_{t_h=12am}^{12pm} bhv_j(t_h) \neq N_j^k \tag{12}$$

Therefore, a conservative approach that preserves the daily total number of boats (N_j^k) is used to calculate the hourly volume. In this approach, N_j^k is distributed starting from the hour slot with the highest probability. The number of boats for this hour slot is calculated by:

$$bhv_j(t_{h\max}) = ceil\left(bPDF_j(t_{h\max}) \times N_j^k\right) \tag{13}$$

In Eq. 13, t_{hmax} refers to the hour slot with the highest probability and function *ceil* calculates the nearest integer in the direction of +infinity. If the remaining number of boats $Nr_j^k = N_j^k - bhv_j(t_{h\max})$ is greater than zero, the same procedure was repeated with the second highest probability hour-slot, except the number of boats is truncated to the nearest integer instead of *ceil*. This process is repeated until all of the boats are distributed throughout the day.

Since all of the boats are assigned to a time slot, the total number of boats for a given day is preserved. Figure 4.2.8.7-2 shows an example application of this procedure for site 7L. The histogram on the left is the sorted bPDF for site 7L and the table on the right shows how 20 boats are distributed starting from the highest-ranking hour slot down to the lowest.

Finally, the boats in the hour slots were randomly assigned to the minutes of the hour by a non-overlapping uniform distribution. It was assumed that each boat event in an hour slot had an equal chance of being in one of the 60 minutes of the hour, and that no boats can share the same minute slot. Thus, each boat record in the simulated dataset has a unique time stamp down to the resolution of minutes.

Figure 4.2.8.7-3 is a bar chart showing the number of boating events for each site during the 15 year-long simulations. The number of sites with the same kernel distribution (e.g. BC-1R, 9R and 12BL) slightly varies due to the added uncertainty. The distribution of the total number or boating events over the river reach is shown in Figure 4.2.8.7-4.

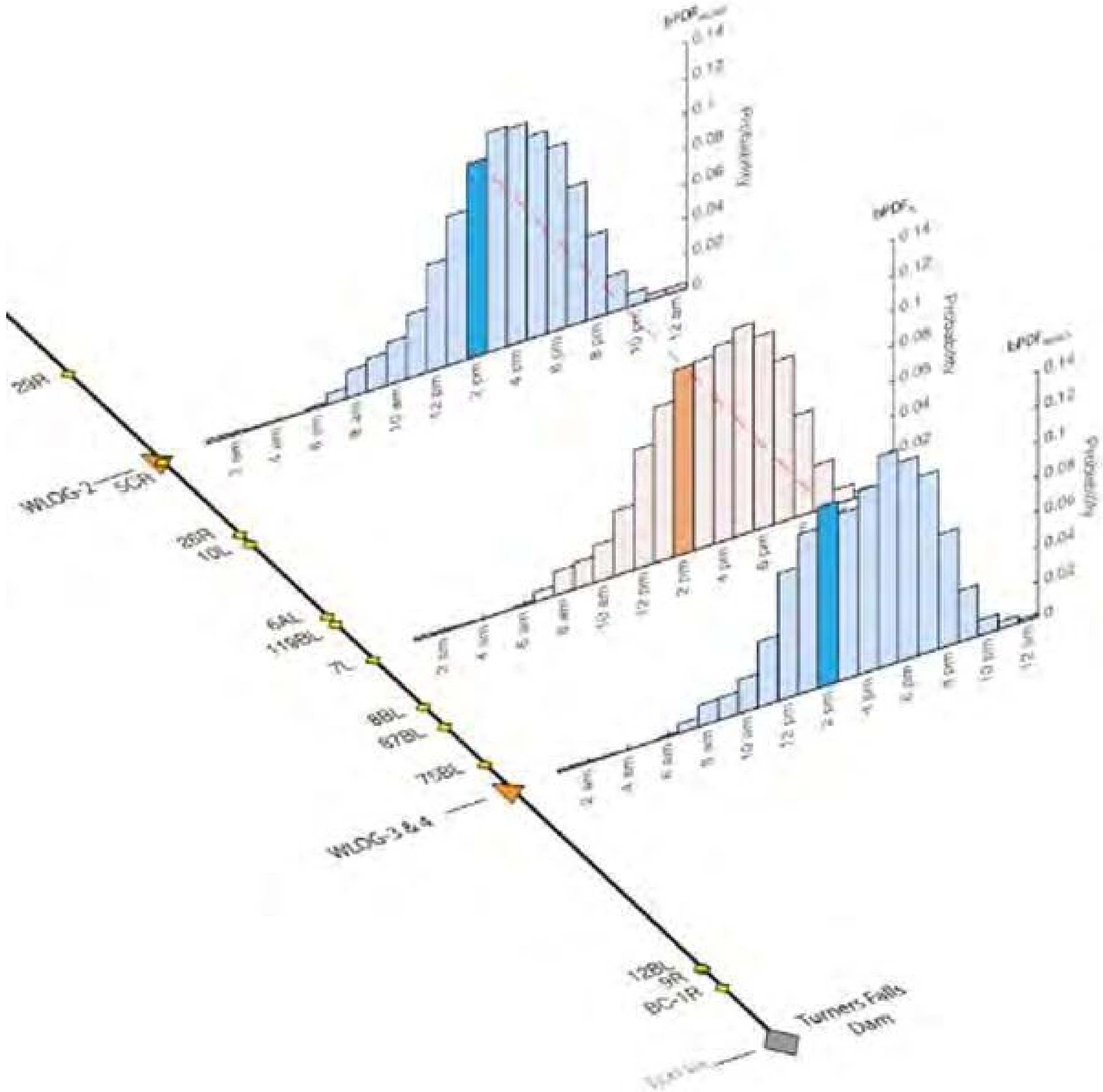

Figure 4.2.8.7-1: Illustration of the bPDFj Interpolations

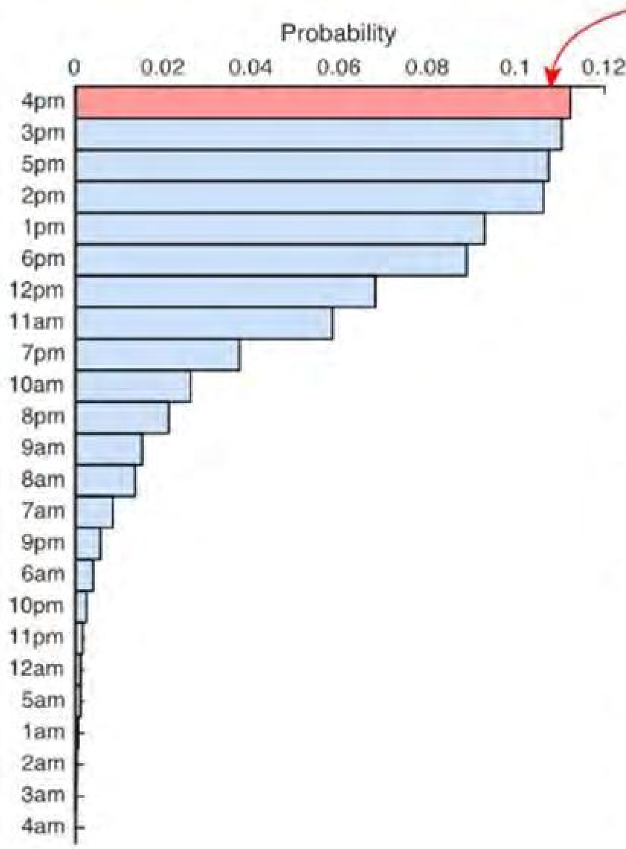

Hour	bPDF	bhv	round(bPDF)	Nr
4 pm	0.1190	2.3798	3	17
3 pm	0.1125	2.2493	2	15
5 pm	0.1104	2.2079	2	13
2 pm	0.1075	2.1503	2	11
1 pm	0.1062	2.1246	2	9
6 pm	0.0930	1.8594	2	7
12 pm	0.0888	1.7758	2	5
11 am	0.0681	1.3619	1	4
7 pm	0.0583	1.1664	1	3
10 am	0.0372	0.7437	1	2
8 pm	0.0261	0.5220	1	1
9 am	0.0212	0.4247	0	0
8 am	0.0151	0.3023	0	0
7 am	0.0136	0.2711	0	0
9 pm	0.0084	0.1686	0	0
6 am	0.0057	0.1131	0	0
10 pm	0.0040	0.0798	0	0
11 pm	0.0024	0.0479	0	0
12 am	0.0015	0.0309	0	0
5 am	0.0011	0.0220	0	0
1 am	0.0011	0.0214	0	0
2 am	0.0006	0.0122	0	0
3 am	0.0002	0.0042	0	0
4 am	0.0002	0.0031	0	0

Figure 4.2.8.7-2: Hourly Distribution for a Day with 20 Boats Passes at Site 7L

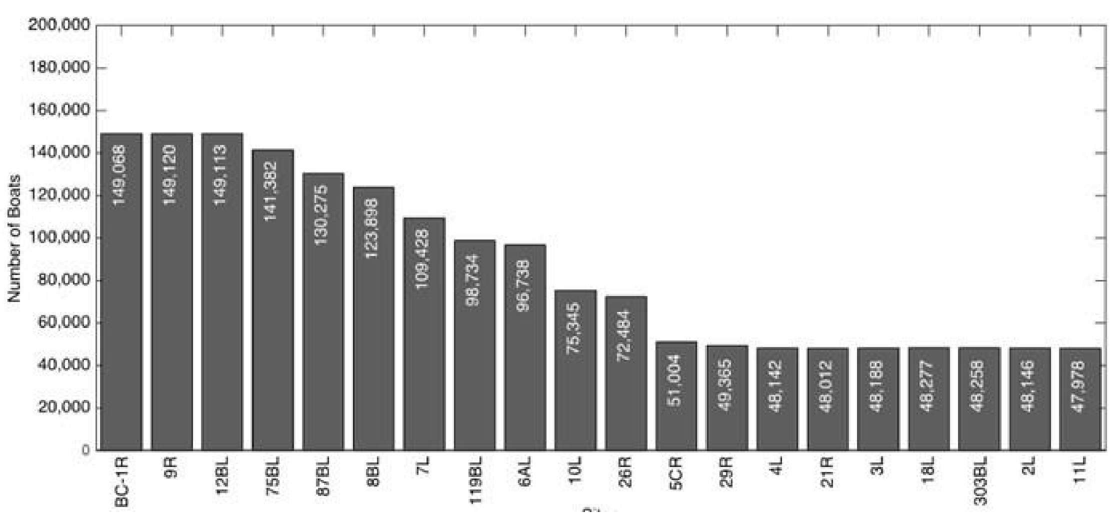

Figure 4.2.8.7-3: Total Number of Boats over the 15-year Period for the 20 Unique Locations (Sites)

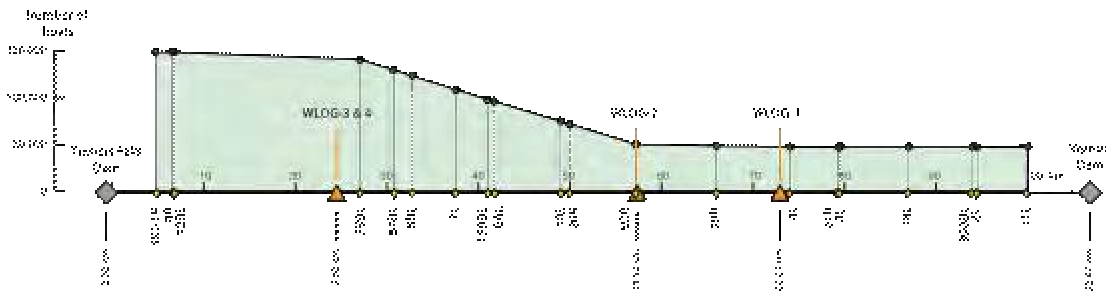

Figure 4.2.8.7-4: The Simulated Number of Boats on an Ideal Day, Distributed Along the Simulation Sites

4.2.8.8 Simulation of Wave Properties

Boat-generated waves were characterized by their maximum height, H_{max} and the wave period (for H_{max}), T_{max}. The manual wave-data input option in the BSTEM Dynamic v2.3, wave model requires a pair of H_{max} and T_{max} for each boating activity. The wave properties, H_{max} and T_{max} mainly depend on the boat speed, size and shape, and water depth. For the simulated boats, these properties were assumed to be similar for the last 15 years, and temporal variations are neglected. However, collected data shows that boat wave properties depend also on the measurement location. Even for the same type of boat, generated wave properties may vary between sites due to river geometry and boat operating conditions. For instance, at wider river sections distance between the sailing line and the shoreline will most likely be longer than that of a narrower section of the river. Because the travel distance of the waves is increased, they will attenuate and spread more due to frequency dispersion and friction. These effects are included in the data generation as uncertainties by using a weighted random-pick procedure. According to this procedure, the likelihood of observing a boat and waves similar to those observed at the measurement sites is inversely proportional to the distance from those measurement sites.

For each of the simulated boating events to be used for BSTEM simulations, a pair of H_{max} and T_{max} was randomly picked from the 12,148 boating events recorded during fieldwork. If the total number of boats simulated for 15 years for a given site j is M_j then $W_A M_j$ of those boats are picked from the measured boating events at wave logger A and $W_B M_j$ of them are picked from wave logger site B. The resulting set of H_{max} and T_{max} pairs are then permuted randomly and assigned to a simulated boating event.

4.2.8.9 Wind Generated Waves

Wave heights of boat-generated waves were 3-4 times higher than the wind-generated waves. This translates to an order of magnitude difference in their energy content since wave energy is a function of wave height squared. Moreover, due to the limited fetch length and sheltering, wind-generated waves are confined in the high frequency band. The energy of the high-frequency waves (or short waves) are concentrated close to the water surface which further limits their contribution in wave erosion.

4.2.9 Sediment Transport

Along with water flowing through river systems, rivers typically transport sediment that has been eroded from the upstream watershed, riverbanks, or the riverbed in response to flow or rainfall events and other processes that erode sediment. Sediment is transported in two modes, in suspension with the water column as it flows downstream (suspended sediment load) and sediment that flows at or near the bed of the river (bedload). Part of the reason for breaking sediment transport into these two components is due to the two methods of traditionally sampling sediment transport: suspended sediment sampling and bedload sampling. For this study emphasis was placed on investigating and evaluating available suspended sediment data collected throughout the TFI. Analysis of suspended sediment data was conducted in order to identify any correlations between flow, suspended sediment concentration, and erosion processes and to independently verify the BSTEM results, to the extent possible.

As part of Study No. 3.1.3 *Sediment Management Plan* (Study No. 3.1.3), FirstLight operated continuous suspended sediment monitors at three locations in the TFI from 2012 to 2015, except during the winter period (due to freezing temperatures). Continuous suspended sediment monitoring equipment which was used included two Laser In-situ Scattering Transmissometry (LISST) HYDRO units (HYDROs) and one LISST-StreamSide (StreamSide) unit. Continuous data was collected on an hourly, or less, basis during the monitoring period. The LISST-HYDROs were installed at the Northfield Mountain Project (initially in the powerhouse and then relocated to the tailrace in 2013) while the StreamSide was installed just upstream of the Rt. 10 Bridge. Additional LISST equipment utilized during Study No. 3.1.3 included the LISST-100X which was used to collect cross-sectional data at the Rt. 10 Bridge and Northfield Mountain tailrace boat barrier line in 2013.

In addition to the LISST instruments, grab samples were taken from the drain hoses of the HYDROs and StreamSide (2012-2015), from the edge-of-water at each LISST instrument (2015), and across the Rt. 10 Bridge over a range of flows (2015). Figures 4.2.9-1 through 4.2.9-4 depict the locations of the various suspended sediment monitoring which occurred as part of Study No. 3.1.3. In-depth discussion and analyses pertaining to this study can be found in the report titled, *Relicensing Study 3.1.3 Northfield Mountain Pumped Storage Project Sediment Management Plan 2015 Summary of Annual Monitoring* filed with FERC in December 2015 (FirstLight, 2015a).

For the purposes of the Causation Study, emphasis was placed on evaluating and analyzing the continuous suspended sediment and grab sample data collected in the vicinity of the Rt. 10 Bridge, more specifically the StreamSide data (2013-2015) and the Rt. 10 Bridge cross-section grab samples (2015). The data collected in the vicinity of the Rt. 10 Bridge allowed for a direct analysis of suspended sediment dynamics in the mainstem Connecticut River (as opposed to the data collected in the Northfield Mountain tailrace which was set back from the mainstem). In-depth discussion pertaining to the analysis of the suspended sediment dataset can be found in Section 5.3.

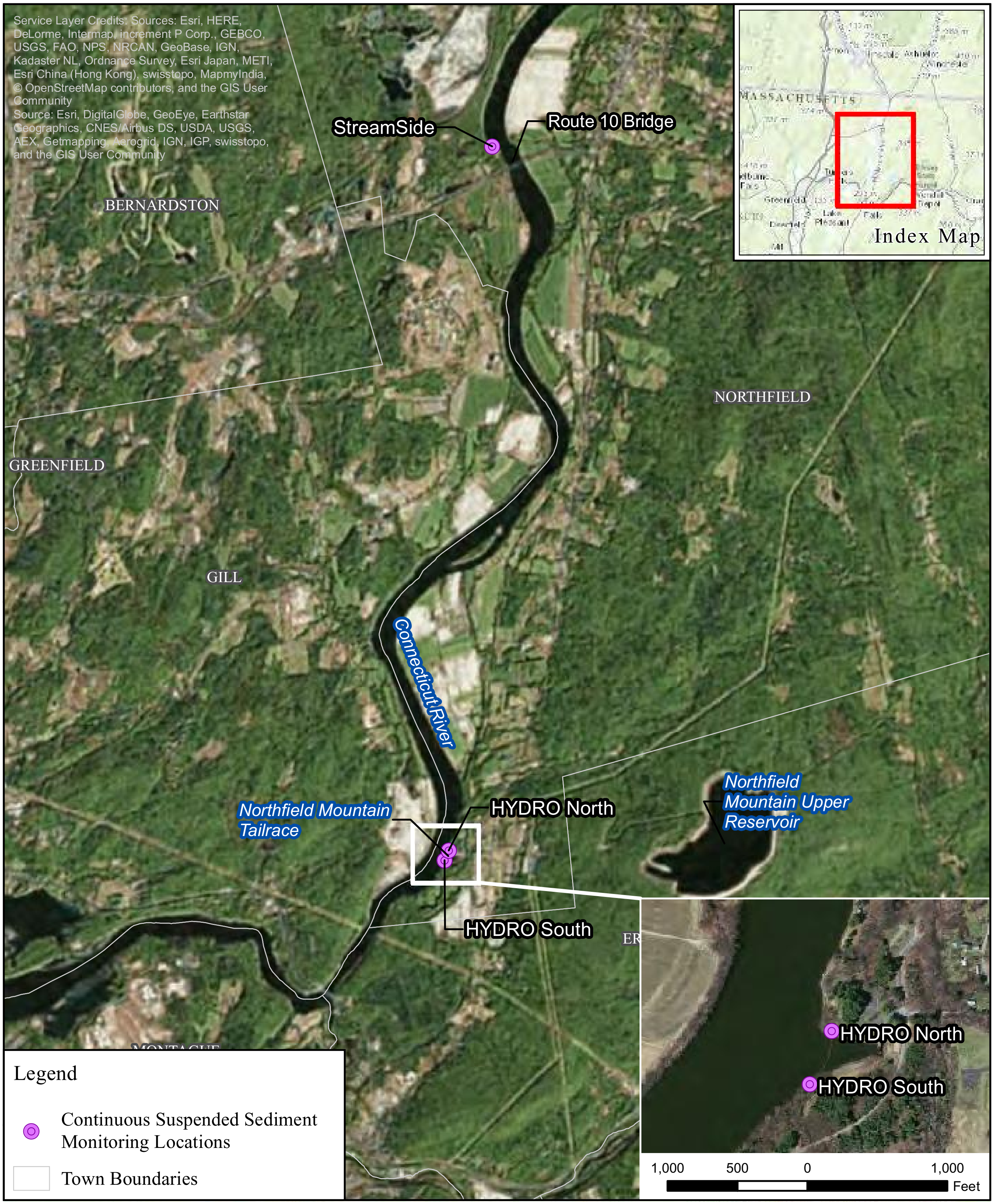

FIRSTLIGHT HYDRO GENERATING COMPANY
Northfield Mountain Pumped Storage Project No. 2485
Turners Falls Hydroelectric Project No. 1889

STUDY 3.1.2

FirstLight Power Resources

N

0 0.5 1 2 Miles

Figure 4.2.9-1:
Locations of LISST Continuous Suspended Sediment Monitors

Path: W:\gis\studies\3_1_2\maps\final_report\figure_4_2_9-1.mxd

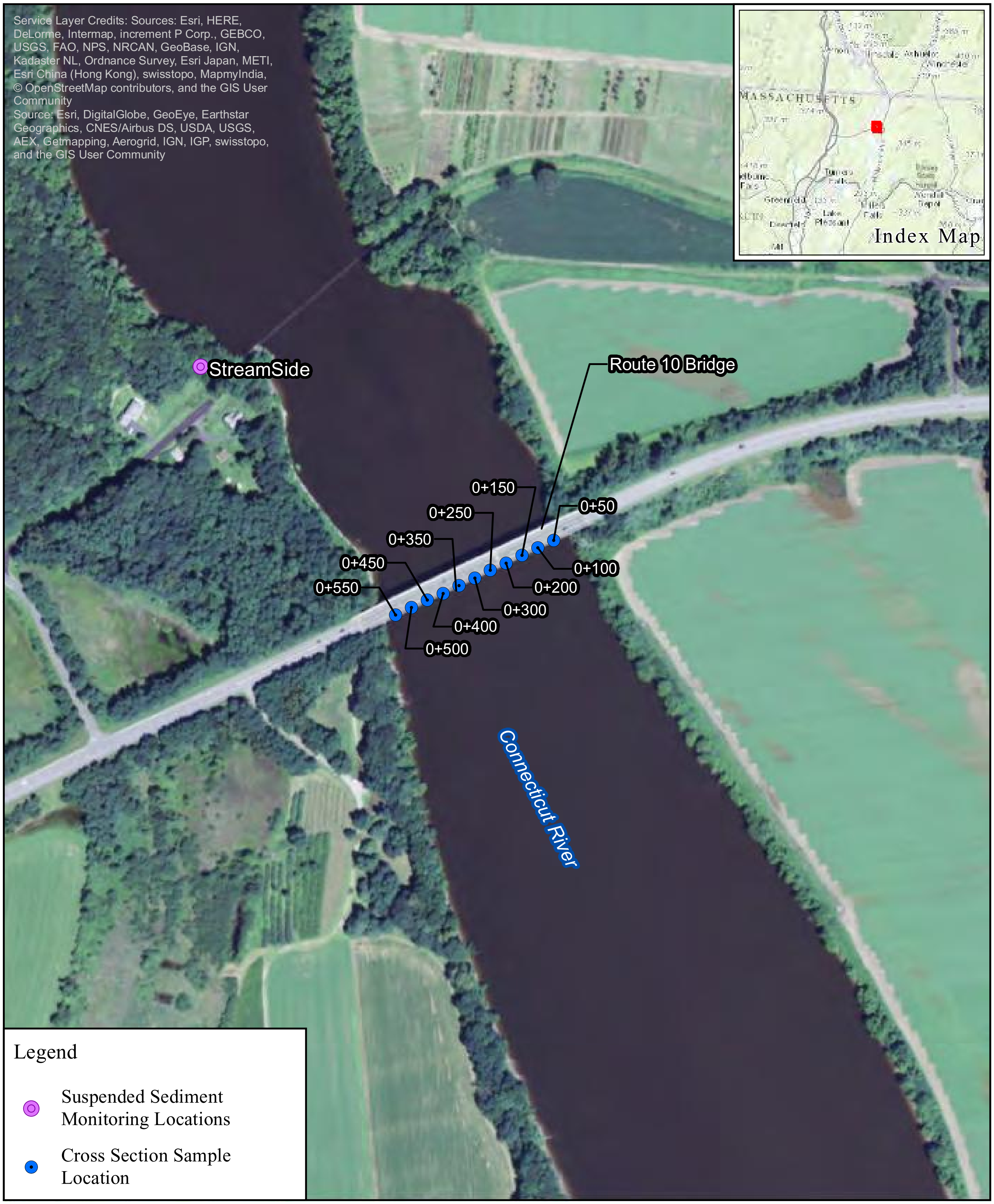

FIRSTLIGHT HYDRO GENERATING COMPANY
Northfield Mountain Pumped Storage Project No. 2485
Turners Falls Hydroelectric Project No. 1889

STUDY 3.1.2

FirstLight Power Resources

N

0 200 400 800 Feet

Figure 4.2.9-2:
Location of LISST-StreamSide and LISST-100X Cross-section

Path: W:\gis\studies\3_1_2\maps\final_report\figure_4_2_9-2.mxd

FirstLight Power Resources

FIRSTLIGHT HYDRO GENERATING COMPANY
Northfield Mountain Pumped Storage Project No. 2485
Turners Falls Hydroelectric Project No. 1889

STUDY 3.1.2

N

0 100 200 400 Feet

Figure 4.2.9-3:
Location of LISST HYDROs and LISST-100X Cross-section

Path: W:\gis\studies\3_1_2\maps\final_report\figure_4_2_9-3.mxd

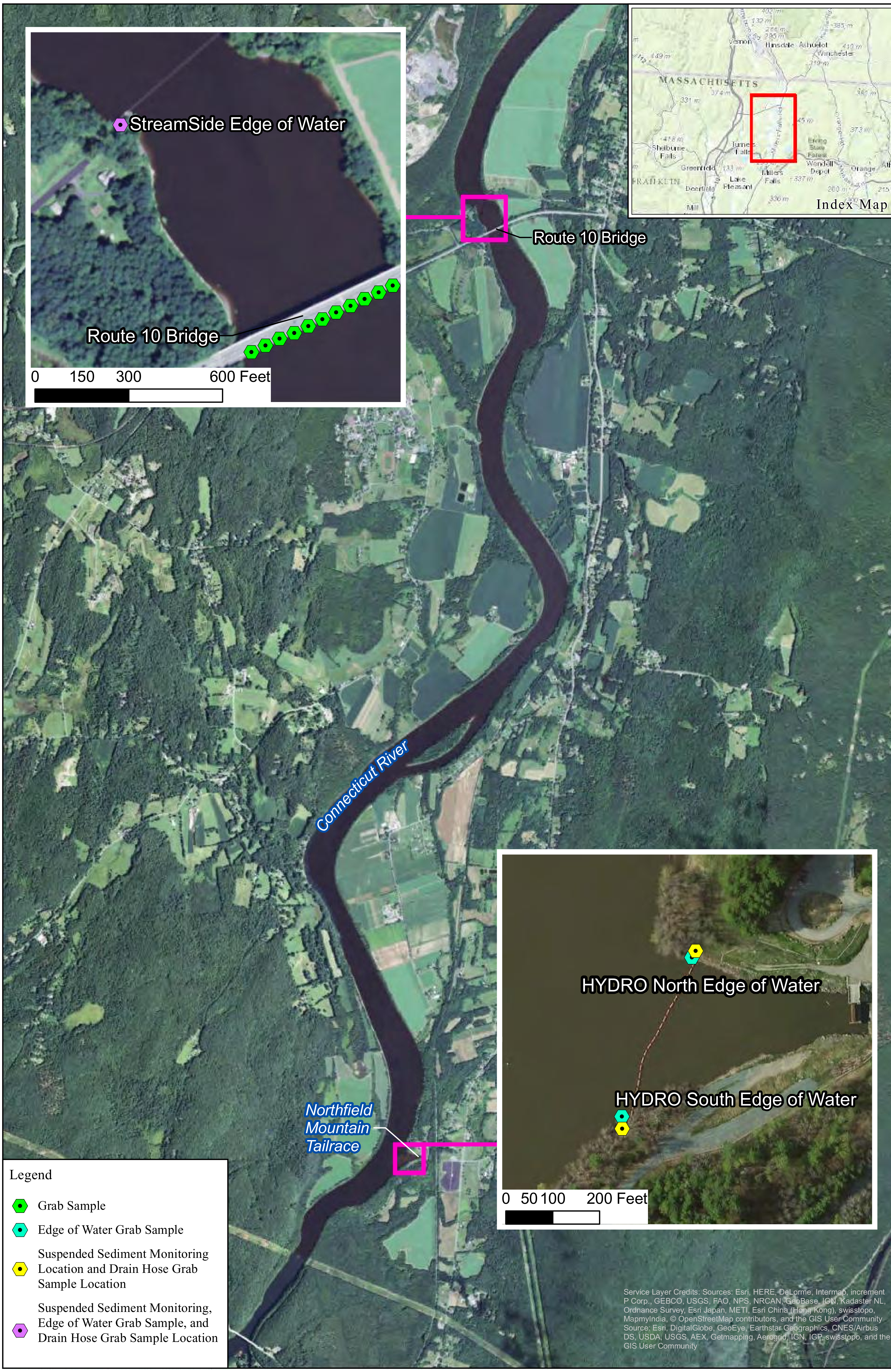

FirstLight Power Resources

FIRSTLIGHT HYDRO GENERATING COMPANY
Northfield Mountain Pumped Storage Project No. 2485
Turners Falls Hydroelectric Project No. 1889

STUDY 3.1.2

N

0 0.25 0.5 1 Miles

Figure 4.2.9-4:
Grab Sampling Locations

Path: W:\gis\studies\3_1_2\maps\final_report\figure_4_2_9-4.mxd

4.2.10 Groundwater Data

Groundwater data was collected in the 1990's to investigate the impact of water level fluctuations on the potential movement of water into and out of riverbanks in the TFI. Pressure transducers to measure water level fluctuations were placed in the river and in three monitoring wells adjacent to the river in the Bennett Meadow area on the west bank of the river a short distance downstream of the Route 10 Bridge. One transducer was placed in the river itself to monitor impoundment fluctuations and the three monitoring wells were placed in a line perpendicular to the riverbank at various distances away from the river (52, 65, and 210 feet back from the edge). Monitoring of these transducers was conducted from mid-July 1997 through February 1998 (see Figure 4.2.10-1). Figures 4.2.10-2 and 4.2.10-3 show these data plotted over time. These groundwater data are provided in Volume III (Appendix I). The findings of this analysis are discussed further in Section 5.5.2.1.

Figure 4.2.10-1: Groundwater Monitoring

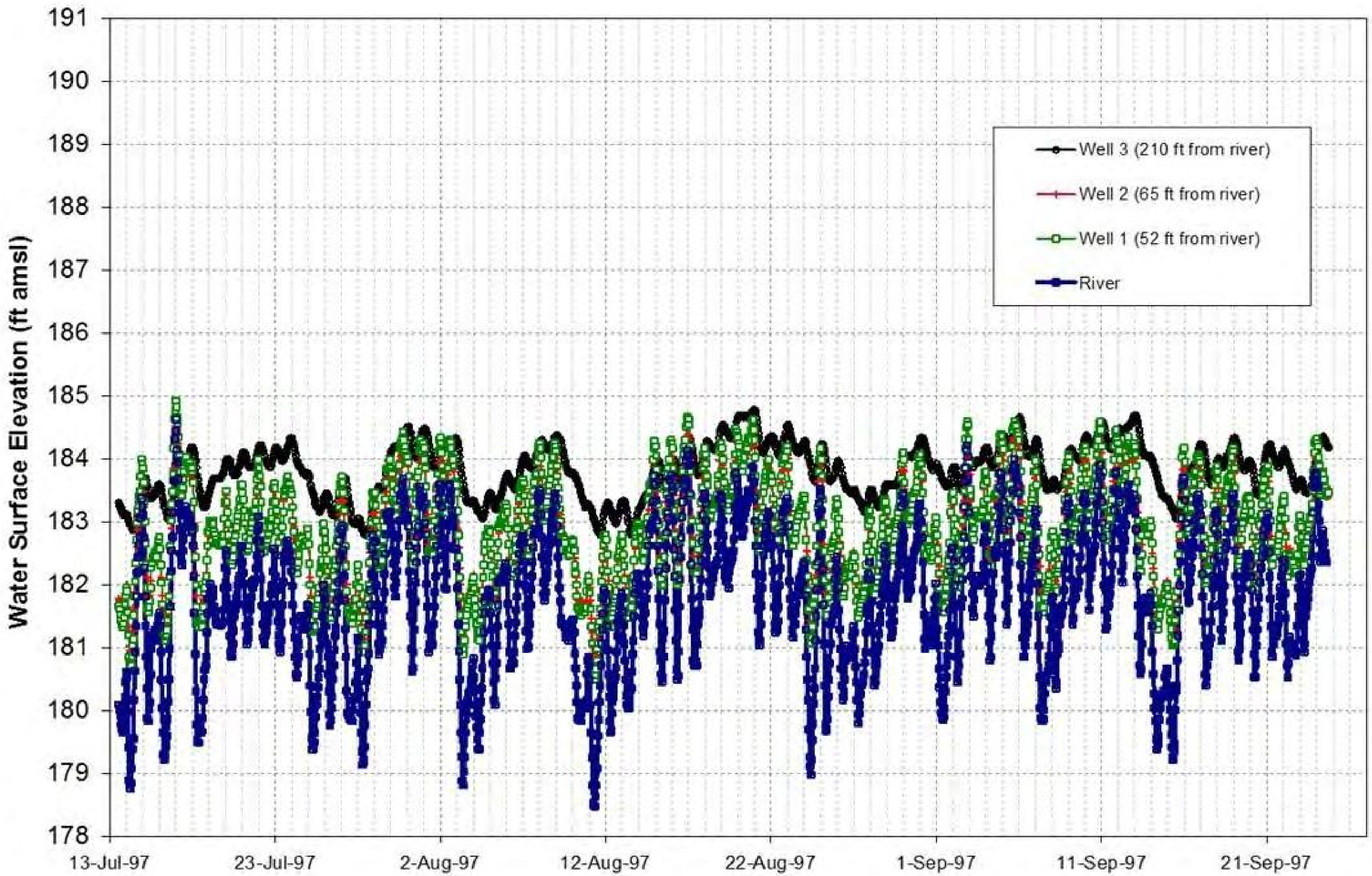

Figure 4.2.10-2: Groundwater Data (July 13, 1997 – September 21, 1997)

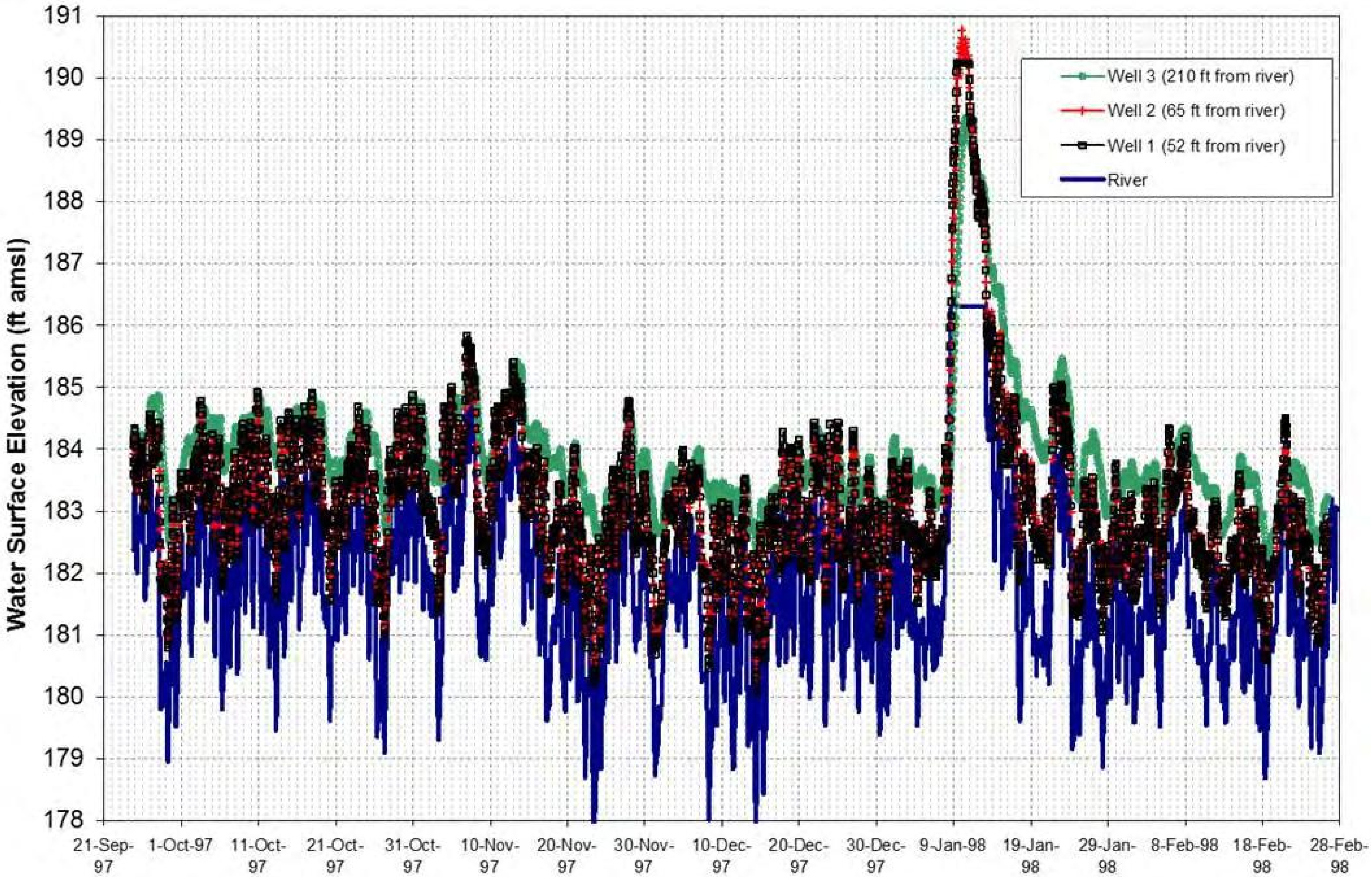

Figure 4.2.10-3: Groundwater Data (September 21, 1997 – February 28, 1998)

4.2.11 Ice

When initially developing the potential causes of erosion discussed in Section 3, ice was listed as a potential secondary cause of erosion. For decades ice had not been a significant factor affecting erosion in the TFI due potentially to the operation of VY located immediately upstream in the Vernon Impoundment. When in operation, VY used water from the Connecticut River for cooling after which heated water was discharged back to the river. The operation of VY may have been the reason why the TFI would rarely ice over completely during the winter months.

In 2013, when Entergy announced the closing of VY by December 29, 2014, FERC issued an Interim ILP schedule for Study Plan Determination. During this period, FirstLight elevated ice from a potential secondary cause of erosion to a potential primary cause of erosion to account for the fact that ice may play a more significant role in riverbank erosion processes in the future. FirstLight filed an addendum to the RSP for Study No. 3.1.2 with FERC in September 2014[32] which highlighted the methodology to be used to more thoroughly examine ice as a potential primary cause of erosion.

In accordance with the RSP addendum, FirstLight completed the following ice related tasks:

- A review was conducted of the USACE, Cold Regions Research and Engineering Laboratory (CRREL) database to document known ice jams recorded on the Connecticut River in the area between Wilder Dam and Turners Falls Dam. CRREL maintains an ice jam database and clearing house. The database was inventoried to determine historic ice jams along the Connecticut River. Similarly, contact was made with the USGS to identify any recorded ice jams or ice floes on the Connecticut River at their gaging stations.

- TransCanada was contacted to determine if it had any historic and/or current information on the timing, extent and duration of sheet ice development and ice-break up in the Wilder and Bellows Falls Impoundments. In addition, information on the thickness of the sheet ice and whether any ice floes have been documented in these impoundments, below the dams, or at the mouths of major tributaries emptying into the impoundments was requested.

- Historic daily air temperature data were obtained to determine any correlation between air temperature and the timing of ice sheet development and break-up for any historic ice formation data collected by TransCanada. Historic air temperature data were also obtained near the TFI. Specific sites from which air temperature data were obtained include:

    - Amherst, MA;
    - Vernon, VT;
    - Keene, NH; and
    - Hanover, NH

  Temperature data obtained at each of these sites is included in Volume III (Appendix J).

- Photographs of ice conditions were taken at a number of predetermined locations throughout the TFI during the winter of 2015/2016, including:

    - Vernon Dam;
    - Confluence of Ashuelot River;

[32] The RSP Addendum addressing the evaluation of ice as a potential primary cause of erosion was filed with FERC as part of the Relicensing Study No. 3.1.2 Initial Study Report Summary.

- Pauchaug Boat Launch;
- Route 10 Bridge;
- Northfield Tailrace;
- French King Bridge;
- Confluence of Millers River; and
- Turners Falls Dam

These sites were selected for two primary reasons: 1) they were easily and safely accessible during winter conditions, and 2) they covered the geographic extent of the TFI. Figure 4.2.11-1 depicts these locations. Photos were taken on:

- December 15, 2015;
- January 5, 2016;
- January 14, 2016;
- January 21, 2016;
- January 28, 2016;
- February 11, 2016;
- February 19, 2016; and
- March 8, 2016

The original intent of the timing of the photographs was to observe: (1) when sheet ice developed; (2) during formation of sheet ice; (3) during ice break-up; and (4) after ice break-up occurred. While ice development was observed during the monitoring period, due to an unseasonably mild winter the TFI never completely iced over. Although the RSP Addendum called for photographs to be taken from December 1 through March 31, ice was not observed at the monitoring sites during the March 8, 2016 site visits. As such, the decision was made to curtail any future site visits.

In addition to the winter 2015/2016 photos, supplemental photos were taken on four occasions during the winter of 2014/2015 to document ice conditions during what was a relatively cold winter.[33] A full set of photographs at all locations is presented in Volume III (Appendix J).

Using the ice and temperature data, correlations between air temperature and ice were developed following a similar approach to that which had been utilized to evaluate ice formation, breakup and subsequent erosion on the Platte River (*Analysis of Ice Formation on the Platte River* (S&A, 1990a), *Physical Process Computer Model of Channel Width and Woodland Changes on the North Platte, South Platte and Platte Rivers* (S&A, 1990b), *Calibration of SEDVEG Model Based on Specific Events from Demography Data* (S&A, 2002)). Additional analysis conducted as part of this study included examining the forces that ice transmits to riverbanks and the type of damages that may potentially occur. These analyses are discussed further in Section 5.5.5.

[33] Supplemental photographs taken during the winter of 2014/2015 were captured on: January 5, January 29, February 25, and March 3, 2015.

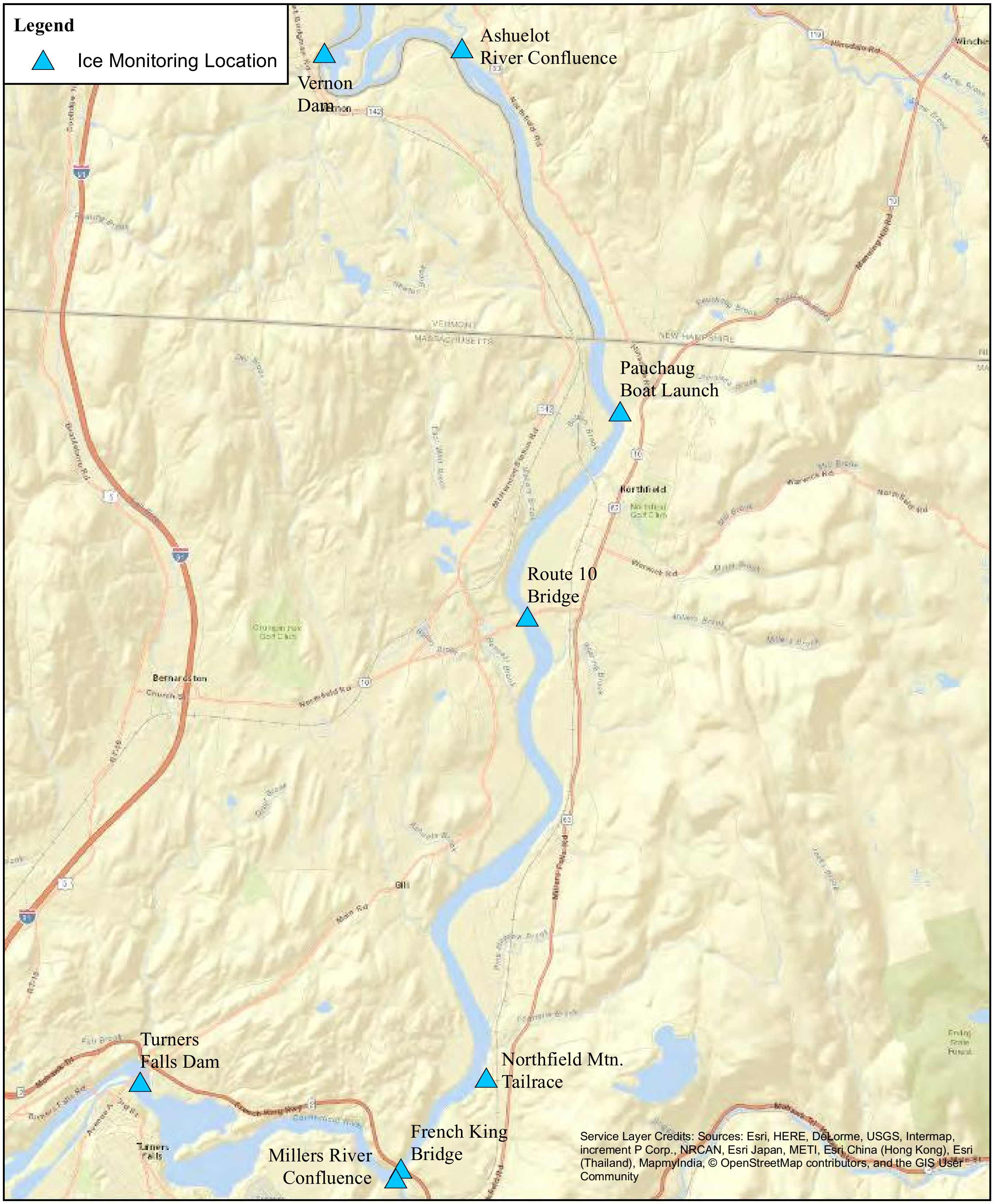

FIRSTLIGHT HYDRO GENERATING COMPANY
Northfield Mountain Pumped Storage Project No. 2485
Turners Falls Hydroelectric Project No. 1889

STUDY 3.1.2

Figure 4.2.11-1:
Ice Monitoring Locations
Winter 2015/2016

Path: W:\gis\studies\3_1_2\maps\final_report\figure_4_2_11-1.mxd

5 DATA ANALYSES & EVALUATION OF THE CAUSES OF EROSION

In order to identify, quantify and rank the causes of erosion in the TFI, a thorough understanding of the forces associated with each primary cause of erosion must be developed. The results of the data analyses presented in this section provides an understanding of: (1) the magnitude of those forces; (2) the vertical location those forces impact the riverbank; (3) the longitudinal location; (4) the duration of the forces; (5) the various types of riverbank materials; and (6) the physical properties of the bank materials that resist hydraulic and geotechnical erosion. The results of the various analyses and modeling described in this section were further used to quantify the relative percentages of the primary causes of erosion at each detailed study site as well as throughout the TFI. While discussion pertaining to the evaluation of the causes of erosion is presented in this section, a summary discussion is also presented in Section 6. All analyses was conducted in accordance with the requirements of the RSP.

BSTEM, including its field collected and hydraulic model input data, was the primary tool used to analyze and evaluate primary causes of erosion in the TFI. BSTEM is a state-of-the-science model which allowed for the analysis of potential primary causes of erosion, including: hydraulic shear stress due to flowing water, water level fluctuations, and boat waves.

In addition to the modeling conducted with BSTEM, supplemental data analyses were conducted as a means of comparison with the BSTEM results. These analyses were used to: (1) investigate the potential primary causes of erosion not included in the BSTEM analysis (i.e. land-use and ice); (2) provide additional analyses of the causes of erosion examined by BSTEM; and (3) to examine secondary causes of erosion present in the TFI (i.e. animals and unique hydraulic and/or geomorphic conditions). Land-use and land management practices were analyzed via geospatial analysis (GIS) and observations made during the 2013 FRR land-based survey. Analysis of the effects of ice was conducted in accordance with the methodology laid out in Section 4.2.11 and the RSP Addendum.

The Hydrology, Hydraulics, and Sediment Transport discussions presented in Sections 5.1, 5.2, and 5.3 respectively, provide the foundation for the BSTEM and supplemental analyses discussed later. BSTEM analyses, including discussion pertaining to input data and results, is presented in Section 5.4. Supplemental analyses are found in Section 5.5, including:

- Hydraulic shear stress (Section 5.5.1);
- Water level fluctuations (Section 5.5.2);
- Boat Waves (Section 5.5.3);
- Land-use and management practices (Section 5.5.4);
- Ice (Section 5.5.5); and
- Animals (Section 5.5.6)

The BSTEM and supplemental analyses discussed in this section, combined with the geomorphic understanding of the Connecticut River discussed in Section 2, represent all components of the three-level approach as discussed in Section 1 and are consistent with the requirements of the RSP.

5.1 Hydrology

In order to understand the erosion processes of the TFI, it is necessary to first understand the hydrology and hydraulics of the study area. As such, this section focuses on the hydrologic characteristics of the TFI in terms of daily flow variations and hourly flow and water level fluctuations. Discussion pertaining to the tools used to evaluate the hydraulics of the TFI can be found in Section 5.2. Evaluation of the hydrologic and hydraulic characteristics of the TFI provides additional information and longer term perspective that is useful in developing an understanding of the patterns and interaction that flow and associated hydropower operations may have on erosion processes.

5.1.1 Hydrologic Setting

While there is no USGS gaging station measuring flow within the TFI, there is a USGS gage on the Connecticut River at Montague, MA (USGS gage no. 01170500), which is located a short distance downstream of Turners Falls Dam. The drainage areas at the Turners Falls Dam and at the Montague gage are 7,163 mi^2 and 7,860 mi^2, respectively; a difference of 697 mi^2. The major tributary between the dam and Montague gage is the Deerfield River with a drainage area of 665 mi^2. Flow on the Deerfield River is regulated from peaking hydroelectric facilities and by two seasonal storage reservoirs located in Vermont. For purposes of this section, the summary of the Montague gage is included to provide a general understanding of the long term average flow regime of the Connecticut River. In addition, FirstLight has maintained an hourly database of flows within the Project area over the past 16 years. This database includes discharges from Vernon Dam, Northfield Mountain Operations, flows over the Turners Falls Dam, and flows to the power canal.

The Connecticut River follows a fairly typical seasonal hydrograph as shown by the mean daily flow from 1904 to 2014 (Figure 5.1.1-1). As shown in this figure, flow at the Montague gage in January through most of February averages just over 10,000 cfs. In late February to early March, the mean flow rises due to spring runoff or freshet peaking in April to about 40,000 cfs. The lowest flow (slightly over 5,000 cfs) occurs during the late summer to early fall.

Another important flow statistic is the annual peak flow as this can be related to flooding and flood related damages. Figure 5.1.1-2 shows the variation in annual peak streamflow for the Connecticut River at Montague from 1904 to 2015. As observed from the Montague gage data, several large floods occurred on the Connecticut River prior to 1940. The largest three floods within the period of record had peak flows of 236,000 cfs (1936), 195,000 cfs (1938), and 179,000 cfs (1928).

The flood of 1936 caused substantial damage and provided the impetus for the construction of flood control reservoirs in the Connecticut River Watershed. In response to the 1936 flood, the USACE completed 9 flood control reservoirs on tributaries to the Connecticut River upstream of Turners Falls Dam between 1941 and 1961 (Table 5.1.1-1). Note that this table does not include mainstem projects such as Moore Dam (completed in 1956) which provides a limited amount of flood storage, or other much smaller local flood mitigation projects. The flood control projects have likely been at least partially responsible for the lower peak flows on the Connecticut River since 1961. Since 1938, no flood peak has exceeded 150,000 cfs with the three highest peaks being: 143,000 cfs (1984), 126,000 cfs (1987), and 127,000 cfs (2011, associated with Tropical Storm Irene).

Most of the analyses used in this study, including BSTEM, were based on hourly hydrologic data from January 1, 2000 to December 31, 2014. This 15-year time period was used for two primary reasons: (1) it was representative of post flood control Connecticut River conditions, and (2) it marked the period of time when the most data was available (i.e. digital FirstLight operations data). In order to determine if the 2000-2014 analysis period was representative of longer term conditions, FirstLight investigated changes in the shape of the flow duration curves and average flows for four time periods:

- 1904-2014 (representing the entire period of record other than 2015);
- 1904-1960 (pre-flood control through flood control development period);
- 1961-2014 (post-flood control period); and
- 2000-2014 (BSTEM modeling period)

As shown in Figure 5.1.1-3, the average yearly peak flow for the 1961-2014 period is 83,600 cfs, 14,000 cfs less than the average yearly peak flow for the 1904-1960 period (97,600 cfs). Table 5.1.1-2 provides the mean daily flows for the four periods. While the average yearly peak flow for the 1961-2014 and 2000-2014 time periods are approximately 7,000 cfs less compared to the 1904-2014 period, and 13,000 to 14,000 cfs less than the 1904-1960 time period; the mean daily flow is higher during these same periods compared to the overall and earlier time periods. This shows that peak flows have been reduced by approximately 8% compared to the overall time period. This is likely due to the previously mentioned flood control projects; contrasted to the time period (2000-2014) for which the mean daily flows are approximately 16% higher.

Flow duration curves based on the mean daily flows for these same periods are plotted in Figures 5.1.1-4 and 5.1.1-5. Figure 5.1.1-4 presents the full range of flows from approximately 1,000 to 240,000 cfs and exceedance percentages from 0 to 100%; while Figure 5.1.1-5 focuses on the upper 2% of the flow range. The slight shift observed for the different time periods can at least be partially explained by the effects of the flood control projects as previously discussed.

The flow duration curve for the 2000-2014 time period is quite similar to the recent, longer post flood control time period (1961-2014) indicating that the 2000-2014 flow regime is representative of the longer time period and reflects the effect that flood control projects now have in the Connecticut River Basin. Using the 2000-2014 time period for flow statistics and for analysis of erosion is supported by this comparison of flows in other time periods in the historic record.

Table 5.1.1-1: Flood Control Dams – Connecticut River

Flood Control Dam	Tributary Watershed	Date Completed	Flood Control Volume (acre-ft)
Union Village	Ompompanoosuc	1950	38,054
North Hartland	Ottauquechee	1961	71,198
North Springfield	Black	1960	51,250
Ball Mountain	West	1961	54,626
Townshend	West	1961	33,758
Surry Mountain	Ashuelot	1941	32,530
Otter Brook	Ashuelot	1958	17,493
Birch Hill	Millers	1942	50,023
Tully	Millers	1949	22,004

Table 5.1.1-2: Average Flows – Connecticut River at Montague

Time Period	Mean Daily Flow (cfs)
1904-2014	14,300
1904-1960	13,800
1961-2014	14,900
2000-2014	16,600

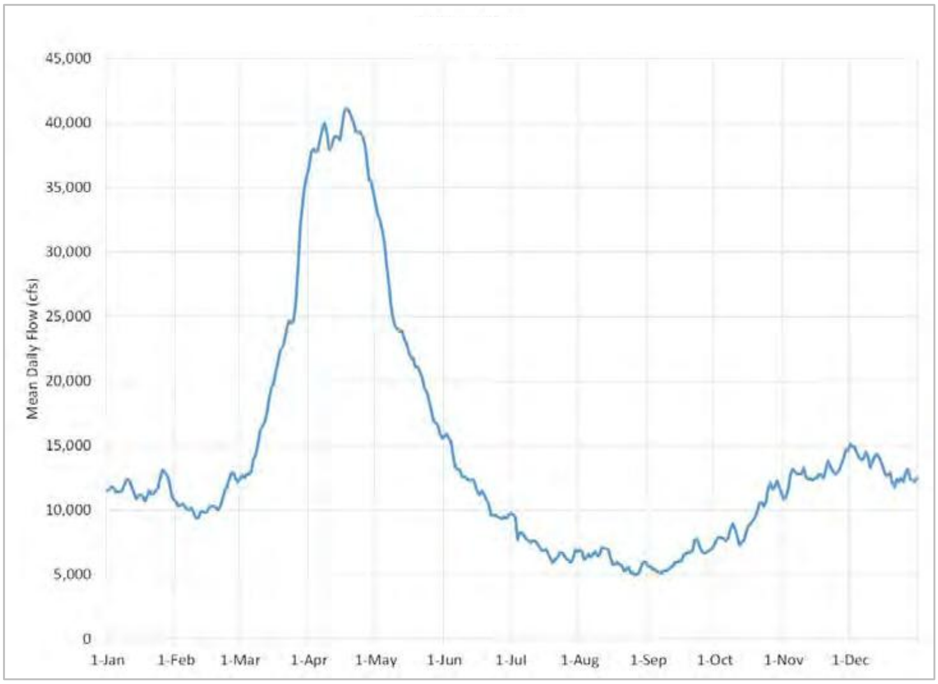

Figure 5.1.1-1: Average Annual Hydrograph – Connecticut River at Montague

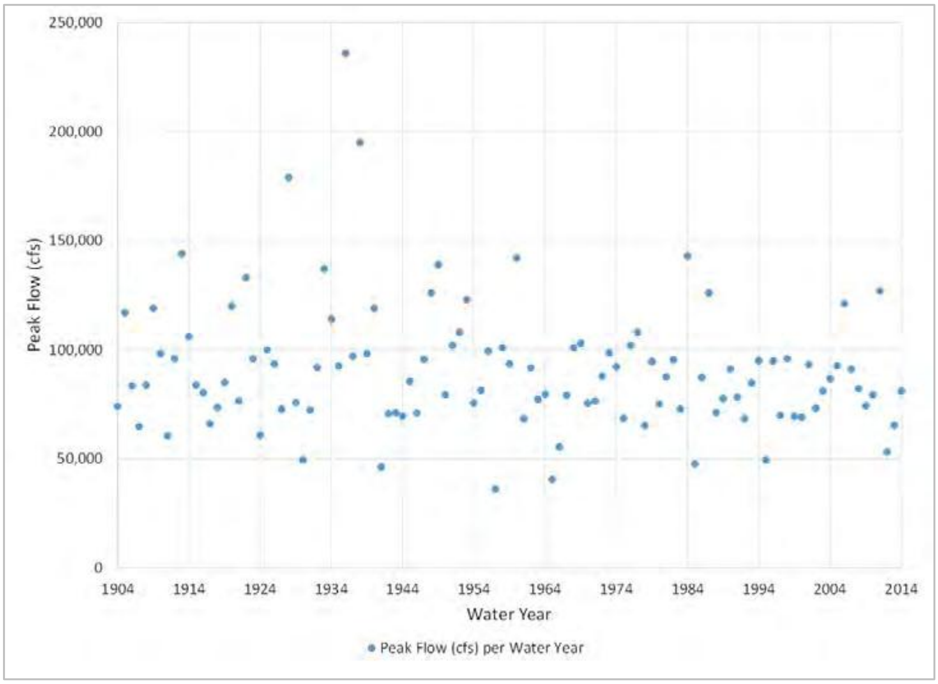

Figure 5.1.1-2: Annual Peak Streamflow on the Connecticut River at Montague, MA (USGS)

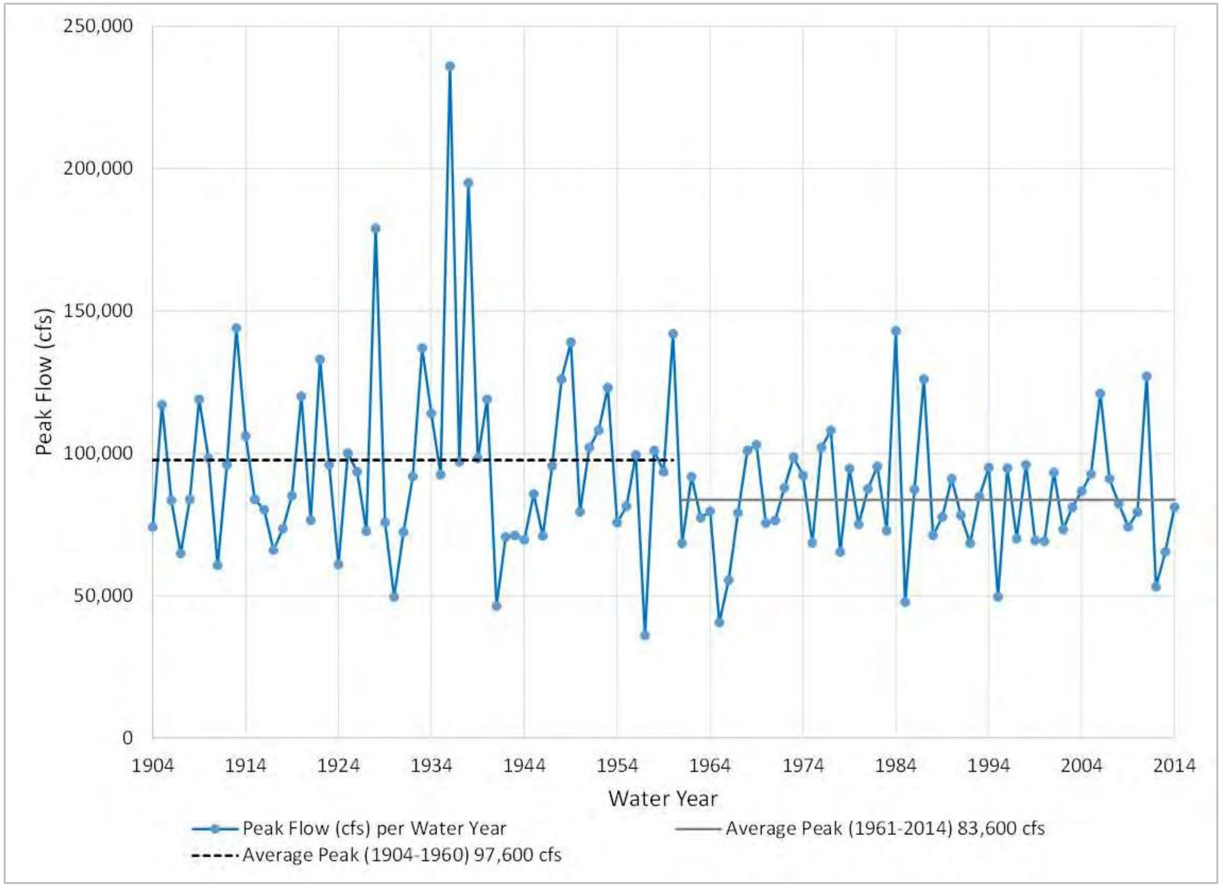

Figure 5.1.1-3: Connecticut River Peak and Average Peak Flows at Montague, MA (USGS)

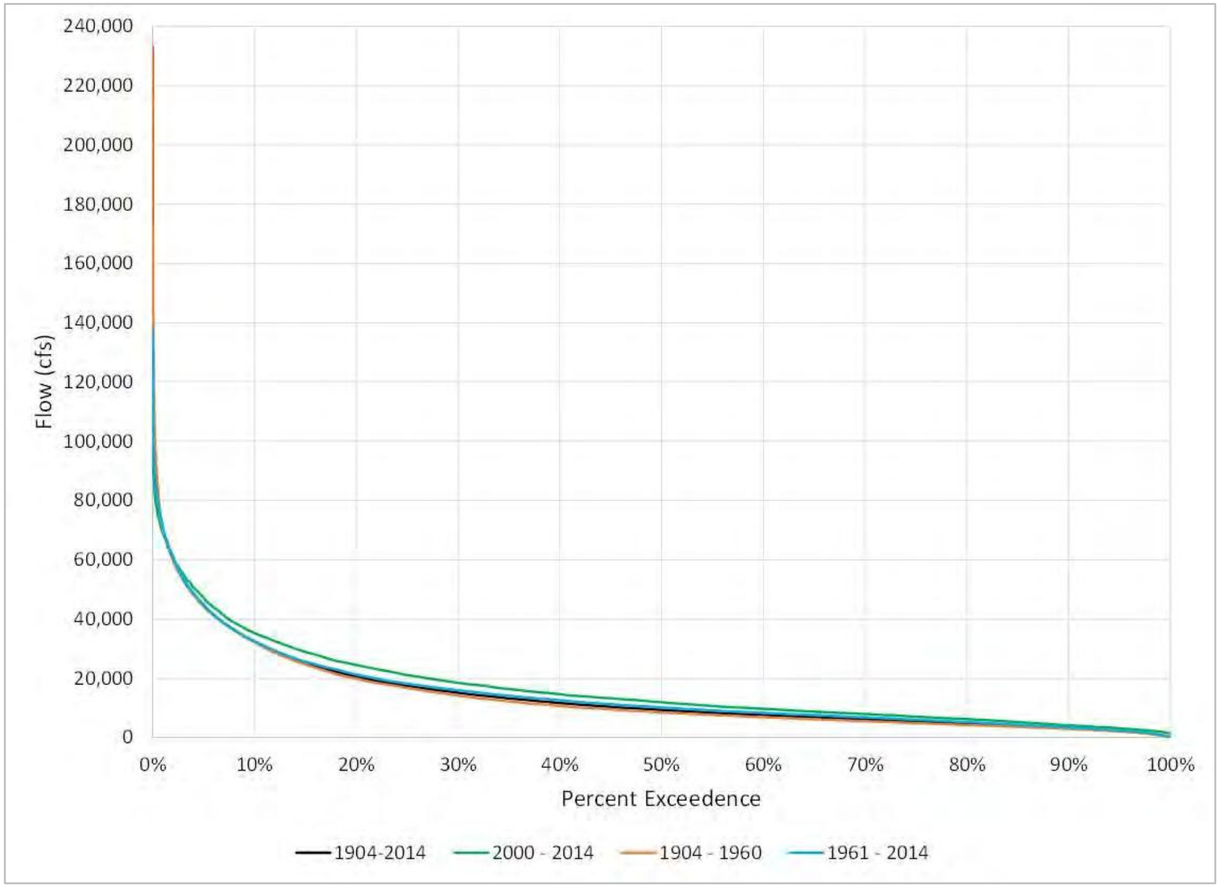

Figure 5.1.1-4: Flow-Duration Curves: Connecticut River at Montague, MA (USGS)

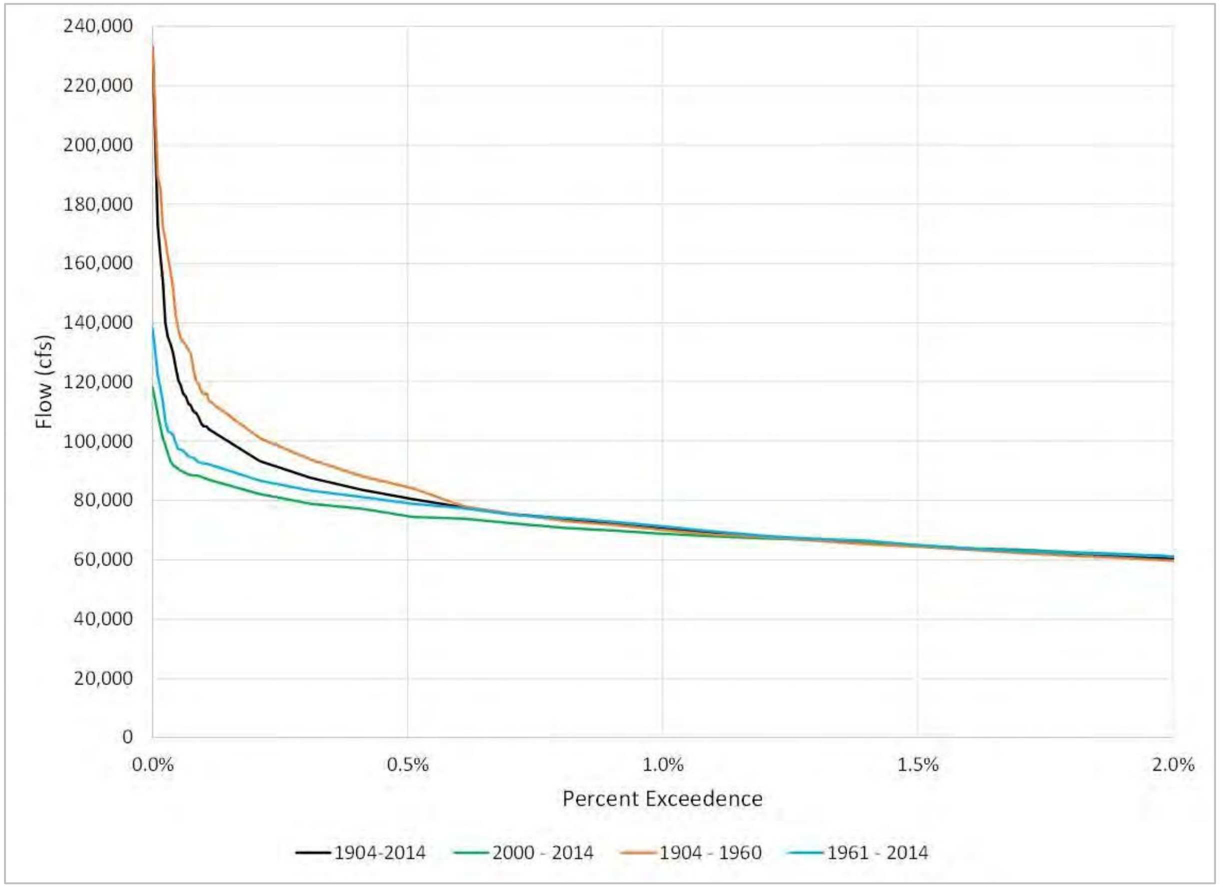

Figure 5.1.1-5: Flow-Duration Curves: Connecticut River at Montague, MA (USGS). 0 to 2 percent exceedance

5.1.2 Daily Flow Variations

The flow on the Connecticut River on a mean daily basis over an annual cycle is unsteady and highly variable. To further understand the variability of flow in the Connecticut River, an annual hydrograph based on the mean daily flow at the Montague USGS gage was developed for 2014 (Figure 5.1.2-1). In addition to the mean daily flow for 2014, the figure also shows the mean daily flow for the 2000-2014 period (note that for the 2000-2014 period all Jan 1, Jan 2, and Dec 31 mean daily flows were averaged to create a long term hydrograph). This hydrograph demonstrates the significant variability in flow over time with changes in flow ranging from a few thousand cfs to several tens of thousands of cfs occurring over relatively short periods of time (days to several days). The mean daily flow peaked at about 80,000 cfs in mid-April 2014. Many other peaks also occurred during 2014 including during late December at about 50,000 cfs and other flow events over 25,000 cfs at numerous other times through the year. During the summer and fall, the flow generally averaged less than 10,000 cfs. The 2014 hydrograph shows considerable variability in flow especially on a weekly basis due mostly to the variability of natural flows, which is typical for the Connecticut River.

Volume III (Appendix K) presents the annual hydrographs for the Connecticut River at Montague, MA from 2000 through 2014; Table 5.1.2-1 summarizes peak flow and variability of these annual hydrographs. The hydrographs from 2000 through 2014, as presented in Volume III and Table 5.1.2-1, typically show a primary peak along with multiple secondary peak flow events occurring each year. Over the period from 2000 through 2014 there were 88 peak flows exceeding 40,000 cfs. On average there were approximately 6 peak flow events greater than 40,000 cfs per year during this period but the number of peaks per year over 40,000 ranged from one in 2012 to 11 in 2006.

Table 5.1.2-1: Summary Mean Daily Annual Hydrographs of the Connecticut River at Montague, MA 2000-2014

Calendar Year	Mean Daily Peak Flow	Summer Maximum (June-Sept)	Comments
2000	66,600 cfs 12/18	Multiple summer peaks (2 > 30,000 cfs, 2 > 20,000 cfs)	Multiple secondary peaks in the spring (3 peaking at about 60,000 cfs, 1 > 50,000 cfs)
2001	88,300 cfs 4/24	One significant peak > 40,000 cfs in early June then primarily less than 10,000 cfs the rest of the summer	Other than the primary spring peak and one early summer peak, flow most of the rest of the year was less than 10,000 cfs
2002	68,200 cfs 4/16	One summer peak in early June > 45,000 cfs	A primary spring peak with two secondary spring peaks in the 40,000 to 50,000 cfs range
2003	80,500 cfs 10/30	One summer peak reaching about 30,000 cfs	Four secondary peaks over 50,000 cfs, one in the spring and three in the fall and early winter
2004	82,700 cfs 4/2	Only three peaks over 20,000 cfs, all in September	Three peaks over 40,000 cfs, two in the spring and one in December
2005	102,000 cfs 10/9	One peak in June just under 40,000 cfs	Multiple peaks in the spring and fall ranging from 50,000 to 90,000 cfs range
2006	81,600 cfs 1/19	Three early summer peaks over 30,000 cfs with one over 50,000 cfs	Numerous winter, spring, and late fall peaks over 40,000 cfs
2007	88,600 4/17	One summer peak in early June over 20,000 cfs	Two peaks over 50,000 cfs, one in January, one late March
2008	78,700 cfs 4/14	Two summer peaks > 50,000 cfs	Multiple spring and winter peaks over 40,000 cfs
2009	66,500 cfs 4/5	One summer peak over 50,000 cfs in early August	Two peaks over50,000 cfs, one in October and one in December
2010	74,300 cfs 3/31	No summer peaks over 20,000 cfs	An additional peak over 70,000 cfs in March and five peaks over 40,000 cfs in the fall and winter.
2011	118,000 cfs 8/29	Other than on 8/29, only one peak over 30,000 cfs, about 75,000 cfs on 9/8	One peak slightly over 80,000 cfs in April and numerous other peaks over 40,000 cfs in the fall, winter and spring
2012	42,100 cfs 4/24	Over than a peak slightly over 30,000 cfs in early June, no other peaks above 20,000 cfs	Several peaks over 30,000 cfs in the late fall, winter and spring.
2013	56,300 cfs 7/4	An additional peak over 50,000 cfs in mid-June	Five peaks over 40,000 cfs in the winter and spring
2014	79,200 cfs 4/17	Four peaks over 20,000 cfs, none over 30,000 cfs	Four peaks over 40,000 cfs in the winter and spring

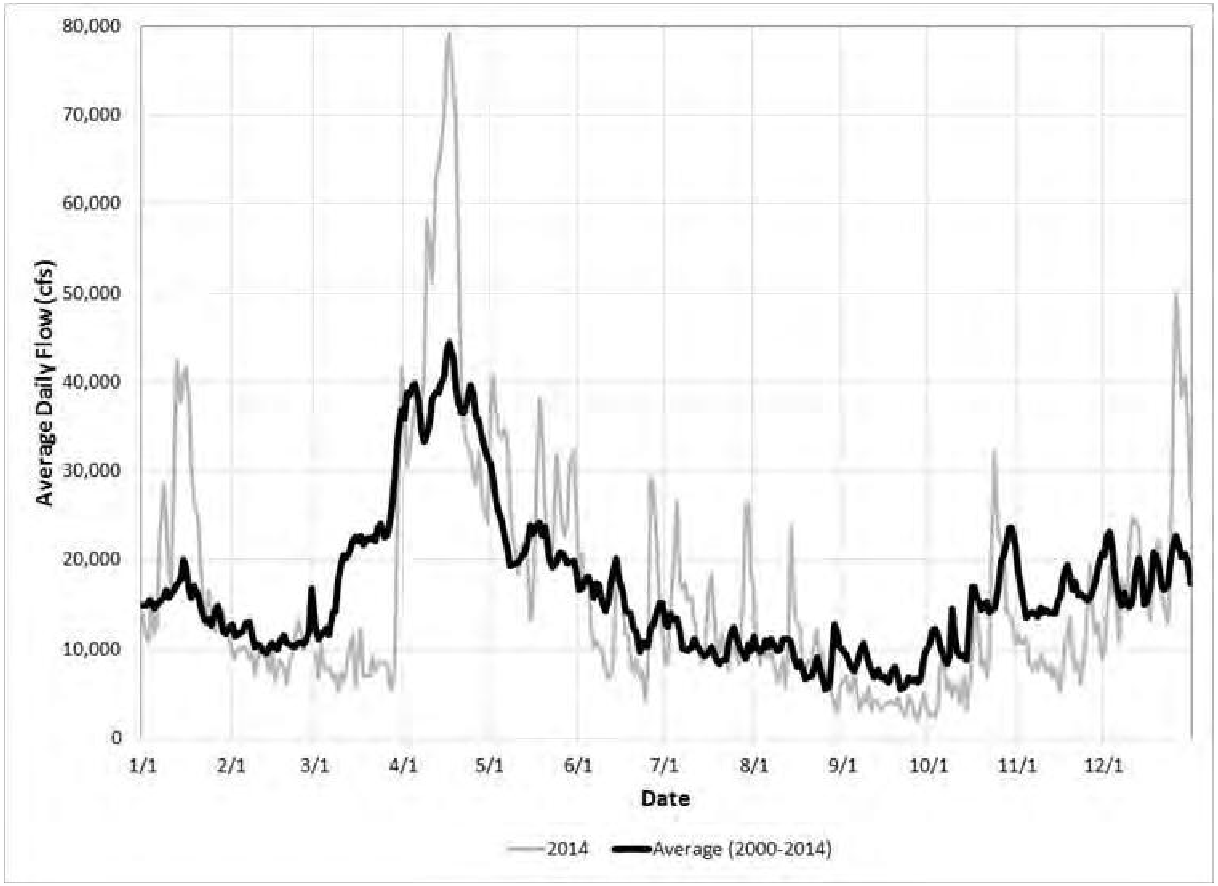

Figure 5.1.2-1: Annual Hydrograph 2014, Connecticut River at Montague, MA (USGS)

5.1.3 Hourly Flow and Water Level Fluctuations

Examination of mean daily flows reported by the USGS at the Montague Gage does not describe the intraday variability of flow on the Connecticut River, especially in the TFI. In order to more fully understand flow and water level variations examination of these data on an hourly time basis is required. Most dams on the Connecticut River having hydropower facilities operate as peaking generation facilities. Under inflow conditions below their generating hydraulic capacities, these facilities often store water in their impoundments on a daily cycle to allow them to generate additional electricity during portions of the day when the power demand and market prices increase. Table 5.1.3-1 provides an overview of the hydraulic capacity of the Vernon, Northfield Mountain, and Turners Falls Hydroelectric Projects.

The main source of inflow into the TFI is TransCanada's Vernon Hydroelectric Project, which normally operates as a peaking facility when inflows are low. The drainage area of the Connecticut River at Vernon Dam is 6,266 mi^2, the station has a total hydraulic capacity[34] of 17,130 cfs, and a minimum flow requirement of 1,250 cfs. The drainage area at Turners Falls Dam is 7,163 mi^2, 897 mi^2 larger than at Vernon Dam. Two main tributaries flow into the TFI, the Ashuelot River about 2 miles below Vernon Dam, and the Millers River, about 4 miles above Turners Falls Dam. Table 5.1.3-2 summarizes the two USGS gages on these tributaries. These gages capture most of the drainage area of the tributaries and 88% of the incremental drainage area between Vernon Dam and Turners Falls Dam.

Northfield Mountain uses the TFI as its lower reservoir and its tailrace, which is located about 5.2 miles upstream of the Turners Falls Dam. Northfield Mountain has 4 reversible pump/turbines that at maximum, can pump at 15,200 cfs or can discharge 20,000 cfs. The Upper Reservoir currently has a FERC maximum usable storage capacity of 12,318 acre-ft. Given this, the Project can pump at maximum capacity for 9.8 hours and generate at maximum capacity for 7.5 hours; however, in reality, the Project rarely pumps or generates at its maximum capacity or utilizes all of the Upper Reservoir volume in a single day.

FirstLight's current FERC license allows the TFI water level to be fluctuated within a 9-foot band between a minimum water surface elevation of 176 and a maximum of 185 ft. NGVD 1929[35], as measured at the Turners Falls Dam. This 9-foot water level fluctuation provides about 16,150 acre-ft. of storage, if fully utilized; however, FirstLight rarely fluctuates the TFI by more than 4 feet in a day even though the TFI acts as the lower reservoir for Northfield Mountain and the headpond for the power canal (which leads to the generation facilities at Station No. 1 and Cabot Station). During normal operations when inflow to the TFI is less than about 17,000 cfs, FirstLight manages the water surface elevation and storage in the TFI to limit spillage at the Turners Falls Dam while allowing efficient generation and pumping cycles at Northfield Mountain and generation at the Turners Falls Project. The combined hydraulic generation capacity of Vernon and Northfield Mountain is 37,130 cfs, much greater than the Cabot and Station No. 1 combined hydraulic generation capacity of 15,938 cfs. Therefore, FirstLight normally operates the TFI water surface elevation such that by early to mid-morning the water surface elevation is at a low for the day after pumping associated with Northfield Mountain. Based on hourly data, the median water surface elevation at the Turners Falls Dam is 181.3, but the normal daily variations in the water level in the TFI downstream of French King Gorge is between 1 and 3 feet. During times when the naturally routed inflow to the TFI is above 30,000 cfs, an agreement between the USACE and FirstLight requires that the water surface elevation at the dam be lowered (but not below an elevation of 176 ft.) to limit flooding upstream of the dam.

As discussed in the March 2015 report for Relicensing Study No. 3.2.2 *Hydraulic Study of Turners Falls Impoundment, Bypass Reach, and Below Cabot* (the Hydraulic Study), at higher flows (i.e., above 30,000 cfs) the natural constriction at the French King Gorge becomes a hydraulic control affecting water levels in

---

[34] Hydraulic capacity is the maximum flow that can be run through the turbines to generate electricity. Flow greater than this magnitude is discharged over the spillway.

[35] All elevations mentioned in Section 5.1 reference the vertical datum NGVD 1929 (US Feet)

the mid and upper sections of the TFI. Therefore at higher flows, the effects of water level management at the Turners Falls Dam by FirstLight becomes much less of a controlling influence of the water surface elevations in the middle and upper parts of the TFI (FirstLight, 2015b).

As part of the hydraulic modeling associated with this study, FirstLight modeled 15 years (January 1, 2000 to December 31, 2014) of inflow and operational data to develop historical water levels throughout the TFI. Figure 5.1.3-1 provides the elevation duration curves for five key locations within the TFI. This figure does not show the extreme highest water levels reached during this time period such as a peak elevation at the Vernon Tailrace of 204.58 ft during Tropical Storm Irene in August of 2011 or the water levels during the shutdown of Northfield Mountain from May to November 2010.

Flow fluctuations on a fifteen minute basis are shown in Figure 5.1.3-2 from the Vernon Hydroelectric Project, Northfield Mountain Project, prorated inflow from the Ashuelot and Millers Rivers, and the corresponding water level at the Turners Falls Dam during a 10 day period from August 24, 2014 to September 3, 2014. This period represents a low flow period, typical Vernon peaking operations, and typical Northfield Mountain operations. At Vernon, peaking power flow releases of normally 6,000 to 10,000 cfs typically started in the early afternoon and continued into the early evening before dropping down to slightly below 2,000 cfs. During this time period inflow from the Ashuelot and Millers Rivers was low and stable and normally in the 200 to 300 cfs range. Northfield Mountain was active with pumping starting normally around midnight and continuing until about 8 am at rates between 10,000 and 15,000 cfs. Generation at Northfield Mountain normally started at about 11 am and continued until early evening. The water level at the Turners Falls Dam showed the effects of the inflow from Vernon, with a travel time delay and a quicker response to pumping or generation at Northfield Mountain. Not shown on this graph is the varying water releases to the power canal which ranged from a minimum flow of about 3,000 cfs to maximum peaking releases often over 10,000 cfs, generally in a similar timeframe as Vernon.

From 2012 to 2015, FirstLight had 10 or more water level recorders throughout the TFI for use in numerous relicensing studies. Figure 5.1.3-3 provides a plot of 10 water level recorders for the same time period as shown in Figure 5.1.3-2 (August 24 to September 3, 2014). The water level data show the variations in water level associated with peaking power operation flow releases from the Vernon Hydroelectric Project combined with the peaking power operations at the Turners Falls Dam and Northfield Mountain. As seen in Figure 5.1.3-3, there is a hydraulic control upstream of Stebbins Island which prevents the water level near Vernon Dam from falling below an elevation of about 181.3 even under low flow conditions from Vernon and low TFI levels. The magnitude of water level fluctuations at all 10 locations shown on Figure 5.1-3-3 is about 3.5 feet on most of the days.

During moderate to high flow events hydroelectric generation operations shift from a peaking power operation mode to a run-of-river mode as the flow exceeds the hydraulic capacity of the power plants at Vernon Dam and Turners Falls (17,130 cfs at Vernon and 15,938 cfs at Turners Falls). Flows in excess of the generating capacity are discharged at the dams. During high flow periods in excess of 30,000 cfs, per an agreement with the USACE, FirstLight lowers the water level at the Turners Falls Dam (but not below El. 176) to limit high water in the Barton Cove area and to a lesser extent, the middle section of the TFI. If we consider the hydraulic capacity of Vernon Dam as approximately 17,000 cfs at the upstream end of the TFI and that Northfield Mountain can provide an additional 20,000 cfs, flows in excess of 37,000 cfs can be considered "natural" high-flow events in the lower impoundment. At flows above 65,000 cfs as per an agreement with the USACE, if Northfield Mountain is operating, the combined usable volume of the Upper Reservoir and the TFI is required to be kept constant in order to limit discharges from Northfield Mountain adding to the outflow from Turners Falls Dam. As a result of this agreement, if Northfield Mountain is operating during such high flows the hydrologic effect in the TFI is minor.

An example of a recent moderate to high flow event occurred during April 2014 when flow in the Connecticut River exceeded the hydraulic capacity at both Vernon and Turners Falls Dams and peak discharge from Vernon reached almost 70,000 cfs. As shown in Figure 5.1.3-4, the discharge at Vernon on April 18 was about 65,000 cfs, falling to about 25,000 cfs by April 27. Figure 5.1.3-4 provides the water surface elevations during this time period at 6 locations within the TFI. As demonstrated in the figure, at higher flows the hydraulic constriction at French King Gorge, about 3 miles upstream of the Turners Falls Dam, limits the effect of the water level at the dam on the water level at the middle and upper portions of the TFI. For example, at a Vernon discharge of 62,000 cfs, the water surface elevation at Vernon Tailrace was about 198.5 ft, about 192.0 ft at the Rt. 10 Bridge, and about 190.0 ft at the Northfield Tailrace, while the water elevation at the Turners Falls Dam was about 181.0 ft.

Table 5.1.3-1: Hydraulic Capacities of the Vernon, Northfield Mountain, and Turners Falls Hydroelectric Projects

Project Name	Hydraulic Capacity (cfs)
Vernon	17,130
Northfield Mountain (Pumping)	15,200
Northfield Mountain (Generating)	20,000
Turners Falls	15,938

Table 5.1.3-2: USGS Gage Information of the Ashuelot and Millers Rivers

Gage No.	Gage Name	Period of Record	Gage Drainage Area	Total River Drainage Area
01161000	Ashuelot River at Hinsdale, NH	1907-current	420 mi^2	420 mi^2
01166500	Millers River at Erving, MA	1915-current	372 mi^2	390 mi^2

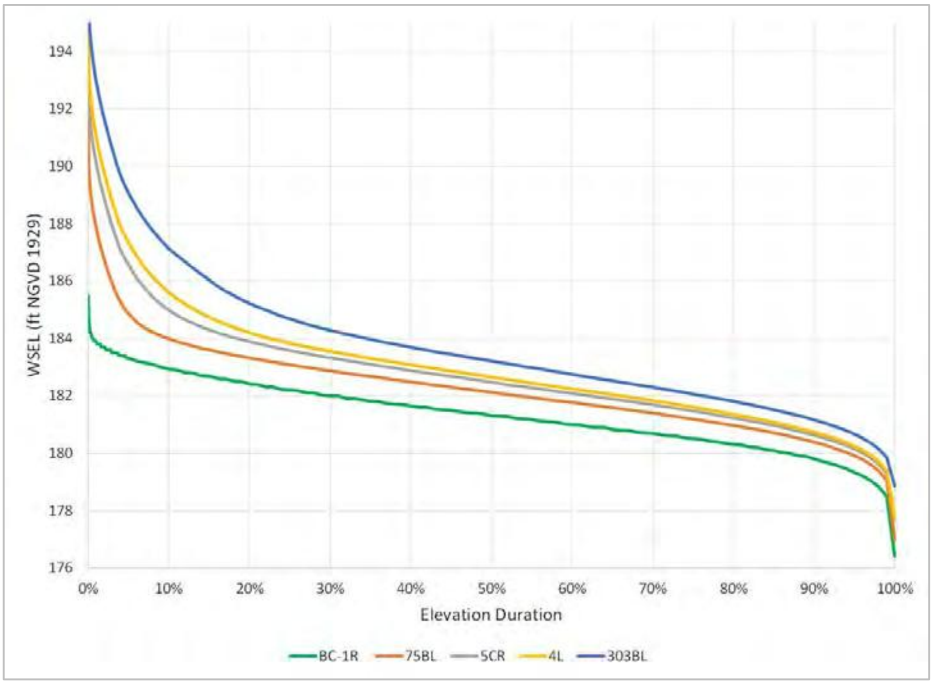

Figure 5.1.3-1: Elevation Duration Curves within the Turners Falls Impoundment (2000-2014)

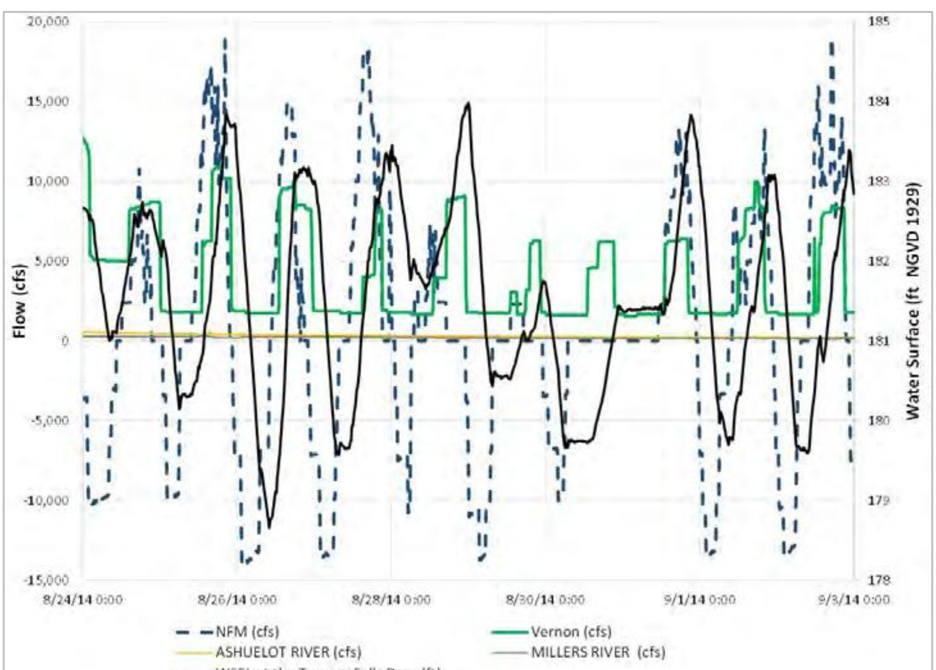

Figure 5.1.3-2: Turners Falls Impoundment Conditions for August 24 – September 3, 2014

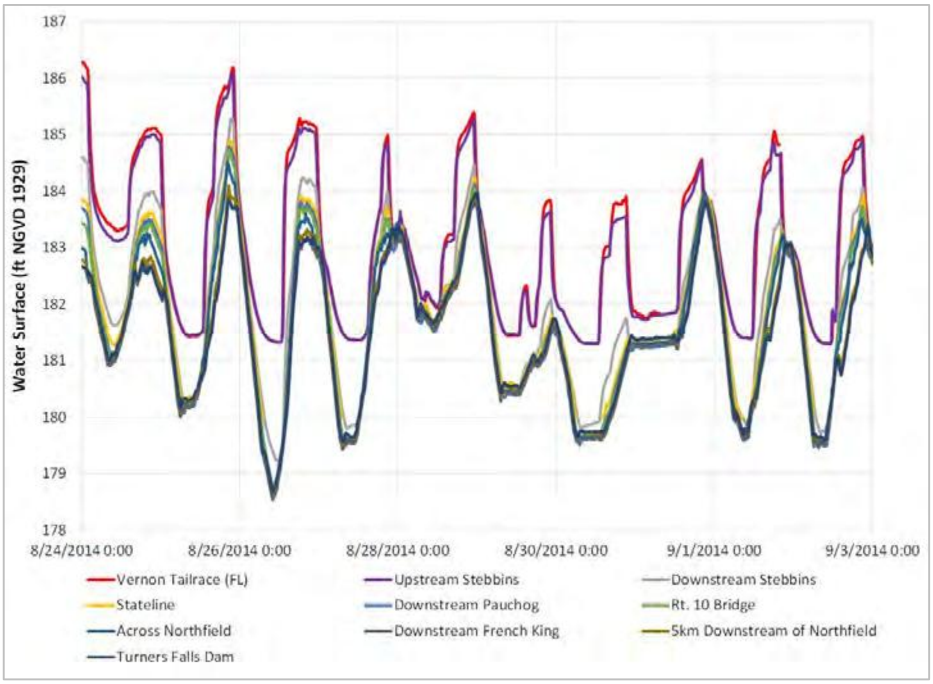

Figure 5.1.3-3: Turners Falls Impoundment Water Surface Elevations for August 24 – September 3, 2014

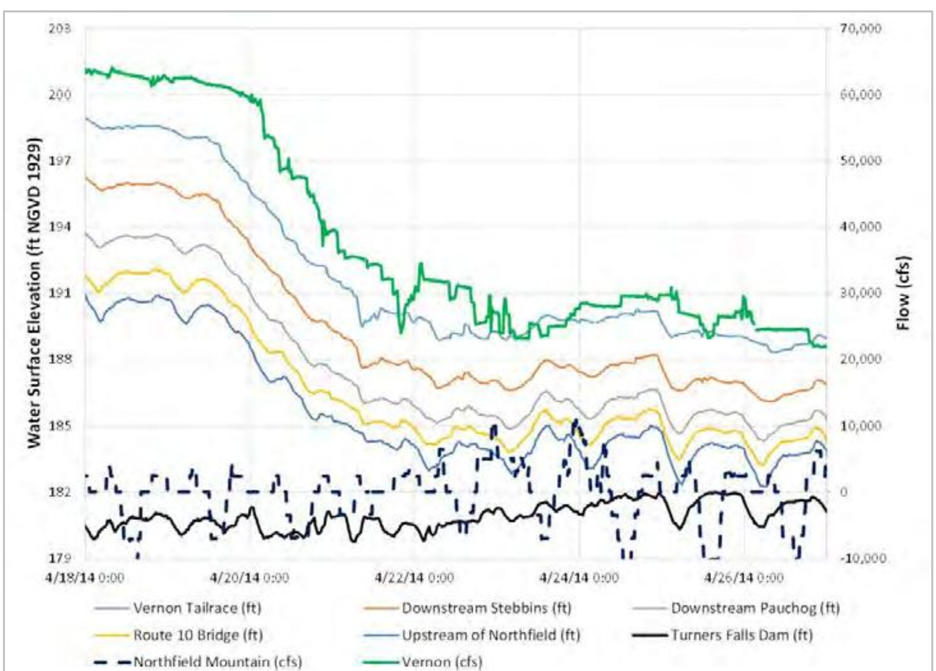

Figure 5.1.3-4: Turners Falls Impoundment Water Surface Elevations for April 18-27, 2014

Location and Duration of Hydraulic Forces

Discussion in this section focuses on the location and duration of hydraulic forces, or more specifically, on the duration at which various water surface elevations are equaled or exceeded and the corresponding location of the water surface relative to bank position.

As noted in USACE (1979), the forces acting on the bank can be broken into two categories: (1) those acting near the surface of the flow, and (2) those acting with the greatest intensity nearer the bottom of the submerged banks. Figures 5.1.3-5 through 5.1.3-7 present examples of this dynamic. Given that erosion processes associated with (1) hydraulic shear stress due to flowing; (2) water level fluctuations due to hydropower operations; (3) boat waves; and (4) ice occur at and below the water surface it is vital to understand where on the riverbank the water surface rests and for what duration.

TFI riverbanks are typically characterized by a lower and upper riverbank. The lower bank is typically a flat, beach-like feature that is submerged or experiences daily water level fluctuations during low to moderate flows as a result of hydropower peaking operations. Depending on its location in the TFI, the lower bank may or may not be vegetated. As one moves away from the normal edge-of-water, the lower bank transitions to an upper bank; the toe of which is clearly identifiable on most cross-section plots. The upper bank is typically steep, has some degree of vegetation, and is usually above the water surface except during high flows. Figure 5.1.3-8 provides an example of a typical TFI lower and upper bank configuration.

The distinction between the lower and upper bank is an important one given that the BSTEM modeling results and the results of the supplemental analyses found that forces acting at the water surface and along the submerged banks typically do not cause erosion at lower flows and minimal erosion at moderate flows when the water surface rests on the lower bank (i.e., below the toe of the upper bank). It is not until the water surface rises and rests on the upper bank during high flow events that riverbank erosion potentially commences; even then the flow threshold to initiate erosion was found to be greater than 37,000 cfs at the majority of detailed study sites.

Although peaking hydropower operations can result in water level fluctuations up to 4 feet over the course of a day, during low to moderate flow periods the water surface typically rests on the lower bank. To determine the amount of time the TFI water surface rests on the lower bank vs. the upper bank a water level duration analysis was conducted at a subset of the 25 detailed study sites. The 5 sites chosen spanned the geographic extent of the TFI, were located in areas with varying hydraulic characteristics, and were found to be representative of the other sites in proximity to them. The results of this analysis found the following:

- At Site BC-1R (at HEC-RAS transect 3518), the water surface rests on the lower bank (defined as that portion of the bank below El. 184.0) 99% of the time;
- At Site 75BL (at HEC-RAS transect 25845), the water surface rests on the lower bank (defined as that portion of the bank below El. 184.0) 90% of the time;
- At Site 5CR (at HEC-RAS transect 56235), the water surface rests on the lower bank (defined as that portion of the bank below El. 184.0) 82% of the time;
- At Site 4L (at HEC-RAS transect 72416), the water surface rests on the lower bank (defined as that portion of the bank below El. 184.0) 78% of the time; and
- At Site 303BL (at HEC-RAS transect 93012), the water surface rests on the lower bank (defined as that portion of the bank below El. 185.0) 79% of the time

As observed above, the water level rests on the lower bank the vast majority of the time at all locations, however, as one moves upstream the water level rests on the lower bank less than in the downstream reaches.

The relationship between location in the TFI and the duration of which the water level rests on the lower bank is a result of the TFI becoming more riverine as you move in the upstream direction. Figure 5.1.3-1 demonstrated the results of the water-level duration analysis at each location previously mentioned.

To further understand the location and duration of hydraulic forces on the bank, stage-discharge relationships were developed at the same sites where the water level duration analyses were conducted to determine at what flow the water surface reaches the upper bank. TFI flow duration curves for the individual locations based on hourly data for the period 2000-2014 were then analyzed to determine the percent of time flows of that magnitude occur in the TFI. The results of this analysis found:

- At Site BC-1R, the water surface is largely a function of the water level as controlled by FirstLight at the Turners Falls Dam, so there is not a distinct stage vs discharge relationship in this part of the TFI;
- At Site 75BL, where the water level can still be a function of the Turners Falls Dam water surface elevation, the water surface generally reaches the upper bank at flows of about 32,000 cfs or greater. This flow is equaled or exceeded about 10% of the time;
- At Site 5CR, the water surface reaches the upper bank at flows of about 23,000 cfs or greater. This flow is equaled or exceeded about 18% of the time;
- At Site 4L, the water surface reaches the upper bank at flows of about 17,000 cfs or greater. This flow is equaled or exceeded about 22% of the time; and
- At Site 303BL, the water surface reaches the upper bank at flows of about 17,500 cfs or greater. This flow is equaled or exceeded about 21% of the time

Figure 5.1.3-9 demonstrates the generalized stage-discharge relationships developed at each site other than BC-1R. At lower elevations at these four sites, the observed and modeled stage storage graph is a scatter plot due to the influence of the water surface elevation at Turners Falls Dam. Figures 5.1.3-10 and 5.1.3-11 depict the flow duration curve for the four sites for the period 2000-2014. These figures show that the high flow regime is very similar at all four sites; however, at flows below about 20,000 cfs there is more of a variation in the flow regime at 75BL (near Northfield Mountain) due to the effects of pumping and generation cycles.

The final step in this analysis was to compare the upper bank flow and water level analysis against the 95% erosion flow threshold (i.e., the flow above which 95% of all erosion occurs at a given site) derived from the BSTEM modeling results at each site (discussed later in the report). The 95% erosion flow threshold for each site was then compared against the flow duration curve to determine the amount of time that flow may be equaled or exceeded. To provide context, the corresponding water surface elevation for the erosion threshold was compared against the elevation of the toe of the upper bank. This analysis found:

- At sites 75BL, 5CR, and 303BL the 95% erosion flow threshold is near or exceeds the natural high flow threshold (37,000 cfs for Sites 75BL and 5CR, 17,130 cfs for Site 303BL), the water surface elevation rests at, or several feet above, the toe of the upper bank, and the percent of time the 95% erosion flow threshold is exceeded is less than 10% (7%, 4%, and 3%, respectively);
- While the 95% erosion flow threshold is noticeably lower at site 4L (~7,000 cfs), the 50% erosion flow threshold (i.e., the flow above which the majority of erosion occurs at a given site) is about 83,500 cfs which equates to a water surface elevation of 195 and is exceeded <1% of the time, however at this site the calculated erosion is very low (0.017 $ft^3/ft/y$); and

- Analysis of BC1-R was not possible given that a reliable stage-discharge relationship could not be developed for this location.

The results of the analyses discussed above are summarized in Table 5.1.3-3. As observed in the table, and to summarize, the water level rests on the lower bank the vast majority of the time. The period of time in which the water surface rests on the lower bank also coincides with the periods when Vernon, Northfield Mountain, and/or Turners Falls are typically operating in a peaking mode (i.e. low and moderate flow periods). This is significant given that the majority of erosion in the TFI only occurs once the water level reaches the upper bank. Furthermore, the 95% erosion flow threshold is near or exceeds the natural high flow threshold at three of the five sites and only occurs 3-7% of the time at those sites.[36] This finding is consistent at the majority of sites throughout the TFI. The results from this analysis clearly indicate: (1) the importance of the water surface elevation and its corresponding location on the bank; (2) the importance of the duration of those water surface elevations; and (3) that the window for the majority of erosion to occur is quite small and well beyond the flows at which hydropower operations have an impact on flow or water level.

Table 5.1.3-3: Detailed Study Site Hydrologic Analysis

Detailed Study Site	Toe of Upper Bank – El.*	Water Level Duration		Flow to Reach Upper Bank (cfs)	% Time Flow is Exceeded	95% Erosion Flow Threshold (cfs, from BSTEM)	% Time Threshold Flow is Exceeded	Corresponding Threshold WSEL
		% Time on Lower Bank	% Time on Upper Bank					
BC-1R	184	99	1	NA	NA	I	NA	NA
75 BL	184	90	10	32,000	10	33,800	7%	184
5CR	184	82	18	23,000	18	47,900	4%	188
4L	184	78	22	17,000	22	7,000	60%	181
303BL	185	79	21	17,500	21	53,200	3%	192

*NGVD29, Feet I = Indeterminate

[36] The exception to this is Site 4L where the 95% flow threshold is 6,991 cfs. Further examination of this site indicates that the average rate of annual erosion is 0.017 ft^3/ft/yr., making it the third lowest rate of erosion of all sites in the TFI. Although the 95% flow threshold at this site is very low, it is a product of how little erosion is actually occurring. By contrast, the 50% erosion flow threshold at this site was found to be 83,527 cfs which equates to a water surface elevation of El. 195, exceeded <1% of the time. It should also be noted that the erosion flow threshold at site BC-1R could not be established given that a reliable relationship between stage and discharge could not be developed in the Barton Cove area.

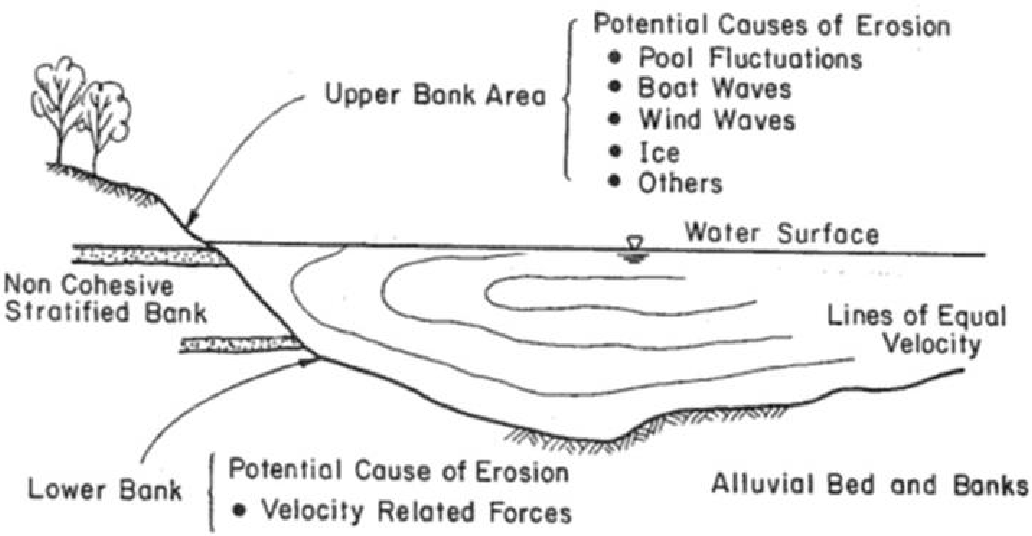

Figure 5.1.3-5: Assumed Initial Channel Conditions (USACE, 1979)

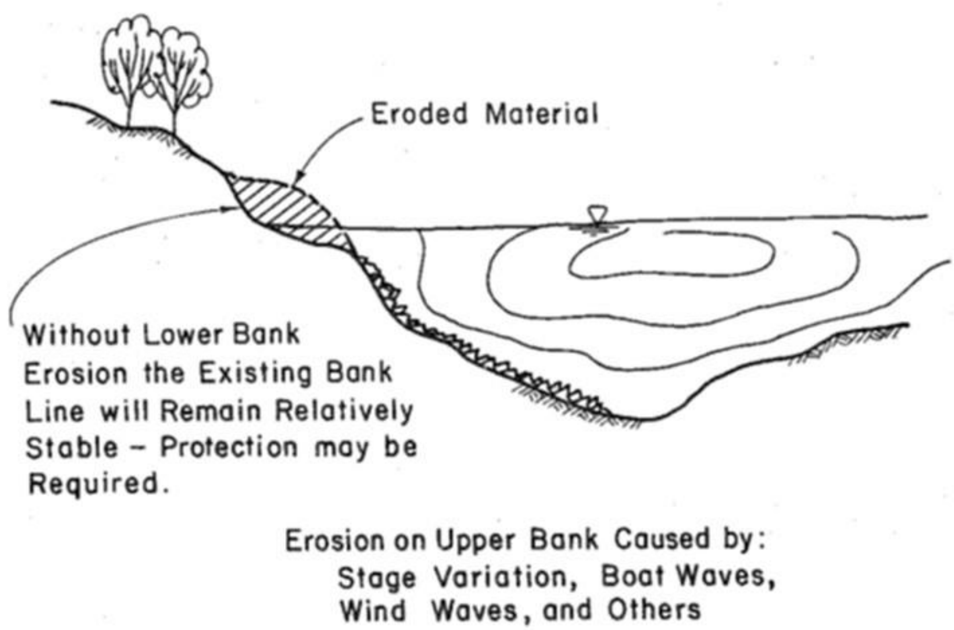

Figure 5.1.3-6: Potential Bank Line Geometry by Erosive Force Acting on the Bank near the Water Surface (USACE, 1979)

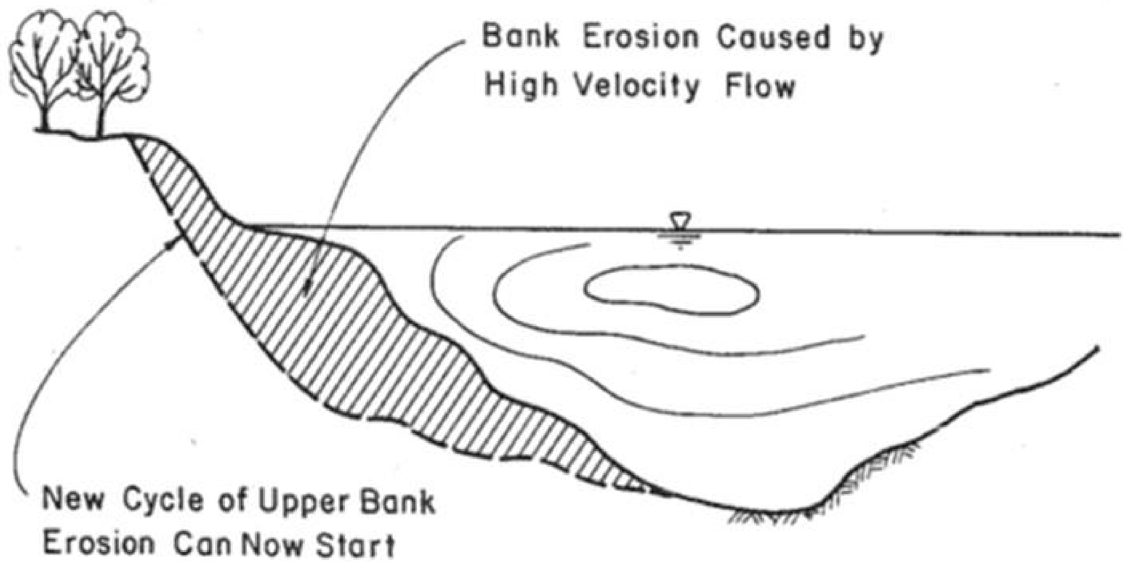

Figure 5.1.3-7: Bank Erosion Caused by Flood Stage High Velocity Flow (USACE, 1979)

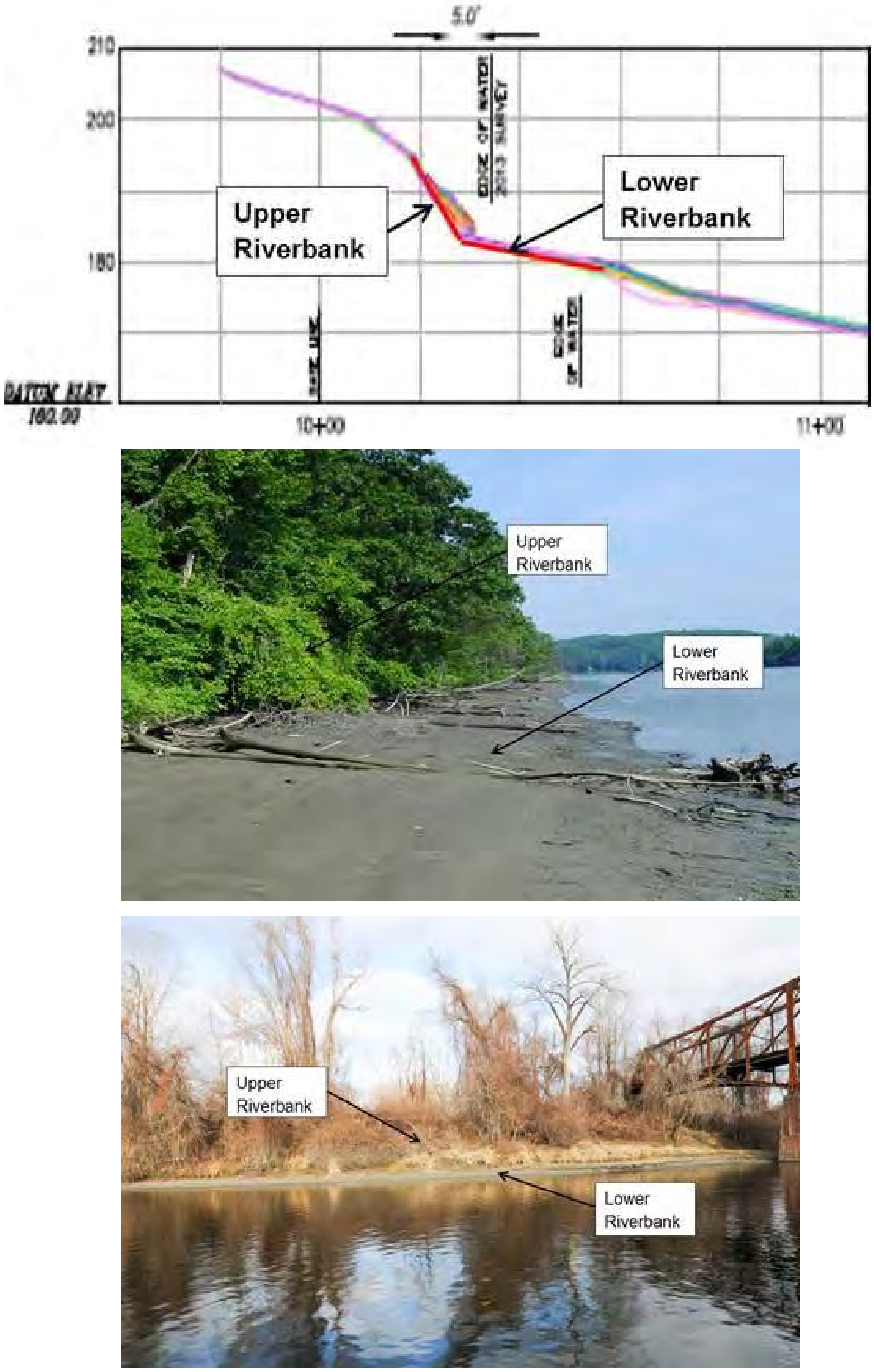

Figure 5.1.3-8: TFI Lower and Upper Riverbank Example

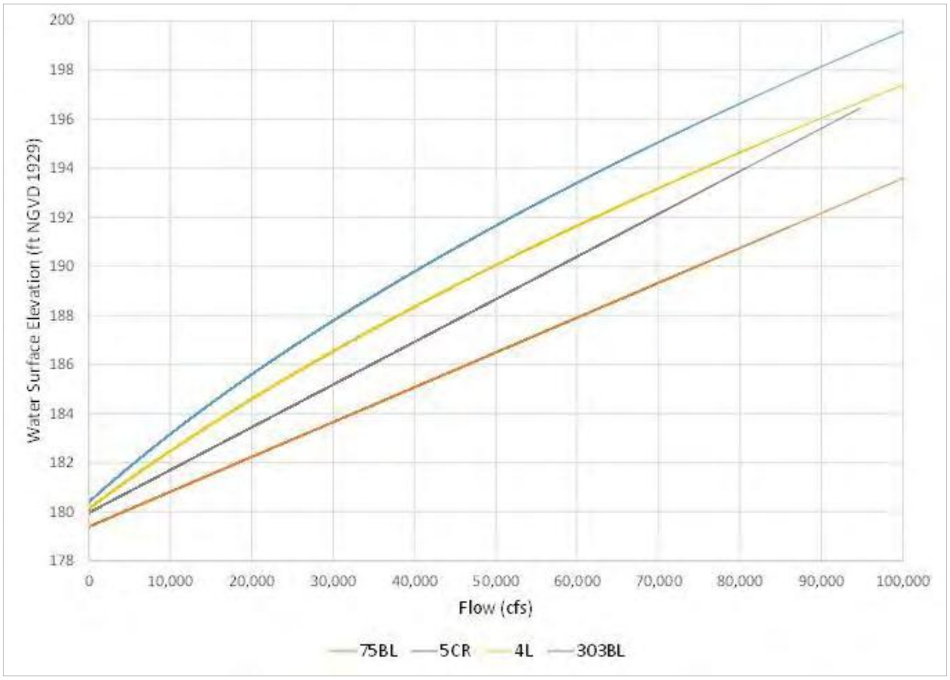

Figure 5.1.3-9 Generalized Stage vs Discharge Trendlines for 75BL, 5CR, 4L, and 303BL

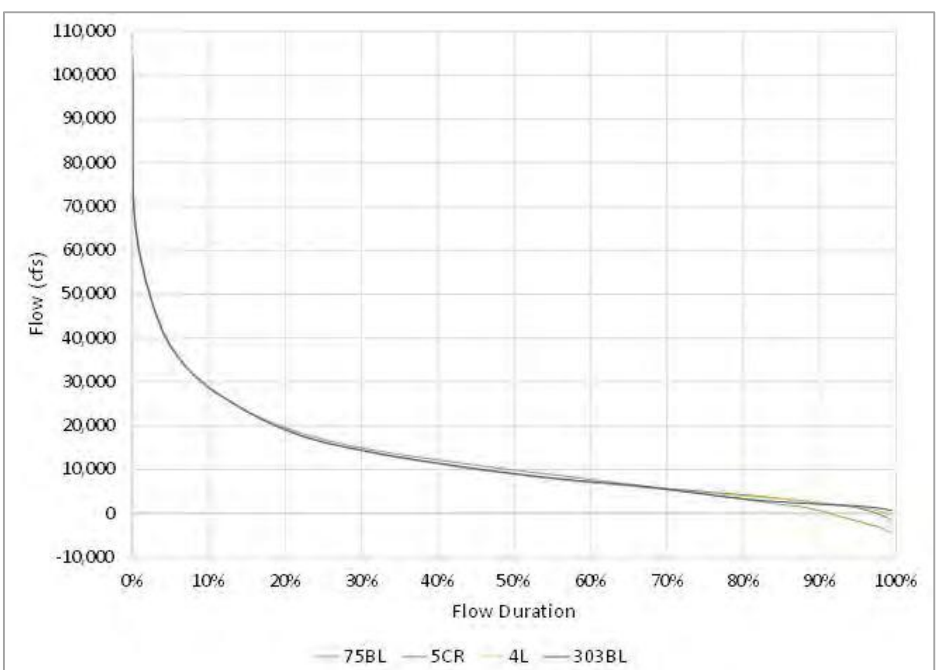

Figure 5.1.3-10 Flow Duration Curves for 75BL, 5CR, 4L, and 303BL

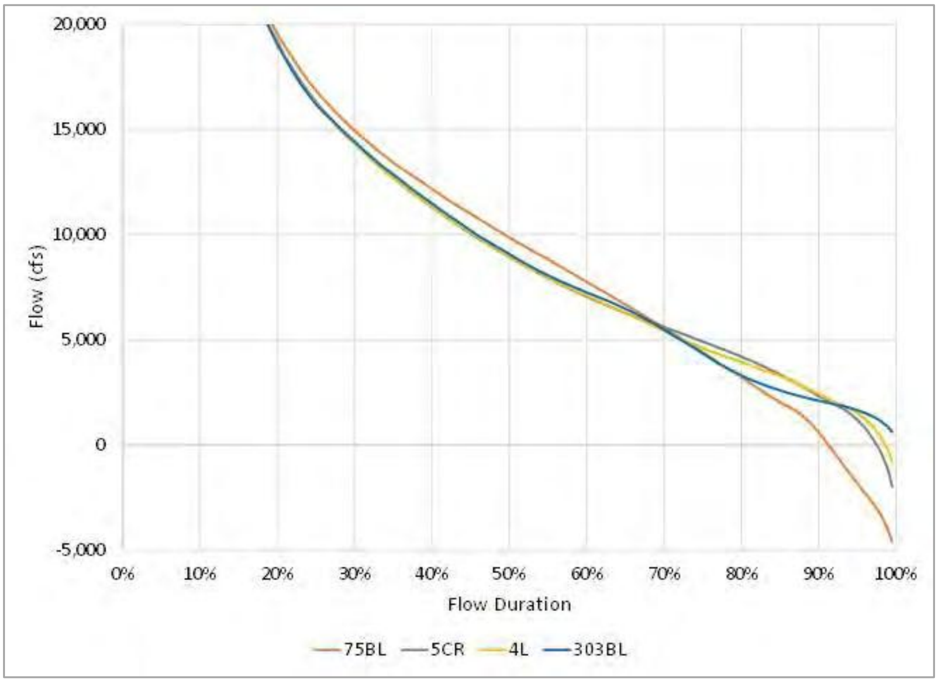

Figure 5.1.3-11 Zoomed in Flow Duration Curves for 75BL, 5CR, 4L, and 303BL

5.1.3.1 Hydrologic Effect of Northfield Mountain Operations

In order to understand the effect Northfield Mountain operations have on flow and water level fluctuations in the TFI, a number of historic time periods and modeled operational scenarios were analyzed. As presented below, analysis focused on two flow thresholds, (1) when the daily average inflow from Vernon Dam was below 18,000 cfs, and (2) when the daily average inflow from Vernon Dam exceeded 18,000 cfs. During these time periods the corresponding Project operations were investigated and the hydrologic effect at a number of detailed study sites was determined.

The low to moderate flow threshold (i.e., <18,000 cfs) was chosen as it represented a flow value just above the hydraulic capacities of Vernon (17,130 cfs) and Turners Falls (15,938 cfs) that would also take into consideration typical inflow from the Ashuelot and Millers Rivers. The moderate to high flow threshold (i.e., >18,000 cfs) was chosen as it represents conditions when Vernon operates in run-of-river mode (i.e., inflow equals outflow) and, as flow increases, the French King Gorge becomes the hydraulic control for the mid and upper TFI, as opposed to water level management at the Turners Falls Dam.

Flow and water level fluctuations during these flow periods were analyzed at the same subset of detailed study sites previously discussed, including:

- BC-1R: entrance to Barton Cove – low to moderate flow analysis only
- 75BL: just downstream of the Northfield Mountain tailrace
- 5CR: just downstream of the Rt. 10 Bridge
- 4L: downstream of the Pauchaug Boat Launch
- 303BL: between Upper Island and Stebbins Island

The transects associated with these detailed study sites were chosen as they covered the geographic extent of the TFI and were each located near one of the three hydropower projects on the TFI. Given that the results of the hydraulic model indicate that the French King Gorge becomes the hydraulic control for the mid and upper portion of the TFI at flows greater than 30,000 cfs (and potentially as low as 20,000 cfs), this analysis was not conducted at Site BC-1R for the moderate to high flow analysis.

Finally, it is important to reiterate that the flow thresholds used for this analysis refer to the inflow from Vernon and not the total TFI flow (i.e., without flow associated with Northfield Mountain operations). Depending on Northfield Mountain operations and the location in the TFI, the total flow can vary by as much as -15,200 cfs during pumping operations or +20,000 cfs during generation. For example, the inflow from Vernon at a given time could be 18,000 cfs, however, if Northfield Mountain is generating with 4 units the flow at site 75BL at that same time could be 38,000 cfs. This distinction will be important to remember when reviewing the BSTEM results found in Section 5.4.

Low to Moderate Flow Analysis (<18,000 cfs)

Northfield Mountain was not operational from May to November 2010 to allow for sediment removal in the Upper Reservoir. Examination of the modeled TFI water surface elevations during this time allows FirstLight to estimate the effects of water level variation within the TFI without Northfield Mountain's pumping and generation cycles. Although this analysis provides an idea of the effects of Northfield Mountain operations on flow and water level fluctuations during low flow conditions, it should be noted that also during this time FirstLight was not managing the water level at Turners Falls Dam as they typically would. That is, typical water level management at the Turners Falls Dam is based partially on Northfield Mountain's likely operational schedule. Figure 5.1.3.1-1 provides a representative time period (late June to early August) in 2010 with Vernon's inflow and modeled water surfaces at 5 detailed study sites in the TFI. This graph shows that Vernon's base flow was about 2,000 cfs, peaking flow normally about 8,000 cfs with water level variation in the TFI normally about a foot per day.

In order to compare the May through November 2010 period when Northfield Mountain was not operational, the Vernon hydrologic and generation records were reviewed to find a similar May through November period. Upon review of the available information, the May to November 2012 period appeared to be similar to the 2010 period in terms Vernon generation and flow average. Table 5.1.3.1-1 provides a comparison of the monthly generation and flow values from Vernon for the May-November period for 2010 and 2012. While the correlation shown in Table 5.1.3.1-1 is not exact it is as close as was possible for recent years that are representative of current operations at Northfield Mountain. In addition to the monthly average generation and flows from Vernon, FirstLight also investigated if the mean daily flow, as measured at the Montague gage was similar for 2012 as it was for 2010 during the May-November time period. Figure 5.1.3.1-2 shows that similar to 2010, the daily flow at Montague was generally lower than average and other than in May and October, the 2010 and 2012 periods lacked the peak flows in the summer and higher than average flow periods that were common in 2008, 2009, 2011, 2013, and 2014. Based on these factors the 2012 period was used as a comparison.

Figure 5.1.3.1-3 provides an example of the flows from Vernon and Northfield Mountain and modeled water surface elevations at the 5 transects for July 20 – August 8, 2012, a low inflow period. This figure shows that daily water surface elevation fluctuations were about 3 feet on most days.

The hourly TFI water surface elevations from HEC-RAS were then used to analyze the maximum daily water surface elevation variation in the TFI at the five detailed study sites for the May to November 2010 and 2012 periods. In addition, two other periods were analyzed: (1) the entire period of record (2000-2014) other than May 1 – October 31, 2010, and (2) the entire period of record (2000-2014) other than May 1 – October 31, 2010 when the mean daily flow was less than 18,000 cfs from Vernon. The additional analysis using the full period of record were conducted to provide context. Given this, four datasets were analyzed for this analysis:

- The entire period of record (2000-2014) other than May1-Oct 31, 2010;
- The entire period of record (2000-2014) other than May 1-October 31, 2010 but only when the mean daily flow was less than 18,000 cfs from Vernon;
- The May 1 – October 31, 2010 period when the mean daily flow was less than 18,000 cfs from Vernon; and
- The May 1 – October 31, 2012 period when the mean daily flow was less than 18,000 cfs from Vernon.

18,000 cfs was chosen as the divider since it is slightly over the maximum generation capacity at Vernon (thus accounting for some inflow from the Ashuelot and Millers Rivers) and at those levels both the Vernon and Turners Falls Projects would be operating as a run of river. Only 18 days in the May 1 – October 31, 2010 period had a mean daily Vernon discharge above 18,000 cfs and 15 days in the same period in 2012. Figures 5.1.3.1-4 through 5.1.3.1-8 provide plots of how common the range of daily water surface elevation variations (at 0.4' intervals) are at the five transects. These plots show a similar general relationship for the daily extent of water surface elevation fluctuation at all 5 locations. For example, at 75BL near Northfield Mountain when the Vernon daily average flow is less than 18,000 cfs Figure 5.1.3.1-5 shows:

- For the May – November 2010 period: 60% of the daily WSEL variations were less than 0.8 feet, and 95% were less than 1.6 feet;

- For the May – November 2012 period: 20% of the daily WSEL variations were less than 1.6 feet and about 95% were less than 3.6 feet; and

- For all of the days (other than May – November 2010) that were modeled: 15% of the daily WSEL variations were less than 1.6 feet and about 95% were less than 4.0 feet.

As shown on the figures, when comparing the 95% value at each location for the 2010 and 2012 periods the combined effect of Northfield Mountain operations and Turners Falls Dam water level management accounts for approximately a 2 ft. fluctuation in water levels at the 5 detailed study sites.

Figure 5.1.3.1-9 provides a frequency curve for daily water surface elevation variation at 75BL near Northfield Mountain for days when Vernon had a mean daily flow of less than 18,000 cfs and over 18,000 cfs. This figure shows that, as expected, during days when Vernon flows are less than 18,000 cfs the daily water surface elevation variation is larger than during days with higher flows from Vernon.

Analysis of the May-November 2010 period combined with the modeled historical fluctuation analysis indicate that during low to moderate flows all three hydroelectric projects (Vernon, Northfield Mountain, and Turners Falls) affect flow and water levels in the TFI. During these periods, Vernon can discharge up to 17,130 cfs when peaking which, when combined with outflow from Northfield Mountain and water level management at Turners Falls Dam, can effect flow and water level fluctuations throughout the entire TFI. Vernon discharges were observed to affect water level fluctuations by up to a foot during the analysis period. The combined influences of Northfield Mountain operational cycles and management of the water level at the Turners Falls Dam for releases to the power canal are likely to have an effect on water level fluctuations of larger than one foot and generally in the two foot range, during low to moderate flow periods.

As previously noted, the flow thresholds established for this analysis were based on a mean daily flow from Vernon of 18,000 cfs. Depending on the location in the TFI, the total flow can reach as high as 37,000 cfs if Vernon (17,130 cfs) and Northfield Mountain (20,000 cfs) are generating at maximum capacity. In other words, even though the outflow from Vernon may only be 17,130 cfs, cumulative Vernon and Northfield Mountain operations can effect TFI hydrology up to 37,000 cfs at a given location.

Moderate to High Flow Analysis (>18,000 cfs)

When Vernon outflow exceeds 17,130 cfs both Vernon and Turners Falls operate in run-of-river mode (i.e., inflow is equal to outflow, no peaking). As the flow from Vernon (and the Ashuelot and Millers Rivers) increases, the effect of Turners Falls Dam operations on water surface elevation fluctuations decreases until the French King Gorge constriction become the dominant influence on water surface elevations in the mid and upper TFI. Based on the results of the hydraulic modeling, this typically occurs at flows equal to or greater than 30,000 cfs (but potentially as low as 20,000 cfs). At flows greater than 37,000 cfs, even though Northfield Mountain may still operate, the dominant hydrologic drivers are high inflows and hydraulic constrictions.

In order to determine the hydrologic effect of Northfield Mountain operations during high flow events historic time periods and modeled operational scenarios were analyzed. The period October 1-3, 2011 provides a historic example using actual data when inflow from Vernon exceeded 30,000 cfs and Northfield Mountain operated with a peak generation flow of 12,000 cfs and pumping flow of -10,000 cfs (Figure 5.1.3.1-10). As shown in the figure, historic (i.e., baseline) conditions were plotted against conditions from a HEC-RAS model run when Northfield Mountain was “turned off” (modeling Scenario 1, discussed later in this report in Section 5.2.1). The difference in water surface elevation of the historic condition and Scenario 1 indicate the effect of Northfield Mountain operations on water level at four of the detailed study sites during a high flow period. The results of this analysis found that during the October 1, 2011 generation period, the greatest difference in water surface elevations were observed at, or near, the Northfield Mountain tailrace with progressively smaller differences observed in the upstream direction. Specifically, the analysis demonstrated (from downstream to upstream):

- **Site 75BL**: Observed difference in water surface elevation = 1.2 feet;
- **Site 5CR**: Observed difference in water surface elevation = 0.9 feet;
- **Site 4L**: Observed difference in water surface elevation = 0.7 feet; and
- **Site 303BL**: Observed difference in water surface elevation = 0.5 feet.

Examination of the October 2, 2011 pumping cycle exhibited similar differences in water surface elevation.

For the purpose of this study, a flow of 37,000 cfs at a given location (i.e. not Vernon inflow or naturally routed flow but instead the combined flow of all hydrologic influences) was determined to be the flow threshold at which natural high flows become the dominant driver of hydrologic conditions in the TFI for hydraulic reaches 1, 2, and 3 (hydraulic reaches are discussed in Section 5.4.1.1). For hydraulic reach 4 (upper most portion of the TFI near Vernon) 17,130 cfs was determined to be the natural high flow threshold as this represents the hydraulic capacity of the Vernon Project. 37,000 cfs was chosen as the natural high flow threshold for the majority of the TFI for a number of reasons, including: (1) it exceeds the flows at which the French King Gorge becomes the hydraulic control for the mid and upper portion of the TFI; (2) it exceeds the hydraulic capacity of Vernon; (3) it exceeds the maximum combined hydraulic capacity for Vernon and Northfield Mountain at a given location; and (4) although Northfield Mountain may still operate at flows greater than 37,000 cfs, historical operating records indicate this is less frequent than at lower flows.

In order to determine if 37,000 cfs was an appropriate flow threshold above which could be considered naturally occurring high flows, FirstLight reviewed the available Project operating data for the period 2000-2014 to determine the amount of time the Project operated at flows greater than 30,000 and 37,000 cfs (Table 5.1.3.1-2). As demonstrated in the table, the Project operated from 2000-2014 when flows exceeded 37,000 cfs as follows:

- Generation with 1 or more units occurred 2.6% of the time;
- Generation with 2 or more units occurred 0.82% of the time;
- Generation with 3 or more units occurred 0.14% of the time; and
- Generation with 4 units occurred 0.025% of the time;

This equates to about 9, 3, 0.5, and 0.1 days per year, respectively. Pumping operations when flows exceeded 37,000 cfs were found to follow a similar pattern.

Although FirstLight rarely operates Northfield Mountain when flows are greater than 37,000 cfs, they do still operate it at times and therefore can still have an effect on flows and water levels. In order to understand these potential effects, FirstLight executed four unsteady HEC-RAS model runs at flows of (1) 30,000 cfs; (2) 40,000 cfs; (3) 50,000 cfs; and (4) 60,000 cfs. 30,000 cfs was chosen as the low end of this analysis as it represents the flow at which the French King Gorge becomes the hydraulic control for the mid and upper portions of the TFI; whereas, 60,000 cfs was chosen as the high end of the analysis as it represents flows just below the point at which Northfield Mountain operations are determined by the USACE agreement (65,000 cfs). As a result of the requirements of the USACE agreement Northfield Mountain operations have minimal to no effect on flow or water level fluctuations at flows greater than 65,000 cfs, if the Project operates at all.

During each of the model runs Northfield Mountain operations were modeled as follows:

- **1 & 2 Unit Generation ("typical" gen)**:8 hours at 10,000 cfs (2 generators); and

  8 hours at 5,000 cfs (1 generator)

- **1 & 2 Unit Pumping ("typical" pump)**:8 hours at 7,600 cfs (2 pumps); and

  8 hours at 3,800 cfs (1 pump)

The model runs were used to determine the effects that Northfield Mountain can have on water levels in the TFI by examining the results at the same four detailed study sites previously discussed in this section. The mean daily pumping and generation volume from the Upper Reservoir is about 4,200 acre-feet (about 1/3 of the total storage in the upper reservoir) for the 2000 to 2014 period. The average volume is equivalent to about 5 hours of generation with 2 units and slightly less than 7 hours of pumping with 2 units. However, Northfield Mountain operations often vary in the duration of the pumping and generation and the number of active units due largely to market cost of electricity. Therefore to analyze the effects of more typical pumping and generation cycles, FirstLight analyzed 1 and 2 unit operations at 8 hours a day which are more similar to the operations at Northfield Mountain and 'bounds' the long term daily operational average.

Figures 5.1.3.1-11 through 5.1.3.1-14 show the effects on the modeled water surface elevation at the four locations for the typical modeled scenarios summarized above. As shown on the figures, during more typical Northfield Mountain operations the water surface elevation near the Northfield Mountain tailrace (Site 75BL) could raise by about 1.4 ft or lower by about 1.0 ft. The effects are observed to progressively decrease in the upstream direction with water surface elevation increases on the order of about 0.6 feet and a decrease of about 0.3 ft. near Site 303BL.

Table 5.1.3.1-1: Monthly Generation and Flows at Vernon for 2010 and 2012

Year	Monthly Vernon Generation (MWH)						
	May	Jun	Jul	Aug	Sep	Oct	Average
2010	17,297	9,345	7,265	6,489	3,912	17,200	10,251
2012	20,322	13,912	6,900	4,566	5,709	11,832	10,540
Year	**Monthly Vernon Discharge (cfs)**						
2010	10,965	7,147	4,225	4,204	2,570	20,934	8,341
2012	16,563	9,915	3,625	2,674	3,320	7,400	7,250

Table 5.1.3.1-2: Analysis of Northfield Mountain Operations during High Flows

% of Time	NFM Operations - Gen				NFM Operations – Pump			
	Inflow <30,000 cfs	Inflow <37,000 cfs	Inflow >30,000 cfs	Inflow >37,000 cfs	Inflow <30,000 cfs	Inflow <37,000 cfs	Inflow >30,000 cfs	Inflow >37,000 cfs
4 Units	0.3%	0.3%	<0.05%	<0.05%	3.8%	3.8%	0.2%	0.2%
3 or more units	3.1%	3.2%	0.2%	0.1%	11%	11%	1.1%	0.7%
2 or more units	14%	15%	1.2%	0.8%	18%	19%	2.2%	1.3%
1 or more units	36%	37%	4.3%	2.6%	26%	27%	3.0%	1.9%

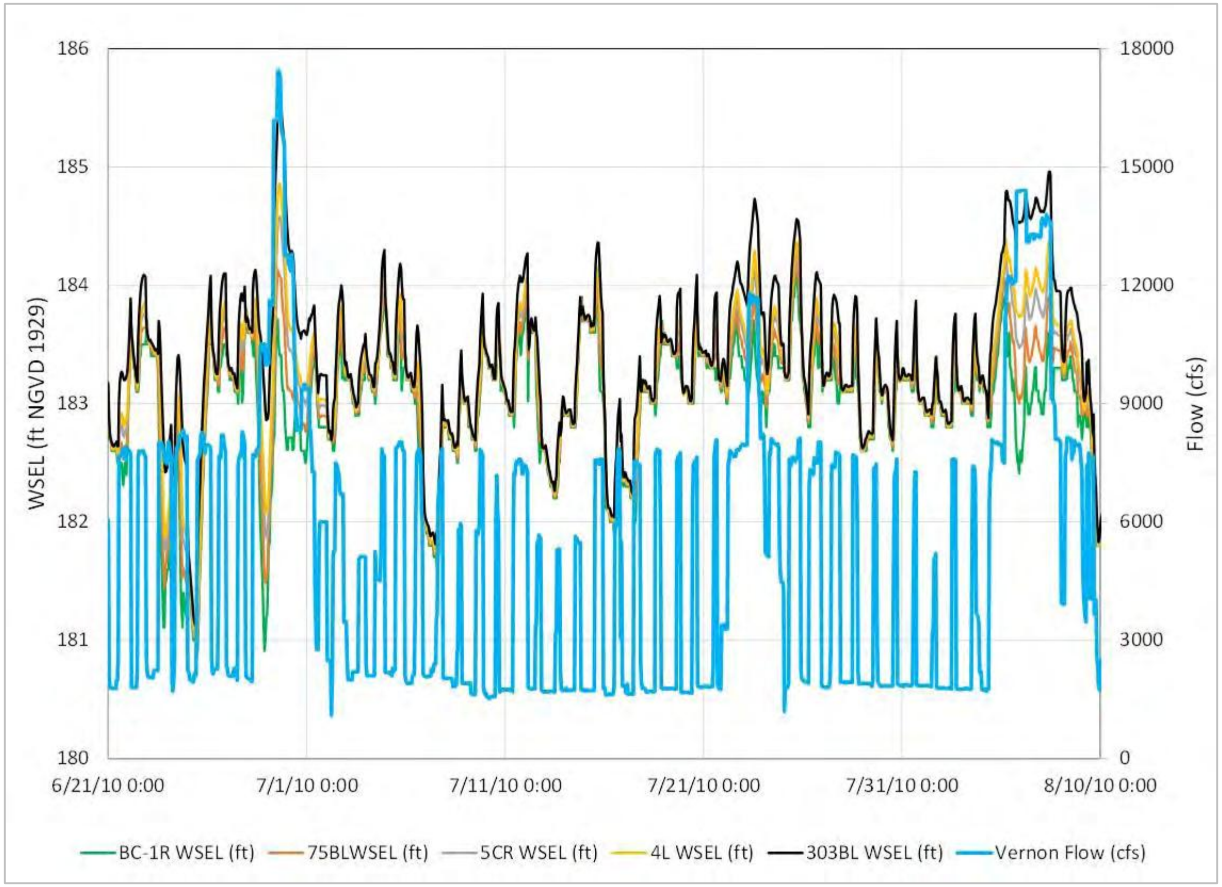

Figure 5.1.3.1-1: Turners Falls Impoundment Modeled Water Surface Elevations for June 21 – August 10, 2010

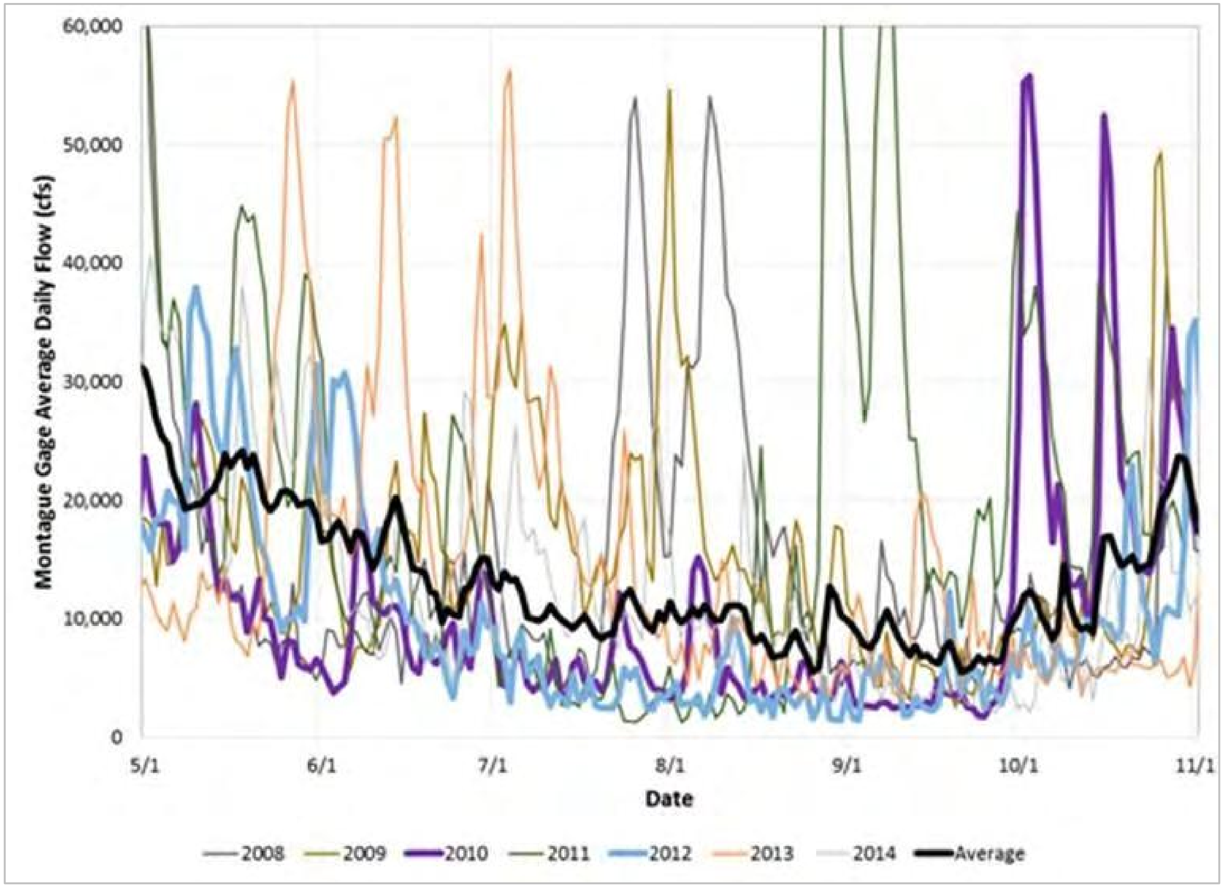

Figure 5.1.3.1-2: Mean Daily Flows at the Montague Gage - May 1 – November 1 for 2008-2014

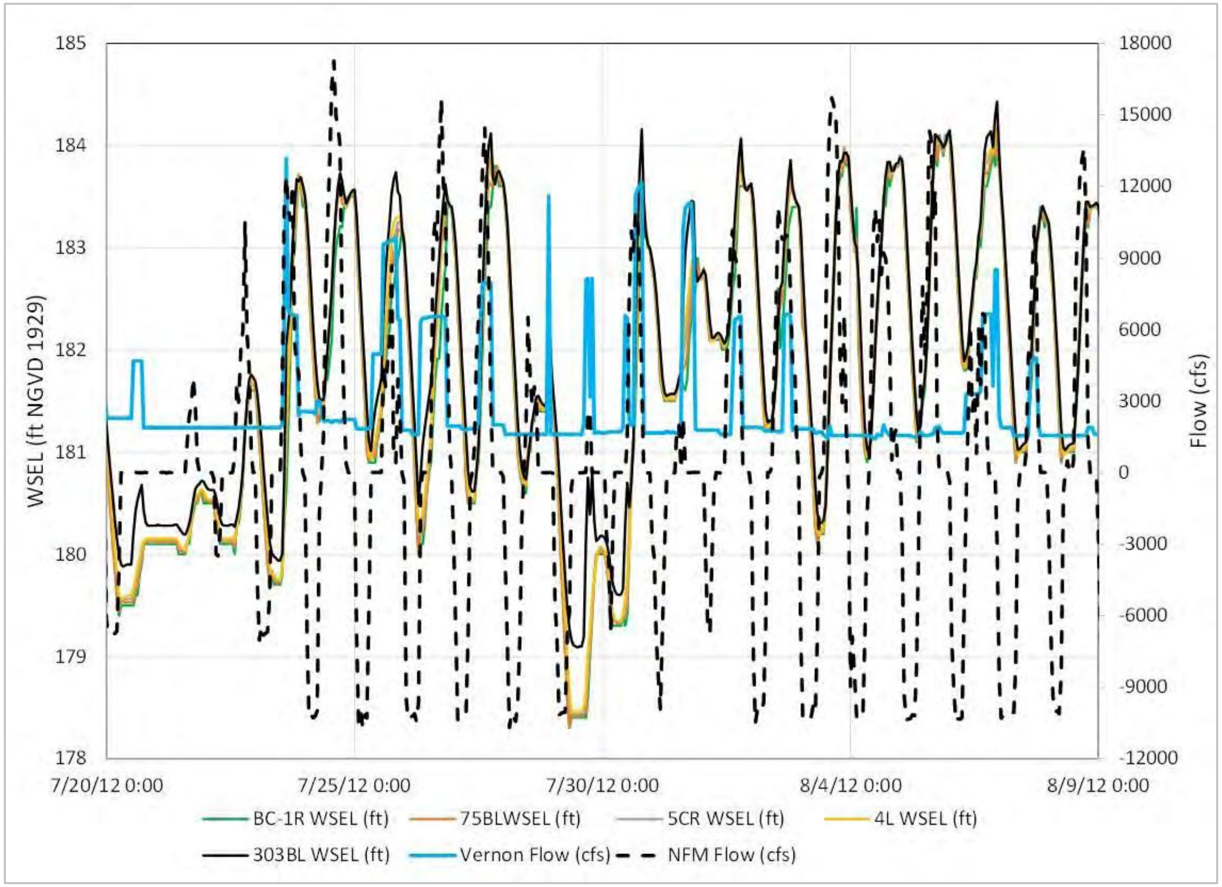

Figure 5.1.3.1-3: Turners Falls Impoundment Modeled Water Surface Elevations – July 20 – August 8, 2012

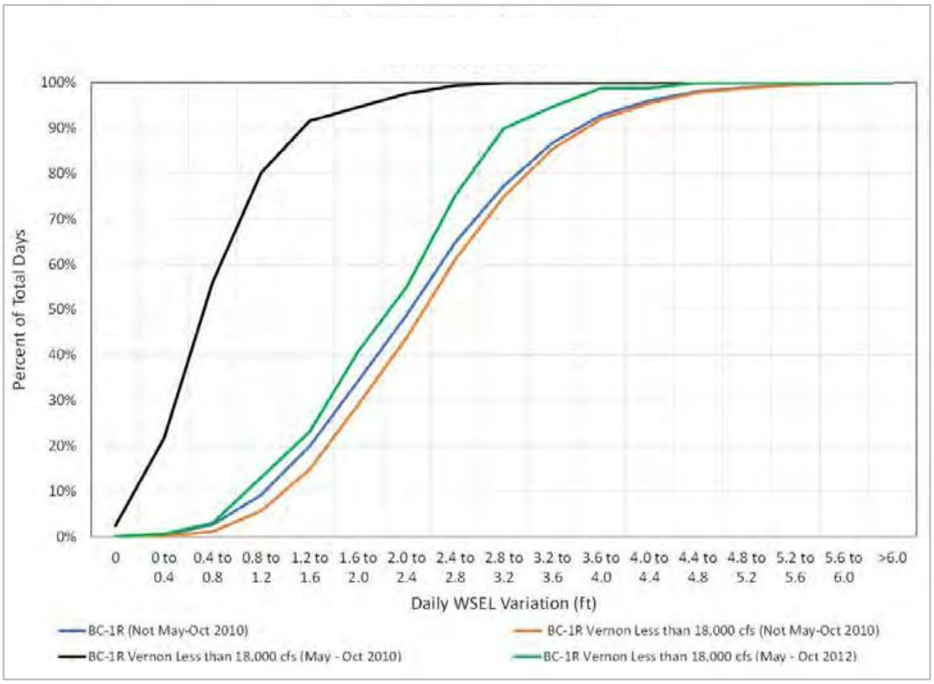

Figure 5.1.3.1-4: Modeled Historical Fluctuations at Transect BC-1R

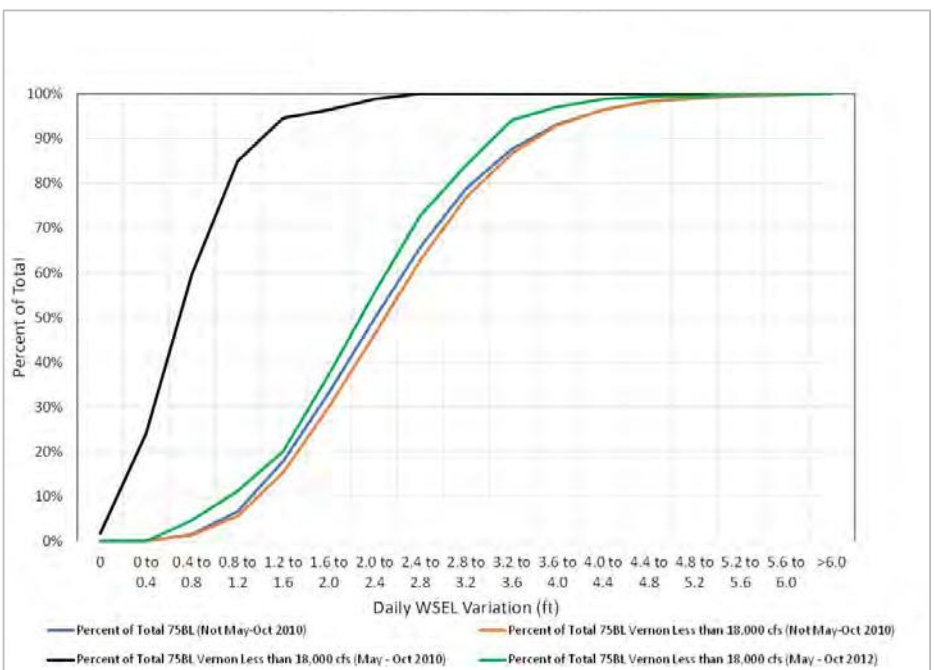

Figure 5.1.3.1-5: Modeled Historical Fluctuations at Transect 75BL

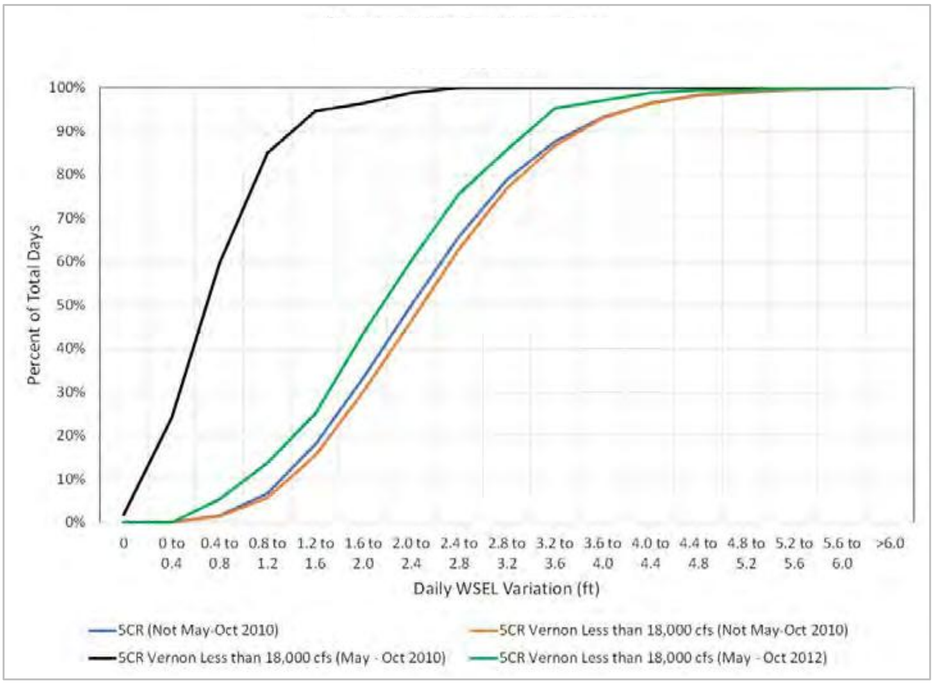

Figure 5.1.3.1-6: Modeled Historical Fluctuations at Transect 5CR

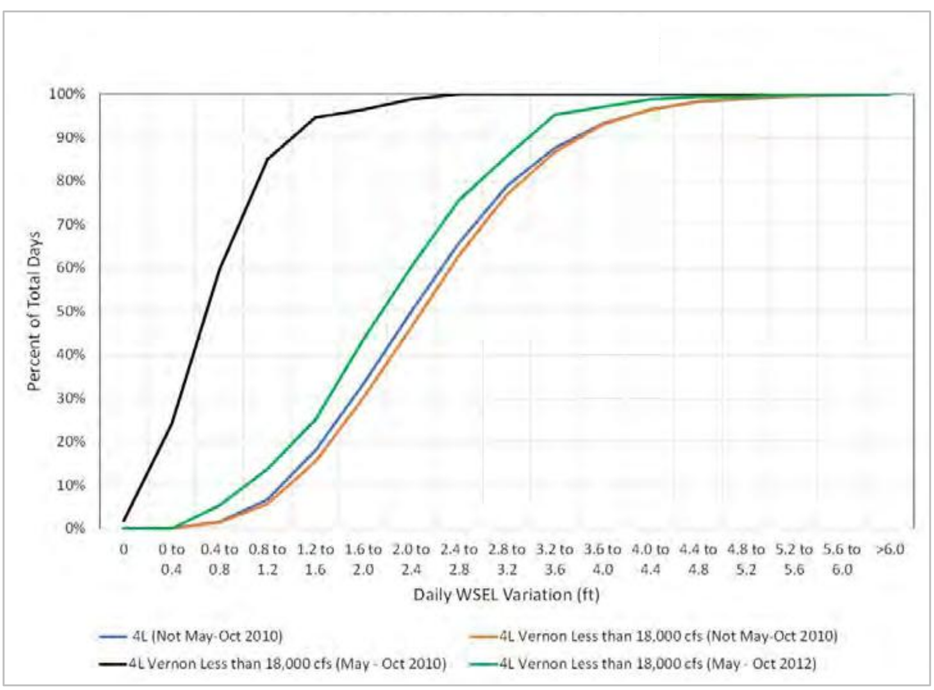

Figure 5.1.3.1-7: Modeled Historical Fluctuations at Transect 4L

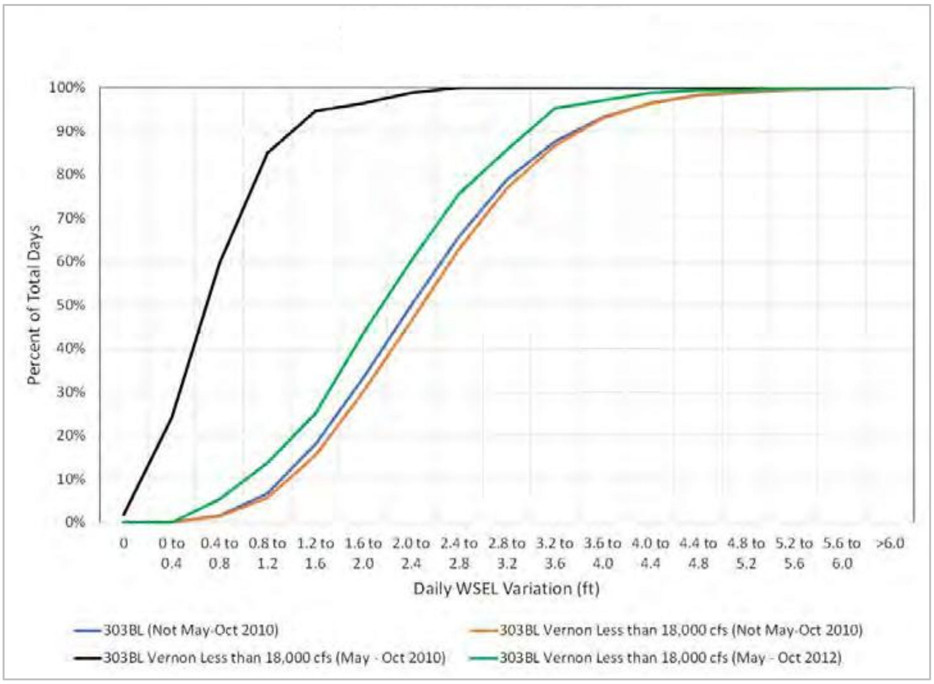

Figure 5.1.3.1-8: Modeled Historical Fluctuations at Transect 303BL

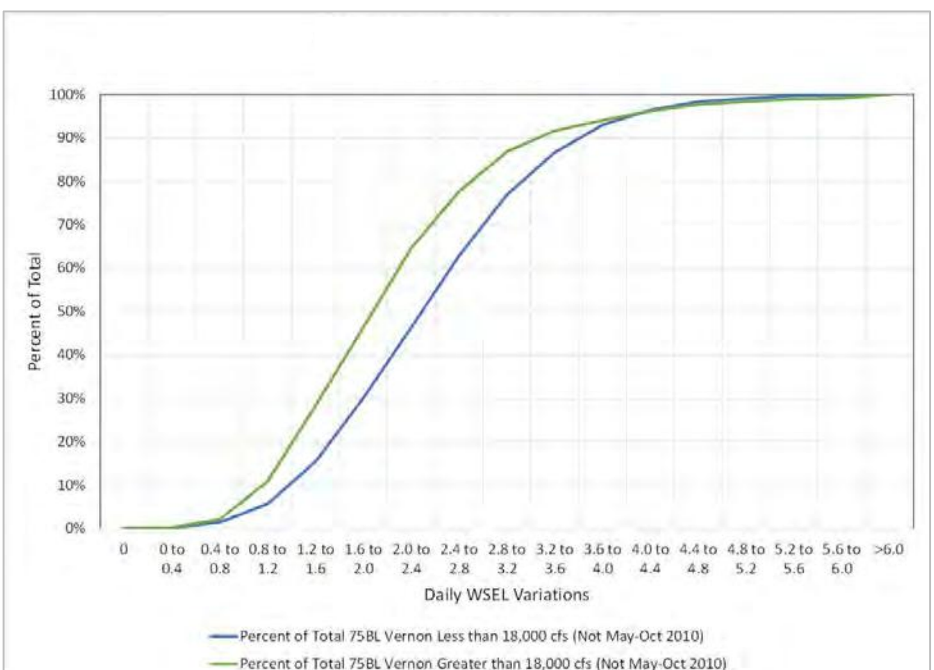

Figure 5.1.3.1-9: Frequency of Daily Water Surface Elevation Variations at Transect 75BL

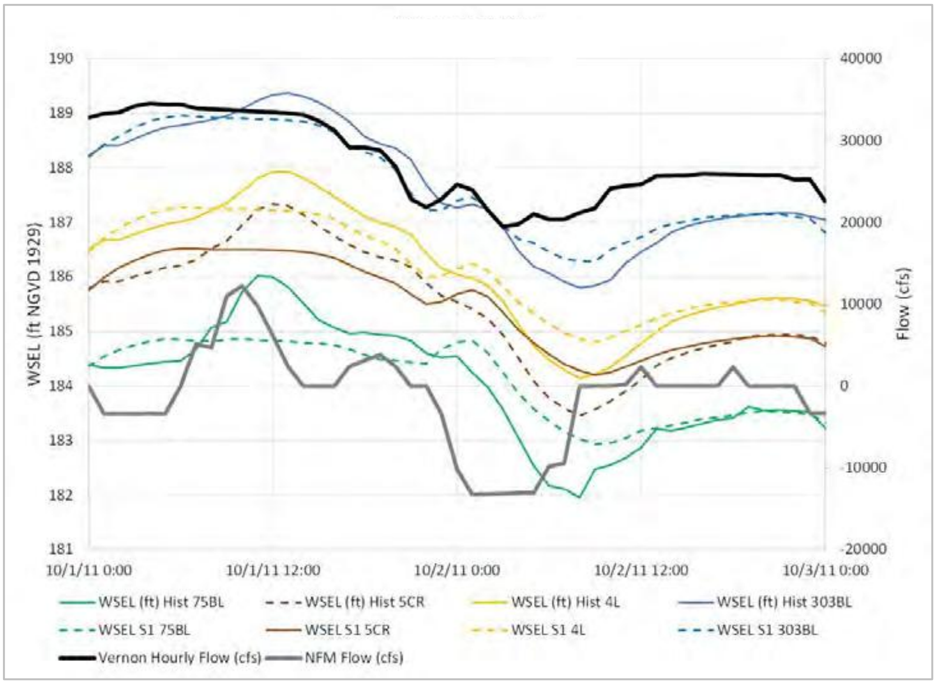

Figure 5.1.3.1-10: Effects of Northfield Mountain Generation during October 1-3, 2011

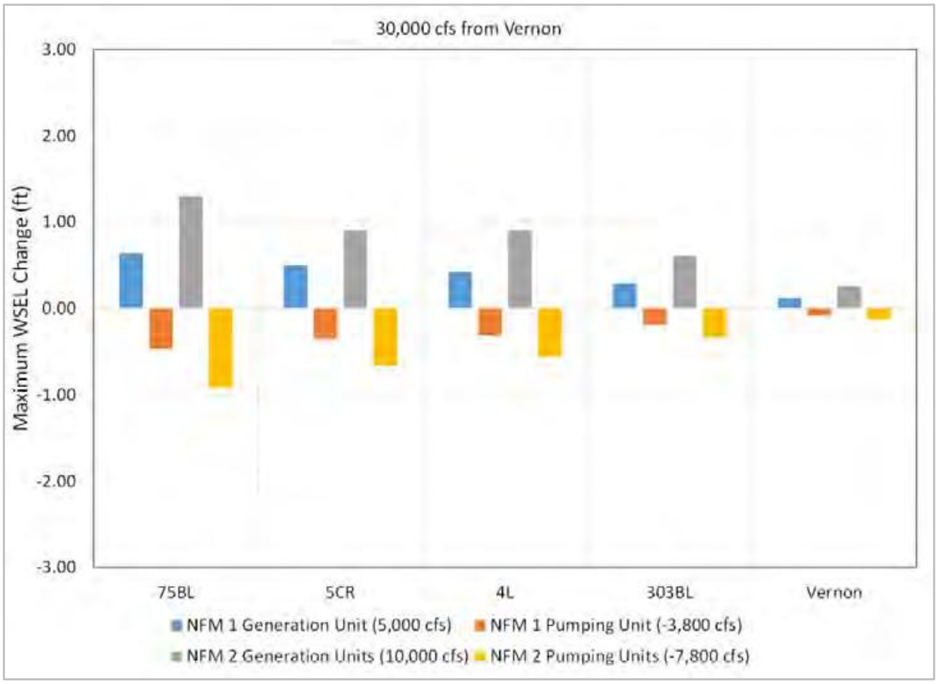

Figure 5.1.3.1-11: Modeled Typical Effects of Northfield Mountain Generation and Pumping during a Vernon inflow of 30,000 cfs

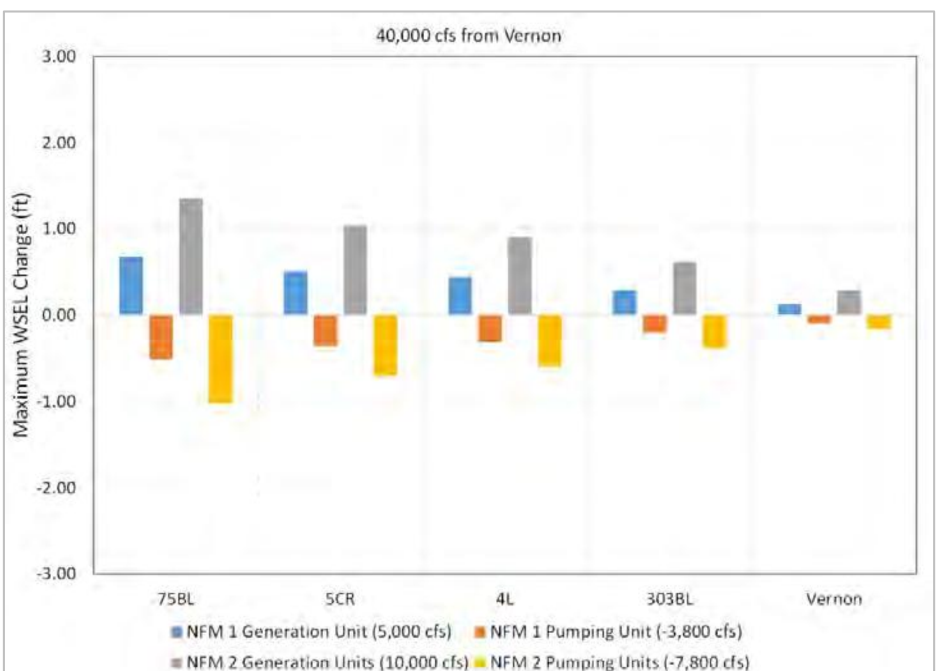

Figure 5.1.3.1-12: Modeled Typical Effects of Northfield Mountain Generation and Pumping during a Vernon inflow of 40,000 cfs

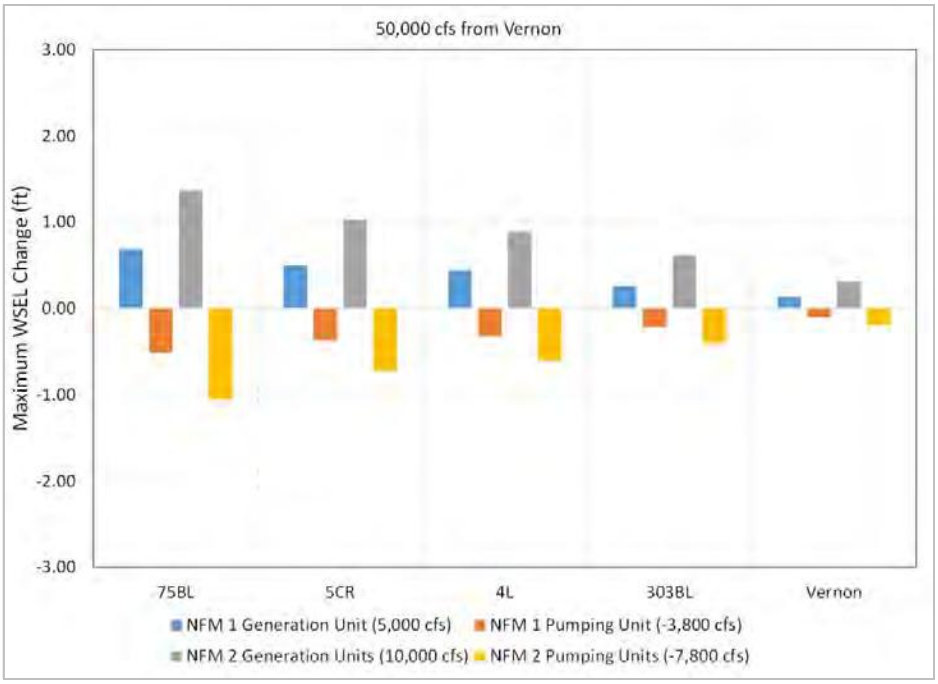

Figure 5.1.3.1-13: Modeled Typical Effects of Northfield Mountain Generation and Pumping during a Vernon inflow of 50,000 cfs

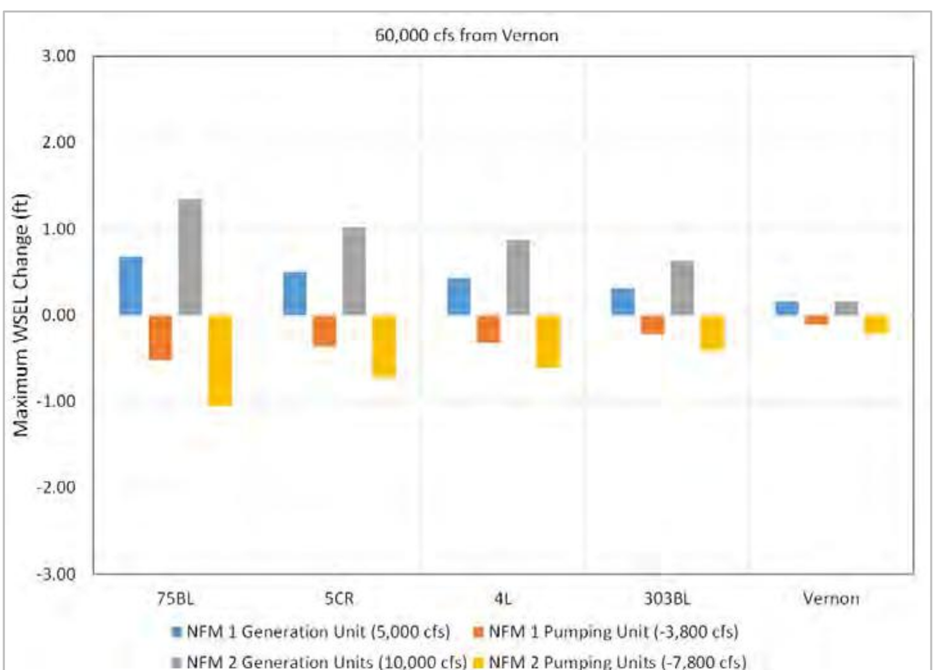

Figure 5.1.3.1-14: Modeled Typical Effects of Northfield Mountain Generation and Pumping during a Vernon inflow of 60,000 cfs

5.2 Hydraulics

Hydraulic modeling using HEC-RAS[37] and River2D [38] were conducted as an integral part of various studies associated with the Turners Falls / Northfield Mountain relicensing, including to provide data for this study. These models determined the water level fluctuations within the TFI that are affected by inflow from the TransCanada's Vernon Project, FirstLight Project operations, and inflows from tributaries. Both models require similar types of input data which included riverbed and bank geometry, flows, and water level data.

Full details of the HEC-RAS model, including the collection of the field data, model setup, model calibration, and analyses were provided in the study report for Study No. 3.2.2 *Hydraulic Study of Turners Falls Impoundment, Bypass Reach and Below Cabot* dated March 2015 (FirstLight, 2015b). The 2-dimensional River2D model was developed for the entire TFI from Vernon to Turners Falls Dam specifically for this study. Once calibrated, a number of production runs were executed to evaluate velocities and shear stresses in the near-bank area at each of the detailed study sites and other areas of interest.

Results from both of these modeling efforts were utilized to determine the water level variation throughout the TFI and shear stresses in the near bank environment. Both the HEC-RAS and River2D models are discussed in more detail in the ensuing sections.

5.2.1 HEC-RAS Modeling

The HEC-RAS model was initially calibrated to the water surface elevations (WSEL) measured at eight water level loggers during two periods when WSEL and flow fluctuations were minor (quasi steady-state conditions). The initial calibration, by adjusting the Manning's n value and the expansion and contraction coefficients, was completed during the following periods:

- May 4-5, 2014: Vernon average flow= 25,785 cfs (high flow event)
- May 8, 2014: Vernon average flow= 17,141 cfs (near Vernon's hydraulic capacity of 17,130 cfs)

Further fine-tuning of the Manning's n values occurred during unsteady-state conditions within the range of accurate flow measurement (turbine operations instead of spillage operations at Vernon) since this is the more common condition in the TFI and is more realistic than the quasi steady-state conditions used for the initial calibration. The flow and WSEL data for the period the water level loggers operated in the TFI were reviewed to identify periods where maximum peaking operations at Vernon and Northfield Mountain cycling occurred. Typically, these conditions occur during low flow, high energy demand periods in the mid-to-late summer. The period selected for further model calibration was August 24 to September 3, 2014, which exemplified peak electrical demand and low flow during non-generation periods.

Section 4 of the March 2015 Study No. 3.2.2 report contains figures of the comparisons of the observed to modeled WSELs for each of the water level logger locations. However, as an example, Figure 5.2.1-1 provides a comparison between the observed and modeled conditions at the Rt. 10 Bridge, near the middle of the TFI. As this figure (and the figures in the March 2015 Study No. 3.2.2 report) indicates, there is an excellent match relative to the magnitude and timing of the observed versus modeled WSELs at the water level loggers. Given the closeness of fit between observed and modeled conditions, the hydraulic model was deemed fully calibrated. Because the hydraulic model is well-calibrated to observed conditions, it was

[37] HEC-RAS Hydrologic Engineering Center River Analysis System is a one-dimensional hydraulic model developed by the USACE.
[38] River2D was developed at the University of Alberta and is a two-dimensional finite element depth averaged hydrodynamic and fish habitat model.

used to predict WSEL's at different locations in the TFI as long as the following data were available: Vernon discharge, USGS gage flows for the Ashuelot and Millers Rivers, Northfield Mountain operational data (pumping or generating flows), and elevation data at the Turners Falls Dam.

In support of the BSTEM modeling efforts associated with this study and the various supplemental analyses which were conducted (including those discussed in Section 5.1), the HEC-RAS model was utilized to generate historic (baseline) water levels and energy grade-line slopes on an hourly basis at the 25 detailed study sites. The Baseline Condition modeling scenario utilized historic upstream inflows at Vernon and tributaries (Ashuelot and Millers Rivers), Northfield Mountain operations, and historic water levels at the Turners Falls Dam. In addition to the Baseline Condition, an additional scenario was developed to provide water level and energy grade-line slope data for the BSTEM modeling at the 25 detailed study sites. The HEC-RAS scenarios used the January 1, 2000 to December 31, 2014 period and historic tributary inflows. The two HEC-RAS modeling scenarios had the following input variables:

- **Baseline Condition**: an hourly model mimicking historic conditions in the TFI.
- **Scenario 1**: an hourly model with Northfield Mountain idle but historic operation at both Vernon and the water level at TFI.

A more in-depth discussion of the scenarios used for the BSTEM modeling are provided in Section 5.4.1.

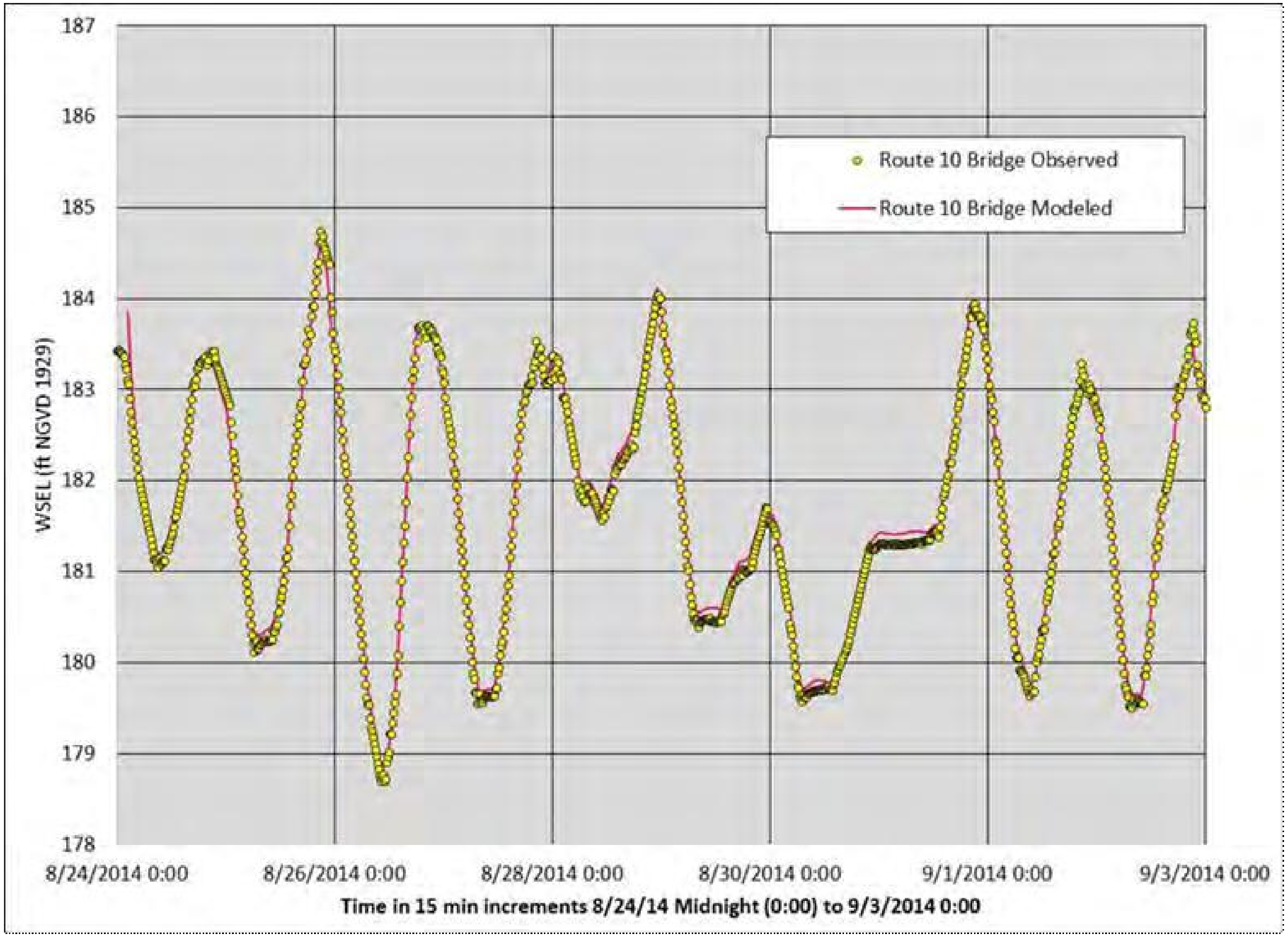

Figure 5.2.1-1 Comparison of Observed and Modeled WSELs at the Route 10 Bridge for the period August 24-September 3, 2014

5.2.2 River2D Modeling

The modeling program River2D was utilized to develop a two-dimensional model of the TFI to evaluate velocities and shear stresses over a range of flows. Due to the size of the TFI, the study area was split into two separate models with approximately 1.25 miles of overlap. This overlap allows for results from the downstream model to be used to define the downstream boundary condition of the upstream model while decreasing the possibility of boundary effects from the upstream boundary of the downstream model. The bed and mesh geometry were built with a finer resolution in the areas immediately surrounding the detailed study sites, while the remainder of the model has a courser resolution adequate for flow conveyance.

The model is intended for steady state evaluations, therefore calibration and verification of the roughness coefficients for each model was performed using observed conditions which were approximated to be steady state. The models were calibrated to an event with a discharge of approximately 31,200 cfs at the Turners Falls Dam, and then verified with three events with discharges at the Turners Falls Dam of approximately 2,500 cfs, 18,600 cfs, and 31,200 cfs. These events represent the full range of available observed flows for which steady state assumptions could be assumed. Calibration and verification at the observed stations was within 0.5 feet throughout the TFI, and generally within 0.25 feet. It should be noted that calibration of hydraulic models to within 0.5 feet is a common industry standard, and that the potential measurement error of the observation stations is approximately 0.2 feet.

Six production runs were performed for a range of conditions, including normal operating conditions, commonly occurring flows that might occur every few years, and more extreme events including the 100-year flood. None of these production runs assumed operation at Northfield Mountain. The primary impact of Northfield Mountain operations on model results at the detailed study sites would be to the range of flows evaluated at particular sites. With the wide range of flows that were analyzed, the exclusion of Northfield Mountain operations in the productions runs is not expected to impact the overall results of the analysis. Further, inclusion of Northfield Mountain operations is not expected to have a significant impact on near bank velocities at any of the detailed study sites for the range of flow conditions analyzed. Existing operations at Turners Falls Dam, and the Federal Emergency Management Agency's (FEMA) Flood Insurance Study (FIS) for Montague in Franklin County, Massachusetts were used to develop the production runs. Table 5.2.2-1 provides an overview of the boundary conditions used for the six production runs. The River2D model does not include bridge decks, but this is not expected to impact the results as water surface elevations remained lower than the bridge low chords reported in the FEMA FIS at all locations along the TFI for all production runs.

The results of the River2D model were used to evaluate velocity and shear stress in the near-bank area at each of the detailed study sites as well as other areas of interest. Discussion related to this analysis can be found in Section 5.5.1.

Table 5.2.2-1: River2D Production Run Boundary Conditions

Production Run	Flow from Vernon Dam (cfs)	Flow from Ashuelot River (cfs)	Flow from Millers River (cfs)	Flow at Turners Falls Dam (cfs)	Water Surface Elevation at Turners Falls Dam (ft)
Generating Capacity at Turners Falls Dam	14,365[1]	840[2]	735[2]	15,940	181.3[3]
Operation Rule Threshold A[4]	27,130[5]	1,495[6]	1,375[7]	30,000[4]	180[4]
Operation Rule Threshold B[4]	58,780[5]	3,245[6]	2,975[7]	65,000[4]	179[4]
10-Year Return Period	87,795[1]	5,845[6]	5,360[8]	99,000[8]	179[9]
50-Year Return Period	119,400[1]	9,860[6]	9,040[8]	138,300[8]	180[10]
100-Year Return Period	134,120[1]	12,300[6]	11,280[8]	157,700[8]	180[10]

Notes:

[1] Vernon flow was calculated as difference between flow at Turners Falls Dam and the combined flow from the Ashuelot and Millers Rivers as follows: $Q_{Ver} = Q_{TF} – (Q_{Ash}+Q_{Mil})$

[2] Mean flow: Ashuelot 1908-2014, Millers 1916-2014

[3] Operating rules state a range of 180.5 to 184.5, 181.3 is the median water level at the dam in the recent decade (Gomez & Sullivan)

[4] Operating rules differ for flows at Turners Falls Dam between 30,000 cfs (Operation Rule Threshold A) and 65,000 cfs (Operation Rule Threshold B). When flows are in this range, the USACE requires that FirstLight drawn the Turners Falls Impoundment elevation down as far as possible, but not below elevation 176 ft. Flows in this range likely have between 1 to 3 year return periods and occur on a relatively frequent basis. Note: during tropical storm Irene the water level at the dam was approximately 179 for flows of approximately 100,000 cfs. Water levels were selected for the various flows depending on flow.

[5] Vernon flow was calculated using the drainage area ratio method presented in the FEMA FIS based on flow at the Turners Falls Dam as follows: $Q_{Ver} = Q_{TF}$*(6266/7165)^.75

[6] Flows for the Ashuelot River were calculated using the drainage area method presented in the FEMA FIS based on flow from the Millers River as follows: $Q_{Ash} = Q_{Mil}$*(440/392)^.75.

[7] Flows for the Millers River were calculated using the drainage area ratio presented in the FEMA FIS based on the difference in flow between the Turners Falls and Vernon Dams as follows: $Q_{Mil} = (Q_{TF}-Q_{Ver})$/[1+(440/392)^.75].

[8] Flows obtained directly from the FEMA FIS.

[9] If the Northfield Mountain Project is not operating and flows at Turners Falls Dam are between 65,000 cfs and 126,000 cfs, the Turners Falls Impoundment should be kept at a constant elevation. Note: during tropical storm Irene the water level at the dam was approximately 179 for flows of approximately 100,000 cfs.

[11] All flows presented in this table were rounded to the nearest 5 cfs.

5.3 Sediment Transport

As discussed in Section 4.2.9, rivers transport sediment that has been eroded from the upstream watershed or riverbanks and river bed in response to flow or rainfall events, as well as other processes that erode sediment. As part of Study No. 3.1.3, FirstLight collected continuous suspended sediment data and grab samples at two locations in the TFI – just upstream of the Rt. 10 Bridge and at the Northfield Mountain tailrace in order to better understand suspended sediment transport dynamics in the TFI.[39] For the purpose of this study, emphasis was placed on evaluating and analyzing the continuous suspended sediment and grab sample data collected in the vicinity of the Rt. 10 Bridge, or more specifically the StreamSide data (2013-2015) and Rt. 10 Bridge cross-section grab samples (2015). The data collected in the vicinity of the Rt. 10 Bridge allowed for a direct analysis of suspended sediment dynamics in the mainstem Connecticut River (as opposed to the data collected in the Northfield Mountain tailrace which was set back from the mainstem).

For the purposes of this study, the data collected and analyzed as part of Study No. 3.1.3 was evaluated to determine any potential relationships between flow, suspended sediment concentration (SSC), and potential erosion and to independently verify the findings of the hydraulic and BSTEM modeling, to the extent possible. Originally, the RSP called for using these data to analyze particle size distribution (PSD) as related to critical shear analysis using Shield's criteria; however, as discussed in the Study No. 3.1.3 December 2015 filing with FERC, the PSD data was not usable and therefore the analysis discussed in the RSP was not possible.

As expected, Study No. 3.1.3 found that suspended sediment measurements collected by the StreamSide and from grab samples collected in the vicinity of the StreamSide pump demonstrate strong correlations between flow and SSC. Over the course of the monitoring period (2013-2015) it was observed that as Connecticut River flows increase so too did SSC (Figure 5.3-1). That is, the highest SSC values were observed during the highest periods of flow while the lowest SSC values were observed during the lowest period of flows. This was a consistent observation for each year data were collected.

As shown in Figure 5.3-1, SSC values were relatively low and without an apparent trend when flows from Vernon Dam were below 12,000 cfs. 95% of SSC measurements observed when flows were below 12,000 cfs were below 14.5 mg/L with a median of 3 mg/L. From 12,000 to 35,000 cfs, SSC values exhibited an increasing trend with a median of 12 mg/L. Finally, SSC values associated with flows greater than 35,000 cfs increased more quickly with flow and were significantly higher with a median of 145 mg/L. The results of this analysis demonstrate that three flow thresholds generally exist in the TFI in regard to SSC values (as measured at the Rt. 10 Bridge): <12,000 cfs (low flow), 12,000-35,000 cfs (moderate flow), and >35,000 cfs (high flow).

As discussed in Section 5.1.3, for the purpose of this study, the flow threshold for natural high flows was determined to be 37,000 cfs for the middle, Northfield Mountain, and lower reaches of the TFI. This value represents the combined maximum hydraulic capacity of Vernon and Northfield Mountain at a given location and also represents flows at which Northfield Mountain operates on a very limited basis, if at all (i.e., less than 3% of the time). Given this, the suspended sediment flow thresholds identified as part of Study No. 3.1.3 are of particular interest as it is observed that significant levels of suspended sediment are not transported until flows reach or exceed the threshold for high flows. While the data collected at the Rt. 10 Bridge represents one location in a ~22 mile long impoundment, BSTEM results discussed in Section

[39] Details pertaining to the data collection efforts at each site were discussed in Section 4.2.9, in-depth discussion and details can further be found in the report titled, *Relicensing Study 3.1.3 Northfield Mountain Pumped Storage Project Sediment Management Plan 2015 Summary of Annual Monitoring* filed with FERC in December 2015.

5.4 observed similar behavior at most detailed study sites. That is, the majority of erosion in the TFI does not occur until flows at a given location exceed 35,000 cfs or higher.

The results of the supplemental cross-section grab samples collected across the Rt. 10 Bridge during the 2015 spring freshet further demonstrate the strong correlation between flow and SSC. Grab samples were collected over four days during the rising limb, on either side of the peak, and across the falling limb of the hydrograph. As shown in Table 5.3-1, as flow increased so too did SSC values with the highest concentrations observed at flows >40,000 cfs and the lowest concentrations at flows <20,000 cfs.

As part of Study No. 3.1.3 investigation then occurred to determine how often these flow thresholds occurred during the study period. Figure 5.3-2 depicts the flow duration curve for Vernon discharge from April through November for the years 2013-2015. As shown on the flow duration curve, flows of 12,000 cfs or less were equaled or exceeded 63% of the time, flows between 12,000-35,000 cfs were equaled or exceeded 32% of the time, while flows greater than 35,000 cfs were equaled or exceeded 5% of the time during the course of the study. In other words, flows of a magnitude when high concentrations were observed occurred only 5% of the time during the study period.

Historic suspended sediment samples and photographs collected during Tropical Storm Irene further demonstrate the strong relationship between flow and SSC values. Figure 5.3-3 demonstrates the contrast between the Millers River and the Connecticut River as affected by Tropical Storm Irene in August 2011. As observed in the figure, the relatively clear water from the Millers River flowed into the sediment laden Connecticut River in a classic, swirling mixing zone. SSC values taken from the Millers River ranged from non-detect (ND, <5 mg/L) to 6.5 mg/L while SSC values measured in the Connecticut River during the same period ranged from 140 to 1,900 mg/L.[40] As a point of comparison, the median SSC value observed during Study No. 3.1.3 for flows greater than 35,000 cfs was 145 mg/L.

Table 5.3-1: Summary of Rt. 10 Bridge Cross-section Grab Samples (2015)

Date	Vernon Discharge (cfs)	Max SSC (mg/L)	Min SSC (mg/L)	Median SSC (mg/L)	StreamSide SSC (mg/L)
4/14/2015	50,536 - 59,700	159	79	108	152
4/17/2015	47,970 - 52,591	106	80	89	82
4/20/2015	41,282 - 42,172	90	30	42	70
4/28/2015	19,112 - 20,437	14	6	12	13

[40] SSC samples collected during Tropical Storm Irene in the Connecticut River were collected as grab samples collected by boat while samples collected from the Millers River were collected as surface grab samples collected at the edge-of-water.

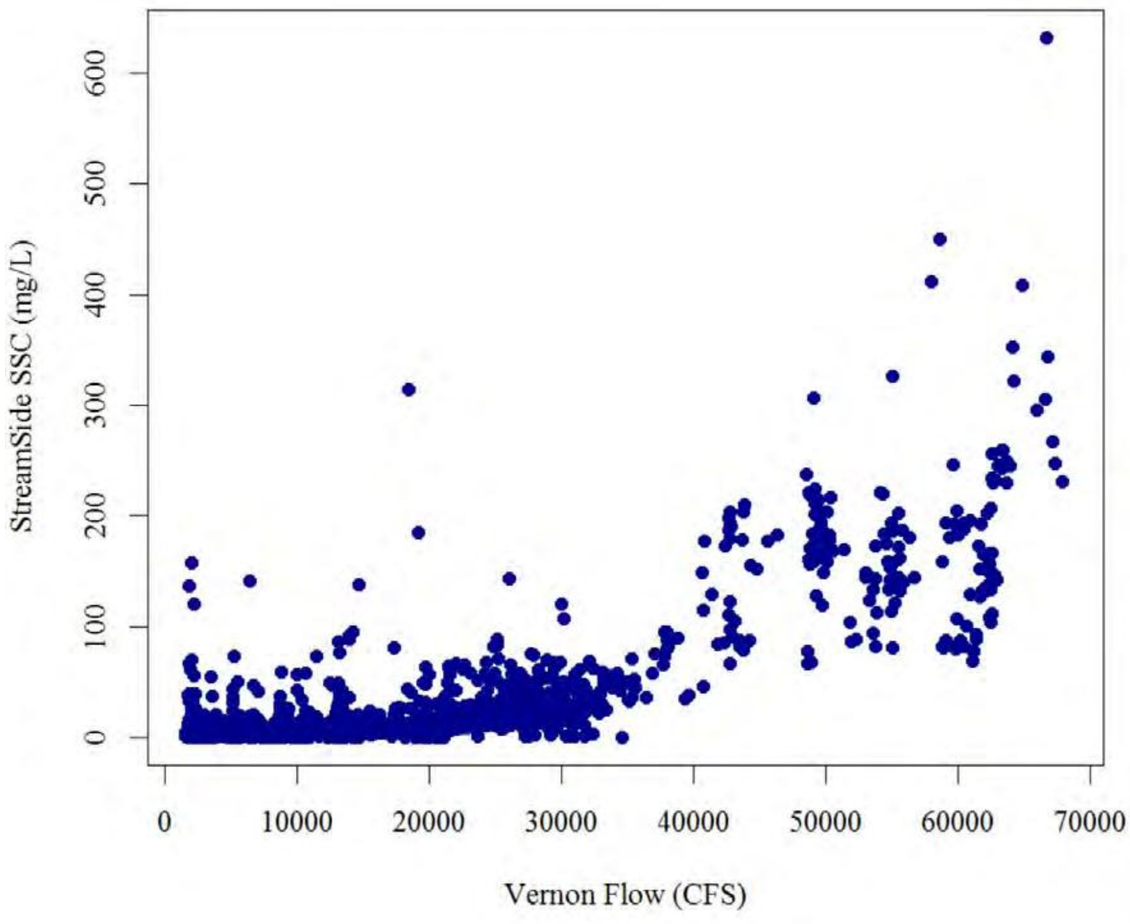

Figure 5.3-1 TFI Impoundment SSC vs. Vernon Discharge (2013-2015)

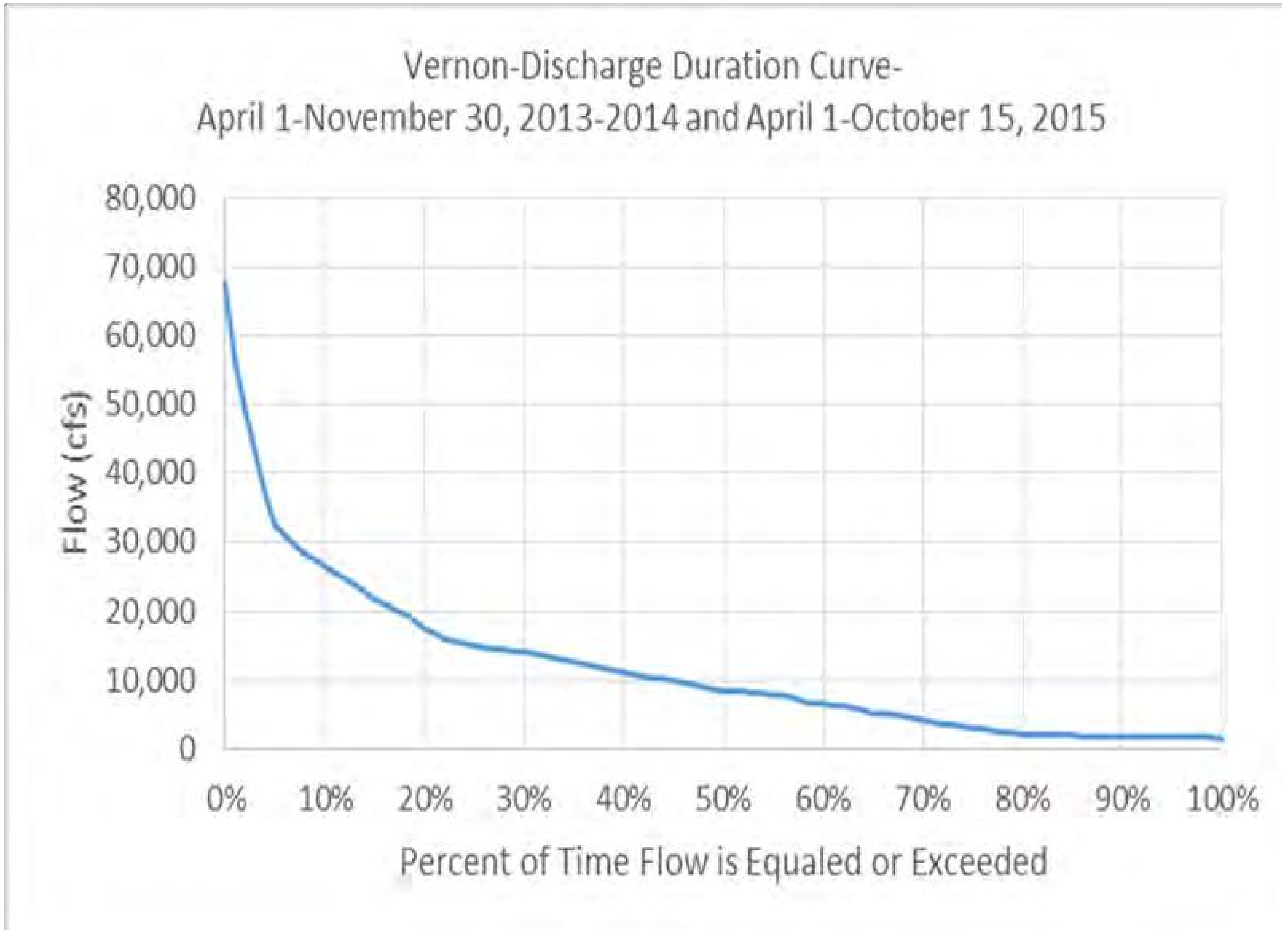

Figure 5.3-2 Flow Duration Curve for the Turners Falls Impoundment

Figure 5.3-3 Millers River Confluence with the Connecticut River (TFI), August 2011

5.4 Analysis of the Causes of Erosion - BSTEM

BSTEM is a state-of-the-science deterministic model that simulates the hydraulic and geotechnical processes responsible for bank erosion, including the effects of vegetation, pore-water pressure, and the confining forces due to flow in the channel. BSTEM was the principal tool used to evaluate the potential primary causes of erosion including hydraulic shear stress due to flowing water, water level fluctuations, and boat waves. Analysis pertaining to the other potential primary causes of erosion (land management practice and ice) are discussed in Section 5.5.

Both the static and dynamic versions of BSTEM have been used worldwide to predict and address issues involving bank erosion. The version used in this study represents the latest version of BSTEM-Dynamic (Ver. 2.3). By dynamic, we mean that instead of relying on a single ”burst” of discharge (a rectangular hydrograph) for a single flow event of given stage and duration, the user is able to input a complete flow series at the time step of their choosing. For this study, a 15-year flow series (2000-2014) was used with both of the modeled scenarios using hourly time steps.

Discussion in this section focuses on BSTEM input data and modeling results. Input data for BSTEM relied on three primary sources: field collected data (as discussed in Section 4); results from both HEC-RAS modeling scenarios; and cross-section surveys which have been conducted annually since 1999. Simulations using the input data discussed below provided the foundation for the BSTEM results and for determining the causes of bank erosion at each detailed study site.

BSTEM results are presented in two ways, (1) as general observations and findings throughout the TFI, and (2) as site-specific results for each detailed study site. BSTEM modeling results are discussed in the context of both hydraulic and geotechnical erosion processes. For the purpose of this study, hydraulic erosion is defined as erosion caused by hydraulic processes. That is, the particle-by-particle entrainment and erosion of surficial sediments when and where the boundary shear stress exerted by the flow exceeds the critical shear stress that characterizes the surficial bank sediments. Hydraulic erosion from river flow or by waves can steepen and undercut bank surfaces leading to a loss of support for the upper part of the bank and making them susceptible to collapse (geotechnical erosion). These processes are most important when shear stresses are highest as during high flows.

Geotechnical erosion is defined as erosion caused directly by gravitational forces as in the collapse of a hillslope or bank. Here, erosion occurs when the downslope, gravitational forces exceed the shearing resistance of the *in situ* materials. Any factors that increase the downslope gravitational forces (such as steepness and weight) or decrease the shearing resistance of the materials (such as generation of positive pore-water pressure) contribute to geotechnical erosion. Pore-water pressure can be generated within the bank by lateral infiltration (depending on the duration the water is at a certain elevation) during rises in stage. This can reduce the frictional component of shear strength (See Volume III - Appendix F). The confining pressure provided by the flow pressing against the bank surface, however, tends to offset this affect. An important point are the relative rates of decreasing stage and groundwater levels during water-level fluctuations because the loss of shear strength combined with a loss of confining pressure (known as the *drawdown* condition) is particularly critical for streambank stability. BSTEM handles these processes by calculating pore-water and confining pressures along potential failure surfaces during each time step of a simulation (See Volume III – Appendix F).

5.4.1 BSTEM Input Data

The required field data that was collected to support BSTEM were discussed in Sections 4.2.5 through 4.2.8. This section focuses on how those data were used and analyzed in support of the model.

5.4.1.1 Hydraulic Input Data

The purpose of the bank-stability modeling was to simulate bank-erosion rates under a range of operational conditions. For example, the Baseline Condition included "normal" peaking operations at Vernon and Northfield Mountain using hourly historical flows and historical water-surface elevations at Turners Falls Dam. Hourly values of water-surface elevations were derived for each of the 25 model locations from 1-D hydraulic modeling using HEC-RAS (Section 5.2.1). Previous versions of BSTEM-Dynamic relied on a single (constant) bed slope to internally calculate shear stress for each time step. To accommodate the more rapidly varying slopes typical during peaking operations, BSTEM-Dynamic was enhanced to allow for input of a unique slope for each time step. Thus, hourly energy slopes calculated in the HEC-RAS model were used for input into BSTEM. Because shear stress is the product of the hydraulic radius, energy slope and unit weight of water, this provided for more accurate evaluations and better temporal resolution of the shear stress calculations along the bank toe and bank face within BSTEM.

Hydraulic inputs provided to BSTEM, including flow elevation and energy slope for each site, provide important information on the forces that can cause particle-by-particle (hydraulic) erosion of the bank materials. As such, the distributions of energy slope along the reach for the Baseline Condition provide a picture of the absolute and relative magnitudes of how these hydraulic forces vary longitudinally along the TFI (Figure 5.4.1.1-1). The median (50^{th} percentile) energy slope for each site is represented by the gray line with 50% of the slopes over the modeling period greater than this value and 50% less. The blue and orange lines represent the 95^{th} and 75^{th} percentiles for each site, respectively. One cannot equate the 95^{th} percentile energy slopes with the greatest boundary shear stresses, however, as these slopes may occur at lower flows where flow depths (and hydraulic radius) are less.

Based on the distribution of the energy grade slope shown in the figure, four hydraulic reaches were identified. These hydraulic reaches included the Upper (Reach 4), Middle (Reach 3), Northfield Mountain (Reach 2), and Lower (Reach 1) reaches.[41] The steepest slopes occur in the "upper" part of the reach (Reach 4) just downstream from Vernon Dam and extending downstream to about station 80,000. That the steepest slopes are in the "upstream reach" is also shown by overlaying the energy slopes for each site in Figure 5.4.1.1-2, with the palest blue color for the most upstream site (11L) and slightly darker shades used for each site progressing downstream. Slopes for the "middle" reach, denoted as Reach 3 (downstream to station 42,000) are generally about an order of magnitude lower. Energy slopes for the Northfield Mountain Reach (Reach 2) are somewhat greater than for both Reaches 3 and the "lower" reach (Reach 1), the latter being the section just above Turners Falls Dam. The effects of operations at both Vernon Dam and Northfield Mountain on energy slopes can be seen (Figure 5.4.1.1-1), keeping in mind that flows above 17,130 cfs are in excess of the hydraulic capacity of Vernon Dam and, therefore, represent run of the river conditions. Figure 5.4.1.1-3 depicts the geographic distribution of the four study reaches in the TFI.

The hydraulic inputs represent only one of the factors determining bank-erosion rates. Quantifying bank-erosion is a matter of quantifying the driving and resisting forces that control the hydraulic and gravitational (geotechnical) processes acting on a bank. The *in situ* field measurements of bank-material properties described in Section 4.2.6 were used to quantify how the bank resists the hydraulic forces provided by the flow and by waves, and the gravitational forces which manifest as bank height and angle. Knowing the resisting forces, including vegetative factors, therefore, allows us to determine the response of each stream bank to a different suite of hydraulic conditions that are generated by different operational scenarios. Understanding the derivation and implications of the hydraulic flow series for each operational scenario is critical to interpretation of BSTEM-derived erosion rates and the causes of bank erosion throughout the reach.

[41] It should be noted that the delineation of the hydraulic reaches using the Energy Grade Line Slope was based on the model results at the 25 detailed study sites.

To better understand the impact various factors have on riverbank erosion processes (i.e. hydropower operations, naturally occurring high flows, etc.) two modeling scenarios were developed from which the results could be compared to tease out causes of erosion. As described above, the Baseline Condition, which includes peaking operations at both Vernon and Northfield Mountain, as well as boat waves, represents the first of two operational scenarios that were simulated to determine the causes of bank erosion throughout the TFI. The non-baseline scenario include various combinations of operations at Vernon and Northfield Mountain (Table 5.4.1.1-1) to help elucidate the roles of upstream flows and peaking operations.

- The **Baseline Condition** (All operating) utilizes measured, historical hourly flows. The resulting hydraulics reflect the combination of natural flows and the peaking operations at both Vernon and Northfield Mountain. Because this flow series represents "existing" conditions over the 2000-2014 period (including waves), it was used for model calibration;

- **Scenario 1** (Vernon operating plus natural flows) also uses historical, hourly data including water levels at the Turners Falls Dam, but in this case, Northfield Mountain is idle. Hydraulics derived from this scenario are the result of natural flows, Vernon operations and water levels at Turners Falls Dam;

It is important to note that the hydraulic time series for the modeled scenarios include all "natural flows" entering the reach between 2000-2014 at its upstream boundary and from tributaries. Simulated erosion rates at each of the 25 sites, therefore, include the effects of these natural hydrologic events during both scenarios. In addition, the simulations included boat waves unless otherwise specified.

Examples of the resulting flow series derived from the HEC-RAS runs are given in Figures 5.4.1.1-4 and 5.4.1.1-5. These examples show the range of flow elevations for the two operational scenarios relative to representative bank sections. Obviously, hydraulic erosion can only occur at locations where the flow can reach and has sufficient shear stress to overcome the resistance of the surficial bank sediments.

Ranges of water-surface elevations for the model scenarios are all comprised of hourly data and are quite similar. Slight variations in these ranges occur due to operational factors (i.e. Northfield Mountain idle) but are not significant, generally 2 feet or less (Figures 5.4.1.1-4 and 5.4.1.1-5). One can also see an extended period during 2010 when Northfield Mountain was not operating. A close up of the water-surface elevations for this year are shown in the vicinity of Northfield Mountain (site 87BL) and the upper reach (site 3R) for the modeled scenarios in Figure 5.4.1.1-6.

In the lower part of the TFI, represented by site 12BL about 6,500 feet upstream of the Turners Falls Dam, flows are restricted to a narrow band near the intersection of the beach/bank toe and the upper bank. This provides opportunity for boat waves to have an effect on undercutting of the bank because their effects are always focused within this narrow range of elevations. Moving upstream we see that the range of flow elevations increases to about 10 feet in Reach 2, 12 feet in Reach 3 to about 15 feet in Reach 4. These ranges do not include the peak flow for the period (102,600 cfs) which occurred as a result of Tropical Storm Irene at 2PM on August 29, 2011. Flow elevations associated with this event increase the range of flow elevations an additional 2 to 5 feet (Figures 5.4.1.1-4 and 5.4.1.1-5).

The band of water level fluctuations generally occurs near the upper portion of the lower bank with peak water surface elevations extending up onto the upper bank. A water surface elevation-duration analysis at a subset of the detailed study sites shows the extent of time that the water surface elevation is above and below the lower to upper bank transition (Section 5.1.3).

Hydraulic data as discussed in this section were input into BSTEM-Dynamic at all 25 sites along the study reach. In those cases where bank-stabilization and/or restoration measures were undertaken, the hydraulic dataset was split in two for model runs to represent pre- and post-restoration bank conditions and geometry. A summary of the range of dates used for each simulation, whether they represent pre- or post-restoration conditions (for those sites that have been modified), and their location along the study reach is shown in Table 5.4.1.1-2.

Table 5.4.1.1-1: Operational Conditions and Associated Hydraulic Data for Each of the Modeled Scenarios

Model Scenario	Time step	Vernon Operations (flow)	NFM Operations (flow)	TFD Operations (elevation)
Baseline	Hourly	Historic	Historic	Historic
S 1	Hourly	Historic	Idle	Historic

Table 5.4.1.1-2: Summary of the Period Encompassing Each of the Hydraulic Datasets used for BSTEM

Site / Condition	Station (ft.)	Dates	
		Start	End
11L	100000	07/15/05	09/10/14
2L-Pre	94500	06/20/00	06/30/12
2L-Post	94500	07/01/12	08/28/14
303BL	94000	01/01/11	08/27/14
18L	87000	01/01/00	08/27/14
3L	79500	01/01/00	08/28/14
3R-Pre	79500	01/01/00	06/30/06
3R-Post	79500	07/01/06	08/28/14
21R	79250	01/01/00	08/27/14
4L	74000	01/01/00	08/28/14
29R	66000	01/01/00	08/27/14
5CR	57250	07/08/02	09/03/14
26R	50000	01/01/00	08/27/14
10L	49000	01/01/00	08/27/14
10R-Post	49000	07/01/01	08/27/14
6AL-Pre	41750	01/01/00	06/30/04
6AL-Post	41750	07/01/04	08/27/14
6AR-Post	41750	06/21/00	08/27/14
119BL	41000	01/01/00	08/27/14
7L	37500	01/01/00	08/26/14
7R	37500	01/01/00	08/26/14
8BL	32750	06/02/00	08/26/14
8BR-Pre	32750	06/02/00	06/30/12
8BR-Post	32750	07/01/12	08/26/14
87BL	30750	01/01/00	08/27/14
75BL	27000	01/01/00	08/27/14
9R-Pre	6750	06/02/00	06/30/08
9R-Post	6750	07/01/08	8/26/14
12BL	6500	01/01/00	08/27/14
BC-1R	4750	06/05/00	08/26/14

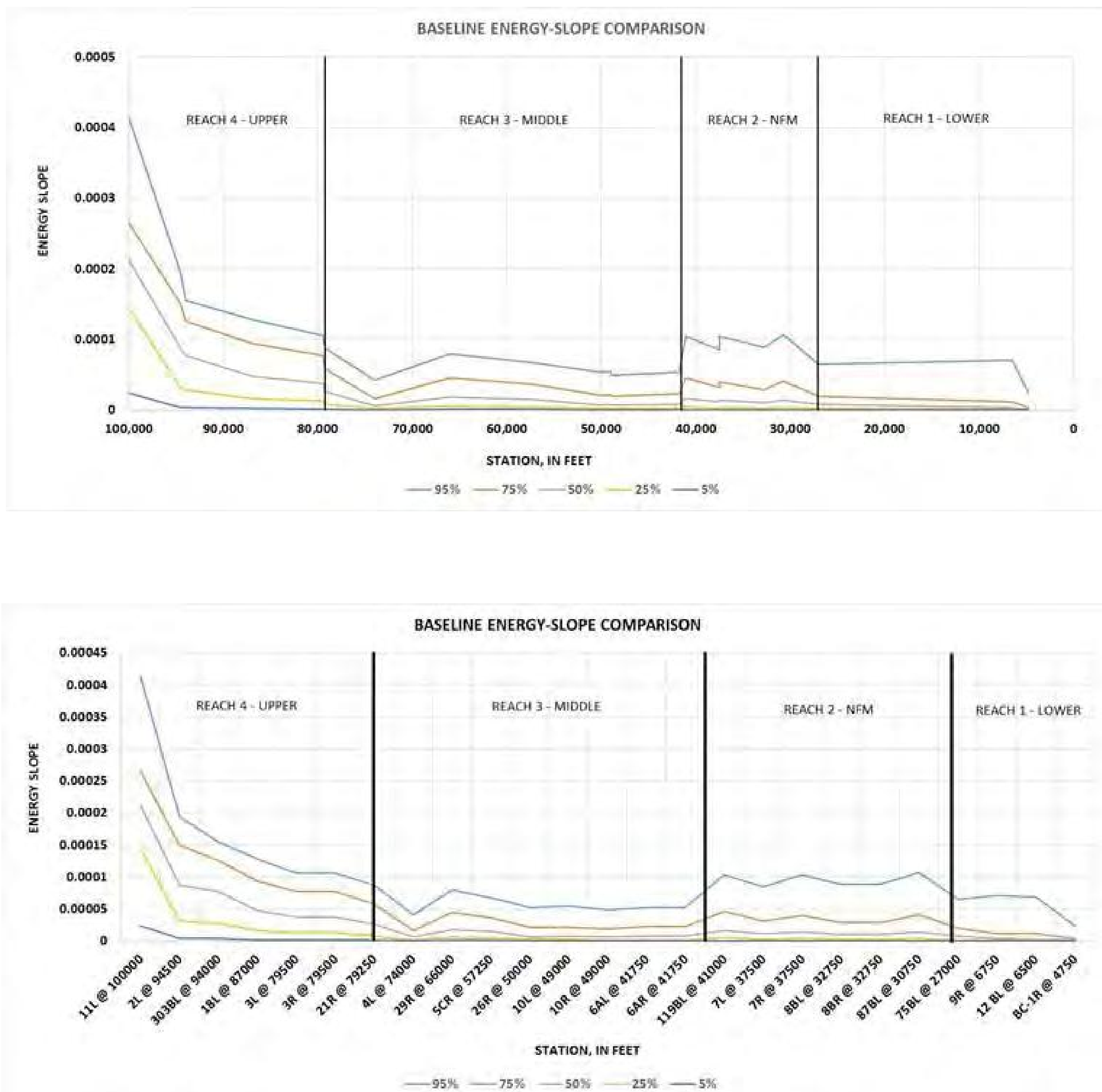

Figure 5.4.1.1-1 Longitudinal variation of energy slopes along the study reach for the Baseline Condition plotted by stationing (Top) and by site number (Bottom)

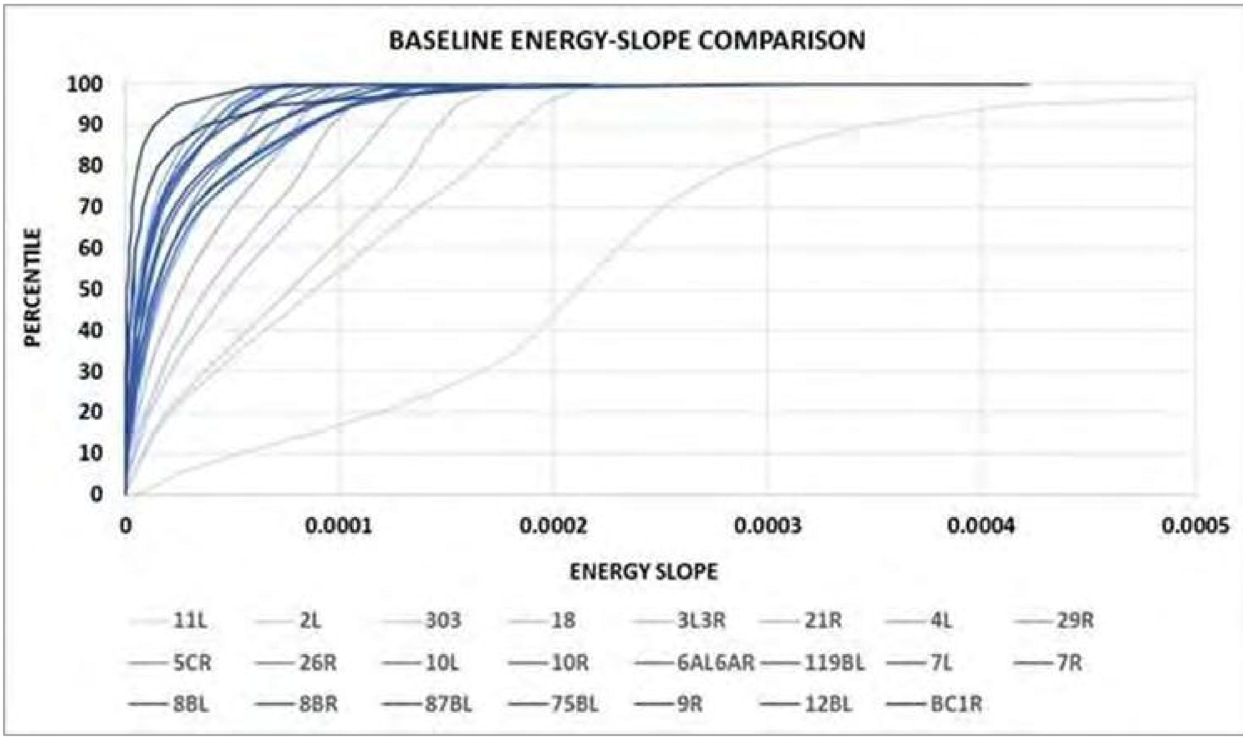

Figure 5.4.1.1-2: Comparison of the Range of Energy Slopes for Each Modeled Site along the Study Reach Showing Steepest Slopes in the "Upstream" Reach

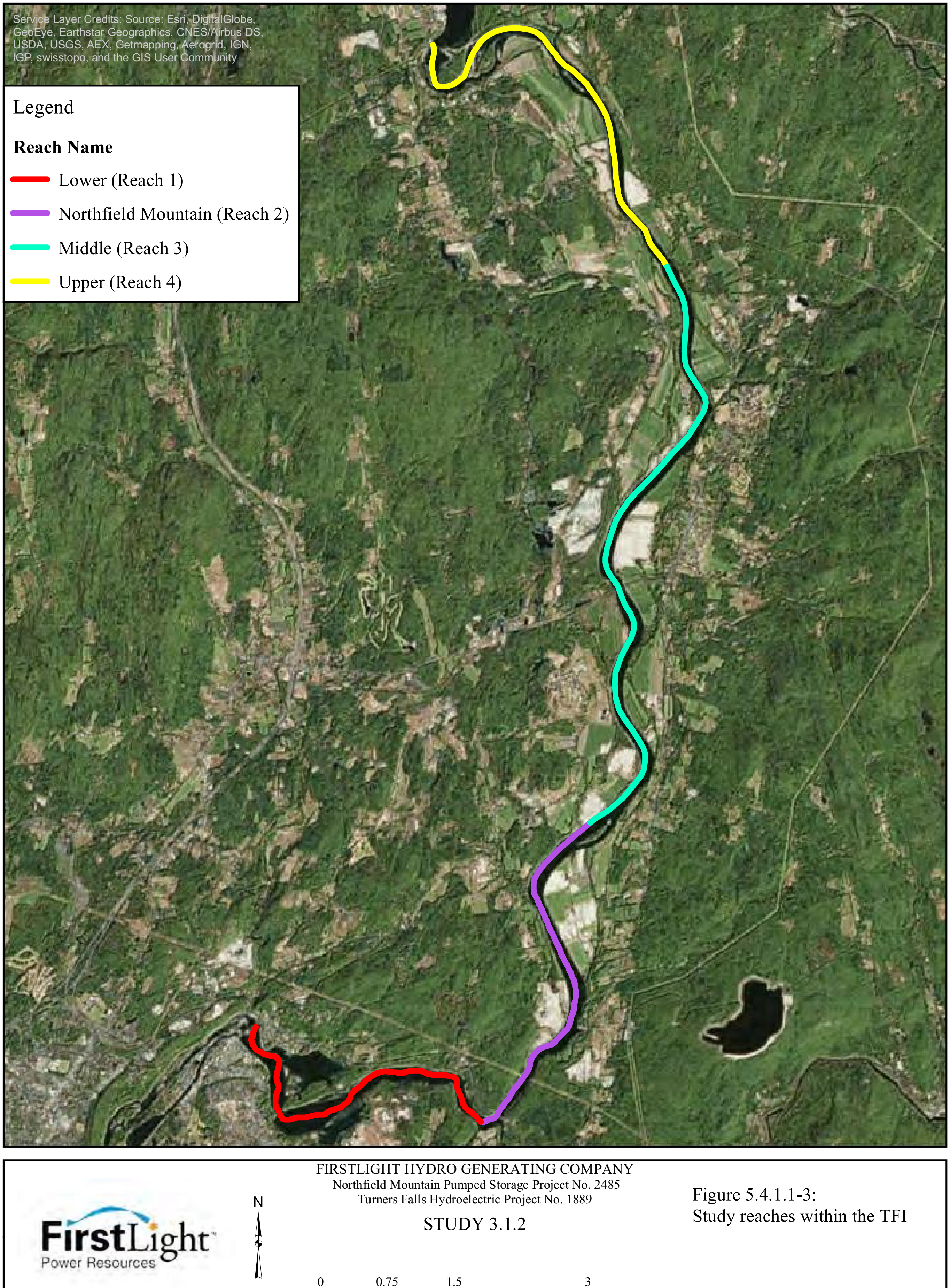

FIRSTLIGHT HYDRO GENERATING COMPANY
Northfield Mountain Pumped Storage Project No. 2485
Turners Falls Hydroelectric Project No. 1889

STUDY 3.1.2

Figure 5.4.1.1-3:
Study reaches within the TFI

FirstLight Power Resources

Path: W:\gis\studies\3_1_2\maps\final_report\figure_5_4_1_1-3.mxd

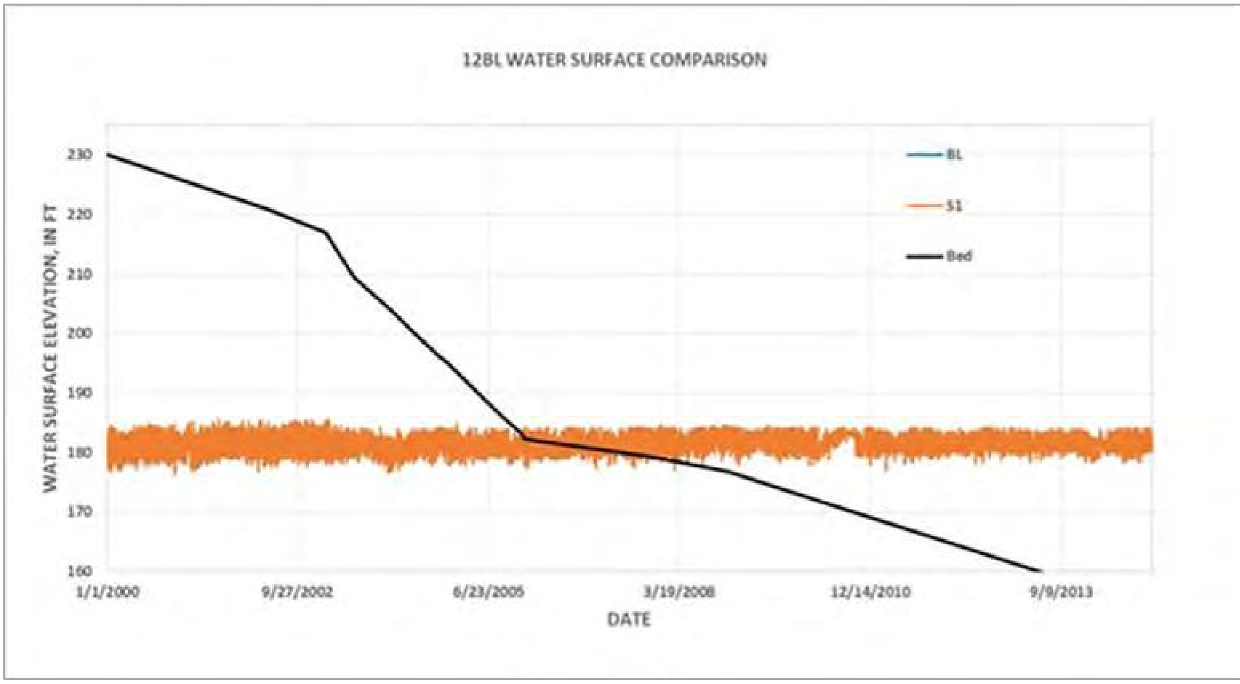

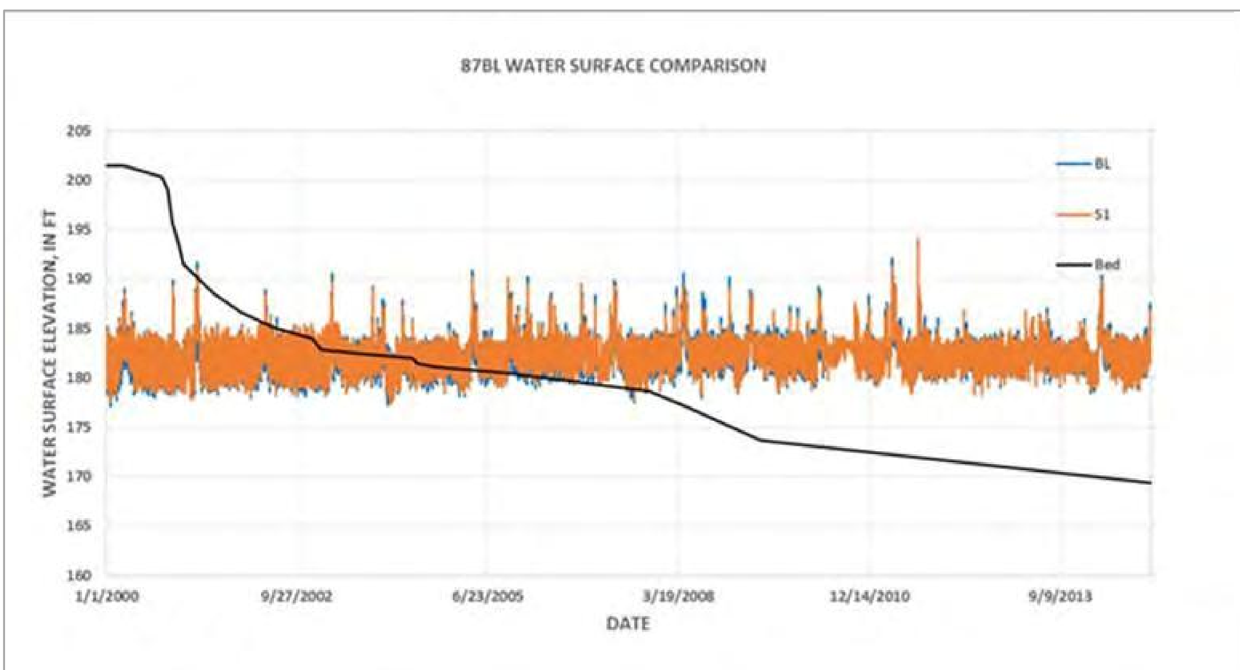

Figure 5.4.1.1-4: Water-surface elevations for representative sites within the Lower Reach (#1; site 12BL), and Northfield Mountain Reach (#2; site 87BL)

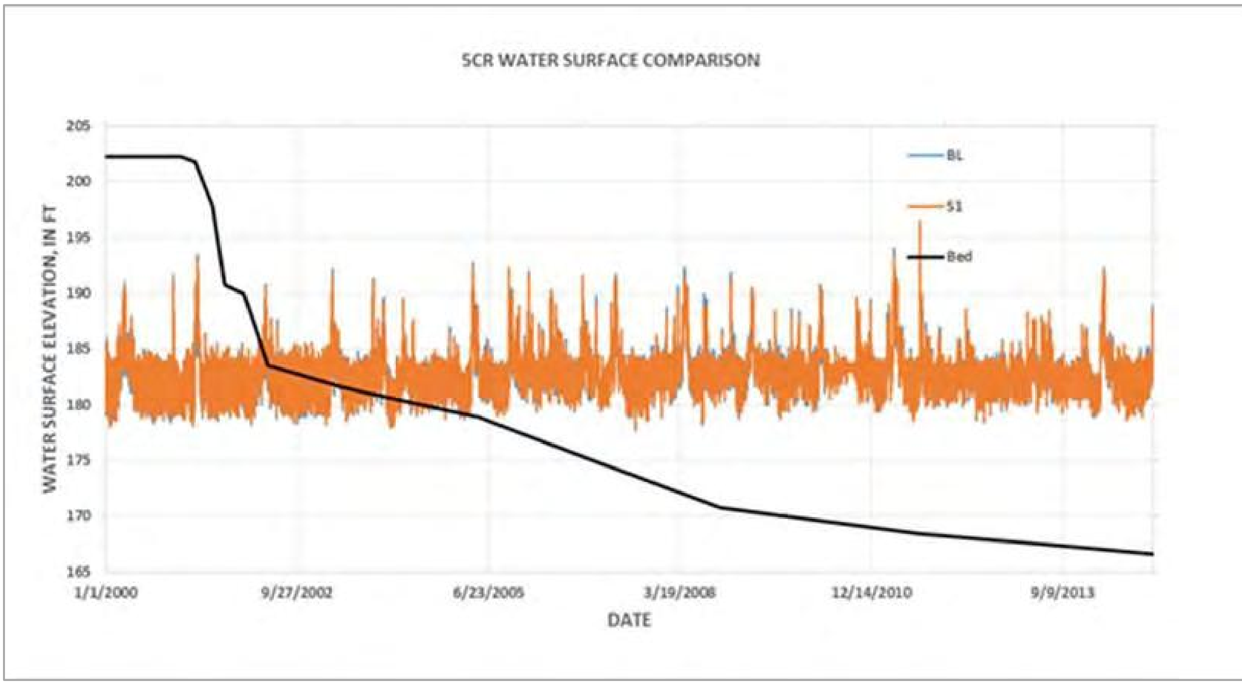

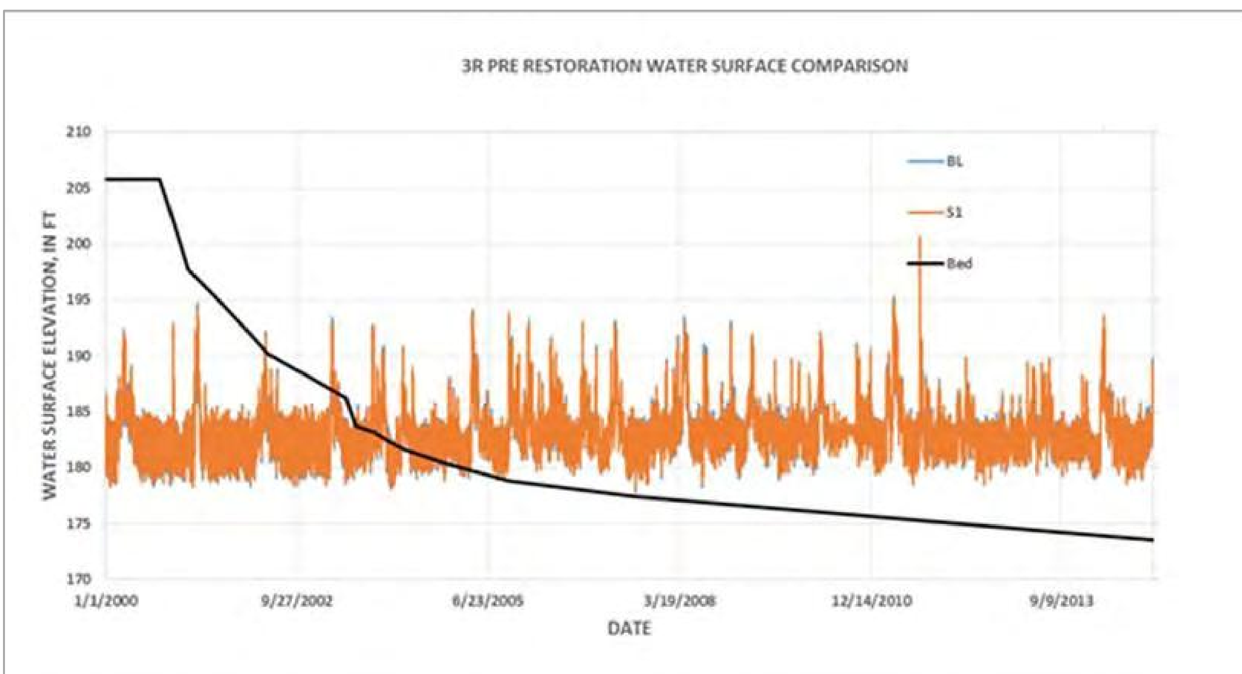

Figure 5.4.1.1-5 Water-surface elevations for representative sites within the Middle Reach (#3; site 5CR) and Upper Reach (#4; site 3R Pre-restoration)

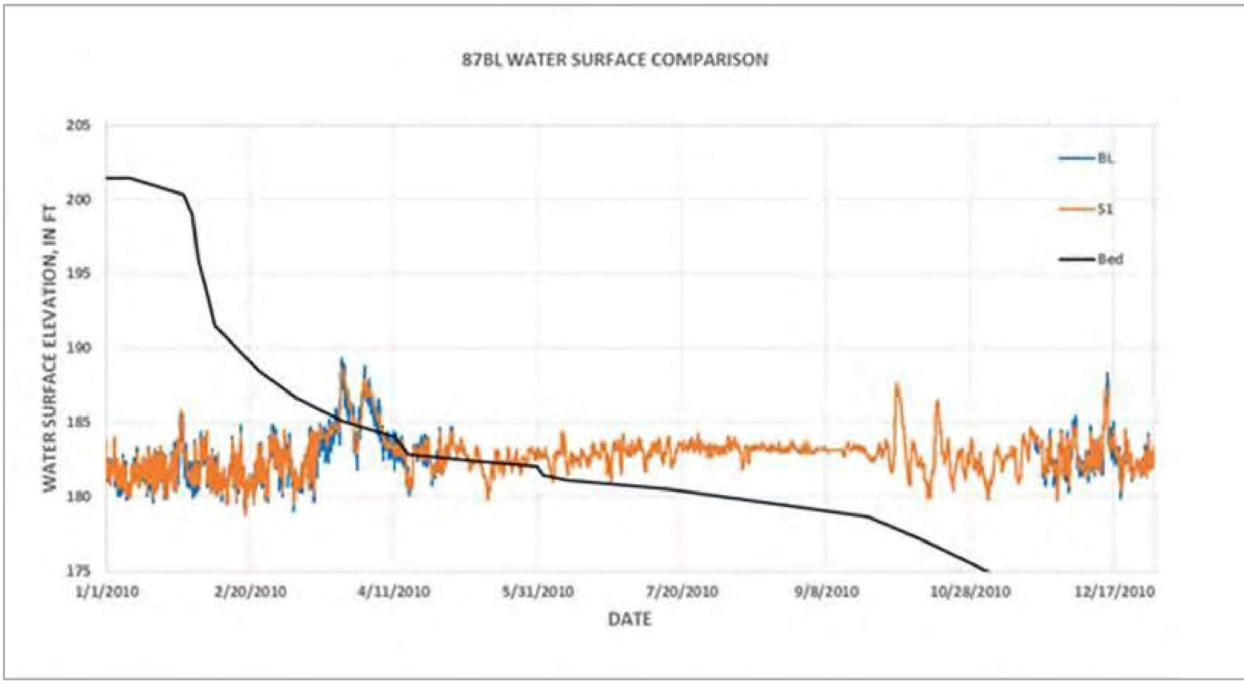

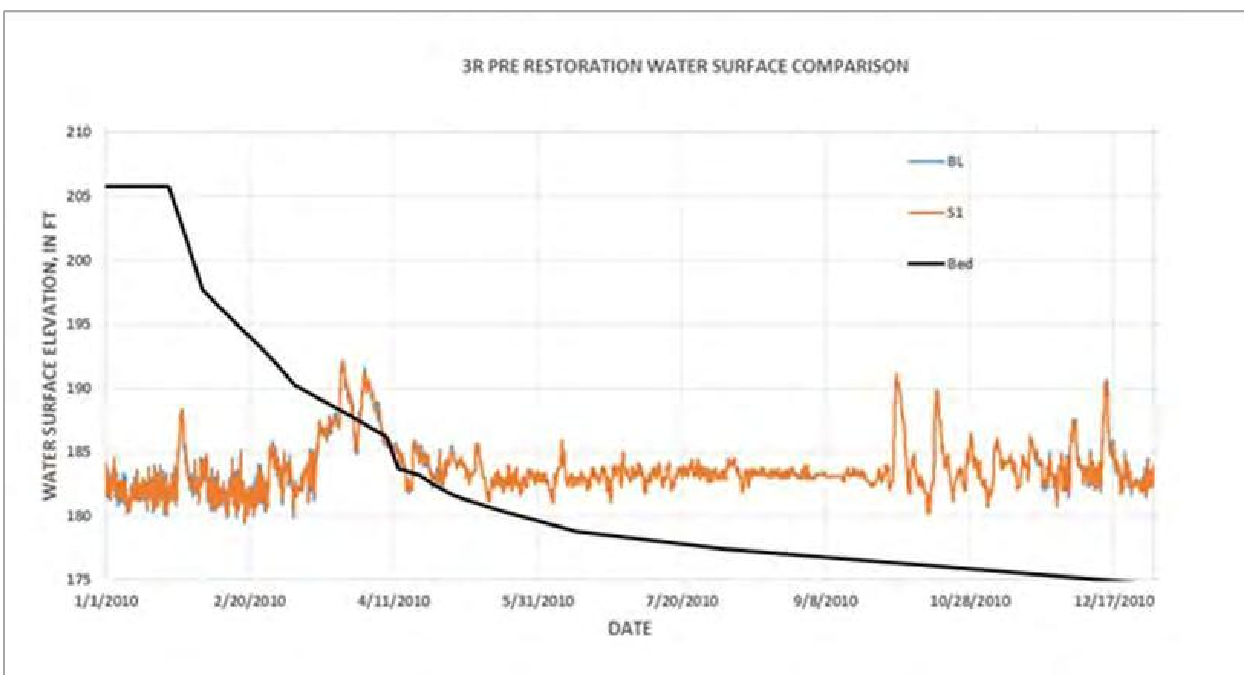

Figure 5.4.1.1-6: Representative 2010 water-surface elevations for Reach 2 (Top) and Reach 4 (Bottom) showing range of stages relative to channel-bank geometry

5.4.1.2 Site Conditions and Bank-Resistance Inputs

Site conditions relevant to bank-stability modeling include aspects of bank geometry (height and steepness), hydraulic and geotechnical resistance, and vegetative conditions. Seven of the sites had stabilization measures applied to the bank at some time during the modeling period (2000-2014) (Table 5.4.1.2-1). As alluded to in the previous section, modeling of these sites included a pre-and post–restoration period, with the output of bank geometry from the pre-restoration run halted and used as input for post-restoration conditions. If bank re-shaping was involved in the stabilization works, that new geometry was used as the starting geometry for the post-restoration simulations. In addition, modifications to other aspects of the bank surface were parameterized for the post-restoration run if needed.

Data on bank-material and vegetation properties for each of the 25 detailed study sites were determined from the *in situ* field investigations described in Section 4. An example of the bank-materials and roughness data are provided for a few sites in Table 5.4.1.2-2 and for the remainder of the sites in Volume III (Appendix L). Layer 5 which is below the minimum water-surface elevation was designated as the "channel bed" and set to be non-erodible because BSTEM is not a sediment-routing model. Data listed under "Toe-Model Data" refer to resistance data for the hydraulic erosion sub model along the entire bank face and not just the bank toe region. Friction angle and cohesion data are derived from the borehole shear tests conducted at each site. Groundwater-flow parameters are estimated according to soil texture, the associated values published by the NRCS (NRCS, 2015) and were discussed in Section 4. Critical shear stress of the surface sediments were obtained from either the Shields criteria for non-cohesive materials using d_{50}, or from jet-test data in the case of fine-grained materials. Summaries of these data and the data-collection methods are also provided in Section 4.

The version of BSTEM-Dynamic used in this study (Ver. 2.3) allowed the user to input a different value of Manning's roughness coefficient (n) for each bank layer. Estimates of n were developed from field observations and from current and historical photographs of each site. Photographs taken during the 2013 FRR and during field data collection associated with this study (2014-2015) represented current conditions while photos taken during the 1998 FRR were used to represent conditions in 2000.

For those sites with historical survey data, the initial bank geometry was obtained directly from the survey data and generally started on 1/1/2000. These sites, shown in bold in Table 5.4.1.2-3 provided an excellent opportunity to calibrate BSTEM by comparing the change in bank geometry at the end of the simulation with the measured change in geometry over the same period. In the general case, the end of the period was 2014 unless otherwise specified. As is customary in hydraulic modeling, Manning's n was the primary calibration parameter, serving to either increase or decrease the effective stress acting on the bank surface. A given calibration run was considered acceptable if the difference between the simulated and measured erosion (in ft^2) over the period was less than the potential survey error.

The potential survey error was termed "total survey variance" (TSV) and was calculated as the product of the slope length times the potential vertical error (Table 5.4.1.2-3). This vertical error was deemed to be about 0.5 feet for all surveys between 2000 and 2006 and about 0.4 feet for all surveys conducted in 2007 and later (R. Howard, written comm., 2015). The approach taken to determine TSV was to:

1. Take the unit survey variance of 0.5 ft^2/ft of slope length (for pre 2001 surveys) and multiply by the sum of the slope lengths undergoing erosion (as determined by the starting and ending surveys) to obtain total survey variance in ft^2.

2. Compare TSV with difference between simulated and "measured" erosion. If that difference is equal to or less than the calculated TSV, the calibration is successful.

For those sites that did not have historical surveys (non-bold in Table 5.4.1.2-3), the bank geometry used for the initial condition was the 2014 surveyed geometry. Hydraulic inputs (water-surface elevation and energy slope) were the same as for the calibration sites and roughness coefficients were estimated as before.

Table 5.4.1.2-1: Bank-stabilization Measures Conducted at the Detailed Study Sites during the Modeling Period

Site #	Project Name	Date Stabilized	Technique
9(R)	Campground	2008	Coir logs or other logs anchored at toe of upper bank, plant vegetation on upper bank
8B(R)	Bathory/Gallagher	2012	Gravel on lower bank along with large woody debris (anchored), planting of vegetation on lower bank
6A(R)	Flagg	2000	Re-shape upper bank to flatter slope, plant vegetation on upper bank, submerged rock toe with aquatic vegetation (which has subsequently accumulated sediment deposits)
6A(L)	Skalski	2004	Re-shape upper bank to flatter slope, plant vegetation on upper bank, coir logs, rock toe below coir logs
10(R)	Urgiel U/S	2001	Re-shape upper bank to flatter slope, plant vegetation on upper bank, coir logs, rock toe below coir logs
3(R)	Kendall	2008	Re-shape upper bank to flatter slope, plant vegetation on upper bank, coir logs, rock toe below coir logs
2(L)	Bonnette Farm	2012	Plant vegetation on upper bank

5CR

	Bank Model Input Data					Groundwater Model Input Data			Toe Model Input Data		Roughness	
Layer Number	*Friction angle f' (degrees)*	*Cohesion c' (kPa)*	*Saturated unit weight (kN/m³)*	*ϕ^b (degrees)*	*Chemical concentration (kg/kg)*	*Hydraulic Conductivity k_{sat} (m/s)*	*van Genuchte n a (1/m)*	*van Genuchte n n*	t_c (Pa)	*k* (cm³/Ns)	*Manning n* ($s/m^{1/3}$)	**Comments**
Layer 1	31.0	2.9	18.0	10.0	-	2.823E-05	1.5073	1.8413	8.70	0.068	0.030	avg MJ 6&7 τc*10 for exposed roots
Layer 2	31.0	2.9	18.0	10.0	-	9.150E-06	0.6577	1.6788	0.87	0.195	0.018	avg MJ 6&7
Layer 3	32.4	5.9	18.0	10.0	-	9.150E-06	0.6577	1.6788	1.03	0.197	0.020	MJ 1
Layer 4	31.4	4.2	18.0	10.0	-	9.150E-06	0.6577	1.6788	0.13	0.555	0.050	beach-toe sample (.18 mm)

3R Post Restoration

	Bank Model Input Data					Groundwater Model Input Data			Toe Model Input Data		Roughness	
Layer Number	*Friction angle f' (degrees)*	*Cohesion c' (kPa)*	*Saturated unit weight (kN/m³)*	*ϕ^b (degrees)*	*Chemical concentration (kg/kg)*	*Hydraulic Conductivity k_{sat} (m/s)*	*van Genuchte n a (1/m)*	*van Genuchte n n*	t_c (Pa)	*k* (cm³/Ns)	*Manning n* ($s/m^{1/3}$)	**Comments**
Layer 1	30.9	1.7	18.0	10.0	-	3.097E-06	2.3570	2.0037	0.66	0.246	0.025	
Layer 2	30.9	1.7	18.0	10.0	-	3.097E-06	2.3570	2.0037	0.66	0.246	0.025	
Layer 3	31.0	2.1	18.0	10.0	-	3.097E-06	2.3570	2.0037	0.66	0.246	0.040	
Layer 4	42.0	0.0	20.0	10.0	-	1.745E-03	3.5237	2.3286	53.46	0.027	0.060	d_{50} RipRap

9R Pre Restoration

	Bank Model Input Data					Groundwater Model Input Data			Toe Model Input Data		Roughness	
Layer Number	*Friction angle f' (degrees)*	*Cohesion c' (kPa)*	*Saturated unit weight (kN/m³)*	*ϕ^b (degrees)*	*Chemical concentration (kg/kg)*	*Hydraulic Conductivity k_{sat} (m/s)*	*van Genuchte n a (1/m)*	*van Genuchte n n*	t_c (Pa)	*k* (cm³/Ns)	*Manning n* ($s/m^{1/3}$)	**Comments**
Layer 1	32.3	3.9	18.0	10.0	-	9.174E-05	3.2066	2.1662	0.09	0.667	0.020	from PS sample (.12 mm) + Rip Root value of 3.9 for c'
Layer 2	33.1	3.6	18.0	10.0	-	9.174E-05	3.2066	2.1662	0.29	11.782	0.016	d50 = 0.41 mm + Rip Root value of 3.6 for c'
Layer 3	28.2	18.3	18.0	10.0	-	9.150E-06	1.6788	2.0037	10.30	5.500	0.016	MJ average (new) + Rip Root value of 3.6 for c'
Layer 4	28.2	14.7	18.0	10.0	-	9.150E-06	1.6788	2.0037	0.21	3.500	0.020	d_{50} = 0.30 mm

Table 5.4.1.2-2: Examples of input bank-material, roughness and additional vegetation data used or BSTEM modeling at sites 5CR, 3R-post-restoration, and 9R pre-restoration

Table 5.4.1.2-3: Summary of BSTEM simulations showing total survey variance (TSV) for calibration runs conducted for the Baseline Condition

Site/Condition	Station (ft.)	Dates		Total Survey Variance (ft^2)
		Start	End	
11L	100000	07/15/05	09/10/14	13.7
2L-Pre	94500	06/20/00	06/30/12	6.2
2L-Post	94500	07/01/12	08/28/14	-
303BL	94000	01/01/00	08/27/14	-
18L	87000	01/01/00	08/27/14	-
3L	79500	01/01/00	08/28/14	17.6
3R-Pre	79500	01/01/00	6/30/06	20.3
3R-Post	79500	07/01/06	08/28/14	8.60
21R	79250	01/01/00	08/27/14	-
4L	74000	01/01/00	08/28/14	4.80
29R	66000	01/01/00	08/27/14	-
5CR	57250	07/08/02	09/03/14	23.2
26R	50000	01/01/00	08/27/14	-
10L	49000	01/01/00	08/27/14	2.81
10R-Post	49000	07/01/01	08/27/14	17.2
6AL-Pre	41750	01/01/00	06/30/04	13.2
6AL-Post	41750	07/01/04	08/27/14	6.60
6AR-Post	41750	06/21/00	08/27/14	4.94
119BL	41000	01/01/00	08/27/14	-
7L	37500	01/01/00	08/26/14	23.6
7R	37500	01/01/00	08/26/14	16.5
8BL	32750	06/02/00	08/26/14	18.5
8BR-Pre	32750	06/02/00	06/30/12	26.0
8BR-Post	32750	07/01/12	08/26/14	1.37
87BL	30750	01/01/00	08/27/14	-
75BL	27000	01/01/00	08/27/14	-
9R-Pre	6750	06/02/00	06/30/08	15.7
9R-Post	6750	07/01/08	08/26/14	14.0
12BL	6500	01/01/00	08/27/14	-
BC-1R	4750	06/05/00	08/26/14	3.78

5.4.2 BSTEM Simulation Results: General

This section brings together the results of the BSTEM simulations at the 25 detailed study sites within the TFI. The locations and stationing of these sites along the TFI are shown in Section 4 along with the flow, geometry and bank-resistance input data used to populate BSTEM for the different scenarios. The flow scenarios represent different operational conditions aimed at determining the role of water-level fluctuations, high flows and boat waves on bank-erosion rates. BSTEM calculates boundary shear stress caused by water-level fluctuations at each time step and at each node along the bank face. To address any issues related to drawdown conditions and effects as a result of hydro-power operations, BSTEM addresses these processes by calculating pore-water and confining pressures along potential failure surfaces during each time step of a simulation.

5.4.2.1 Baseline Conditions

The first set of BSTEM simulations were those for the Baseline Condition so that the calibration parameters could then be used for subsequent model scenarios. As a reminder, the Baseline Condition was designed to represent "existing" conditions, including Vernon and Northfield Mountain operations, natural flows and boat waves. These are the flow conditions that the sites had been subjected to over the 2000 to 2014 period and would serve as a means of comparison with the other flow scenario. Results of the baseline simulations (with waves on) are listed along with the measured erosion for that site (Table 5.4.2.1-1). Note that results from all of the sites have been normalized by dividing the total erosion over the period (in ft^3/ft of channel length) by the number of years of simulation because not all simulation periods were of equal duration. These values are then readily comparable to interpret relative degrees of bank instability along the reach.

For the Baseline Condition, simulated rates of bank erosion along the reach range from very close to zero ft^3/ft/y to 15.4 ft^3/ft/y at site 3R under pre-restoration conditions. Other sites with bank-erosion rates higher than the 75^{th} percentile for the non-restored sites include 5CR (8.6 ft^3/ft/y), 8BR-pre-restoration (7.4 ft^3/ft/y), 3L (6.1 ft^3/ft/y), 119 BL (5.9 ft^3/ft/y) and 9R pre-restoration (5.4 ft^3/ft/y). Of these six highest rates, three of the sites have been restored. Specific information regarding the erosion rates at these and the other sites will be provided in the following section. The spatial distribution of erosion rates along the reach are shown schematically in Figure 5.4.2.1-1.

The median value for all sites and conditions (including restored conditions) along the reach is about 1.2 ft^3/ft/y compared to 2.2 ft^3/ft/y including just the non-restored sites. The difference in the distributions for the Baseline Condition can be clearly seen in the Figure 5.4.2.1-2 showing the greater erosion rates when the restored sites are not included in the data set. Restoration measures have been very effective in reducing bank-erosion rates by about an order of magnitude throughout the reach (Figure 5.4.2.1-2; Middle and Bottom), with an average reduction of 93%. Median bank-erosion rates for the non-restored and restored sites are 1.9 and 0.21 ft^3/ft/y, respectively.

Table 5.4.2.1-1: Results of BSTEM Simulations for the Baseline Condition

Site/Condition[1]	Station	Dates		Total Survey Variance	Measured Erosion[2]	Baseline (Waves on)
	(ft)	Start	End	(ft^2/y)	(ft^2/y)	(ft^2/y)
11L	100000	07/15/05	09/10/14	1.49	0.576	0.297
2L-Pre	94500	06/20/00	06/30/12	0.518	0.904	1.20
2L-Post	94500	07/01/12	08/28/14	-	0.000	0.214
303BL	94000	01/01/00	08/27/14	-	N/A	0.647
18L	87000	01/01/00	08/27/14	-	N/A	1.09
3L	79500	01/01/00	08/28/14	1.20	6.40	6.09
3R-Pre	79500	01/01/00	06/30/06	3.13	16.7	15.4
3R-Post	79500	07/01/06	08/28/14	1.40	0.824	0.285
21R	79250	01/01/00	08/27/14	-	N/A	2.36
4L	74000	01/01/00	08/28/14	0.33	0.154	0.017
29R	66000	01/01/00	08/27/14	-	N/A	1.72
5CR	57250	07/08/02	09/03/14	1.91	7.04	8.61
26R	50000	01/01/00	08/27/14	-	N/A	1.19
10L	49000	01/01/00	08/27/14	0.19	0.140	0.160
10R-Post	49000	07/01/01	08/27/14	1.31	0.115	0.00
6AL-Pre	41750	01/01/00	06/30/04	2.92	2.73	2.67
6AL-Post	41750	07/01/04	08/27/14	0.65	0.456	0.00
6AR-Post	41750	01/01/00	08/27/14	0.35	0.243	0.21
119BL	41000	01/01/00	08/27/14	-	N/A	5.88
7L	37500	01/01/00	08/26/14	1.61	4.48	4.29
7R	37500	01/01/00	08/26/14	1.12	2.28	2.06
8BL	32750	06/02/00	08/26/14	1.30	0.522	0.427
8BR-Pre	32750	06/02/00	06/30/12	2.15	5.93	7.41
8BR-Post	32750	07/01/12	08/26/14	0.64	0.456	0.312
87BL	30750	01/01/00	08/27/14	-	N/A	3.57
75BL	27000	01/01/00	08/27/14	-	N/A	3.76
9R-Pre	6750	06/02/00	06/30/08	1.94	6.26	5.43
9R-Post	6750	07/01/08	08/26/14	2.27	0.472	0.227
12BL	6500	01/01/00	08/27/14	-	N/A	2.22
BC-1R	4750	06/05/00	08/26/14	0.266	0.091	0.190

[1]*Sites shown in bold have been calibrated*
[2] *Measured rates of erosion as determined from field surveys are included for comparison*

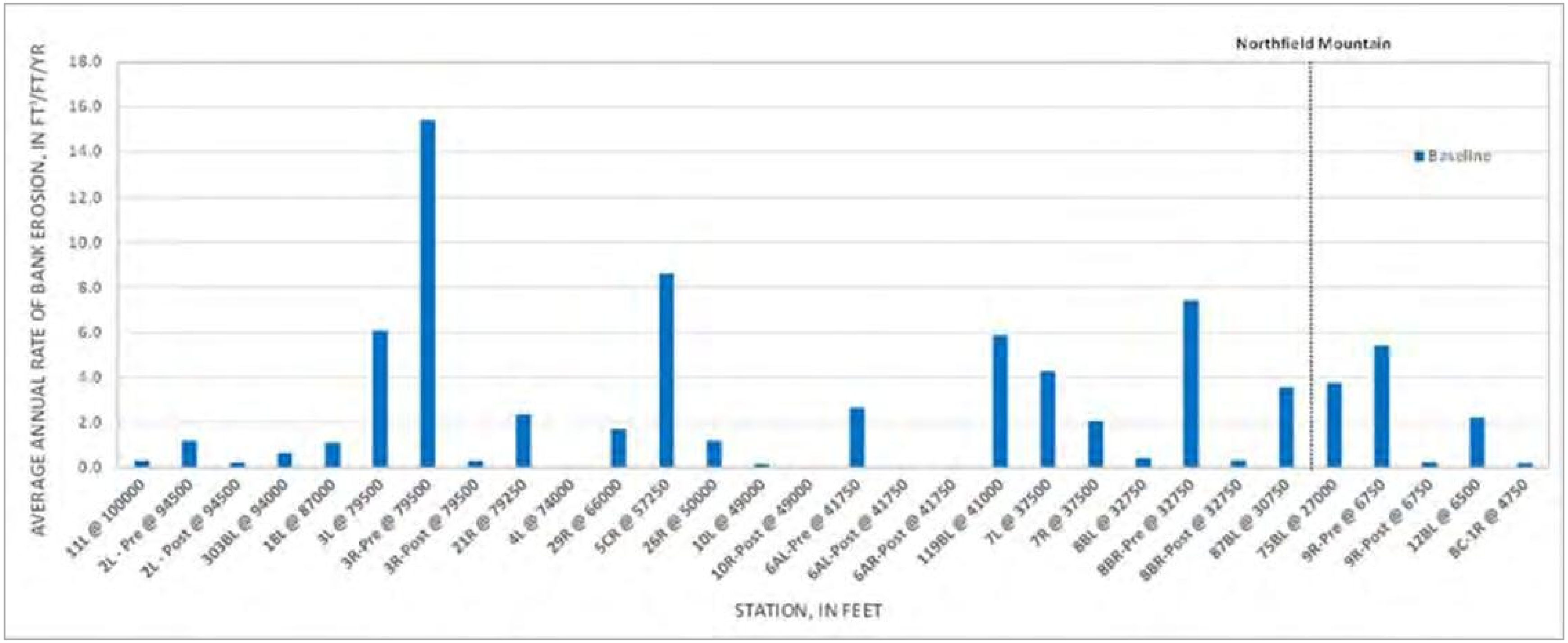

Figure 5.4.2.1-1: Spatial Distribution of Bank-erosion Rates for all Sites under Baseline Conditions

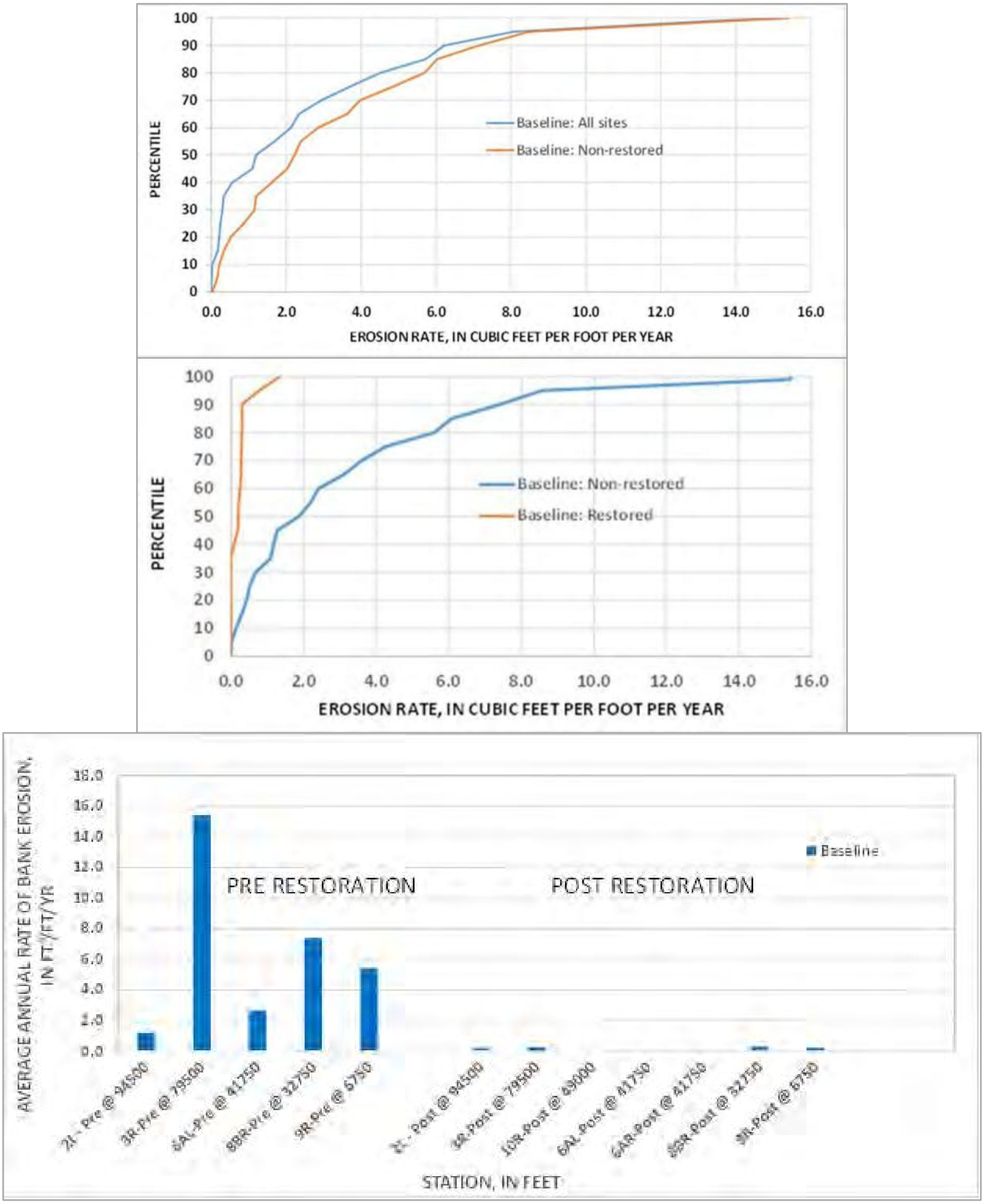

Figure 5.4.2.1-2: Distribution of Bank-erosion Rates for the Baseline Condition for All Sites/conditions versus Non-restored (Top), and for Restored versus Non-restored Simulations (Middle) and Direct Comparison (Bottom)

5.4.2.2 Comparisons with Other Modeling Scenarios

The other bank-erosion scenario modeled with BSTEM (S1) is based on hydraulic inputs representing a range of operational conditions along the TFI. This scenario is described in previous sections with the hydraulic assumptions summarized in Table 5.4.1.1-1. In addition to the basic operational and hydraulic scenarios, an additional Baseline Condition was run for each site with the wave sub-model turned off. Differences between the Baseline Condition with and without waves provided a convenient way to determine the role of boat-generated waves on bank erosion. Perhaps the easiest way to view and interpret the multitude of BSTEM simulations is to view the results in graphical form sorted schematically by station. Figure 5.4.2.2-1 shows the simulated bank-erosion rates (in $ft^3/ft/y$) along the entire study reach for ease of comparison of simulations of different lengths. Vernon Dam would be located at the far left of the plot with Turners Falls Dam at the far right. A numerical summary of these results is provided in Table 5.4.2.2-1.

Several interpretations about bank-erosion rates can be gleaned from Figure 5.4.2.2-1.

- First, is that there are no apparent longitudinal trends as one moves upstream or downstream from either Vernon Dam or Northfield Mountain, or along the reach as a whole.

- Second, erosion rates for the Baseline Condition (with waves) represent the maximum erosion rate at each of the sites. The slightly greater values (by about 1%) for S1 at sites 3R pre-restoration and 87BL should be considered the same as the Baseline as they are within the range of differences in failure geometries over the course of a 15-year simulation.

- Third, the role of boat waves has a small impact starting in the lower TFI (Reach 1) in the vicinity of station 27,000 (site 75BL) and generally increases downstream. This is related to the general lake-like conditions in the lower TFI where water-surface elevations vary across a narrow range (See Figure 5.4.1.1-4; Top from previous section), focusing wave impacts in the zone where the beach/toe intersect the lower-most part of the upper bank. A close up of the erosion at site 12BL (station 6,500) shows the increase in basal undercutting that took place with the "waves on" version of the Baseline Condition in comparison to the simulation without waves (Figure 5.4.2.2-2).

Role of Northfield Mountain Project Operations

One of the ways to determine the role of Northfield Mountain Project operations on bank-erosion rates is to attempt to isolate the effects of the peaking operations from Northfield Mountain at the exclusion of high flows (represented by the hourly data) and boat-generated waves. To accomplish this we subtract the bank-erosion rates predicted for S1 (Vernon operating, hourly peaks, boat waves and Northfield Mountain idle) from the erosion rates predicted for the Baseline Condition. The operational difference between the two scenarios would be manifest as altered hydraulic conditions (and assumedly erosion rates) resulting from operations at Northfield Mountain. As can be seen in Figure 5.4.2.2-3, Project operations as denoted by the orange bars (BL-S1) generally show very small effects. The apparent negative values for the Baseline – S1 Case are the result of slight differences in failure geometries caused by differences in the geometry of hydraulic erosion at several sites (i.e. slightly larger when NFM is idle in these cases).

The exception appears to be at site 8BR pre-restoration (station 32,750) where a large geotechnical failure occurred at a high flow of about 99,000 cfs but only under Baseline Conditions. The other model scenario for the site does not show this failure. Given that mass wasting are not a linear, continuous process such as entrainment of bed sediments under excess stress, it is reasonable that slightly more hydraulic erosion occurred during the Baseline Condition causing the failure. In comparison to site 8L which does not show a dominant impact from Northfield Mountain, 8BR is much steeper and less vegetated. Current and future erosion rates at this site, however, reflect the effect of restoration activities in 2012 that greatly reduced bank-erosion rates from about 7.4 $ft^3/ft/y$ to about 0.3 $ft^3/ft/y$ (Figure 5.4.2.1-2; Bottom).

The only other locations/conditions that show even a minor impact (> 0.1 $ft^3/ft/y$) from Northfield Mountain Project operations are sites 7L at station 37,500 (0.17 $ft^3/ft/y$) and perhaps 119BL at station 41,000 (0.09 $ft^3/ft/y$). These are all very low erosion rates and if considered in the context of average, annual-erosion rates for non-restoration sites under the Baseline Condition, these contributions fall at or below the 10th percentile of erosion rates. At site 7L bank erosion due to Northfield Mountain Project operations (Baseline minus S1) accounts for about 4% of the erosion under Baseline Conditions while 95% of the erosion occurs at flows greater than 47,700 cfs. At site 119BL the contribution from Project operations is about 1.5%.

Overall contributions of Northfield Mountain Project operations on bank-erosion rates can be seen by comparing the BL-S1 erosion rate with the total erosion rate under Baseline Conditions. The contribution in percent (%) is plotted schematically (in orange) by site/station along with the bank-erosion rate (in blue) under the Baseline Condition (Figure 5.4.2.2-3). If looking at just the contributions from Northfield Mountain Project operations (BL-S1), values are generally low (less than 5%) with a few exceptions; sites 10R post-restoration (station 49,000), 6AL post-restoration (station 41,750), 8BR pre- and post-restoration (station 32,750) and 8BL (station 32,750). When including the information on erosion rates as well, we see that aside from 8BR pre-restoration, the remaining sites just mentioned are experiencing very low rates of erosion, with most representing restored conditions (Table 5.4.2.2-2).

Role of Naturally Occurring High Flows

The role of high flows on bank-erosion rates was investigated by analyzing the hourly outputs from each time step in BSTEM. The output data were sorted by the amount of bank erosion during each time step to determine what stages (flow elevations) and discharges were responsible for bank erosion along the reach. The stage data was converted to discharge by developing polynomial regression relations using data from HEC-RAS. An example plot is shown in Figure 5.4.2.2-4 that was used for sites 10R, 10L and 26R; all equations are listed in Table 5.4.2.2-3. Erosion data for each site were thus sorted into 10,000 discharge classes to determine how much erosion had occurred in each discharge class without biasing the classes because of different sizes. Data from each class were then summed to develop a cumulative frequency distribution for each model run.

The resulting database of erosion totals provides us with an opportunity to investigate the relative amounts of erosion that occur at different discharges. A metric that denotes the flows at which the vast majority of the erosion occurs is informative in determining causes. For example, Figure 5.4.2.2-5 shows the discharge at which 95% and 75% of the erosion occurs at flows greater than indicated. Conversely, only 5% of the erosion occurs at flows less than those shown in the top figure. The combined hydraulic capacity of Vernon Dam (17,130 cfs) and Northfield Mountain (20,000 cfs) of roughly 37,000 cfs is shown as the solid black line for the middle, Northfield Mountain, and lower impoundment. A threshold of 17,130 cfs is used to show the hydraulic capacity for the upper impoundment as a result of Vernon Dam only. The figure clearly shows that 95% of the bank-erosion for just about all of the sites, conditions and scenarios occurs at flows much greater than the hydraulic capacity of Vernon Dam. Again, these results need to be taken in the context of the actual amount of erosion that occurs at each site/condition. For example, of the sites where 95% of the erosion occurs at about 10,000 cfs or less including sites 4L, 29R, 10R post-restoration and 6AR post-restoration, only site 29R (station 66,000) had measureable amounts of erosion (about 1.7 $ft^3/ft/y$). Here, the initial condition (2014) of the bank showed a pronounced undercut at the start of the simulation (Figure 5.4.2.2-6). Mass wasting of the cantilever section of the bank occurred soon thereafter, regardless of the magnitude of the flow.

As further evidence of the critical role of high flows on bank-erosion rates, a number of examples of the discharges where bank-erosion occurs are provided in Figure 5.4.2.2-7. In this case we are looking at both the contribution of discharges to cumulative erosion at a particular site as well the individual discharge classes where the erosion occurred. The examples provided are for the following stations:

- Site 3L at station 79,500 where about 6.1 ft^3/ft/y of erosion occurred
- Site 5CR at station 57,250 where 8.6 ft^3/ft/y of erosion occurred;
- Site 6AL pre-restoration at station 41,750 where 2.6 ft^3/ft/y occurred; and
- Site 6AR post-restoration also at 41,750 where only 0.02 ft^3/ft/y).

Vertical sections in the cumulative plots (sold traces) and peaks in the dotted traces generally indicate the occurrence of a mass wasting. These are most likely the result of bank steepening and undercutting during high-flow events. The most significant message to be taken for these plots, similar plots in the section on individual site write-ups (Section 5.4.3), and the results shown in Figure 5.4.2.2-5, is that measureable erosion processes do not begin at the vast majority of sites until flows exceed 25,000 to 30,000 cfs, with many occurring at flows above 60,000 cfs. In the examples shown in Figure 5.4.2.2-7, erosion throughout the range of flows occurred only at the site representing very low erosion rates (6AR post-restoration), indicating that some small amount of particle-by-particle erosion has occurred across the range of flows.

To obtain a clearer understanding of the flows that are responsible for bank erosion in the TFI under Baseline Conditions and to provide further evidence of the importance of high flows on bank-erosion rates data that describes the distribution of responsible flows for each site are shown in Table 5.4.2.2-4. With the exception of site 11L just downstream from Vernon Dam and effected by dam releases, and site 29R where a severe undercut in the existing bank geometry led to a sizeable failure at a relatively low discharge, one can see the bank-erosion was dominated by the high-flow discharges.

Table 5.4.2.2-1: Summary of BSTEM Results for the Various Operational Scenarios

Site/Condition	Station	Dates		Baseline (Waves On)	Baseline (Waves off)	S1
	(ft)	Start	End	($ft^3/ft/y$)	($ft^3/ft/y$)	($ft^3/ft/y$)
11L	100000	7/15/2005	9/10/2014	0.297	0.296	0.303
2L-Pre	94500	6/20/2000	6/30/2012	1.197	1.184	1.194
2L-Post	94500	7/1/2012	8/28/2014	0.214	0.204	0.213
303BL	94000	1/1/2000	8/27/2014	0.647	0.645	0.674
18L	87000	1/1/2000	8/27/2014	1.092	1.092	1.080
3L	79500	1/1/2000	8/28/2014	6.086	6.090	6.042
3R-Pre	79500	1/1/2000	6/30/2006	15.425	15.407	15.458
3R-Post	79500	7/1/2006	8/28/2014	0.285	0.281	0.282
21R	79250	1/1/2000	8/27/2014	2.359	2.291	2.355
4L	74000	1/1/2000	8/28/2014	0.017	0.014	0.017
29R	66000	1/1/2000	8/27/2014	1.718	1.709	1.718
5CR	57250	7/8/2002	9/3/2014	8.606	8.500	8.566
26R	50000	1/1/2000	8/27/2014	1.194	1.145	1.196
10L	49000	1/1/2000	8/27/2014	0.160	0.158	0.158
10R-Post	49000	7/1/2001	8/27/2014	0.000	0.000	0.000
6AL-Pre	41750	1/1/2000	6/30/2004	2.668	2.635	2.736
6AL-Post	41750	7/1/2004	8/27/2014	0.000	0.000	0.000
6AR-Post	41750	6/21/2000	8/27/2014	0.021	0.000	0.020
119BL	41000	1/1/2000	8/27/2014	5.876	5.722	5.789
7L	37500	1/1/2000	8/26/2014	4.291	4.242	4.125
7R	37500	1/1/2000	8/26/2014	2.058	2.037	2.047
8BL	32750	6/2/2000	8/26/2014	0.427	0.427	0.399
8BR-Pre	32750	6/2/2000	6/30/2012	7.415	7.394	1.954
8BR-Post	32750	7/1/2012	8/26/2014	0.312	0.312	0.248
87BL	30750	1/1/2000	8/27/2014	3.568	3.607	3.595
75BL	27000	1/1/2000	8/27/2014	3.755	3.475	3.927
9R-Pre	6750	6/2/2000	6/30/2008	5.426	0.967	5.192
9R-Post	6750	7/1/2008	8/26/2014	0.227	0.002	0.224
12BL	6500	1/1/2000	8/27/2014	2.221	0.239	2.150
BC-1R	4750	6/5/2000	8/26/2014	0.190	0.000	0.189

* Hydraulic assumptions for Scenario 1 (S1) are provided in *Table 5.4.1.1-1*

Table 5.4.2.2-2: Baseline Erosion Rates and Contribution to That Erosion by Project Operations as Determined by Subtracting Erosion Rates For S1 from those of the Baseline Condition

Site/Condition	Station	Total Erosion	Northfield Mtn. Erosion
		Baseline (waves on)	Baseline – S1
		(ft^3/ft)	% Contribution to Baseline
11L	100000	0.297	-2.2%
2L-Pre	94500	1.20	0.2%
2L-Post	94500	0.214	0.4%
303BL	94000	0.647	-4.2%
18L	87000	1.092	1.1%
3L	79500	6.09	0.7%
3R-Pre	79500	15.42	-0.2%
3R-Post	79500	0.285	1.1%
21R	79250	2.36	0.2%
4L	74000	0.017	0.6%
29R	66000	1.72	0.0%
5CR	57250	8.61	0.5%
26R	50000	1.19	-0.1%
10L	49000	0.160	1.1%
10R-Post	49000	0.0003	99.9%[1]
6AL-Pre	41750	2.67	-2.6%
6AL-Post	41750	0.00001	18.9%[1]
6AR-Post	41750	0.021	2.0%
119BL	41000	5.88	1.5%
7L	37500	4.29	3.9%
7R	37500	2.06	0.5%
8BL	32750	0.427	6.6%
8BR-Pre	32750	7.41	73.6%
8BR-Post	32750	0.312	20.4%
87BL	30750	3.57	-0.8%
75BL	27000	3.76	-4.6%
9R-Pre	6750	5.43	4.3%[2]
9R-Post	6750	0.227	1.4%[2]
12BL	6500	2.22	3.2%[2]
BC-1R	4750	0.190	0.2%[2]

1- Even though % Contribution shows a NFM influence the total erosion is almost zero

2 - % in this reach also includes a wave influence

Table 5.4.2.2-3: Stage-discharge Relations Developed from HEC-RAS Data for the Detailed Study Sites

HEC-RAS File	Station	Equation	Type	r^2
98769	11L	$Q = -188.1532x^3 + 33{,}742.6670x^2 – 1{,}998{,}2785x + 39{,}159{,}171.6988$	3-parameter	0.98
93245	2L	$Q = -325.1597x^3 + 57{,}051.4539x^2 -3{,}317{,}743.6127x + 63{,}995{,}507.4672$	3-parameter	0.97
93245	303BL	$Q = -325.1597x^3 + 57{,}051.4539x^2 -3{,}317{,}743.6127x + 63{,}995{,}507.4672$	3-parameter	0.97
85957	18L	$Q = -444.5923x^3 + 77477.8485x^2 – 4480900.9989x + 86050961.3259$	3-parameter	0.96
78453	3L	$Q = -602.1374x^3 + 401{,}357.5191x^2 – 6{,}007{,}824.1090x + 114{,}932{,}875.9390$	3-parameter	0.94
78453	#R	$Q = -602.1374x^3 + 401{,}357.5191x^2 – 6{,}007{,}824.1090x + 114{,}932{,}875.9390$	3-parameter	0.94
78453	21R	$Q = -602.1374x^3 + 401{,}357.5191x^2 – 6{,}007{,}824.1090x + 114{,}932{,}875.9390$	3-parameter	0.94
72416	4L	$Q = -707.4104x^3 + 122{,}336{,}1119x^2 – 7{,}030{,}226.6244x + 134{,}294{,}867.1744$	3-parameter	0.94
64708	29L	$Q = -907.9605x^3 + 156501.7740x^2 – 8968894.6763x + 170937379.1121$	3-parameter	0.92
56235	5CR	$Q = -1{,}098.8039x^3 + 188{,}972.1623x^2 – 10{,}809{,}028.2672x + 205{,}673{,}698.1172$	3-parameter	0.91
47938	26R	$Q = -205.59471389x^6 + 70387.15430583x^5 – 10038404.69817680x^4 + 763370519.39162800x^3 – 32645915306.65530000x^2 + 744424922625.25800000x – 7071331681422.40000000$	6-parameter	0.90
47938	10L	$Q = -205.59471389x^6 + 70387.15430583x^5 – 10038404.69817680x^4 + 763370519.39162800x^3 – 32645915306.65530000x^2 + 744424922625.25800000x – 7071331681422.40000000$	6-parameter	0.90
47938	10L	$Q = -205.59471389x^6 + 70387.15430583x^5 – 10038404.69817680x^4 + 763370519.39162800x^3 – 32645915306.65530000x^2 + 744424922625.25800000x – 7071331681422.40000000$	6-parameter	0.90
39952	6AL	$Q = -245.51028346x^6 + 83995.45306679x^5 – 11971140.24890380x^4 + 909742504.71487900x^3 – 38880163616.77810000x^2 +886013079166.84800000x – 8410935562085.17000000$	6-parameter	0.88
39952	6AR	$Q = -245.51028346x^6 + 83995.45306679x^5 – 11971140.24890380x^4 + 909742504.71487900x^3 – 38880163616.77810000x^2 +886013079166.84800000x – 8410935562085.17000000$	6-parameter	0.88
39952	119BL	$Q = -245.51028346x^6 + 83995.45306679x^5 – 11971140.24890380x^4 + 909742504.71487900x^3 – 38880163616.77810000x^2 +886013079166.84800000x – 8410935562085.17000000$	6-parameter	0.88
36653	7L	$Q = -281.71574298x^6 + 96325.50879321x^5 – 13720463.52509040x^4 + 1042084875.6568000x^3 – 44511028775.98300000x^2 + 1013767141883.29000000x – 9618436642314.27000000$	6-parameter	0.87
36653	7R	$Q = -281.71574298x^6 + 96325.50879321x^5 – 13720463.52509040x^4 + 1042084875.6568000x^3 – 44511028775.98300000x^2 + 1013767141883.29000000x – 9618436642314.27000000$	6-parameter	0.87
30404	8BL	$Q = -314.92075666x^6 + 107664.35596156x^5 – 15333485.42641640x^4 + 1164441334.34417000x^3 – 49730804176.63400000x^2 + 1132505344005.5800000x – 10743643009686.7000000$	6-parameter	0.83
30404	8BR	$Q = -314.92075666x^6 + 107664.35596156x^5 – 15333485.42641640x^4 + 1164441334.34417000x^3 – 49730804176.63400000x^2 + 1132505344005.5800000x – 10743643009686.7000000$	6-parameter	0.83
30404	87BL	$Q = -314.92075666x^6 + 107664.35596156x^5 – 15333485.42641640x^4 + 1164441334.34417000x^3 – 49730804176.63400000x^2 + 1132505344005.5800000x – 10743643009686.7000000$	6-parameter	0.83
25845	75BL	$Q = -453.53388331x^6 -154738.13119984x^5 – 21993407.72848850x^4 + 1666881999.57544000x^3 – 71048965952.00670000x^2 + 1614830996923.93000000x – 15289824117576.90000000$	6-parameter	0.83
4830	12BL	N/A	N/A	N/A
4830	9R	N/A	N/A	N/A
4830	BC1R	N/A	N/A	N/A

Note that stage is in meters (units for BSTEM input) and discharge is in cfs (units for HEC-RAS). Regressions could not be developed for three sites in the lower impoundment due to lack of a relation.

Table 5.4.2.2-4 - Distribution of discharges responsible for 5%, 50% and 95% of the bank erosion at the 25 detailed study sites

Site	Station	Total Erosion Under Baseline, $ft^3/ft/yr$	Baseline Scenario Discharge, cfs		
			95% of Erosion: 5% of erosion occurs at flows greater than	50% of Erosion: 50% of erosion occurs at flows greater than	5 % of Erosion: 95% of erosion occurs at flows greater than
11L	100000	0.297	56869	4985	500
2L - **Pre**	94500	1.197	89294	64854	49906
2L - Post	94500	0.214	71465	65195	51924
303BL	94000	0.647	79881	64684	53194
18L	87000	1.092	73352	54485	17824
3L	79500	6.086	98234	78682	37098
3R-Pre	79500	15.425	73365	61470	39229
3R-Post	79500	0.285	87760	54420	36411
21R	79250	2.359	63852	46345	22928
4L	74000	0.017	95042	83527	6991
29R*	66000	1.718	11968	11968	11923
5CR	57250	8.606	76391	76391	47867
26R	50000	1.194	80503	60282	43294
10L	49000	0.160	98882	79003	58922
10R-Post	49000	0.000	49015	48156	46944
6AL-Pre	41750	2.668	77664	65442	56264
6AL-Post	41750	0.000	65167	63310	62287
6AR-Post	41750	0.021	29662	11191	7051
119BL	41000	5.876	70557	53969	24796
7L	37500	4.291	98753	65338	47731
7R	37500	2.058	98463	65880	53614
8BL	32750	0.427	84451	84138	77997
8BR-Pre	32750	7.415	99458	99458	64443
8BR-Post	32750	0.312	72009	69312	66504
87BL	30750	3.568	63968	42875	17849
75BL	27000	3.755	71586	48054	33822
9R-Pre	6750	5.426	I	I	I
9R-Post	6750	0.227	I	I	I
12BL	6500	2.221	I	I	I
BC-1R	4750	0.190	I	I	I

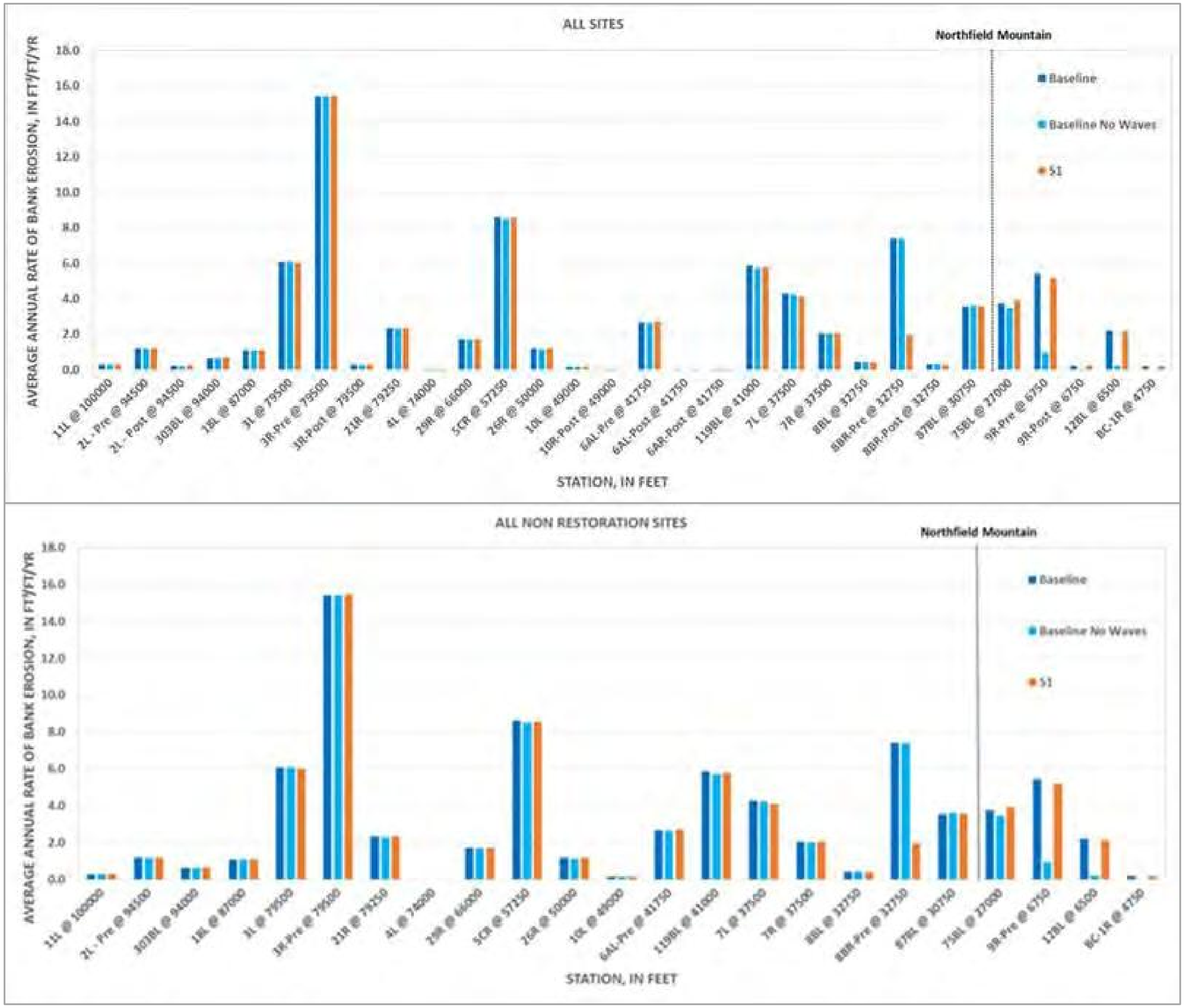

Figure 5.4.2.2-1: Summary of Bank-erosion Rates for All Sites (including restored conditions) and Modeling Scenarios along the Study Reach (Top) and for only the Non-restored Sites/Conditions (Bottom)

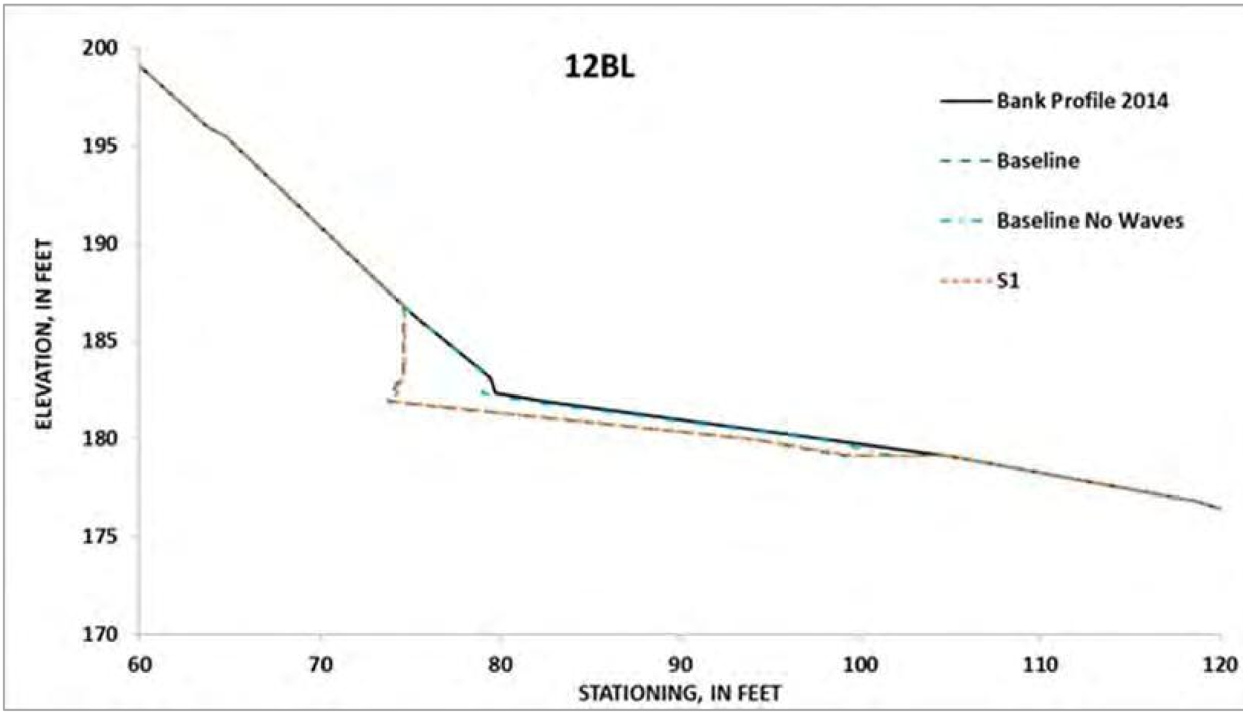

Figure 5.4.2.2-2: Example of the Important Effect of Boat Waves in the Lower TFI (Reach 1) showing the Greater amount of Hydraulic Erosion (Undercutting) between the Baseline Condition with Waves as Compared to the Baseline Condition Without Waves at Site 12BL

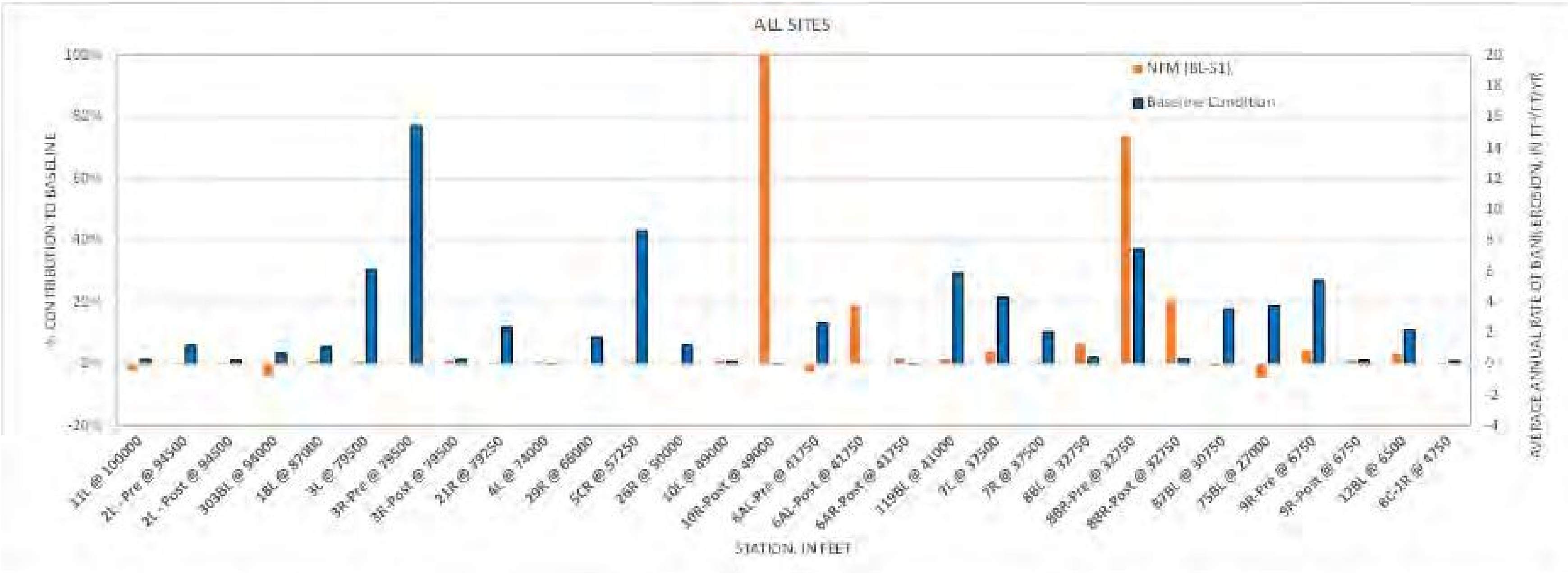

Figure 5.4.2.2-3: Contribution of Erosion Rates Due to Project Operations Compared to Erosion Rates for the Baseline Condition

Results need to be taken in context of the total amount of erosion at a particular site to interpret relative impact of the Project

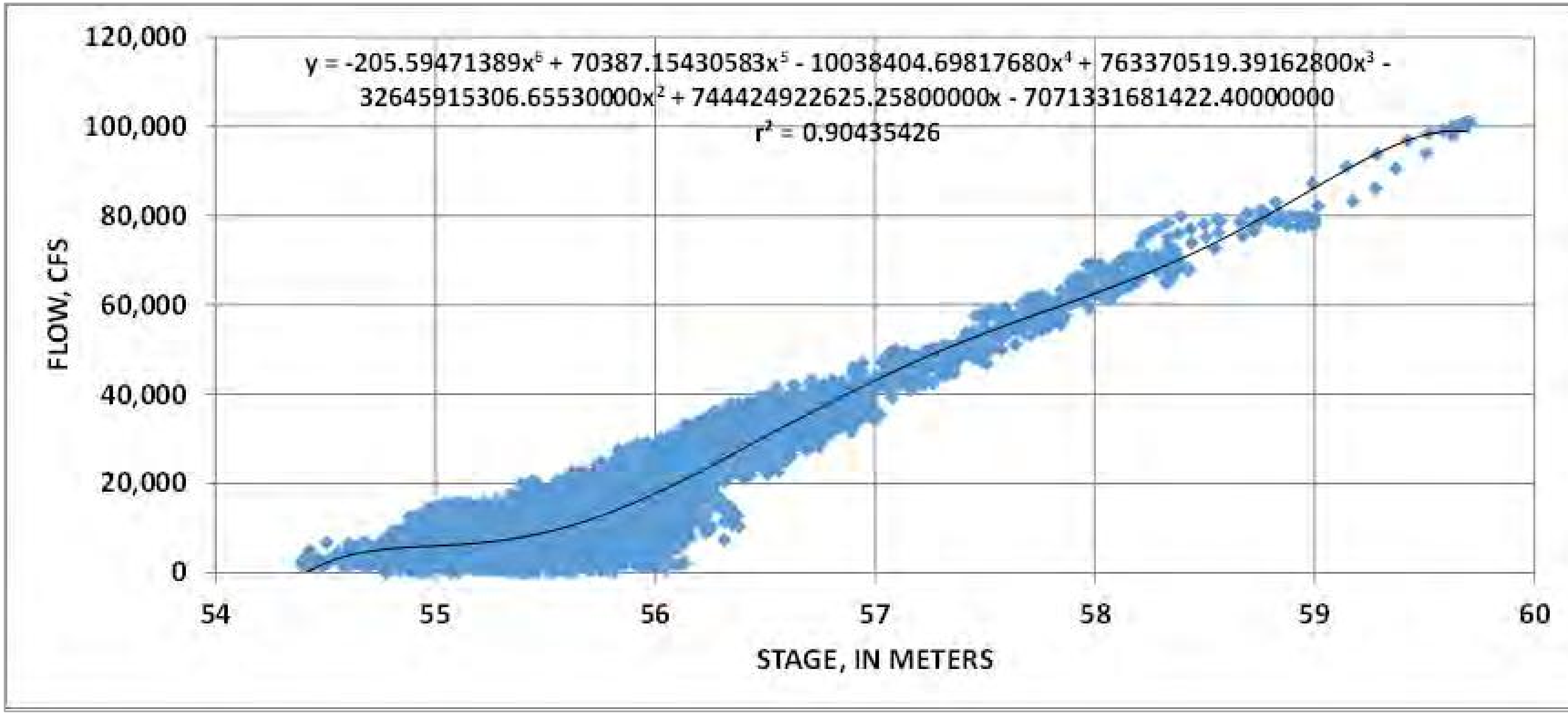

Figure 5.4.2.2-4: Example Stage-discharge Relationship Developed for Sites 10L, 10R and 26R from Hourly HEC-RAS Data

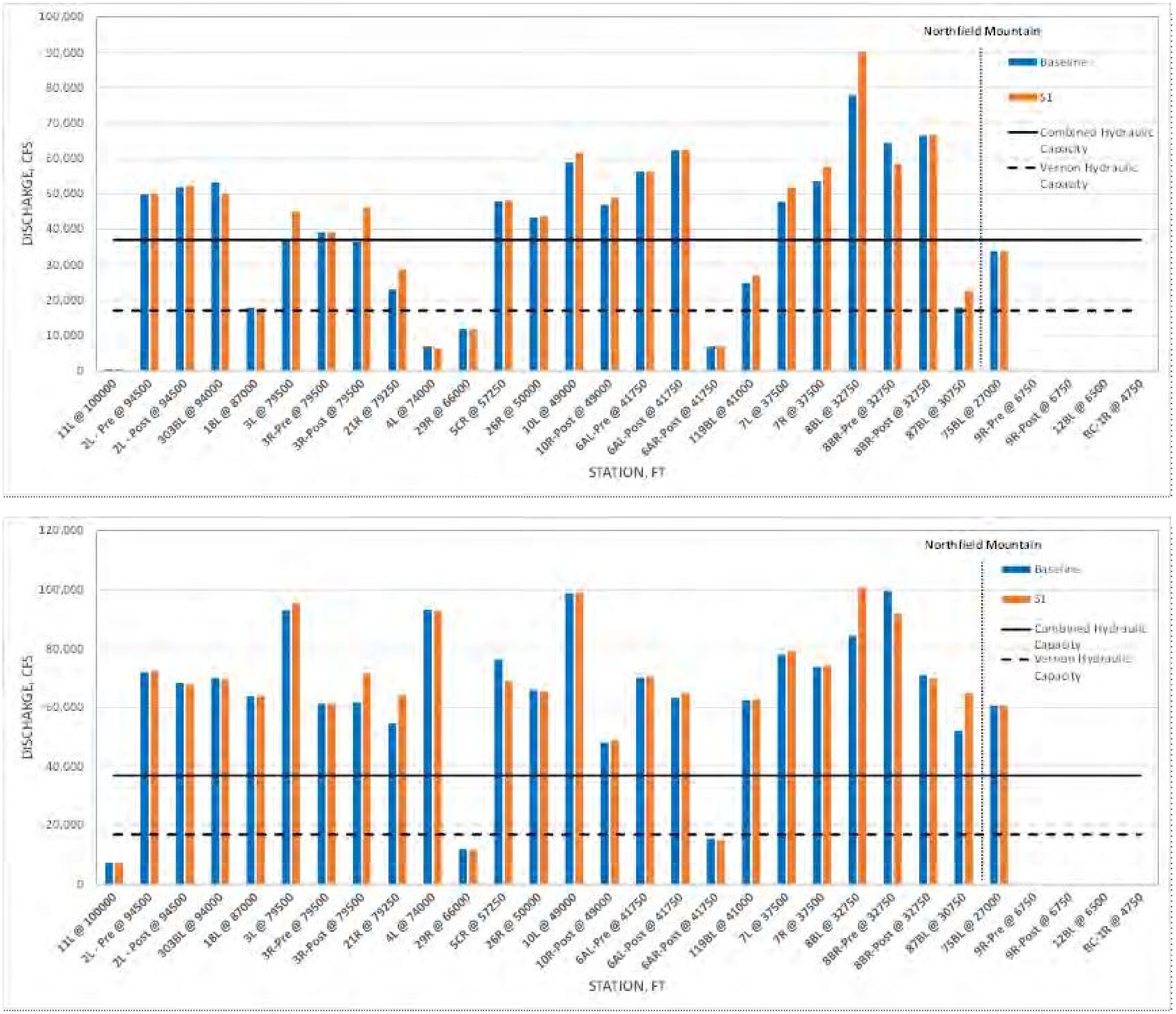

Figure 5.4.2.2-5: Discharge at which 95% of the erosion occurs at flows higher than indicated (Top) and where 75% of the erosion occurs at higher discharges (Bottom)

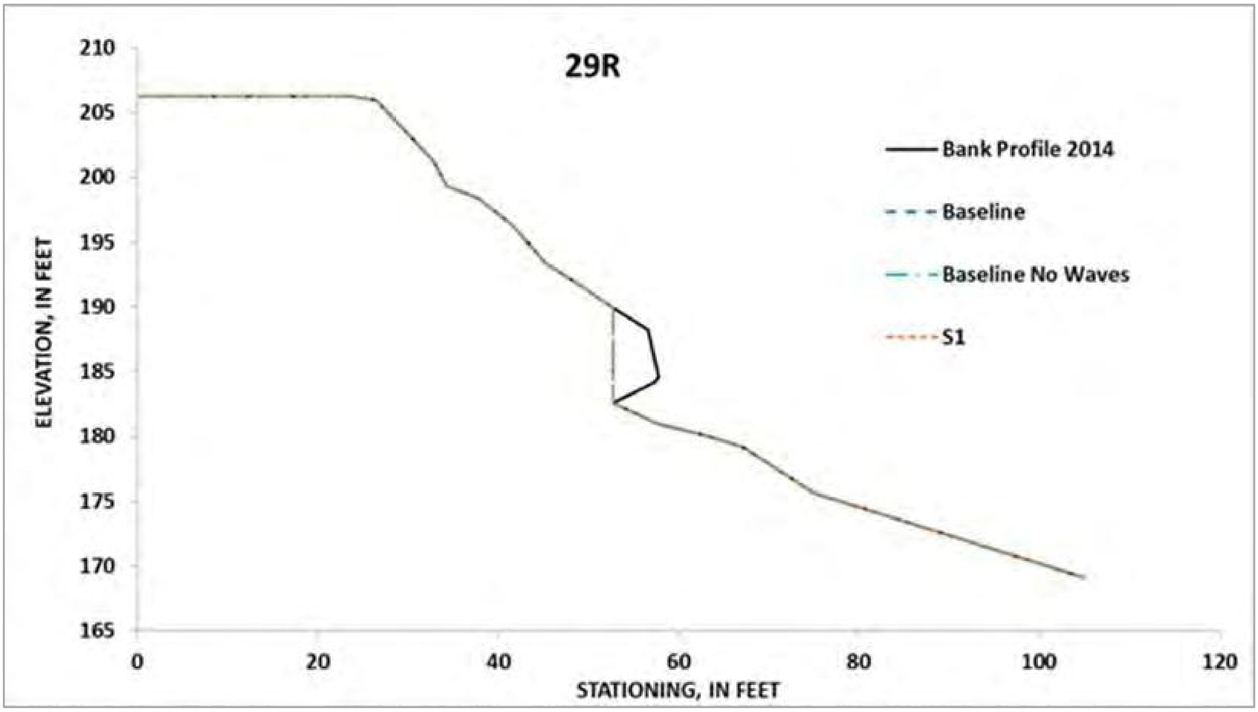

Figure 5.4.2.2-6: Bank profile for site 29R at Station 66,000 Showing Pronounced Undercut at the Start of the Simulations

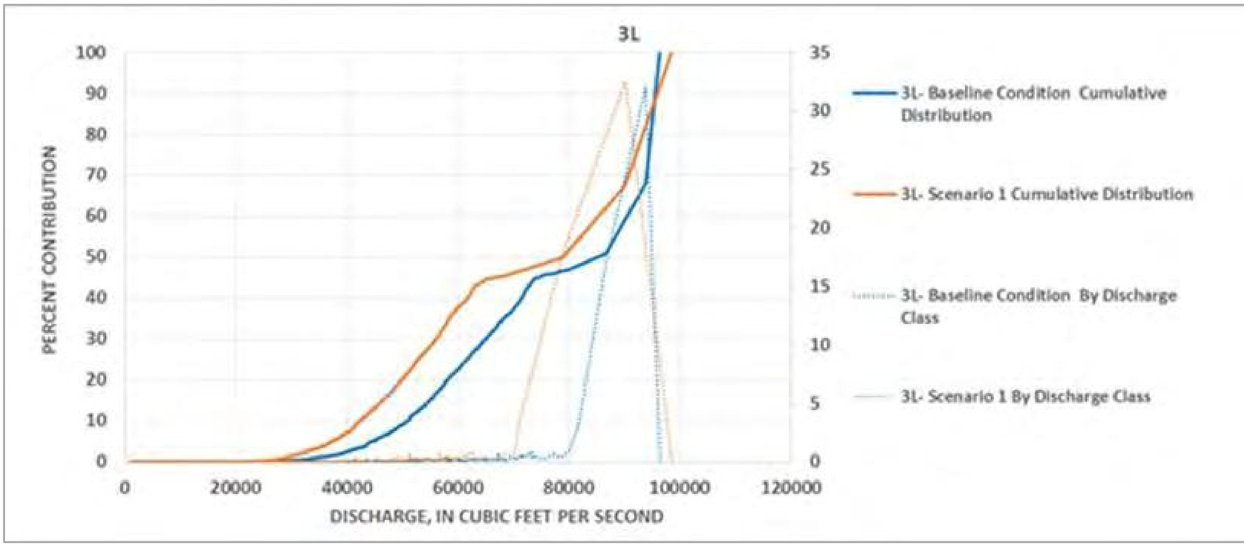

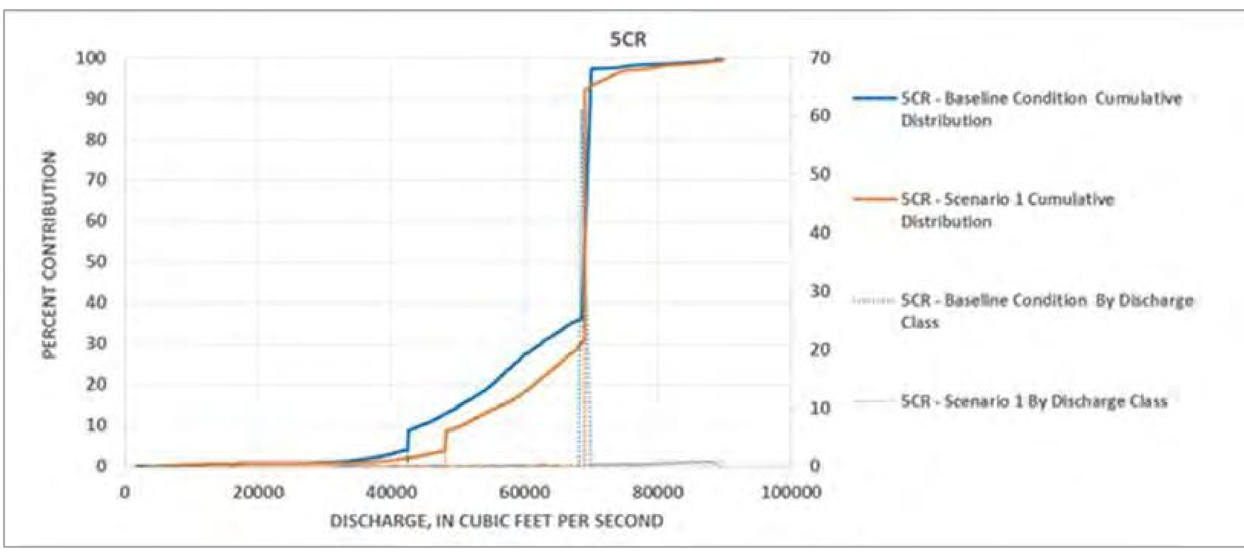

Figure 5.4.2.2-7 (Part 1 of 2): Distribution of Total Erosion at Four Sites According to Discharge Classes

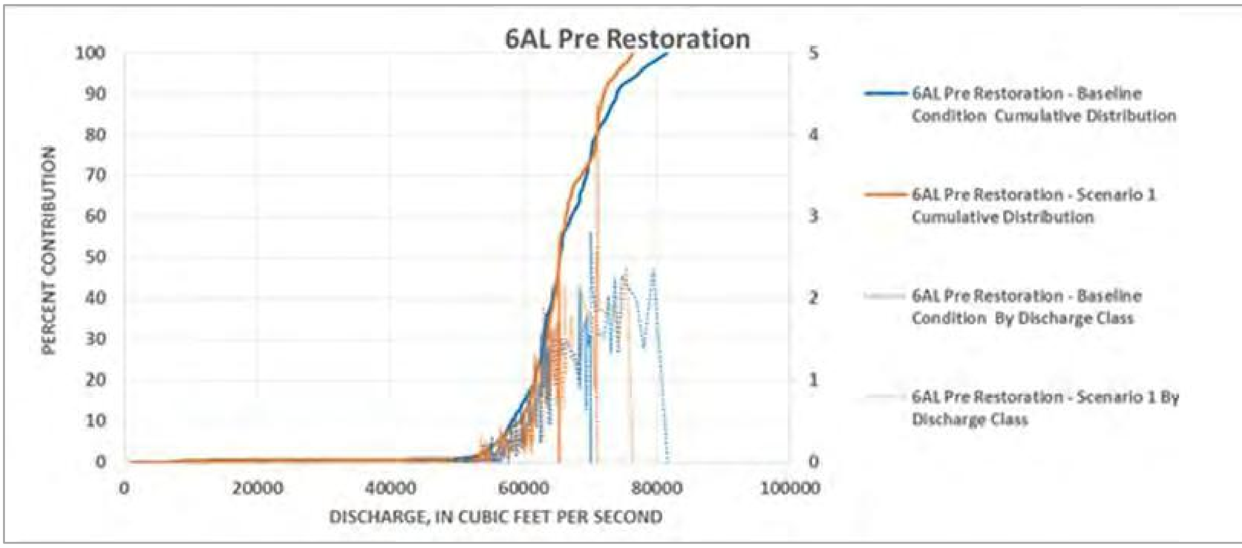

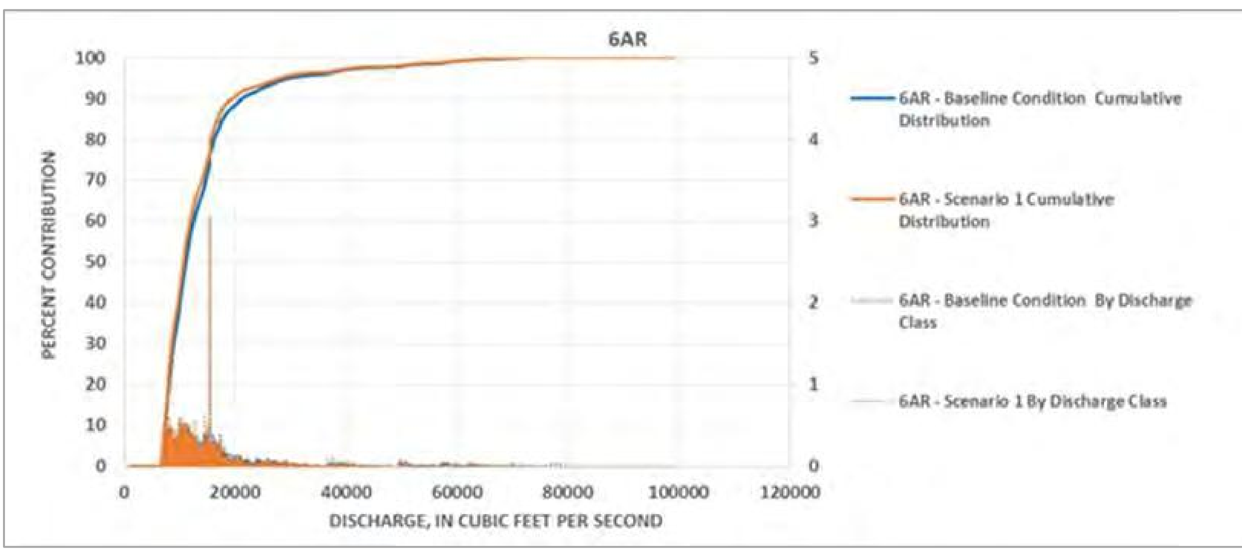

Figure 5.4.2.2-7 (Part 2 of 2): Distribution of Total Erosion at Four Sites According to Discharge Classes

5.4.2.3 Role of Boat-Generated Waves

The role of boat-generated waves for the Baseline Condition was briefly discussed in an earlier section. A plot from site 12BL (Figure 5.4.2.2-2, previous section) was used as an example of the much greater amounts of basal undercutting that can occur in the lower TFI as a result of boat-generated waves. This is related to the fact that water-surface elevations do not vary significantly in the lower TFI, thereby focusing all of the wave energy along a narrow band of elevations along the bank. Because the resulting basal erosion rate is the product of the magnitude of the excess shear stress and the duration of that excess stress at a given bank node, the greater durations provided along this narrow band makes boat-generated waves an important factor in bank erosion at these locations. This helps to explain why boat-generated wave action is not as important a factor in bank erosion rates in other parts of the TFI. As described in a previous chapter on wave characteristics, wind-generated waves in the study reach do not have sufficient energy to cause basal erosion, likely due to short fetches.

Acknowledging the importance of boat-generated waves for the Baseline Condition in the lower TFI led to re-running the other Operational scenarios without waves as well. A comparison of erosion rates with and without boat-generated waves for the four sites in the lower TFI is shown in Figure 5.4.2.3-1. Clearly, erosion rates drop significantly for all scenarios when the effects of waves are removed. As one moves upstream in the TFI, however, the effect is reduced to the point that at site 75BL (station 27,000), there is enough vertical flow variability that differences in erosion rates with and without waves become small (Figure 5.4.2.3-1). A summary of the bank-erosion rates in the lower TFI with and without waves for all Operational scenarios is provided in Table 5.4.2.3-1.

Table 5.4.2.3-1: Summary of bank-erosion rates for sites in the lower impoundment showing differences with and without boat-generated waves

Site/Condition	Station	Dates		Baseline (Waves on)	Baseline (Waves off)	S1 (Waves on)	S1 (Waves off)
	ft	Start	End	$ft^3/ft/y$	$ft^3/ft/y$	$ft^3/ft/y$	$ft^3/ft/y$
75BL	27000	01/01/00	08/27/14	3.76	3.47	3.93	3.72
9R-Pre	6750	06/02/00	06/30/08	5.43	0.97	5.19	0.77
9R-Post	6750	07/01/08	08/26/14	0.23	0.00	0.22	0.00
12BL	6500	01/01/00	08/27/14	2.22	0.24	2.15	0.19
BC-1R	4750	06/05/00	08/26/14	0.19	0.00	0.19	0.00

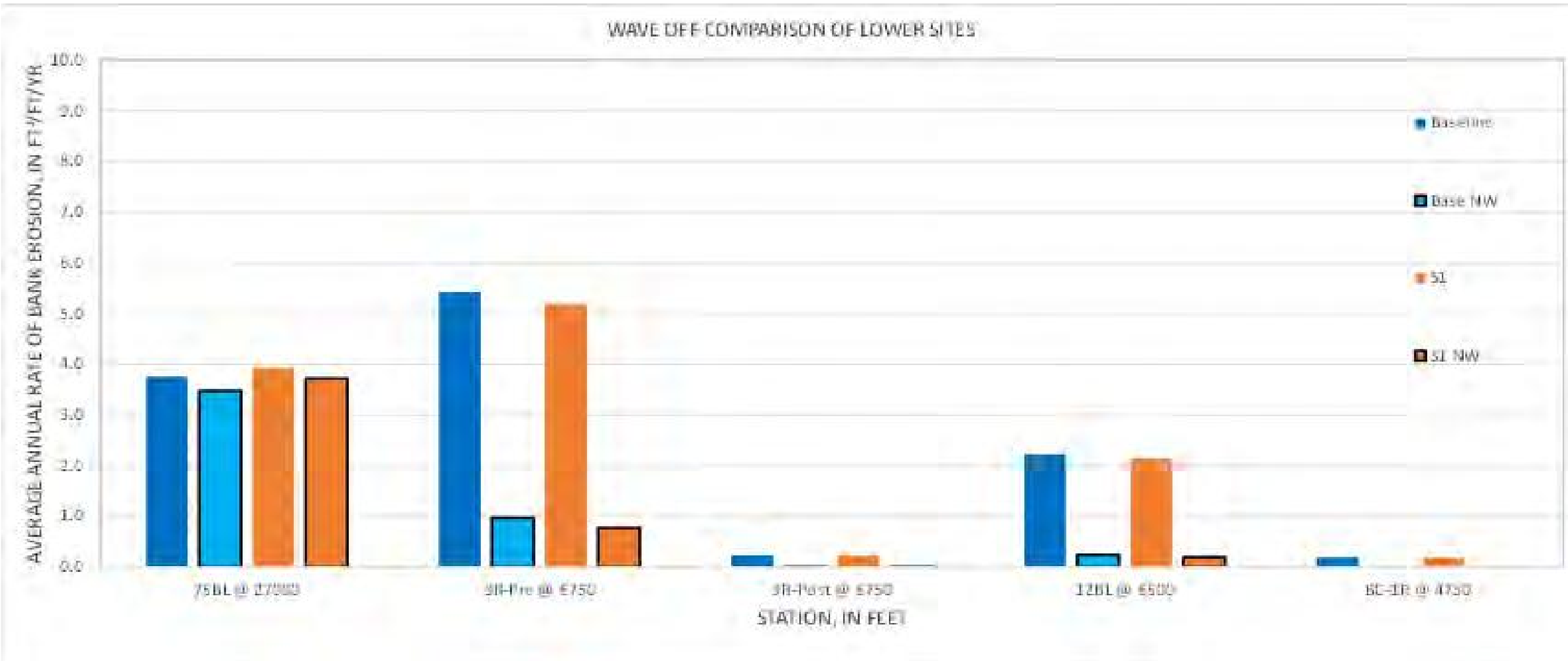

Figure 5.4.2.3-1 Comparison of Bank-erosion Rates with and without Boat-generated Waves for Sites in the Lower Turners Falls Impoundment

5.4.3 BSTEM Simulation Results: Site-Specific Results

The following section provides the results from BSTEM modeling conducted at each of the 25 detailed study sites to investigate the causes of bank erosion along the TFI. Descriptions start with the most upstream site 11L, just below Vernon Dam and continue downstream to BC-1R, just upstream of Turners Falls Dam. The locations and stationing of these sites are shown in Section 4 along with the flow, geometry and bank-resistance input data used to populate BSTEM for the different scenarios. This section discusses general site characteristics and the BSTEM results at each site.

The magnitude and distribution of bank erosion along the study reach is a combination of many factors that control the hydraulic and geotechnical processes that cause erosion. For each site, a comparison of the modeling results for each modeled scenario is presented including a discussion of the controlling factors and processes. The flow scenarios represent different operational conditions aimed at determining the role of water-level fluctuations, high flows and boat waves on bank-erosion rates. BSTEM calculates boundary shear stress caused by water-level fluctuations at each time step and at each node along the bank face. To address any issues related to drawdown conditions and effects as a result of hydro-power operations, BSTEM addresses these processes by calculating pore-water and confining pressures along potential failure surfaces during each time step of a simulation.

As a reminder, BSTEM modeling results are discussed in the context of both hydraulic and geotechnical erosion processes. For the purpose of this study, hydraulic erosion is defined as erosion caused by hydraulic processes. That is, the particle-by-particle entrainment and erosion of surficial sediments when and where the boundary shear stress exerted by the flow exceeds the critical shear stress that characterizes the surficial bank sediments. Hydraulic erosion from river flow or by waves can steepen and undercut bank surfaces leading to a loss of support for the upper part of the bank and making them susceptible to collapse (geotechnical erosion). These processes are most important when shear stresses are highest as during high flows.

Again to reiterate, geotechnical erosion is defined as erosion caused directly by gravitational forces as in the collapse of a hillslope or bank. Here, erosion occurs when the downslope, gravitational forces exceed the shearing resistance of the *in situ* materials. Any factors that increase the downslope gravitational forces (such as steepness and weight) or decrease the shearing resistance of the materials (such as generation of positive pore-water pressure) contribute to geotechnical erosion. Pore-water pressure can be generated within the bank by lateral infiltration (depending on the duration the water is at a certain elevation) during rises in stage. This can reduce the frictional component of shear strength (See Volume III – Appendix F). The confining pressure provided by the flow pressing against the bank surface, however, tends to offset this affect. An important point are the relative rates of decreasing stage and groundwater levels during water-level fluctuations because the loss of shear strength combined with a loss of confining pressure (known as the *drawdown* condition) is particularly critical for streambank stability. BSTEM handles these processes by calculating pore-water and confining pressures along potential failure surfaces during each time step of a simulation (See Volume IIII - Appendix F).

Geotechnical erosion (bank failure) generally does not occur unless there is a change to the equilibrium condition that the bank slope exists in. This change can be an increase in the downslope gravitational forces and/or the resistance of the materials. With streambanks, this change towards disequilibrium and instability is often related to a steepening of the bank by hydraulic action. Whether this steepening or undercutting is related to water-level fluctuations due to hydropower operations or to the shear stress imposed by high flows has been the subject of the analysis in the previous section. Results showed that in almost all cases that the bulk of the erosion occurred during high flows and not during periods of water-level fluctuations due to Project operations.

Model results, along with the measured erosion over the period (normalized by the number of years for each simulation) are shown in Table 5.4.3-1. Hydraulic erosion either from flows or boat-waves that cause undercutting can be a contributing factor in erosion rates by instigating mass failure of the upper bank. Figure 5.4.3-1 shows the relative contributions of hydraulic and geotechnical erosion for all sites and operational scenarios along the study reach. Both the aforementioned Table and Figure provide the backdrop to the individual site write ups that follow.

Table 5.4.3-1: Summary of BSTEM Results for All Detailed Study Sites

Site/Condition	Station	Dates		Baseline (Waves On)	Baseline (Waves off)	S1
	(ft)	Start	End	(ft^3/ft/y)	(ft^3/ft/y)	(ft^3/ft/y)
11L	100000	7/15/2005	9/10/2014	0.297	0.296	0.303
2L-Pre	94500	6/20/2000	6/30/2012	1.197	1.184	1.194
2L-Post	94500	7/1/2012	8/28/2014	0.214	0.204	0.213
303BL	94000	1/1/2000	8/27/2014	0.647	0.645	0.674
18L	87000	1/1/2000	8/27/2014	1.092	1.092	1.080
3L	79500	1/1/2000	8/28/2014	6.086	6.090	6.042
3R-Pre	79500	1/1/2000	6/30/2006	15.425	15.407	15.458
3R-Post	79500	7/1/2006	8/28/2014	0.285	0.281	0.282
21R	79250	1/1/2000	8/27/2014	2.359	2.291	2.355
4L	74000	1/1/2000	8/28/2014	0.017	0.014	0.017
29R	66000	1/1/2000	8/27/2014	1.718	1.709	1.718
5CR	57250	7/8/2002	9/3/2014	8.606	8.500	8.566
26R	50000	1/1/2000	8/27/2014	1.194	1.145	1.196
10L	49000	1/1/2000	8/27/2014	0.160	0.158	0.158
10R-Post	49000	7/1/2001	8/27/2014	0.000	0.000	0.000
6AL-Pre	41750	1/1/2000	6/30/2004	2.668	2.635	2.736
6AL-Post	41750	7/1/2004	8/27/2014	0.000	0.000	0.000
6AR-Post	41750	6/21/2000	8/27/2014	0.021	0.000	0.020
119BL	41000	1/1/2000	8/27/2014	5.876	5.722	5.789
7L	37500	1/1/2000	8/26/2014	4.291	4.242	4.125
7R	37500	1/1/2000	8/26/2014	2.058	2.037	2.047
8BL	32750	6/2/2000	8/26/2014	0.427	0.427	0.399
8BR-Pre	32750	6/2/2000	6/30/2012	7.415	7.394	1.954
8BR-Post	32750	7/1/2012	8/26/2014	0.312	0.312	0.248
87BL	30750	1/1/2000	8/27/2014	3.568	3.607	3.595
75BL	27000	1/1/2000	8/27/2014	3.755	3.475	3.927
9R-Pre	6750	6/2/2000	6/30/2008	5.426	0.967	5.192
9R-Post	6750	7/1/2008	8/26/2014	0.227	0.002	0.224
12BL	6500	1/1/2000	8/27/2014	2.221	0.239	2.150
BC-1R	4750	6/5/2000	8/26/2014	0.190	0.000	0.189

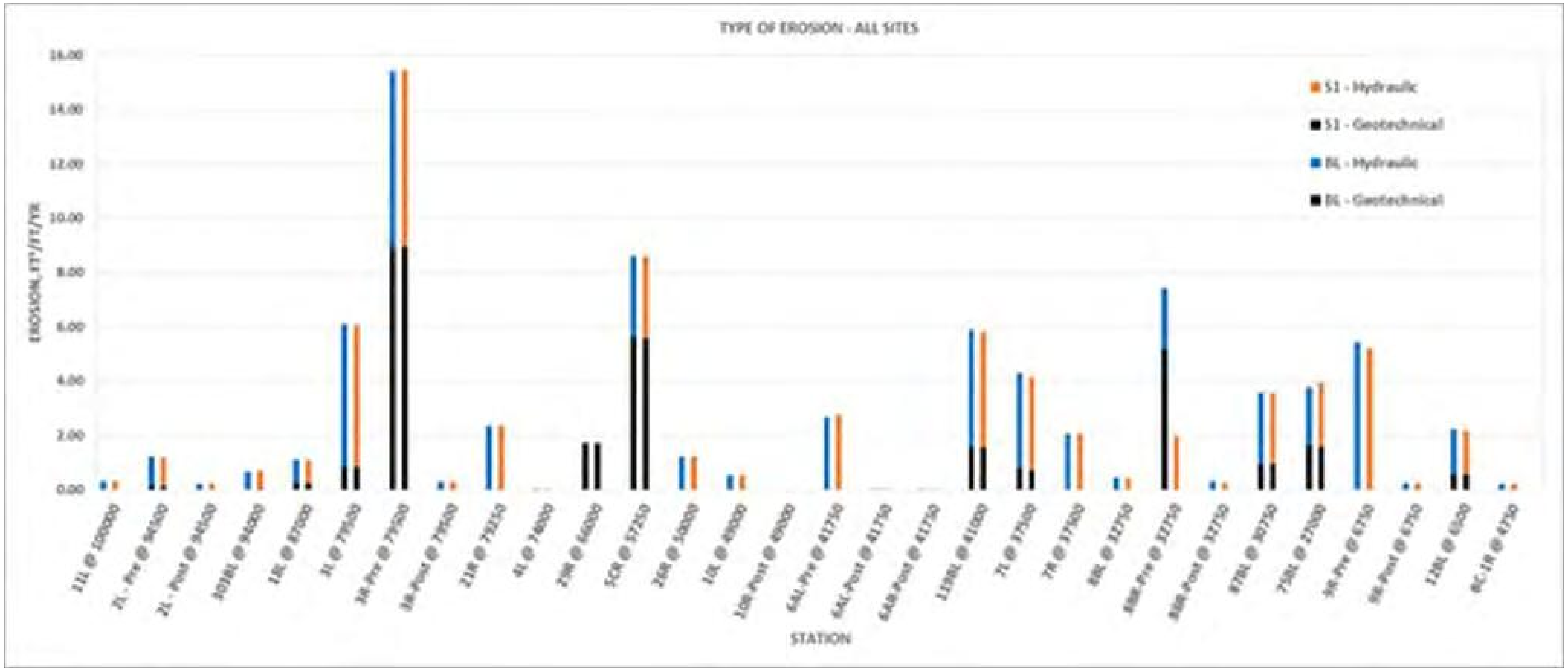

Figure 5.4.3-1: Bank-erosion Rates for all Sites, Conditions and Modeling Scenarios shown schematically from Upstream to Downstream along the Study Reach

Results represented by the vertical bars are separated into erosion by hydraulic (black sections) and geotechnical (mass failure) processes

5.4.3.1 Site 11L

The river at site 11L has steep, heavily vegetated banks, located at station 100,000, at Stebbins Island, roughly 7,000 ft downstream of Vernon Dam (Figure 5.4.3.1-1). The bank is roughly 27 feet tall with a silt loam toe and upper bank. The bank is vegetated with grasses, shrubs, Black and Yellow Birch, Eastern Hemlock, and Red Maple trees. The first surveyed cross section for site 11L was taken on 7/15/2005, and was therefore used as the starting point for the model.

BSTEM runs at this site show that under the Baseline Condition, 2.72 ft^3 of erosion occurred per foot of bank, during the 2005-2014 flow period, averaging 0.297 $ft^3/ft/y$ (Table 5.4.3-1). This results in the 10^{th} lowest erosion rate for the Baseline Condition, placing it between the 30^{th} and 35^{th} percentiles of erosion rates along the reach. The modeling also indicates that all 100% (0.297 $ft^3/ft/y$) of the erosion is due directly to hydraulic processes, and none of the bank erosion is the result of larger geotechnical failures.

The Baseline Condition (Waves off) resulted in 0.296 $ft^3/ft/y$, with 0.303 $ft^3/ft/y$ for Scenario 1. This resulted in the percent reductions in erosion rates of -2.2% for Scenario 1 (Figure 5.4.3.1-2). Baseline simulations with waves off showed virtually no reduction in erosion indicating that boat waves have little effect on erosion processes at this site. Because of this, all of the remaining scenarios were simulated with boat waves on.

For the Baseline Condition, 89.4% of the total erosion at site 11L occurs at flows below 17,130 cfs (Figure 5.4.3.1-3). These flows are well within the range of the hydraulic capacity of Vernon Dam. The remaining contributions to erosion are 10.4% due to high flows over the 17,130 cfs threshold and a very small 0.2% due to waves. Table 5.4.3.1-1 denotes the flows above which 95%, 50%, and 5% of all erosion occurs at the site as well as the amount of time those flows were exceeded for each year in the modeling period.

Table 5.4.3.1-1: Flow Exceedance Calculations for Site 11L

Site 11L	Percent of Erosion		
	95%	**50%**	**5%**
	Flow (cfs)		
Year	**56,869**	**4,985**	**500**
2000	0.90%	63.90%	100.00%
2001	2.50%	45.30%	99.99%
2002	0.30%	63.10%	99.95%
2003	1.10%	71.40%	100.00%
2004	0.10%	73.00%	99.99%
2005	1.60%	79.50%	99.99%
2006	1.10%	89.80%	100.00%
2007	2.60%	70.00%	100.00%
2008	2.40%	89.30%	100.00%
2009	0.50%	82.90%	100.00%
2010	0.60%	72.60%	100.00%
2011	3.80%	79.40%	100.00%
2012	NA	61.90%	99.99%
2013	0.10%	72.20%	100.00%
2014	1.80%	71.90%	100.00%

NA: Not Applicable since flows did not reach this value

Figure 5.4.3.1-1: Photos at Site 11L

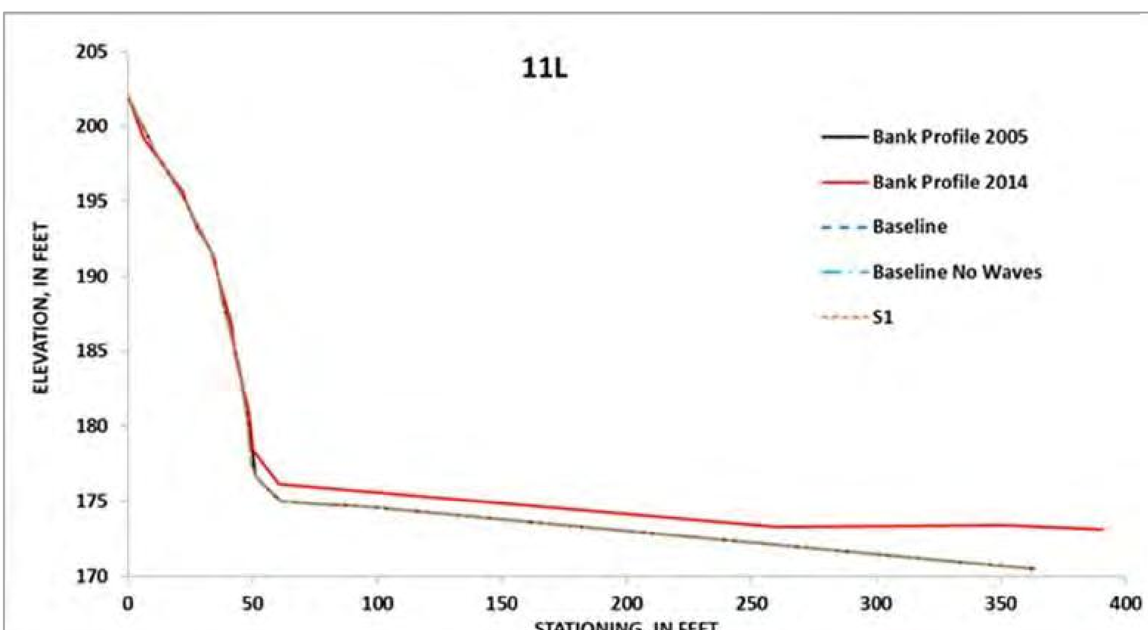

Figure 5.4.3.1-2: Simulated, future unit-erosion for the Baseline Condition (with boat waves on and off) and Scenario 1 at site 11L for the period 2005-2014

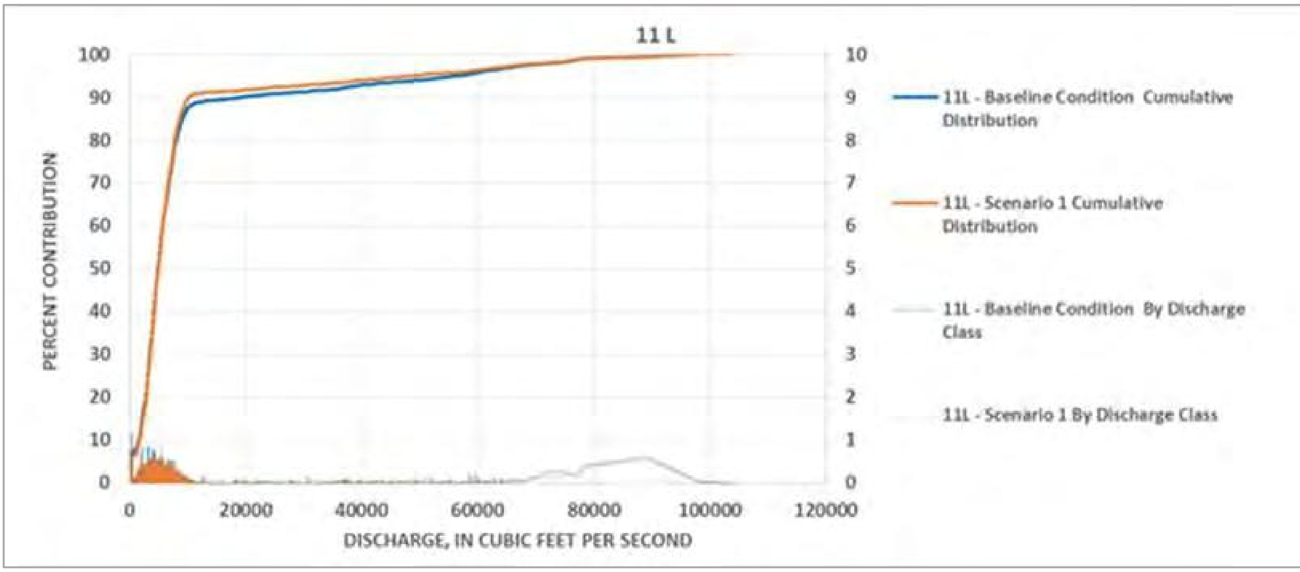

Figure 5.4.3.1-3: Simulated, percent contribution of total erosion by discharge for the Baseline Condition and Scenario 1 at site 11L for the period 2005-2014

5.4.3.2 Site 2L Pre-Restoration

The river at site 2L Pre-restoration (at station 94,500) has steep to vertical, very sparsely vegetated, moderately-high banks. The site is located, at the Bonnette Farm, just below the mouth of the Ashuelot River, south of Stebbins Island. The bank is roughly 16 feet tall, with a silty-sand bank and beach. Moderate vegetation was noted in the 2013 FRR for the Upper Riverbank slope, with very sparse to no vegetation on the lower riverbank slope (Figure 5.4.3.2-1).

BSTEM runs at this site show that under the Baseline Condition, 14.4 ft^3 of erosion occurred per foot of bank, during the 2000 to 2012 flow period prior to restoration, averaging 1.20 ft^3/ft/y (Table 5.4.3-1). This results in the 15th highest erosion rate for the Baseline Condition, placing it between the 50th and 55th percentiles of erosion rates along the reach. The modeling also indicates that 88% (1.05 ft^3/ft/y) of the erosion is due directly to hydraulic processes, whereas the other 12% (0.147 ft^3/ft/y) is the result of geotechnical processes and associated mass failures.

The Baseline Condition (Waves off) resulted in 1.18 ft^3/ft/y, with 1.19 ft^3/ft/y for Scenario 1 (Note- while this site did show a small reduction in erosion between the BL and S1 Scenarios the total reduction in erosion is well below the measureable/significant rate of 0.163 ft^3/ft/yr). This resulted in the following percent reductions in erosion rates compared to the Baseline Condition: 1.04 % under the Baseline Waves off Condition and 0.23% for Scenario 1 (Figure 5.4.3.2-2 and Figure 5.4.3.2-3). Baseline simulations with waves off showed virtually no reduction in erosion, indicating that boat-generated waves had little effect on erosion processes at this site. Because of this Scenario 1 was simulated with boat waves on. For the Baseline Condition, 98.7% of the total erosion occurs at flows of 17,130 cfs or greater (Figure 5.4.3.2-4). The hydraulic erosion gradually builds across the range of flows between 50,000 cfs and 75,000 cfs, at which point a significant geotechnical failure occurs at the extreme high flows. Through this analysis we can conclude that those flows greater than the hydraulic capacity at Vernon are accounting for most of the total erosion. This is supported by the small reductions in erosion rates for the various scenarios (compared to Baseline). Table 5.4.3.2-1 denotes the flows above which 95%, 50%, and 5% of all erosion occurs at the site as well as the amount of time those flows were exceeded for each year in the modeling period.

Table 5.4.3.2-1: Flow Exceedance Calculations for Site 2L

Site 2L	Percent of Erosion		
	95%	50%	5%
	Flow (cfs)		
Year	71,465	65,195	51,924
2000	NA	0.10%	1.30%
2001	0.80%	1.60%	3.20%
2002	NA	0.10%	0.50%
2003	NA	0.20%	2.10%
2004	NA	NA	0.50%
2005	0.40%	0.70%	2.90%
2006	0.10%	0.30%	1.90%
2007	NA	0.50%	2.80%
2008	NA	0.50%	4.00%
2009	NA	NA	1.20%
2010	NA	NA	1.70%
2011	1.00%	2.10%	5.00%
2012	NA	NA	NA
2013	NA	NA	0.10%
2014	NA	0.80%	2.40%

NA: Not Applicable since flows did not reach this value

Figure 5.4.3.2-1: Photo at Site 2L Pre Restoration

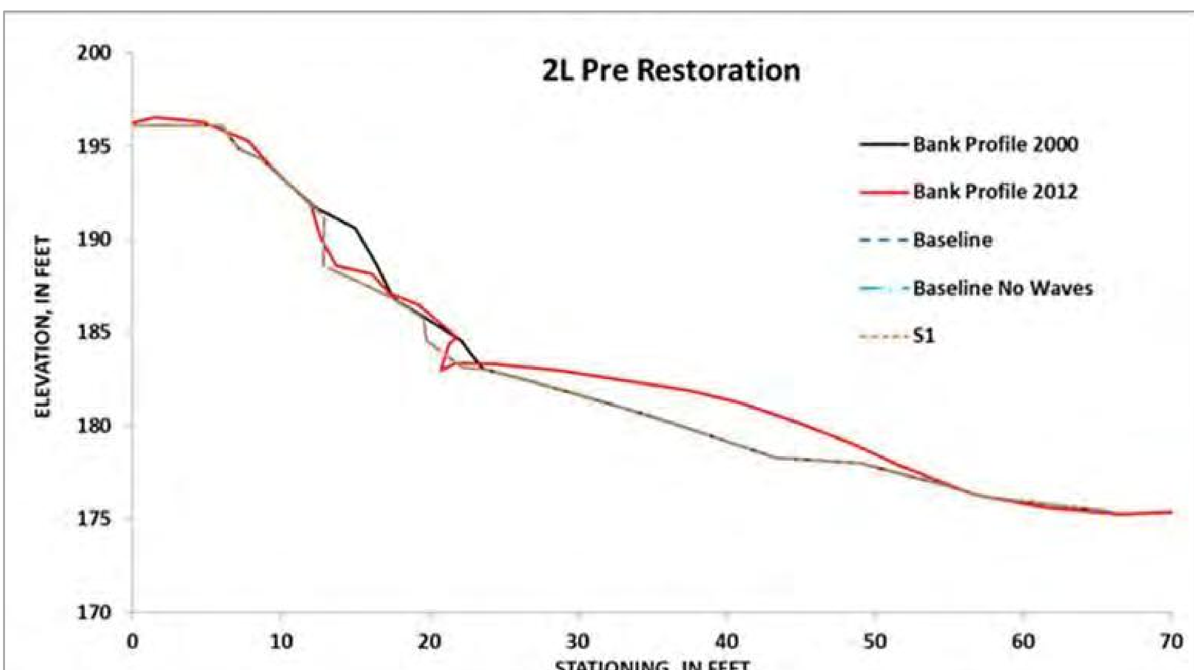

Figure 5.4.3.2-2: Simulated, future unit-erosion for the Baseline Condition (with boat waves on and off) and Scenario 1 at site 2L Pre Restoration for the period 2000-2012

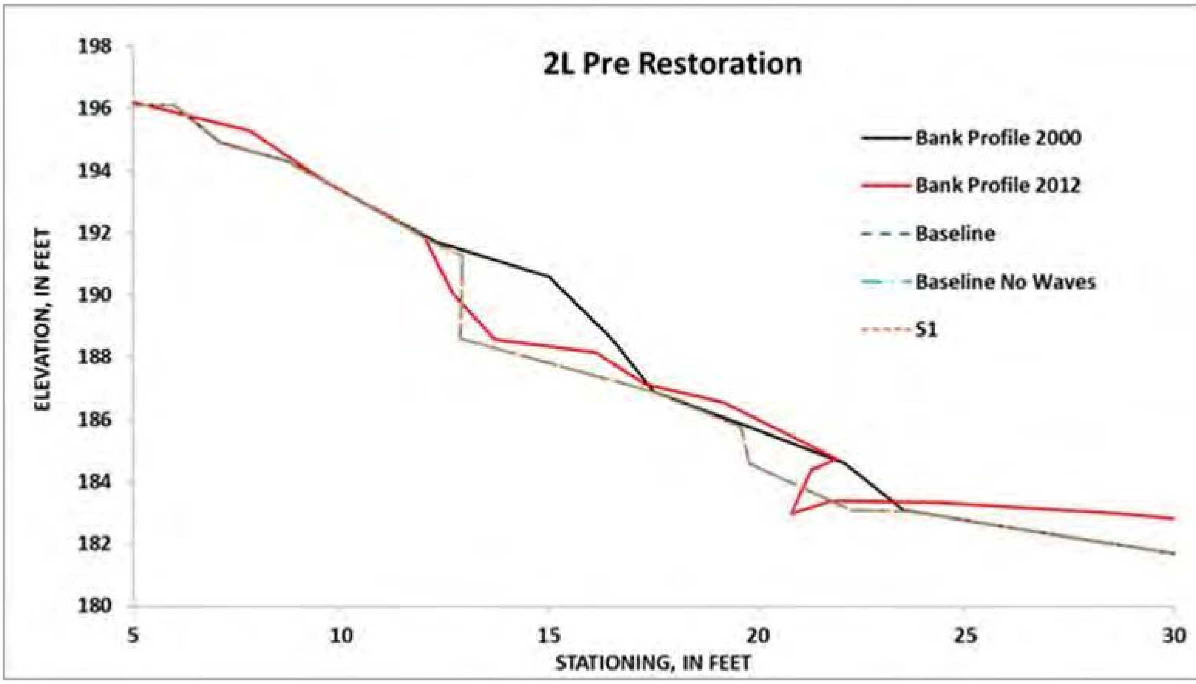

Figure 5.4.3.2-3: Simulated, future erosion for the Baseline Condition (with boat waves on and off) and Scenario 1 at site 2L Pre Restoration for the period 2000-2012. Zoomed in at area of erosion for illustrative purposes.

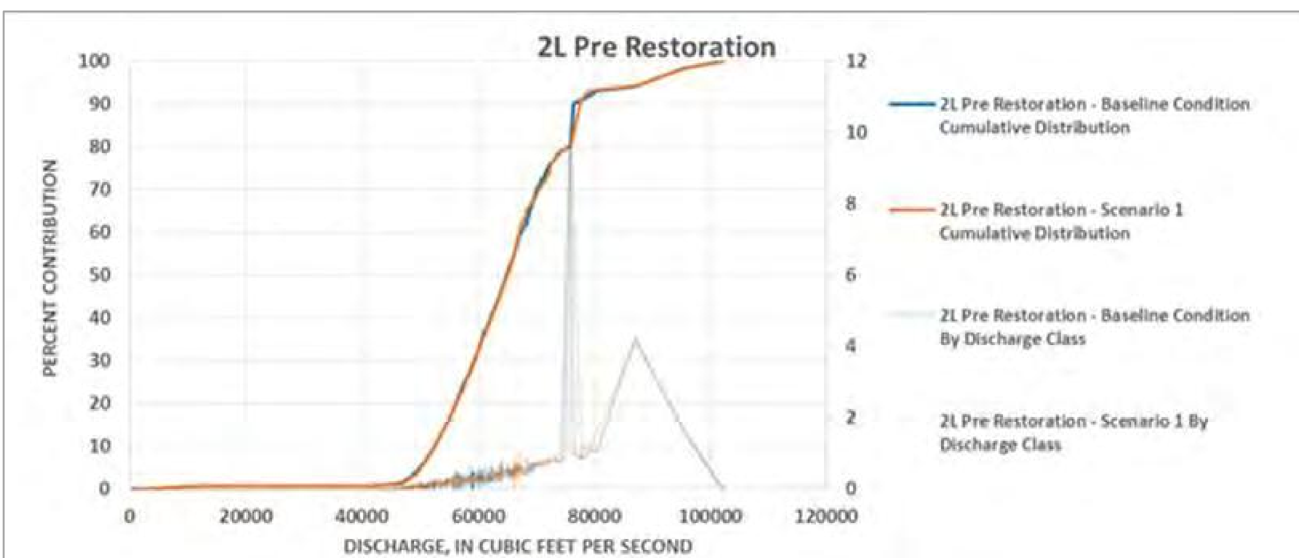

Figure 5.4.3.2-4: Simulated, percent contribution of total erosion by discharge for the Baseline Condition and Scenario 1 at site 2L for the period 2000-2012

5.4.3.3 Site 2L Post Restoration

The river at site 2L (station 94,500) Post Restoration has steep to vertical, heavily vegetated, moderately high banks. It is located at the Bonnette Farm, just below the mouth of the Ashuelot River, south of Stebbins Island. The bank is roughly 16 feet tall, with a silty sand bank and beach. The re-planted bank is heavily vegetated with grasses and large shrubs (Figure 5.4.3.3-1).

BSTEM runs at this site show that under the Baseline Condition, 0.463 ft^3 of erosion occurred per foot of bank, during the 2012 to 2014 flow period after restoration activities, averaging 0.214 ft^3/ft/y (Table 5.4.3-1). This results in the 7th lowest erosion rate for the Baseline Condition, placing it between the 20th and 25th percentiles of erosion rates along the reach. The modeling also indicates that all 100% (0.214 ft^3/ft/y) of the erosion is due directly to hydraulic processes, and none of the bank erosion is the result of geotechnical failures.

The Baseline Condition (Waves off) resulted in 0.204 ft^3/ft/y of erosion, with 0.213 ft^3/ft/y for Scenario 1 (Note- while this site did show a small reduction in erosion between the BL and S1 Scenarios the total reduction in erosion is well below the measureable/significant rate of 0.163 ft^3/ft/yr). This resulted in the following percent reductions in erosion rates: 4.65% for Baseline Wave off and 0.37% for Scenario 1 (Figure 5.4.3.3-2). Baseline simulations with waves off showed very little reduction in erosion.

For the Baseline Condition, 98.7% of the total erosion occurs at flows of about 17,130 cfs or greater (Figure 5.4.3.3-3). The minimal hydraulic erosion that did occur was between 36,000 cfs and 70,000 cfs, well above the hydraulic capacity of Vernon Dam, and can therefore be attributed to high flows. Table 5.4.3.3-1 denotes the flows above which 95%, 50%, and 5% of all erosion occurs at the site as well as the amount of time those flows were exceeded for each year in the modeling period.

Based on the reduction from Pre-Restoration to Post-Restoration, we can conclude that the site is eroding at a much slower rate, and that the restoration activities succeed in doing their intended function. In general, there is virtually no erosion at this site now.

Table 5.4.3.3-1: Flow Exceedance Calculations for Site 2L

Site 2L	Percent of Erosion		
	95%	50%	5%
	Flow (cfs)		
Year	71,465	65,195	51,924
2000	NA	0.10%	1.30%
2001	0.80%	1.60%	3.20%
2002	NA	0.10%	0.50%
2003	NA	0.20%	2.10%
2004	NA	NA	0.50%
2005	0.40%	0.70%	2.90%
2006	0.10%	0.30%	1.90%
2007	NA	0.50%	2.80%
2008	NA	0.50%	4.00%
2009	NA	NA	1.20%
2010	NA	NA	1.70%
2011	1.00%	2.10%	5.00%
2012	NA	NA	NA
2013	NA	NA	0.10%
2014	NA	0.80%	2.40%

NA: Not Applicable since flows did not reach this value

Figure 5.4.3.3-1: Photos at Site 2L Post Restoration

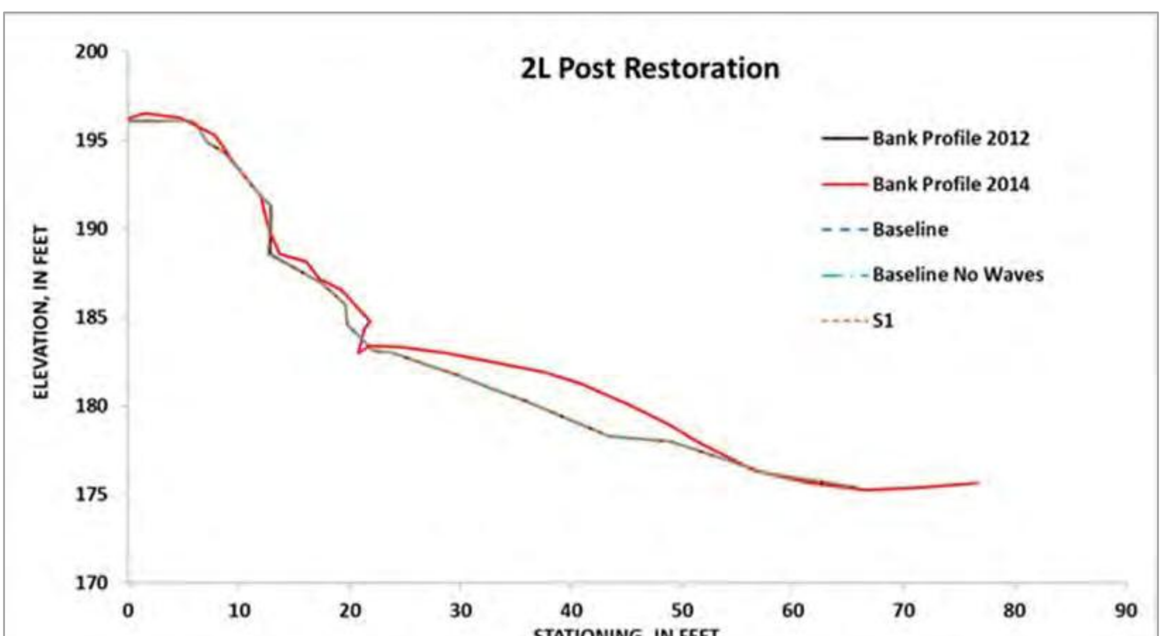

Figure 5.4.3.3-2: Simulated, future unit-erosion for the Baseline Condition (with boat waves on and off) and Scenario 1 at Site 2L Post Restoration for the period 2005-2014

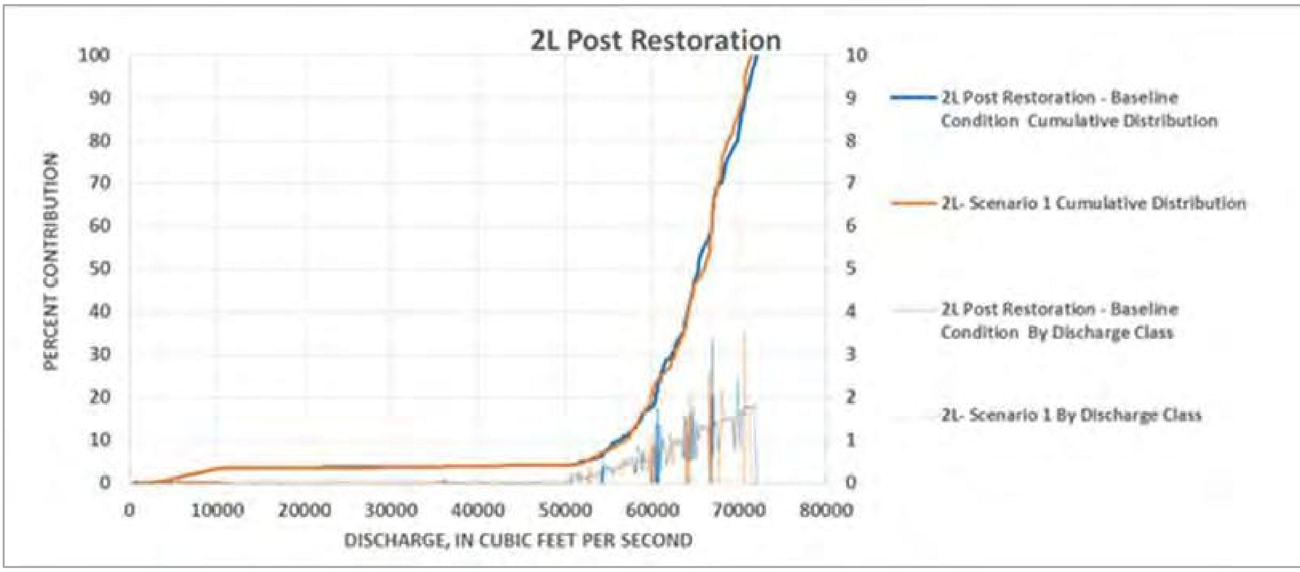

Figure 5.4.3.3-3: Simulated, percent contribution of total erosion by discharge for the Baseline Condition and Scenario 1 at site 2L for the period 2012-2014

5.4.3.4 Site 303BL

The river at site 303BL has steep to vertical, sparsely vegetated banks, located at station 94,000, downstream of Stebbins Island, immediately downstream of site 2L. The bank is roughly 16 feet tall with a sandy toe (d_{50}=0.11mm) and a silty bank face. The bank is vegetated mostly with grasses and small shrubs, but contains a few American elm, Green ash, and Silver maple trees. A significant amount of bare soil and exposed roots were noted on the bank face, and undercutting was present. No historical cross sections exist for this site. The site was surveyed in 2014 and this geometry was used as a starting point for the model runs (Figure 5.4.3.4-1).

BSTEM runs at this site show that under the Baseline Condition, 9.48 ft^3 of erosion occurred per foot of bank, during the 2000-2014 flow period, averaging 0.647 ft^3/ft/y (Table 5.4.3-1). This results in the 18th highest erosion rate for the Baseline Condition, placing it between the 40th and 45th percentiles of erosion rates along the reach. The modeling also indicates that 96% (0.622 ft^3/ft/y) of the erosion is due directly to hydraulic processes, whereas only 4% (0.025 ft^3/ft/y) is the result of geotechnical processes and associated mass failures. Bank undercutting and a large number of exposed roots were noted during fieldwork, supporting the predicted high percentage of hydraulic erosion compared to geotechnical erosion.

The Baseline Condition (Waves off) resulted in 0.645 ft^3/ft/y, with 0.674 ft^3/ft/y for Scenario 1. This resulted in the following percent reductions (compared to the Baseline Condition) in erosion rates: 0.34% and -4.23% for Baseline Wave off and Scenario 1, respectively (Figure 5.4.3.4-2 and Figure 5.4.3.4-3). Baseline simulations with waves off showed virtually no reduction in erosion indicating that boat waves have little effect on erosion processes at this site. Because of this, all of the remaining scenario was simulated with boat waves on.

For the Baseline Condition, 95% of the total erosion occurs at flows of about 53,000 cfs or greater (Figure 5.4.3.4-4). Hydraulic erosion and small failures occurred between 53,000 and 80,000, at which point a larger (though still relatively small) failure occurred, resulting in the remaining 10% of total erosion at those extreme high flows. Through this analysis we can conclude that the high flows greater than the hydraulic capacity at Vernon Dam, Northfield Mountain, and Turners Falls are accounting for most of the total erosion at this site. Table 5.4.3.4-1 denotes the flows above which 95%, 50%, and 5% of all erosion occurs at the site as well as the amount of time those flows were exceeded for each year in the modeling period.

It should be noted that at this site, Scenario 1 showed greater erosion than the Baseline Condition. One possible cause for this is the variation in flows from peaking operations for Scenario 1. These flows created a geotechnical failure (4.2% of the total) at a flow of about 45,000 cfs, still above the hydraulic capacity of the dam. This failure did not occur for the Baseline Condition. The failure is likely due to the rapid decrease in water surface elevation after extreme high flows at a stage of 196.33 ft (79,000 cfs) (Figure 5.4.3.4-5). If we only look at the hydraulic erosion both scenarios produce the same amount (Figure 5.4.3-1), it was the one geotechnical failure under the Scenario 1 conditions that resulted in the increase in erosion. This failure may have occurred due to the lack of fluctuation of water surface leading up to the high flow event. The shear velocities are focused on a narrower range of the bank under the Scenario 1 conditions, it is possible that this caused a weakening in the bank that did not occur under the Baseline Conditions.

Table 5.4.3.4-1: Flow Exceedance Calculations for Site 303BL

Site 303BL	Percent of Erosion		
	95%	50%	5%
	Flow (cfs)		
Year	79,881	64,684	53,194
2000	NA	0.20%	1.30%
2001	NA	1.70%	2.90%
2002	NA	0.10%	0.50%
2003	NA	0.40%	1.90%
2004	NA	NA	0.30%
2005	NA	0.70%	2.40%
2006	NA	0.40%	1.80%
2007	NA	0.50%	2.70%
2008	NA	0.50%	3.60%
2009	NA	NA	1.10%
2010	NA	NA	1.30%
2011	0.40%	2.30%	4.70%
2012	NA	NA	NA
2013	NA	NA	0.10%
2014	NA	0.80%	2.20%

NA: Not Applicable since flows did not reach this value

Figure 5.4.3.4-1 Photos at site 303BL

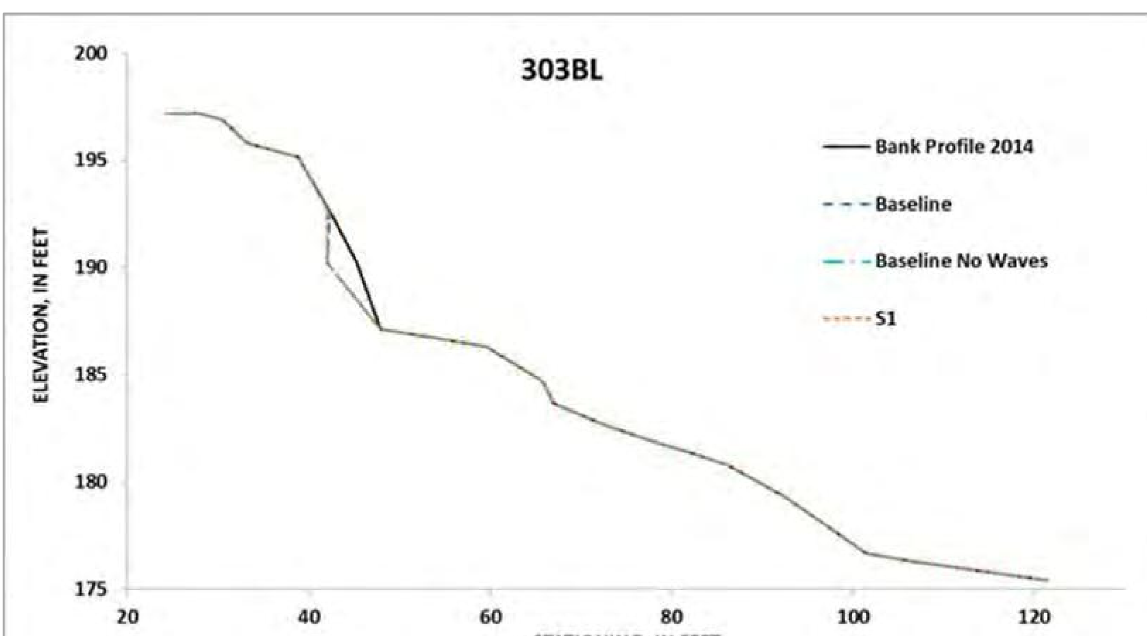

Figure 5.4.3.4-2: Simulated, future unit-erosion for the Baseline Condition (with boat waves on and off) and Scenarios 1 at site 303BL for the period 2000-2014

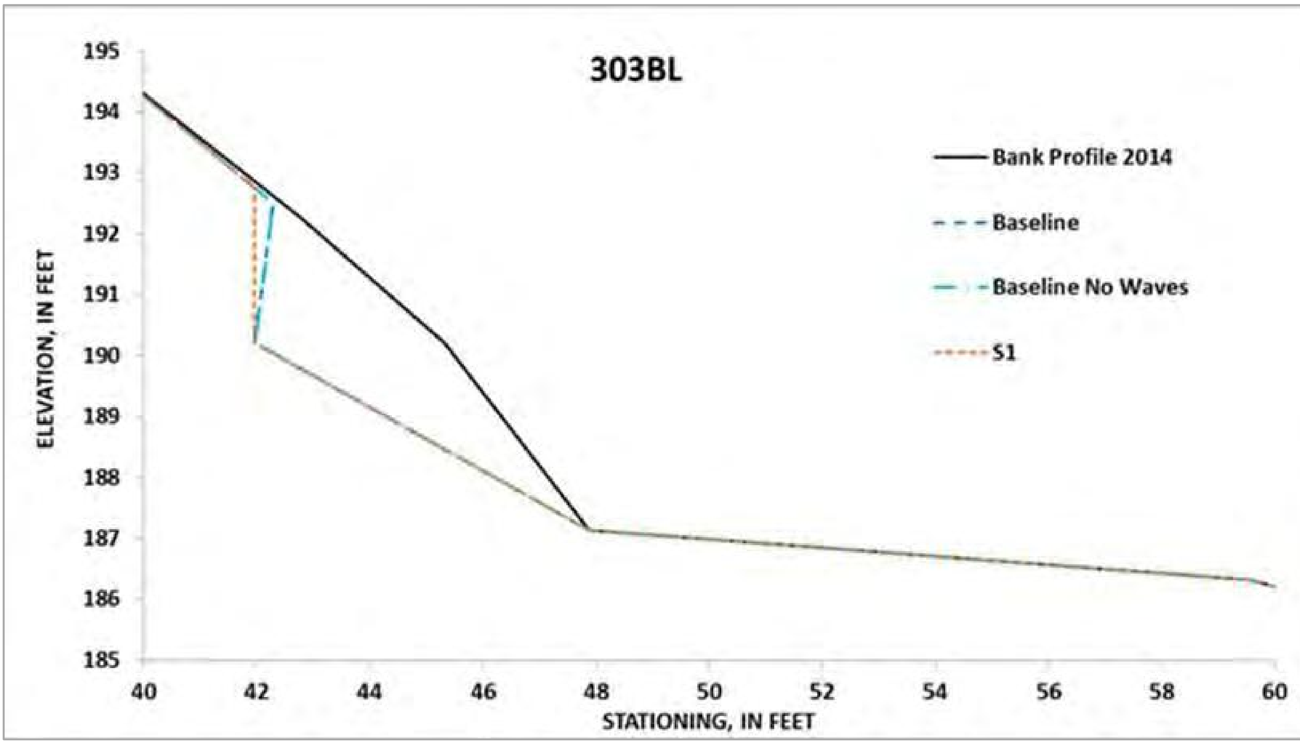

Figure 5.4.3.4-3: Simulated, future erosion for the Baseline Condition (with boat waves on and off) and Scenarios 1 at site 303BLfor the period 2000-2014. Zoomed in at area of erosion for illustrative purposes.

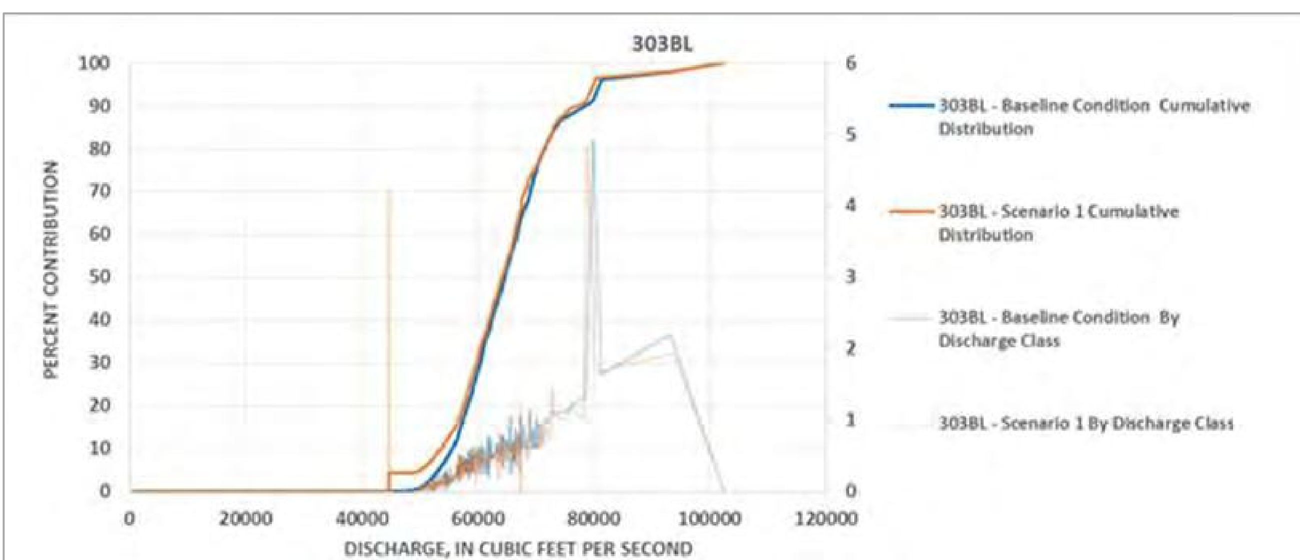

Figure 5.4.3.4-4: Simulated, percent contribution of total erosion by discharge for the Baseline Condition and Scenarios 1 at site 303BL for the period 2000-2014

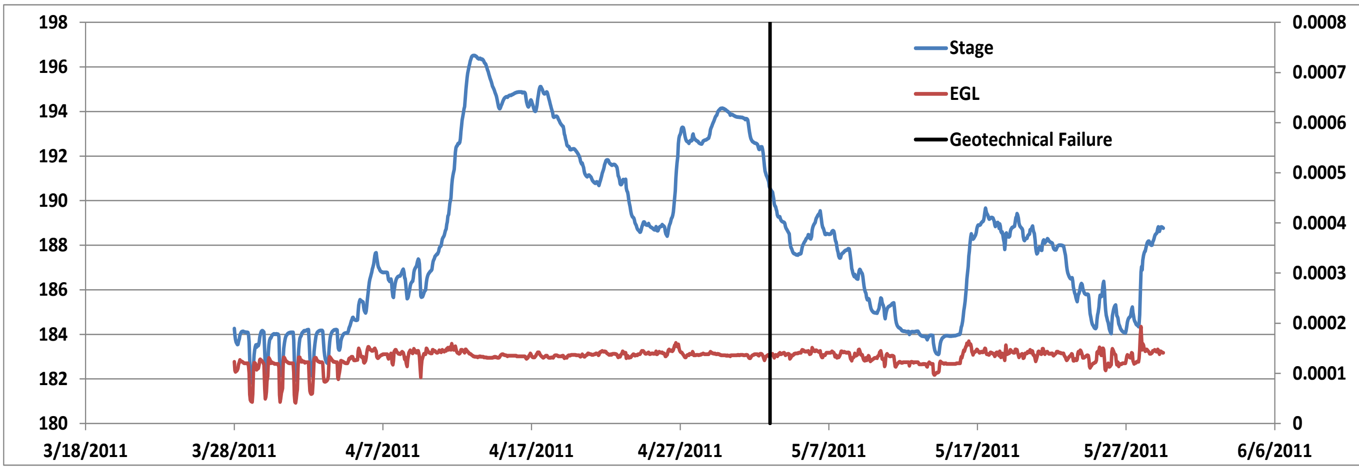

Figure 5.4.3.4-5: Stage and Energy Grade Line (EGL) of flows at Site 303BL under Scenario 1 around the time of the geotechnical failure on 05/03/2011 at 1:00AM (denoted by vertical black line).

5.4.3.5 Site 18BL

The river at site 18BL has steep to vertical, sparsely vegetated banks. It is located at station 87,000, roughly 5,000 ft downstream of Upper Island. The bank is roughly 23 feet tall, with a sandy-loam bank toe and bank face. The bank is vegetated mostly with grasses and small shrubs, but contains a few American elm, American sycamore, Green ash, and Red oak trees. A significant amount of bare soil and exposed roots were noted on the bank face, and undercutting was present. No historical cross sections existed for this site. A 2014 survey was used as the starting geometry for the model runs (Figure 5.4.3.5-1).

BSTEM runs at this site show that under the Baseline Condition, 16.0 ft^3 of erosion occurred per foot of bank during the 2000-2014 flow period, averaging 1.09 ft^3/ft/y (Table 5.4.3-1). This results in the 17th highest erosion rate for the Baseline Condition, placing it between the 40th and 45th percentiles of erosion rates along the reach. The modeling also indicates that 76% (0.83 ft^3/ft/y) of the erosion is due directly to hydraulic processes, whereas remaining 24% (0.26 ft^3/ft/y) is the result of geotechnical processes and associated mass failures. This is also shown in (Figure 5.4.3.5-4), as a very gradual smooth shape, with few large spikes that would indicate the prevalence of mass wasting.

The Baseline Condition (Waves off) resulted in 1.09 ft^3/ft/y, with 1.08 ft^3/ft/y for Scenario 1 (Figure 5.4.3.5-2 and Figure 5.4.3.5-3). This resulted in a 1.1% reduction in erosion rates for Scenario 1 (Note- while this site did show a small reduction in erosion between the BL and S1 Scenarios the total reduction in erosion is well below the measureable/significant rate of 0.163 ft^3/ft/yr). As Baseline Condition (Waves off) scenario illustrated a zero reduction in erosion, it was concluded that boat waves had no impact on bank stability, and the remaining scenarios were not conducted with boat-waves off.

For the Baseline Condition, 98% of the total erosion occurs at flows of about 17,130 cfs or greater (Figure 5.4.3.5-4). There are two significant geotechnical failures that occur at 18,000 cfs and 27,000 cfs which account for the majority of the geotechnical erosion at site 18BL. The distribution of hydraulic erosion gradually builds between 27,000 and 80,000 cfs, where they begin to taper off at the extreme high flows. Through this analysis we can conclude that those flows greater than the hydraulic capacity at Vernon Dam are accounting for most of the total erosion. Table 5.4.3.5-1 denotes the flows above which 95, 50, and 5% of all erosion occurs at the site as well as the amount of time those flows were exceeded for each year.

Table 5.4.3.5-1: Flow Exceedance Calculations for Site 18BL

Site 18BL	Percent of Erosion		
	95%	**50%**	**5%**
	Flow (cfs)		
Year	**73,352**	**54,485**	**17,824**
2000	NA	1.20%	22.60%
2001	0.40%	2.70%	9.30%
2002	NA	0.40%	15.90%
2003	NA	1.60%	26.50%
2004	NA	0.20%	15.30%
2005	0.20%	2.20%	30.70%
2006	0.10%	1.50%	33.10%
2007	NA	2.70%	19.10%
2008	NA	3.30%	30.40%
2009	NA	0.80%	23.50%
2010	NA	1.00%	21.80%
2011	0.90%	4.50%	31.00%
2012	NA	NA	12.30%
2013	NA	0.10%	16.80%
2014	NA	2.10%	20.70%

NA: Not Applicable since flows did not reach this value

Figure 5.4.3.5-1 Photos at site 18BL

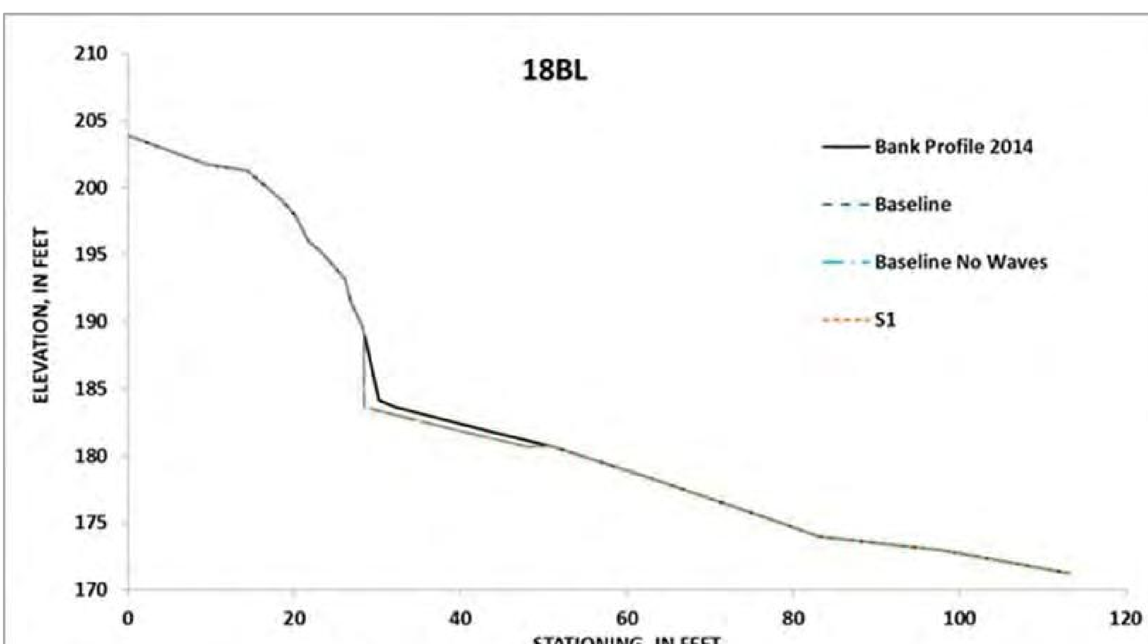

Figure 5.4.3.5-2: Simulated, future unit-erosion for the Baseline Condition (with boat waves on and off) and Scenarios 1 at site 18BL for the period 2000-2014

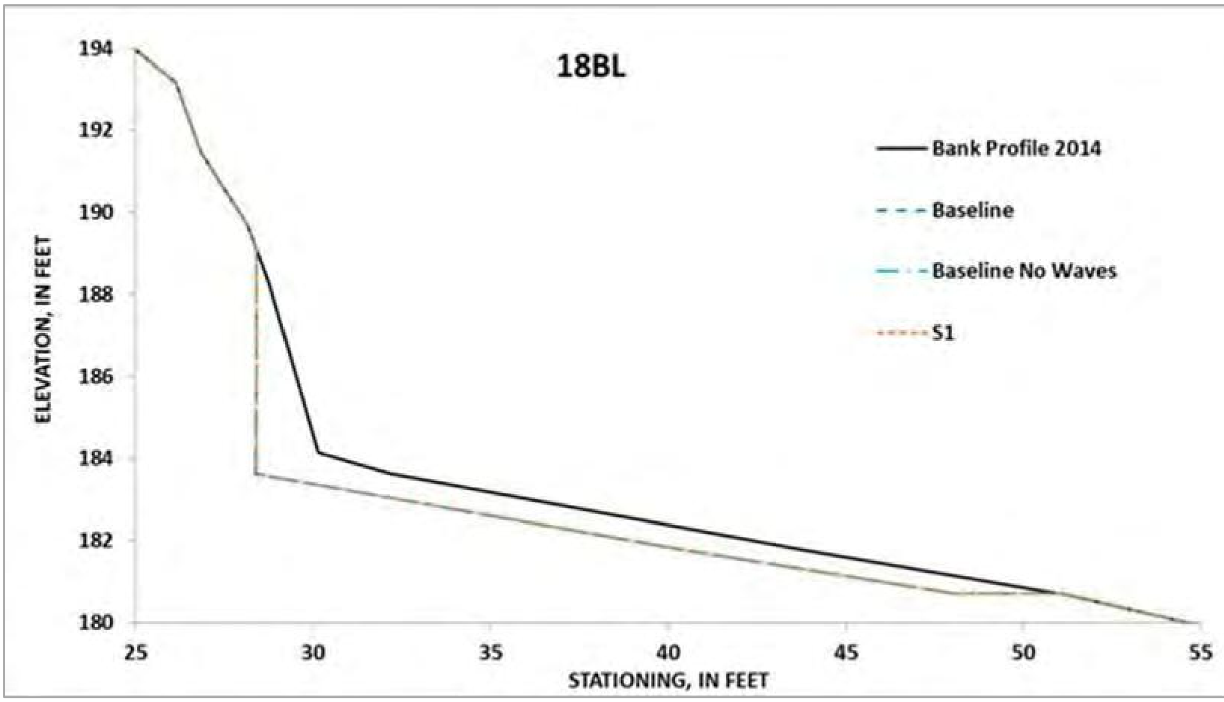

Figure 5.4.3.5-3: Simulated, future erosion for the Baseline Condition (with boat waves on and off) and Scenarios 1 at site 18BL for the period 2000-2014. Zoomed in at area of erosion for illustrative purposes.

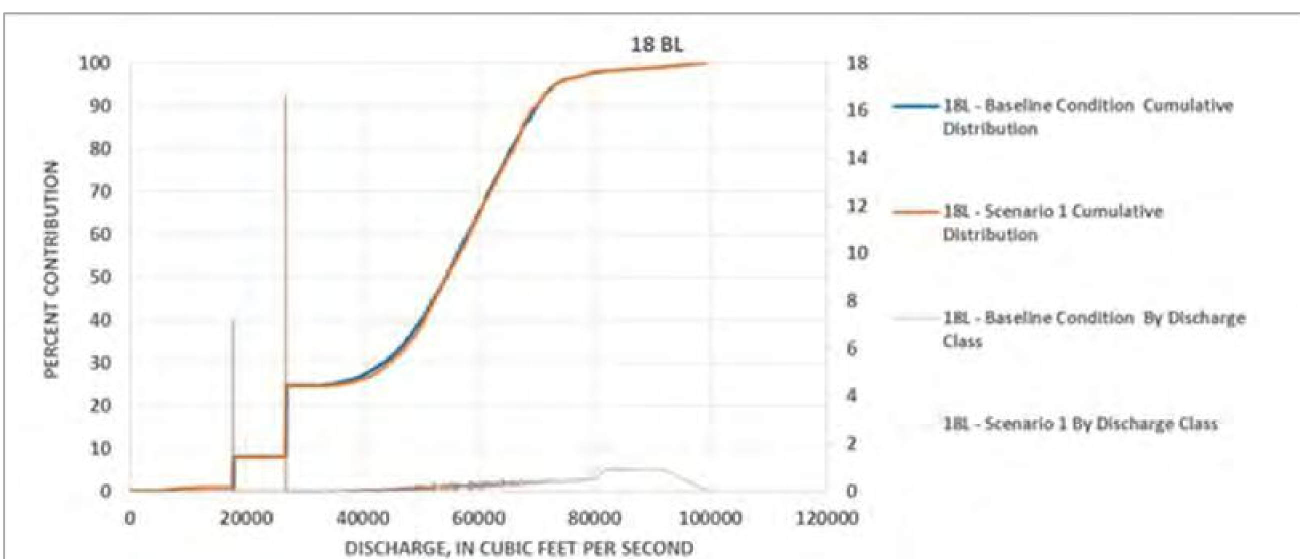

Figure 5.4.3.5-4: Simulated, percent contribution of total erosion by discharge for the Baseline Condition and Scenarios 1 at site 18BL for the period 2000-2014

5.4.3.6 Site 3L

The river at site 3L (station 79,500) has slightly more gradual, heavily vegetated banks, and is located north of the Massachusetts-Vermont border, just north of site 21R. The bank is roughly 20 feet tall, with a sandy-loam bank toe and upper bank. The bank is vegetated with grasses, shrubs, and large American elms, Green ash, Hickory and Northern red oak trees (Figure 5.4.3.6-1).

BSTEM runs at this site show that under the Baseline Condition, 89.2 ft^3 of erosion occurred per foot of bank during the 2000-2014 flow period, averaging 6.09 ft^3/ft/y (Table 5.4.3-1). This results in the 4th highest erosion rate for the Baseline Condition, placing it between the 85th and 90th percentiles of erosion rates along the reach. The modeling also indicates that 86% (5.25 ft^3/ft/y) of the erosion is due directly to hydraulic processes, whereas the remaining 14% (0.84 ft^3/ft/y) is the result of geotechnical processes and associated mass failures.

The Baseline Condition (Waves off) resulted in 6.09 ft^3/ft/y, with 6.04 ft^3/ft/y for Scenario 1 (Note- while this site did show a small reduction in erosion between the BL and S1 Scenarios the total reduction in erosion is well below the measureable/significant rate of 0.163 ft^3/ft/yr). This resulted in a percent reduction in erosion rates for Scenario 1 of 0.7% (Figure 5.4.3.6-2). As Baseline Condition (Waves off) scenario showed a zero reduction in erosion, it was concluded that boat waves are not having a significant impact on bank stability, and the remaining scenario was not considered with boat waves off. For the Baseline Condition, 95% of the total erosion occurs at flows of about 37,000 cfs or greater (Figure 5.4.3.6-3). There is some hydraulic erosion and small failures between 35,000 and 78,000, at which point significant failures occur, resulting in 50% of the total erosion at site 3L. Through this analysis we can conclude that those flows greater than the hydraulic capacity at Vernon are accounting for most of the total erosion.

Table 5.4.3.6-1 denotes the flows above which 95%, 50%, and 5% of all erosion occurs at the site as well as the amount of time those flows were exceeded for each year in the modeling period.

Table 5.4.3.6-1: Flow Exceedance Calculations for Site 3L

Site 3L	Percent of Erosion		
	95%	50%	5%
	Flow (cfs)		
Year	98,234	78,682	37,098
2000	NA	NA	5.20%
2001	NA	NA	5.10%
2002	NA	NA	2.70%
2003	NA	NA	6.50%
2004	NA	NA	1.70%
2005	NA	NA	9.00%
2006	NA	NA	7.40%
2007	NA	NA	5.00%
2008	NA	NA	11.60%
2009	NA	NA	4.00%
2010	NA	NA	6.30%
2011	0.20%	0.60%	10.40%
2012	NA	NA	0.50%
2013	NA	NA	1.80%
2014	NA	NA	3.90%

NA: Not Applicable since flows did not reach this value

Figure 5.4.3.6-1 Photos at site 3L

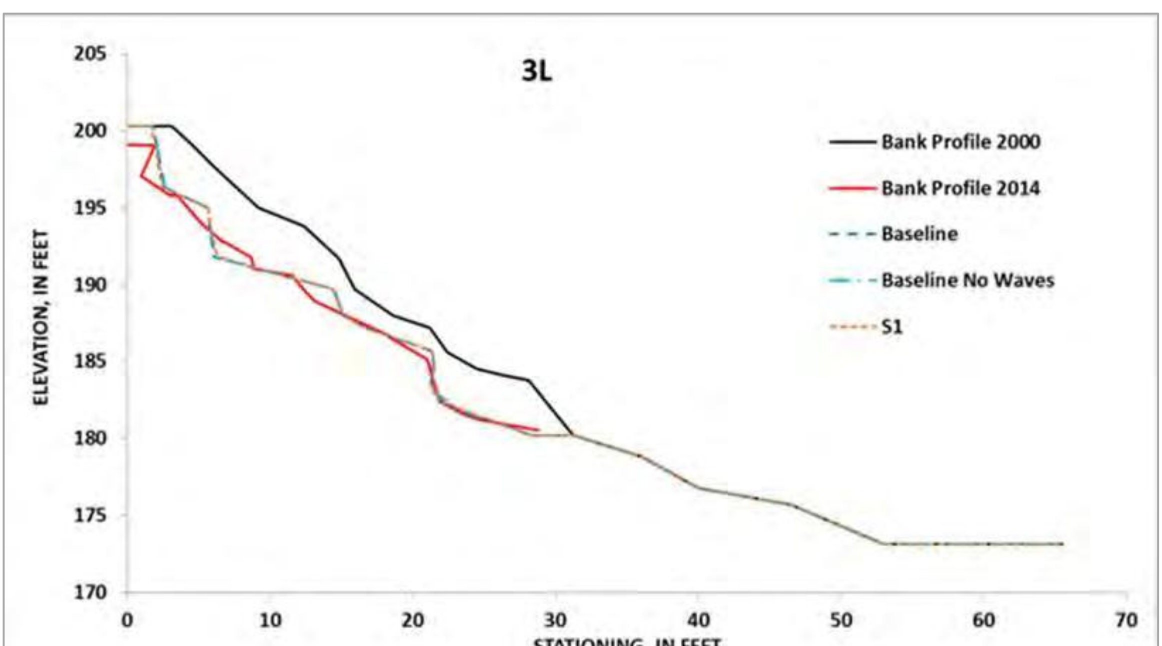

Figure 5.4.3.6-2: Simulated, future unit-erosion for the Baseline Condition (with boat waves on and off) and Scenarios 1 at site 3L for the period 2000-2014

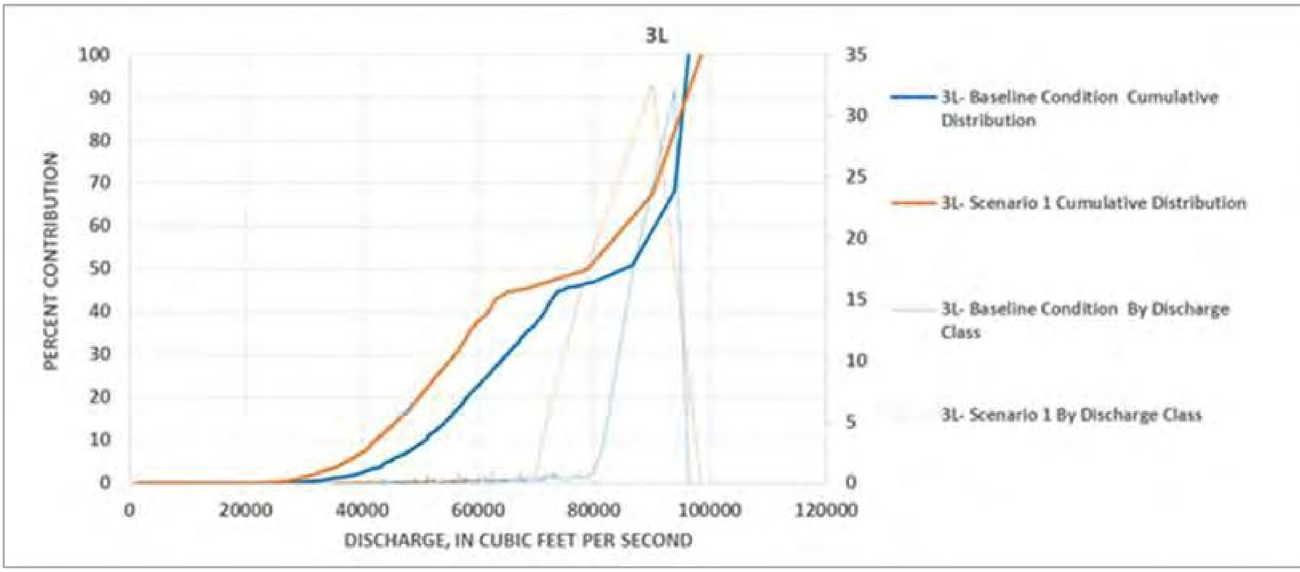

Figure 5.4.3.6-3: Simulated, percent contribution of total erosion by discharge for the Baseline Condition and Scenarios 1 at site 3L for the period 2000-2014

5.4.3.7 Site 3R Pre-Restoration

The river at site 3R Pre-Restoration has steep to vertical, very sparsely vegetated banks and is the same stationing (79,500) as site 3L, above. The bank is roughly 26 feet tall, with a silty-sand bank and beach. Observations from 1998 indicate active and extensive erosion with overhanging banks and notches (Figure 5.4.3.7-1).

BSTEM runs at this site show that under the Baseline Condition, about 100 ft^3 of erosion occurred per foot of bank, during the 2000 to 2006 flow period prior to restoration, averaging 15.4 ft^3/ft/y (Table 5.4.3-1). This results in the highest erosion rate for the Baseline Condition, placing it between the 95th and 100th percentiles of erosion rates along the reach. The modeling also indicates that 42% (6.51 ft^3/ft/y) of the erosion is due directly to hydraulic processes, whereas the other 58% (8.91 ft^3/ft/y) is the result of geotechnical processes and associated mass failures.

The Baseline Condition (Waves off) resulted in 15.4 ft^3/ft/y, with 15.5 ft^3/ft/y for Scenario 1. This resulted in the following percent reductions in erosion rates: 0.113% and -0.219% for Baseline Wave off and Scenario 1, respectively (Figure 5.4.3.7-2). Baseline simulations with waves off showed very little reduction in erosion indicating that boat waves have little effect on erosion processes at this site. Because of this, all of the remaining scenarios were simulated with boat waves on.

For the Baseline Condition, 95% of the total erosion occurs at flows of about 32,000 cfs or greater (Figure 5.4.3.7-3). The hydraulic erosion occurs across the range of flows between 32,000 cfs and 61,000 cfs, at which point a large geotechnical failure occurs resulting in roughly 65% of the total erosion at site 3R prior to restoration activities. Through this analysis we can conclude that those flows greater than the hydraulic capacity at Vernon are accounting for most of the total erosion.

Table 5.4.3.7-1 denotes the flows above which 95%, 50%, and 5% of all erosion occurs at the site as well as the amount of time those flows were exceeded for each year in the modeling period.

Table 5.4.3.7-1: Flow Exceedance Calculations for Site 3R Pre-Restoration

Site 3R	Percent of Erosion		
	95%	50%	5%
	Flow (cfs)		
Year	**87,760**	**54,420**	**36,411**
2000	NA	1.20%	5.30%
2001	NA	2.70%	5.40%
2002	NA	0.40%	2.90%
2003	NA	1.70%	6.90%
2004	NA	0.30%	1.90%
2005	NA	2.20%	9.40%
2006	NA	1.50%	7.80%
2007	NA	2.70%	5.20%
2008	NA	3.30%	12.00%
2009	NA	0.80%	4.20%
2010	NA	1.00%	6.60%
2011	0.30%	4.50%	11.10%
2012	NA	NA	0.50%
2013	NA	0.10%	2.00%
2014	NA	2.10%	4.20%

NA: Not Applicable since flows did not reach this value

Right bank, 1998

Figure 5.4.3.7-1 Photos from 1998 at site 3R Pre Restoration (Labeled as 1998 FRR/ECP-Site 9)

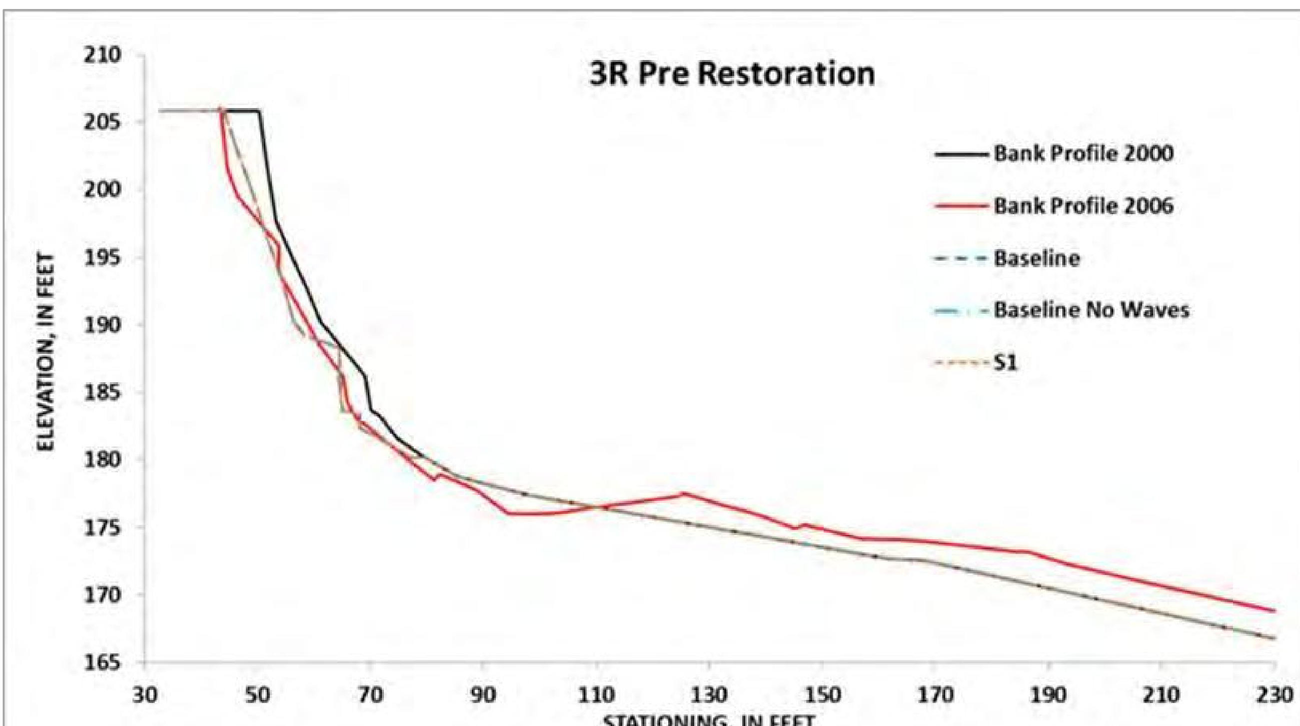

Figure 5.4.3.7-2: Simulated, future unit-erosion for the Baseline Condition (with boat waves on and off) and Scenarios 1 at site 3R for the period 2000-2006

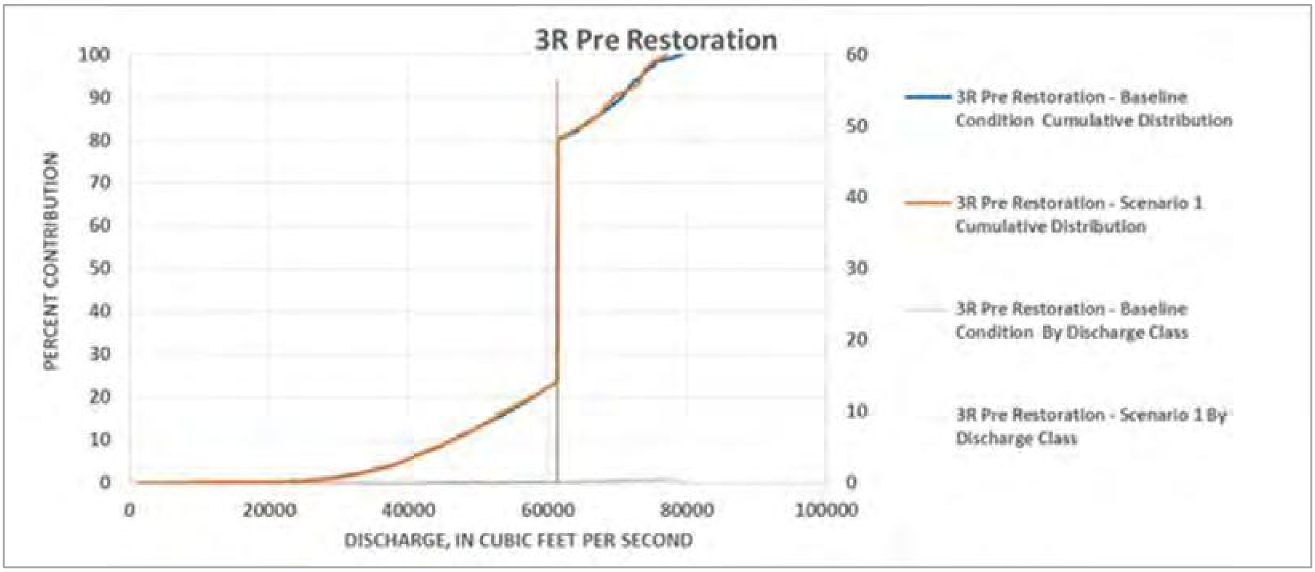

Figure 5.4.3.7-3: Simulated, percent contribution of total erosion by discharge for the Baseline Condition and Scenario 1 at site 3R for the period 2000-2006

5.4.3.8 Site 3R Post Restoration

The river at site 3R Post Restoration has slightly more gradual, heavily vegetated banks, located at station 79,500, north of the Massachusetts-Vermont border, just north of site 21R. The bank is roughly 26 feet tall, with a placed rock toe designed to reduce hydraulic erosion (d_{50} = 55 mm) and a silt loam bank. The replanted bank is heavily vegetated with large shrubs and the bank top is planted in corn (Figure 5.4.3.8-1).

BSTEM runs at this site show that under the Baseline Condition, 1.75 ft^3 of erosion occurred per foot of bank, during the 2006 to 2014 flow period after restoration activities, averaging 0.285 ft^3/ft/y (Table 5.4.3-1). This results in the 9th lowest erosion rate for the Baseline Condition, placing it between the 20th and 25th percentiles of erosion rates along the reach. The modeling also indicates that all 100% (0.285 ft^3/ft/y) of the erosion is due directly to hydraulic processes, and none of the bank erosion is the result of larger geotechnical failures. The minimal amount of hydraulic erosion that is occurring is within the level of the placed rock at the toe, indicating that the rock may be slightly undersized for the flows.

The Baseline Condition (Waves off) resulted in 0.281 ft^3/ft/y, with 0.282 ft^3/ft/y for Scenario 1 (Note- while this site did show a small reduction in erosion between the BL and S1 Scenarios the total reduction in erosion is well below the measureable/significant rate of 0.163 ft^3/ft/yr). This resulted in the following percent reductions in erosion rates: 1.4% and 1.1% for Baseline Wave off and Scenario 1, respectively (Figure 5.4.3.8-2). Baseline simulations with waves off showed very little reduction in erosion, it was concluded that boat waves have little effect on erosion processes at this site. Because of this, all of the remaining scenarios were simulated with boat waves on.

For the Baseline Condition, 97.5% of the total erosion occurs at flows of 17,130 cfs or greater (Figure 5.4.3.8-3). The minimal hydraulic erosion that did occur was between 36,000 cfs and 70,000 cfs. As there is almost no erosion below the operating capacity of Vernon, those flows above the peaking operations look to be the cause of the minimal erosion at this site. Based on the reduction in erosion rates from pre-restoration to post-restoration conditions, we can conclude that the restoration work was highly successful. In general there is currently no active erosion taking place at this site. Table 5.4.3.8-1 denotes the flows above which 95%, 50%, and 5% of all erosion occurs at the site as well as the amount of time those flows were exceeded for each year in the modeling period.

Table 5.4.3.8-1: Flow Exceedance Calculations for Site 3R Post Restoration

Site 3R	Percent of Erosion		
	95%	50%	5%
	Flow (cfs)		
Year	**87,760**	**54,420**	**36,411**
2000	NA	1.20%	5.30%
2001	NA	2.70%	5.40%
2002	NA	0.40%	2.90%
2003	NA	1.70%	6.90%
2004	NA	0.30%	1.90%
2005	NA	2.20%	9.40%
2006	NA	1.50%	7.80%
2007	NA	2.70%	5.20%
2008	NA	3.30%	12.00%
2009	NA	0.80%	4.20%
2010	NA	1.00%	6.60%
2011	0.30%	4.50%	11.10%
2012	NA	NA	0.50%
2013	NA	0.10%	2.00%
2014	NA	2.10%	4.20%

NA: Not Applicable since flows did not reach this value

Figure 5.4.3.8-1 Photos at site 3R Post Restoration

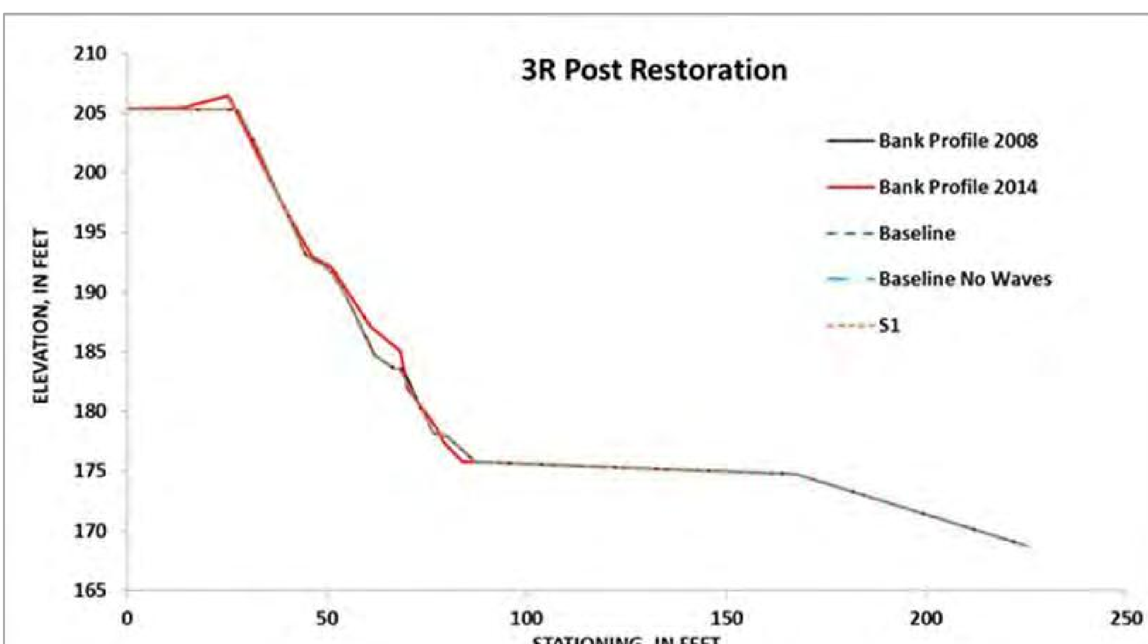

Figure 5.4.3.8-2: Simulated, future unit-erosion for the Baseline Condition (with boat waves on and off) and Scenarios 1 at site 3R for the period 2006-2014

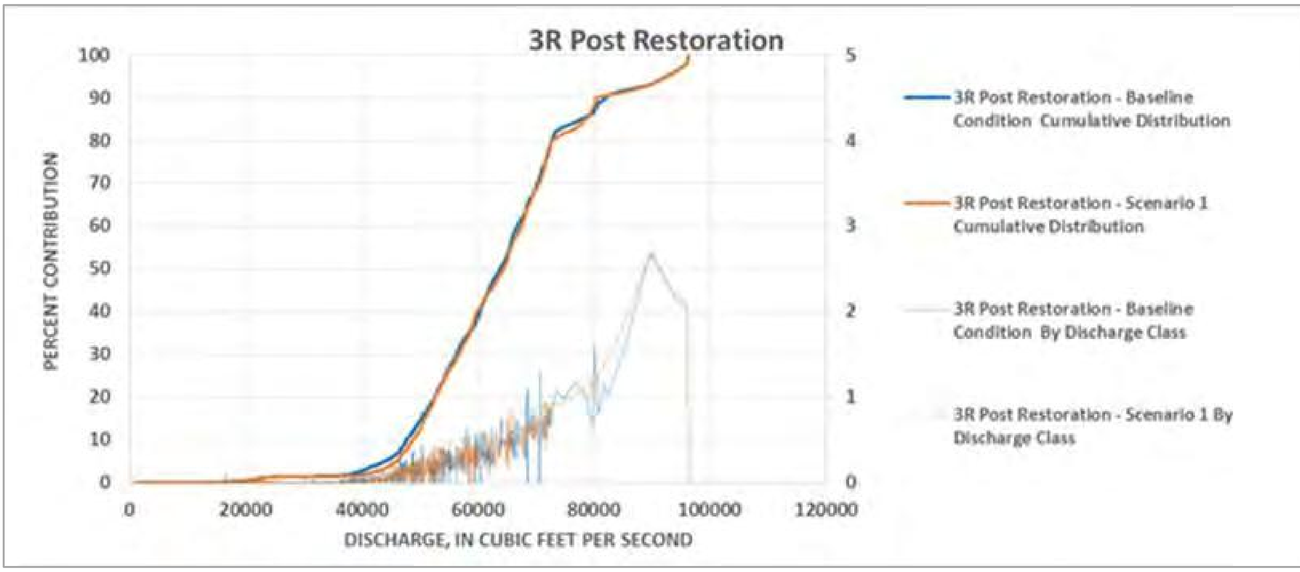

Figure 5.4.3.8-3: Simulated, percent contribution of total erosion by discharge for the Baseline Condition and Scenarios 1 at site 3R for the period 2006-2014

5.4.3.9 Site 21R

The river at site 21R has a steep bank face, sparsely vegetated banks, and is located at station 79,250, just north of the Massachusetts-Vermont Border. The bank is roughly 27 feet tall, with a sandy-loam bank toe and upper bank. The bank is vegetated mostly with grasses and small shrubs, but contains a few American basswood, Green ash, and Northern red oak trees. A significant amount of bare soil was noted on the bank face. No historical cross sections existed for this site. A survey conducted in 2014 was used as the initial bank geometry for the model runs (Figure 5.4.3.9-1).

BSTEM runs at this site show that under the Baseline Condition, 34.6 ft^3 of erosion occurred per foot of bank, during the 2000-2014 flow period, averaging 2.36 ft^3/ft/y (Table 5.4.3-1). This results in the 11th highest erosion rate for the Baseline Condition, placing it between the 65th and 70th percentiles of erosion rates along the reach. The modeling also indicates that all 100% (2.36 ft^3/ft/y) of the erosion is due directly to hydraulic processes, and that none of the bank erosion is the result of larger geotechnical failures.

The Baseline Condition (Waves off) resulted in 2.29 ft^3/ft/y, with 2.35 ft^3/ft/y for Scenario 1 (Note- while this site did show a small reduction in erosion between the BL and S1 Scenarios the total reduction in erosion is well below the measureable/significant rate of 0.163 ft^3/ft/yr). This is a reduction in erosion of 2.9% for Baseline Wave off and 0.2% for Scenario 1(Figure 5.4.3.9-2 to Figure 5.4.3.9-3). As Baseline Condition (Waves off) scenario illustrated a very little reduction in erosion, it was concluded that boat waves are not having a significant impact on bank stability, and the remaining scenarios were not considered with boat waves off.

For the Baseline Condition, 96.8% of the total erosion occurs at flows of about 17,130 cfs or greater (Figure 5.4.3.9-4). Though there is some small amount of hydraulic erosion at site 21R below about 12,000 cfs, the rate of hydraulic erosion drastically increases at about 23,000 cfs, climbing steadily until 65,000 cfs, and then dropping off at the extreme high flows. Table 5.4.3.9-1 denotes the flows above which 95%, 50%, and 5% of all erosion occurs at the site as well as the amount of time those flows were exceeded for each year in the modeling period. Through this analysis we can conclude that high flows above the hydraulic capacity of Vernon are accounting for most of the total erosion.

Table 5.4.3.9-1: Flow Exceedance Calculations for Site 21R

Site 21R	Percent of Erosion		
	95%	50%	5%
	Flow (cfs)		
Year	**63,852**	**46,345**	**22,928**
2000	0.20%	2.60%	15.10%
2001	1.70%	3.80%	8.20%
2002	0.10%	1.20%	10.60%
2003	0.60%	3.40%	18.50%
2004	NA	0.80%	8.40%
2005	0.70%	5.10%	23.20%
2006	0.40%	2.80%	21.00%
2007	0.80%	3.50%	13.30%
2008	0.60%	6.10%	22.10%
2009	NA	2.20%	13.90%
2010	NA	3.10%	15.30%
2011	2.50%	6.80%	25.20%
2012	NA	0.30%	7.80%
2013	NA	0.30%	12.10%
2014	0.90%	2.90%	15.80%

NA: Not Applicable since flows did not reach this value

Figure 5.4.3.9-1: Photos at site 21R

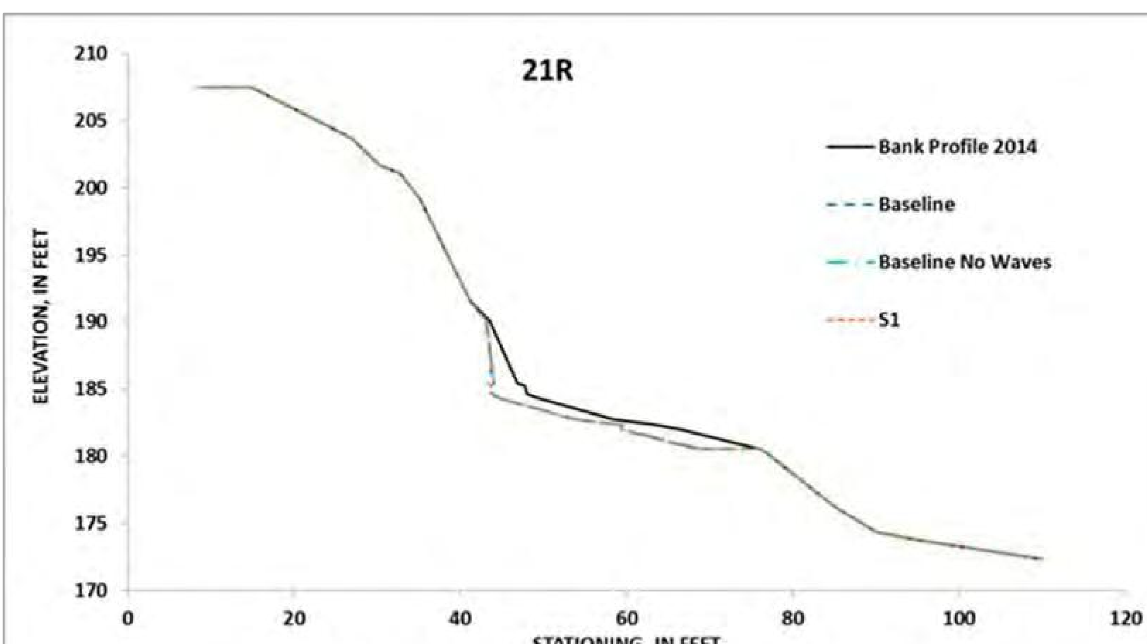

Figure 5.4.3.9-2: Simulated, future unit-erosion for the Baseline Condition (with boat waves on and off) and Scenarios 1 at site 21R for the period 2000-2014

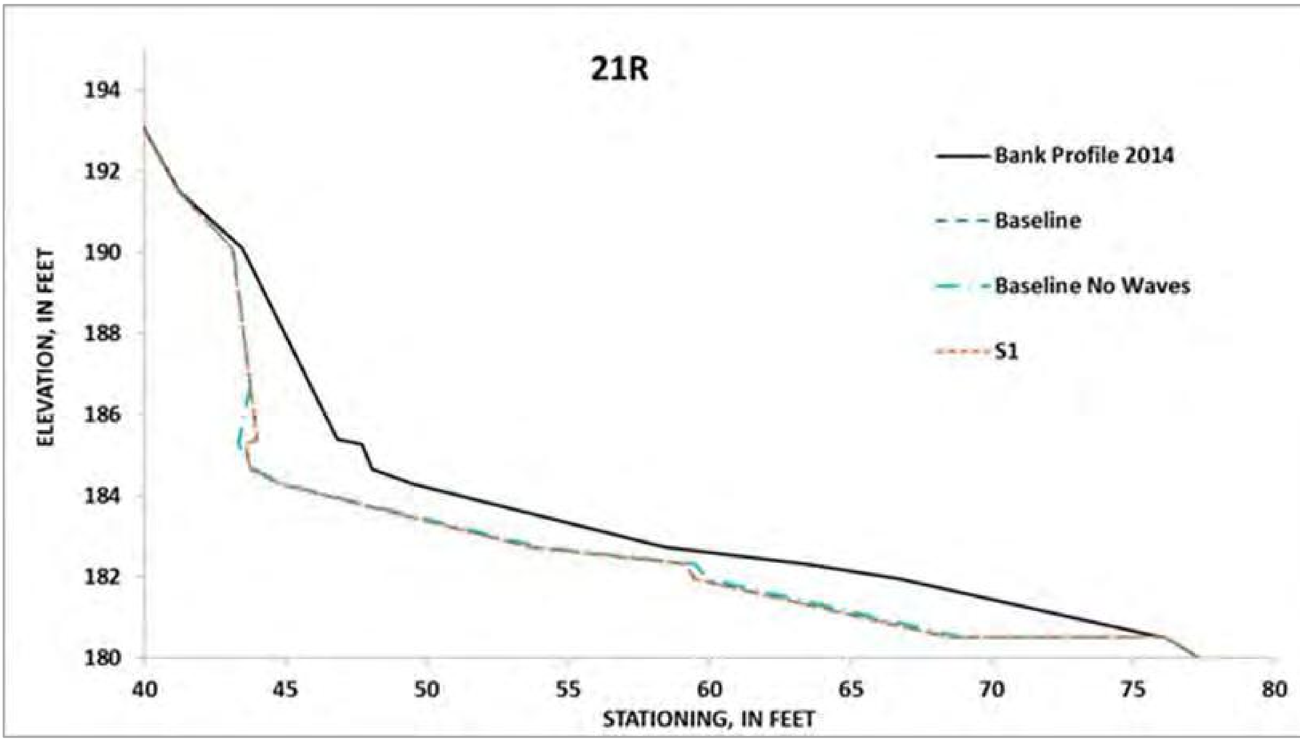

Figure 5.4.3.9-3: Simulated, future erosion for the Baseline Condition (with boat waves on and off) and Scenarios 1 at site 21Rfor the period 2000-2014. Zoomed in at area of erosion for illustrative purposes.

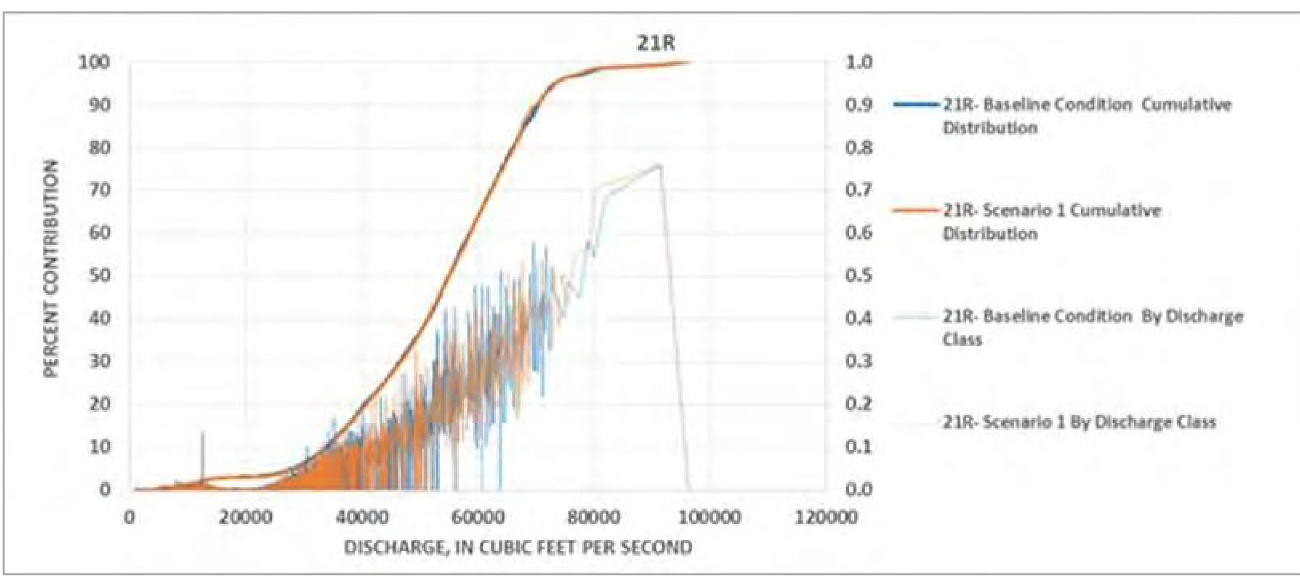

Figure 5.4.3.9-4: Simulated, percent contribution of total erosion by discharge for the Baseline Condition and Scenarios 1 at site 21R for the period 2000-2014

5.4.3.10 Site 4L

The river at site 4L, located at station 74,000 has a gradual bank face, sparsely vegetated banks, and is immediately upstream of the Pauchaug Boat Ramp. The bank is roughly 16 feet tall, with deposits of sandy-loam at the bank toe. The surface of the upper bank is also composed of sandy loam and the bank is vegetated predominantly with grasses and small shrubs, but contains a few American elm, Ashleaf and Silver maple trees (Figure 5.4.3.10-1).

BSTEM runs at this site show that under the Baseline Condition, 0.25 ft^3 of erosion occurred per foot of bank, during the 2000-2014 flow period, averaging 0.017 ft^3/ft/y (Table 5.4.3-1). This results in the 3rd lowest erosion rate for the Baseline Condition, placing it between the 5th and 10th percentiles of erosion rates along the reach. The modeling also indicates that all 100% (0.0173 ft^3/ft/y) of the erosion is due directly to hydraulic processes, and that none of the bank erosion is the result of geotechnical failures.

The Baseline Condition (Waves off) resulted in 0.0136 ft^3/ft/y, with 0.017 ft^3/ft/y for Scenario 1. This resulted in reduction in erosion rates of 21.4% and 0.6% for Baseline Wave off and Scenario 1 (Figure 5.4.3.10-2). Although erosion rates are quite low at this site as it is in a depositional environment, comparison of the "waves on" and "waves off" conditions under Baseline hydraulics shows that boat waves are a factor at this site. This is not surprising given its proximity to the boat ramp. Still, because of the generally low erosion rates, the remaining scenarios were not considered with boat waves off.

The erosion modeled at this site does not account for the depositional material that has been placed at the toe. The model does not recognize depositional material, and the slight erosion that is happening under the Baseline Condition, is happening at the toe. As material from the bank toe is being eroded, the river is re-depositing additional sediment to compensate. In general though, very little erosion is occurring at this site.

For the Baseline Condition, 95% of the total erosion occurs at flows of only 7,000 cfs or greater (Figure 5.4.9.10-3). This number is again misleading because of the material deposited since the original survey in 2000. However the greater percentage of erosion is occurring at those extreme high flows, and might indicate that material is being eroded during those high flow events, and re-deposited during more normal flow periods. Though the model output is indicating that some slight erosion is occurring within operation flows, the beach has been continually aggrading over the modeling period with increased roughness from establishing grasses at the bank toe.

Table 5.4.3.10-1 denotes the flows above which 95%, 50%, and 5% of all erosion occurs at the site as well as the amount of time those flows were exceeded for each year in the modeling period.

Table 5.4.3.10-1: Flow Exceedance Calculations for Site 4L

Site 4L	Percent of Erosion		
	95%	50%	5%
	Flow (cfs)		
Year	**95,042**	**83,527**	**6,991**
2000	NA	NA	52.90%
2001	NA	NA	35.00%
2002	NA	NA	51.60%
2003	NA	NA	60.60%
2004	NA	NA	59.90%
2005	NA	NA	67.40%
2006	NA	NA	80.80%
2007	NA	NA	61.90%
2008	NA	NA	80.10%
2009	NA	NA	76.70%
2010	NA	NA	67.40%
2011	0.20%	0.30%	73.00%
2012	NA	NA	53.20%
2013	NA	NA	62.40%
2014	NA	NA	63.40%

NA: Not Applicable since flows did not reach this value

Figure 5.4.3.10-1 Photos at site 4L

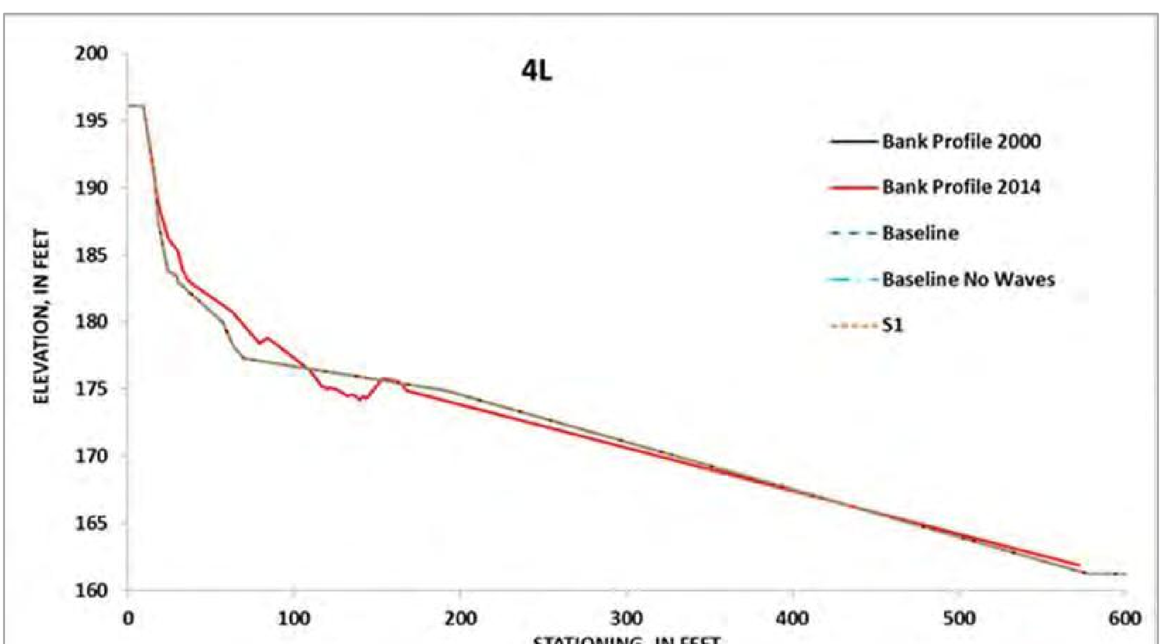

Figure 5.4.3.10-2: Simulated, future unit-erosion for the Baseline Condition (with boat waves on and off) and Scenarios 1 at site 4L for the period 2000-2014

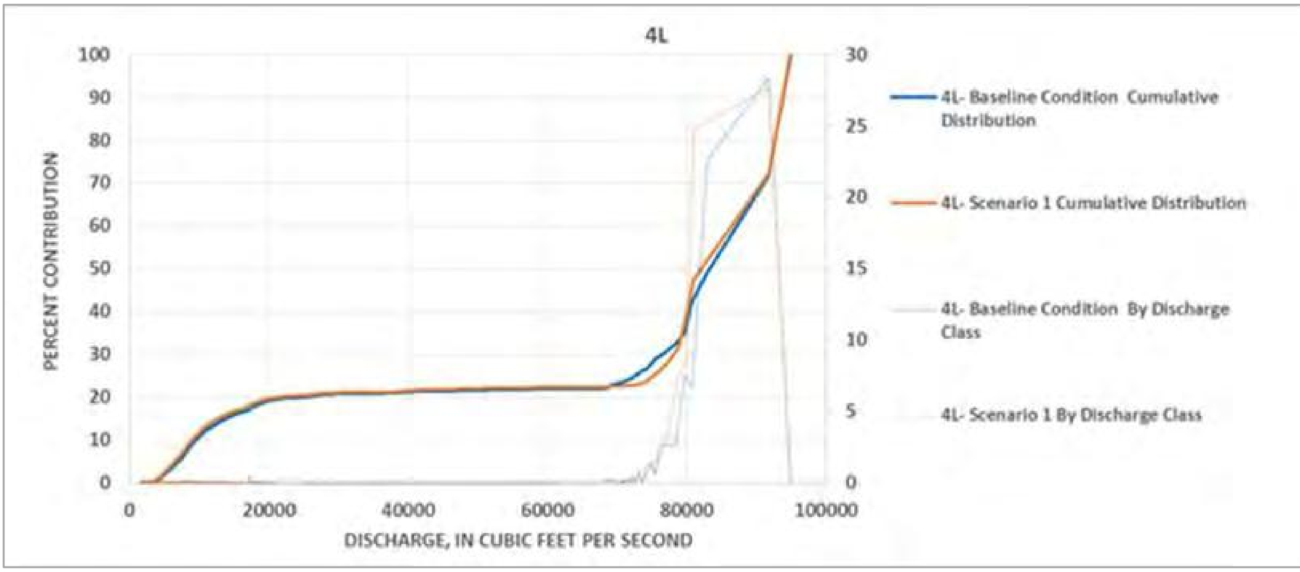

Figure 5.4.3.10-3: Simulated, percent contribution of total erosion by discharge for the Baseline Condition and Scenarios 1 at site 4L for the period 2000-2014

5.4.3.11 Site 29R

The river at site 29R (at station 66,000) has a steep bank face, sparsely vegetated banks, and is located between Mallory Brook and the Pauchaug Boat Ramp. The bank is roughly 26 feet tall, with a sandy loam toe and upper bank slope. The bank contains only patchy vegetation with Green ash and Silver maple trees. A significant amount of bare soil was noted on the bank face. No historical cross sections exist for this site, however this site was surveyed in 2014 and this was used as the initial geometry for the model runs (Figure 5.4.3.11-1).

BSTEM runs at this site show that under the Baseline Condition, 25.2 ft^3 of erosion occurred per foot of bank during the 2000-2014 flow period, averaging 1.72 ft^3/ft/y (Table 5.4.3-1). This results in the 14th highest erosion rate for the Baseline Condition, placing it between the 55th and 60th percentiles of erosion rates along the reach. The modeling also indicates that only 1% (about 0.009 ft^3/ft/y) of the erosion is due directly to hydraulic processes, whereas the other 99% (1.71 ft^3/ft/y) is the result of geotechnical processes and associated mass failures. Looking at the starting cross section, with the existing undercut, it becomes obvious that a large geotechnical failure is imminent (Figure 5.4.3.11-2). In fact, failure of the upper bank here represents the single, significant erosion event at this site that occurred early on in the simulation period.

The Baseline Condition (Waves off) resulted in 1.71 ft^3/ft/y, with 1.72 ft^3/ft/y for Scenario 1. As Baseline Condition (Waves off) scenario illustrated a very little reduction in erosion, it was concluded that boat waves are not having a significant impact on bank stability, and the remaining scenarios were not considered with boat waves off. Under all scenarios, the same soil block failed, indicating that this was likely to occur with minor additional undercutting under any flow scenario. For the Baseline Condition, 95% of the total erosion occurs at flows of 12,000 cfs or greater (Figure 5.4.3.11-3). This coincides with the previous analysis of the results, indicating that there is an imminent bank failure due at site 29R in the near future. Once this block fails, additional undercutting could further destabilize the upper part of the bank.

Table 5.4.3.11-1 denotes the flows above which 95%, 50%, and 5% of all erosion occurs at the site as well as the amount of time those flows were exceeded for each year in the modeling period.

Table 5.4.3.11-1: Flow Exceedance Calculations for Site 29R

Site 29R	Percent of Erosion		
	95%	50%	5%
	Flow (cfs)		
Year	**11,968**	**11,968**	**11,923**
2000	31.10%	31.10%	31.20%
2001	11.40%	11.40%	11.50%
2002	27.60%	27.60%	27.70%
2003	37.60%	37.60%	37.80%
2004	26.30%	26.30%	26.40%
2005	43.80%	43.80%	44.00%
2006	58.10%	58.10%	58.30%
2007	32.80%	32.80%	32.90%
2008	50.10%	50.10%	50.40%
2009	54.50%	54.50%	54.80%
2010	47.40%	47.40%	47.60%
2011	55.30%	55.30%	55.50%
2012	32.00%	32.00%	32.20%
2013	38.10%	38.10%	38.40%
2014	37.50%	37.50%	37.70%

NA: Not Applicable since flows did not reach this value

Figure 5.4.3.11-1 Photos at site 29R

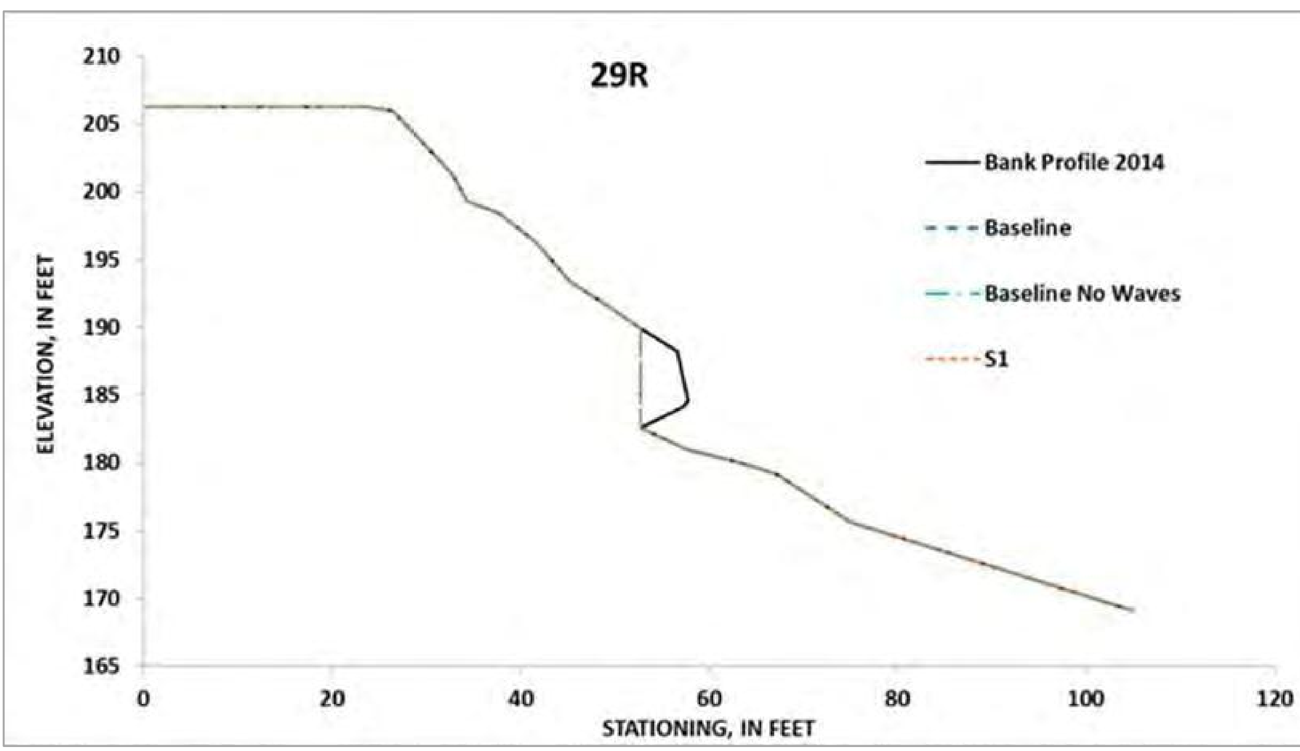

Figure 5.4.3.11-2: Simulated, future unit-erosion for the Baseline Condition (with boat waves on and off) and Scenarios 1 at site 29R for the period 2000-2014

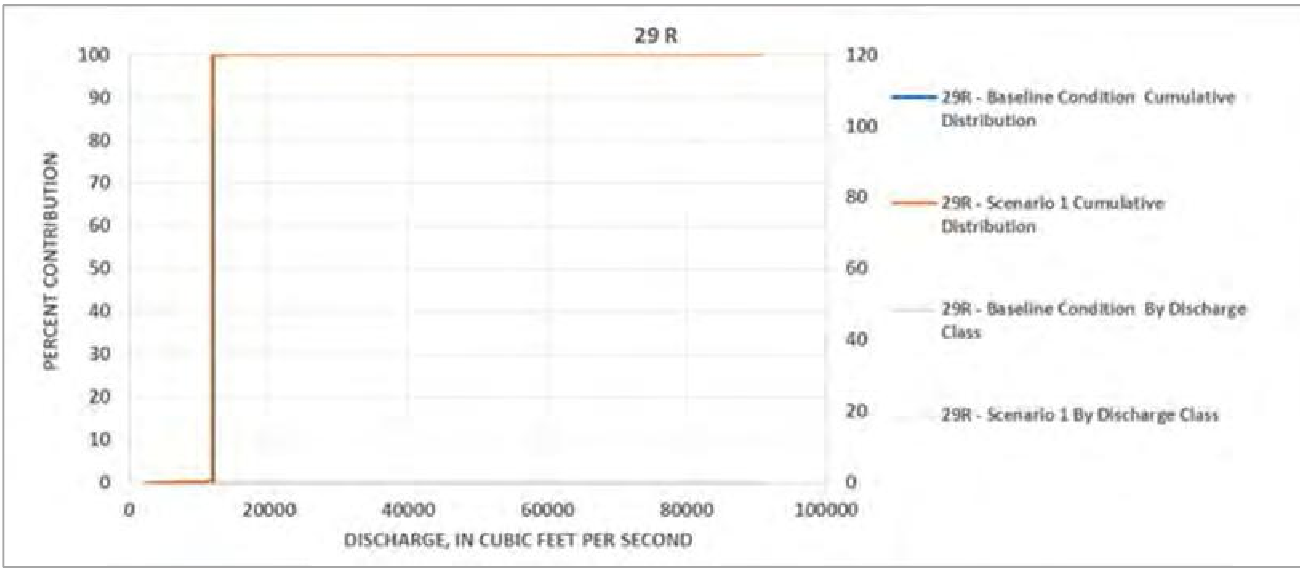

Figure 5.4.3.11-3: Simulated, percent contribution of total erosion by discharge for the Baseline Condition and Scenarios 1 at site 29R for the period 2000-2014

5.4.3.12 Site 5CR

The river at site 5CR (station 57,250) has a steep bank face, which is sparsely vegetated, and is located immediately downstream of the Route 10 Bridge. The bank is roughly 23 feet tall, with a loamy sand toe and bank, and the upper part of the bank consisting of a sandy loam. The bank is vegetated with small shrubs, American basswood, Green ash, and Red and Sugar maple trees. The first historic cross section for site 5CR was taken on 7/8/2002, and was, therefore, used as the initial geometry for modeling (Figure 5.4.3.12-1).

BSTEM runs at this site show that under the Baseline Condition, 105 ft^3 of erosion occurred per foot of bank, during the 2002-2014 flow period, averaging 8.61 ft^3/ft/y (Table 5.4.3-1). This results in the 2nd highest erosion rate for the Baseline Condition, placing it between the 95th and 99th percentiles of erosion rates along the reach. The modeling also indicates that roughly 35% (about 3.0 ft^3/ft/y) of the erosion is due directly to hydraulic processes, whereas the other 65% (5.6 ft^3/ft/y) is the result of geotechnical processes and associated mass failures.

The Baseline Condition (Waves off) resulted in 8.50 ft^3/ft/y, with 8.57 ft^3/ft/y for Scenario 1 (Figure 5.4.3.12-2 to Figure 5.4.3.12-3). This resulted in the following percent reductions in erosion rates: 1.23% and 0.46% for Baseline Wave off and Scenario 1 (Note- while this site did show a small reduction in erosion between the BL and S1 Scenarios the total reduction in erosion is well below the measureable/significant rate of 0.163 ft^3/ft/yr). Since waves accounted for only about 1% of the total erosion under the Baseline Condition the remaining scenarios were not considered with boat waves off.

For the Baseline Condition, 95% of the total erosion occurs at flows of about 48,000 cfs or greater (Figure 5.4.3.12-4). Although there is some limited hydraulic erosion at flows below 37,000 cfs, a significant geotechnical failure occurs at 48,000 cfs, with additional hydraulic erosion occurring through 76,000 cfs. At this flow, a large geotechnical failure occurs resulting in roughly 65% of the total erosion at site 5CR. Through this analysis we can conclude that those flows greater than the hydraulic capacity of Vernon and Northfield Mountain are accounting for most of the total erosion. Table 5.4.3.12-1 denotes the flows above which 95%, 50%, and 5% of all erosion occurs at the site as well as the amount of time those flows were exceeded for each year in the modeling period.

Table 5.4.3.12-1: Flow Exceedance Calculations for Site 5CR

Site 5 CR	Percent of Erosion		
	95%	50%	5%
	Flow (cfs)		
Year	76,391	76,391	47,867
2000	NA	NA	2.30%
2001	NA	NA	3.70%
2002	NA	NA	1.10%
2003	NA	NA	2.90%
2004	NA	NA	0.70%
2005	NA	NA	4.30%
2006	0.10%	0.10%	2.30%
2007	NA	NA	3.30%
2008	NA	NA	5.70%
2009	NA	NA	1.80%
2010	NA	NA	2.80%
2011	0.80%	0.80%	6.20%
2012	NA	NA	0.20%
2013	NA	NA	0.20%
2014	NA	NA	2.70%

NA: Not Applicable since flows did not reach this value

Figure 5.4.3.12-1 Photos at site 5CR

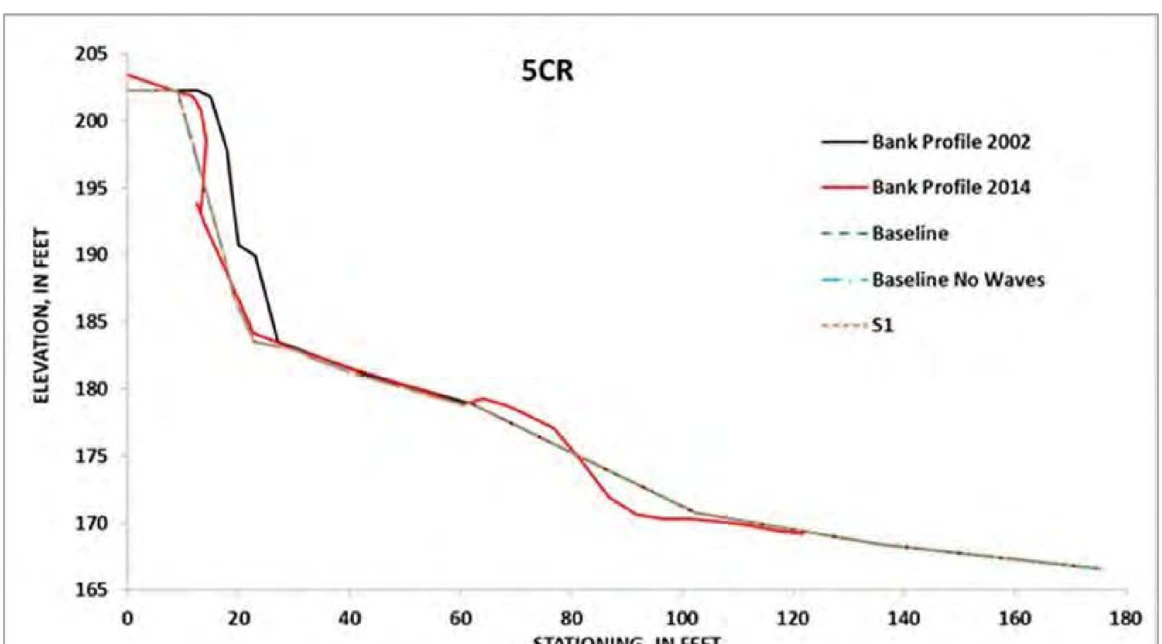

Figure 5.4.3.12-2: Simulated, future unit-erosion for the Baseline Condition (with boat waves on and off) and Scenarios 1 at site 5CR for the period 2002-2014

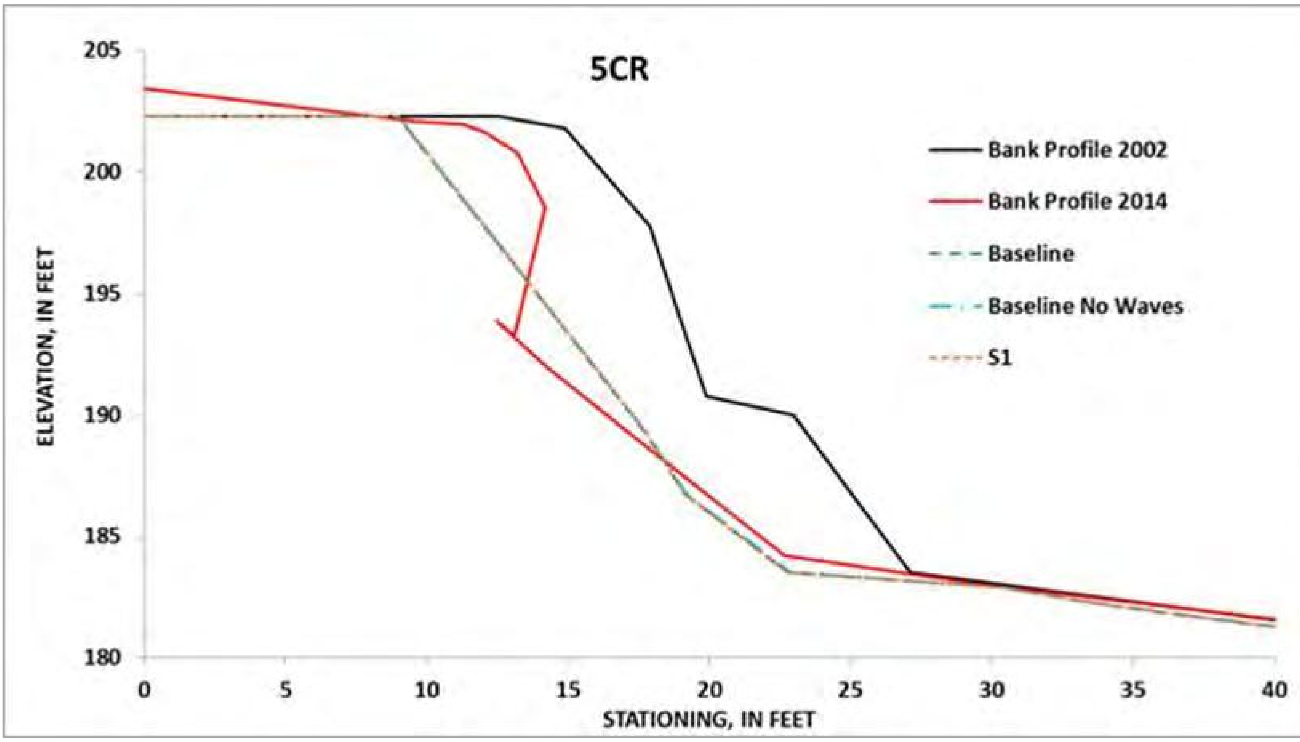

Figure 5.4.3.12-3: Simulated, future erosion for the Baseline Condition (with boat waves on and off) and Scenarios 1 at site 5CR for the period 2002-2014. Zoomed in at area of erosion for illustrative purposes

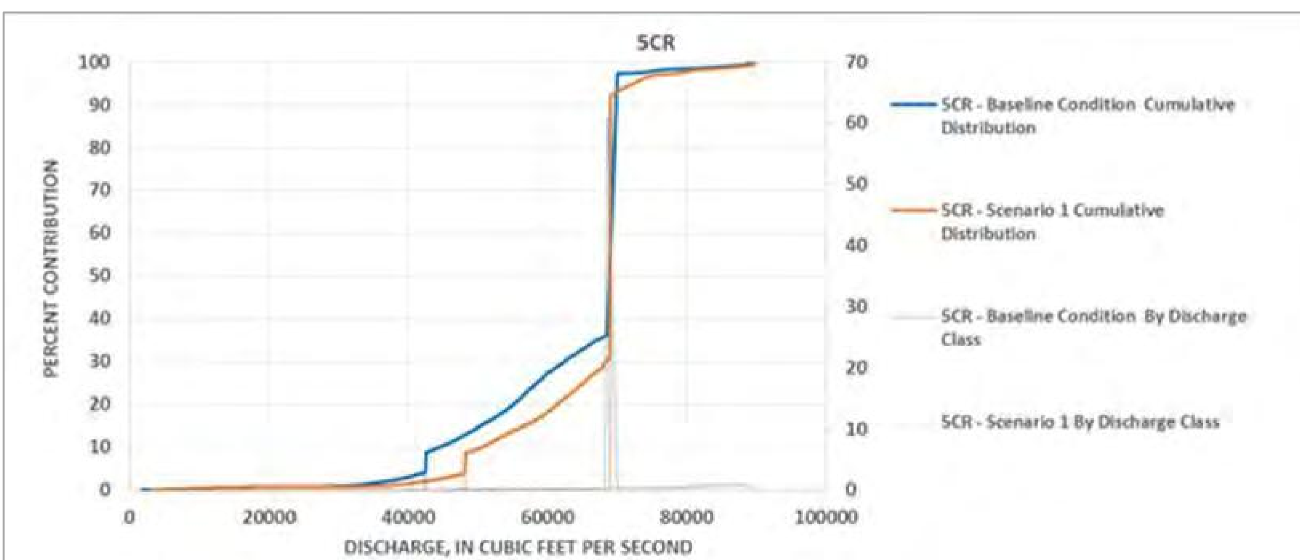

Figure 5.4.3.12-4: Simulated, percent contribution of total erosion by discharge for the Baseline Condition and Scenarios 1 - 3 at site 5CR for the period 2002-2014

5.4.3.13 Site 26R

The river at site 26R (station 50,000) has a steep bank face which is sparsely vegetated. The site is located between Kidds Island and the mouth of Bennett Brook. The bank is roughly 28 feet tall, with a loamy-sand toe and bank, and the upper portion of the bank consisting of a sandy loam. The bank is vegetated with Hickory, Northern red oak, Sugar and Red maples, and White birch trees. No historical cross sections exist for this site, requiring the 2014 survey to be used as the initial geometry for the model runs (Figure 5.4.3.13-1).

BSTEM runs at this site show that under the Baseline Condition, 17.5 ft^3 of erosion occurred per foot of bank, during the 2000-2014 flow period, averaging 1.194 ft^3/ft/y (Table 5.4.3-1). This results in the 16th highest erosion rate for the Baseline Condition, placing it between the 45th and 50th percentiles of erosion rates along the reach. The modeling also indicates that all 100% (1.19 ft^3/ft/y) of the erosion is due directly to hydraulic processes, and none of the bank erosion is the result of larger geotechnical failures.

The Baseline Condition (Waves off) resulted in 1.145 ft^3/ft/y, with 1.196 ft^3/ft/y for Scenario 1 (Figure 5.7.13-2 to Figure 5.7.13-3). This resulted in the following percent reductions in erosion rates: 4.1% and -0.123%, for Baseline Wave off and Scenario 1 respectively. These differences are relatively small indicting little difference in erosion rates across all operational scenarios. As Baseline Condition (Waves off) scenario illustrated a very little reduction in erosion, it was concluded that boat waves are not having a significant impact on bank stability, and the remaining scenarios were not considered with boat waves off.

For the Baseline Condition, 96% of the total erosion occurs at flows of about 37,000 cfs or greater (Figure 5.4.3.13-4). Though there is some limited hydraulic erosion at flows below 37,000 cfs, the erosion rate (albeit moderate) drastically increases at 43,000 cfs and is maintained through 70,000 cfs. Through this analysis we can conclude that those flows greater than the combined hydraulic capacity of Vernon and Northfield Mountain are accounting for most of the total erosion. Table 5.4.3.13-1 denotes the flows above which 95%, 50%, and 5% of all erosion occurs at the site as well as the amount of time those flows were exceeded for each year in the modeling period.

Table 5.4.3.13-1: Flow Exceedance Calculations for Site 26R

Site 26R	Percent of Erosion		
	95%	50%	5%
	Flow (cfs)		
Year	**80,503**	**60,282**	**43,294**
2000	NA	0.40%	3.20%
2001	NA	2.20%	4.00%
2002	NA	0.10%	1.70%
2003	NA	0.80%	4.50%
2004	NA	NA	1.00%
2005	NA	0.90%	6.10%
2006	NA	0.70%	4.00%
2007	NA	1.80%	3.80%
2008	NA	1.10%	7.70%
2009	NA	0.20%	2.80%
2010	NA	0.20%	3.80%
2011	0.40%	3.20%	7.50%
2012	NA	NA	0.30%
2013	NA	NA	0.60%
2014	NA	1.40%	3.20%

NA: Not Applicable since flows did not reach this value

Figure 5.4.3.13-1 Photos at site 26R

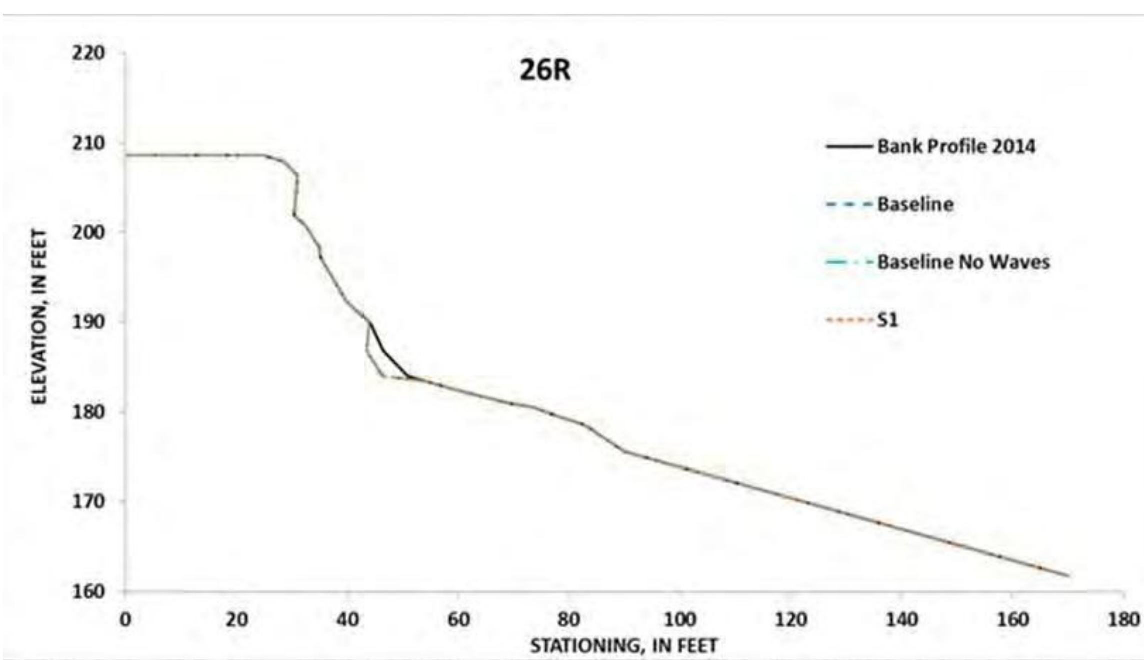

Figure 5.4.3.13-2: Simulated, future unit-erosion for the Baseline Condition (with boat waves on and off) and Scenarios 1 at site 26R for the period 2000-2014

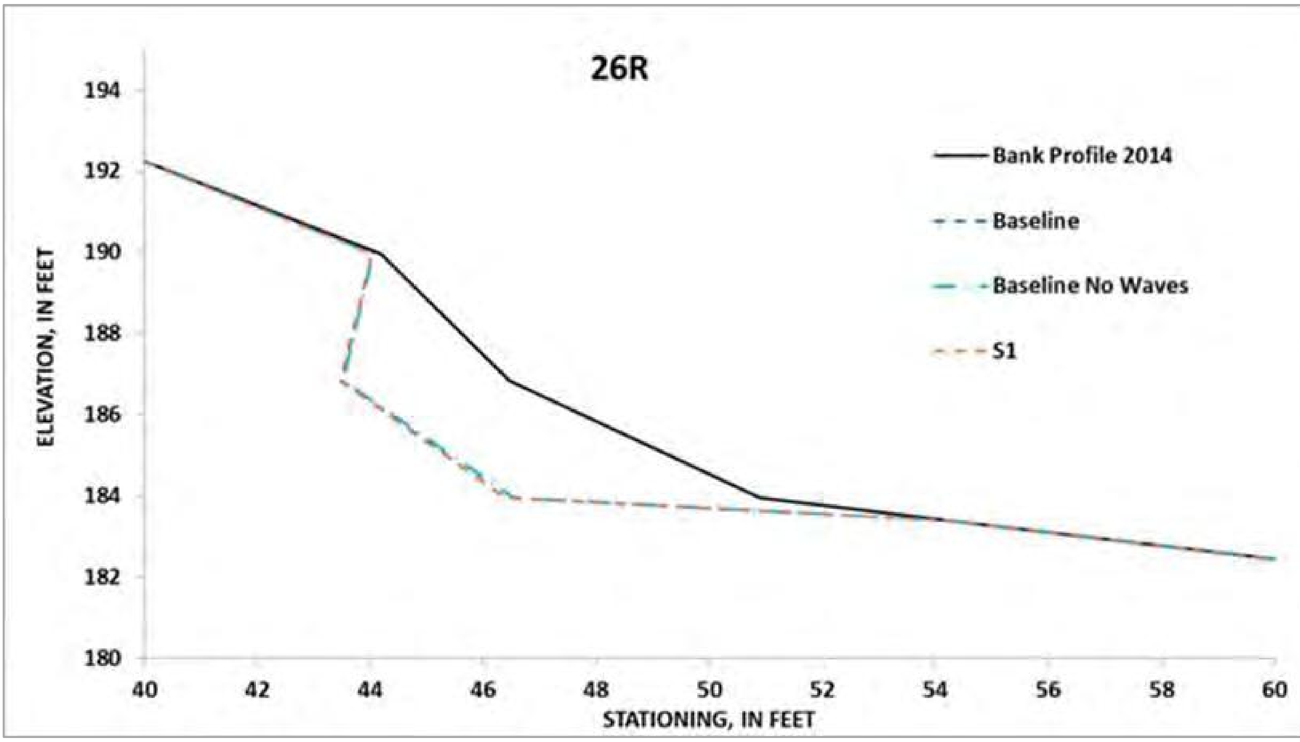

Figure 5.4.3.13-3: Simulated, future erosion for the Baseline Condition (with boat waves on and off) and Scenarios 1 at site 26Rfor the period 2000-2014. Zoomed in at area of erosion for illustrative purposes.

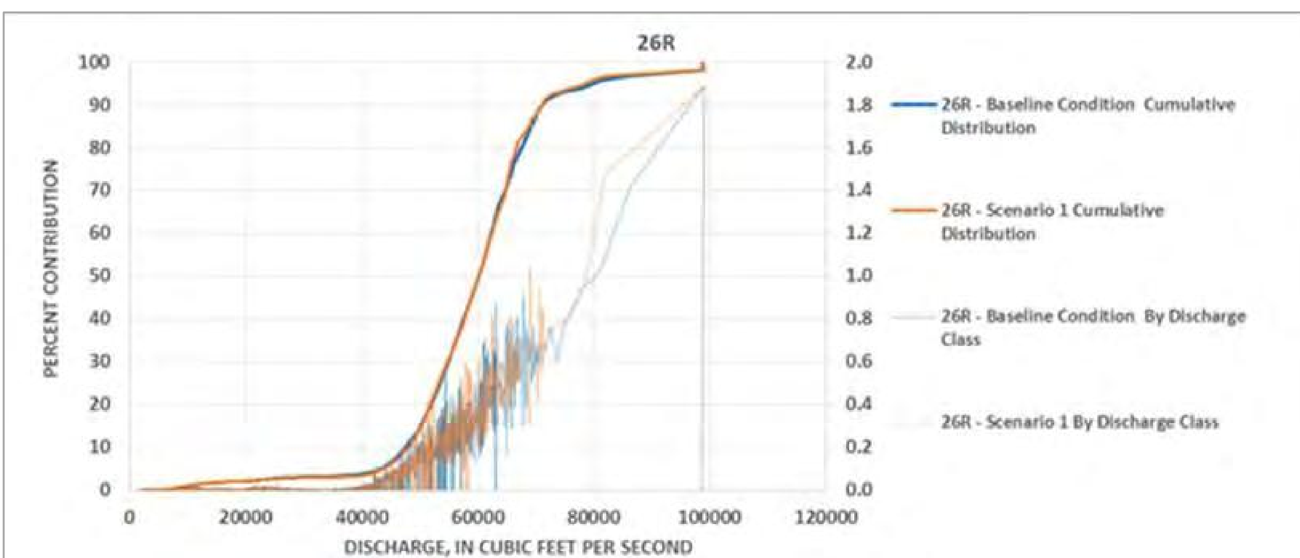

Figure 5.4.3.13-4: Simulated, percent contribution of total erosion by discharge for the Baseline Condition and Scenarios 1 at site 26R for the period 2000-2014

5.4.3.14 Site 10L

The river at site 10L has a gradual bank face, moderately vegetated banks and is located at station 49,000, roughly 6,000 ft upstream of Kidds Island. The bank is roughly 14 feet tall, with a deposited sandy-loam toe and a bank comprised of sand and sandy loam. The bank is vegetated mostly with grasses and shrubs, with large Green ash and Silver maple trees. Behind the upper bank lies a corn field (Figure 5.4.3.14-1).

BSTEM runs at this site show that under the Baseline Condition, 2.34 ft^3 of erosion occurred per foot of bank, during the 2002-2014 flow period, averaging 0.160 ft^3/ft/y (Table 5.4.3-1). This results in the 5th lowest erosion rate for the Baseline Condition, placing it between the 10th and 15th percentiles of erosion rates along the reach. The modeling also indicates that all 100% (0.160 ft^3/ft/y) of the erosion is due directly to hydraulic processes, and none of the bank erosion is the result of geotechnical failures.

The Baseline Condition (Waves off) resulted in 0.1583 ft^3/ft/y, with 0.1579 ft^3/ft/y for Scenario 1 (Figure 5.4.3.14-2 to Figure 5.4.3.14-3). This resulted in the following percent reductions in erosion rates: 0.87% and 1.10%, for Baseline Wave off and Scenario 1. As the Baseline Condition (Waves off) scenario illustrated a very little reduction in erosion, it was concluded that boat waves are not having a significant impact on bank stability, and the remaining scenarios were not considered with boat waves off.

Predicted erosion at this site does not account for the deposition of material at the bank toe (Figure 5.4.3.14-4). Since BSTEM is not a sediment-routing model and as such, it does not predict fluvial deposition. Still, the small amount of erosion that is simulated under the Baseline Condition, represents undercutting at the bank toe. As material from the toe is eroded, however, additional sediment is re-deposited. Thus, little net erosion occurs at this site. Differences in predicted erosion rates are minor given the low rates. For the Baseline Condition, 95% of the total erosion occurs at flows of 59,000 cfs or greater (Figure 5.4.3.14-5). Table 5.4.3.14-1 denotes the flows above which 95%, 50%, and 5% of all erosion occurs at the site as well as the amount of time those flows were exceeded for each year in the modeling period. Though there is some minor erosion within operational flow limits, this number is somewhat misleading because of the net deposition of material since the original survey in 2000 (Figure 5.4.3.14-2). The beach has been generally aggrading continually during the modeled period.

Table 5.4.3.14-1: Flow Exceedance Calculations for Site 10L

Site 10 L	Percent of Erosion		
	95%	50%	5%
	Flow (cfs)		
Year	**98,882**	**79,003**	**58,922**
2000	NA	NA	0.60%
2001	NA	NA	2.30%
2002	NA	NA	0.10%
2003	NA	NA	0.90%
2004	NA	NA	NA
2005	NA	NA	1.20%
2006	NA	NA	0.80%
2007	NA	NA	2.40%
2008	NA	NA	1.70%
2009	NA	NA	0.30%
2010	NA	NA	0.30%
2011	0.20%	0.50%	3.40%
2012	NA	NA	NA
2013	NA	NA	0.10%
2014	NA	NA	1.40%

NA: Not Applicable since flows did not reach this value

Figure 5.4.3.14-1 Photos at site 10L

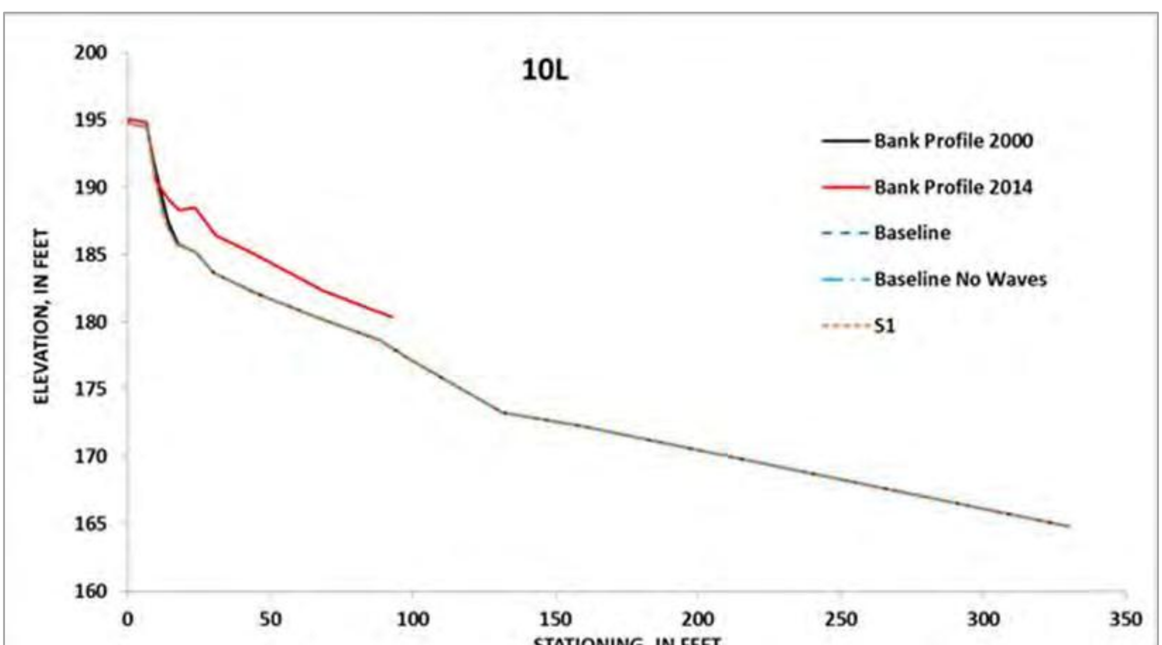

Figure 5.4.3.14-2: Simulated, future unit-erosion for the Baseline Condition (with boat waves on and off) and Scenarios 1 at site 10L for the period 2000-2014

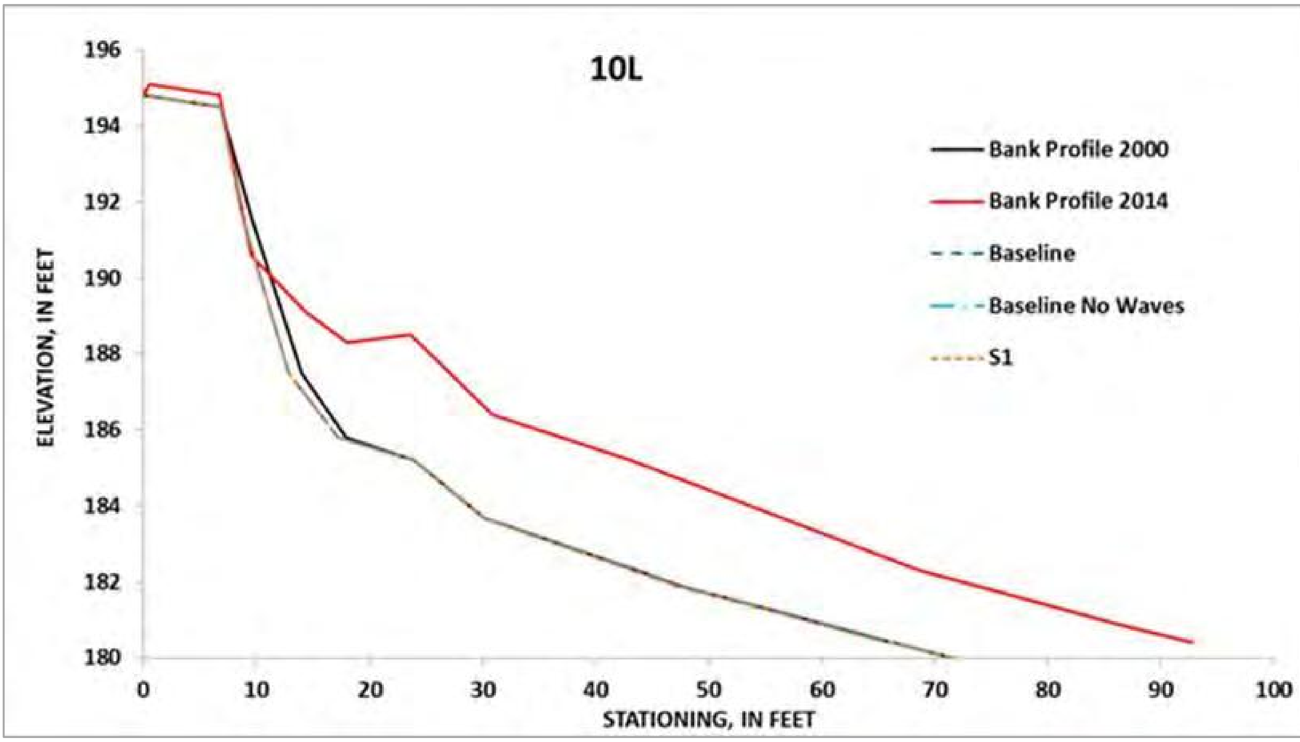

Figure 5.4.3.14-3: Simulated, future erosion for the Baseline Condition (with boat waves on and off) and Scenarios 1 at site 10Lfor the period 2000-2014. Zoomed in at area of erosion for illustrative purposes.

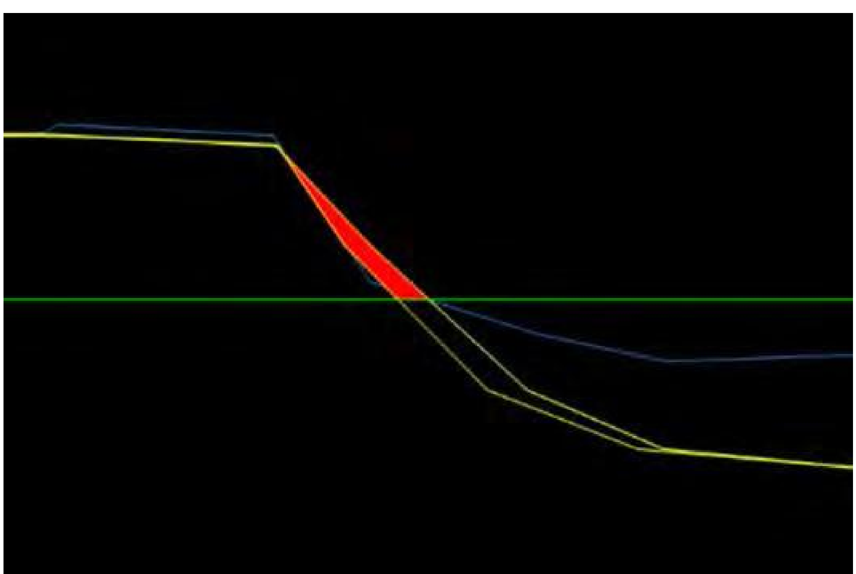

Figure 5.7.14-4 Calculated Erosion above Depositional Layer

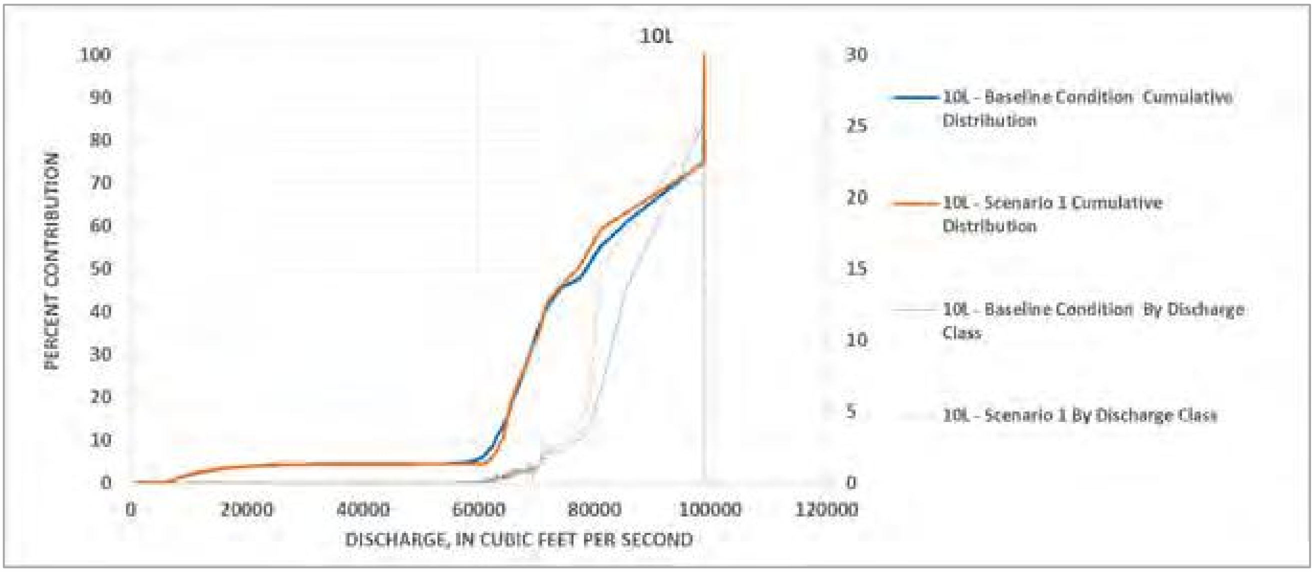

Figure 5.3.3.14-5: Simulated, percent contribution of total erosion by discharge for the Baseline Condition and Scenarios 1 at site 10L for the period 2000-2014

5.4.3.15 Site 10R

The river at site 10R has steep, heavily vegetated banks. The site is located at station 49,000, nearly 6,000 ft upstream of Kidds Island. The bank is roughly 31 feet tall, with a rock toe (d_{50}=59 mm) and a sandy-loam bank. The replanted bank is heavily vegetated with large shrubs, Northern red oak, and Eastern cottonwood. As 10R was restored in 2001, no Pre-Restoration simulation was conducted for this site (Figure 5.4.3.15-1).

BSTEM runs for the Post Restoration condition at this site show that under the Baseline Condition, 3.7E-03 ft^3 of erosion occurred per foot of bank, during the 2001 to 2014 flow period after restoration, averaging 2.8E-04 ft^3/ft/y (Table 5.4.3-1). This represents virtually no erosion and is the 2^{th} lowest erosion rate for the Baseline Condition. The modeling also indicates that all 100% (2.82E-04 ft^3/ft/y) of the erosion is due directly to hydraulic processes, and that there are no geotechnical failures.

The Baseline Condition (Waves off) resulted in 2.83E-04 ft^3/ft/y, with 3.96E-07 ft^3/ft/y for Scenario 1 (Figure 5.4.3.15-2). This resulted in reductions in erosion rates of -0.4% for Baseline Wave off and 99.9% for Scenario 1. Baseline simulations with waves off showed virtually no reduction in erosion, it was concluded that boat waves have little effect on erosion processes at this site. Because of this, all of the remaining scenarios were simulated with boat waves on.

Erosion values at this site are so low that comparisons of rates are meaningless. Fundamentally, there is no bank erosion at this site and the restoration works have been very successful. For the Baseline Condition, 95% of the total erosion occurs at flows of about 47,000 cfs or greater (Figure 5.4.3.15-3). Table 5.4.3.15-1 denotes the flows above which 95%, 50%, and 5% of all erosion occurs at the site as well as the amount of time those flows were exceeded for each year in the modeling period.

Table 5.4.3.15-1: Flow Exceedance Calculations for Site 10R

Site 10R	Percent of Erosion		
	95%	50%	5%
	Flow (cfs)		
Year	**49,015**	**48,156**	**46,944**
2000	2.10%	2.20%	2.40%
2001	3.70%	3.70%	3.80%
2002	1.10%	1.10%	1.10%
2003	2.60%	2.80%	3.20%
2004	0.60%	0.70%	0.80%
2005	4.00%	4.20%	4.70%
2006	2.20%	2.30%	2.60%
2007	3.20%	3.30%	3.50%
2008	5.20%	5.50%	5.90%
2009	1.60%	1.80%	2.00%
2010	2.40%	2.70%	2.90%
2011	5.80%	6.00%	6.50%
2012	0.20%	0.20%	0.20%
2013	0.10%	0.20%	0.30%
2014	2.70%	2.70%	2.80%

NA: Not Applicable since flows did not reach this value

Figure 5.4.3.15-1 Photos at site 10R Post Restoration

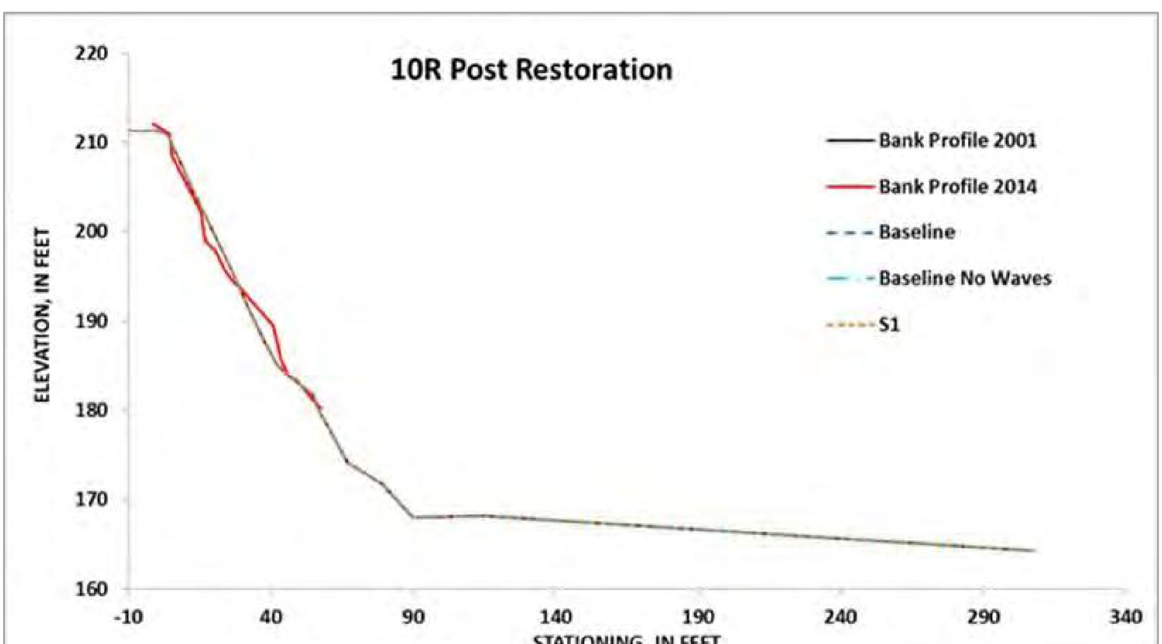

Figure 5.4.3.15-2: Simulated, future unit-erosion for the Baseline Condition (with boat waves on and off) and Scenarios 1 at site 10R for the period 2001-2014

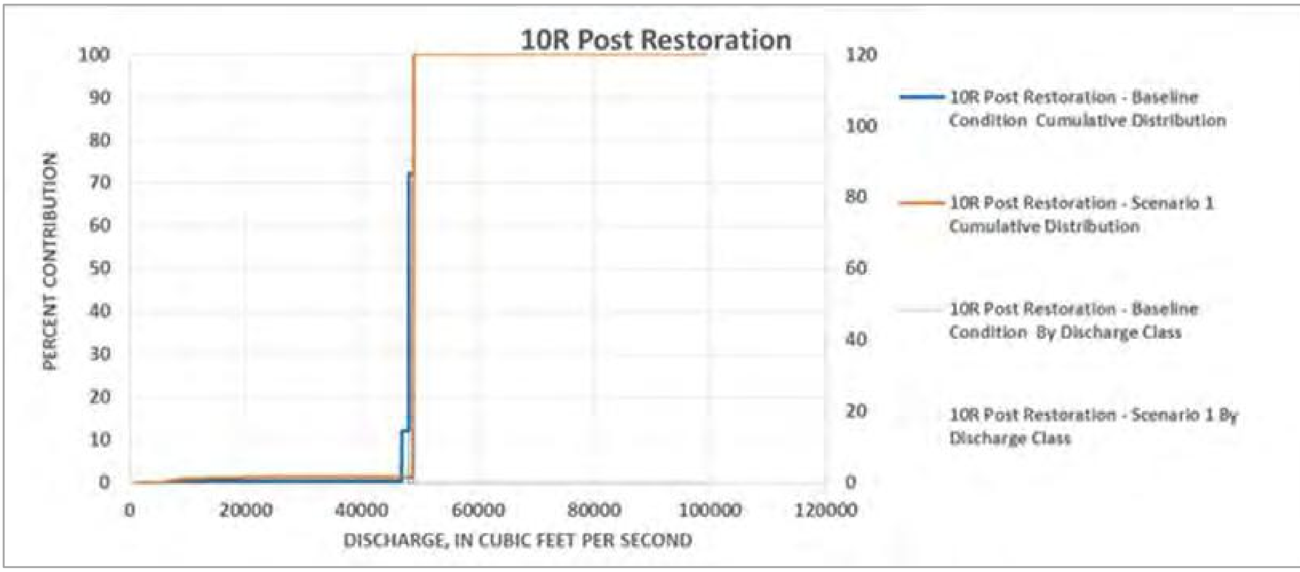

Figure 5.4.3.15-3: Simulated, percent contribution of total erosion by discharge for the Baseline Condition and Scenarios 1 at site 10R for the period 2001-2004

5.4.3.16 Site 6AL – Pre-Restoration

The river at site 6AL Pre-Restoration has steep, to overhanging banks with little vegetation. The site is located at station 41,750, roughly halfway up Kidds Island. The bank is about 37 feet tall, with a silty-sand bank and beach. Observations from 1998 indicate active and extensive erosion with exposed roots, overhanging bank, and leaning trees (Figure 5.4.3.16-1).

BSTEM runs at this site for the Pre-Restoration Condition show that under the Baseline Condition, 12.0 ft^3 of erosion occurred per foot of bank, during the 2000 to 2004 flow period prior to restoration, averaging 2.67 ft^3/ft/y (Table 5.4.3-1). This results in the 10^{th} highest erosion rate for the Baseline Condition, placing it between the 65^{th} and 70^{th} percentiles of erosion rates along the reach. The modeling also indicates that all 100% (2.67 ft^3/ft/y) of the erosion is due directly to hydraulic processes, and none of the bank erosion is the result of larger geotechnical failures.

The Baseline Condition (Waves off) resulted in 2.64 ft^3/ft/y, with 2.74 ft^3/ft/y for Scenario 1 (Figure 5.4.3.16-2 to Figure 5.4.3.16-3). This resulted in the following percent reductions in erosion rates: 1.2% and -2.57% for Baseline Wave off and Scenario 1 respectively. Baseline simulations with waves off showed virtually no reduction in erosion, it was concluded that boat waves have little effect on erosion processes at this site. Because of this, all of the remaining scenarios were simulated with boat waves on.

For the Baseline Condition, 95% of the total erosion occurs at flows of about 56,000 cfs or greater (Figure 5.4.3.16-4). Table 5.4.3.16-1 denotes the flows above which 95%, 50%, and 5% of all erosion occurs at the site as well as the amount of time those flows were exceeded for each year in the modeling period. The hydraulic erosion occurs across the range of flows above 56,000 cfs. Through this analysis we can conclude that those flows greater than the combined hydraulic capacity of Vernon and Northfield Mountain were accounting for most of the total erosion.

.Table 5.4.3.16-1: Flow Exceedance Calculations for Site 6L Pre-Restoration

Site 6AL	Percent of Erosion		
	95%	50%	5%
	Flow (cfs)		
Year	**65,167**	**63,310**	**62,287**
2000	0.10%	0.20%	0.30%
2001	1.60%	1.90%	1.90%
2002	0.10%	0.10%	0.10%
2003	0.20%	0.60%	0.60%
2004	NA	NA	NA
2005	0.70%	0.80%	0.80%
2006	0.30%	0.40%	0.50%
2007	0.50%	1.00%	1.30%
2008	0.50%	0.60%	0.70%
2009	NA	NA	0.10%
2010	NA	NA	0.10%
2011	2.20%	2.60%	3.00%
2012	NA	NA	NA
2013	NA	NA	NA
2014	0.80%	1.00%	1.10%

NA: Not Applicable since flows did not reach this value

Left bank, 1998

Figure 5.4.3.16-1 Photos at site 6AL Pre Restoration (Labeled as 1998 FRR/ECP-Site 6)

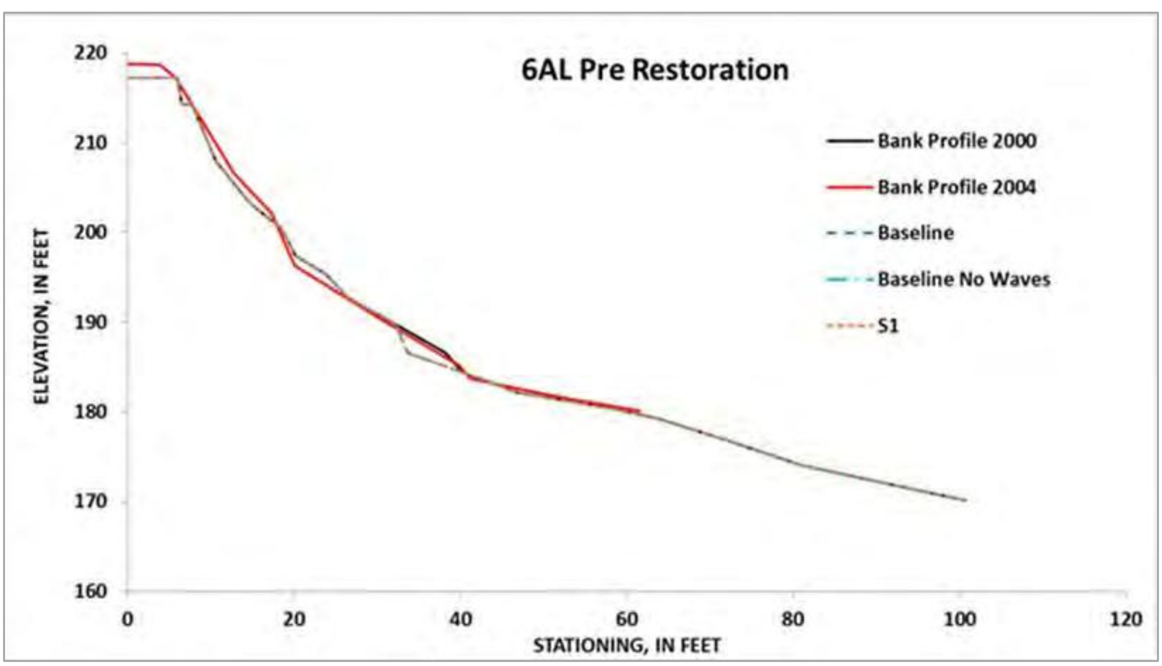

Figure 5.4.3.16-2: Simulated, future unit-erosion for the Baseline Condition (with boat waves on and off) and Scenarios 1 at site 6AL for the period 2000-2004

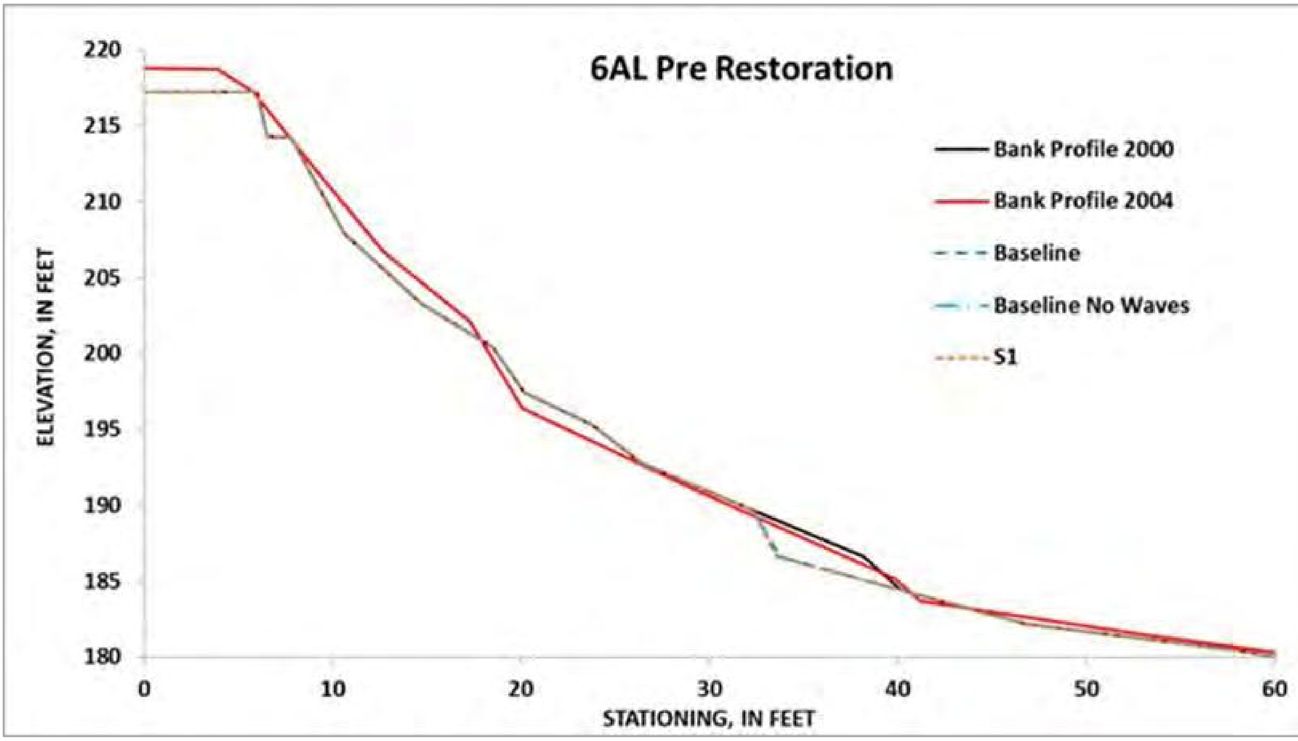

Figure 5.4.3.16-3: Simulated, future erosion for the Baseline Condition (with boat waves on and off) and Scenarios 1 at site 6AL for the period 2000-2004. Zoomed in at area of erosion for illustrative purposes.

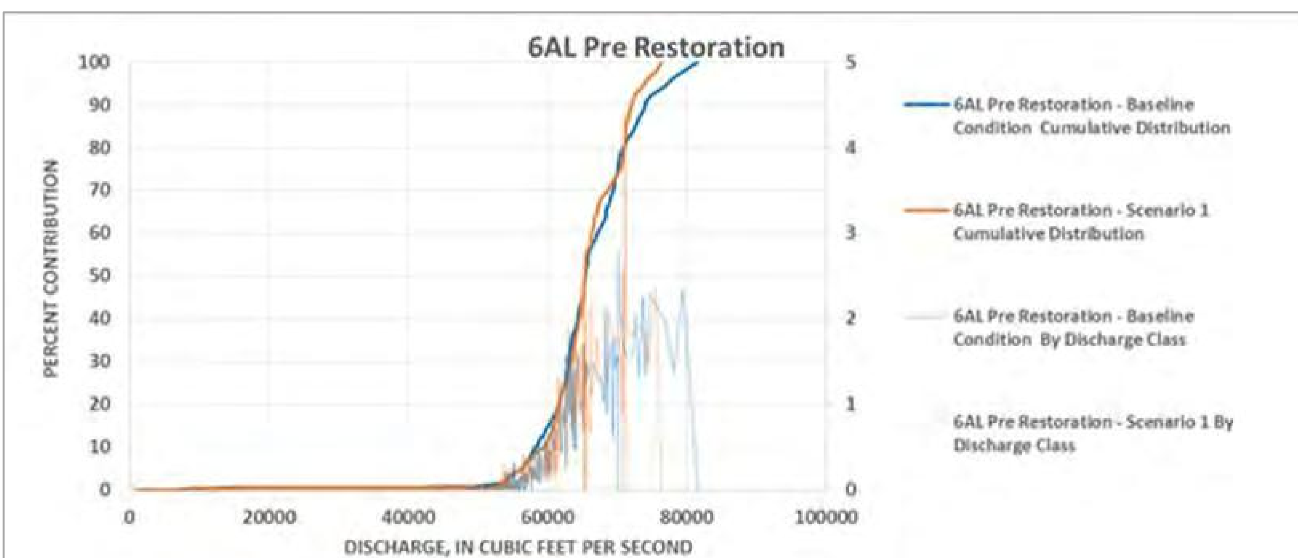

Figure 5.4.3.16-4: Simulated, percent contribution of total erosion by discharge for the Baseline Condition and Scenarios 1 at site 6AL for the period 2000-2004

5.4.3.17 Site 6AL – Post Restoration

The Post Restoration condition at site 6AL is characterized by steep, heavily vegetated banks. The bank is roughly 37 feet tall, with a rock toe (d_{50}=55 mm) and a silt loam bank. The replanted bank is heavily vegetated with large shrubs, Northern red oak, and Sugar maple (Figure 5.4.3.17-1).

BSTEM runs at this site show that the restoration activities have been highly successful with erosion rates under the Baseline Condition of 5.5E-05 ft^3 per foot of bank, during the 2004 to 2014 flow period, averaging 5.45E-06 ft^3/ft/y (Table 5.4.3-1). This results in the lowest erosion rate for the Baseline Condition. The modeling also indicates that all 100% (5.45E-06 ft^3/ft/y) of the erosion is due directly to hydraulic processes, and there are no geotechnical failures.

The Baseline Condition (Waves off) resulted in 0.00E+00 ft^3/ft/y, with 4.42E-06 ft^3/ft/y for Scenario 1 (Figure 5.4.3.17-2). Baseline simulations with waves off showed virtually no reduction in erosion, it was concluded that boat waves have little effect on erosion processes at this site. Because of this, all of the remaining scenarios were simulated with boat waves on.

For the Baseline Condition, 95% of the total erosion occurs at flows of about 62,000 cfs or greater (Figure 5.4.3.17-3). The minimal hydraulic erosion that did occur was between 62,000 cfs and 66,000 cfs. Table 5.4.3.17-1 denotes the flows above which 95%, 50%, and 5% of all erosion occurs at the site as well as the amount of time those flows were exceeded for each year in the modeling period. In summary, there is virtually no erosion at this site.

Table 5.4.3.17-1: Flow Exceedance Calculations for Site 6AL Post Restoration

Site 6AL	Percent of Erosion		
	95%	50%	5%
	Flow (cfs)		
Year	65,167	63,310	62,287
2000	0.10%	0.20%	0.30%
2001	1.60%	1.90%	1.90%
2002	0.10%	0.10%	0.10%
2003	0.20%	0.60%	0.60%
2004	NA	NA	NA
2005	0.70%	0.80%	0.80%
2006	0.30%	0.40%	0.50%
2007	0.50%	1.00%	1.30%
2008	0.50%	0.60%	0.70%
2009	NA	NA	0.10%
2010	NA	NA	0.10%
2011	2.20%	2.60%	3.00%
2012	NA	NA	NA
2013	NA	NA	NA
2014	0.80%	1.00%	1.10%

NA: Not Applicable since flows did not reach this value

Figure 5.4.3.17-1 Photos at site 6AL Post Restoration

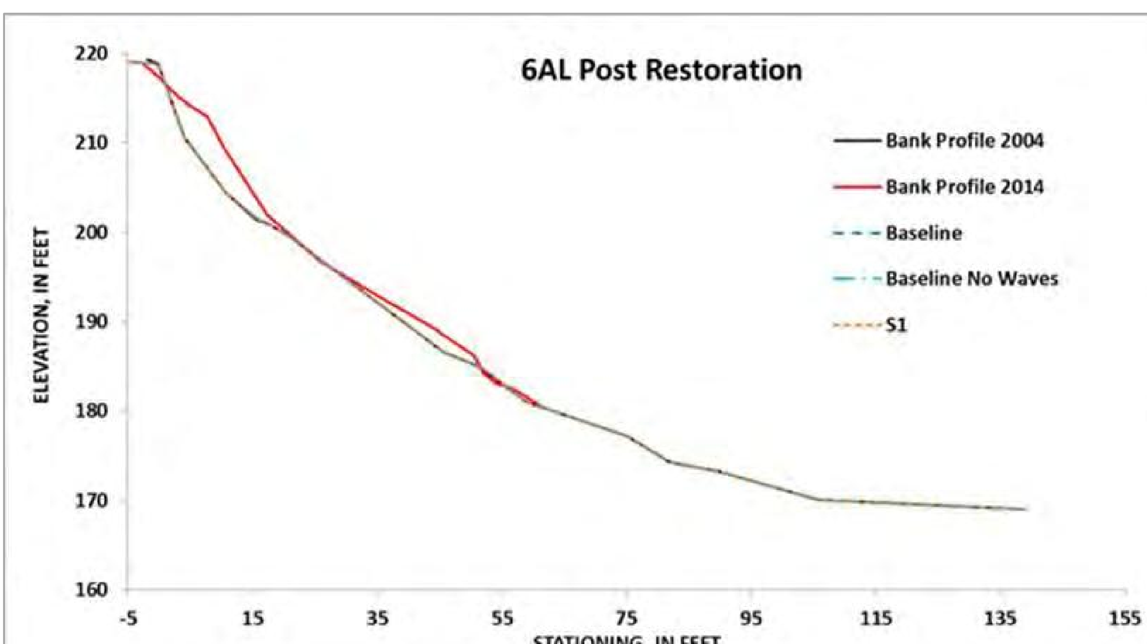

Figure 5.4.3.17-2: Simulated, future unit-erosion for the Baseline Condition (with boat waves on and off) and Scenarios 1 at site 6AL for the period 2004-2014

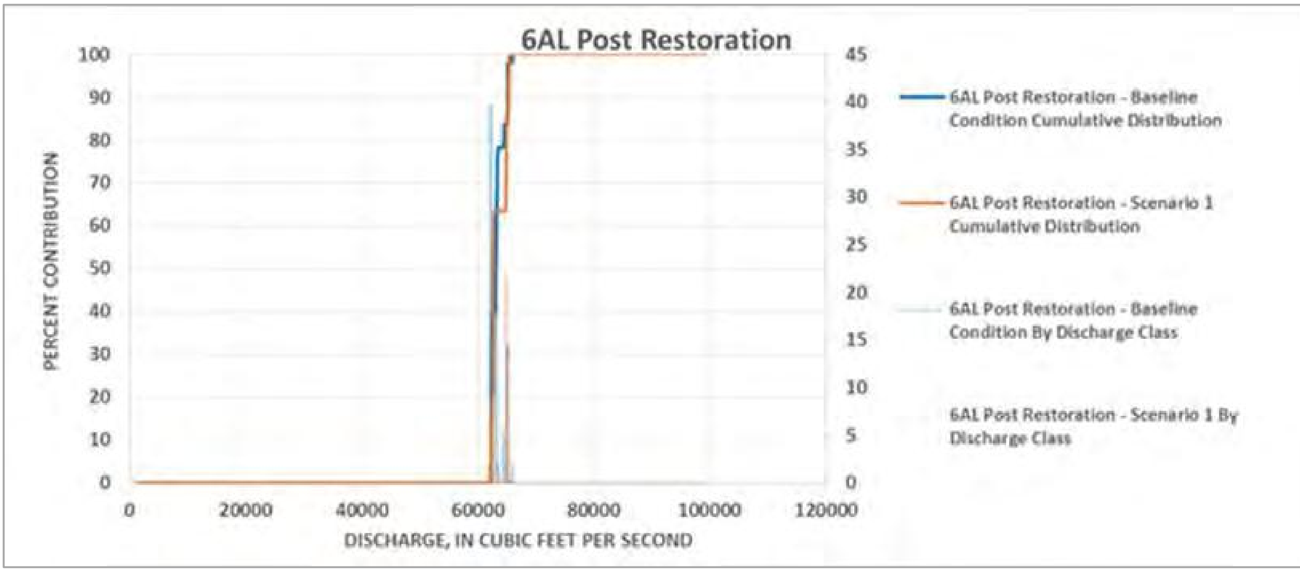

Figure 5.4.3.17-3: Simulated, percent contribution of total erosion by discharge for the Baseline Condition and Scenarios 1 at site 6AL for the period 2004-2014

5.4.3.18 Site 6AR

The river at site 6AR is across the channel from 6AL at station 41,750. The silt-loam bank is about 25 feet tall, and is characterized by steep, heavily vegetated banks and a rock toe (d_{50}=55 mm) that was part of the restoration works undertaken in 2000. The replanted bank is heavily vegetated with large shrubs, Northern red oak, and Sugar maple. As 6AR was restored in 2000, no Pre-Restoration simulation was conducted for this site (Figure 5.4.3.18-1).

BSTEM runs for the Post Restoration Condition at this site show that under the Baseline Condition, 0.295 ft^3 of erosion occurred per foot of bank, during the 2000 to 2014 flow period after restoration, averaging 0.0209 ft^3/ft/y (Table 5.4.3-1). This results in the 4th lowest erosion rate for the Baseline Condition, placing it between the 10th and 15th percentiles of erosion rates along the reach. The modeling also indicates that all 100% (0.021 ft^3/ft/y) of the erosion is due directly to hydraulic processes, and none of the bank erosion is the result of larger, geotechnical failures.

The Baseline Condition (Waves off) resulted in 0.000201 ft^3/ft/y, with 0.0204 ft^3/ft/y for Scenario 1 (Figure 5.4.3.18-2). This resulted in a reduction in erosion of 2.0% for Scenario 1. Baseline simulations with waves off showed a large % reduction in erosion but overall the amount of erosion at 6AR is so small that it was concluded that boat waves have little effect on erosion processes at this site. Because of this, all of the remaining scenarios were simulated with boat waves on.

Although the vast majority of the simulated bank erosion occurs at flows within the combined operational range of Vernon Dam and Northfield Mountain, with 95% of the total erosion for the Baseline Condition occurring at flows of 7,000 cfs or greater (Figure 5.4.3.18-3), this does not indicate that Project operations are causing significant bank erosion. Erosion rates here are very low and represent hydraulic scour of deposited material at the bank toe. Observations indicate that there is a net deposition of material here from fluvial deposition. Table 5.4.3.18-1 denotes the flows above which 95%, 50%, and 5% of all erosion occurs at the site as well as the amount of time those flows were exceeded for each year in the modeling period.

Table 5.4.3.18-1: Flow Exceedance Calculations for Site 6AR

Site 6AR	Percent of Erosion		
	95%	50%	5%
	Flow (cfs)		
Year	29,662	11,191	7,051
2000	8.80%	33.40%	52.70%
2001	7.10%	12.50%	34.70%
2002	5.70%	29.60%	51.00%
2003	10.40%	39.90%	60.30%
2004	4.40%	28.00%	59.40%
2005	14.50%	45.90%	66.40%
2006	13.60%	62.40%	80.30%
2007	7.30%	34.70%	60.70%
2008	15.50%	53.80%	79.80%
2009	6.30%	58.70%	76.50%
2010	10.00%	50.90%	67.30%
2011	18.60%	58.80%	72.70%
2012	2.60%	35.70%	53.00%
2013	5.50%	40.90%	62.00%
2014	9.40%	42.10%	63.10%

NA: Not Applicable since flows did not reach this value

Figure 5.4.3.18-1 Photos at site 6AR Post Restoration

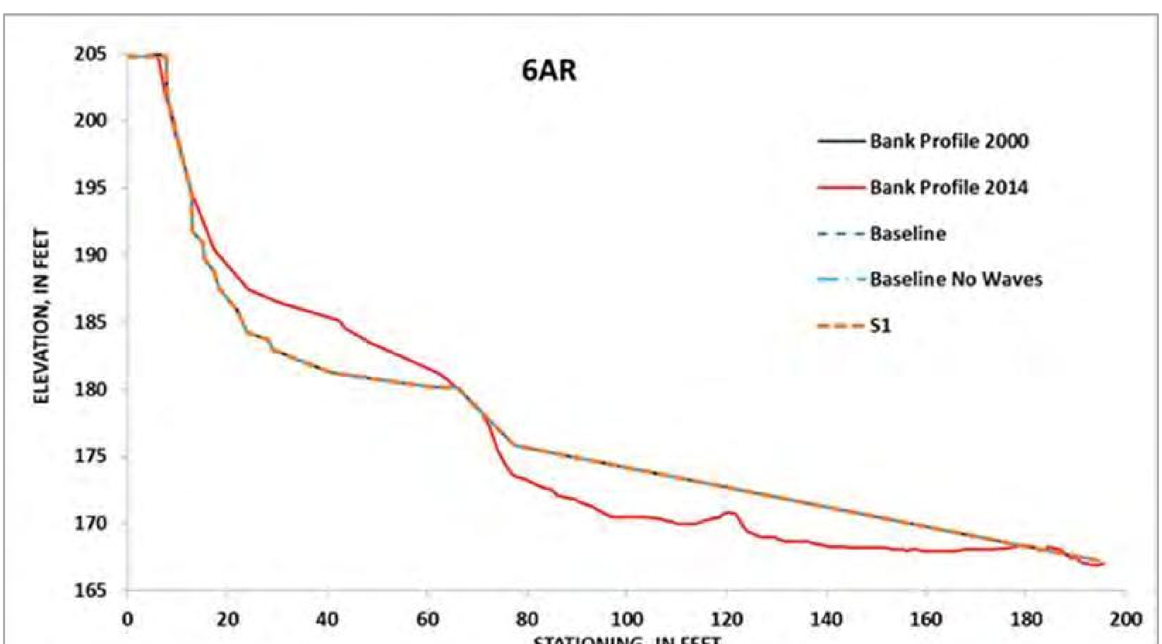

Figure 5.4.3.18-2: Simulated, future unit-erosion for the Baseline Condition (with boat waves on and off) and Scenarios 1 at site 6AR for the period 2000-2014

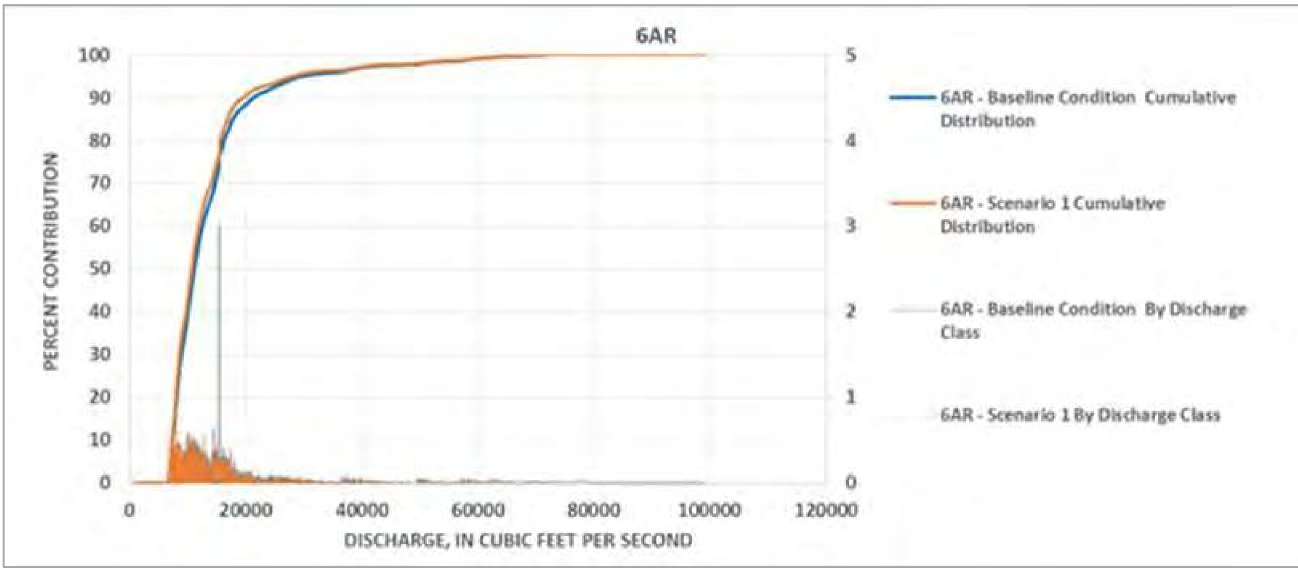

Figure 5.4.3.18-3: Simulated, percent contribution of total erosion by discharge for the Baseline Condition and Scenarios 1 at site 6AR for the period 2000-2014

5.4.3.19 Site 119BL

The river at site 119BL (station 41,000) has steep, partially vegetated banks, located near the downstream limit of Kidds Island. The bank is just under 30 feet tall, with silty-sand toe material with a d_{50} of 0.068 mm. Large Ashleaf maples spread out over most of the upper bank, with short grasses under the canopy. The lower bank, though highly vegetated, shows signs of erosion, with exposed roots, and soft saturated soils. No historical cross sections exist for this site. As a result, the 2014 survey was used as the initial geometry for the model runs (Figure 5.4.3.19-1).

BSTEM runs at this site show that under the Baseline Condition 86.1 ft^3 of erosion occurred per feet of bank, during the 2000 to 2014 flow period modeled, averaging 5.88 ft^3/ft/y (Table 5.4.3-1). This results in the 5th highest erosion amongst the model sites, placing it between the 85th and 90th percentiles of erosion rates along the reach. The modeling also indicates that roughly 73% (4.26 ft^3/ft/y) of erosion is due to hydraulic processes, whereas the other 27% (1.62 ft^3/ft/y) is due to geotechnical processes and mass failures. This is also shown in the Percent Contribution of Total Erosion by Discharge plot for Site 119BL (Figure 5.4.3.19-4), as the graph has a very gradual smooth shape, with few large spikes indicating mass wasting.

The Baseline Condition (Waves off) resulted in 5.72 ft^3/ft/y, with 5.79 ft^3/ft/y for Scenario 1 (Figure 5.4.3.19-2 and Figure 5.4.3.19-3). This resulted in the following percent reduction in erosion rates as compared to the Baseline Condition: 2.61% and 1.47%, for Baseline Wave off and Scenario 1. As the Baseline Condition (Waves off) scenario illustrated a very little reduction in erosion, it was concluded that boat waves are not having a significant impact on bank stability, and the remaining scenarios were not considered with boat waves off.

During the Baseline Condition, 83% of the total erosion occurs at flows of 37,000 cfs or greater (Figure 5.4.3.19-4). The plot shows erosion throughout the range of flows above 37,000 cfs, greater than the combined hydraulic capacity of Vernon and Northfield Mountain. This supports the conclusion that naturally occurring high flows are the biggest factor in bank erosion at Site 119BL. The resulting bank geometry is such that a 4-foot vertical face is developed that could continue to retreat, leading to collapse of the upper part of the bank in the future (Figure 5.4.3.19-2 and Figure 5.4.3.19-3). Moderate flows (17,000 – 37,000 cfs) contribute 13.1% of erosion. Evaluating the moderate flow contribution to the total erosion it was determined that Northfield Mountain operations occurred 7% of the time over the modeled period of record. This equates to 0.9% of the total erosion during the moderate flows. The Northfield Mountain contribution was adjusted by this 0.9% to better estimate contributions from the Project and resulting in a total erosion of 2.4%.

Table 5.4.3.19-1 denotes the flows above which 95%, 50%, and 5% of all erosion occurs at the site as well as the amount of time those flows were exceeded for each year in the modeling period.

Table 5.4.3.19-1: Flow Exceedance Calculations for Site 119BL

Site 119BL	Percent of Erosion		
	95%	50%	5%
	Flow (cfs)		
Year	**70,557**	**53,969**	**24,796**
2000	0.10%	1.30%	14.10%
2001	0.90%	2.90%	7.80%
2002	NA	0.60%	10.00%
2003	0.10%	1.90%	16.60%
2004	NA	0.30%	7.70%
2005	0.50%	2.40%	20.70%
2006	0.20%	1.40%	19.20%
2007	0.20%	2.70%	12.80%
2008	0.30%	3.60%	22.80%
2009	NA	1.10%	14.70%
2010	NA	1.20%	15.00%
2011	1.10%	4.70%	24.10%
2012	NA	NA	7.20%
2013	NA	0.10%	11.40%
2014	0.20%	2.20%	14.80%

NA: Not Applicable since flows did not reach this value

Figure 5.4.3.19-1 Photos at site 119BL

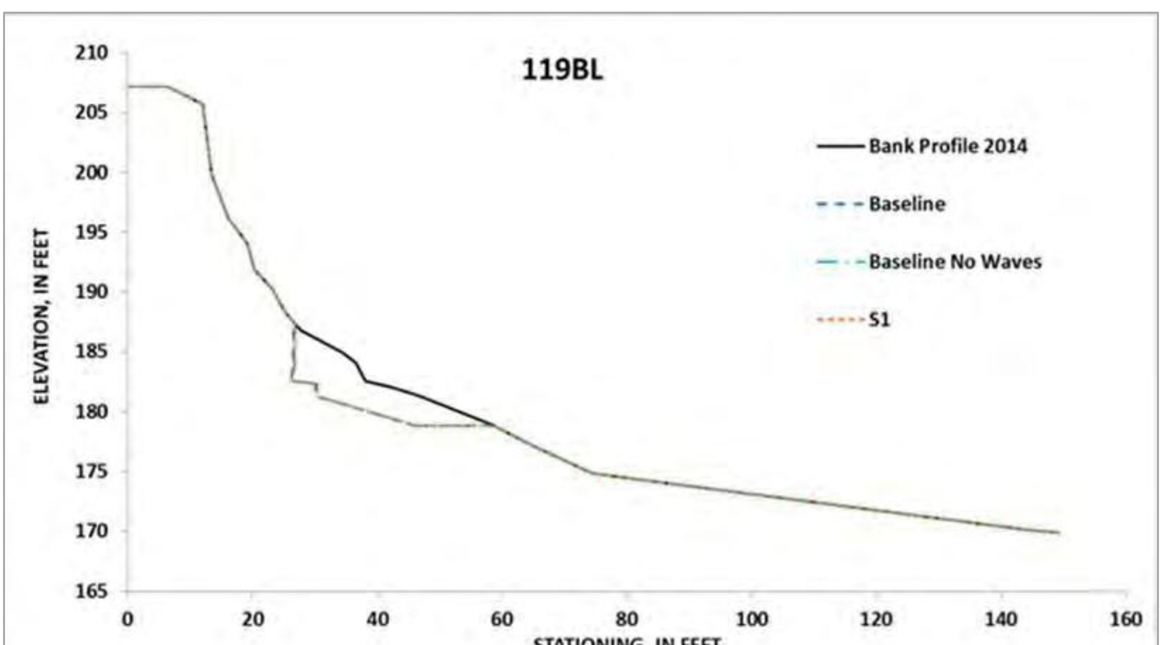

Figure 5.4.3.19-2: Simulated, future unit-erosion The Baseline Condition and Scenario 1(both with boat waves on and boat waves off) at site 119BL for the period 2000-2014

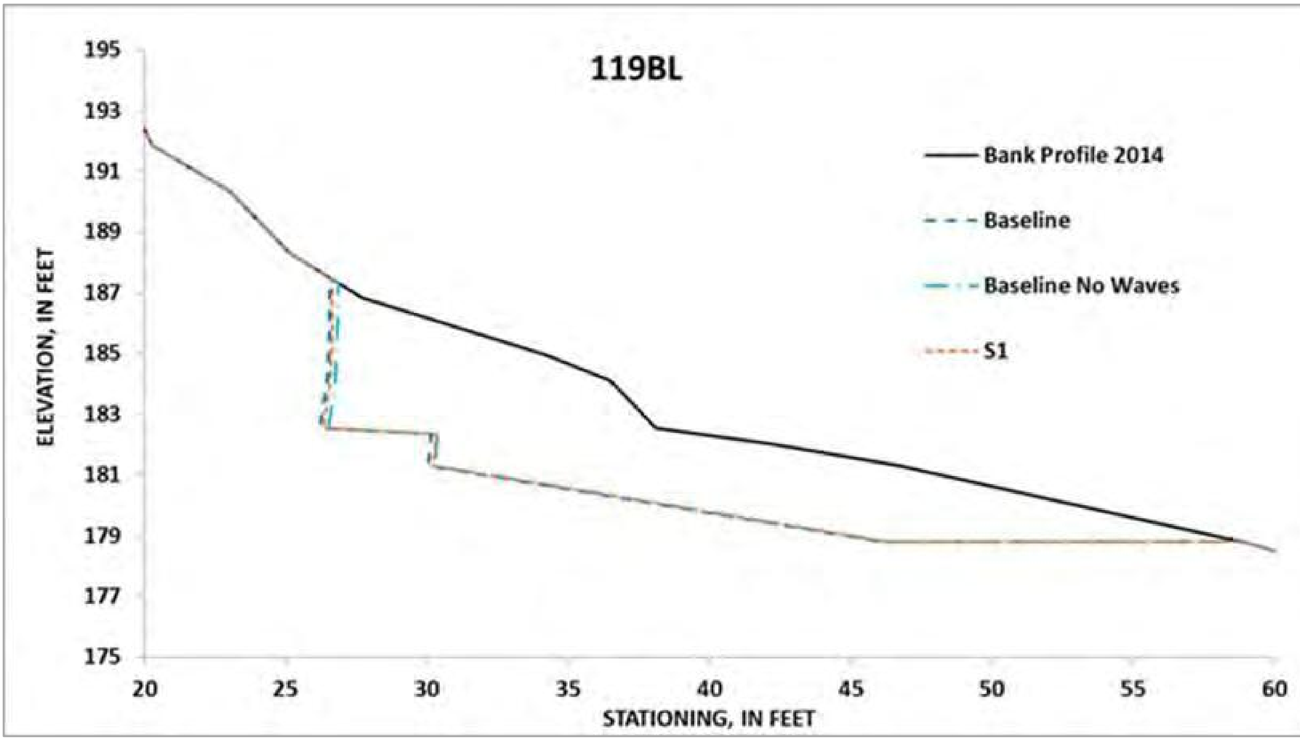

Figure 5.4.3.19-3: Simulated, future unit-erosion The Baseline Condition and Scenario 1 (both with boat waves on and boat waves off) at site 119BL for the period 2000-2014. Zoomed in at area of erosion for illustrative purposes

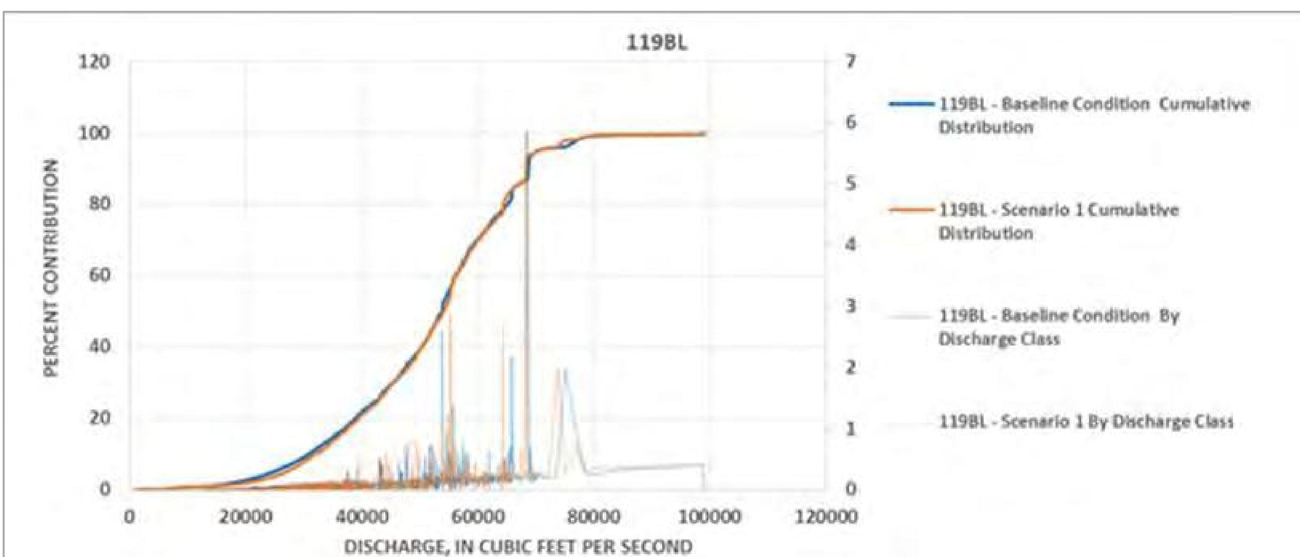

Figure 5.4.3.19-4: Simulated, future percent contribution of total erosion by discharge for Baseline Condition and Scenario 1 at site 119BL for the period 2000-2014

5.4.3.20 Site 7L

The river at site 7L has steep, partially vegetated banks. Located at station 37,500, between Kidds Island and the Northfield Mountain Tailrace, the bank is roughly 28 feet tall, with a sandy toe and a sandy-loam upper bank. The bank slope is highly vegetated with American basswood and Northern red oak. The bank top is similarly vegetated with the addition of small grasses growing under the canopy (Figure 5.4.3.20-1).

BSTEM runs at this site show that under the Baseline Condition, 62.9 ft^3 of erosion occurred per foot of bank, during the 2000 to 2014 flow period, averaging 4.29 ft^3/ft/y (Table 5.4.3-1). This results in the 7th highest erosion rate for the Baseline Condition, placing it between the 75th and 80th percentiles of erosion rates along the reach. The modeling also indicates that roughly 81% (3.48 ft^3/ft/y) of the erosion is due directly to hydraulic processes, whereas the other 19% (0.81 ft^3/ft/y) is the result of geotechnical processes and associated mass failures.

The Baseline Condition (Waves off) resulted in 4.24 ft^3/ft/y, with 4.13 ft^3/ft/y for Scenario 1 (Figure 5.4.3.20-2 to Figure 5.4.3.20-3). This resulted in the following percent reductions in erosion rates: 1.15% and 3.89% for Baseline Wave off and Scenario 1 respectively. As the Baseline Condition (Waves off) scenario illustrated only a 1% reduction in erosion from the waves on condition, it is clear that boat waves have little to no effect on erosion rates at this site. Because of this, the remaining scenarios were not considered with boat waves off.

For the Baseline Condition, 95% of the total erosion occurs at flows of about 47,700 cfs or greater (Figure 5.4.3.20-4). Table 5.4.3.20-1 denotes the flows above which 95%, 50%, and 5% of all erosion occurs at the site as well as the amount of time those flows were exceeded for each year in the modeling period. Hydraulic erosion is fairly consistent across the range of flows above 40,000 cfs, with 75% occurring between about 40,000 cfs and 80,000 cfs, and 25% of the total erosion happening above 80,000 cfs. Through this analysis we can conclude that high flows greater than the combined hydraulic capacity of Vernon Dam and Northfield Mountain are accounting for most of the total erosion.

Table 5.4.3.20-1: Flow Exceedance Calculations for Site 7L

Site 7L	Percent of Erosion		
	95%	50%	5%
	Flow (cfs)		
Year	98,753	65,338	47,731
2000	NA	0.20%	2.30%
2001	NA	1.40%	3.70%
2002	NA	0.10%	1.20%
2003	NA	0.50%	3.20%
2004	NA	NA	0.70%
2005	NA	0.70%	4.50%
2006	NA	0.40%	2.60%
2007	NA	0.80%	3.30%
2008	NA	0.90%	5.80%
2009	NA	0.10%	2.00%
2010	NA	0.10%	2.80%
2011	0.20%	2.20%	6.50%
2012	NA	NA	0.20%
2013	NA	0.10%	0.40%
2014	NA	0.80%	2.70%

NA: Not Applicable since flows did not reach this value

Figure 5.4.3.20-1 Photos at site 7L

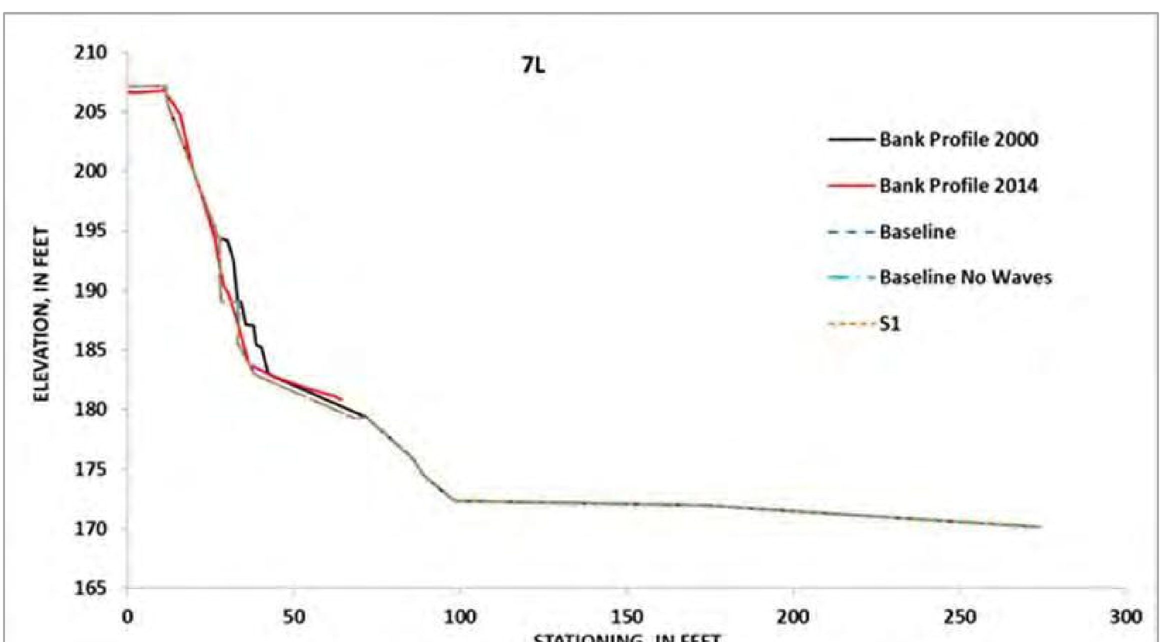

Figure 5.4.3.20-2: Simulated, future unit-erosion for the Baseline Condition (with boat waves on and off) and Scenario 1 at site 7L for the period 2000-2014

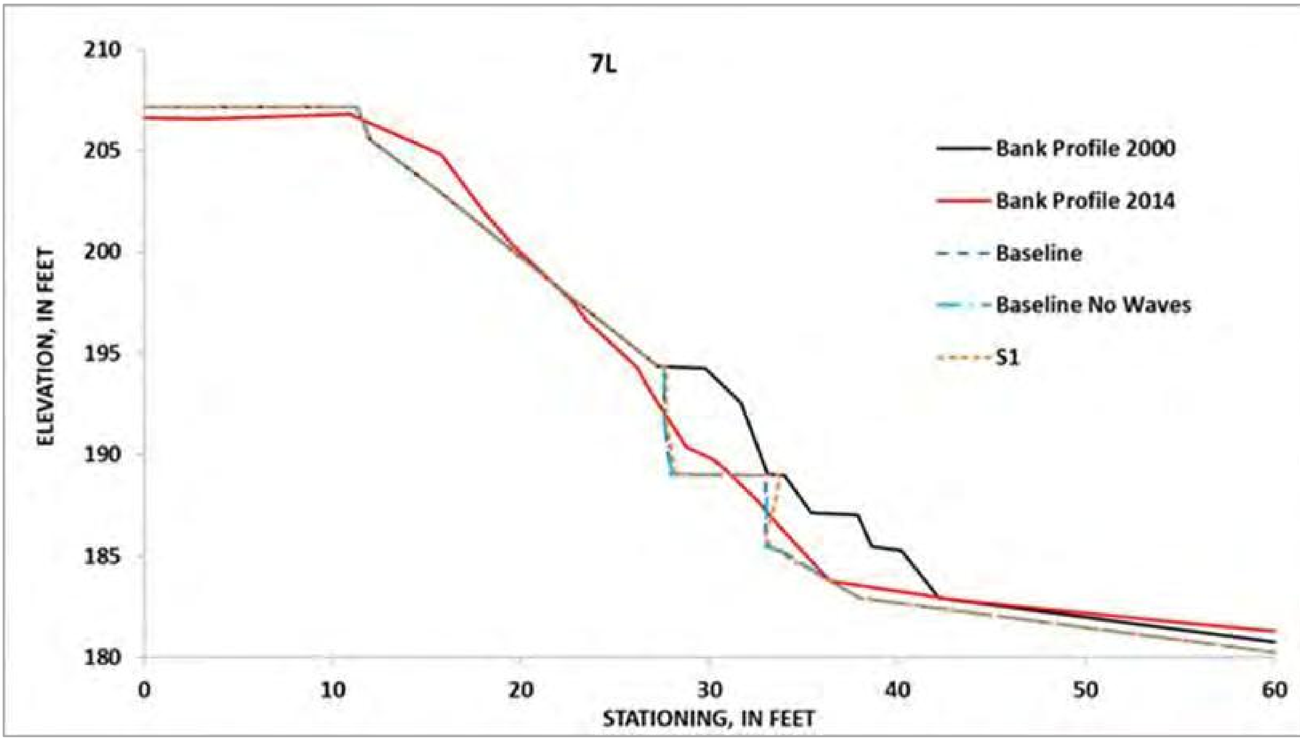

Figure 5.4.3.20-3: Simulated, future erosion for the Baseline Condition (with boat waves on and off) and Scenario 1 at site 7L for the period 2000-2014. Zoomed in at area of erosion for illustrative purposes

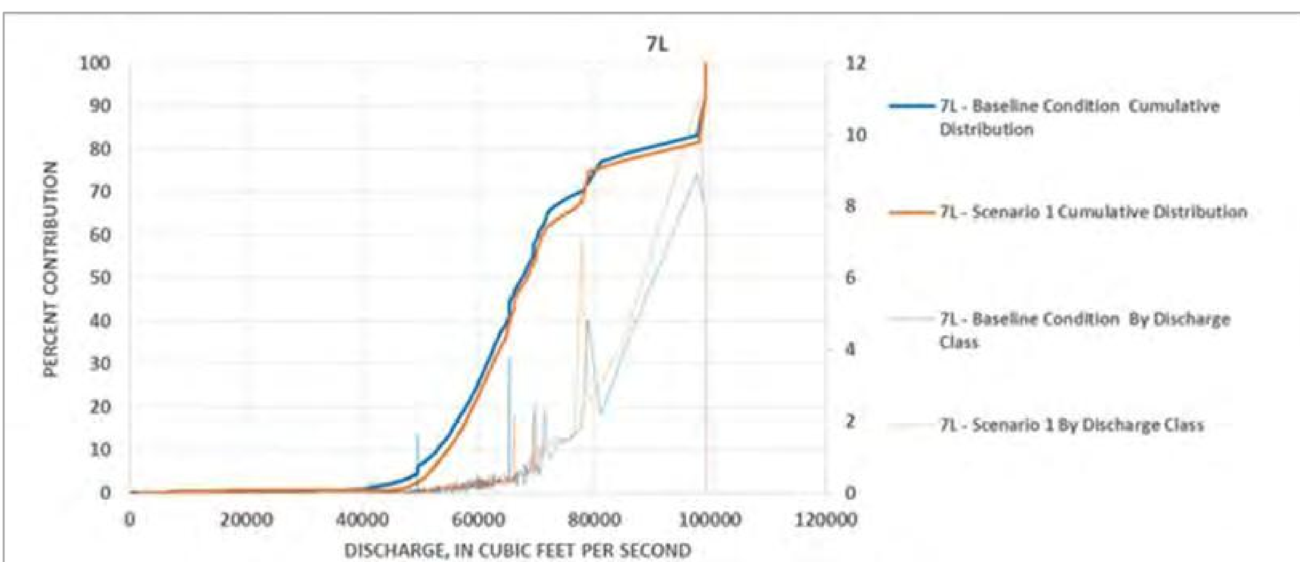

Figure 5.4.3.20-4: Simulated, percent contribution of total erosion by discharge for the Baseline Condition and Scenario 1 at site 7L for the period 2000-2014

5.4.3.21 Site 7R

Site 7R (station 37,500) is located between Kidds Island and the Northfield Mountain Tailrace, just upstream of Dry Brook. The site has steep, partially vegetated banks that are roughly 24 feet tall, with a sandy toe and a sandy-loam upper bank. The bank is vegetated with 20 to 50 year-old Hemlock, Pine, and Silver maple. There was a significant amount of bare soil noted on the upper bank, likely due to the dense tree canopy (Figure 5.4.3.21-1).

BSTEM runs at this site show that under the Baseline Condition, 30.1 ft^3 of erosion occurred per foot of bank, during the 2000 to 2014 flow period, averaging 2.06 ft^3/ft/y (Table 5.4.3-1). This results in the 13th highest erosion rate for the Baseline Condition, placing it between the 55th and 60th percentiles of erosion rates along the reach. The modeling also indicates that all 100% (2.06 ft^3/ft/y) of the erosion is due directly to hydraulic processes, and none of the bank erosion is the result of larger, geotechnical failures.

The Baseline Condition (Waves off) resulted in 2.04 ft^3/ft/y, with 2.05 ft^3/ft/y for Scenario 1 (Figure 5.4.3.21-2 to Figure 5.4.3.21-3). This resulted in reductions in erosion rates of 1.0% and 0.53% for Baseline Wave off and Scenario 1 respectively. As Baseline simulations with waves off showed virtually no reduction in erosion, it was concluded that boat waves have little effect on erosion processes at this site.

To further support the important role of high flows in bank-erosion rates, for the Baseline Condition, 95% of the total erosion occurs at flows of about 53,500 cfs or greater (Figure 5.4.3.21-4). Table 5.4.3.21-1 denotes the flows above which 95%, 50%, and 5% of all erosion occurs at the site as well as the amount of time those flows were exceeded for each year in the modeling period. The hydraulic erosion looks to be fairly consistent across the range of flows above 40,000 cfs, with 75% occurring between 40,000 cfs and 75,000 cfs, and 25% of the total erosion occurring above 75,000 cfs. Through this analysis we can conclude that those flows greater than the combined hydraulic capacity of Vernon and Northfield Mountain are accounting for most of the total erosion.

Table 5.4.3.21-1: Flow Exceedance Calculations for Site 7R

Site 7R	Percent of Erosion		
	95%	**50%**	**5%**
	Flow (cfs)		
Year	**98,463**	**65,880**	**53,614**
2000	NA	0.20%	1.30%
2001	NA	1.40%	3.00%
2002	NA	0.10%	0.60%
2003	NA	0.40%	2.00%
2004	NA	NA	0.30%
2005	NA	0.60%	2.50%
2006	NA	0.30%	1.50%
2007	NA	0.70%	2.70%
2008	NA	0.80%	3.80%
2009	NA	0.10%	1.10%
2010	NA	0.10%	1.30%
2011	0.20%	2.00%	4.80%
2012	NA	NA	NA
2013	NA	0.10%	0.10%
2014	NA	0.70%	2.20%

NA: Not Applicable since flows did not reach this value

Figure 5.4.3.21-1 Photos at site 7R

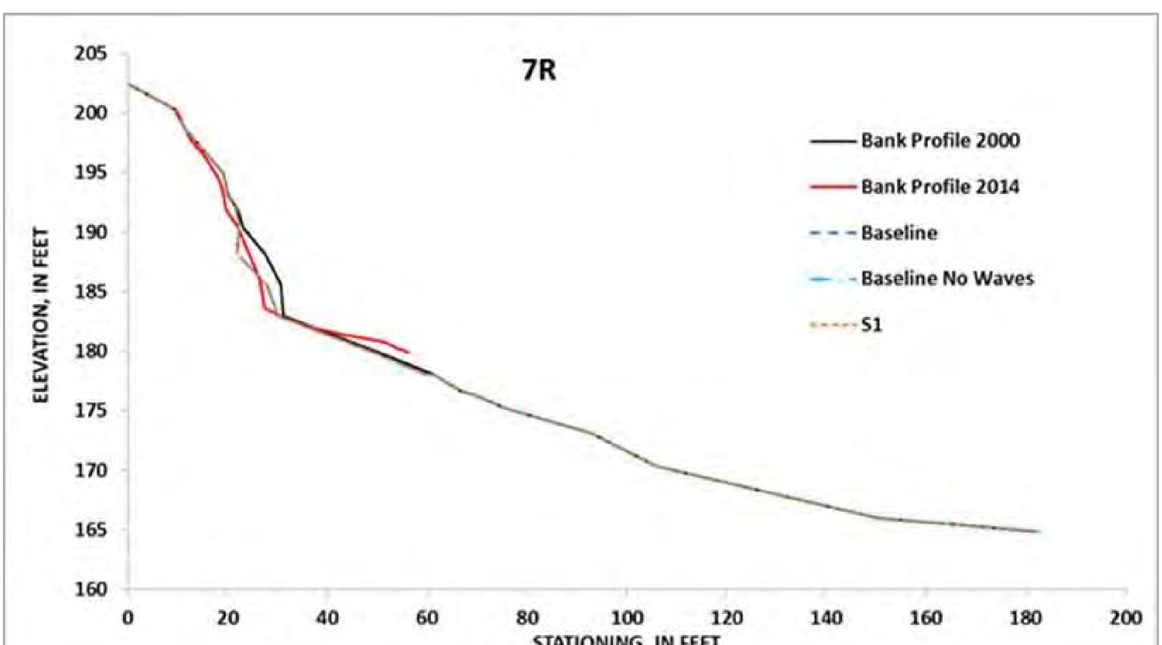

Figure 5.4.3.21-2: Simulated, future unit-erosion for the Baseline Condition (with boat waves on and off) and Scenario 1 at site 7R for the period 2000-2014

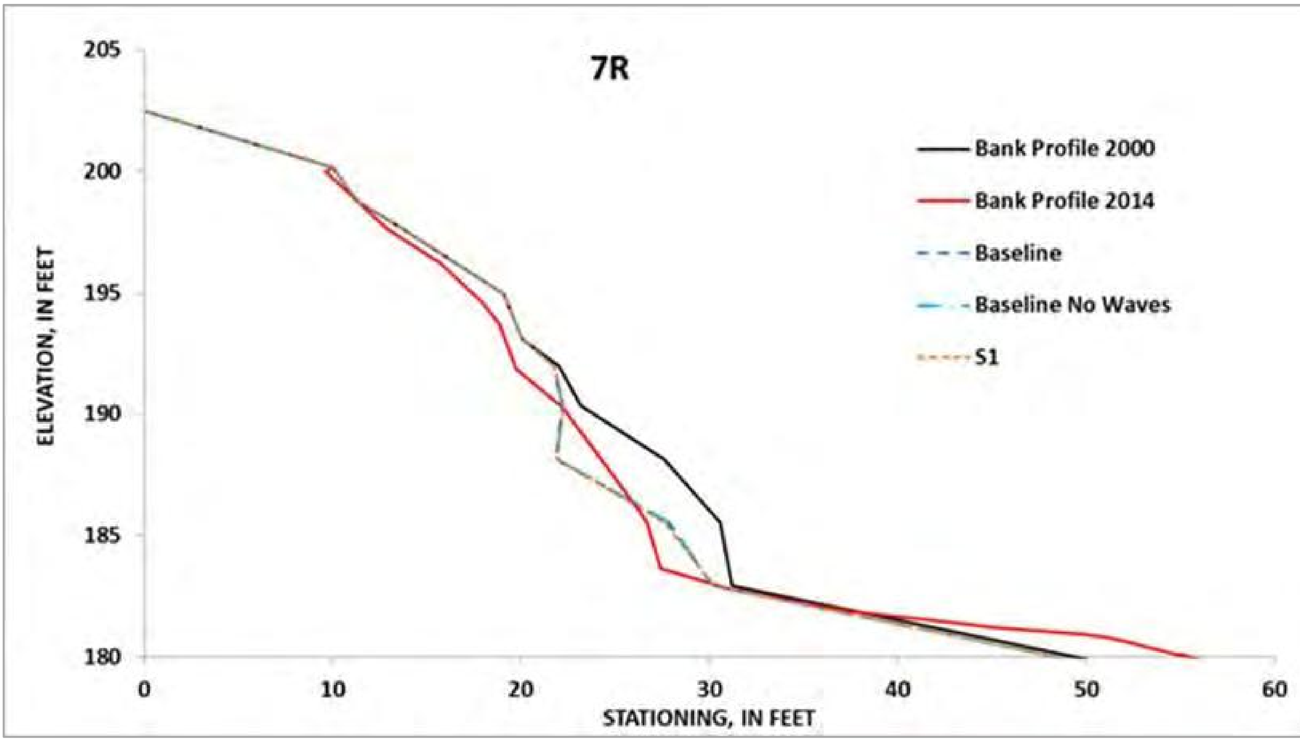

Figure 5.4.3.21-3: Simulated, future erosion for the Baseline Condition (with boat waves on and off) and Scenario 1 at site 7R for the period 2000-2014. Zoomed in at area of erosion for illustrative purposes

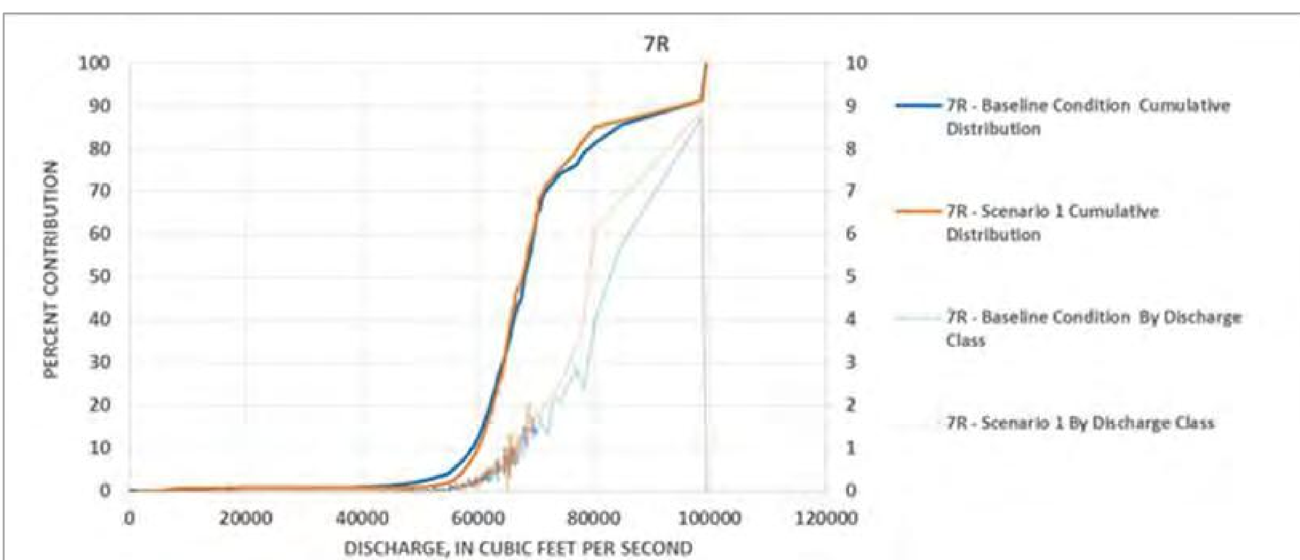

Figure 5.4.3.21-4: Simulated, percent contribution of total erosion by discharge for the Baseline Condition and Scenario 1 at site 7R for the period 2000-2014

5.4.3.22 Site 8BL

The river at site 8BL (station 32,750) has steep, vegetated banks and is located between Kidds Island and the Northfield Mountain Tailrace, just upstream of Pine Meadow Brook. The bank is roughly 24 feet tall, with a sandy toe and a sandy-loam upper bank. The bank is highly vegetated with 20 to 50 year old Hemlock, Pine, and Silver maple. There was a significant amount of bare soil noted, likely due to the dense tree canopy (Figure 5.4.3.22-1).

BSTEM runs at this site show that under the Baseline Condition, 6.09 ft^3 of erosion occurred per foot of bank, during the 2000 to 2014 flow period, averaging 0.43 ft^3/ft/y (Table 5.4.3-1). This results in the 19th highest erosion rate for the Baseline Condition, placing it between the 35th and 40th percentiles of erosion rates along the reach. The modeling also indicates that all 100% (0.428 ft^3/ft/y) of the erosion is due directly to hydraulic processes, and none of the bank erosion is the result of geotechnical processes and associated mass failures.

The Baseline Condition (Waves off) resulted in 0.43 ft^3/ft/y, with 0.40 ft^3/ft/y for Scenario 1(Figure 5.4.3.22-2 to Figure 5.4.3.22-3). This resulted in the following percent differences in erosion rates relative to the Baseline Condition: 0.09% and 6.6%, for Baseline Wave off and Scenario 1, respectively. As the Baseline Condition (Waves off) scenario illustrated a very little reduction in erosion, it was concluded that boat waves are not having a significant impact on bank stability, and the remaining scenarios were not considered with boat waves off.

The important role of high flows in bank-erosion rates can be seen in the Baseline Condition erosion results, 93% of the total erosion occurs at flows of 37,000 cfs or greater (Figure 5.4.3.22-4). Table 5.4.3.22-1 denotes the flows above which 95%, 50%, and 5% of all erosion occurs at the site as well as the amount of time those flows were exceeded for each year in the modeling period. Through this analysis we can conclude that those flows greater than the combined hydraulic capacity of Vernon and Northfield Mountain are accounting for most of the total erosion with a small percent of erosion (6.6%) contributed by Northfield Mountain Project operations.

Table 5.4.3.22-1: Flow Exceedance Calculations for Site 8BL

Site 8BL	Percent of Erosion		
	95%	50%	5%
	Flow (cfs)		
Year	84,451	84,138	77,997
2000	NA	NA	NA
2001	0.10%	0.10%	0.30%
2002	NA	NA	NA
2003	NA	NA	NA
2004	NA	NA	NA
2005	NA	NA	0.10%
2006	NA	NA	NA
2007	NA	NA	NA
2008	NA	NA	0.10%
2009	NA	NA	NA
2010	NA	NA	NA
2011	0.40%	0.40%	0.60%
2012	NA	NA	NA
2013	NA	NA	NA
2014	NA	NA	NA

NA: Not Applicable since flows did not reach this value

Figure 5.4.3.22-1 Photos at site 8BL

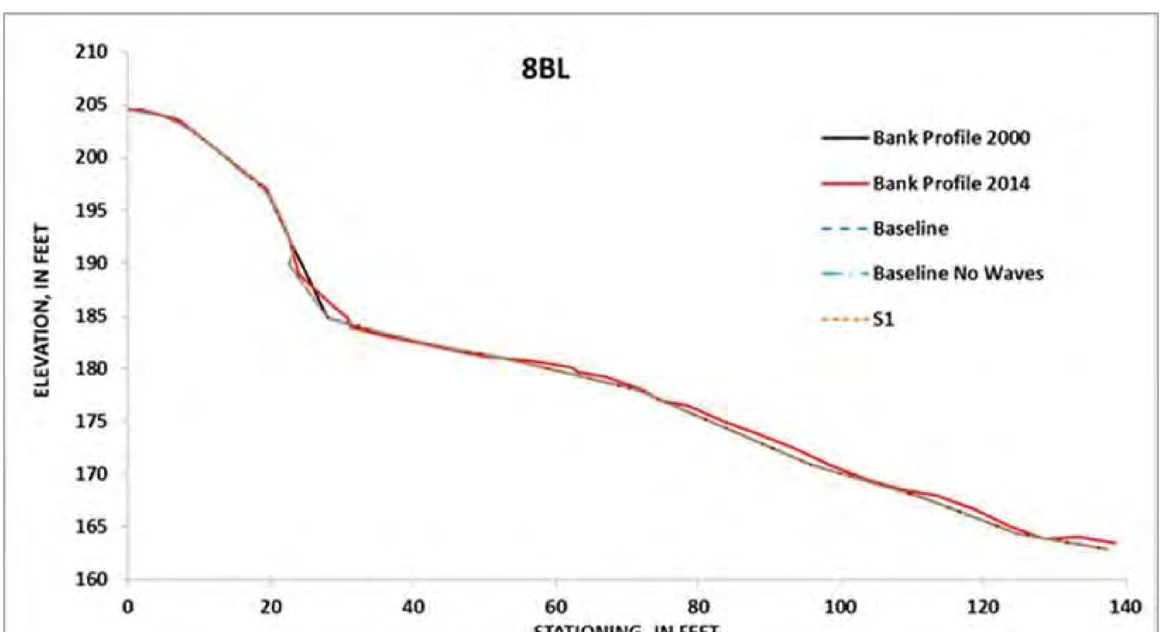

Figure 5.4.3.22-2: Simulated, future unit-erosion for the Baseline Condition (with boat waves on and off) and Scenario 1 at site 8BL for the period 2000-2014

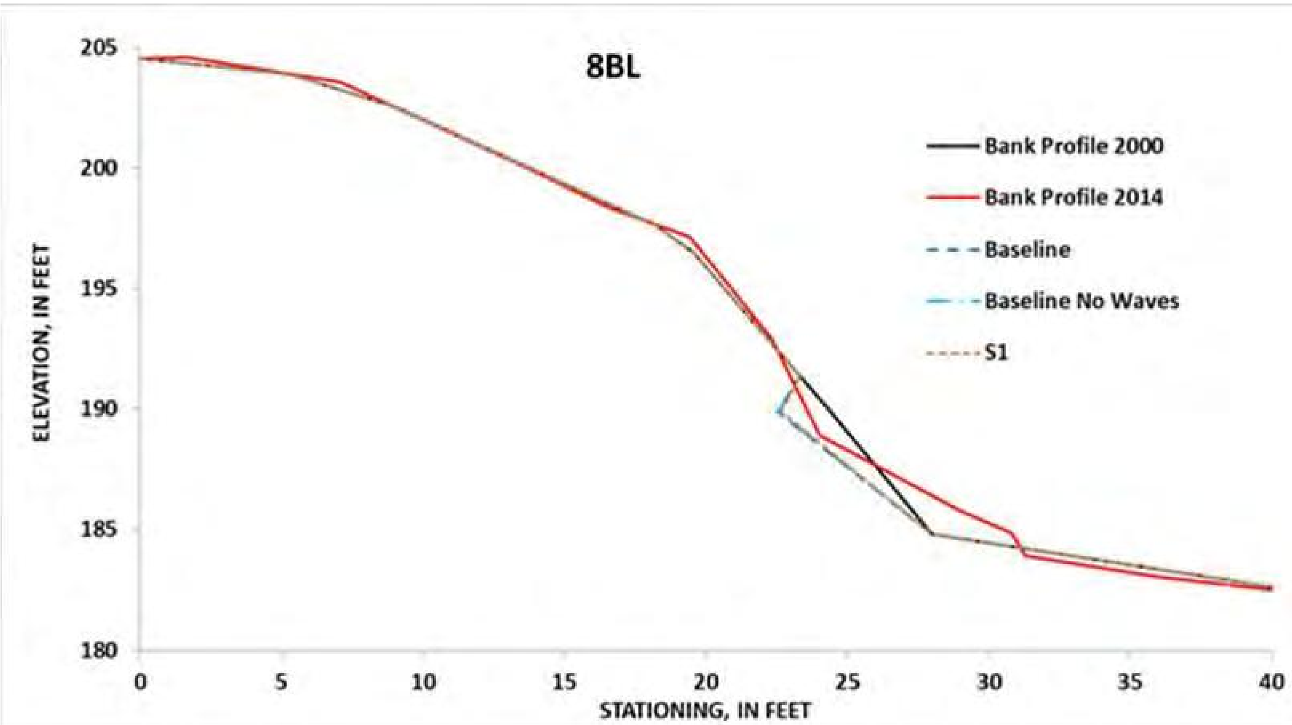

Figure 5.4.3.22-3: Simulated, future erosion for the Baseline Condition (with boat waves on and off) and Scenario 1 at site 8BL for the period 2000-2014. Zoomed in at area of erosion for illustrative purposes

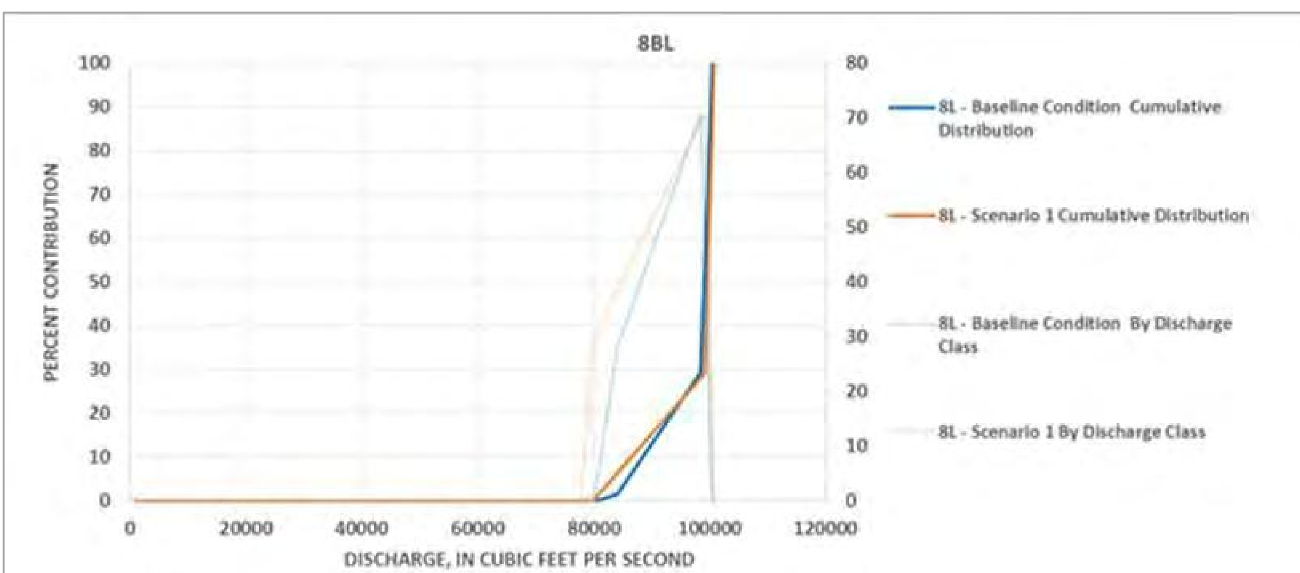

Figure 5.4.3.22-4: Simulated, percent contribution of total erosion by discharge for the Baseline Condition and Scenario 1 at site 8BL for the period 2000-2014

5.4.3.23 Site 8BR – Pre-Restoration

The river at site 8BR (station 32,750) has steep, sparsely vegetated banks and is located between Kidds Island and Northfield Mountain Tailrace, just upstream of Pine Meadow Brook. The bank is roughly 19 feet tall, with a sandy toe and a sandy-loam upper bank. The bank is thinly vegetated with Northern red oak and Green ash. There was also significant amount of bare soil noted (Figure 5.4.3.23-1).

BSTEM runs for the Pre-Restoration Condition at this site show that under the Baseline Condition, 89.6 ft^3 of erosion occurred per foot of bank, during the 2000 to 2012 flow period prior to restoration, averaging 7.42 ft^3/ft/y (Table 5.4.3-1). This results in the 3rd highest erosion rate for the Baseline Condition, placing it between the 90th and 95th percentiles of erosion rates along the reach. The modeling also indicates that roughly 30% (2.23 ft^3/y) of the erosion is due to hydraulic processes, whereas the other 70% (5.19 ft^3/y) is the result of geotechnical processes and associated mass failures.

The Baseline Condition (Waves off) resulted in 7.39 ft^3/ft/y, with 1.95 ft^3/ft/y for Scenario 1 (Figure 5.4.3.23-2 to Figure 5.4.3.23-3). This resulted in the following percent reductions in erosion rates: 0.28% and 73.6% for Baseline Wave off and Scenario 1, respectively. The drastic difference between bank-erosion rates for the Baseline Condition and Scenarios 1, can be attributed to what happened at 8R during Hurricane Irene in 2011. As this site is in the Northfield Mountain reach, it appears that a significant failure occurs during Baseline Conditions that does not occur during the other Operational scenario when the effects of Northfield Mountain are not included. This difference is attributed to the lack of rapid fluctuations in water-surface elevations for Scenario 1 (because Northfield Mountain is idle) (Figure 5.4.3.23-4). The figure shows that a large failure occurs here under the Baseline Condition, when peaking operations are combined with extreme high flows.

As the Baseline Condition (Waves off) scenario illustrated a very small reduction in erosion compared to waves on, it was concluded that boat waves are not having a significant impact on bank stability, and the remaining scenarios were not considered with boat waves off.

For the Baseline Condition, 95% of the total erosion occurs at flows of about 64,000 cfs or greater (Figure 5.7.23-5). Table 5.4.3.23-1 denotes the flows above which 95%, 50%, and 5% of all erosion occurs at the site as well as the amount of time those flows were exceeded for each year in the modeling period. There is a significant geotechnical failure at extreme high flow (near 99,000 cfs) which accounts for the bulk of the geotechnical erosion, whereas hydraulic erosion is fairly consistent across the range of flows above 50,000 cfs. This large geotechnical failure happens at the extremely high flow during Hurricane Irene but is not present in the Scenario 1 results suggesting that 73.6% of the erosion at this site is due to Northfield Mountain operations.

Table 5.4.3.23-1: Flow Exceedance Calculations for Site 8BR Pre-Restoration

Site 8BR	Percent of Erosion		
	95%	50%	5%
	Flow (cfs)		
Year	**72,009**	**69,312**	**66,504**
2000	NA	0.10%	0.20%
2001	0.80%	1.00%	1.30%
2002	NA	NA	0.10%
2003	0.10%	0.20%	0.40%
2004	NA	NA	NA
2005	0.50%	0.50%	0.60%
2006	0.10%	0.20%	0.30%
2007	0.10%	0.30%	0.50%
2008	0.20%	0.40%	0.70%
2009	NA	NA	0.10%
2010	NA	0.10%	0.10%
2011	0.90%	1.30%	1.90%
2012	NA	NA	NA
2013	NA	NA	0.10%
2014	0.10%	0.40%	0.60%

NA: Not Applicable since flows did not reach this value

Figure 5.4.3.23-1 Photos at site 8BR Pre Restoration (Labeled as 1998 FRR/ECP-Site 16)

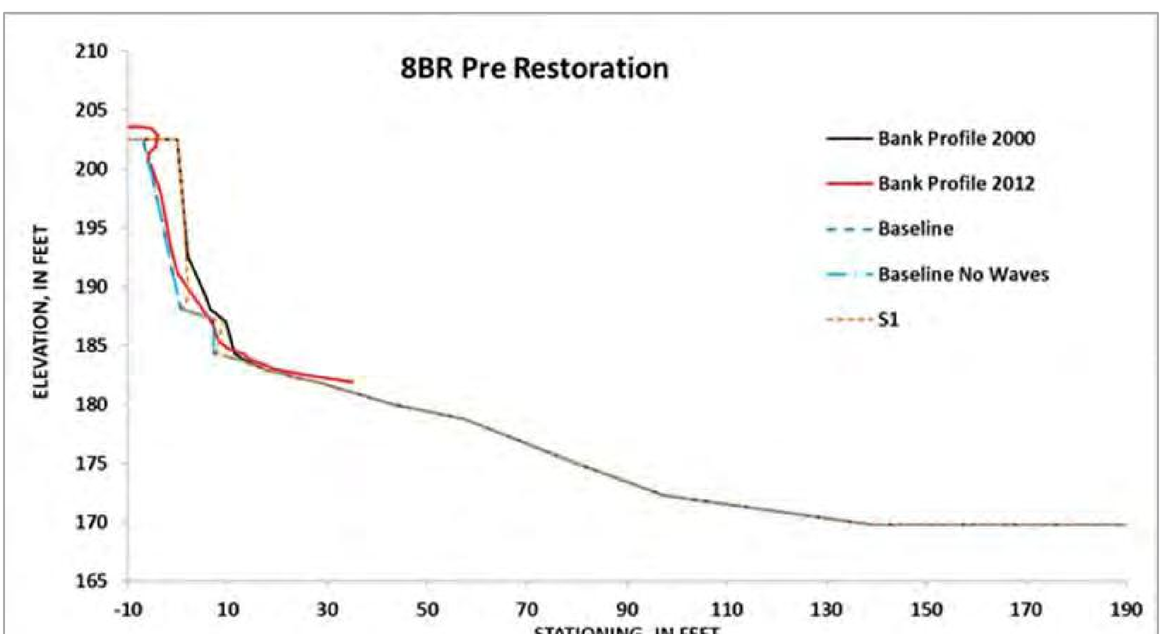

Figure 5.4.3.23-2: Simulated, future unit-erosion for the Baseline Condition (with boat waves on and off) and Scenario 1 at site 8BR for the period 2000-2012

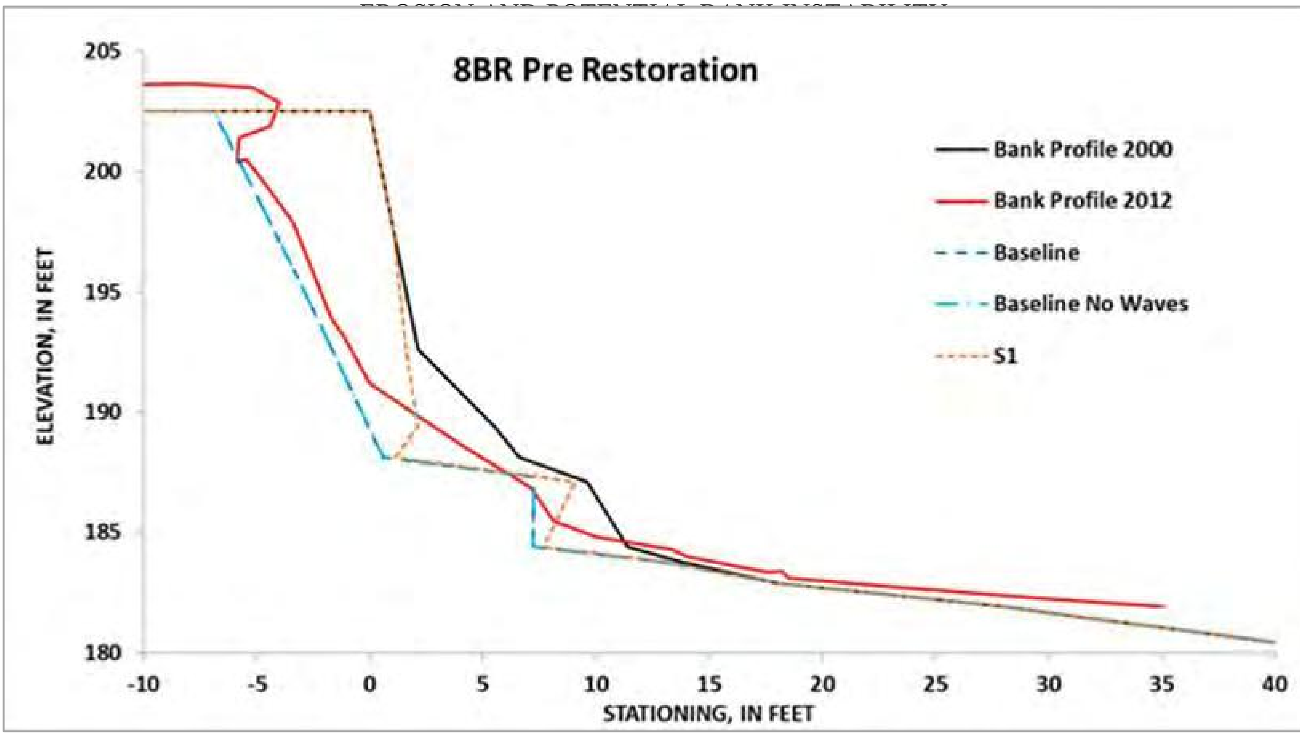

Figure 5.4.3.23-3: Simulated, future erosion for the Baseline Condition (with boat waves on and off) and Scenario 1 at site 8BR for the period 2000-2012. Zoomed in at area of erosion for illustrative purposes

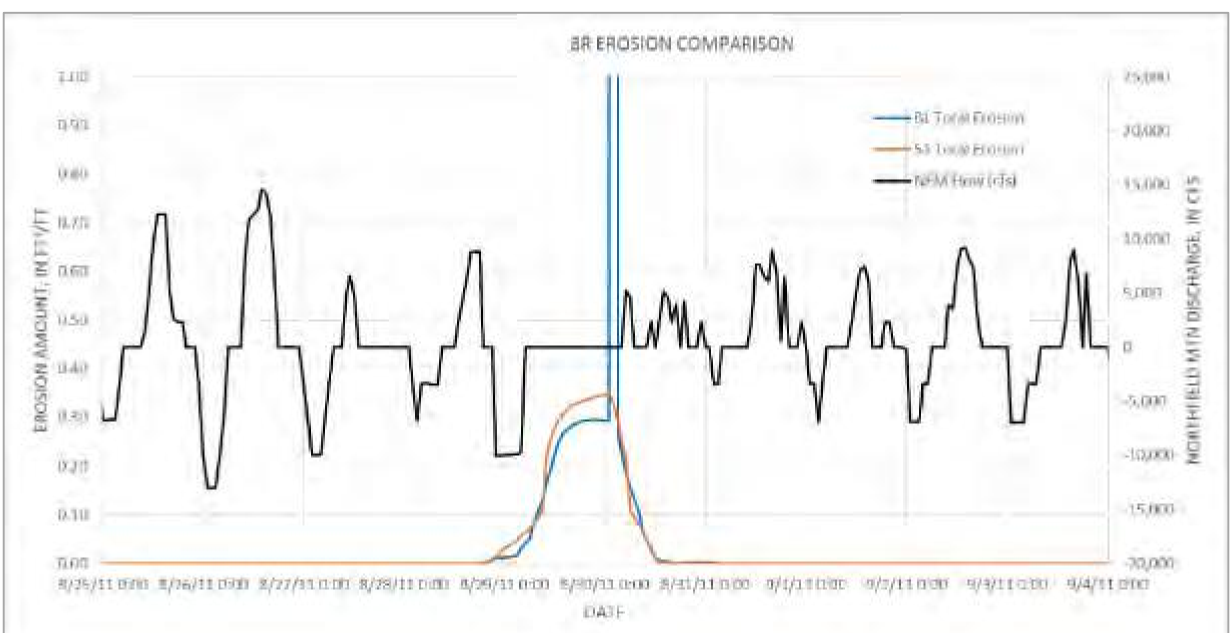

Figure 5.7.23-4 – Timing of large, geotechnical failure during Hurricane Irene for the Baseline Condition but not during Scenario 1 when NFM is idle.

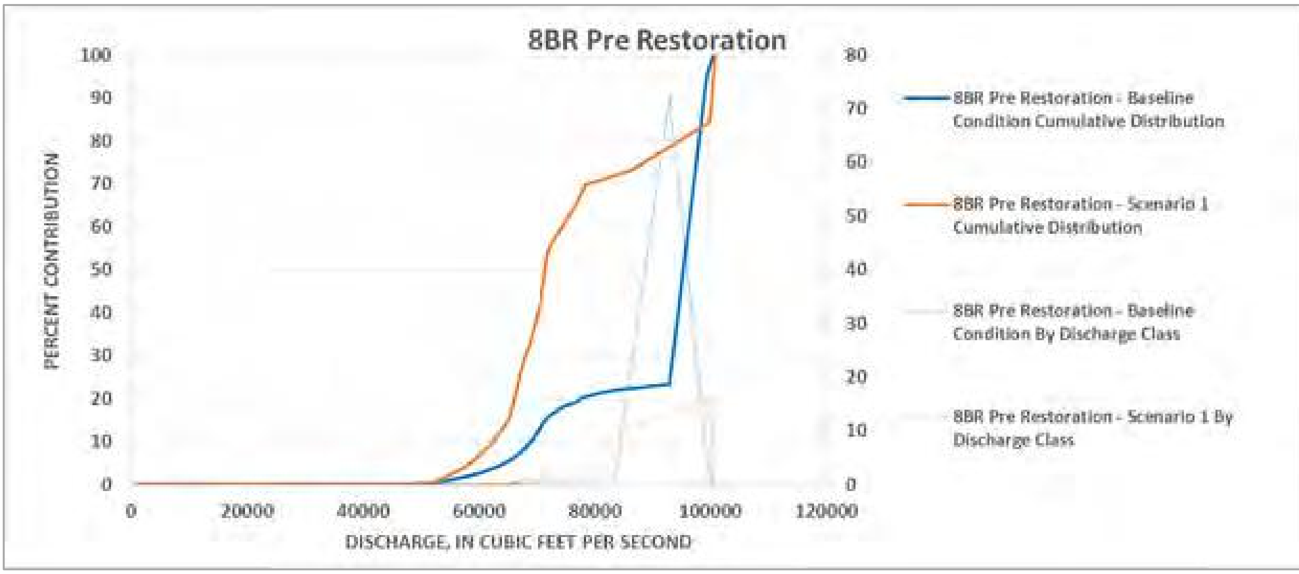

Figure 5.4.3.23-5: Simulated, percent contribution of total erosion by discharge for the Baseline Condition and Scenario 1 at site 8BR for the period 2000-2012

5.4.3.24 Site 8BR – Post Restoration

For the Post Restoration condition at site 8R gravel materials (d_{50} = 13 mm) were placed on the bank toe along with anchored, large woody debris. Vegetation was also added to the lower bank (Figure 5.4.3.24-1).

BSTEM runs at this site show that under the Baseline Condition, 0.671 ft^3 of erosion occurred per foot of bank, during the 2012-2014 flow period post restoration, averaging 0.312 $ft^3/ft/y$ (Table 5.4.3-1). This results in the 11th lowest erosion rate for the Baseline Condition, placing it between the 30th and 35th percentiles of erosion rates along the reach. The modeling also indicates that all 100% (0.31 $ft^3/ft/y$) of the erosion is due directly to hydraulic processes that are occurring just above the placed materials. None of the bank erosion appears to be the result of geotechnical processes and associated mass failures.

The Baseline Condition (Waves off) resulted in 0.312 $ft^3/ft/y$, with 0.248 $ft^3/ft/y$ for Scenario 1 (Figure 5.4.3.24-2 to Figure 5.4.3.24-3). This resulted in the differences in erosion rates relative to the Baseline Condition of 0.0% and 20.4%, for Baseline Wave off and Scenario 1 respectively. As Baseline Condition (Waves off) scenario illustrated no reduction in erosion, it was concluded that boat waves are not having a significant impact on bank stability, and the remaining scenarios were not considered with boat waves off.

For the Baseline Condition, 95% of the total erosion occurs at flows of about 66,000 cfs or greater (Figure 5.4.3.24-4). Table 5.4.3.24-1 denotes the flows above which 95%, 50%, and 5% of all erosion occurs at the site as well as the amount of time those flows were exceeded for each year in the modeling period. The hydraulic erosion is fairly consistent across the range of flows above 50,000 cfs. Through this analysis we can conclude that those flows greater than the combined hydraulic capacity of Vernon and Northfield Mountain are accounting for most of the total erosion. Scenario 1 contributes 20.4% of the erosion and suggests that Northfield Mountain is a contributing factor to the total erosion.

Table 5.4.3.24-1: Flow Exceedance Calculations for Site 8BR Post Restoration

Site 8BR	Percent of Erosion		
	95%	50%	5%
	Flow (cfs)		
Year	72,009	69,312	66,504
2000	NA	0.10%	0.20%
2001	0.80%	1.00%	1.30%
2002	NA	NA	0.10%
2003	0.10%	0.20%	0.40%
2004	NA	NA	NA
2005	0.50%	0.50%	0.60%
2006	0.10%	0.20%	0.30%
2007	0.10%	0.30%	0.50%
2008	0.20%	0.40%	0.70%
2009	NA	NA	0.10%
2010	NA	0.10%	0.10%
2011	0.90%	1.30%	1.90%
2012	NA	NA	NA
2013	NA	NA	0.10%
2014	0.10%	0.40%	0.60%

NA: Not Applicable since flows did not reach this value

Figure 5.4.3.24-1 Photos at site 8BR Post Restoration

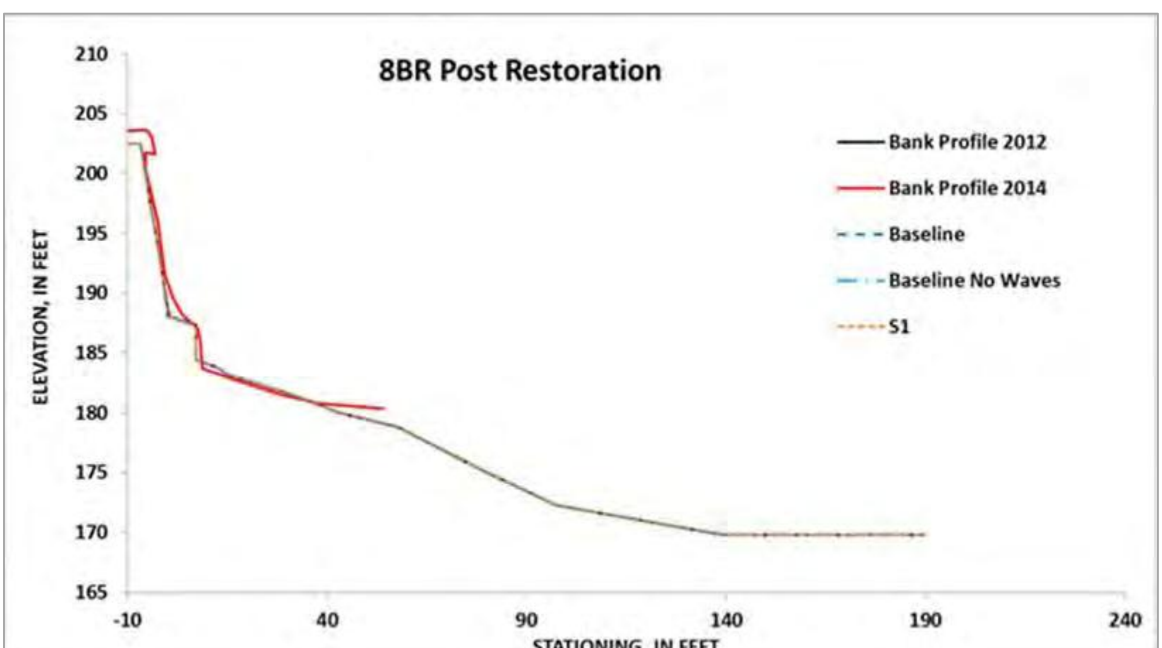

Figure 5.4.3.24-2: Simulated, future unit-erosion for the Baseline Condition (with boat waves on and off) and Scenario 1 at site 8BR Post Restoration for the period 2012-2014

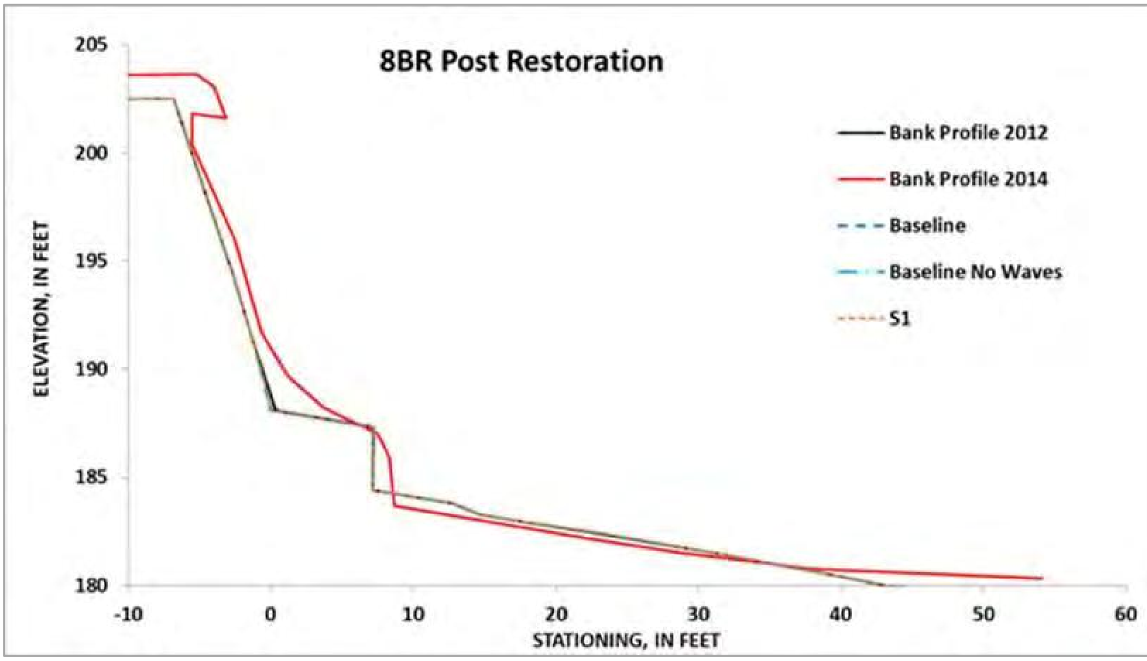

Figure 5.4.3.24-3: Simulated, future erosion for the Baseline Condition (with boat waves on and off) and Scenario 1 at site 8BR Post Restoration for the period 2012-2014. Zoomed in at area of erosion for illustrative purposes

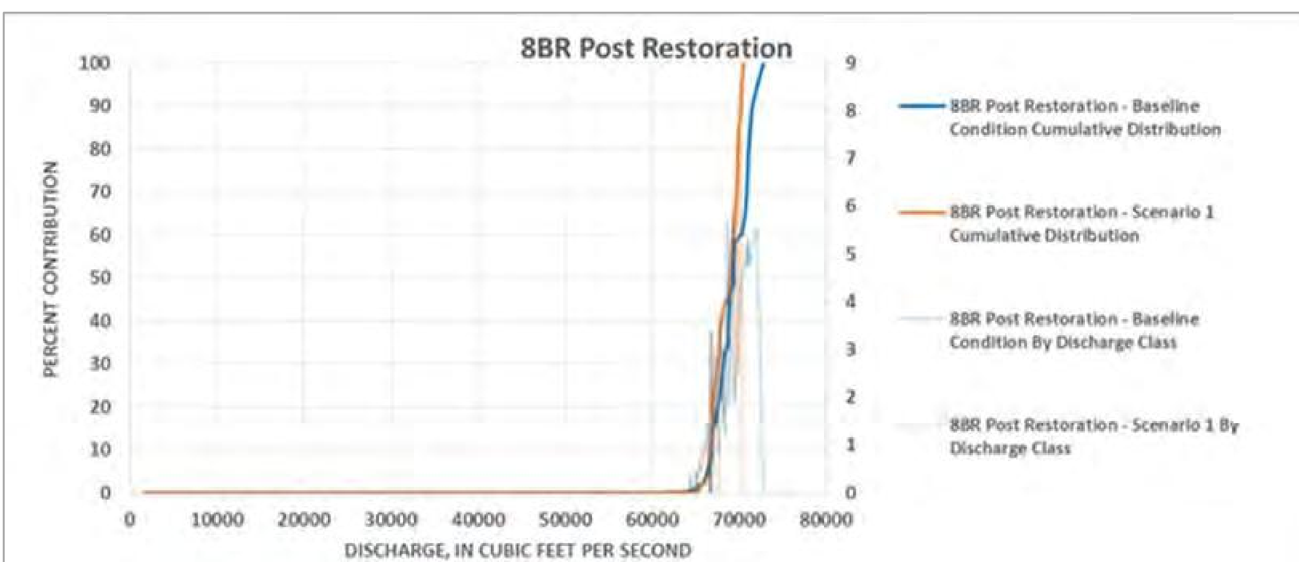

Figure 5.4.3.24-4: Simulated, percent contribution of total erosion by discharge for the Baseline Condition and Scenario 1 at site 8BR Post Restoration for the period 2012-2014

5.4.3.25 Site 87BL

The river at site 87BL (station 30,750) has a steep bank face with an extensive beach, sparsely vegetated banks (Figure 5.4.3.25-1). The site is located between Kidds Island and Northfield Mountain Tailrace, just downstream of Pine Meadow Brook. The bank is roughly 20 feet tall, with a sandy-loam toe and a silt-loam bank. The bank is vegetated with tall grasses and a few American elms. There was a significant amount of bare soil noted. The toe material appears to be depositional. No historical cross sections existed for this site and a 2014 survey was used, therefore, as the initial bank geometry for modeling.

BSTEM runs at this site show that under the Baseline Condition, 52.3 ft^3 of erosion occurred per foot of bank, during the 2000-2014 flow period, averaging 3.57 $ft^3/ft/y$ (Table 5.4.3-1). The modeling also indicates that roughly 73% (2.6 ft^3/y) of the erosion is due directly to hydraulic processes, whereas the other 27% (0.96 ft^3/y) is the result of geotechnical processes and associated mass failures. This reach had higher energy grade line slopes than reach 1 and reach 3. We can see that 87BL has the 9th highest erosion rate and is in the 70th to 75th percentile of erosion rates.

The Baseline Condition (Waves off) resulted in 3.61 $ft^3/ft/y$, with 3.60 $ft^3/ft/y$ for Scenario 1 (Figure 5.4.3.25-2 to Figure 5.4.3.25-3). This resulted in the following percent differences in erosion rates relative to the Baseline Condition: -1.01% and -0.76% for Baseline Wave off and Scenario 1, respectively. As Baseline Condition (Waves off) scenario and Scenario 1 resulted in a slightly higher erosion rate (about 1%) that is certainly within model limitations and does not indicate that erosion would be greater without boat waves and Northfield Mountain operations.

Erosion rates for all Operational scenarios are similar. For the Baseline Condition, 80% of the total erosion occurs at flows of about 37,000 cfs or greater (Figure 5.4.3.25-4). Table 5.4.3.25-1 denotes the flows above which 95%, 50%, and 5% of all erosion occurs at the site as well as the amount of time those flows were exceeded for each year in the modeling period. The geotechnical failures that account for the 27% of the total erosion, occur at the extreme high flows, whereas hydraulic erosion is fairly consistent across the range of flows above 10,000 cfs, resulting in undercutting of the lower bank (Figures 5.4.3.25-2 and Figures 5.4.3.25-3). Evaluating the moderate flow contribution to the total erosion it was determined that Northfield Mountain operations occurred about 17% of the time over the modeled period of record. This equates to about 3.5% of the total erosion during the moderate flows. The Northfield Mountain contribution was adjusted by this 3.5% to better estimate contributions from the project resulting in a total contribution of about 3%.

Table 5.4.3.25-1: Flow Exceedance Calculations for Site 87BL Post Restoration

Site 87BL	Percent of Erosion		
	95%	50%	5%
	Flow (cfs)		
Year	63,968	42,875	17,849
2000	0.30%	3.80%	24.40%
2001	1.60%	4.50%	12.60%
2002	0.10%	1.80%	20.00%
2003	0.60%	4.40%	28.20%
2004	0.10%	1.20%	17.80%
2005	0.70%	6.50%	33.10%
2006	0.50%	4.50%	36.70%
2007	1.00%	3.90%	23.90%
2008	1.20%	8.10%	36.20%
2009	0.10%	2.90%	32.30%
2010	0.20%	4.30%	25.50%
2011	2.30%	8.00%	36.80%
2012	NA	0.40%	18.10%
2013	0.10%	0.80%	22.90%
2014	0.90%	3.30%	27.50%

NA: Not Applicable since flows did not reach this value

Figure 5.4.3.25-1 Photos at site 87BL Post Restoration

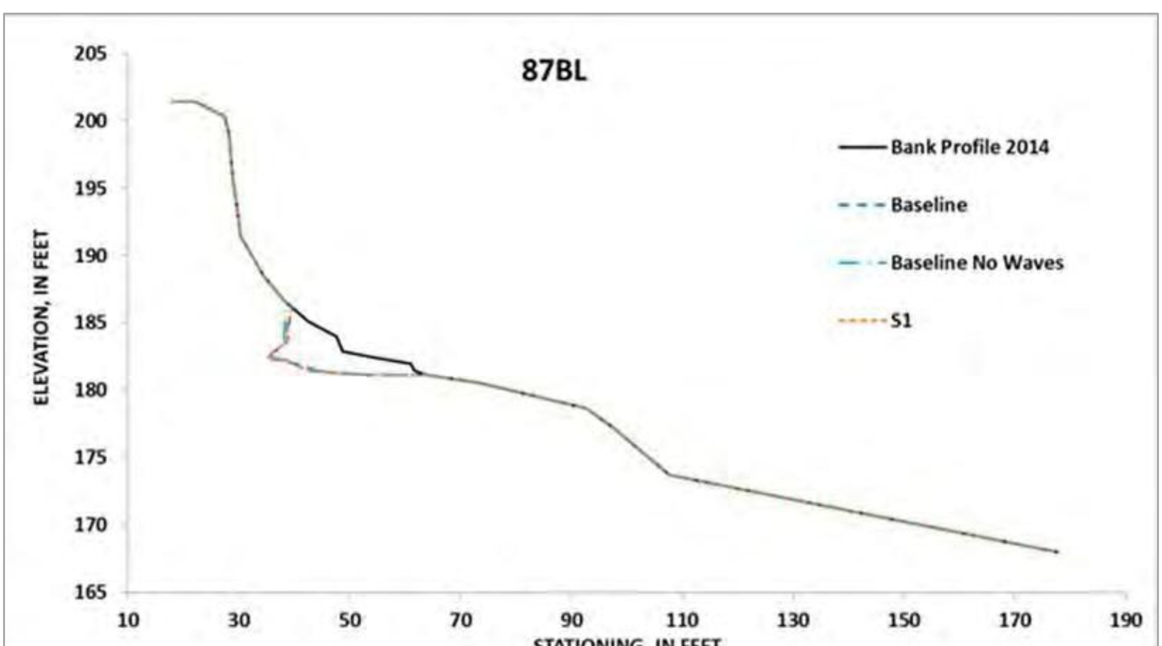

Figure 5.4.3.25-2: Simulated, future unit-erosion for the Baseline Condition (with boat waves on and off) and Scenario 1 at site 87BL for the period 2000-2014

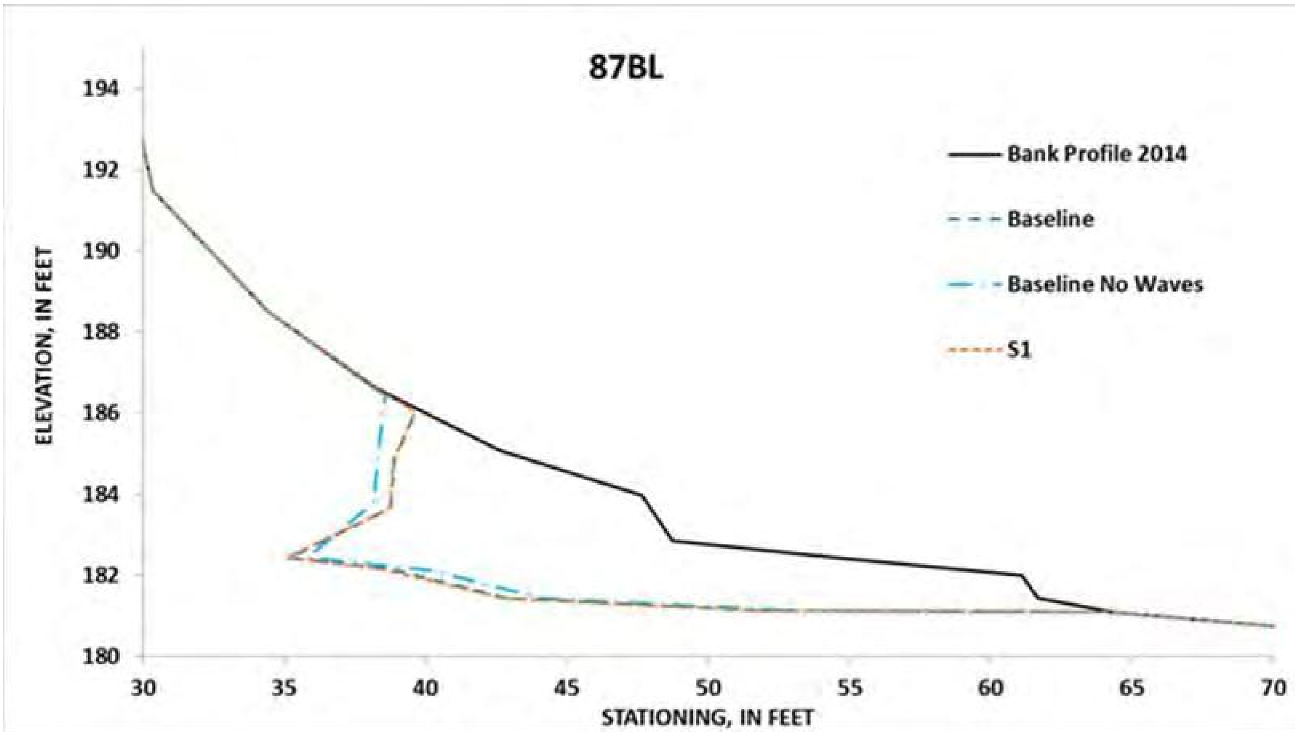

Figure 5.4.3.25-3: Simulated, future erosion for the Baseline Condition (with boat waves on and off) and Scenario 1 at site 87BL for the period 2000-2014. Zoomed in at area of erosion for illustrative purposes

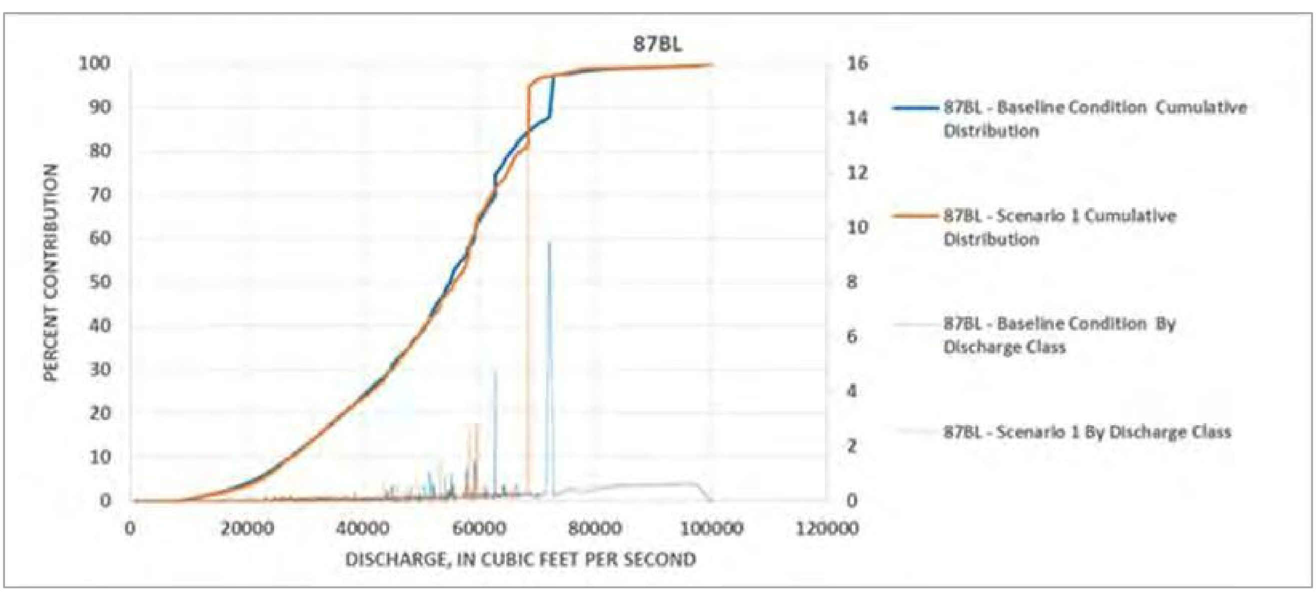

Figure 5.4.3.25-4: Simulated, percent contribution of total erosion by discharge for the Baseline Condition and Scenario 1 at site 87BL for the period 2000-2014

5.4.3.26 Site 75BL

The river at site 75BL (station 27,000) has steep, partially vegetated banks and is located immediately downstream of the Northfield Mountain Tailrace. The bank is roughly 65 feet tall, and the toe material ranges from coarse sand to large cobbles. Large Eastern hemlocks cover most of the upper bank, however the lower bank, shows signs of erosion, with lots of exposed roots. No historical cross sections exist for this site, however this site was surveyed in 2014 as a starting point for the model runs (Figure 5.4.3.26-1).

BSTEM runs at this site show that under the Baseline Condition, 55.0 ft^3 of erosion occurred per foot of bank, during the 2000 to 2014 flow period, averaging 3.76 $ft^3/ft/y$ (Table 5.4.3-1). This results in the 8th highest erosion rate for the Baseline Condition, placing it between the 75th and 80th percentiles of erosion rates along the reach. The modeling also indicates that roughly 56% (2.10 ft^3/y) of the erosion is due directly to hydraulic processes, whereas the other 44% (1.66 ft^3/y) is the result of geotechnical processes and associated mass failures.

For Scenario 1, 3.93 $ft^3/ft/y$ of erosion occurred (Figure 5.4.3.26-2 to Figure 5.4.3.26-3) resulting in a percent difference in erosion rate relative to the Baseline Condition of -4.6%. The Baseline Condition (Waves off) resulted in 3.48 $ft^3/ft/y$. Bank-erosion rates for the Baseline Condition with boat waves was 7.5% greater than without waves, a small, but measurable amount. Because of this, Scenario 1 was also run without the effects of boat waves. With waves off Scenario 1 resulted in 3.72 $ft^3/ft/y$. A comparison of results showed that bank-erosion rates were about 5.3% greater with boat waves than without for Scenario 1. As these numbers are not drastically different from the runs with the boat waves turned on, this location is likely at or near the upstream limit of where boat waves are having a significant impact on bank stability.

For the Baseline Condition, 79.5% of the total erosion occurs at flows of about 37,000 cfs or greater (Figure 5.4.3.26-4). Table 5.4.3.26-1 denotes the flows above which 95%, 50%, and 5% of all erosion occurs at the site as well as the amount of time those flows were exceeded for each year in the modeling period. There are two significant geotechnical failures that account for the bulk of the geotechnical erosion, whereas hydraulic erosion is fairly consistent across the range of flows above 37,000 cfs, with a larger peak between 48,000 and 72,000 cfs. Through this analysis we can conclude that those flows greater than the combined hydraulic capacity of Vernon and Northfield Mountain are accounting for most of the total erosion. The same additional moderate flow analysis completed for site 119BL and 87BL was performed on this site. Moderate flows at 75BL contribute about 13% of the total erosion. Northfield Mountain operations were reviewed and determined to occur about 1.2% of the time over the period of record under moderate flows. This equates to about 0.16% additional contribution by Northfield Mountain resulting in no significate change to the Scenario 1 results.

It should be noted that at this site, the Baseline Condition flows did not result in the greatest amount of erosion. One possible cause for this is that the peaking operations at Northfield Mountain are creating greater fluctuations in water surface elevations than would be created under a run-of-river scenario. By elimination of these fluctuations as seen in Scenario 1 this causes the shear stresses to be focused on a narrower band of the bank cross section, resulting in slightly higher hydraulic erosion which could cause an increase in the size of the individual bank failures.

Table 5.4.3.26-1: Flow Exceedance Calculations for Site 75BL

Site 75BL	Percent of Erosion		
	95%	**50%**	**5%**
	Flow (cfs)		
Year	**71,586**	**48,054**	**33,822**
2000	0.10%	2.30%	7.00%
2001	0.80%	3.70%	5.90%
2002	NA	1.20%	4.20%
2003	0.10%	3.10%	8.60%
2004	NA	0.70%	3.10%
2005	0.50%	4.40%	11.40%
2006	0.10%	2.50%	10.50%
2007	0.10%	3.20%	5.90%
2008	0.30%	5.70%	13.70%
2009	NA	1.90%	5.40%
2010	NA	2.70%	7.80%
2011	1.00%	6.40%	14.20%
2012	NA	0.20%	1.30%
2013	NA	0.30%	3.80%
2014	0.20%	2.60%	6.30%

NA: Not Applicable since flows did not reach this value

Figure 5.4.3.26-1 Photos at site 75BL

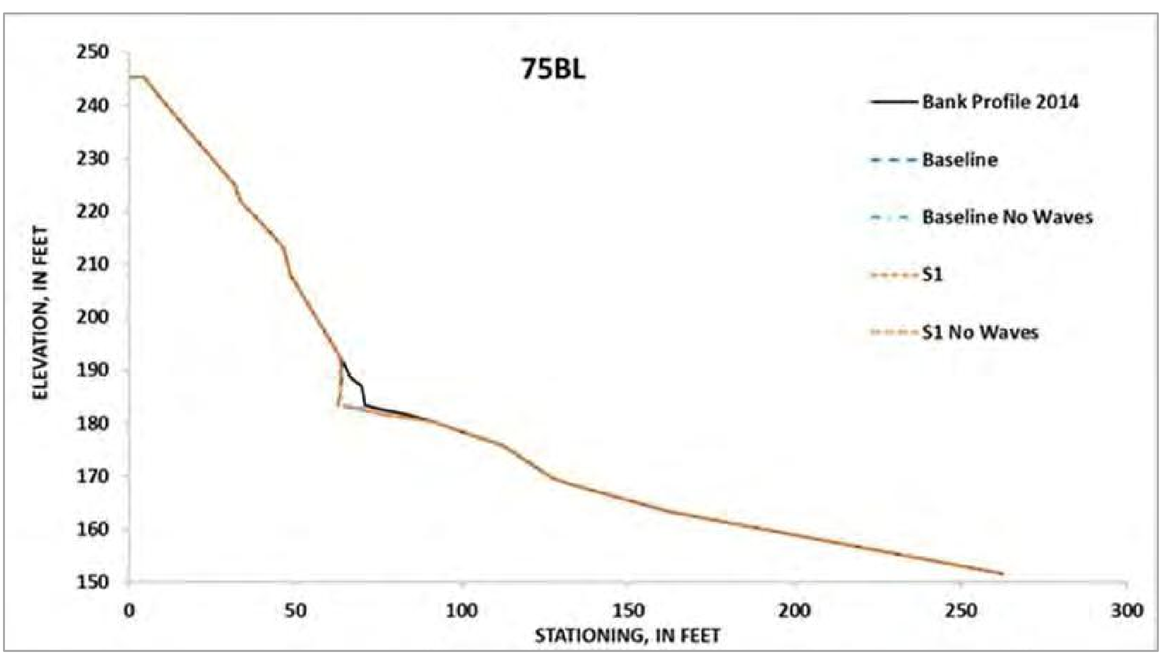

Figure 5.4.3.26-2: Simulated, future unit-erosion for the Baseline Condition (with boat waves on and off) and Scenario 1 at site 75BL for the period 2000-2014

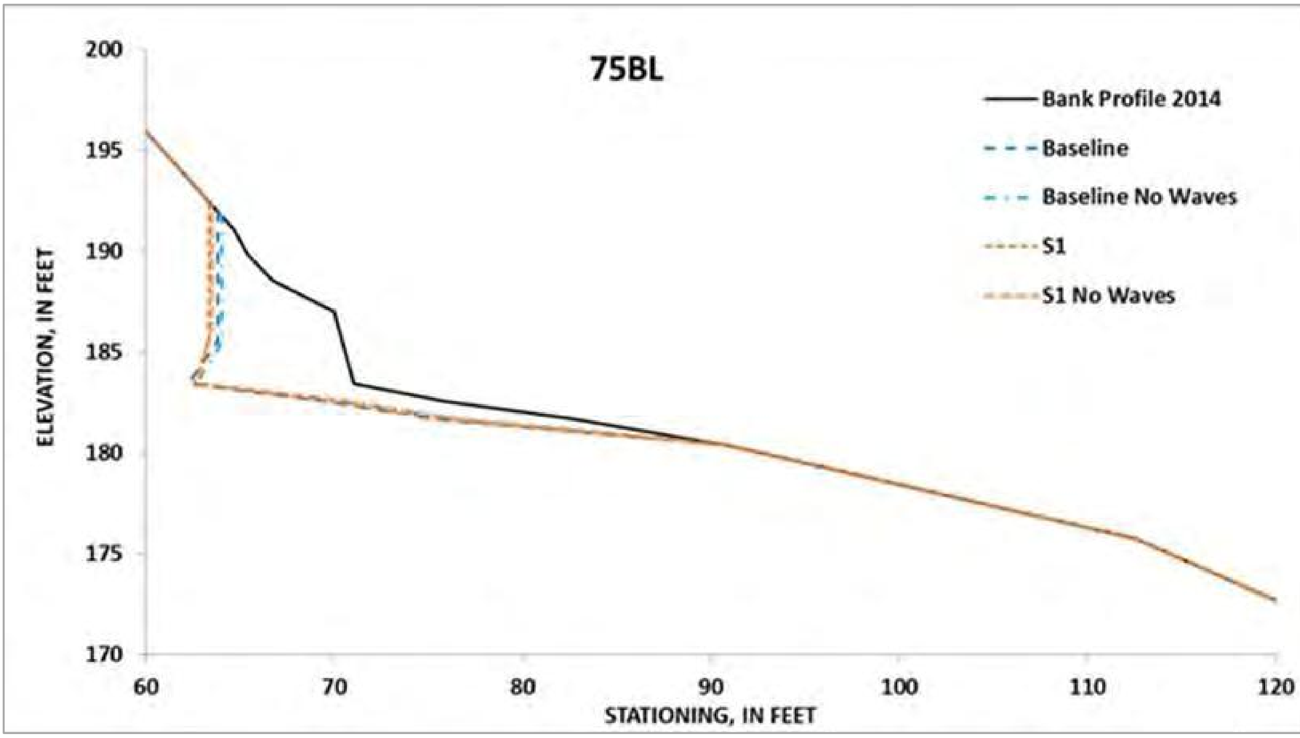

Figure 5.4.3.26-3: Simulated, future erosion for the Baseline Condition (with boat waves on and off) and Scenario 1 at site 75BL for the period 2000-2014. Zoomed in at area of erosion for illustrative purposes

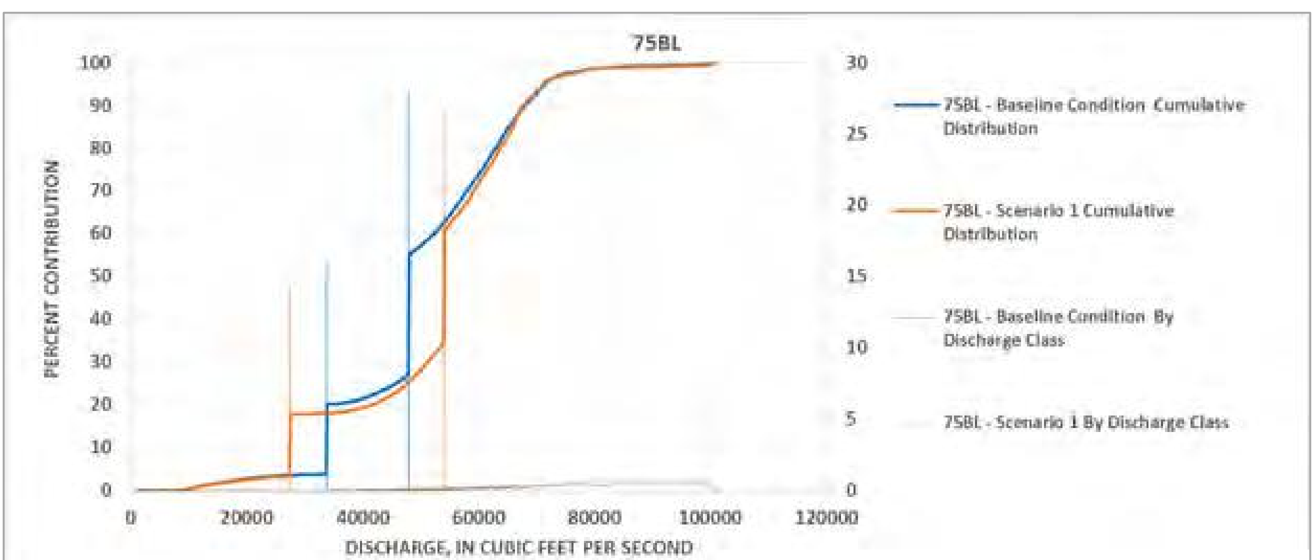

Figure 5.4.3.26-4: Simulated, percent contribution of total erosion by discharge for the Baseline Condition and Scenario 1 at site 75BL for the period 2000-2014

5.4.3.27 Site 9R Pre-Restoration

The river at site 9R (station 6,750) has moderately steep, sparsely vegetated banks and is located on the south side of the Barton Cove Campground. The bank is roughly 61 feet tall, with a sandy toe and a sandy-loam upper bank. The bank is thinly vegetated with Northern red oak, American basswood, and Green ash trees. There was a significant amount of bare soil noted on the bank face, likely due to the large trees and canopy cover (Figure 5.4.3.27-1).

BSTEM runs at this site for the Pre-restoration condition show that under the Baseline Condition, 43.8 ft^3 of erosion occurred per foot of bank, during the 2000 to 2008 flow period prior to restoration, averaging 5.43 ft^3/ft/y (Table 5.4.3-1). This results in the 6^{th} highest erosion rate for the Baseline Condition, placing it between the 80^{th} and 85^{th} percentiles of erosion rates along the reach. The modeling also indicates that all of the erosion is due directly to hydraulic processes.

Scenario 1 produced an erosion rate of 5.19 ft^3/ft/y (Figure 5.4.3.27-2 to Figure 5.4.3.27-4) resulting in a difference in an erosion rate relative to the Baseline Condition of 4.3%. Without the impact of boat waves, erosion rates for the Baseline Condition (Waves off) resulted in 0.967 ft^3/ft/y, indicating that boat-generated waves are an important contributor to erosion at this site. As there was a large difference between the Baseline Condition (Waves on) and Baseline Condition (Waves off), Scenario 1 was also investigated for the waves-off condition. With waves off the bank-erosion rate for Scenario 1 was 0.77 ft^3/ft/y. While the Baseline Condition had 82% more erosion with boat waves, Scenario 1 showed that bank-erosion rates were greater by 85% with waves.

Overall the difference between Baseline and S1 was found to be 4%; however, determining the causes of erosion at this site is not as simple as subtracting Baseline and S1, as was done at other sites. The difference in impact from boat waves between the Baseline Condition (82%) and S1 (85%) demonstrates how waves influence the erosion in this reach. When Northfield Mountain is set to idle (S1), erosion due to boat waves is 3% greater than if Northfield Mountain is online. In other words, it would appear that the effect of waves on the bank is reduced with Northfield Mountain operating. When taking boat waves into consideration, the actual percent reduction in erosion with the S1 Scenario is likely closer to 1%. This results in an S1 erosion amount of 0.075 ft^3/ft/y, which is lower than the measurable/significant rate of 0.163 ft^3/ft/y. Another factor compounding the S1 results in this area is the downstream boundary condition used to simulate the Turner Falls Dam. The historic dam operations were used as the boundary condition for S1 which resulted in potentially more TFI fluctuations than may have occurred had Northfield Mountain actually been idle. The increased water level fluctuations modeled in S1 may have actually led to less hydraulic erosion than would have occurred had the TFI been fluctuated less given that the location of the water surface on the bank varied more than it would have historically which would have prevented the repeated undercutting of the bank at the same location.

The proximity of the site to Turner Falls Dam precluded the development of a reliable stage-discharge relation. Because of this the high flow analysis which is based on the erosion amounts within a given range of discharges was not run for this site. Instead, stage was used (Figure 5.4.3.27-4). Still, it is clear that boat-generated waves are a dominant factor in erosion rates in the lower TFI producing 82% of the erosion. While moderate to high flow erosion rates could not be determined for this site, based on the trend throughout the TFI in reaches 2, 3, and 4 it is likely that moderate to high flows still play a role in total erosion.

Figure 5.4.3.27-1 Photos at site 9R Pre Restoration (Photo from 2013 FRR)

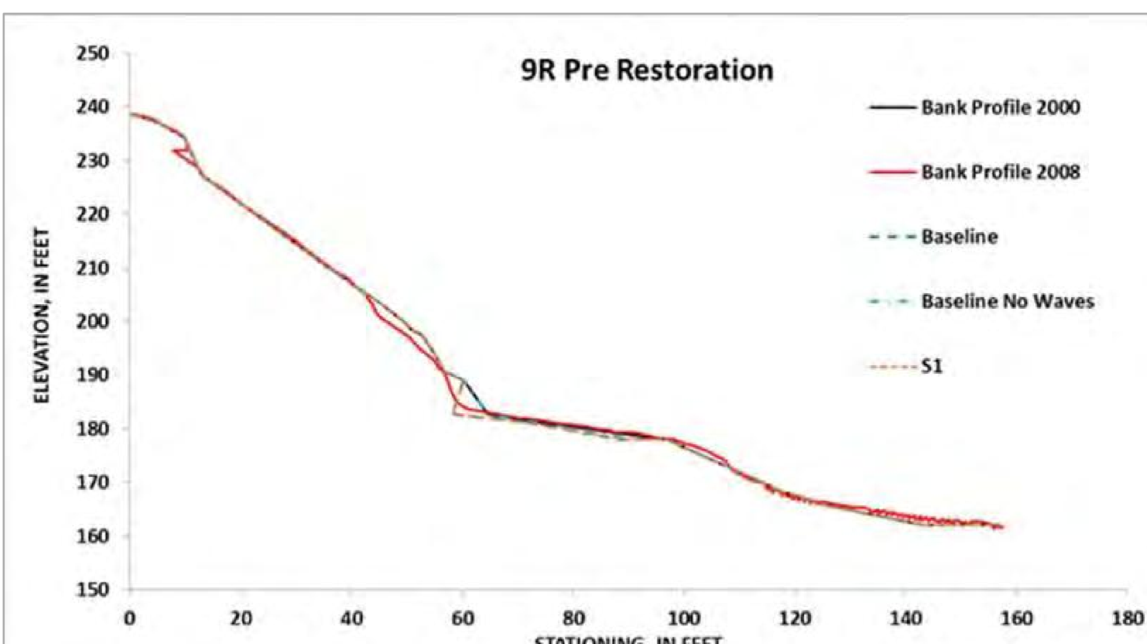

Figure 5.4.3.27-2: Simulated, future unit-erosion for the Baseline Condition and Scenario 1 (with boat waves on) at site 9R Pre Restoration for the period 2000-2008

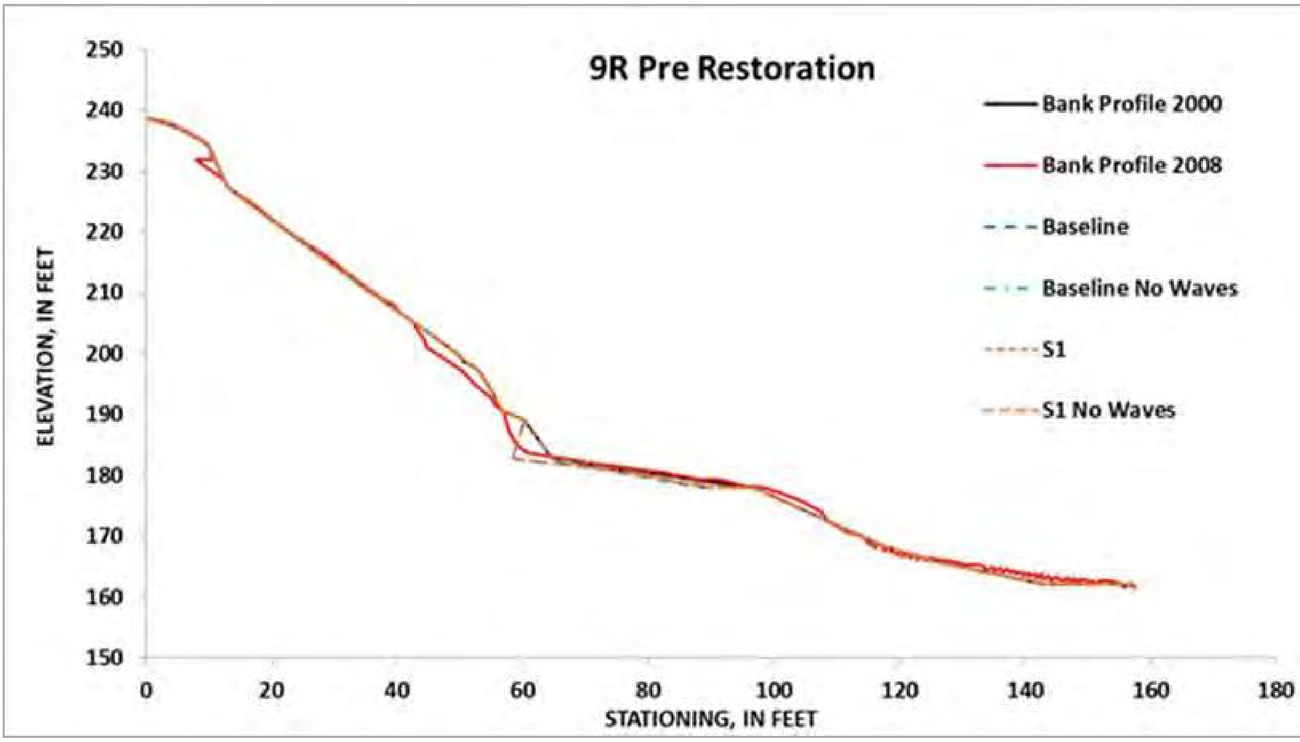

Figure 5.4.3.27-3: Simulated, future unit-erosion for the Baseline Condition (with boat waves on and off) and Scenario 1 at site 9R Pre Restoration for the period 2000-2008

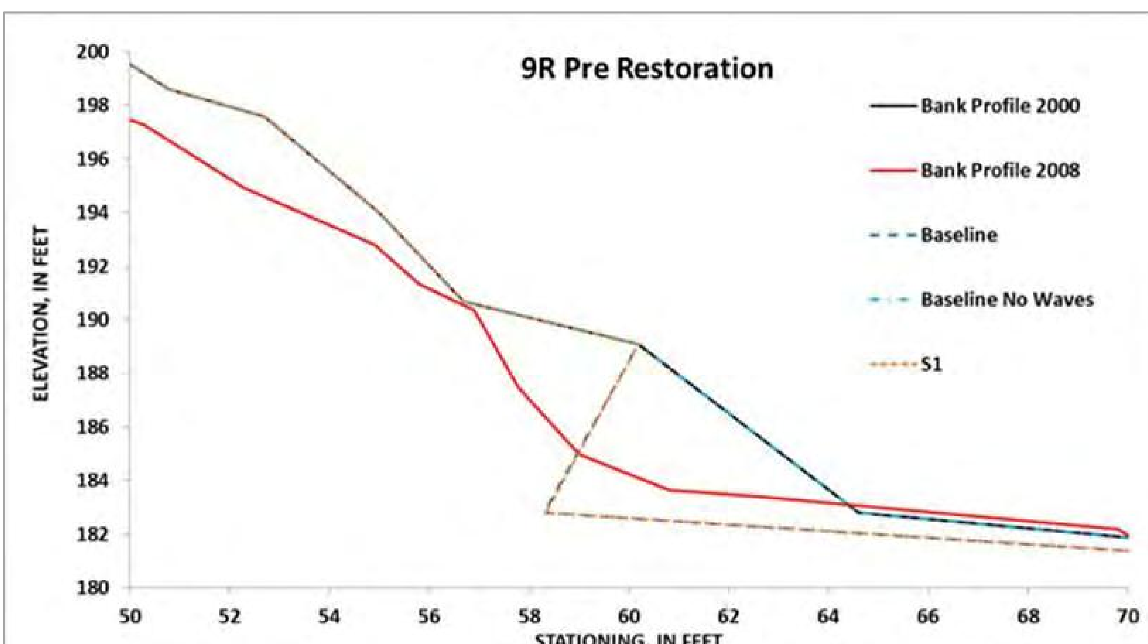

Figure 5.4.3.27-4: Simulated, future erosion for the Baseline Condition and Scenario 1 (with boat waves on) at site 9R Pre Restoration for the period 2000-2008. Zoomed in at area of erosion for illustrative purposes

Figure 5.4.3.27-5: Simulated, percent contribution of total erosion by stage for the Baseline Condition and Scenario 1 at site 9R Pre Restoration for the period 2000-2008. As no stage-discharge relationship could be developed, stage was used

5.4.3.28 Site 9R Post Restoration

As part of the site restoration in 2008, coir or other logs were anchored at the bank toe. Vegetation was also planted on the upper bank (Figure 5.4.3.28-1). As there was no bank reshaping at this site as part of the restoration, the model inputs were only adjusted to account for the toe protection and vegetation. The output cross section from the 9R Pre-Restoration model was used as the starting section for the 9R Post Restoration model.

BSTEM runs at this site show that for Post-restoration under the Baseline Condition, 1.40 ft^3 of erosion occurred per foot of bank, during the 2008 to 2014 flow period, averaging 0.227 ft^3/ft/y (Table 5.4.3-1). This results in the 8th lowest erosion rate for the Baseline Condition, placing it between the 20th and 25th percentiles of erosion rates along the reach. The modeling also indicates that all of the erosion is due directly to hydraulic processes.

Scenario 1 had a resulting erosion amount of 0.224 ft^3/ft/y (Figure 5.4.3.28-2). The Baseline Condition (Waves off) resulted in 0.002 ft^3/ft/y, indicating a substantial reduction in bank-erosion rates with the removal of the impacts from boat-generated waves. As there was a large difference between the Baseline Condition (Waves on) and Baseline Condition (Waves off), Scenario 1 was investigated for the waves off condition as well. This resulted in 1.50 x10-3 ft^3/ft/y of erosion for Scenario 1 (Note- while this site did show a small reduction in erosion between the BL and S1 Scenarios the total reduction in erosion is well below the measureable/significant rate of 0.163 ft^3/ft/yr). The highest water surface elevation for this period occurred at 184.5 ft. Most of the measured erosion for this site appears to occur above 190 feet. This erosion does not appear to be a function of the TFI hydraulics. For erosion to be present above the high water line, toe erosion would need to occur and then a geotechnical failure would occur above. The toe for this site, based on survey data, has not eroded significantly since the restoration to the point where a geotechnical failure would occur.

As a stage-discharge relation could not be developed for site 9R the high flow analysis is presented according to stage data only (Figure 5.4.3.28-3). Boat-generated waves are a dominant factor in erosion rates at this site producing 99% of the erosion.

Figure 5.4.3.28-1 Photos at site 9R Post Restoration

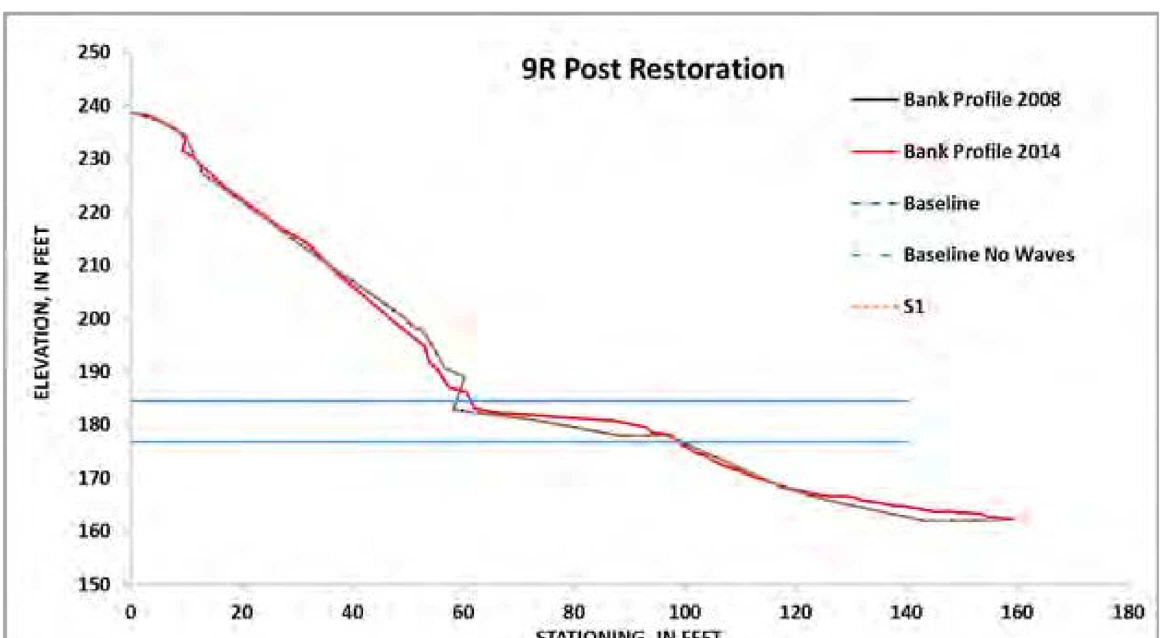

Figure 5.4.3.28-2: Simulated, future unit-erosion for the Baseline Condition (with boat waves on and off) and Scenario 1 at site 9R Post Restoration for the period 2008-2014, with a minimum water surface elevation of 176.9 feet and a maximum water surface elevation of 184.5 feet.

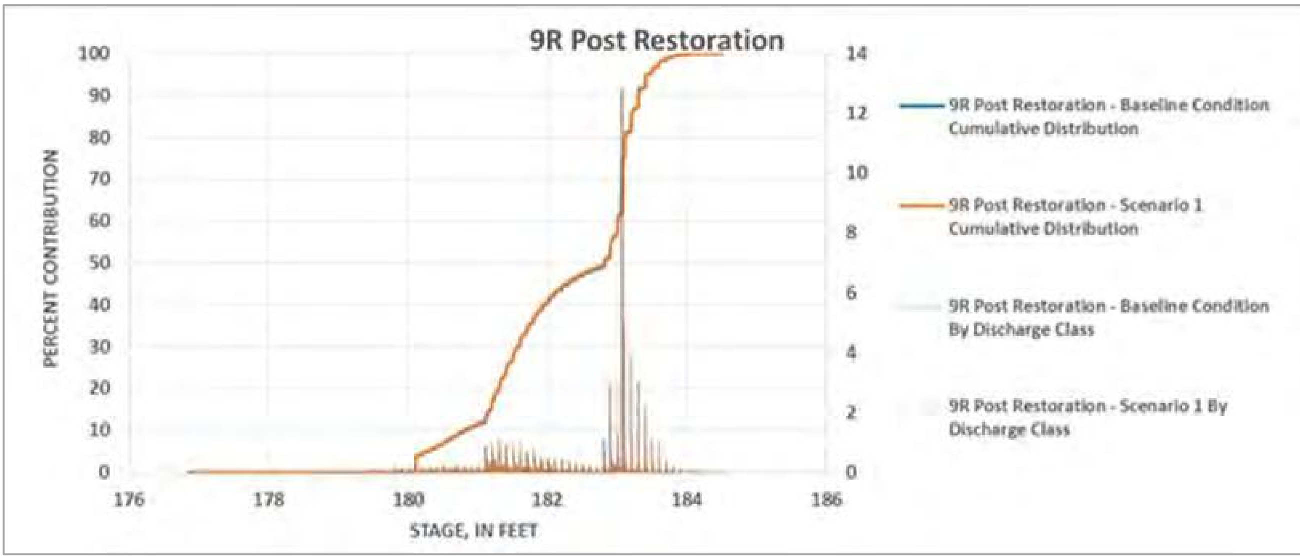

Figure 5.4.3.28-3: Simulated, percent contribution of total erosion by stage for the Baseline Condition and Scenario 1 at site 9R Post Restoration for the period 2008-2014. As no stage-discharge relationship could be developed, stage was used.

5.4.3.29 Site 12BL

The river at site 12BL (station 6,500) has steep, heavily vegetated banks, and is located slightly downstream and across the river from site 9R. The bank is roughly 51 feet tall, and the toe material consists of coarse sand. Large Birch, Oak, and Hemlock cover most of the upper bank. Parts of the lower bank, however, show signs of erosion, with sloughed material against the in-situ bank face (Figure 5.4.3.29-1). No historical cross sections exist for this site thus a 2014 survey was used as the initial geometry for the model runs.

BSTEM runs at this site show that under the Baseline Condition, 32.6 ft^3 of erosion occurred per foot of bank, during the 2000 to 2014 flow period, averaging 2.22 ft^3/ft/y (Table 5.4.3-1). This results in the 12th highest erosion rate for the Baseline Condition, placing it between the 60th and 65th percentiles of erosion rates along the reach. The modeling also indicates that roughly 74% (1.65 ft^3/y) of the erosion is due directly to hydraulic processes, whereas the other 26% (0.57 ft^3/y) is the result of geotechnical processes and associated mass failures.

For Scenario 1, 2.15 ft^3/ft/y of erosion occurred (Figure 5.4.3.29-2 to Figure 5.4.3.29-4) resulting in about 3% of the total erosion (Note- while this site did show a small reduction in erosion between the BL and S1 Scenarios the total reduction in erosion is well below the measureable/significant rate of 0.163 ft^3/ft/yr). With the lower variability in water surface fluctuations at this site we see a bigger wave influence. The Baseline Condition (Waves off) resulted in 0.239 ft^3/ft/y representing about 89% of the total erosion, attesting to the important role of boat-generated waves in inducing erosion at this site. As Baseline Condition (Waves off) scenario illustrated a significant reduction in erosion, Scenario 1 was also run without the effects of boat waves. With waves off the model run for Scenario 1 resulted in 0.194 ft^3/ft/y. Clearly, boat waves are significant for all Operational scenarios and, therefore, protection of the bank-toe region could limit further bank erosion at this site.

As a stage-discharge relation could not be developed for site 12BL, the high flow analysis is presented according to stage data only (Figure 5.4.3.29-5). Boat-generated waves are a dominant factor in erosion rates at this site producing 89% of the erosion. While moderate to high flow erosion rates could not be determined for this site, based on the trend throughout the impoundment in reaches 2, 3, and 4 it is likely that moderate to high flows still play a contributing role in total erosion.

Figure 5.4.3.29-1 Photos at site 12BL

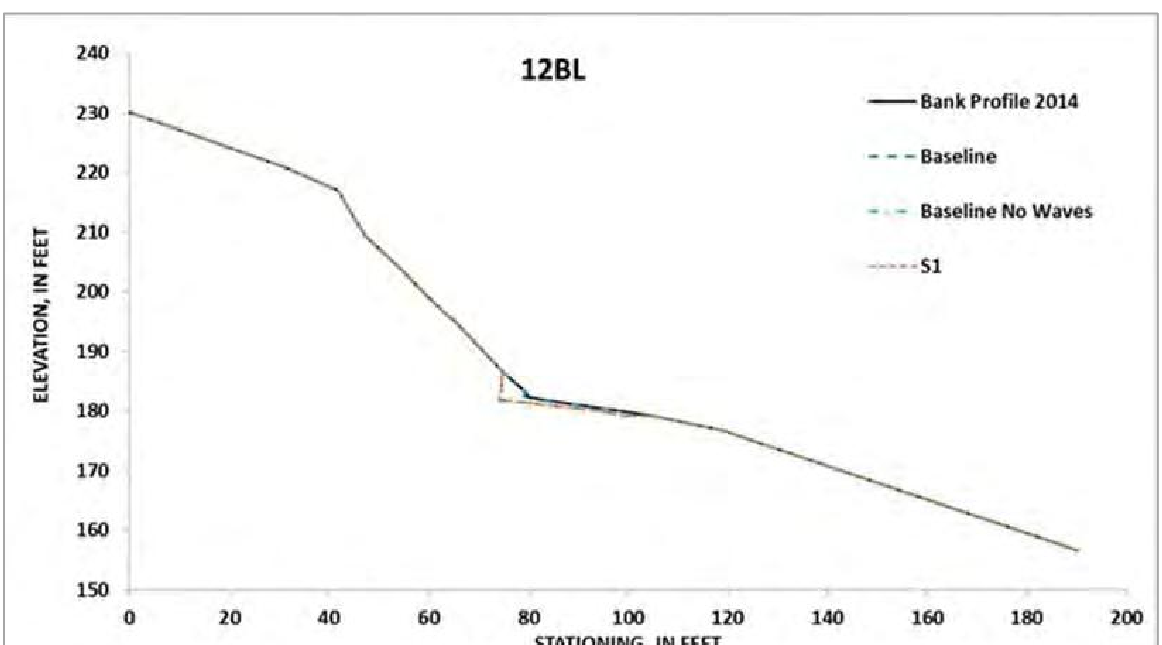

Figure 5.4.3.29-2: Simulated, future unit-erosion for the Baseline Condition and Scenario 1 (with boat waves on) at site 12BL for the period 2000-2014

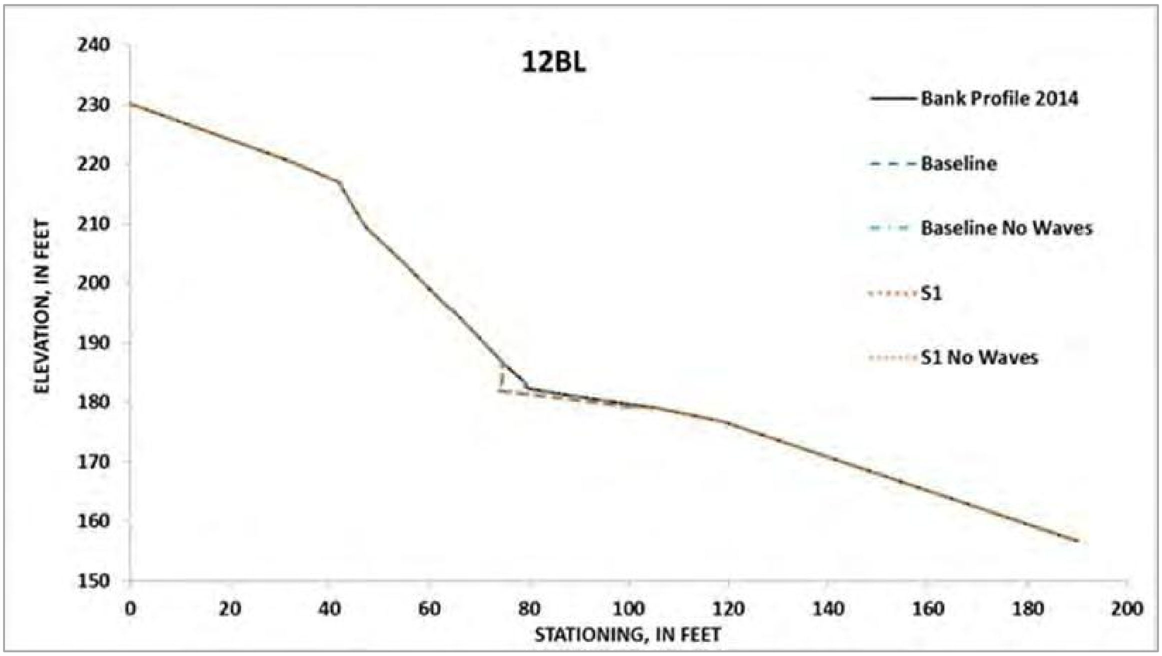

Figure 5.4.3.29-3: Simulated, future unit-erosion for the Baseline Condition (with boat waves on and off) and Scenario 1 at site 12BL for the period 2000-2014

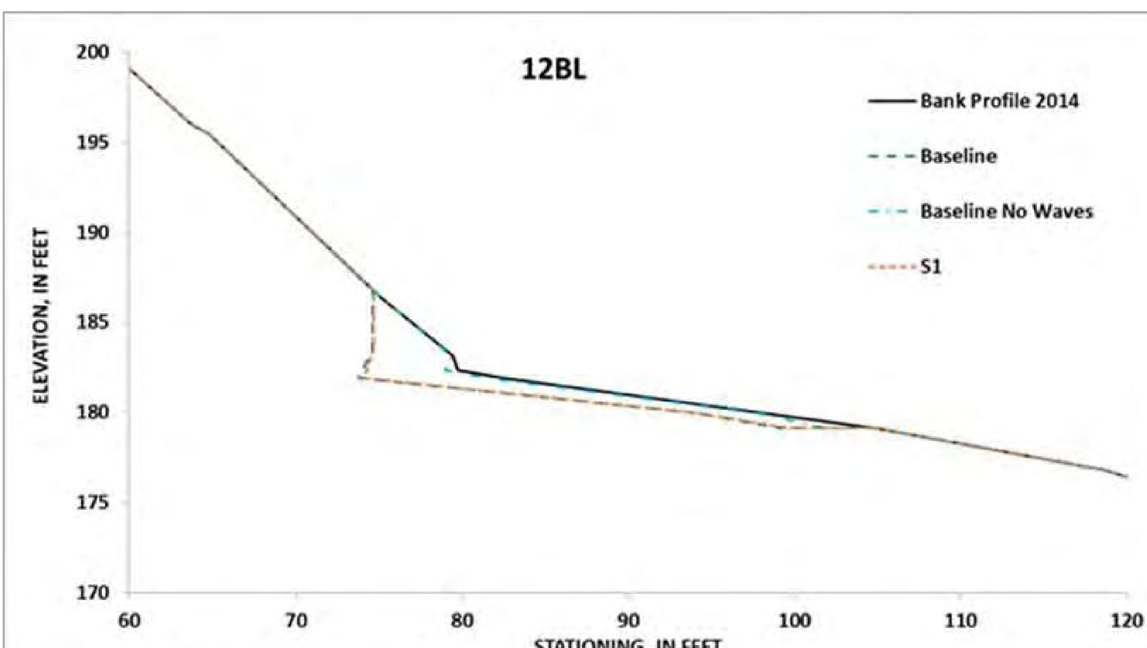

Figure 5.4.3.29-4: Simulated, future erosion for the Baseline Condition and Scenario 1 (with boat waves on) at site 12BL for the period 2000-2014. Zoomed in at area of erosion for illustrative purposes.

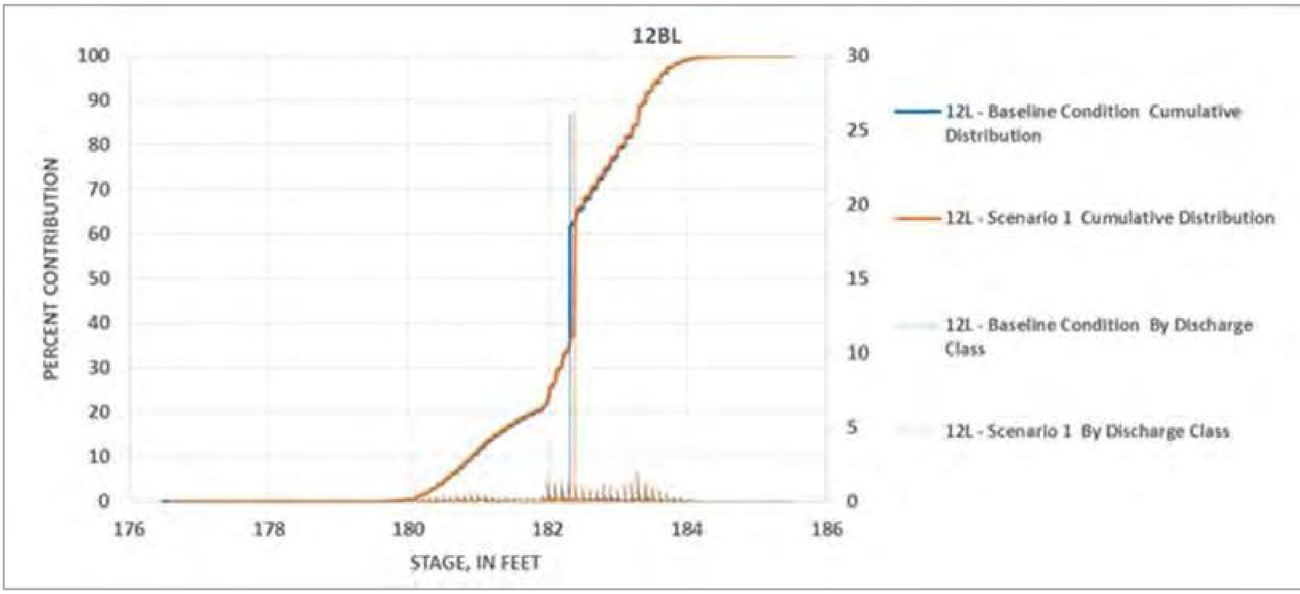

Figure 5.4.3.29-5: Simulated, percent contribution of total erosion by stage for the Baseline Condition and Scenario 1 at site 12BL for the period 2000-2014. As no stage-discharge relationship could be developed, stage was used.

5.4.3.30 Site BC-1R

The river at site BC-1R (station 4,750) has moderately steep, heavily vegetated banks and is located on the north side of the Barton Cove Campground, immediately upstream of the Turners Falls Dam. The bank is roughly 20 feet tall, with a silty-loam toe and a sandy upper bank. The bank face and bank top are heavily vegetated with Black birch, Eastern hemlock, Eastern white pine, and Northern red oak trees. There was a significant amount of bare soil noted on the bank face, likely due to the large trees and canopy cover (Figure 5.4.3.30-1).

BSTEM runs at this site show that under the Baseline Condition, 2.70 ft^3 of erosion occurred per foot of bank, during the 2000 to 2014 flow period, averaging 0.190 $ft^3/ft/y$ (Table 5.4.3-1). This results in the 6th lowest erosion rate for the Baseline Condition, placing it between the 15th and 20th percentiles of erosion rates along the reach. The modeling also indicates that 100% of the bank erosion is due directly to hydraulic processes, and none of the bank erosion is the result of mass failures.

For Scenario 1, 0.189 $ft^3/ft/y$, of erosion occurred (Figure 5.4.3.30-2 to Figure 5.4.3.30-3) resulting in the percent reduction in erosion rates of 0.237%. With the lower variability in water surface fluctuations at this site we see a bigger wave influence. As there was a large difference between the Baseline Condition (Waves on) and Baseline Condition (Waves off), Scenario 1 was investigated for the waves-off condition as well. This resulted in virtually no erosion with 8.42x10-9 $ft^3/ft/y$. Thus, boat-generated waves are the dominant cause (almost 100%) for the small amount of bank erosion at this site.

As a stage-discharge relation could not be developed for site BC-1R, the high flow analysis is shown with stage data only (Figure 5.4.3.30-4).

Figure 5.4.3.30-1 Photos at site BC1R

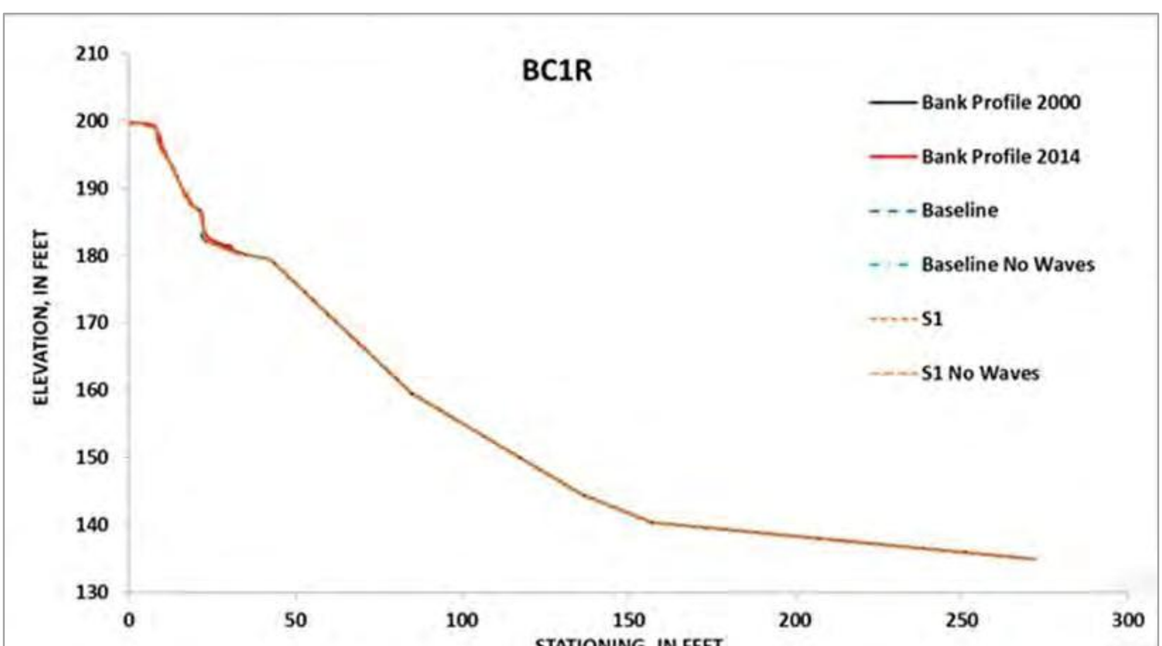

Figure 5.4.3.30-2: Simulated, future unit-erosion for the Baseline Condition (with boat waves on and off) and Scenario 1 at site BC-1R for the period 2000-2014

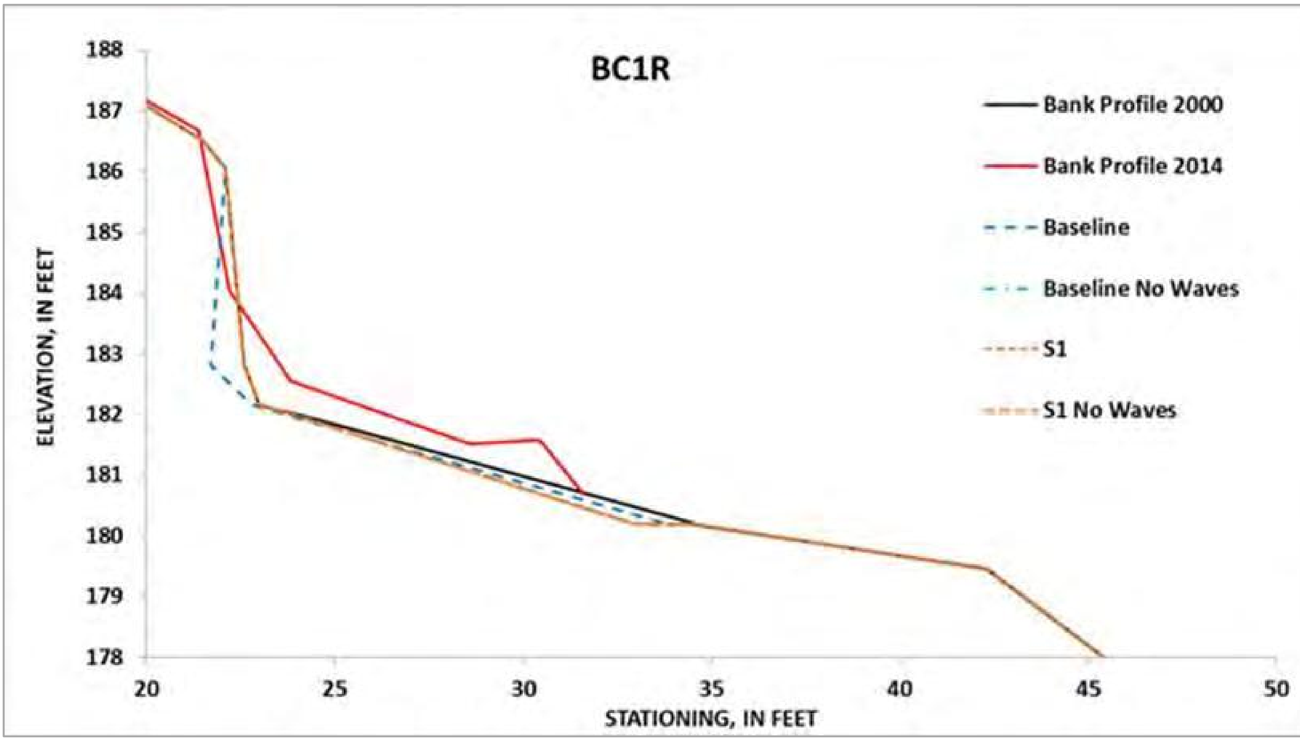

Figure 5.4.3.30-3: Simulated, future erosion for the Baseline Condition (with boat waves on and off) and Scenario 1 at site BC-1R for the period 2000-2014. Zoomed in at area of erosion for illustrative purposes

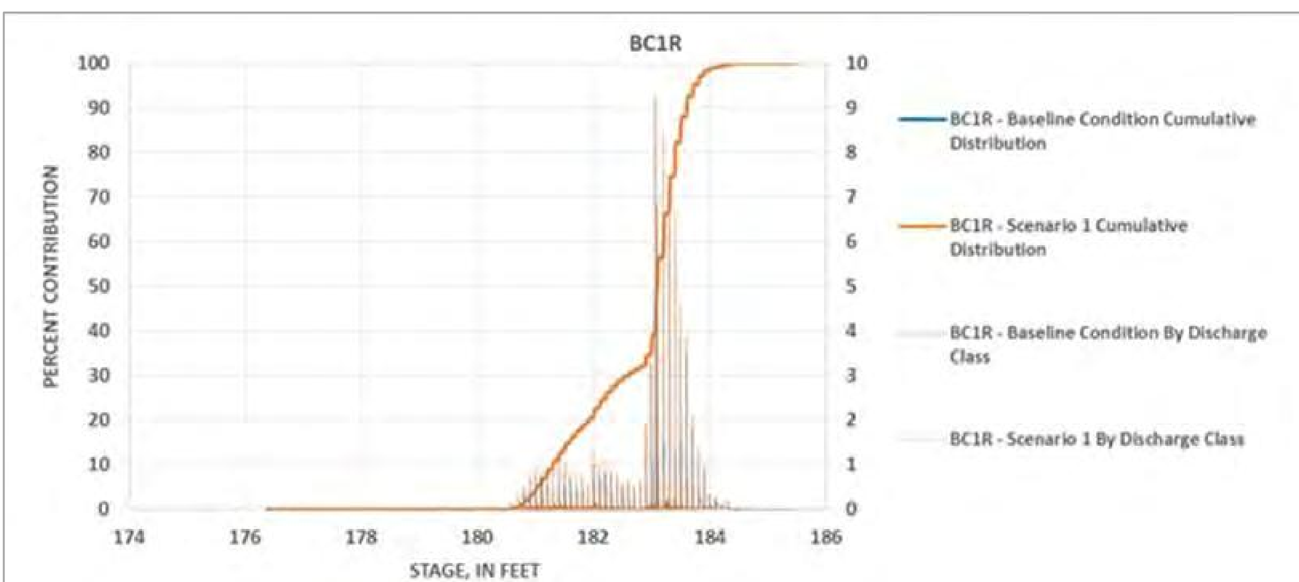

Figure 5.4.3.30-4: Simulated, percent contribution of total erosion by stage for the Baseline Condition and Scenario 1 at site BC-1R for the period 2000-2014. As no stage-discharge relationship could be developed, stage was used.

5.5 Analysis of the Causes of Erosion – Supplemental Analyses

Supplemental analyses discussed in this section served three primary purposes: (1) to serve as a means of comparison against the BSTEM results discussed in the previous section; (2) to investigate the potential primary causes of erosion not included in the BSTEM analysis (i.e. land management practices and ice); and (3) to examine secondary causes of erosion present in the TFI (i.e. animals and unique hydraulic and/or geomorphic conditions).

5.5.1 Hydraulic Shear Stress

Flowing water imparts a force on the river banks (i.e. hydraulic shear stress) which is counteracted by forces which resist sediment movement (i.e. primarily the weight of the soil particles in non-cohesive sediment, or physiochemical inter-particle forces in cohesive sediment). The comparison of these forces dictates if hydraulic erosion and sediment transport occur. Hydraulic erosion occurs on a particle by particle basis when the hydraulic shear stress (i.e. boundary shear stress) exceeds a threshold resistive force (i.e. critical shear stress), causing sediment particles to be dislodged and transported downstream. Further discussion on the estimation of the critical shear stress (τ_c) was provided in Section 4 (i.e. Sections 4.2.6.2 and 4.2.6.6), while the bed shear stress (τ_o) can be computed as follows:

$$\tau_o = \rho * u_*^2 \qquad (3)$$

Where τ_o is the boundary shear stress (i.e. hydraulic shear stress), ρ is the density of water, and u_* is the shear velocity.

5.5.1.1 <u>Analysis of velocity and shear stress data – Detailed Study Sites</u>

Table 5.5.1.1-1 provides a comparison of τ_c with τ_o at 23 of the detailed study sites for the six River2D production runs discussed earlier in Section 5 (i.e. Section 5.2.2). The critical shear stress presented in this table represents the median τ_c obtained from the jet test data for each site as presented in Table 4.2.6.6-1. For the computation of the bed shear stress, this analysis assumed a water density appropriate for water with a temperature of approximately 60 degrees Fahrenheit (i.e. 998.9 kg/m^3), while the shear velocity was obtained from the River2D production runs discussed in earlier in Section 5. The River2D results indicate that the hydraulic shear stress is only sufficient to cause erosion when flows at Turners Falls Dam exceed approximately 30,000 cfs (i.e. Operation Rule Threshold A), and may be insufficient to cause erosion at approximately half of the detailed study sites under a 100-year return period event. It should be noted that the River2D results are being compared to the median critical shear value, which means that some erosion may still occur.

Table 5.5.1.1-1: Comparison of Critical Shear Stress and River2D Bed Shear Stress at Detailed Study Sites[42]

Detailed Study Site	Critical Shear Stress, τ_c	Bed Shear Stress, τ_o					
		Generating Capacity at Turners Falls Dam	Operation Rule Threshold A	Operation Rule Threshold B	10-Year Return Period	50-Year Return Period	100-Year Return Period
2L	0.137	0.00	0.00	0.30	0.78	2.00	2.95
3L	0.777	0.00	0.01	0.32	0.26	0.01	0.18
3R	0.639	0.00	0.00	0.03	0.06	0.43	1.33
4L	0.106	0.00	0.09	0.80	2.58	3.44	3.74
5CR	1.03	0.00	0.00	0.06	0.17	0.45	0.98
6AL	0.64	0.00	0.00	0.04	0.13	0.13	0.08
6AR	0.475	0.01	0.09	1.50	1.82	2.29	2.46
7L	0.748	0.05	0.25	0.81	1.38	1.86	2.34
7R	7.14	0.00	0.00	0.01	0.11	0.18	0.22
8BL	3.33	0.00	0.00	0.04	0.14	0.56	0.88
8BR	0.627	0.01	0.06	0.13	0.21	0.59	0.88
9R	10.3	0.00	0.00	0.02	0.14	0.74	1.34
10L	0.585	0.00	0.00	0.11	0.41	0.06	0.17
10R	3.47	0.00	0.01	0.23	0.59	1.37	1.71
11L	2.91	0.00	0.02	0.89	0.58	0.01	0.03
18L	3.27	0.00	0.00	0.03	0.07	0.15	0.22
21R	0.1945	0.00	0.00	0.18	0.30	0.71	1.66
26R	0.024	0.00	0.00	0.14	0.20	0.39	0.48
29R	1.51	0.00	0.00	0.05	0.19	0.73	1.09
75BL	3.41	0.00	0.00	0.12	0.02	0.08	0.14
87BL	0.082	0.00	0.00	0.01	0.01	0.04	0.23
119BL	0.0025	0.00	0.00	0.00	0.05	0.29	0.61
303BL	2.49	0.00	0.00	0.12	0.08	0.08	0.45

[42] Refer to Table 5.2.2-1 for flow thresholds associated with the six bed shear stress categories.

5.5.1.2 Analysis of velocity and shear stress data – Unique Hydraulic Conditions

A one dimensional model assumes that flow is evenly distributed, however, this only holds true for a straight channel with symmetrical cross section geometry and roughness which is not typically the case in a natural river system. The River2D results provided insight into the distribution of flow within the channel, leading to unique hydraulic characteristics which can impact the potential for erosion.

When a channel changes direction, the velocity is higher on the outside of the bend as opposed to the inside of a bend. This leads to a higher chance for erosion on the outside of the bend, and a higher chance for sediment to be deposited on the inside of the bend. Sometimes the distribution of flow in a channel can vary with the magnitude of the flow, as shown in Figure 5.5.1.2-1. Access to other flow paths (e.g. the island in the figure) redistributes flow within the river, which in this case resulted in lower velocities along the bank near Site 11L. Such occurrences help to explain how the bed shear stress can be lower despite a higher total flow in the river. The ultimate impact to bank erosion caused by flow distribution may depend on the severity of bends in the river, channel geometry (e.g. alternate flow paths), the magnitude of flow, nearby bank materials, and other factors.

Additionally, significant changes in channel geometry, whether natural (e.g. rock outcrops or deep chasms) or manmade (e.g. bridge abutments and piers) can impact the flow distribution. Natural chasms exist within the Connecticut River, such as the more than 120 foot deep King Philip's Abyss and French King Hole located approximately 3 miles upstream of the Turners Falls Dam. The River2D model indicates that eddies are formed due to these chasms, as shown in Figure 5.5.1.2-2. Similarly, the model indicates that eddies form approximately 5 miles downstream of Vernon Dam, immediately downstream of an old bridge (i.e. whose deck has been removed, but abutments and piers remain), as shown in Figure 5.5.1.2-3. This figure shows that the magnitude and presence of recirculation can also be impacted by the magnitude of flow in the river.

Previous reports submitted to FERC have documented eddying downstream of Vernon Dam and near the Route 10 Bridge. Figure 5.5.1.2-4 shows an example of eddying in these areas despite the model using a coarser mesh resolution (i.e. as discussed in Section 5.2.2) near Vernon Dam and upstream of the Route 10 Bridge. The eddying downstream of Vernon Dam was noted to be more significant with increased flow, while the eddying in the vicinity of the Route 10 bridge was noted both upstream and downstream of the bridge depending on the flow. While other locations along the Connecticut River also exhibited eddying, only select examples were included for reporting purposes. The ultimate impact to bank erosion caused by changes in channel geometry (i.e. natural or manmade) may depend on the eddy location, the magnitude of flow, nearby bank materials, and other factors.

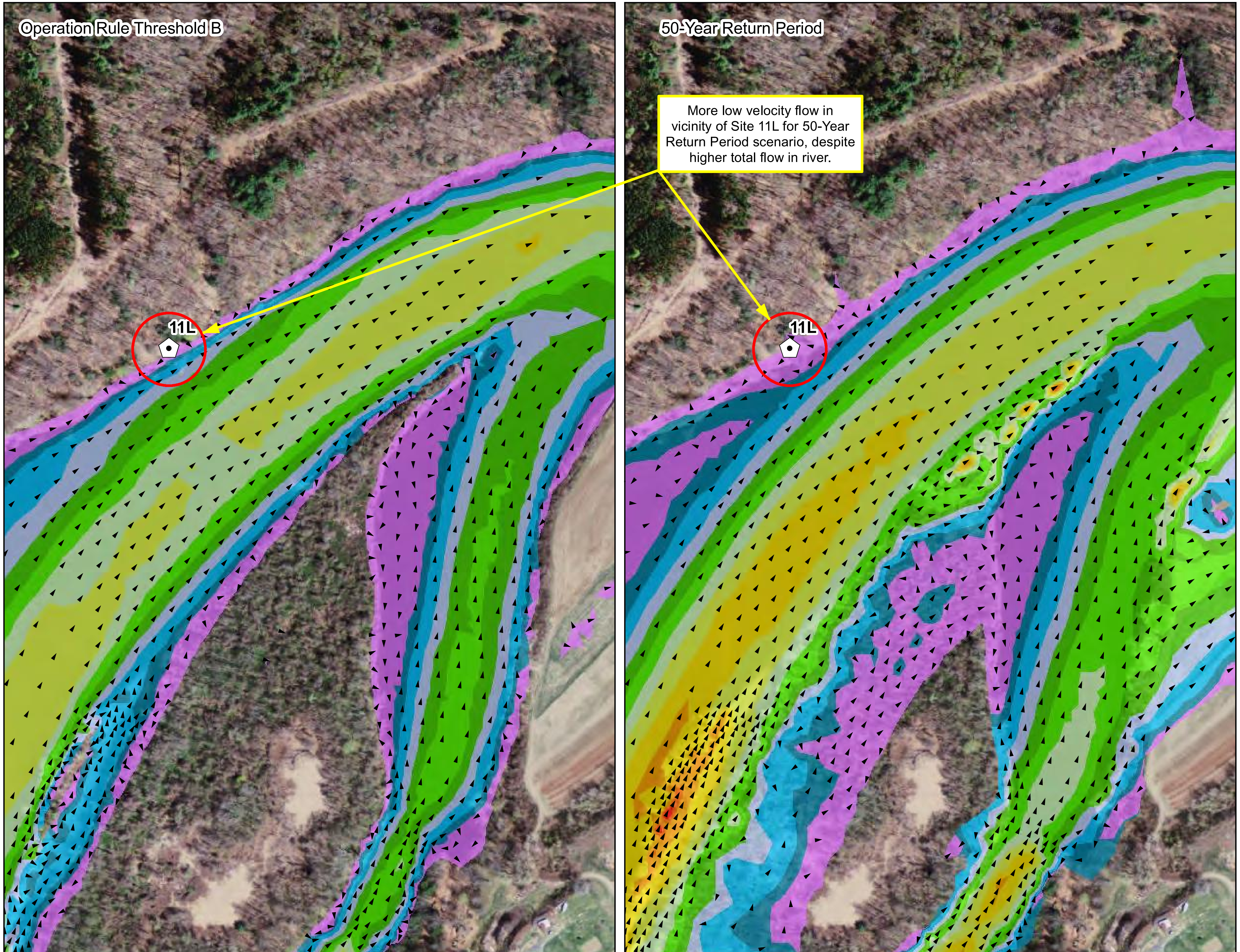

FIRSTLIGHT HYDRO GENERATING COMPANY
Northfield Mountain Pumped Storage Project No. 2485
Turners Falls Hydroelectric Project No. 1889

STUDY 3.1.2

Figure 5.5.1.2-1:
Impact of Flow Magnitude
on Flow Distribution

Legend

- Erosion Study Site
- Velocity Direction

Velocity Magnitude

- >10 (ft/s)
- 9 - 10 (ft/s)
- 8 - 9 (ft/s)
- 7 - 8 (ft/s)
- 6 - 7 (ft/s)
- 5 - 6 (ft/s)
- 4 - 5 (ft/s)
- 3 - 4 (ft/s)
- 2 - 3 (ft/s)
- 1 - 2 (ft/s)
- 0.5 - 1 (ft/s)
- 0 - 0.5 (ft/s)

N

Service Layer Credits: Sources: Esri, HERE, DeLorme, Intermap, increment P Corp., GEBCO, USGS, FAO, NPS, NRCAN, GeoBase, IGN, Kadaster NL, Ordnance Survey, Esri Japan, METI, Esri China (Hong Kong), swisstopo, MapmyIndia, © OpenStreetMap

0 150 300 600 Feet

1 inch = 300 feet

FirstLight Power Resources

Path: W:\gis\studies\3_1_2\maps\final_report\figure_5_5_1_2-1.mxd

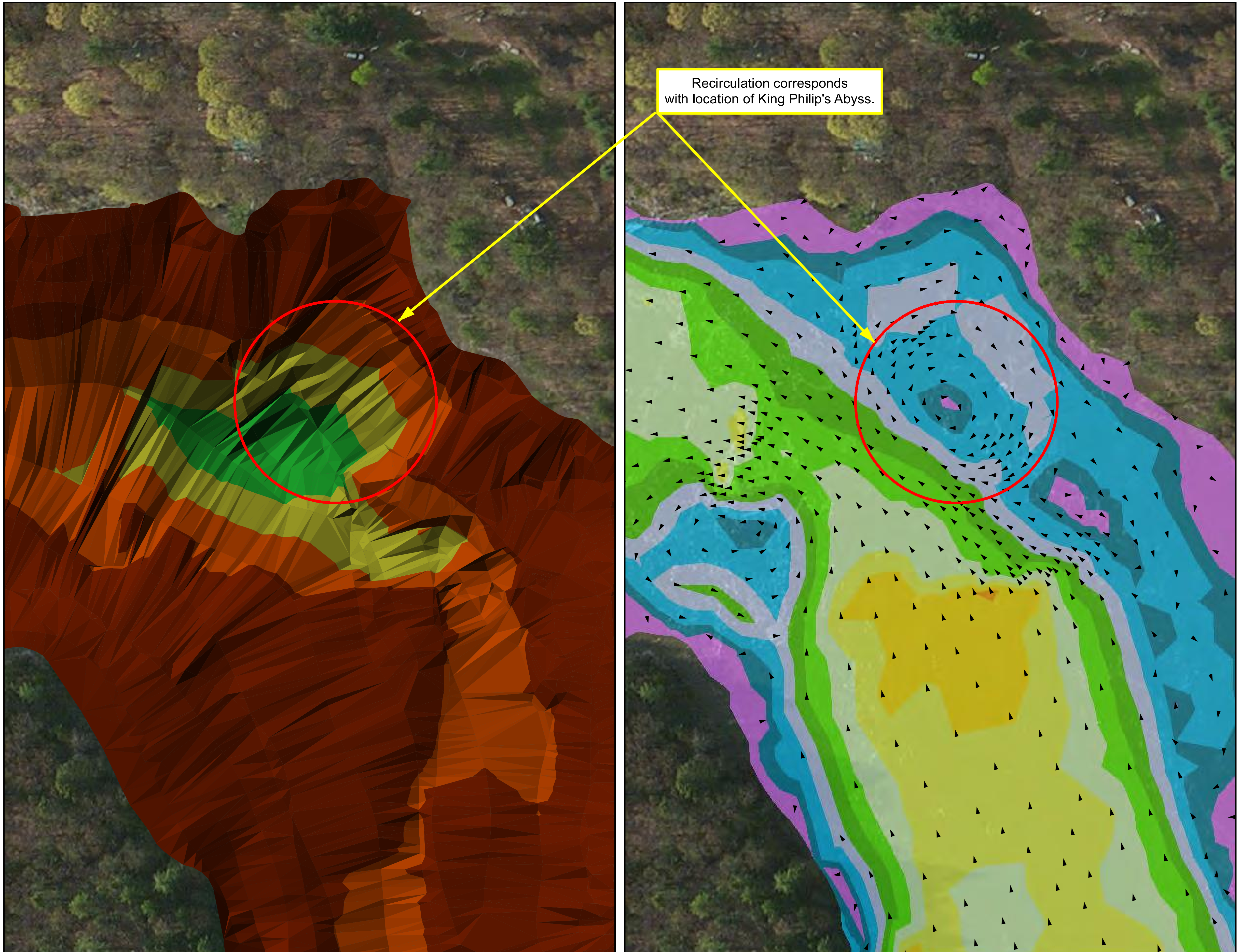

FIRSTLIGHT HYDRO GENERATING COMPANY
Northfield Mountain Pumped Storage Project No. 2485
Turners Falls Hydroelectric Project No. 1889

STUDY 3.1.2

Figure 5.5.1.2-2:
Eddy Formation in
King Philip's Abyss

Legend

Erosion Study Site

Velocity Direction

Velocity Magnitude

- >10 (ft/s)
- 9 - 10 (ft/s)
- 8 - 9 (ft/s)
- 7 - 8 (ft/s)
- 6 - 7 (ft/s)
- 5 - 6 (ft/s)
- 4 - 5 (ft/s)
- 3 - 4 (ft/s)
- 2 - 3 (ft/s)
- 1 - 2 (ft/s)
- 0.5 - 1 (ft/s)
- 0 - 0.5 (ft/s)

Bathymetry

- 240 - 272.309
- 210 - 240
- 180 - 210
- 150 - 180
- 120 - 150
- 90 - 120
- 60 - 90
- 30 - 60
- 0 - 30

N

Service Layer Credits: Sources: Esri, HERE, DeLorme, Intermap, increment P Corp., GEBCO, USGS, FAO, NPS, NRCAN, GeoBase, IGN, Kadaster NL, Ordnance Survey, Esri Japan, METI, Esri China (Hong Kong), swisstopo, MapmyIndia, © OpenStreetMap

0 50 100 200 Feet

1 inch = 100 feet

Path: W:\gis\studies\3_1_2\maps\final_report\figure_5_5_1_2-2.mxd

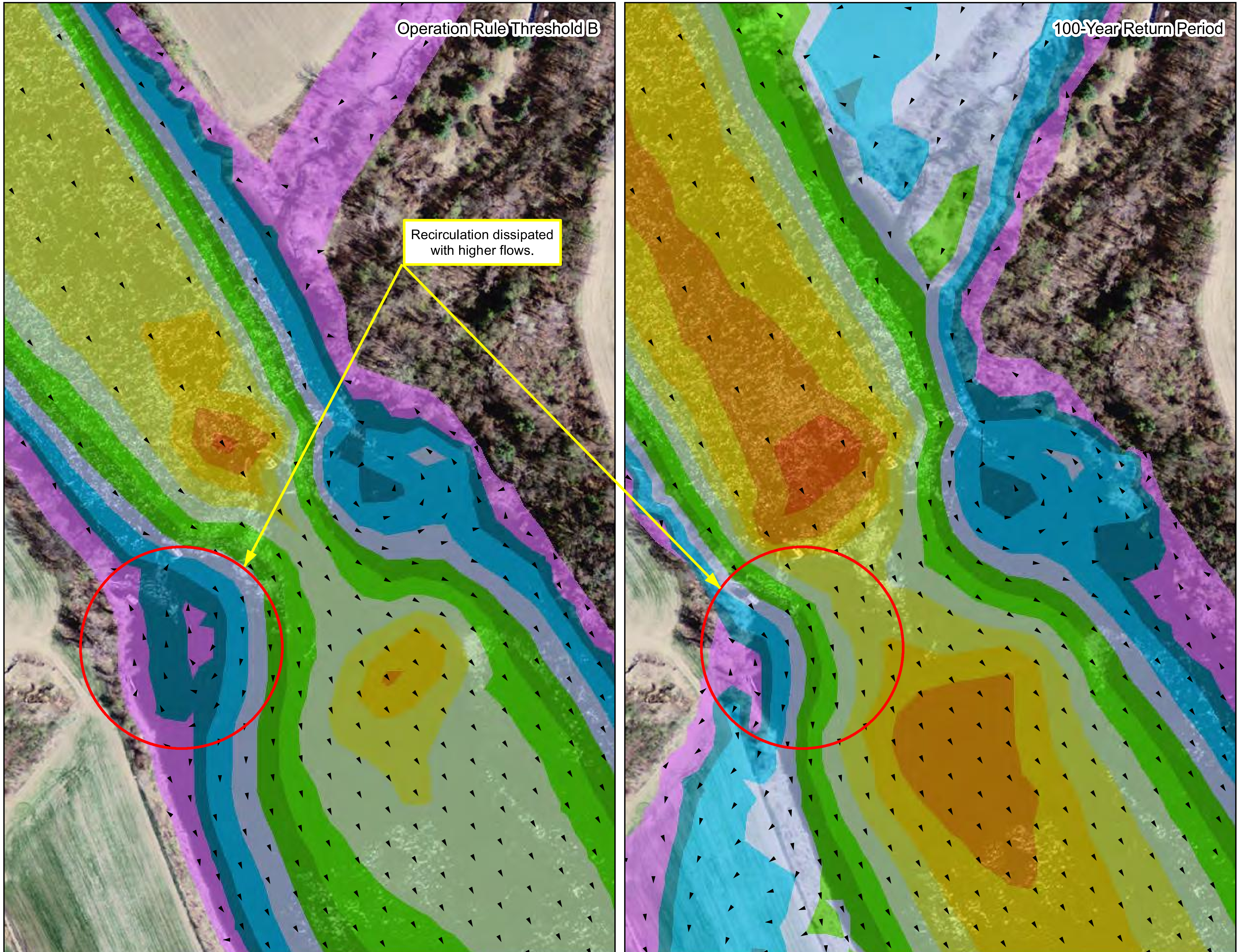

FIRSTLIGHT HYDRO GENERATING COMPANY
Northfield Mountain Pumped Storage Project No. 2485
Turners Falls Hydroelectric Project No. 1889

STUDY 3.1.2

Figure 5.5.1.2-3:
Impact of Flow Magnitude
on Eddies

Legend

N

Erosion Study Site

Velocity Direction

Velocity Magnitude

- >10 (ft/s)
- 9 - 10 (ft/s)
- 8 - 9 (ft/s)
- 7 - 8 (ft/s)
- 6 - 7 (ft/s)
- 5 - 6 (ft/s)
- 4 - 5 (ft/s)
- 3 - 4 (ft/s)
- 2 - 3 (ft/s)
- 1 - 2 (ft/s)
- 0.5 - 1 (ft/s)
- 0 - 0.5 (ft/s)

Service Layer Credits: Sources: Esri, HERE, DeLorme, Intermap, increment P Corp., GEBCO, USGS, FAO, NPS, NRCAN, GeoBase, IGN, Kadaster NL, Ordnance Survey, Esri Japan, METI, Esri China (Hong Kong), swisstopo, MapmyIndia, © OpenStreetMap

0 90 180 360 Feet

1 inch = 180 feet

FirstLight Power Resources

Path: W:\gis\studies\3_1_2\maps\final_report\figure_5_5_1_2-3.mxd

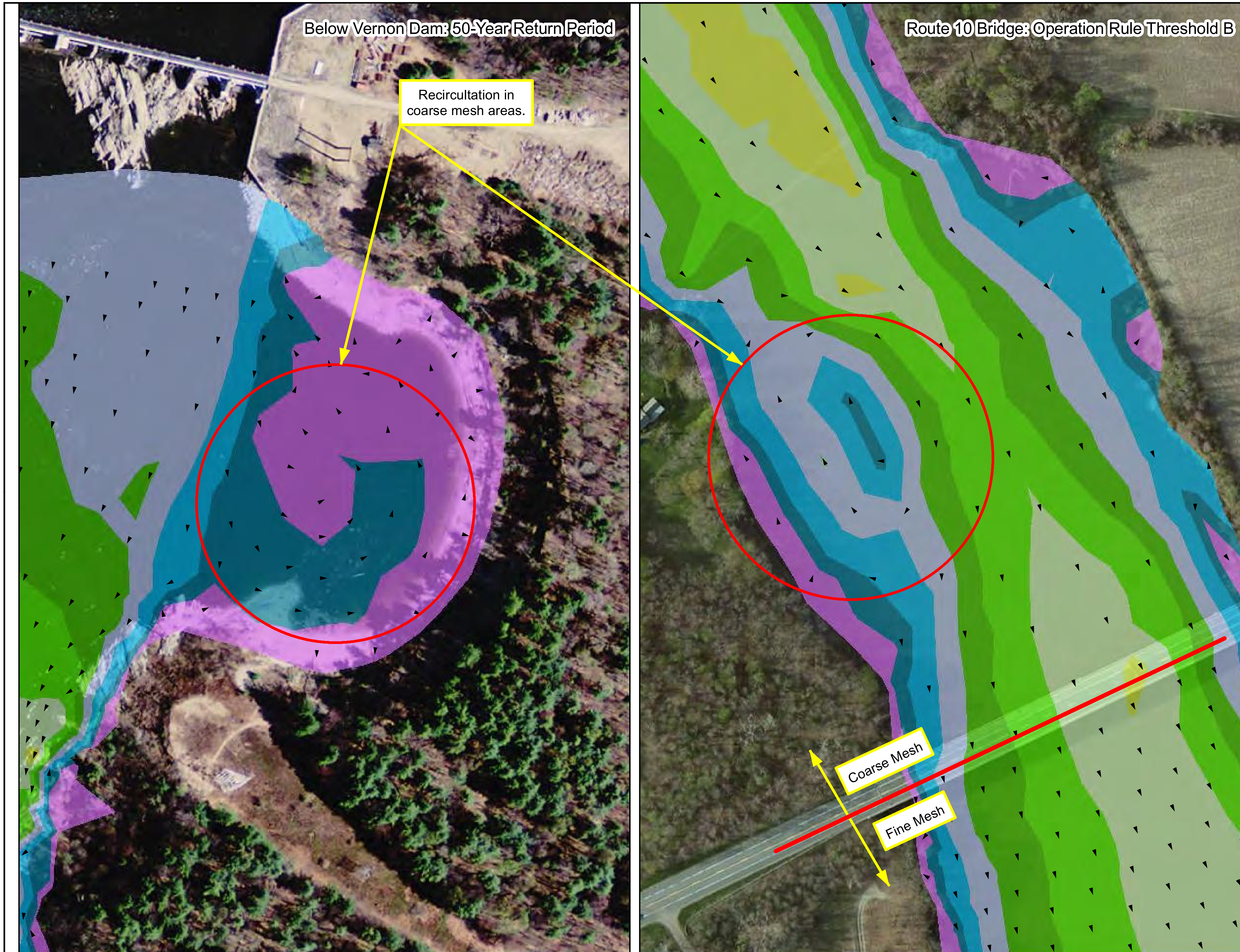

FIRSTLIGHT HYDRO GENERATING COMPANY
Northfield Mountain Pumped Storage Project No. 2485
Turners Falls Hydroelectric Project No. 1889

STUDY 3.1.2

Figure 5.5.1.2-4:
Eddying in Areas of
Coarse Resolution

Legend

N

- Erosion Study Site
- Velocity Direction

Velocity Magnitude

- >10 (ft/s)
- 9 - 10 (ft/s)
- 8 - 9 (ft/s)
- 7 - 8 (ft/s)
- 6 - 7 (ft/s)
- 5 - 6 (ft/s)
- 4 - 5 (ft/s)
- 3 - 4 (ft/s)
- 2 - 3 (ft/s)
- 1 - 2 (ft/s)
- 0.5 - 1 (ft/s)
- 0 - 0.5 (ft/s)

Service Layer Credits: Sources: Esri, HERE, DeLorme, Intermap, increment P Corp., GEBCO, USGS, FAO, NPS, NRCAN, GeoBase, IGN, Kadaster NL, Ordnance Survey, Esri Japan, METI, Esri China (Hong Kong), swisstopo, MapmyIndia, © OpenStreetMap

0 75 150 300 Feet

1 inch = 150 feet

FirstLight Power Resources

Path: W:\gis\studies\3_1_2\maps\final_report\figure_5_5_1_2-4.mxd

5.5.2 Water Level Fluctuations

Water level fluctuations associated with hydropower operations was one of the potential primary causes of erosion identified in the RSP. Section 5.1, and more specifically Section 5.1.3, presented an in-depth look at the complex hydrologic characteristics of the TFI and the hydrologic impacts the Vernon, Northfield Mountain, and Turners Falls hydropower projects have on TFI water levels. The results of the BSTEM modeling discussed in Section 5.4 also took into consideration the impact that water level fluctuations can have on bank stability and erosion processes. Analysis of supplemental groundwater data is presented in this section to examine what impact, if any, water level fluctuations have on groundwater levels and bank stability. The information presented in this section, combined with the information presented in Sections 5.1 and 5.4, provides a comprehensive understanding of water level fluctuations in the TFI and their potential role in bank stability and erosion processes.

The water surface elevation of a river varies depending on the magnitude of flow as a result of typical hydrologic factors including rainfall events and snowmelt. In addition, TFI water levels fluctuate on a shorter term basis as a result of four primary reasons:

1. Natural variability in inflows from upstream as well as from tributary inputs including key tributaries such as the Ashuelot and Millers Rivers;

2. Variable releases from the Vernon Hydroelectric Project;

3. Variable releases from the Turners Falls Hydroelectric Project resulting in water level fluctuations upstream of the Turners Falls Dam; and/or

4. Pumping and generation associated with the Northfield Mountain Project

As previously discussed, when flows are below the hydraulic capacity of the Turners Falls Project (15,938 cfs) and Vernon Project (17,130 cfs), the projects operate in a peaking power mode. During this mode of operation impoundment levels are allowed to rise upstream of the dam(s) during off-peak hours temporarily storing water for power production during peak hours. Power production during peak hours increases the flows through the power plants thus increasing the water level in the river downstream of the dam(s) while also decreasing the impoundment level upstream of the dam(s). When flow in the river is greater than the hydraulic capacity of the hydropower projects, the projects tend to generate at capacity in a run-of-river mode (i.e., inflow equals outflow) with the remaining water being passed over the dam(s). Additionally, Northfield Mountain can operate virtually independent of the flow through the TFI with a maximum generating capacity of 20,000 cfs and pumping capacity of 15,200 cfs, but common operations are not at the maximum capacities.

As discussed in Section 5.1.3, depending on flows and hydropower project operating conditions, water level management at the Turners Falls Dam and operation of Northfield Mountain can impact water levels and flows as far upstream as Vernon. Similarly, Vernon operations can impact water levels and flows as far downstream as the Turners Falls Dam. While some impacts from these projects can be observed a significant distance upstream or downstream from their location, the most significant hydrologic influences are typically localized within the general proximity to a given project with that projects impact dampening in the upstream or downstream direction. This is especially true at high flows (i.e., flows greater than the erosion thresholds observed in BSTEM) where it was observed that water level fluctuations due to hydropower operations at Northfield Mountain were typically on the order of 1.2 ft. at Site 75BL yet only 0.5 ft. at Site 303BL.

5.5.2.1 Groundwater Analysis

The relationship between groundwater levels and river water levels can affect the movement of water through the riverbank via seepage/piping in a narrow zone adjacent to the river. When the groundwater level is higher than the river water level, there is a gradient causing water in the ground to move towards the river. Water tends to move from the river into the ground when river water levels exceed adjacent groundwater levels. The hydraulic conductivity of the soil and the extent of voids or larger spaces between soil particles dictates the speed of water traveling through the soil matrix. Groundwater and river water level data were collected and analyzed in order to better understand these processes.

As discussed in Section 4.2.10, groundwater data were collected in the river as well as at 3 groundwater monitoring wells adjacent to the river in the vicinity of the Rt. 10 Bridge. The groundwater monitoring wells were setback from the edge of water approximately 52, 65, and 210 feet. The complete set of data was plotted and graphs of the entire period from July 13, 1997 through February 28, 1998 are found in Volume III (Appendix I). The corresponding flow for this period of time at the Montague gage shows that the flow ranged from approximately 2,000 to 75,000 cfs, covering periods of low flow with typical hydropower operations as well as a high flow event (Figure 5.5.2.1-1).

Examples of the data from a period of relatively low water and higher water show the response of the groundwater levels to the variations in river water level (Figures 5.5.2.1-2 and 5.5.2.1-3). As observed in the figures, the data show that the ground water closely follows the pattern of water level variations in the river at the two monitoring wells closest to the river. At the well further away from the river, the pattern of hourly fluctuations is damped out but follows the overall rising and falling trends in the river. For the vast majority of the time, the ground water level is higher than water levels in the river indicating a general gradient of groundwater flow towards the river. During the high flow event, the water level in the river rises above the groundwater levels, temporarily reversing the groundwater gradient from the river into the riverbank.

Observation of the data presented above indicates that water moves quite freely into and out of the riverbank. This demonstrates a limited opportunity for significant drawdown effects, particularly during "normal" operations since the water drains out of the soil at essentially the same rate as the decrease in river level. There are no field observations to suggest that groundwater seepage effects due to fluctuating water levels cause failure of riverbanks to any significant degree. In addition to the groundwater analysis described above, soil moisture data were collected and analyzed at the detailed study sites in support of the BSTEM modeling. BSTEM modeling also analyzed the potential impact of water level fluctuations on bank stability via its built-in near bank groundwater model. The findings of the supplemental analysis described above are generally consistent with the findings from the BSTEM modeling efforts and data analysis that showed very limited drawdown effects.

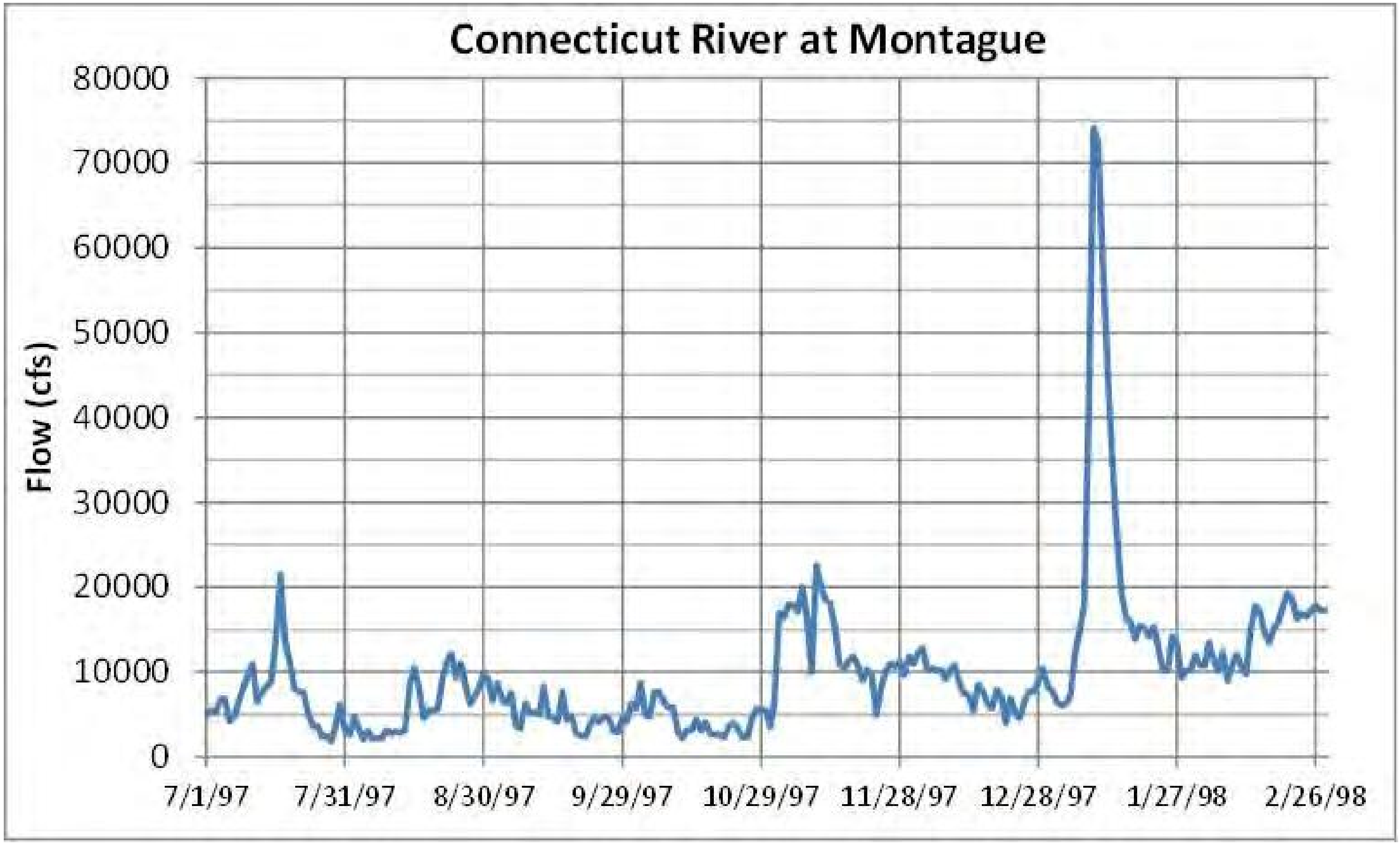

Figure 5.5.2.1-1: Connecticut River at Montague, July 1, 1997 – February 28, 1998

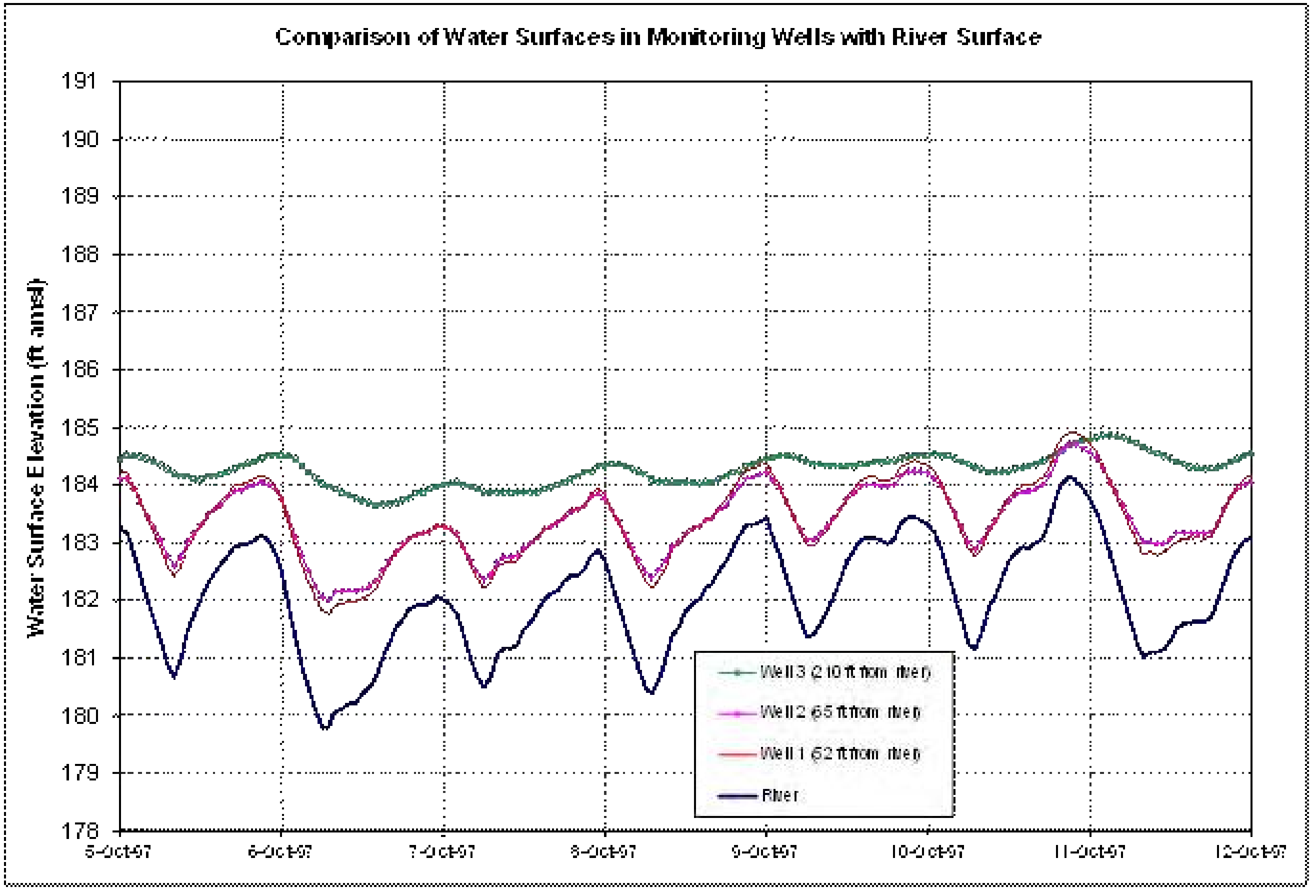

Figure 5.5.2.1-2: Water Level Monitoring Data, October 5-12, 1997

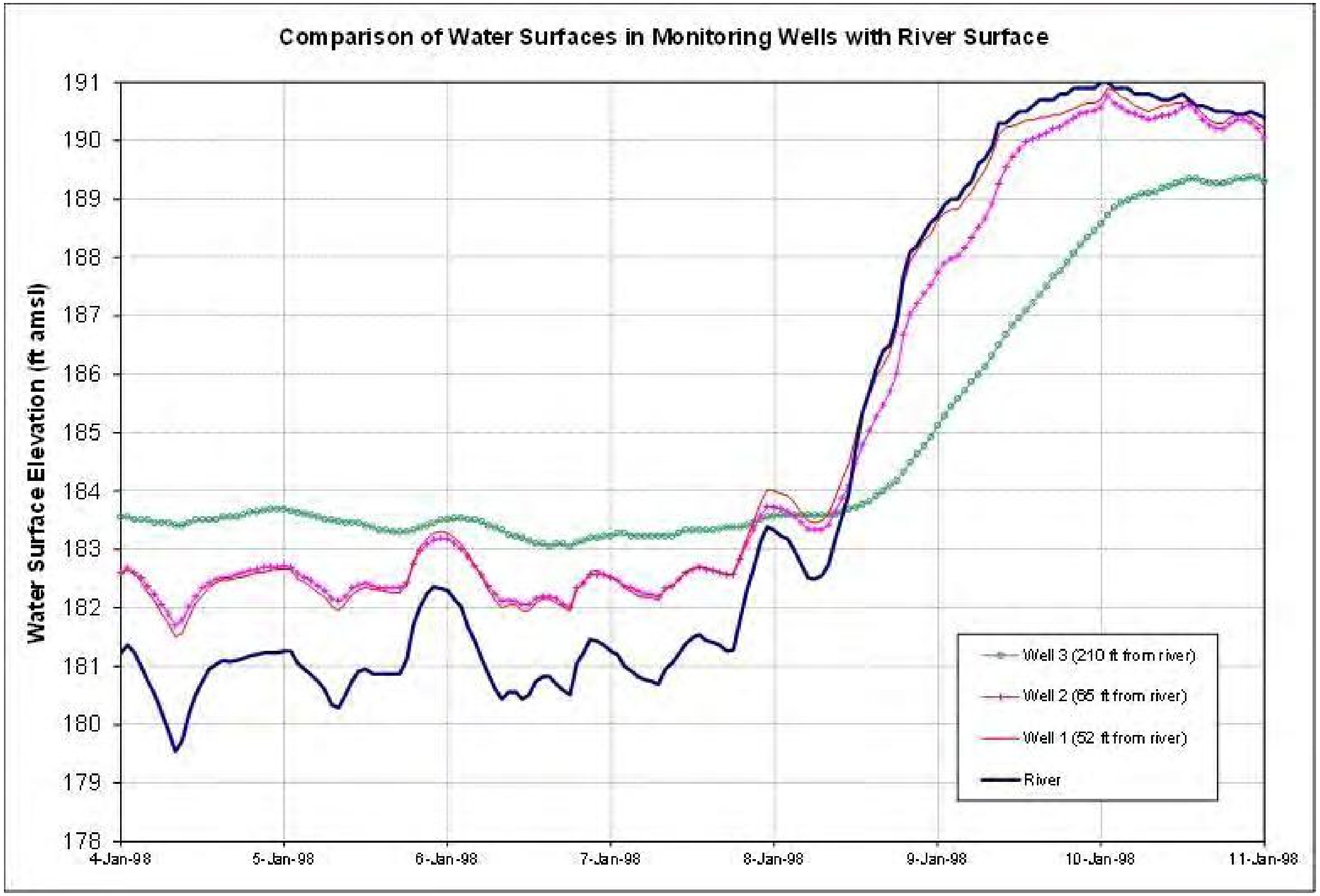

Figure 5.5.2.1-3: Water Level Monitoring Data, January 4-11, 1998

5.5.3 Boat Waves

As discussed in Section 4.2.8 and again in Section 5.4.2, boat waves were investigated in-depth and incorporated for analysis in BSTEM during the study period. In addition to the BSTEM related analysis of boat waves, supplemental boat wave data collected in the 1990's were analyzed as part of this study. This section discusses the results of the non-BSTEM boat wave analysis in order to provide additional context regarding the impact boat waves have on riverbank erosion in the TFI.

The adverse effect of boat wakes and associated waves as they impact the riverbank is acknowledged by the Connecticut River Joint Commissions, supported by Rivers and Trails Conservation Assistance Program of the National Park Service, through the Connecticut River Valley Partnership Program in a guide entitled, "River Dynamics and Erosion." This document states, *"Waves or wakes washing away soil at the base of the bank will undercut it, particularly if it is unvegetated, allowing the unsupported bank material above to collapse into the stream."* The effect of waves is also documented in the scientific literature, an example of which is found in "Experimental measurements of river-bank erosion caused by boat-generated waves on the Gordon river, Tasmania," 1993, Gerald C. Nanson, Axel Von Krusenstierna, Edward A. Bryant and Martin R. Renilson in which they acknowledge that erosion of natural river banks by boat-generated waves is an increasingly serious problem on the navigable reaches of many rivers (Nanson *et al*., 1993).

Episodes of erosion as a result of boat waves are readily observable on the Connecticut River. Furthermore, boat waves have been observed to play a role in creating instability and causing erosion in the TFI. In July 1997, and again in July 1998, S&A investigated the role boat wakes have on riverbank erosion in the TFI. The findings of that investigation are presented in the sections below.

July 1997 Observations

Data on boat waves and their effect on the riverbank were collected on July 12th and 13th, 1997 on the right bank across from Kidds Island and on the right bank downstream of the Route 10 Bridge. The water level in the TFI ranged from about El. 182 down to about El. 180 over the course of the day. The flows released from Vernon ranged from approximately 1,000 to 10,000 cfs. These flow and TFI conditions placed the water level on the lower bank or beach area rather than on the upper bank. At several locations, a temporary staff gage was installed in the water to document wave amplitude and frequency by video tape. Suspended sediment samples were also collected in the area where the waves impacted the riverbank. Figure 5.5.3-1 shows the temporary staff gage and video camera set up to record wave activity. Additional video was taken focusing on the wave activity and bank response.

The rate of rise and fall of the water level due to water level fluctuations was compared to the rate of rise and fall of the water level due to boat waves. Data collected show that boat waves impact the shore at a frequency of once every 1.2 to 1.95 seconds. The maximum amplitude of the initial boat waves recorded by the video camera was generally on the order of several tenths of a foot (approximately 0.2 to 0.4 feet). Timing and amplitude data were determined from analysis of the video of the waves on the staff gage. Some waves that were not recorded on video tape were estimated to have amplitudes as large as about one foot. Based on these data, the rate of rise and fall of the water level based on boat waves is approximately 0.2 to 0.66 feet per second (or 720 to 2400 feet per hour over the limited range of wave from crest to trough). This can be compared with the rate of rise and fall of the TFI fluctuations that are generally on the order of a few tenths of a foot per hour. The rate of change in water level for boat waves therefore ranges from about 1,000 to 10,000 times larger than for TFI fluctuations caused by variability in flow or hydropower operations. Compared against high rates of water level fluctuation that occur less frequently, the ratio of boat wave induced change to TFI level induced change would be smaller than the factor of 1,000 times. Compared against the low rates of TFI water level change that occurs more frequently, the ratio would be even greater than the factor of 10,000. This demonstrates that boat waves are orders of magnitude more intense in terms of rapidity of change of water level than TFI fluctuations caused by variability of flow or hydropower operations.

In addition, water level fluctuations cause no horizontal impact to the riverbank; the water level simply rises and falls slowly. Boat waves, on the other hand, are traveling toward the riverbank at a significant rate of speed causing an impact against the bank as well as an intense rise and fall of water level. Hours of video tape have been collected showing the slow rise and fall of water level associated with hydropower fluctuations without any observable erosion. In contrast, hours of video tape have been collected showing significant erosion due to boat waves.

A series of six photos showing the sequence of a wave impacting the lower riverbank over a period of about 2 seconds is found in Figure 5.5.3-2a through c. Given that the general water level that day was on the lower riverbank, as the waves moved towards the bank they would break on the lower bank and erode a short notch into the bank. As each progressive wave would impact this small notch, some of the vertical face would frequently break off and collapse onto the beach where the water would move sediment particles back down the beach where they would generally deposit. During these low flow conditions the downstream velocity of the flow was negligible so no significant downstream transport of the detached and mobile sediment occurred. Even during this period of relatively low flow and water surface elevation, there was evidence of larger notches cut by the waves in the transition area between the lower and upper riverbanks (Figure 5.5.3-3).

Suspended sediment samples were collected by dip sampling near the water surface at the bank line when boat waves were impacting against the riverbank. These samples represent sediment concentrations in this limited area in the brief window of time when boat waves directly impacted against the riverbanks causing erosion. Near-bank SSC values when boat waves impacted the riverbank ranged from a few hundred to 20,000 mg/L and averaged approximately 9,800 mg/L. By contrast, average near-bank SSC values during non-boat conditions over a wide range of flows (including much higher flow events up to approximately 80,000 cfs) was approximately 66 mg/L (with a range from <5 to 280 mg/L). Based on these data, SSC values observed during boat events is about 148 (9,800/66=148) times greater than suspended sediment samples collected during non-boat events.

Comparisons between the near-bank sediment concentrations affected by boats and without boats are shown in Figures 5.5.3-4 and 5.5.3-5. The first graph is plotted on an arithmetic scale. Because the sediment concentrations are so high for the samples collected during boat events, the sediment concentrations during non-boat events are located very near the axis as if they were virtually zero (even though they range from 5 to 280 mg/L). Plotting the data using this scale shows the dramatic difference between sediment concentrations collected during boat and non-boat events. The second graph (Figure 5.5.3-5) shows the same data plotted with sediment concentrations on a semi-logarithmic scale. This way, the magnitudes of the concentrations for boat and non-boat events can be distinguished.

The majority of the samples collected during the July 1997 field investigation were collected from within the breaking waves where sediment concentrations are highest. These samples represent: (1) the immediate impact of the breaking waves on the lower bank, (2) the resulting erosion of sediment as the wave impacts against and breaks away segments of bank, and (3) the eroded sediment churning into suspension in the immediate area of the breaking wave. Samples collected from within the breaking wave are shown in the vertical row at flows in the range of approximately 7,400 to 9,300 cfs in Figure 5.5.3-4. Also observed in this figure are the two samples collected on 5/7/97 when the flow ranged from about 29,000 to 30,000 cfs. These samples were not collected directly from within the breaking boat waves but in the general vicinity of the wave. As a result the concentrations were in the few hundred mg/L range as opposed to in the thousands or tens of thousands range. While not as high as the values collected in the breaking wave, they were on the same order of magnitude or higher than those samples collected during non-boat events at significantly higher flows.

Figure 5.5.3-1: Video Camera and Temporary Staff Gage

Figure 5.5.3-2a: Boat Wave Data Collection, July 1997

Figure 5.5.3-2b: Boat Wave Data Collection, July 1997

Figure 5.5.3-2c: Boat Wave Data Collection, July 1997

Figure 5.5.3-3: Notching Due to Boat Waves

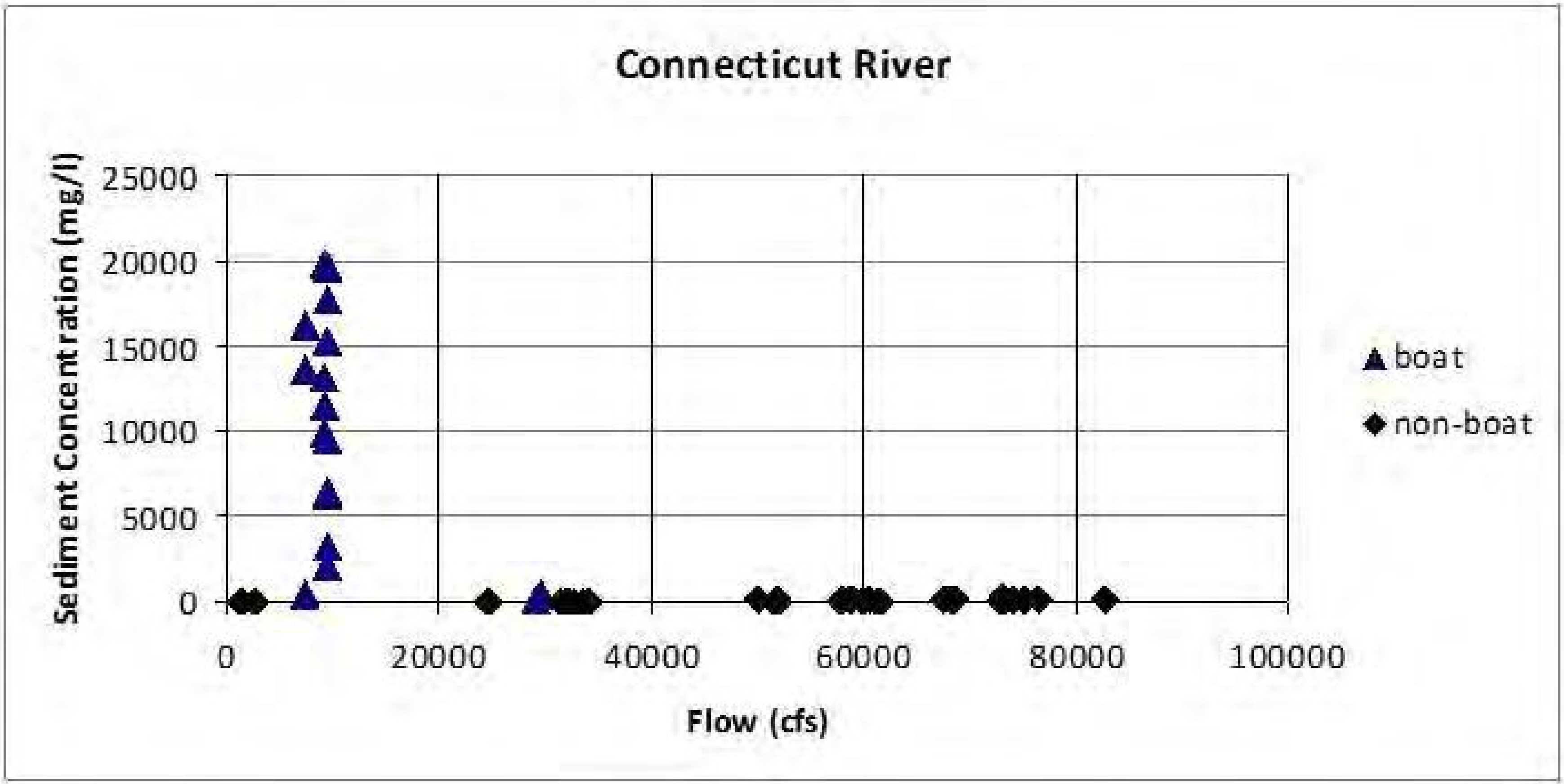

Figure 5.5.3-4 Comparison of Boat vs. Non-Boat Suspended Sediment Concentrations (arithmetic)

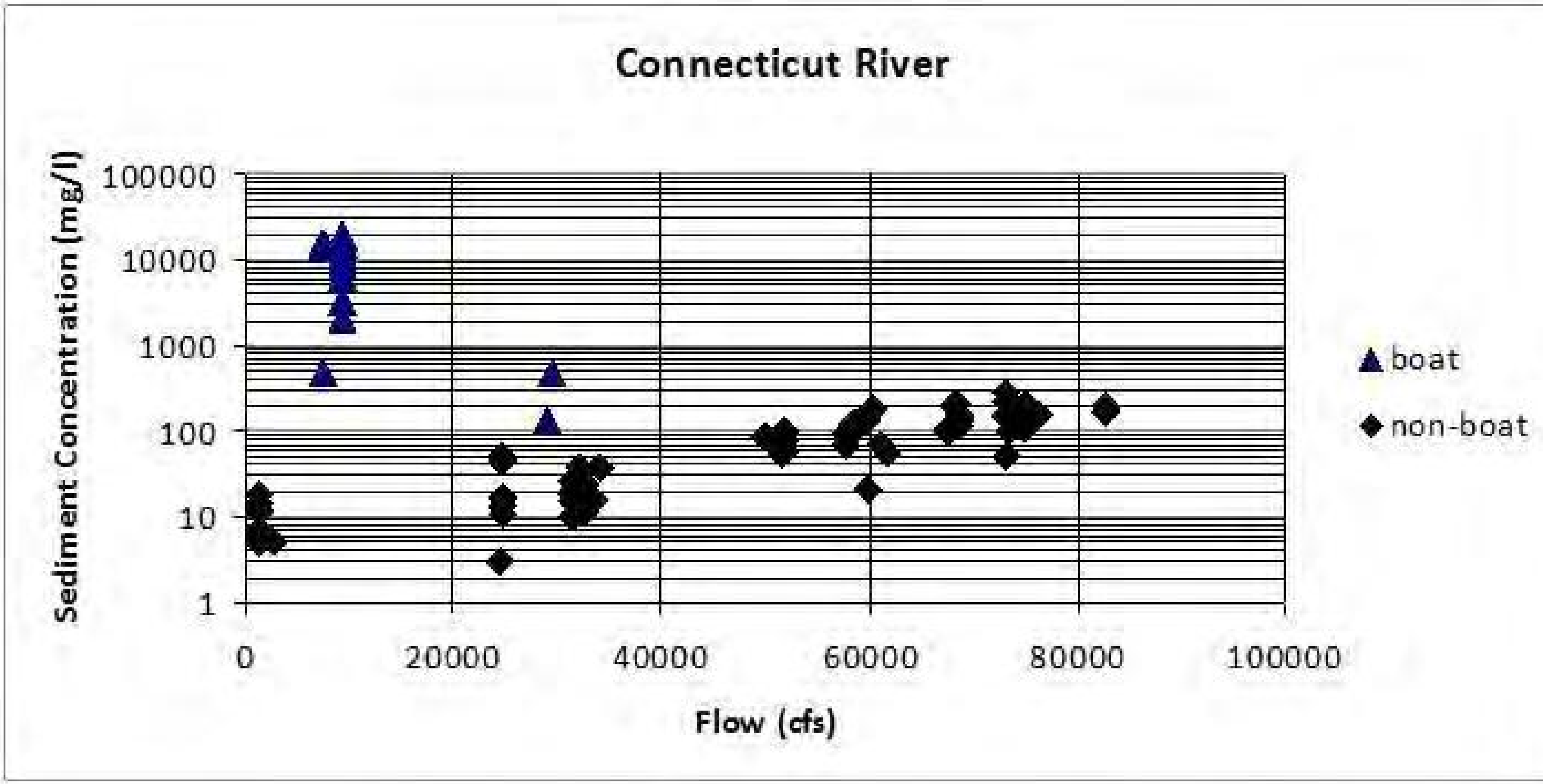

Figure 5.5.3-5 Comparison of Boat vs. Non-Boat Suspended Sediment Concentrations (log)

July 2008 Observations

Boat waves were again monitored during July 26th and 27th, 2008 on the right bank across the river from the Northfield Mountain Tailrace utilizing the same approach with a staff gage and video to analyze the effect of boat waves on riverbank erosion. During these days the flow was relatively high, with Vernon discharge between 48,000 to 50,000 cfs during the day and dropping to about 41,000 cfs at night on July 26th. On July 27th, the flow continued receding from a high of about 42,000 cfs to 34,000 cfs. The water level at Turners Falls Dam was kept between El. 178.8 to 181 during the survey. Thus, the water level at the dam was kept low during this relatively high flow event. The water level at the Northfield tailrace ranged from El. 184.2 to 187.2, dictated by the natural riverine constriction at the French King Gorge. There was no hydropower generation for several hours each day around the middle of the day and no peaking power operations at Vernon or Turners Falls since the flow exceeded the hydraulic generating capacity. As a result of the relatively high flows, the water level was generally above the lower riverbank or beach area for most of these two days and was therefore located on the upper riverbank.

The boat traffic was relatively light for a weekend in July due to cool temperatures and occasional rain. Despite the light boat traffic, significant erosion was observed due to boat waves. Figures 5.5.3-6a and 5.5.3-6b) show a sequence of boat wave impact and erosion photos captured from the video taken these two days. This sequence of photos covers a period of about 10 seconds. The first photo in the sequence shows that a piece of riverbank about 4 to 6 inches in thickness and about a foot or more in height was being undercut by waves at its base had begun to crack loose from the riverbank. As the waves continue to impact the base of this riverbank the crack widens and then the piece falls into the turbulent water. Because the water level was on the upper bank, boat waves undercut the bank and easily caused pieces of bank to fail. As a result, erosion was quite significant over this two day period at the observation site. Hours of video tape are available showing the significant and progressive erosion that resulted from boat waves that impacted the upper bank during a moderately high flow event in July 2008. During these two days, no significant erosion was observed due to the current or the slow rise and fall of the water surface. Significant erosion was observed consistently, however, whenever boat waves impacted and undercut the riverbank. This can be clearly seen in the DVD documenting the study.

After the water had receded further, a photograph of this same area shows that about 4 vertical benches were eroded into the riverbank as waves impacted the bank at different levels as the water level varied with flow (Figure 5.5.3-7). Note that tree roots are observed dangling beneath the overhanging bank at the top of the photograph. It is apparent that other higher flow events have eroded this riverbank resulting in the overhanging bank. A view from a little farther out shows the notches cut into the riverbank by boat waves and the hanging roots from the undercut tree above the portion of the bank recently impacted by boat waves (Figure 5.5.3-8).

Figure 5.5.3-6a: Boat Wave Erosion Sequence

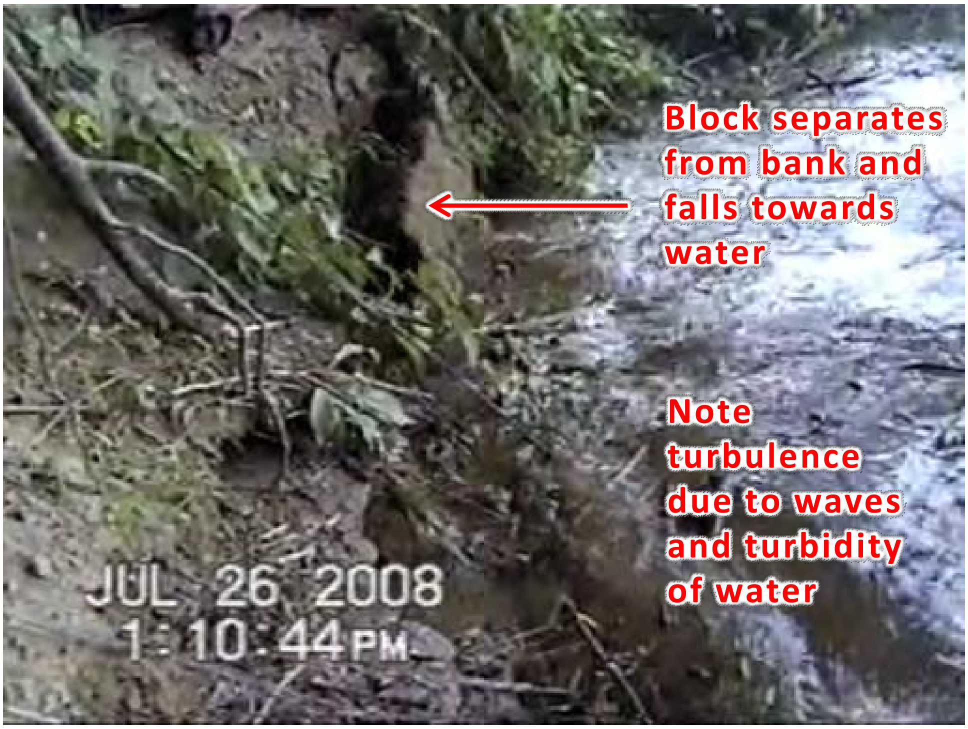

Figure 5.5.3-6b: Boat Wave Erosion Sequence

Figure 5.5.3-7: Example of Boat Wave Erosion

Figure 5.5.3-8: Example of Boat Wave Erosion

Summary of Boat Wave Observations

When the water level is on the lower bank (beach) and boat waves occur, erosion limited in size and damage to the overall riverbank occurs (as shown in Figures 5.5.3-2 a through c). Under conditions with waves breaking on the beach, erosion is typically on the order of an inch or two high and may move on the order of an inch up to a foot in an episode of erosion up the beach. The sediment movement, in this scenario; is from wherever on the beach the wave breaks, down to lower portions of the beach. Since the waves break on the beach, the upper riverbank is not undercut to any significant degree.

On the other hand, when the water level is on the upper bank, boat waves break against a much steeper slope on the upper bank and waves, under this scenario; can and do cause significant erosion and damage to the riverbank. As shown in Figures 5.5.3-6a through b, blocks of sediment on the order of a foot high and several inches back into the bank are broken loose from the upper bank which then fall and disintegrate into individual particles as they hit the turbulent water below. A portion of this eroded material may stay on the upper beach, but when flows are high, the velocity of flow is correspondingly higher than low flow conditions and some of the sediment that is produced by wave action on the upper bank is then transported downstream and away from the beach. Again, no direct erosion of the upper riverbank was observed due to the current or the slowly rising or falling water levels. Significant erosion was observed whenever boat waves impacted and undercut the upper riverbank.

In 2015 detailed boat traffic and wave data were collected as discussed in Section 4.2.8. As part of this data collection effort, cameras were placed on three bridges throughout the TFI to document boat traffic over time. Images from this effort provide further perspective into the fact that boat waves cause some erosion along the riverbanks of the TFI. Figures 5.5.3-9 through 5.5.3-12, taken from the French King Bridge, provide evidence of the impact boat waves can have on erosion. As illustrated by the arrow in the figures, the waves breaking on the shore from the recently passed boat appear to result in a sediment plume emanating from the riverbank. As time progresses so too does the size of the plume.

Figure 5.5.3-9: Plume of Suspended Sediment Begins from Bank Erosion Induced by Waves

Figure 5.5.3-10: Suspended Sediment Plume Expands

Figure 5.5.3-11: Further Expansion of Suspended Sediment Plume

Figure 5.5.3-12: Suspended Sediment Plume Expands Farther Out From Banks

5.5.4 Land Management Practices and Anthropogenic Influences to the Riparian Zone

As part of the 2013 FRR, land-use practices within 200 ft. of adjacent riverbanks throughout the TFI were identified and classified through a combination of desktop GIS analysis and field investigation/validation. In advance of field investigation, preliminary analysis of aerial photographs (2011) was conducted to: (1) determine the width of the riparian buffer; (2) develop a list of predetermined land-use categories that would be used during the field classification; and (3) identify other pertinent land-use information that would be useful during the field survey. Land-use GIS layers from MassGIS were also referenced to complement the preliminary analysis.

Following completion of preliminary analysis land-uses adjacent to TFI riverbanks were identified for an area of approximately 200 feet horizontally from the top of the slope. Land-use categories identified during this process included:

- Agriculture (intensive (e.g., row crops) and pasture/hay)
- Barren (little or no vegetation growth)
- Developed (houses or other impermeable land uses)
- Riparian Buffer Forest (statistics for different widths (0-25 ft., 25-50 ft., 50-100 ft., 100-200 ft., and >200 ft.))
- Wetland (non-forested)
- Restored Banks
- Transportation (roads, bridges, railroad)

Table 5.5.4-1 provides a summary of the land-use classifications identified in the TFI while Table 5.5.4-2 includes summary statistics regarding the width of the forested riparian buffer throughout the TFI. Maps denoting the various land-use classifications throughout the TFI can be found in Figure 5.5.4-1.

Various types and degrees of erosion found in the TFI can be observed at locations with a wide variety of adjacent land-uses. The strongest correlation between land-use and erosion has been observed in agricultural areas. Agriculture along the river typically is located on relatively flat floodplain terraces with only a narrow or virtually non-existent zone of riparian vegetation (Figure 5.5.4-2). Riparian vegetation along a river corridor plays a significant role in riverbank stability as it damps out or attenuates hydraulic forces of flowing water or waves as well as providing structure to bind soils together through its root system. To the extent that riparian vegetation is adversely affected, riverbank stability is likewise adversely affected.

As observed in Tables 5.5.4-1 and 5.5.4-2, 27.5% of TFI riverbanks were classified as either cropland or pasture with 38% of riverbanks exhibiting a riparian buffer less than 50 ft. Frequently riverbanks in areas with narrow or non-existent riparian buffers consist of steep to overhanging banks consisting of silty/sandy soils that are easily erodible unless sufficient vegetation is present to reinforce the soil and provide some buffering of hydraulic forces. An example of erosion that has occurred where the agricultural land-use exists can be seen in Figure 5.5.4-3.

In addition to narrow riparian zones, agricultural irrigation practices can impact riverbank processes. In relatively recent years, irrigation has been increasingly utilized on a number of agricultural fields adjacent to the Connecticut River (Figures 5.5.4-4 and 5.5.4-5). Some irrigation water comes from groundwater pumping and some comes directly from the river (Figures 5.5.4-6a -c). Water is applied on relatively flat terraces adjacent to the river where agricultural fields have been developed. Irrigation water is used to supplement rainfall which adds to wetter soil conditions. Some of the irrigation water provides water to crops and in this process a portion of the water goes to evapo-transpiration while some of it infiltrates deeper into the soil and flows back towards the river. Irrigation therefore increases soil moisture and the quantity of water that may seep through the banks which could adversely affect riverbank stability in these localized areas.

When significant rainfall occurs, water may pond on relatively flat agricultural fields and infiltrate into the ground (Figures 5.5.4-7 through 5.5.4-13, 9/30/2015). This adds to soil saturation (compared to hillslopes where more rainfall tends to occur as runoff and less infiltration into the soil). A greater degree of saturation in these soils would then result in additional seepage through the riverbank and back to the river.

In addition to agriculture, erosion has also been observed in areas where houses and other associated development are located in close proximity to the river. An example of erosion in close proximity to a house is shown in Figure 5.5.4-14. As shown in the figure undercutting, overhanging bank, and exposed roots were observed at this location in close proximity to the structure. In several instances where houses have been built close to the river, riparian vegetation has also been cleared which can adversely affect riverbank stability. An example of this is shown in Figure 5.5.4-15.

As observed in Figure 5.5.4-1, many of the eroded sites where stabilization has occurred in accordance with the ECP are found at locations where the adjacent land-use is classified as either agricultural or some other type of development. This indicates the adverse effect land-use and land management practices can have on riverbank stability.

Table 5.5.4-1: Summary of Turners Falls Impoundment Land-use (200-ft Buffer)

Land-use	Acres	Percentage of Total
Cropland	275	26
Pasture	15	1.5
Barren	1	<0.5
Developed	86	8
Transportation	22	2
Forest	631	60
Non-forested wetland	4	0.5
Restored	11	1

Table 5.5.4-2: Forested Riparian Buffer Widths (within 500 ft.)

Width (ft.)	Length (mi)	Percentage of Total
0-25	14	31
25-50	3	7
50-100	5	11
100-200	7	15
200-500	16	36

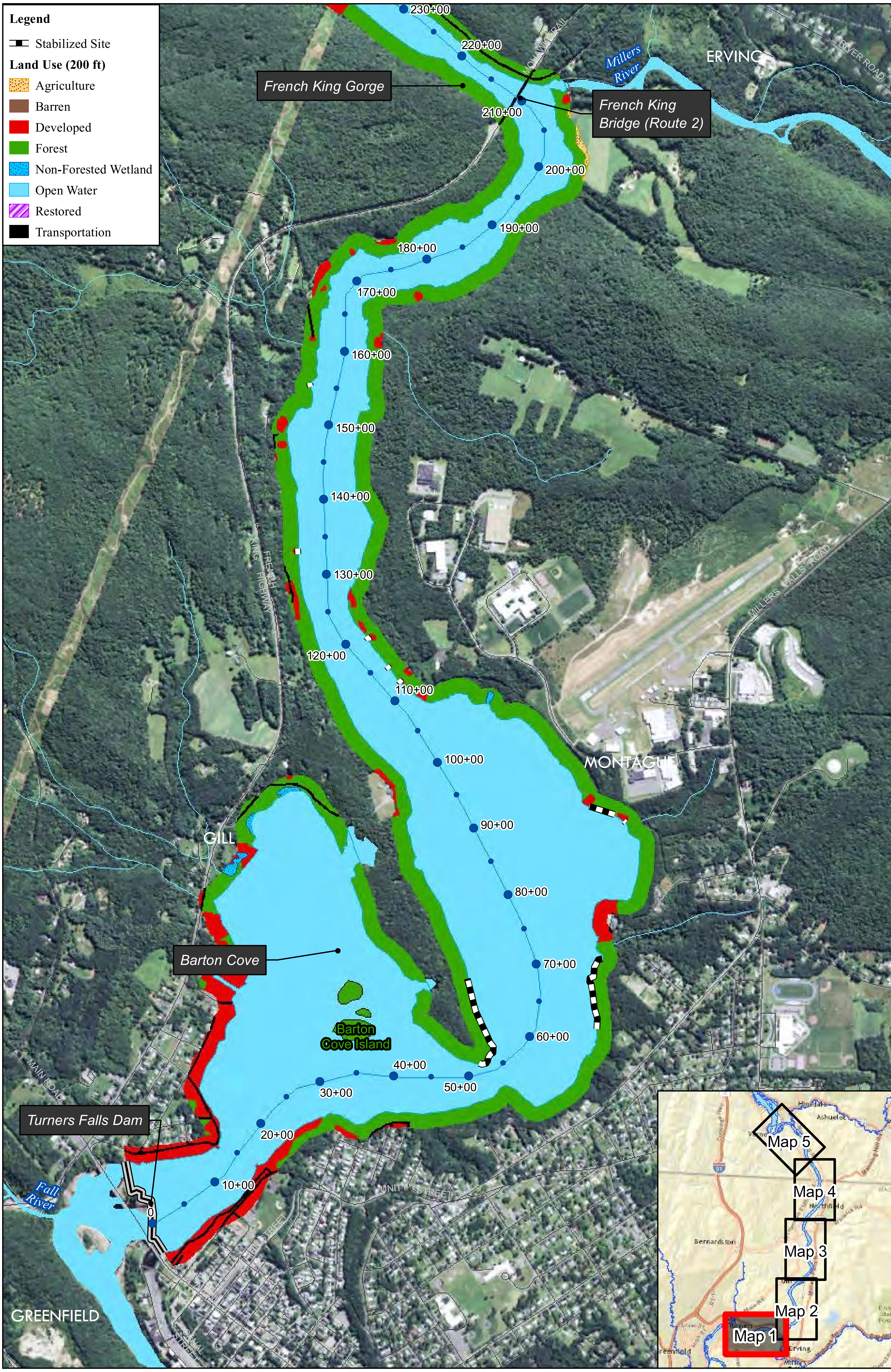

FIRSTLIGHT HYDRO GENERATING COMPANY
Northfield Mountain Pumped Storage Project No. 2485
Turners Falls Hydroelectric Project No. 1889

STUDY 3.1.2

0 625 1,250 2,500 Feet

Figure 5.5.4-1:
Turners Falls Impoundment
Land-use (2013 FRR)
Map 1

Service Layer Credits: Sources: Esri, HERE, DeLorme, USGS, Intermap, increment P Corp., NRCAN, Esri Japan, METI, Esri China (Hong Kong), Esri (Thailand), MapmyIndia, © OpenStreetMap contributors, and the GIS User Community
Source: Esri, DigitalGlobe, GeoEye, Earthstar Geographics, CNES/Airbus DS, USDA, USGS,

Path: W:\gis\studies\3_1_2\maps\final_report\figure_5_5_4-1.mxd

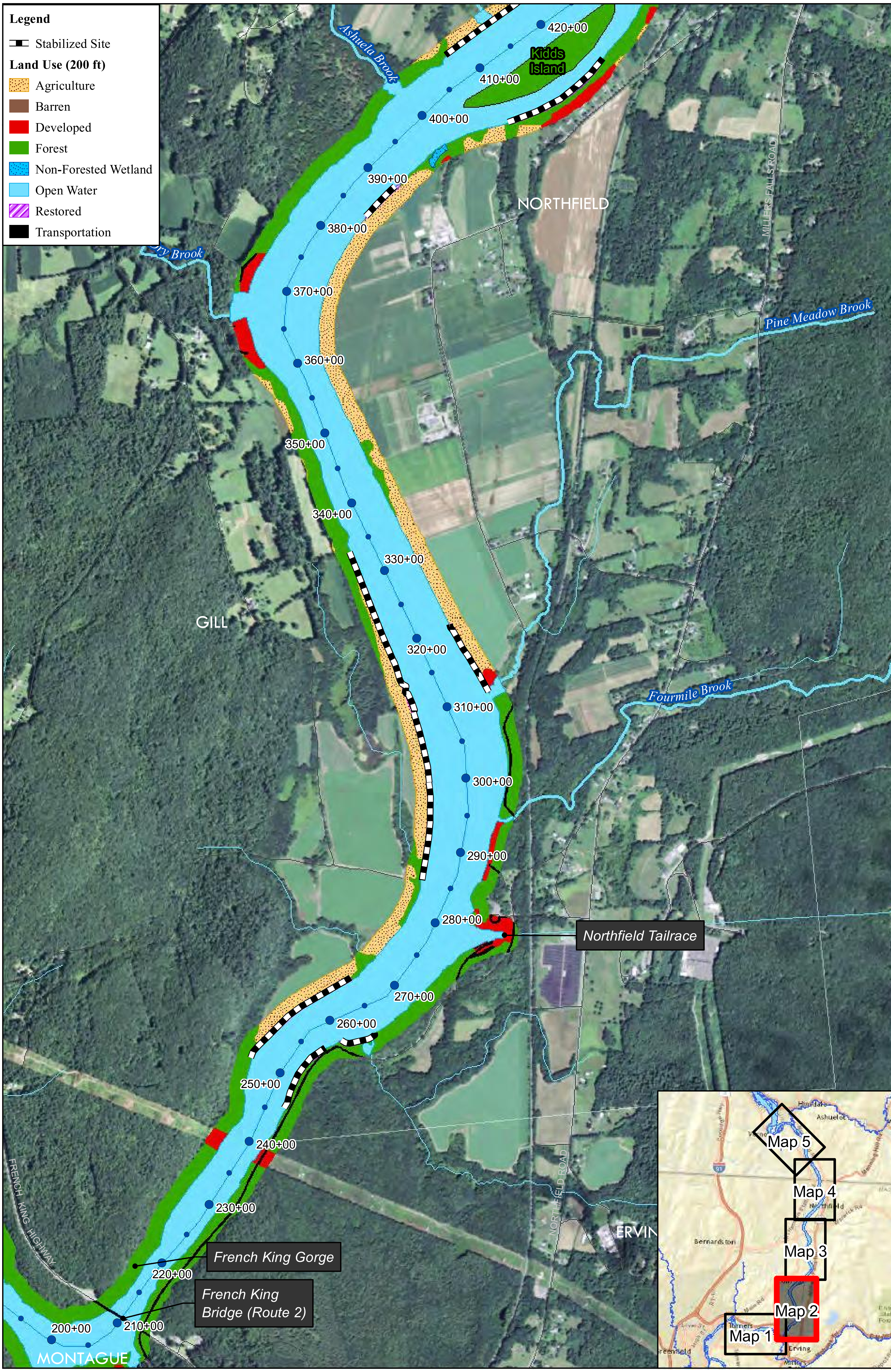

FirstLight Power Resources

N

FIRSTLIGHT HYDRO GENERATING COMPANY
Northfield Mountain Pumped Storage Project No. 2485
Turners Falls Hydroelectric Project No. 1889

STUDY 3.1.2

0 625 1,250 2,500 Feet

Figure 5.5.4-1:
Turners Falls Impoundment
Land-use (2013 FRR)
Map 2

Service Layer Credits: Sources: Esri, HERE, DeLorme, USGS, Intermap, increment P Corp., NRCAN, Esri Japan, METI, Esri China (Hong Kong), Esri (Thailand), MapmyIndia, © OpenStreetMap contributors, and the GIS User Community
Source: Esri, DigitalGlobe, GeoEye, Earthstar Geographics, CNES/Airbus DS, USDA, USGS,

Path: W:\gis\studies\3_1_2\maps\final_report\figure_5_5_4-1.mxd

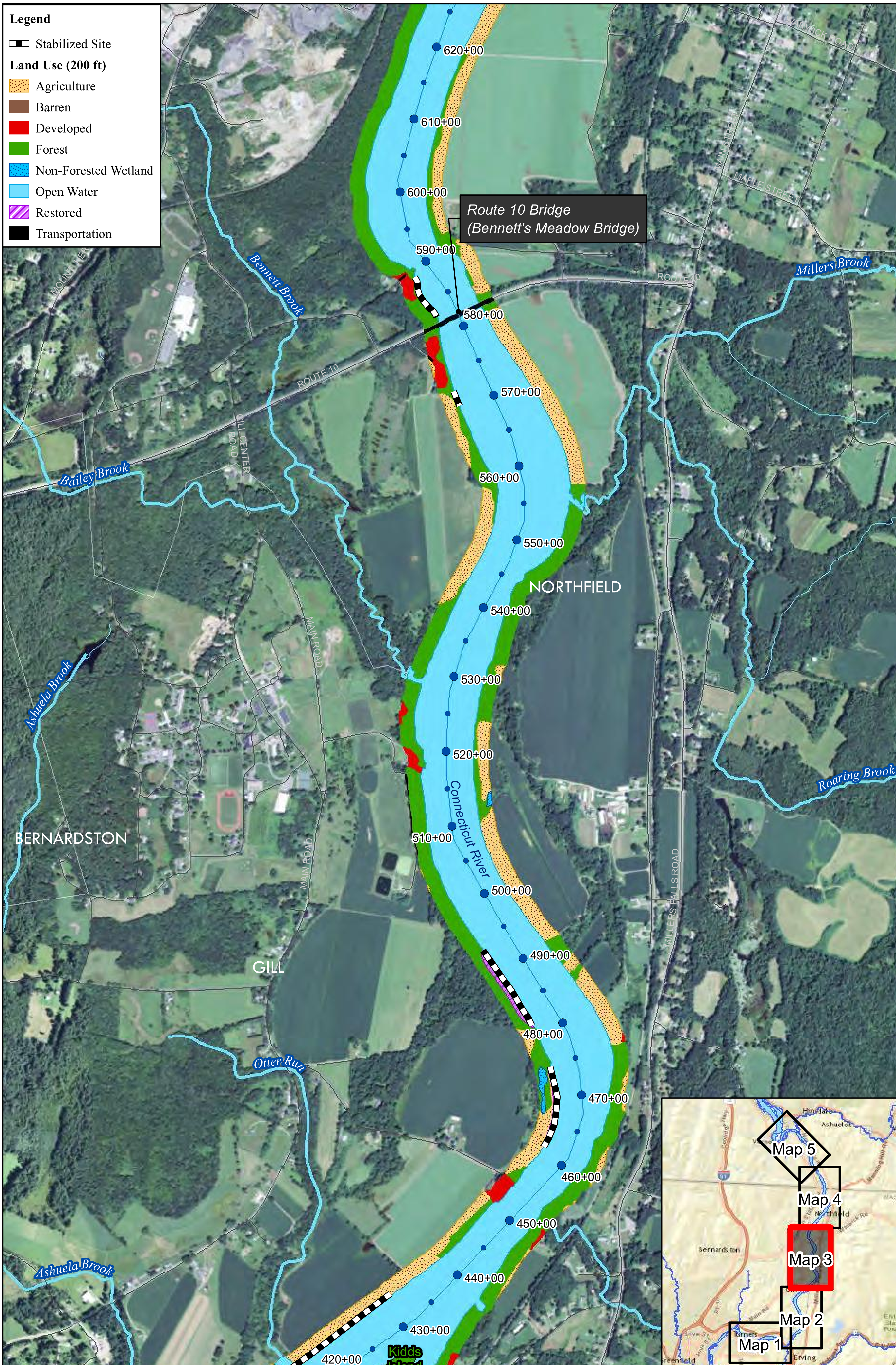

FIRSTLIGHT HYDRO GENERATING COMPANY
Northfield Mountain Pumped Storage Project No. 2485
Turners Falls Hydroelectric Project No. 1889

STUDY 3.1.2

FirstLight Power Resources

N

0 625 1,250 2,500 Feet

Figure 5.5.4-1:
Turners Falls Impoundment
Land-use (2013 FRR)
Map 3

Service Layer Credits: Sources: Esri, HERE, DeLorme, USGS, Intermap, increment P Corp., NRCAN, Esri Japan, METI, Esri China (Hong Kong), Esri (Thailand), MapmyIndia, © OpenStreetMap contributors, and the GIS User Community
Source: Esri, DigitalGlobe, GeoEye, Earthstar Geographics, CNES/Airbus DS, USDA, USGS,

Path: W:\gis\studies\3_1_2\maps\final_report\figure_5_5_4-1.mxd